

REVIEW OF THE QCD SUM RULES FOR EXOTIC STATES

Zhi-Gang Wang¹

Department of Physics, North China Electric Power University, Baoding 071003, P. R. China

Abstract

We review the exotic states, such as the X , Y , Z , T and P states, and present their possible assignments based on the QCD sum rules. We present many predictions which can be confronted to the experimental data in the future to diagnose the exotic states. Furthermore, we also mention other theoretical methods.

Contents

1	Introduction	2
1.1	Overview	2
1.2	$X(3872)$	2
1.3	$X(3915)$, $X(3940)$, $Y(3940)$, $Z(3930)$, $X(4160)$, $X(3860/3960)$	3
1.4	$\eta_c(3945)$, $h_c(4000)$, $\chi_{c1}(4010)$, $h_c(4300)$	4
1.5	$X(4140)$, $X(4274)$, $X(4500/4475)$, $X(4700/4710)$, $X(4685/4650)$, $X(4630/4800)$	4
1.6	$X(4350)$	5
1.7	$X_0(2900)$, $X_1(2900)$, $T_{c\bar{s}}(2900)$	5
1.8	$X(5568)$	5
1.9	$X(6600)$, $X(6900)$, $X(7300)$	6
1.10	$Y(4260/4230)$, $Y(4360/4320)$, $Y(4390)$, $Y(4500)$, $Y(4660)$, $Y(4710/4750/4790)$	6
1.11	$Z_c(3900/3885)$, $Z_c(4020/4025)$, $Z_{cs}(3985/4000)$, $Z_{cs}(4123)$, $Z_{cs}(4220)$	7
1.12	$Z_1(4050)$, $Z_1(4250)$, $Z_c(4100)$	8
1.13	$Z_c(4430)$, $Z_c(4600)$	9
1.14	$Z_c(4200)$, $Z_{c\bar{s}}(4600)$, $Z_{c\bar{s}}(4900)$, $Z_{c\bar{s}}(5200)$	9
1.15	$Z_b(10610)$, $Z_b(10650)$, $Y(10750)$	9
1.16	$T_{cc}(3875)$	10
1.17	$P_c(4312)$, $P_c(4380)$, $P_c(4440)$, $P_c(4457)$, $P_c(4337)$, $P_{cs}(4338)$, $P_{cs}(4459)$	10
2	Theoretical methods and possible assignments	11
2.1	Threshold cusps, Triangle singularities or genuine Resonances	11
2.2	Dynamical Generated Resonances and Molecular States	14
2.3	$Q\bar{Q}$ states with coupled channel effects	14
2.4	Hybrid and Tetraquark states in Born-Oppenheimer approximation	15
2.5	Tetraquarks in diquark models	16
2.6	Tetraquark states from Lattice QCD	18
2.7	Tetraquark (molecular) states with the QCD sum rules	19
3	Are QCD sum rules reliable to explore multiquark states	21
4	Energy scale dependence of the QCD sum rules	30
5	$\bar{3}3$ type hidden-heavy tetraquark states	37
5.1	Tetraquark states with positive parity	38
5.2	Tetraquark states with the first radial excitation	55
5.3	Tetraquark states with negative parity	59
5.4	Tetraquark states with explicit P-wave	69
6	$\bar{3}3$ type doubly heavy tetraquark states	74

¹E-mail: zgwang@aliyun.com.

7	$\bar{3}3$ type fully heavy tetraquark states	78
8	11 type hidden/doubly heavy tetraquark states	82
8.1	11 type hidden heavy tetraquark states	85
8.2	11 type doubly heavy tetraquark states	95
9	Hidden heavy pentaquark states	100
9.1	$\bar{3}33$ type hidden heavy pentaquark states	102
9.2	11 type hidden heavy pentaquark states	119
10	Singly-heavy tetraquark and pentaquark states	126
10.1	Singly-heavy tetraquark states	126
10.2	Single-heavy pentaquark states	128
11	Strong decays of exotic states	135
11.1	Strong decays of the $Y(4500)$ as an example	138
11.2	Light-cone QCD sum rules for the $Y(4500)$ as an example	149

1 Introduction

1.1 Overview

In 1964, Gell-Mann suggested that multi-quark states beyond the minimal valence quark constituents $q\bar{q}$ and qqq maybe exist [1], a quantitative model for the tetraquark states with the quark contents $qq\bar{q}\bar{q}$ was developed by Jaffe using the MIT bag model in 1977 [2, 3]. Latter, the five-quark baryons with the quark contents $qqqq\bar{q}$ were developed [4], while the name pentaquark was introduced by Lipkin [5]. The QCD allows the existence of multi-quark states and hybrid states which contain not only quarks but also gluonic degrees of freedom [6, 7, 8].

Before observation of the $X(3872)$ by the Belle collaboration in 2003 [9], the most promising and most hot subject is the nature of the light mesons below 1 GeV, are they traditional 3P_0 states, tetraquark states or molecular states? [2, 3, 10, 11, 12, 13]. In fact, the observation of the $X(3872)$ stimulates more motivations and curiosities in the nature of the light scalar mesons [14, 15, 16, 17, 18, 19, 20, 21, 22, 23, 24, 25], for more references, see the reviews [26, 27, 28]. However, it is an un-resolved problem until now. Firstly, let us see the experimental data on the exotic states pedagogically and dogmatically in the order X , Y , Z , T and P sequentially. There have been several reviews with emphasis on different aspects [29, 30, 31, 32, 33, 34, 35, 36, 37, 38, 39, 40, 41, 42, 43].

1.2 $X(3872)$

In 2003, the Belle collaboration observed a narrow charmonium-like state $X(3872)$ with the mass $3872.0 \pm 0.6 \pm 0.5$ MeV near the $D\bar{D}^*$ threshold in the $\pi^+\pi^-J/\psi$ mass spectrum in the exclusive decay processes $B^\pm \rightarrow K^\pm\pi^+\pi^-J/\psi$ [9]. The evidences for the decay modes $X(3872) \rightarrow \gamma J/\psi, \gamma\psi'$ observed by the Belle and BaBar collaborations imply the positive charge conjunction $C = +$ [44, 45, 46]. Angular correlations between final state particles $\pi^+\pi^-J/\psi$ analyzed by the CDF, Belle and LHCb collaborations favor the $J^{PC} = 1^{++}$ assignment [47, 48, 49, 50]. It is a possible candidate for the tetraquark state [51, 52, 53, 54, 55, 56, 57, 58], (not) molecular state ([59]) [60, 61, 62, 63, 64, 65, 66, 67, 68, 69, 70, 71, 72, 73, 74, 75, 76, 77, 78], (not) traditional charmonium $\chi_{c1}(2P)$ ([79]) [80, 81, 82], threshold cusp [83], etc. However, none of those available assignment has won an overall consensus, its nature is still under heated debates, the very narrow width and exotic branching fractions make it a hot potato. yet, and the door remains open for another binding mechanism.

1.3 $X(3915)$, $X(3940)$, $Y(3940)$, $Z(3930)$, $X(4160)$, $X(3860/3960)$

In 2005, the Belle collaboration observed the $Y(3940)$ in the B -decays $B \rightarrow KY(3940) \rightarrow K\omega J/\psi$ [84], later, the BaBar collaboration confirmed the $Y(3940)$ in the $\omega J/\psi$ mass spectrum with a mass about 3.915 GeV in the decays $B \rightarrow K\omega J/\psi$ [85, 86].

In 2007, the Belle collaboration observed the $X(3940)$ in the process $e^+e^- \rightarrow J/\psi X(3940)$ with the subprocess $X(3940) \rightarrow D^*\bar{D}$ [87]. In 2008, the Belle collaboration confirmed the $X(3940)$ in the same process, and observed the $X(4160)$ in the subprocess $X(4160) \rightarrow D^*\bar{D}^*$ [88].

In 2010, the $X(3915)$ was observed in the process $\gamma\gamma \rightarrow J/\psi\omega$ by the Belle collaboration [89], then the BaBar collaboration determined its quantum numbers $J^P = 0^+$ [90], it is a good candidate for the conventional charmonium $\chi_{c0}(2P)$. The $Y(3940)$ and $X(3915)$ could be the same particle, and is denoted as the $\chi_{c0}(3915)$ with the assignment $J^{PC} = 0^{++}$ in *The Review of Particle Physics* [91].

In 2006, the $Z(3930)$ was observed in the process $\gamma\gamma \rightarrow J/\psi\omega$ by the Belle collaboration [92], then confirmed by the BaBar collaboration in the same process [93], the two collaborations both determined its quantum numbers to be $J^{PC} = 2^{++}$, and it is widely assigned as the $\chi_{c2}(3930)$.

In 2017, the Belle collaboration performed a full amplitude analysis of the process $e^+e^- \rightarrow J/\psi D\bar{D}$, and observed a new charmonium-like state $X^*(3860)$ which decays to the $D\bar{D}$ pair, the measured mass and width are 3862_{-32}^{+26+40} MeV and $201_{-67}^{+154+88}$ MeV, respectively [94]. The $J^{PC} = 0^{++}$ hypothesis is favored over the 2^{++} hypothesis at the level of 2.5σ , and the Belle collaboration assigned the $X^*(3860)$ as an alternative $\chi_{c0}(2P)$ state [94].

In 2020, the LHCb collaboration performed an amplitude analysis of the $B^+ \rightarrow D^+D^-K^+$ decays and observed that it is necessary to include the $\chi_{c0}(3930)$ and $\chi_{c2}(3930)$ with the $J^{PC} = 0^{++}$ and 2^{++} respectively in the D^+D^- channel, and to include the $X_0(2900)$ and $X_1(2900)$ with the $J^P = 0^+$ and 1^- respectively in the D^-K^+ channel [95, 96]. The measured Breit-Wigner masses and widths are

$$\begin{aligned}\chi_{c0}(3930) &: M = 3923.8 \pm 1.5 \pm 0.4 \text{ MeV}; \Gamma = 17.4 \pm 5.1 \pm 0.8 \text{ MeV}, \\ \chi_{c2}(3930) &: M = 3926.8 \pm 2.4 \pm 0.8 \text{ MeV}; \Gamma = 34.2 \pm 6.6 \pm 1.1 \text{ MeV},\end{aligned}\quad (1)$$

and the $\chi_{c0}(3915)$ and $\chi_{c0}(3930)$ can be identified as the $\chi_{c0}(2P)$.

In 2023, the LHCb collaboration announced the observation of the $X(3960)$ in the $D_s^+D_s^-$ mass spectrum in the $B^+ \rightarrow D_s^+D_s^-K^+$ decays, and the assignment $J^{PC} = 0^{++}$ is favored [97], the measured Breit-Wigner mass and width are $3956 \pm 5 \pm 10$ MeV and $43 \pm 13 \pm 8$ MeV, respectively.

The thresholds of the $D_s^+D_s^-$ and D^+D^- are 3938 MeV and 3739 MeV, respectively, which favors assigning the $X(3960)$ and $\chi_{c0}(3930)$ as the same particle. However, the ratio of the branching fractions [97],

$$\frac{\Gamma(X \rightarrow D^+D^-)}{\Gamma(X \rightarrow D_s^+D_s^-)} = 0.29 \pm 0.09 \pm 0.10 \pm 0.08, \quad (2)$$

implies the exotic nature of this state, as it is harder to excite an $s\bar{s}$ pair from the vacuum compared with the $u\bar{u}$ or $d\bar{d}$ pair, and the traditional charmonium states predominantly decay into the $D\bar{D}$ and $D^*\bar{D}^*$ states rather than into the $D_s\bar{D}_s$ and $D_s^*\bar{D}_s^*$ states. In addition, there is no room for the $X(3860)$, so at least one of the $X(3860)$, $X(3915)$, $\chi_{c0}(3930)$ and $X(3960)$ should be exotic state.

For example, the updated nonrelativistic potential mode (NR) and Godfrey-Isgur relativized potential model (GI) indicate that the 2P charmonium states have the masses (NR; GI)[98],

$$\begin{aligned}\chi_{c2}(2P) &: 3972 \text{ MeV}, 3979 \text{ MeV}, \\ \chi_{c1}(2P) &: 3925 \text{ MeV}, 3953 \text{ MeV}, \\ \chi_{c0}(2P) &: 3852 \text{ MeV}, 3916 \text{ MeV},\end{aligned}\quad (3)$$

even the assignments of the $\chi_{c0}(2P)$ and $\chi_{c2}(2P)$ are not comfortable enough.

1.4 $\eta_c(3945)$, $h_c(4000)$, $\chi_{c1}(4010)$, $h_c(4300)$

In 2024, the LHCb collaboration explored the decays $B^+ \rightarrow D^{*+}D^-K^+$ and $D^{*-}D^+K^+$, and observed four charmonium(-like) states $\eta_c(3945)$, $h_c(4000)$, $\chi_{c1}(4010)$ and $h_c(4300)$ with the quantum numbers $J^{PC} = 0^{-+}, 1^{+-}, 1^{++}$ and 1^{+-} respectively in the $D^{*\pm}D^\mp$ mass spectrum [99]. The measured Breit-Wigner masses and widths are

$$\begin{aligned}\eta_c(3945) : M &= 3945_{-17}^{+28} {}_{-28}^{+37} \text{ MeV}, \Gamma = 130_{-49}^{+92} {}_{-70}^{+101} \text{ MeV}, \\ h_c(4000) : M &= 4000_{-14}^{+17} {}_{-22}^{+29} \text{ MeV}, \Gamma = 184_{-45}^{+71} {}_{-61}^{+97} \text{ MeV}, \\ \chi_{c1}(4010) : M &= 4012.5_{-3.9}^{+3.6} {}_{-3.7}^{+4.1} \text{ MeV}, \Gamma = 62.7_{-6.4}^{+7.0} {}_{-6.6}^{+6.4} \text{ MeV}, \\ h_c(4300) : M &= 4307.3_{-6.6}^{+6.4} {}_{-4.1}^{+3.3} \text{ MeV}, \Gamma = 58_{-16}^{+28} {}_{-25}^{+28} \text{ MeV}.\end{aligned}\quad (4)$$

The updated nonrelativistic potential mode (NR) and Godfrey-Isgur relativized potential model (GI) indicate that the 3S/2P/3P charmonium states have the masses (NR; GI) [98],

$$\begin{aligned}\eta_c(3S) &: 4043 \text{ MeV}, 4064 \text{ MeV}, \\ \chi_{c1}(2P) &: 3925 \text{ MeV}, 3953 \text{ MeV}, \\ \chi_{c1}(3P) &: 4271 \text{ MeV}, 4317 \text{ MeV}, \\ h_c(2P) &: 3934 \text{ MeV}, 3956 \text{ MeV}, \\ h_c(3P) &: 4279 \text{ MeV}, 4318 \text{ MeV},\end{aligned}\quad (5)$$

the assignments $\eta_c(3945)$, $h_c(4000)$ and $\chi_{c1}(4010)$ in Ref.[99] are rather marginal.

1.5 $X(4140)$, $X(4274)$, $X(4500/4475)$, $X(4700/4710)$, $X(4685/4650)$, $X(4630/4800)$

In 2009, the CDF collaboration observed the $X(4140)$ in the $J/\psi\phi$ mass spectrum in the $B^+ \rightarrow J/\psi\phi K^+$ decays with a significance larger than 3.8σ [100]. In 2011, the CDF collaboration confirmed the $Y(4140)$ in the $B^\pm \rightarrow J/\psi\phi K^\pm$ decays with a significance greater than 5σ , and observed an evidence for the $X(4274)$ with an approximate significance of 3.1σ [101]. In 2013, the CMS collaboration also confirmed the $X(4140)$ in the $B^\pm \rightarrow J/\psi\phi K^\pm$ decays [102].

In 2016, the LHCb collaboration performed the first full amplitude analysis of the $B^+ \rightarrow J/\psi\phi K^+$ decays, confirmed the $X(4140)$ and $X(4274)$ in the $J/\psi\phi$ mass spectrum, and determined the spin-parity to be $J^P = 1^+$ [103, 104]. Moreover, the LHCb collaboration observed two new particles $X(4500)$ and $X(4700)$ in the $J/\psi\phi$ mass spectrum, and determined the spin-parity to be $J^P = 0^+$ [103, 104]. The measured masses and widths are

$$\begin{aligned}X(4140) : M &= 4146.5 \pm 4.5_{-2.8}^{+4.6} \text{ MeV}, \Gamma = 83 \pm 21_{-14}^{+21} \text{ MeV}, \\ X(4274) : M &= 4273.3 \pm 8.3_{-3.6}^{+17.2} \text{ MeV}, \Gamma = 56 \pm 11_{-11}^{+8} \text{ MeV}, \\ X(4500) : M &= 4506 \pm 11_{-15}^{+12} \text{ MeV}, \Gamma = 92 \pm 21_{-20}^{+21} \text{ MeV}, \\ X(4700) : M &= 4704 \pm 10_{-24}^{+14} \text{ MeV}, \Gamma = 120 \pm 31_{-33}^{+42} \text{ MeV}.\end{aligned}\quad (6)$$

If they are tetraquark states, their quark constituents must be $cs\bar{c}\bar{s}$. The S-wave $J/\psi\phi$ systems have the quantum numbers $J^{PC} = 0^{++}, 1^{++}, 2^{++}$, while the P-wave $J/\psi\phi$ systems have the quantum numbers $J^{PC} = 0^{-+}, 1^{-+}, 2^{-+}, 3^{-+}$. The LHCb's data rule out the 0^{++} or 2^{++} $D_s^{*+}D_s^{*-}$ molecule assignments.

In 2021, the LHCb collaboration performed an improved full amplitude analysis of the exclusive process $B^+ \rightarrow J/\psi\phi K^+$, observed the $X(4685)$ ($X(4630)$) in the $J/\psi\phi$ mass spectrum with the $J^P = 1^+$ (1^-) and Breit-Wigner masses and widths,

$$\begin{aligned}X(4685) : M &= 4684 \pm 7_{-16}^{+13} \text{ MeV}, \Gamma = 126 \pm 15_{-41}^{+37} \text{ MeV}, \\ X(4630) : M &= 4626 \pm 16_{-110}^{+18} \text{ MeV}, \Gamma = 174 \pm 27_{-73}^{+134} \text{ MeV},\end{aligned}\quad (7)$$

furthermore, they observed the $Z_{cs}(4000)$ and $Z_{cs}(4220)$ with the $J^P = 1^+$ in the $J/\psi K^+$ mass spectrum and confirmed the four old particles [105].

In 2024, the LHCb collaboration performed the first full amplitude analysis of the decays $B^+ \rightarrow \psi(2S)K^+\pi^+\pi^-$, and they developed an amplitude model with 53 components comprising 11 hidden-charm exotic states, for example, the $X(4475)$, $X(4650)$, $X(4710)$ and $X(4800)$ in the $\psi(2S)\rho^0(770)$ mass spectrum with the $J^P = 0^+, 1^+, 0^+$ and 1^- , respectively, the $X(4800)$ is just an effective description of generic partial wave-function [106].

The $X(4475)$, $X(4650)$, $X(4710)$ and $X(4800)$ have the isospin $(I, I_3) = (1, 0)$, while the $X(4500)$, $X(4685)$, $X(4700)$ and $X(4630)$ have the isospin $(I, I_3) = (0, 0)$ according the final states $\psi(2S)\rho^0(770)$ and $J/\psi\phi$. A possible explanation is that those states are genuinely different states, if the $X(4475)$ state is the $c\bar{c}(u\bar{u} - d\bar{d})$ isospin partner of the $X(4500)$ interpreted as the $c\bar{c}s\bar{s}$ state, one would generally expect a larger mass difference of $M_{X(4500)} - M_{X(4475)} \approx 200$ MeV rather than several MeV.

1.6 $X(4350)$

In 2010, the Belle collaboration measured the process $\gamma\gamma \rightarrow \phi J/\psi$ for the $\phi J/\psi$ mass distributions and observed a narrow peak of $8.8^{+4.2}_{-3.2}$ events with a significance of 3.2σ [107]. The mass and width are $(4350.6^{+4.6}_{-5.1} \pm 0.7)$ MeV and $(13.3^{+17.9}_{-9.1} \pm 4.1)$ MeV respectively. However, the $X(4350)$ is not confirmed by other experiments.

1.7 $X_0(2900)$, $X_1(2900)$, $T_{c\bar{s}}(2900)$

In 2020, the LHCb collaboration reported a narrow peak in the $D^- K^+$ invariant mass spectrum in the decays $B^\pm \rightarrow D^+ D^- K^\pm$ [95, 96]. The peak could be reasonably parameterized in terms of two Breit-Wigner resonances:

$$\begin{aligned} X_0(2900) &: J^P = 0^+, M = 2866 \pm 7 \pm 2 \text{ MeV}, \Gamma = 57 \pm 12 \pm 4 \text{ MeV}; \\ X_1(2900) &: J^P = 1^-, M = 2904 \pm 5 \pm 1 \text{ MeV}, \Gamma = 110 \pm 11 \pm 4 \text{ MeV}. \end{aligned} \quad (8)$$

They are the first exotic hadrons with fully open flavor, the valence quarks or constituent quarks are $ud\bar{c}\bar{s}$ [95, 96]. The narrow peak can be assigned as the diquark-antidiquark type tetraquark state with the $J^P = 0^+$ [108, 109, 110, 111], or its radial/orbital excitation [112], or non tetraquark state [113], $D^* \bar{K}^*$ molecular state [111, 114, 115, 116, 117, 118], triangle singularity [119], etc.

In 2023, the LHCb collaboration observed the tetraquark candidates $T_{c\bar{s}}^{0/++}(2900)$ with the spin-parity $J^P = 0^+$ in the processes $B^+ \rightarrow D^- D_s^+ \pi^+$ and $B^0 \rightarrow \bar{D}^0 D_s^+ \pi^-$ with the significance larger than 9σ [120, 121]. The measured Breit-Wigner masses and widths are

$$\begin{aligned} T_{c\bar{s}}^0(2900) &: M = 2.892 \pm 0.014 \pm 0.015 \text{ GeV}, \Gamma = 0.119 \pm 0.026 \pm 0.013 \text{ GeV}, \\ T_{c\bar{s}}^{++}(2900) &: M = 2.921 \pm 0.017 \pm 0.020 \text{ GeV}, \Gamma = 0.137 \pm 0.032 \pm 0.017 \text{ GeV}, \end{aligned} \quad (9)$$

respectively, and they belong to a new type of open-charm tetraquark states with the c and \bar{s} quarks. The $\bar{X}_0(2900)$, $T_{c\bar{s}}^0(2900)$ and $T_{c\bar{s}}^{++}(2900)$ can be accommodated in the light flavor $SU(3)_F$ symmetry sextet.

1.8 $X(5568)$

In 2016, the D0 collaboration observed a narrow structure $X(5568)$ in the decays $X(5568) \rightarrow B_s^0 \pi^\pm$ with significance of 5.1σ [122]. The mass and natural width are $5567.8 \pm 2.9^{+0.9}_{-1.9}$ MeV and $21.9 \pm 6.4^{+5.0}_{-2.5}$ MeV, respectively. The $B_s^0 \pi^\pm$ systems consist of two quarks and two antiquarks of four different flavors, just like the $T_{c\bar{s}}(2900)$ with the $J^P = 0^+$ observed 7 years later in the $D_s^+ \pi^+ / D_s^+ \pi^-$ mass spectrum by the LHCb collaboration [120, 121]. The D0 collaboration fitted

the $B_s^0\pi^\pm$ systems with the S-wave Breit-Wigner parameters, the favored assignments are $J^P = 0^+$, but the assignments $J^P = 1^+$ cannot be excluded according to decays $X(5568) \rightarrow B_s^*\pi^+ \rightarrow B_s^0\pi^+\gamma$, where the low-energy photon is not detected. It can be assigned as a $usb\bar{d}$ tetraquark state with the $J^{PC} = 0^{++}$ [123, 124, 125, 126, 127], however, the $X(5568)$ is not confirmed by the LHCb, CMS, ATLAS and CDF collaborations [128, 129, 130, 131].

1.9 $X(6600)$, $X(6900)$, $X(7300)$

In 2020, the LHCb collaboration reported evidences of two fully-charm tetraquark candidates in the $J/\psi J/\psi$ mass spectrum [132]. They observed a broad structure above the $J/\psi J/\psi$ threshold ranging from 6.2 to 6.8 GeV and a narrow structure at about 6.9 GeV with the significance of larger than 5σ . In addition, they also observed some vague structures around 7.2 GeV.

In 2023, the ATLAS collaboration observed statistically significant excesses in the $J/\psi J/\psi$ channel, which are consistent with a narrow resonance at about 6.9 GeV and a broader structure at much lower mass. And they also observed a statistically significant excess at about 7.0 GeV in the $J/\psi\psi'$ channel [133].

In 2024, the CMS collaboration observed three resonant structures in the $J/\psi J/\psi$ mass spectrum with the masses 6638_{-38}^{+43+16} MeV, 6847_{-28}^{+44+48} MeV and 7134_{-25}^{+48+41} MeV, respectively [134]. While in the no-interference model, the measured Breit-Wigner masses and widths are [134],

$$\begin{aligned} X(6600) : M &= 6552 \pm 10 \pm 12 \text{ MeV}, \Gamma = 124_{-26}^{+32} \pm 33 \text{ MeV}, \\ X(6900) : M &= 6927 \pm 9 \pm 4 \text{ MeV}, \Gamma = 122_{-21}^{+24} \pm 18 \text{ MeV}, \\ X(7300) : M &= 7287_{-18}^{+20} \pm 5 \text{ MeV}, \Gamma = 95_{-40}^{+59} \pm 19 \text{ MeV}. \end{aligned} \quad (10)$$

The two-meson pairs J/ψ , J/ψ' , $\psi'\psi'$, $h_c h_c$, $\chi_{c0}\chi_{c0}$, $\chi_{c1}\chi_{c1}$ and $\chi_{c2}\chi_{c2}$ lie at 6194 MeV, 6783 MeV, 7372 MeV, 7051 MeV, 6829 MeV, 7021 MeV and 7112 MeV, respectively [91], it is difficult to assign the $X(6600)$, $X(6900)$ and $X(7300)$ as the charmonium-charmonium molecular states without introducing coupled channel effects.

1.10 $Y(4260/4230)$, $Y(4360/4320)$, $Y(4390)$, $Y(4500)$, $Y(4660)$, $Y(4710/4750/4790)$

In 2005, the BaBar collaboration studied the initial-state radiation process $e^+e^- \rightarrow \gamma_{ISR}\pi^+\pi^- J/\psi$ and observed the $Y(4260)$ in the $\pi^+\pi^- J/\psi$ mass spectrum, the measured mass and width are $(4259 \pm 8_{-6}^{+2})$ MeV and $(88 \pm 23_{-4}^{+6})$ MeV, respectively [137]. Subsequently the $Y(4260)$ was confirmed by the Belle and CLEO collaborations [138, 139], the Belle collaboration also observed an evidence for a very broad structure $Y(4008)$ in the $\pi^+\pi^- J/\psi$ mass spectrum.

In 2007, the Belle collaboration studied the initial-state radiation process $e^+e^- \rightarrow \gamma_{ISR}\pi^+\pi^-\psi'$, and observed the $Y(4360)$ and $Y(4660)$ in the $\pi^+\pi^-\psi'$ mass spectrum at $(4361 \pm 9 \pm 9)$ MeV with a width of $(74 \pm 15 \pm 10)$ MeV and $(4664 \pm 11 \pm 5)$ MeV with a width of $(48 \pm 15 \pm 3)$ MeV, respectively [140, 141], then the $Y(4660)$ was confirmed by the BaBar collaboration [142].

In 2008, the Belle collaboration studied the initial-state radiation process $e^+e^- \rightarrow \gamma_{ISR}\Lambda_c^+\Lambda_c^-$, observed a clear peak $Y(4630)$ in the $\Lambda_c^+\Lambda_c^-$ mass spectrum just above the $\Lambda_c^+\Lambda_c^-$ threshold, and determined the mass and width to be (4634_{-7-8}^{+8+5}) MeV and (92_{-24-21}^{+40+10}) MeV, respectively [143]. Thereafter, the $Y(4660)$ and $Y(4630)$ are taken as the same particle according to the uncertainties of the masses and widths, for example, in *The Review of Particle Physics* [91].

In 2014, the BESIII collaboration searched for the production of $e^+e^- \rightarrow \omega\chi_{cJ}$ with $J = 0, 1, 2$, and observed a resonance in the $\omega\chi_{c0}$ cross section, the measured mass and width are $4230 \pm 8 \pm 6$ MeV and $38 \pm 12 \pm 2$ MeV, respectively [144].

In 2016, the BESIII collaboration measured the cross sections of the process $e^+e^- \rightarrow \pi^+\pi^-h_c$, and observed two structures, the $Y(4220)$ has a mass of $4218.4 \pm 4.0 \pm 0.9$ MeV and a width of $66.0 \pm 9.0 \pm 0.4$ MeV respectively, and the $Y(4390)$ has a mass of $4391.6 \pm 6.3 \pm 1.0$ MeV and a width of $139.5 \pm 16.1 \pm 0.6$ MeV respectively [145].

Also in 2016, the BESIII collaboration precisely measured the cross section of the process $e^+e^- \rightarrow \pi^+\pi^-J/\psi$ and observed two resonant structures, which agree with the $Y(4260)$ and $Y(4360)$, respectively. The first resonance has a mass of $4222.0 \pm 3.1 \pm 1.4$ MeV and a width of $44.1 \pm 4.3 \pm 2.0$ MeV, while the second one has a mass of $4320.0 \pm 10.4 \pm 7.0$ MeV and a width of $101.4^{+25.3}_{-19.7} \pm 10.2$ MeV [146].

In 2022, the BESIII collaboration observed two resonant structures in the K^+K^-J/ψ mass spectrum, one is the $Y(4230)$ and the other is the $Y(4500)$, which was observed for the first time with the Breit-Wigner mass and width $4484.7 \pm 13.3 \pm 24.1$ MeV and $111.1 \pm 30.1 \pm 15.2$ MeV, respectively [147].

In 2023, the BESIII collaboration observed three enhancements in the $D^{*-}D^{*0}\pi^+$ mass spectrum in the Born cross sections of the process $e^+e^- \rightarrow D^{*0}D^{*-}\pi^+$, the first and third resonances are the $Y(4230)$ and $Y(4660)$, respectively, while the second resonance has the Breit-Wigner mass and width $4469.1 \pm 26.2 \pm 3.6$ MeV and $246.3 \pm 36.7 \pm 9.4$ MeV, respectively, and is roughly compatible with the $Y(4500)$ [148].

Also in 2023, the BESIII collaboration observed three resonance structures in the $D_s^{*+}D_s^{*-}$ mass spectrum, the two significant structures are consistent with the $\psi(4160)$ and $\psi(4415)$, respectively, while the third structure is new, and has the Breit-Wigner mass and width 4793.3 ± 7.5 MeV and 27.1 ± 7.0 MeV, respectively, therefore is named as $Y(4790)$ [149].

Also in 2023, the BESIII collaboration observed a new resonance $Y(4710)$ in the K^+K^-J/ψ mass spectrum with a significance over 5σ , the measured Breit-Wigner mass and width are $4708^{+17}_{-15} \pm 21$ MeV and $126^{+27}_{-23} \pm 30$ MeV, respectively [150].

In 2024, the BESIII collaboration measured the Born cross sections for the processes $e^+e^- \rightarrow \omega\chi_{c1}$ and $\omega\chi_{c2}$, and observed the well established $\psi(4415)$ in the $\omega\chi_{c2}$ mass spectrum [151]. In addition, they observed a new resonance in the $\omega\chi_{c1}$ mass spectrum, and measured the mass and width as $4544.2 \pm 18.7 \pm 1.7$ MeV and $116.1 \pm 33.5 \pm 1.7$ MeV, respectively, which are also roughly compatible with the $Y(4500)$.

Also in 2024, the BESIII collaboration studied the processes $e^+e^- \rightarrow \omega X(3872)$ and $\gamma X(3872)$, and observed that the relatively large cross section for the $e^+e^- \rightarrow \omega X(3872)$ process is mainly due to the enhancement about 4.75 GeV, which maybe indicate a potential structure in the $e^+e^- \rightarrow \omega X(3872)$ cross section [152]. If the enhancement is confirmed in the future by enough experimental data, there maybe exist another Y state, the $Y(4750)$.

We should bear in mind, in 2023, the BESIII collaboration studied the process $e^+e^- \rightarrow \Lambda_c^+\Lambda_c^-$ at twelve center-of-mass energies from 4.6119 to 4.9509 GeV, determined the Born cross sections and effective form-factors with unprecedented precision, and obtained flat cross sections about 4.63 GeV, which does not indicate the resonant structure $Y(4630)$ [153].

The charmonium-like candidates $Y(4260/4230)$, $Y(4360/4320)$, $Y(4390)$, $Y(4500)$, $Y(4660)$ and $Y(4710/4750/4790)$ with the $J^{PC} = 1^{--}$ overwhelm the accommodating capacity of the traditional $c\bar{c}$ model.

1.11 $Z_c(3900/3885)$, $Z_c(4020/4025)$, $Z_{cs}(3985/4000)$, $Z_{cs}(4123)$, $Z_{cs}(4220)$

In 2013, the BESIII collaboration studied the process $e^+e^- \rightarrow \pi^+\pi^-J/\psi$ at a center-of-mass energy of 4.260 GeV, and observed a structure $Z_c^\pm(3900)$ in the $\pi^\pm J/\psi$ mass spectrum with a mass of $(3899.0 \pm 3.6 \pm 4.9)$ MeV and a width of $(46 \pm 10 \pm 20)$ MeV [154], at the same time, the Belle collaboration studied the process $e^+e^- \rightarrow \gamma_{ISR}\pi^+\pi^-J/\psi$ using initial-state radiation, and observed a structure $Z_c^\pm(3900)$ in the $\pi^\pm J/\psi$ mass spectrum with a mass of $(3894.5 \pm 6.6 \pm 4.5)$ MeV and a width of $(63 \pm 24 \pm 26)$ MeV [155]. Then this structure was confirmed by the CLEO collaboration [156].

Also in 2013, the BESIII collaboration studied the process $e^+e^- \rightarrow (D^*\bar{D}^*)^\pm\pi^\mp$ at $\sqrt{s} = 4.26$ GeV, and observed a structure $Z_c^\pm(4025)$ near the $(D^*\bar{D}^*)^\pm$ threshold in the π^\mp recoil mass spectrum [159]. The measured mass and width are $(4026.3 \pm 2.6 \pm 3.7)$ MeV and $(24.8 \pm 5.6 \pm 7.7)$ MeV, respectively [159]. Slightly later, the BESIII collaboration studied the process $e^+e^- \rightarrow$

$\pi^+\pi^-h_c$ at \sqrt{s} from 3.90 GeV to 4.42 GeV, and observed a distinct structure $Z_c(4020)$ in the $\pi^\pm h_c$ mass spectrum, the measured mass and width are $(4022.9 \pm 0.8 \pm 2.7)$ MeV and $(7.9 \pm 2.7 \pm 2.6)$ MeV, respectively [160].

In 2014, the BESIII collaboration studied the process $e^+e^- \rightarrow \pi D\bar{D}^*$ at $\sqrt{s} = 4.26$ GeV, and observed a distinct charged structure $Z_c(3885)$ in the $(D\bar{D}^*)^\pm$ mass spectrum [157]. The measured mass and width are $(3883.9 \pm 1.5 \pm 4.2)$ MeV and $(24.8 \pm 3.3 \pm 11.0)$ MeV, respectively, and the angular distribution of the $\pi Z_c(3885)$ system favors the assignment $J^P = 1^+$ [157].

We tentatively identify the $Z_c(3900)$ and $Z_c(3885)$ as the same particle according to the uncertainties of the masses and widths [56]. In 2017, the BESIII collaboration established the spin-parity of the $Z_c(3900)$ to be $J^P = 1^+$ [158].

In 2021, the BESIII collaboration observed an excess near the $D_s^- D^{*0}$ and $D_s^{*-} D^0$ thresholds in the K^+ recoil-mass spectrum with the significance of 5.3σ in the processes $e^+e^- \rightarrow K^+(D_s^- D^{*0} + D_s^{*-} D^0)$ [161]. The Breit-Wigner mass and width of the new structure $Z_{cs}(3985)$ were measured as $3985.2_{-2.0}^{+2.1} \pm 1.7$ MeV and $13.8_{-5.2}^{+8.1} \pm 4.9$ MeV, respectively.

The $Z_c(3885)$ and $Z_{cs}(3985)$ have similar production modes,

$$\begin{aligned} e^+e^- &\rightarrow Z_c^-(3885)\pi^+ \rightarrow (D\bar{D}^*)^-\pi^+, \\ e^+e^- &\rightarrow Z_{cs}^-(3985)K^+ \rightarrow (D_s^- D^{*0} + D_s^{*-} D^0)K^+, \end{aligned} \quad (11)$$

and they should be cousins and have similar properties.

Also in 2021, the LHCb collaboration reported two new exotic states with the valence quarks $c\bar{c}u\bar{s}$ in the $J/\psi K^+$ mass spectrum in the decays $B^+ \rightarrow J/\psi\phi K^+$ [105]. The most significant state $Z_{cs}^+(4000)$ has a mass of $4003 \pm 6_{-14}^{+4}$ MeV, a width of $131 \pm 15 \pm 26$ MeV, and the spin-parity $J^P = 1^+$, while the broader state $Z_{cs}^+(4220)$ has a mass of $4216 \pm 24_{-30}^{+43}$ MeV, a width of $233 \pm 52_{-73}^{+97}$ MeV, and the spin-parity $J^P = 1^+$ or 1^- (with a 2σ difference in favor of the first hypothesis) [105]. Considering the large difference between the widths, the $Z_{cs}(3985)$ and $Z_{cs}(4000)$ are unlikely to be the same particle.

In 2023, the BESIII collaboration reported an excess of the $Z_{cs}^-(4123) \rightarrow D_s^{*-} D^{*0}$ candidate at a mass of $(4123.5 \pm 0.7 \pm 4.7)$ MeV with a significance of 2.1σ in the process $e^+e^- \rightarrow K^+ D_s^{*-} D^{*0} + c.c.$ [162]. The $Z_{cs}^-(4123)$ is consistent with the tetraquark state with the valence quarks $c\bar{c}s\bar{u}$, spin-parity $J^{PC} = 1^{+-}$, a mass 4.11 ± 0.08 GeV and a width 22.71 ± 1.65 MeV predicted in previous work based on the QCD sum rules [163].

The charmonium-like states $Z_c(3900/3885)$, $Z_c(4020/4025)$, $Z_{cs}(3985/4000)$, $Z_{cs}(4123)$ and $Z_{cs}(4220)$ have non-zero electric charge, and are excellent candidates for the tetraquark (molecular) states.

1.12 $Z_1(4050)$, $Z_1(4250)$, $Z_c(4100)$

In 2008, the Belle collaboration reported the first observation of two resonance-like structures $Z_1^+(4050)$ and $Z_2^+(4250)$ exceeding 5σ in the $\pi^+\chi_{c1}$ mass spectrum near 4.1 GeV in the exclusive decays $\bar{B}^0 \rightarrow K^-\pi^+\chi_{c1}$ [165]. The Breit-Wigner masses and widths are $M_1 = 4051 \pm 14_{-41}^{+20}$ MeV, $\Gamma_1 = 82_{-17}^{+21} +_{-22}^{+47}$ MeV, $M_2 = 4248_{-29}^{+44} +_{-35}^{+180}$ MeV and $\Gamma_2 = 177_{-39}^{+54} +_{-61}^{+316}$ MeV, respectively. However, the BaBar collaboration observed no evidence for the $Z_1^+(4050)$ and $Z_2^+(4250)$ states in the $\pi^+\chi_{c1}$ mass spectrum in the exclusive decays $\bar{B}^0 \rightarrow \pi^+\chi_{c1}K^-$ and $B^+ \rightarrow \pi^+\chi_{c1}K_S^0$ [166].

In 2018, the LHCb collaboration observed an evidence for the $\eta_c\pi^-$ resonant structure $Z_c(4100)$ with the significance larger than 3σ in a Dalitz plot analysis of the $B^0 \rightarrow \eta_c K^+\pi^-$ decays, the measured mass and width are $4096 \pm 20_{-22}^{+18}$ MeV and $152 \pm 58_{-35}^{+60}$ MeV respectively [167]. The assignments $J^P = 0^+$ and 1^- are both consistent with the experimental data. However, the $Z_c(4100)$ is not confirmed by other experiments until now.

1.13 $Z_c(4430)$, $Z_c(4600)$

In 2007, the Belle collaboration observed a distinct peak in the $\pi^\pm\psi'$ mass spectrum in the decays $B \rightarrow K\pi^\pm\psi'$, the mass and width are $(4433 \pm 4 \pm 2)$ MeV and (45_{-13}^{+18+30}) MeV, respectively [168]. In 2009, the Belle collaboration observed a signal for the decay $Z(4430)^+ \rightarrow \pi^+\psi'$ from a Dalitz plot analysis of the decays $B \rightarrow K\pi^+\psi'$ [169]. In 2013, the Belle collaboration performed a full amplitude analysis of the decays $B^0 \rightarrow \psi'K^+\pi^-$ to reach the favored assignments $J^P = 1^+$ [170].

In 2014, the LHCb collaboration analyzed the $B^0 \rightarrow \psi'\pi^-K^+$ decays by performing a four-dimensional fit of the amplitude, and provided the first independent confirmation of the $Z^-(4430)$ resonance and established its spin-parity $J^P = 1^+$. The measured Breit-Wigner mass and width are $(4475 \pm 7_{-25}^{+15})$ MeV and $(172 \pm 13_{-34}^{+37})$ MeV, respectively [171], which excludes the possibility of assigning the $Z_c(4430)$ as the D^*D_1 molecular state with the spin-parity $J^P = 0^-$ [172], although it lies near the D^*D_1 threshold.

The Okubo-Zweig-Iizuka supper-allowed decays

$$\begin{aligned} Z_c(3900) &\rightarrow J/\psi\pi, \\ Z'_c(4430) &\rightarrow \psi'\pi \end{aligned} \quad (12)$$

are expected to take place easily, and the energy gaps have the relation $M_{Z'_c} - M_{Z_c} = m_{\psi'} - m_{J/\psi}$, the $Z_c(4430)$ can be assigned as the first radial excitation of the $Z_c(3900)$ [52, 173, 174], which was proposed before the J^P of the $Z_c(3900)$ were determined by the BESIII collaboration [158].

In 2019, the LHCb collaboration performed an angular analysis of the weak decays $B^0 \rightarrow J/\psi K^+\pi^-$, examined the $m(J/\psi\pi^-)$ versus the $m(K^+\pi^-)$ plane, and observed two possible resonant structures in the vicinity of the energies $m(J/\psi\pi^-) = 4200$ MeV and 4600 MeV, respectively [175], the structure $Z_c(4600)$ has not been confirmed by other experiments yet. According to the mass gaps $M_{Z_c(4600)} - M_{Z_c(4020)} \approx M_{Z_c(4430)} - M_{Z_c(3900)}$, we can tentatively assign the $Z_c(4600)$ as the first radial excitation of the $Z_c(4020)$ [176, 177].

1.14 $Z_c(4200)$, $Z_{\bar{c}s}(4600)$, $Z_{\bar{c}s}(4900)$, $Z_{\bar{c}s}(5200)$

In 2014, the Belle collaboration analyzed the decays $\bar{B}^0 \rightarrow K^-\pi^+J/\psi$ and observed a resonance $Z_c(4200)$ in the $J/\psi\pi^+$ mass spectrum with a statistical significance more than 6.2σ , the measured mass and width are 4196_{-29-13}^{+31+17} MeV and $370_{-70-132}^{+70+70}$ MeV, respectively, the preferred assignment is $J^P = 1^+$ [178].

In 2019, the LHCb collaboration performed an angular analysis of the decays $B^0 \rightarrow J/\psi K^+\pi^-$, examined the $m(J/\psi\pi^-)$ versus the $m(K^+\pi^-)$ plane, and observed two structures in the vicinity of the energies $m(J/\psi\pi^-) = 4200$ MeV and 4600 MeV, respectively [179].

In 2024, the LHCb collaboration performed the first full amplitude analysis of the decays $B^+ \rightarrow \psi(2S)K^+\pi^+\pi^-$, and they developed an amplitude model with 53 components comprising 11 hidden-charm exotic states, for example, the $Z_c(4200)$ and $Z_c(4430)$ in the $\psi(2S)\pi^+$ mass spectrum with the $J^P = 1^+$; the $Z_{\bar{c}s}(4600)$ and $Z_{\bar{c}s}(4900)$ in the $\psi(2S)K^*(892)$ mass spectrum with the $J^P = 1^+$, which might be the radial excitations of the $Z_{\bar{c}s}(4000)$ in the scenario of tetraquark states with the valence constituents $c\bar{c}d\bar{s}$; the $Z_{\bar{c}s}(4000)$, $Z_c(4055)$ and $Z_{\bar{c}s}(5200)$ are effective descriptions of generic partial wave-functions with the $J^P = 1^+$, 1^- and 1^- , respectively [106]. The spin-parity of the $Z_c(4200)$ is determined to be 1^+ for the first time with a significance exceeding 5σ .

1.15 $Z_b(10610)$, $Z_b(10650)$, $Y(10750)$

In 2011, the Belle collaboration reported the first observation of the $Z_b(10610)$ and $Z_b(10650)$ in the $\pi^\pm\Upsilon(1,2,3S)$ and $\pi^\pm h_b(1,2P)$ mass spectra associated with a single charged pion in the $\Upsilon(5S)$ decays, the quantum numbers $I^G(J^P) = 1^+(1^+)$ are favored [180]. Subsequently, the Belle collaboration updated the measured parameters $M_{Z_b(10610)} = (10607.2 \pm 2.0)$ MeV, $M_{Z_b(10650)} =$

(10652.2 ± 1.5) MeV, $\Gamma_{Z_b(10610)} = (18.4 \pm 2.4)$ MeV and $\Gamma_{Z_b(10650)} = (11.5 \pm 2.2)$ MeV, respectively [181]. In 2013, the Belle collaboration observed the $\Upsilon(5S) \rightarrow \Upsilon(1, 2, 3S)\pi^0\pi^0$ decays for the first time, and obtained the neutral $Z_b^0(10610)$ in a Dalitz analysis of the decays to the final states $\Upsilon(2, 3S)\pi^0$ [182].

In 2019, the Belle collaboration observed a resonance structure $Y(10750)$ in the $e^+e^- \rightarrow \Upsilon(nS)\pi^+\pi^-$ ($n = 1, 2, 3$) cross sections [183]. The Breit-Wigner mass and width are $10752.7 \pm 5.9^{+0.7}_{-1.1}$ MeV and $35.5^{+17.6}_{-11.3} +^{3.9}_{-3.3}$ MeV, respectively. The $Y(10750)$ is observed in the $\Upsilon(nS)\pi^+\pi^-$ mass spectrum with $n = 1, 2, 3$, its quantum numbers are $J^{PC} = 1^{--}$.

The Belle II collaboration confirmed the $Y(10750)$ in the processes $e^+e^- \rightarrow \omega\chi_{b1}(1P)$, $\omega\chi_{b2}(1P)$ [184], $\pi^+\pi^-\Upsilon(1S)$, $\pi^+\pi^-\Upsilon(2S)$ [185], and observed no evidence in the processes $e^+e^- \rightarrow \omega\eta_b(1S)$, $\omega\chi_{b0}(1P)$ [186], $\pi^+\pi^-\Upsilon(3S)$ [185].

1.16 $T_{cc}(3875)$

In 2021, the LHCb collaboration formally announced observation of the exotic state $T_{cc}^+(3875)$ just below the D^0D^{*+} threshold [187, 188]. The Breit-Wigner mass and width are $\delta M_{BW} = -273 \pm 61 \pm 5^{+11}_{-14}$ KeV below the D^0D^{*+} threshold and $\Gamma_{BW} = 410 \pm 165 \pm 43^{+18}_{-38}$ KeV [187, 188]. The exotic state $T_{cc}^+(3875)$ is consistent with the ground isoscalar tetraquark state with the valence quarks $cc\bar{u}\bar{d}$ and spin-parity $J^P = 1^+$, and exploring the DD mass spectrum disfavors interpreting the $T_{cc}^+(3875)$ as an isovector state. The observation of the $T_{cc}^+(3875)$ is a great breakthrough beyond the Ξ_{cc}^{++} for hadron physics, and it is the first doubly-charmed tetraquark candidate with the typical quark configuration $cc\bar{u}\bar{d}$, it is a very good candidate for the tetraquark (molecular) state having doubly-charm.

1.17 $P_c(4312)$, $P_c(4380)$, $P_c(4440)$, $P_c(4457)$, $P_c(4337)$, $P_{cs}(4338)$, $P_{cs}(4459)$

In 2015, the LHCb collaboration observed two exotic structures $P_c(4380)$ and $P_c(4450)$ in the $J/\psi p$ mass spectrum in the $\Lambda_b^0 \rightarrow J/\psi K^- p$ decays [189]. The $P_c(4380)$ has a mass of $4380 \pm 8 \pm 29$ MeV and a width of $205 \pm 18 \pm 86$ MeV, while the $P_c(4450)$ has a mass of $4449.8 \pm 1.7 \pm 2.5$ MeV and a width of $39 \pm 5 \pm 19$ MeV. The preferred spin-parity assignments of the $P_c(4380)$ and $P_c(4450)$ are $J^P = \frac{3}{2}^-$ and $\frac{5}{2}^+$, respectively [189].

In 2019, the LHCb collaboration studied the $\Lambda_b^0 \rightarrow J/\psi K^- p$ decays with a data sample, which is an order of magnitude larger than that previously analyzed, and observed a narrow pentaquark candidate $P_c(4312)$ in the $J/\psi p$ mass spectrum. Furthermore, the LHCb collaboration confirmed the pentaquark structure $P_c(4450)$, and observed that it consists of two narrow overlapping peaks $P_c(4440)$ and $P_c(4457)$ [190]. The measured masses and widths are

$$\begin{aligned} P_c(4312) : M &= 4311.9 \pm 0.7^{+6.8}_{-0.6} \text{ MeV}, \Gamma = 9.8 \pm 2.7^{+3.7}_{-4.5} \text{ MeV}, \\ P_c(4440) : M &= 4440.3 \pm 1.3^{+4.1}_{-4.7} \text{ MeV}, \Gamma = 20.6 \pm 4.9^{+8.7}_{-10.1} \text{ MeV}, \\ P_c(4457) : M &= 4457.3 \pm 0.6^{+4.1}_{-1.7} \text{ MeV}, \Gamma = 6.4 \pm 2.0^{+5.7}_{-1.9} \text{ MeV}. \end{aligned} \quad (13)$$

In 2021, the LHCb collaboration reported an evidence of a hidden-charm pentaquark candidate $P_{cs}(4459)$ with the strangeness $S = -1$ in the $J/\psi \Lambda$ mass spectrum with a significance of 3.1σ in the $\Xi_b^- \rightarrow J/\psi K^- \Lambda$ decays [191], the Breit-Wigner mass and width are

$$P_{cs}(4459) : M = 4458.8 \pm 2.9^{+4.7}_{-1.1} \text{ MeV}, \Gamma = 17.3 \pm 6.5^{+8.0}_{-5.7} \text{ MeV}, \quad (14)$$

and the spin-parity have not been determined yet up to now.

In 2022, the LHCb collaboration observed an evidence for a structure $P_c(4337)$ in the $J/\psi p$ and $J/\psi \bar{p}$ systems in the $B_s^0 \rightarrow J/\psi p \bar{p}$ decays with a significance about $3.1 - 3.7\sigma$ depending on the J^P hypothesis [192], the Breit-Wigner mass and width are

$$P_c(4337) : M = 4337^{+7+2}_{-4-2} \text{ MeV}, \Gamma = 29^{+26+14}_{-12-14} \text{ MeV}. \quad (15)$$

Its existence is still need confirmation and its spin-parity are not measured yet.

In 2023, the LHCb collaboration observed an evidence for a new structure $P_{cs}(4338)$ in the $J/\psi\Lambda$ mass distribution in the $B^- \rightarrow J/\psi\Lambda\bar{p}$ decays [193], the measured Breit-Wigner mass and width are

$$P_{cs}(4338) : M = 4338.2 \pm 0.7 \pm 0.4 \text{ MeV}, \Gamma = 7.0 \pm 1.2 \pm 1.3 \text{ MeV}, \quad (16)$$

and the favored spin-parity is $J^P = \frac{1}{2}^-$.

The $P_{cs}(4338)$ and $P_{cs}(4459)$ are observed in the $J/\psi\Lambda$ mass spectrum, they have the isospin $I = 0$, as the strong decays conserve isospin. The $P_c(4312)$, $P_c(4380)$, $P_c(4440)$, $P_c(4457)$, $P_{cs}(4459)$ and $P_{cs}(4338)$ lie slightly below or above the thresholds of the charmed meson-baryon pairs $\bar{D}\Sigma_c$, $\bar{D}\Sigma_c^*$, $\bar{D}^*\Sigma_c$, $\bar{D}^*\Sigma_c^*$, $\bar{D}\Xi'_c$ ($\bar{D}\Xi_c^*$, $\bar{D}^*\Xi_c$, $\bar{D}^*\Xi'_c$) and $\bar{D}\Xi_c$, respectively. It is difficult to identify the $P_c(4337)$ as the molecular state without resorting to the help of large coupled-channel effects due to lacking nearby meson-baryon thresholds.

2 Theoretical methods and possible assignments

There have been tremendous progresses on the hadron spectrum containing two heavy quarks experimentally since the observation of the $X(3872)$. It is surprising that many resonant structures lie around thresholds of a pair of heavy hadrons. Are they threshold cusps, triangle singularity or genuine resonances? As there always exist threshold cusps at the S-wave thresholds or triangle singularities near the thresholds. Firstly, let us see the outcomes based on the (non)relativistic effective field theory.

2.1 Threshold cusps, Triangle singularities or genuine Resonances

Not all peaks in the invariant mass distributions are resonances, they often arise due to the nearby kinematical singularities of the transition amplitudes in the complex energy plane. Those singularities (or Landau singularities) occur when the intermediate particles are on the mass-shell. The simplest case is the cusp at the normal two-body thresholds, there always exist a cusp at the S-wave threshold of two particles coupling to the final states, while a more complicated case is the so-called triangle singularity. They maybe produce observable effects if the involved interactions are strong enough, sometimes, even mimic the behavior of a resonance. It is important to distinguish kinematic singularities from genuine resonances. We would like give an example concerning the exotic states $Y(4260)$ and $Z_c(3900)$ to illustrate their possible assignments of the threshold cusps, triangle singularities and genuine resonances.

The threshold cusp is determined by masses of the involved particles, how strong the cusp depends on detailed dynamics and the cusp could be rather dramatic if there is a nearby pole, thus it plays an important role in studying the exotic states [194]. For example, the $X(3872)$, $Z_c(3900)$, $Z_c(4020)$, $Z_b(10610)$ and $Z_b(10650)$ lie near the $D^0\bar{D}^{*0}$, $D\bar{D}^*$, $D^*\bar{D}^*$, $B\bar{B}^*$ and $B^*\bar{B}^*$ thresholds, respectively, their quantum numbers are the same as the corresponding S-wave meson pairs though the J^{PC} of the $Z_c(4020)$ have not been fully determined yet [91].

The $X(3872)$ was assigned to be a threshold cusp by Bugg [83], subsequently, he realized that the very narrow line shapes in the $J/\psi\rho$ and $D^0\bar{D}^{*0}$ channels could not be fitted with only a threshold cusp, and a resonance or virtual state pole was necessary [195].

In a modified threshold cusp model [196, 197], see the Feynman diagram shown in Fig.1 as an example, both the inelastic ($J/\psi\pi$, $h_c\pi$) and elastic ($D\bar{D}^*$, $D^*\bar{D}^*$) decay modes were considered for the $Z_c(3900)$ and $Z_c(4020)$, analogous discussions are applied to the $Z_b(10610)$ and $Z_b(10650)$. A Gaussian form-factor was chosen for all the vertices including the tree-level ones. Then the experimental data for the $J/\psi\pi$ and $D\bar{D}^*$ mass spectra for the $Z_c(3900)$ and the $D^*\bar{D}^*$ and $h_c\pi$ mass spectra for the $Z_c(4020)$ could be fitted very good, no exotic resonances are not required to

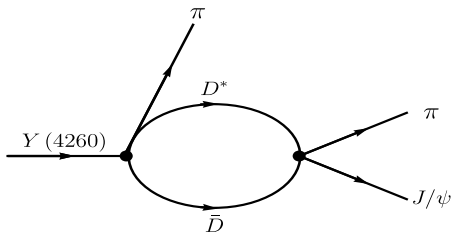


Figure 1: A Feynman diagram for the decay $Y(4260) \rightarrow J/\psi\pi^+\pi^-$ may lead to threshold cusp.

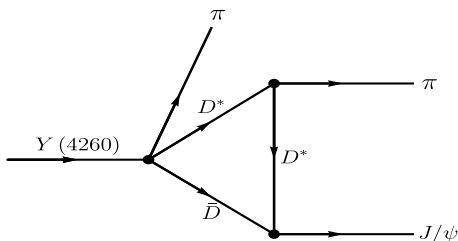


Figure 2: A Feynman diagram for the decay $Y(4260) \rightarrow J/\psi\pi^+\pi^-$ in the ISPE mechanism.

account for the experimental data. However, the fitting quality depends crucially on the cutoff parameter in the Gaussian form-factor.

The triangle singularity is determined by the masses of the intermediate particles plus the invariant masses of the external ones, therefore the triangle singularities are sensitive to the kinematic variables, the peak position and peak shape change according to the variations of the external energies. More precisely, the triangle singularities are determined by the scalar triangle loop integral, which does not depend on the orbital angular momentum for each vertex, however, sharp triangle singularity peaks are constrained to the S-wave internal particles, as momentum power factor weakens the singular behavior in other cases [194].

In the initial single-pion emission (ISPE) mechanism, the triangle singularities appear as threshold cusps, see Fig.2 for a typical Feynman diagram. This mechanism was suggested firstly to study the exotic structures $Z_b(10610)$ and $Z_b(10650)$, Chen and Liu introduced a dipole form-factor to accompany the exchanged B -meson propagator and took account of the $B\bar{B}$, $B\bar{B}^*$, $B^*\bar{B}$ and $B^*\bar{B}^*$ triangle loop diagrams, and produced sharp cusps right around the $Z_b(10610)$ and $Z_b(10650)$ structures in the $\Upsilon(1S, 2S, 3S)\pi$ and $h_b(1P, 2P)\pi$ mass spectra, and observed no cusp at the $B\bar{B}$ threshold [198]. Similarly, Chen, Liu and Matsuki took account of the $D\bar{D}$, $D\bar{D}^*$, $D^*\bar{D}$ and $D^*\bar{D}^*$ triangle loop diagrams and the intermediate $f_0(600)$ and $f_0(980)$ to study the decays $Y(4260) \rightarrow J/\psi\pi\pi$, and observed two peaks, the $Z_c(3900)$ and its reflection [199].

In Ref.[200], Dong, Guo and Zou show that the threshold cusp appears as a peak only for channels with attractive interaction, and the cusp's width is inversely proportional to the reduced mass for the relevant threshold. There should be threshold structures at any threshold of a $q\bar{Q}$ and $Q\bar{q}$ (Qqq) pair, which have attractive interaction at threshold, in the invariant mass distribution of a $Q\bar{Q}$ state and a $q\bar{q}$ (qqq) state coupling to the $q\bar{Q}$ and $Q\bar{q}$ (Qqq) pair, and the structure becomes more pronounced if there is a near-threshold pole.

In Ref.[201], Liu and Li suppose the $Y(4260)$ as a $D_1\bar{D}$ molecular state to study its decays, see Fig.3 as an example, and observe that under special kinematic configurations, the triangle

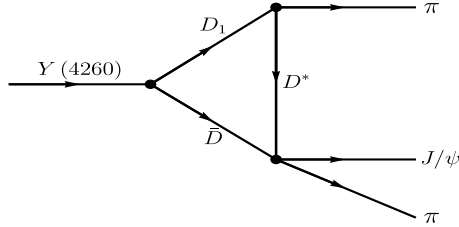


Figure 3: The Feynman diagram for the decays $Y(4260) \rightarrow J/\psi\pi^+\pi^-$.

singularity maybe occur in the re-scattering amplitude, which can change the threshold behavior significantly. Obvious threshold enhancements or narrow cusp structures appear quite naturally without introducing a genuine resonance, but cannot exclude existence of a genuine resonance.

If the $Y(4260)$ have a large $D_1\bar{D}$ molecular component, the decays $Y(4260) \rightarrow J/\psi\pi^+\pi^-$ can occur through the re-scattering process [202, 203, 204], see Fig.3. The singularity regions provide an ideal environment for forming bound states or resonances. Although the $Y(4260)$ lies slightly below the $D_1(2420)\bar{D}$ threshold, the triangle singularity in the $J/\psi\pi^\pm$ invariant mass of the re-scattering amplitude is still near the physical boundary and can influence the $J/\psi\pi^\pm$ invariant mass distribution around the $D^*\bar{D}$ threshold significantly [202]. Despite the importance of the triangle diagram contribution, it is insisted that a $Z_c(3900)$ resonance was still needed in order to fit to the narrow peak observed in experiments [201, 202].

The resonance pole can be incorporated by constructing a unitarized coupled-channel scattering T -matrix by fitting to the experimental data, the best fit still demand the T -matrix to have a resonant or virtual pole near the $D\bar{D}^*$ threshold, which can be interpreted as the $Z_c(3900)$ [205]. The molecule assignment provides a natural explanation for the resonance-like structure $Z_c(3900)$ in the $Y(4260)$ decays [204, 205], the kinematic threshold cusp cannot produce a narrow peak in the invariant mass distribution in the elastic channel in contrast with a genuine S-matrix pole [206].

In a similar scenario, Szczepaniak suggests that the $Z_c(3900)$ peak could be attributed to the $D_0^*(2300)\bar{D}^*D$ loop instead of the $D_1(2420)\bar{D}D^*$ loop, which is in the physical region by neglecting the width of the $D_0^*(2300)$ [207]. The triangle singularities can produce enhancement potentially in the amplitude consistent with the experimental data qualitatively.

In Ref.[208], Chen, Du and Guo perform a unified description of the $\pi^+\pi^-$ and $J/\psi\pi^+\pi^-$ mass distributions for the $e^+e^- \rightarrow J/\psi\pi^+\pi^-$ and the D^0D^{*-} mass distribution for the $e^+e^- \rightarrow D^0D^{*-}\pi^+$ at $\sqrt{s} = 4.23$ and 4.26 GeV. They take account of the open-charm meson loops containing triangle singularities, the $J/\psi\pi-D\bar{D}^*$ coupled-channel interaction respecting unitarity, and the strong $\pi\pi-K\bar{K}$ final-state interaction using dispersion relations, which lead to a precise determination of the pole mass and width ($3880.7 \pm 1.7 \pm 22.4$) MeV and ($35.9 \pm 1.4 \pm 15.3$) MeV, respectively, and indicate the molecular and non-molecular components are of similar importance for the structure $Z_c(3900)$.

Precisely measuring the near threshold structures play an important role in diagnosing the heavy-hadron interactions, therefore understanding the puzzling hidden-charm and hidden-bottom structures. Furthermore, it is important to search for the resonant structures in processes free of triangle singularities, such as the photo-production and pion-induced production processes in the e^+e^- and pp collisions [209, 210, 211].

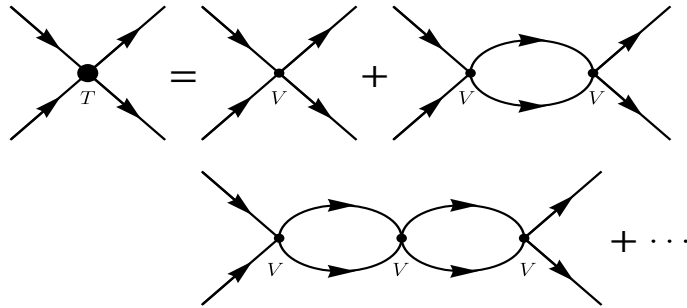


Figure 4: Summing the two-meson loops through the Bethe-Salpeter equation.

2.2 Dynamical Generated Resonances and Molecular States

If we take the traditional heavy mesons as the elementary degrees of freedom, then we construct the heavy meson effective Lagrangian according to the chiral symmetry, hidden-local symmetry and heavy quark symmetry. It is easy to obtain the two-meson scattering amplitudes V . Then we have three choices:

Firstly, we unitarize the amplitudes by taking account of the intermediate two-meson loops with the coupled channel effects through the Bethe-Salpeter or Lippmann-Schwinger equation with on-shell factorization [212, 213],

$$T = [1 - V G]^{-1} V, \quad (17)$$

where the G is the loop function, see Fig.4 for a diagrammatical representation. Then explore the analytical properties of the full amplitudes T , and try to find the poles in the complex Riemann sheets, such as the bound states, virtual states and resonances. Such discussions are applied to the baryon-meson systems directly.

Bound states appear as poles on the physical sheet, and only appear on the real s -axis below the lowest threshold by causality. Virtual states also appear on the real s -axis, however, on the unphysical Riemann sheet. Resonances appear as poles on an unphysical Riemann sheet close to the physical one with non-zero imaginary part, and they appear in conjugate pairs. For example, the loosely bound states $X(3872)$, $Y(3940)$, $Z_c(3900)$, $Z_b(10610)$, $Z_b(10650)$ [66, 70, 214, 215, 216, 217], the hidden-charm pentaquark resonances [218, 219, 220, 221, 222]. We usually apply Weinberg's compositeness condition to estimate the hadronic molecule components [223, 224, 225, 226, 227].

Secondly, we take the scattering amplitudes V as interaction kernels, solve the quasi-potential Bethe-Salpeter or Lippmann-Schwinger equation with the coupled channel effects directly, then explore the analytical properties of the full amplitudes [228, 229, 230, 231, 232, 233], or obtain the bound energies directly to estimate the bound states [71, 234, 235, 236, 237, 238].

Thirdly, we reduce the scattering amplitudes to interaction potentials in the momentum space in terms of the Breit approximation and introduce monopole form-factors associated with the exchanged particles. Generally, we should introduce form-factor in each interaction vertex, which reflects the off-shell effect of the exchanged meson and the structure effect, because the components of the molecular state and exchanged mesons are not elementary particles. Then we perform the Fourier transformation to obtain the potential in the coordinate space, finally we solve the Schrodinger equation directly to obtain the binding energy [59, 239, 240, 241, 242, 243, 244, 245, 246, 247, 248, 249].

2.3 $Q\bar{Q}$ states with coupled channel effects

In the famous GI model, the charmonium $\chi_{c1}(2^3P_1)$ has the mass about 3953 MeV [80], which is about 100 MeV above the $X(3872)$, which lies near the $D^0\bar{D}^{*0}$ threshold, the strong coupling

to the nearby threshold maybe lead to some DD^* molecular configuration. Furthermore, pure charmonium assignment cannot interpret the high $\gamma\psi'$ decay rate [250].

We can extend the constituent quark models to include the meson-meson Fock components, and write the physical charmonium (bottomonium) states in terms of $|\Psi\rangle$,

$$|\Psi\rangle = \sum_{\alpha} c_{\alpha} |\psi_{\alpha}\rangle + \sum_{\beta} \chi_{\beta}(P) |\phi_1 \phi_2 \beta\rangle \quad (18)$$

where the $|\psi_{\alpha}\rangle$ are the $Q\bar{Q}$ eigenstates, the ϕ_i are $Q\bar{q}$ or $q\bar{Q}$ eigenstates, $|\phi_1 \phi_2 \beta\rangle$ are the two-meson state with β quantum numbers, and the $\chi_{\beta}(P)$ is the relative wave function between the two mesons. Then we solve the Schrodinger equation directly [251, 252, 253, 254, 255, 256, 257, 258].

2.4 Hybrid and Tetraquark states in Born-Oppenheimer approximation

Due to the large ratio of the mass of a nucleus to that of the electron, the electrons respond almost instantaneously to the motion of the nuclei. The energy of the electrons combined with the repulsive Coulomb energy of the nuclei defines a Born-Oppenheimer potential. Accordingly, due to the large ratio of the heavy-quark mass m_Q to the energy scale Λ_{QCD} associated with the gluon field, the gluons respond almost instantaneously to the motion of the heavy quarks Q and \bar{Q} [259, 260, 261, 262, 263, 264].

In the static limit, the Q and \bar{Q} serve as two color-sources separated by a distance r , the ground-state flavor-singlet Born-Oppenheimer potential $V_{\Sigma_g^+}(r)$ is defined by the minimal energy of the gluonic configurations, whose small and large r limiting behaviors are qualitatively compatible with the simple phenomenological Cornell potential, thus the $V_{\Sigma_g^+}(r)$ describes the traditional heavy quarkonium states. The excited Born-Oppenheimer potentials $V_{\Gamma}(r)$ are defined as the minimal energies of the excited configurations for the gluon and light-quark fields with the quantum numbers Γ [259, 260, 261].

The hybrid states $\bar{Q}GQ$ are energy levels of a heavy quark pair $Q\bar{Q}$ in the excited flavor-singlet Born-Oppenheimer potentials, the hybrid potentials. Juge, Kuti and Morningstar calculated many flavor-singlet potentials using the quenched lattice QCD [265]. There have been some works on the lowest lying hybrid potentials using lattice QCD with two flavors of dynamical Wilson fermions [266, 267]. At large r , the hybrid potential $V_{\Gamma}(r)$ is a flux-tube extending between the Q and \bar{Q} . At small r , the hybrid potential approaches the repulsive color-Coulomb potential between a Q and \bar{Q} in a color-octet state. In the limit $r \rightarrow 0$, the Q and \bar{Q} sources reduce to a single local color-octet $Q\bar{Q}$ source. The energy levels of the flavor-singlet gluon and light-quark field configurations bound to a static color-octet source are called static hybrid mesons. The most effective pictorial representation of the hybrid states is the flux-tube model. Lattice QCD simulations show that two static quarks Q and \bar{Q} at large distances are confined by approximately cylindrical regions of the color fields [265, 266, 267].

The $\bar{Q}Q\bar{q}q$ tetraquark states are energy levels in the Born-Oppenheimer potentials with nonsinglet (excited singlet) flavor quantum numbers, the tetraquark potentials, which are distinguished by the quantum numbers, $u\bar{u} \pm d\bar{d}$, $u\bar{d}$, $d\bar{u}$, $s\bar{q}$, $s\bar{s}$, etc. At large r , the minimal-energy configuration consists of two static mesons localized near the Q and \bar{Q} sources. At small r , the minimal-energy configuration is the flavor-singlet Σ_g^+ potential accompanied by one or two pions (two or three pions), depending on the quantum numbers Γ . There have been works on the energies of static adjoint mesons using the quenched lattice QCD [268]. The static adjoint mesons are energy levels of the light-quark and gluon fields with nonsinglet flavor quantum numbers bound to a static color-octet source.

The heavy quark motion is restored by solving the Schrodinger equation in each of those potentials, and many X , Y and Z mesons could be assigned as the bound states in the Born-Oppenheimer potentials [259, 260, 261, 262, 263, 264].

2.5 Tetraquarks in diquark models

If we take the quarks in color triplet $\mathbf{3}$ as the basic constituents, then we could construct the hadrons according to the $SU(3)$ symmetry. For the traditional mesons,

$$q_{\mathbf{3}} \otimes \bar{q}_{\bar{\mathbf{3}}} \rightarrow [\bar{q}q]_{\mathbf{1}}. \quad (19)$$

For the traditional baryons,

$$q_{\mathbf{3}} \otimes q_{\mathbf{3}} \otimes q_{\mathbf{3}} \rightarrow [qqq]_{\mathbf{1}}. \quad (20)$$

For the tetraquark molecular states,

$$q_{\mathbf{3}} \otimes \bar{q}_{\bar{\mathbf{3}}} \otimes q_{\mathbf{3}} \otimes \bar{q}_{\bar{\mathbf{3}}} \rightarrow [\bar{q}q]_{\mathbf{1}}[\bar{q}q]_{\mathbf{1}} \oplus [\bar{q}q]_{\mathbf{8}}[\bar{q}q]_{\mathbf{8}} \rightarrow [\bar{q}q\bar{q}q]_{\mathbf{1}} \oplus [\bar{q}q\bar{q}q]_{\mathbf{1}}, \quad (21)$$

and we usually call the color singlet-singlet type structures as the molecular states. For the tetraquark states,

$$q_{\mathbf{3}} \otimes q_{\mathbf{3}} \otimes \bar{q}_{\bar{\mathbf{3}}} \otimes \bar{q}_{\bar{\mathbf{3}}} \rightarrow [qq]_{\bar{\mathbf{3}}}[\bar{q}\bar{q}]_{\mathbf{3}} \oplus [qq]_{\mathbf{6}}[\bar{q}\bar{q}]_{\bar{\mathbf{6}}} \rightarrow [qq\bar{q}\bar{q}]_{\mathbf{1}} \oplus [qq\bar{q}\bar{q}]_{\mathbf{1}}, \quad (22)$$

and we usually call the color antitriplet-triplet type structures as the tetraquark states. For the pentaquark molecular states,

$$q_{\mathbf{3}} \otimes q_{\mathbf{3}} \otimes q_{\mathbf{3}} \otimes q_{\mathbf{3}} \otimes \bar{q}_{\bar{\mathbf{3}}} \rightarrow [qqq]_{\mathbf{1}}[\bar{q}q]_{\mathbf{1}} \rightarrow [qqqq\bar{q}]_{\mathbf{1}}. \quad (23)$$

For the pentaquark states,

$$q_{\mathbf{3}} \otimes q_{\mathbf{3}} \otimes q_{\mathbf{3}} \otimes q_{\mathbf{3}} \otimes \bar{q}_{\bar{\mathbf{3}}} \rightarrow [qq]_{\bar{\mathbf{3}}}[qq]_{\bar{\mathbf{3}}}[\bar{q}]_{\bar{\mathbf{3}}} \rightarrow [qqqq\bar{q}]_{\mathbf{1}}. \quad (24)$$

If we take the viewpoint of the quantum field theory, the scattering amplitude for one-gluon exchange is proportional to,

$$\left(\frac{\lambda^a}{2}\right)_{ij} \left(\frac{\lambda^a}{2}\right)_{kl} = -\frac{N_c+1}{4N_c} t_{ik}^A t_{lj}^A + \frac{N_c-1}{4N_c} t_{ik}^S t_{lj}^S, \quad (25)$$

where

$$\begin{aligned} t_{ik}^A t_{lj}^A &= \delta_{ij} \delta_{kl} - \delta_{il} \delta_{kj} = \varepsilon_{mik} \varepsilon_{mjl} \\ t_{ik}^S t_{lj}^S &= \delta_{ij} \delta_{kl} + \delta_{il} \delta_{kj}, \end{aligned} \quad (26)$$

the λ^a is the Gell-Mann matrix, the i, j, k, m and l are color indexes, the N_c is the color number, and $N_c = 3$ in the real world. The negative sign in front of the antisymmetric antitriplet $\bar{\mathbf{3}}$ indicates the interaction is attractive, which favors formation of the diquarks in color antitriplet, while the positive sign in front of the symmetric sextet $\mathbf{6}$ indicates the interaction is repulsive, which disfavors formation of the diquarks in color sextet.

In this sub-section, we would like focus on the tetraquark states, as the extension to the pentaquark states is straightforwardly. Now we define the color factor,

$$\widehat{C}_i \cdot \widehat{C}_j = \frac{\lambda_i^a}{2} \cdot \frac{\lambda_j^a}{2}, \quad (27)$$

where the subscripts i and j denote the quarks, $\langle \widehat{C}_i \cdot \widehat{C}_j \rangle = -\frac{2}{3}$ and $\frac{1}{3}$ for the $\bar{\mathbf{3}}$ and $\mathbf{6}$ diquark $[qq]$, respectively, and $\langle \widehat{C}_i \cdot \widehat{C}_j \rangle = -\frac{4}{3}$ and $\frac{1}{6}$ for the $\mathbf{1}$ and $\mathbf{8}$ quark-antiquark $\bar{q}q$, respectively. If we define $\widehat{C}_{12} \cdot \widehat{C}_{34} = \left(\widehat{C}_1 + \widehat{C}_2\right) \cdot \left(\widehat{C}_3 + \widehat{C}_4\right)$, then $\langle \widehat{C}_{12} \cdot \widehat{C}_{34} \rangle = -\frac{4}{3}$ and $-\frac{10}{3}$ for the $\bar{\mathbf{33}}$ and $\mathbf{6\bar{6}}$ type tetraquark states. It is feasible to take both the $\bar{\mathbf{33}}$ and $\mathbf{6\bar{6}}$ diquark configurations to explore the tetraquark states, while the preferred or usually taken configuration is of the $\bar{\mathbf{33}}$ type.

The color-spin Hamiltonian can be written as [269],

$$H = - \sum_{i \neq j} \kappa_{ij} S_i \cdot S_j \frac{\lambda_i^a}{2} \cdot \frac{\lambda_j^a}{2}, \quad (28)$$

the color factor $\frac{\lambda_i^a}{2} \cdot \frac{\lambda_j^a}{2}$ can be absorbed into the chromomagnetic couplings κ_{ij} after taking matrix elements between the $\bar{\mathbf{3}}\mathbf{3}$ type tetraquark states.

In 2004, Maiani et al introduced the simple spin-spin Hamiltonian,

$$H = 2m_{[cq]} + 2(\kappa_{cq})_{\bar{\mathbf{3}}} [(S_c \cdot S_q) + (S_{\bar{c}} \cdot S_{\bar{q}})] + 2\kappa_{q\bar{q}} (S_q \cdot S_{\bar{q}}) + 2\kappa_{c\bar{q}} [(S_c \cdot S_{\bar{q}}) + (S_{\bar{c}} \cdot S_q)] + 2\kappa_{c\bar{c}} (S_c \cdot S_{\bar{c}}), \quad (29)$$

to study the hidden-charm tetraquark states in the diquark model, where the m_{cq} is the charmed diquark mass [51]. They took the $X(3872)$ with the $J^{PC} = 1^{++}$ tetraquark state as the basic input and predicted a mass spectrum for the $\bar{\mathbf{3}}\mathbf{3}$ type hidden-charm tetraquark states with the $J^{PC} = 0^{++}, 1^{+-}$ and 2^{++} . Maiani et al assigned the $J^{PC} = 1^{+-}$ charged resonance in the $Y(4260) \rightarrow \pi^+ \pi^- J/\psi$ decays as the $X(3882)$ or $Z(3882)$ according to the BESIII and Belle data, however, there is no evidence for the lower resonance $X(3754)$ or $Z(3754)$ [270]. In fact, in the Type-I diquark model, see the Hamiltonian in Eq.(29) [51], the predicted masses 3754 MeV and 3882 MeV for the $J^{PC} = 1^{+-}$ states are smaller than that of the tetraquark candidates $Z_c(3900)$ and $Z_c(4020)$ observed later, respectively [154, 155, 157, 159, 160].

In 2005, Maiani et al assigned the $Y(4260)$ to be the first orbital excitation of the $[cs][\bar{c}\bar{s}]$ state by including the spin-orbit interaction, and obtained a crucial prediction that the $Y(4260)$ should decay predominantly in $D_s \bar{D}_s$ channel [271]. The decay model $Y(4260) \rightarrow D_s \bar{D}_s$ has not been observed yet up to now. In 2009, Drenska, Faccini and Polosa investigated the $[cs][\bar{c}\bar{s}]$ tetraquark states with the $J^{PC} = 0^{++}, 0^{-+}, 0^{--}, 1^{++}, 1^{+-}, 1^{-+}$ and 1^{--} by computing the mass spectrum and decay modes [272].

In 2014, Maiani et al restricted the dominant spin-spin interactions to the ones within each diquark, and simplify the effective Hamiltonian,

$$H = 2m_{[cq]} + 2\kappa_{cq} [(S_c \cdot S_q) + (S_{\bar{c}} \cdot S_{\bar{q}})], \quad (30)$$

which could describe the hierarchy of the $X(3872)$, $Z_c(3900)$, $Z_c(4020)$ very well in the scenario of tetraquark states [52], furthermore, they introduced a spin-orbit interaction to interpret the Y states,

$$H = M_{00} + B_c \frac{L^2}{2} - 2aL \cdot S + 2\kappa_{cq} [(S_c \cdot S_q) + (S_{\bar{c}} \cdot S_{\bar{q}})], \quad (31)$$

where the M_{00} , B_c and a are parameters to be fitted experimentally. Then they sorted the states in terms of $|S_{qc}, S_{\bar{q}\bar{c}}; S, L; J\rangle$, and assigned the $Y(4008)$, $Y(4260)$, $Y(4290/4220)$ and $Y(4630)$ to be the vector tetraquark states $|0, 0; 0, 1; 1\rangle$, $\frac{1}{\sqrt{2}}(|1, 0; 1, 1; 1\rangle + |0, 1; 1, 1; 1\rangle)$, $|1, 1; 0, 1; 1\rangle$ and $|1, 1; 2, 1; 1\rangle$, respectively. The effective Hamiltonian, see Eq.(30), is referred to as the Type-II diquark model. Then the $[cs][\bar{c}\bar{s}]$ mass spectrum was explored [273], and applied to study the LHCb's $J/\psi\phi$ resonances [274].

In 2017, Maiani, Polosa and Riquer introduced the hypothesis that diquarks and antidiquarks in tetraquarks are separated by a potential barrier to answer long standing questions challenging the diquark-antidiquark model of exotic resonances [275].

In 2018, Ali et al analyzed the hidden-charm P-wave tetraquarks in the diquark model using an effective Hamiltonian incorporating the dominant spin-spin, spin-orbit and tensor interactions,

$$H = 2m_{\mathcal{D}} + \frac{B_{\mathcal{D}}}{2} L^2 + 2a_Y L \cdot S + b_Y (3S_1 \cdot \vec{n} S_2 \cdot \vec{n} - S_1 \cdot S_2) + 2\kappa_{cq} (S_q \cdot S_c + S_{\bar{q}} \cdot S_{\bar{c}}), \quad (32)$$

where $\vec{n} = \frac{\vec{r}}{r}$, the S_1 and S_2 are the spins of the diquark \mathcal{D} and antiquark $\bar{\mathcal{D}}$, respectively, the $m_{\mathcal{D}}$, B_Y , a_Y and b_Y are parameters to be fitted experimentally [276]. And their updated analysis indicate that it is favorable to assign the $Y(4220)$, $Y(4330)$, $Y(4390)$, $Y(4660)$ as the vector tetraquark states $|0, 0; 0, 1; 1\rangle$, $\frac{1}{\sqrt{2}}(|1, 0; 1, 1; 1\rangle + |0, 1; 1, 1; 1\rangle)$, $|1, 1; 0, 1; 1\rangle$ and $|1, 1; 2, 1; 1\rangle$, respectively.

In 2021, Maiani, Polosa and Riquer suggested that the $Z_{cs}(3985)$ and $Z_{cs}(4003)$ are two different particles, and there exist two $SU(3)_f$ nonets with the $J^{PC} = 1^{++}$ and 1^{+-} , respectively, thus could assign the The $X(3872)$, $Z_c(3900)$, $Z_{cs}(3985)$, $Z_{cs}(4003)$ and $X(4140)$ consistently [277].

Again, let us turn to the chromomagnetic interaction model, see Eq.(28), and choose the $\bar{\mathbf{33}}$ plus $\mathbf{66}$ configurations and $\mathbf{11}$ plus $\mathbf{88}$ configurations as two independent representations (or basis) respectively to explore the mass spectrum of the exotic states and their decay channels, and have obtained many successful descriptions [278, 279, 280, 281, 282].

In the dynamical diquark picture, Brodsky, Hwang and Lebed assume that the $\mathcal{D}\bar{\mathcal{D}}$ pair forms promptly at the production point, and rapidly separates due to the kinematics of the production process, as the diquark and antiquark are colored objects, they cannot separate asymptotically far apart; they create a color flux tube or string between them. If sufficient energy is available, the string would break to create an additional $q\bar{q}$ pair, and rearrange into a baryon-antibaryon pair, for example, the $\Lambda_c\bar{\Lambda}_c$ pair. The overlap of the wave-functions between the quark and antiquark is suppressed greatly, due to the large spatial separation between the diquark and antiquark pair, therefore, the transition rate is suppressed and leads to small exotic widths [53]. The exotic mass spectrum is calculated in this picture [283, 284, 285, 286, 287, 288].

In the relativized quark model, the Hamiltonian can be written as,

$$H = \sum_{i=1}^4 (p_i^2 + m_i^2)^{1/2} + \sum_{i<j} V_{ij}^{\text{conf}} + \sum_{i<j} V_{ij}^{\text{oge}} \quad (33)$$

where the V_{ij}^{conf} is the linear confining potential, the V_{ij}^{oge} is the one-gluon exchange potential including a Coulomb and a hyperfine term. Then the $\bar{\mathbf{33}}$ type configurations or both the $\bar{\mathbf{33}}$ and $\mathbf{66}$ type configurations are taken into account to solve the Schrodinger equations to obtain the mass spectrum [289, 290, 291, 292, 293, 294, 295, 296, 297].

In the quasipotential approach, Ebert et al take the $\bar{\mathbf{33}}$ -type configurations to study the hidden-charm (hidden-bottom, charm-bottom or fully-heavy) tetraquark mass spectrum by solving the Schrodinger type equations, where an effective one-gluon exchange potential plus a linear confining potential are adopted [298, 299, 300, 301].

In the constituent quark model, all possible quark configurations satisfying the Pauli principle are explored by solving the Schrodinger equation with the potential kernel containing the confinement plus one-gluon-exchange plus (or not plus) one-meson-exchange interactions [302, 303, 304, 305, 306, 307, 308, 309], while in the color flux-tube model, a multi-body interacting confinement potential instead of a two-body interacting confinement potential is chosen [310, 311].

2.6 Tetraquark states from Lattice QCD

Lattice QCD provides rather accurate and reliable calculations for the hadrons which lie well below strong-decay threshold and do not decay strongly, the physics information is commonly extracted from the discrete energy spectrum. The physical system for specified quantum numbers is created from the vacuum $|0\rangle$ using an operator \mathcal{O}_j^\dagger at time $t=0$, then this system propagates for a time t before being annihilated by an operator \mathcal{O}_i . We perform the spectral decomposition to express the correlators $C_{ij}(t)$ in terms of the energies E_n and overlaps Z_j^n of the eigenstates $|n\rangle$,

$$C_{ij}(t) = \langle 0 | \mathcal{O}_i(t) \mathcal{O}_j^\dagger(0) | 0 \rangle = \sum_n Z_i^n Z_j^{n*} e^{-E_n t}, \quad (34)$$

$Z_i^n \equiv \langle 0 | \mathcal{O}_i | n \rangle$. We calculate the correlators $C_{ij}(t)$ on the lattice and use their time-dependence to extract the E_n and Z_n^i [312, 313]. The lattice QCD has been applied extensively to study the exotic states [314, 315, 316, 317, 318, 319, 320, 321].

In the energy region near or above the strong decay thresholds, we infer the masses of the bound states and resonances from the finite-volume scattering matrix of one-channel elastic or multiple-channel inelastic scattering. Various approaches with varying degrees of mathematical rigour have been used in the simulations [322]. The simplest example is a one-channel elastic scattering with the partial wave l , where we parameterize the scattering matrix $S(p)$ satisfying unitarity $SS^\dagger = 1$ in terms of the phase shift $\delta_l(p)$,

$$\begin{aligned} S(p) &= e^{2i\delta_l(p)} = 1 + 2iT(p), \\ T(p) &= \frac{1}{\cot(\delta_l(p)) - i}, \end{aligned} \quad (35)$$

we can extract the phase shift $\delta_l(p)$ for the S-wave scattering using the well-established and rigorous Luscher's relation [323, 324, 325], which applies for the elastic scattering below and above threshold. The phase shifts $\delta(p)$ provide copious information about the masses of resonances and bound states. In the vicinity of a hadronic resonance with a mass m_R and a width Γ , the cross section has a Breit-Wigner-type shape with the value $\delta(s = m_R^2) = \frac{\pi}{2}$,

$$T(p) = \frac{-\sqrt{s} \Gamma(p)}{s - m_R^2 + i\sqrt{s} \Gamma(p)} = \frac{1}{\cot \delta(p) - i}. \quad (36)$$

Below and above threshold, the $p \cot \delta(p)$ can be expanded by the effective range approximation,

$$p \cot \delta(p) = \frac{1}{a} + \frac{1}{2} r p^2, \quad (37)$$

where the a is the scattering length and the r is the effective range. On the other hand, the bound state (B) is realized when the scattering amplitude $T(p)$ has a pole at the value $p_B = i|p_B|$,

$$T = \frac{1}{\cot(\delta(p_B)) - i} = \infty, \quad (38)$$

the location of this shallow bound state can be obtained by parameterizing $\delta(p)$ near the threshold and finding the p_B which satisfies $\cot(\delta(p_B)) = i$. Most of the exotic candidates are above several two-hadron thresholds, and have more than one decay channels, which requires determining the scattering matrix for the coupled-channel nonelastic scattering matrix elements [327, 328, 329, 330].

The HALQCD collaboration used the HALQCD approach to extract the coupled-channel scattering matrix [331, 332], the HALQCD approach is based on the lattice determination of the potential $V(r)$ between different channels, then employs the Nambu-Bethe-Salpeter equation to extract the masses of the bound states.

2.7 Tetraquark (molecular) states with the QCD sum rules

The QCD sum rules were introduced by Shifman, Vainshtein and Zakharov in 1979 to investigate mesons [333, 334], and its extension to baryons was done afterwards by Ioffe [335]. the QCDSR is an analytic method and fully relativistic. The basic idea of the QCD sum rule formalism is to approach the bound state problem in QCD from the asymptotic freedom side, *i.e.*, to start at short distances, where the quark-gluon dynamics is essentially perturbative, and move to larger distances where the hadronic states are formed, including non-perturbative effects step by step, and using some approximate procedure to extract information on hadronic properties.

A generic two-point correlation function is given by

$$\Pi(p^2) \equiv i \int d^4x e^{ip \cdot x} \langle 0 | T[J(x)J^\dagger(0)] | 0 \rangle, \quad (39)$$

where $J(x)$ are the local composite operators builded up from quarks and gluons fields with specified quantum numbers, the T is the time ordered product between the operators.

We can take into account the QCD degrees of freedom, quarks and gluon fields, and calculate the correlation function using Wilson's operator product expansion in order to separate the physics of short and long-range distances.

$$\Pi(p^2) = \sum_n C_n(p^2, \mu) \langle \mathcal{O}_n(\mu) \rangle, \quad (40)$$

where the $C_n(p^2, \mu)$ is the Wilson's coefficients, which encode perturbative contributions, the $\langle \mathcal{O}_n(\mu) \rangle$ are the expectation values of the composite local operators with the dimension n . The short-distance contributions at $p^2 > \mu^2$ are included in the coefficients $C_n(p^2, \mu)$, the long-distance contributions at $p^2 < \mu^2$ are absorbed into the vacuum condensates $\langle \mathcal{O}_n(\mu) \rangle$. If $\mu \gg \Lambda_{QCD}$, the Wilson coefficients $C_n(p^2, \mu)$ depend only on short-distance dynamics, while the long-distance effects are taken into account by the vacuum condensates $\langle \mathcal{O}_n(\mu) \rangle$. The lowest condensate is vacuum expectation of the unit operator $\langle \mathcal{O}_0(\mu) \rangle = 1$ associated with the perturbative contribution. The vacuum condensates with dimensions $n = 3, 4, 5, 6, \dots$ are quark condensate $\langle \bar{q}q \rangle$, gluon condensate $\langle \frac{\alpha_s GG}{\pi} \rangle$, mixed condensate $\langle \bar{q}g_s \sigma Gq \rangle$, four-quark condensate $\langle \bar{q}q \rangle^2, \dots$, which parameterize the nonperturbative effects or the soft gluons and quarks.

We obtain the Källén-Lehmann representation through dispersion relation at the QCD side or at the quark-gluon degrees of freedom,

$$\Pi_{QCD}(p^2) = \frac{1}{\pi} \int_{\Delta^2}^{\infty} ds \frac{\text{Im}\Pi_{QCD}(s)}{s - p^2}, \quad (41)$$

where the Δ^2 denotes the threshold.

At the hadron degrees of freedom, we insert a complete set of intermediate hadronic states $|n\rangle$ with the same quantum numbers as the current operators $J(x)$ into the correlation functions $\Pi(p^2)$ and take account of the current-hadron couplings to the analytical expressions, again we obtain the Källén-Lehmann representation through dispersion,

$$\Pi_H(p^2) = \frac{1}{\pi} \int_{\Delta^2}^{\infty} ds \frac{\text{Im}\Pi_H(s)}{s - p^2}, \quad (42)$$

where

$$\rho_H(s) = \frac{\text{Im}\Pi_H(s)}{\pi} = \sum_n |0|J(0)|n\rangle|^2 \delta(s - M_n^2), \quad (43)$$

where the subscript H denote the hadron side.

According to the Quark-Hadron duality, we introduce the continuum threshold parameters s_0 , and match the QCD side with hadron side of the correlation functions $\Pi(p^2)$,

$$\frac{1}{\pi} \int_{\Delta^2}^{s_0} ds \frac{\text{Im}\Pi_H(s)}{s - p^2} = \frac{1}{\pi} \int_{\Delta^2}^{s_0} ds \frac{\text{Im}\Pi_{QCD}(s)}{s - p^2}. \quad (44)$$

An important point is the choice of the continuum threshold, s_0 . It is a physical parameter that should be determined from the hadronic spectrum. Then we perform the Borel transformation,

$$\Pi(T^2) = \mathcal{B}[\Pi(P^2)] \equiv \lim_{\substack{P^2, n \rightarrow \infty \\ P^2/n = T^2}} \frac{(P^2)^{n+1}}{(n)!} \left(-\frac{d}{dP^2} \right)^n \Pi(P^2), \quad (45)$$

to obtain the QCD sum rules,

$$\frac{1}{\pi} \int_{\Delta^2}^{s_0} ds \text{Im}\Pi_H(s) \exp\left(-\frac{s}{T^2}\right) = \frac{1}{\pi} \int_{\Delta^2}^{s_0} ds \text{Im}\Pi_{QCD}(s) \exp\left(-\frac{s}{T^2}\right). \quad (46)$$

where the T^2 is the Borel parameter. If only the ground state is taken, then $\frac{\text{Im}\Pi_H(s)}{\pi} = |\langle 0|J(0)|H\rangle|^2 \delta(s - M_H^2) = \lambda_H^2 \delta(s - M_H^2)$, we obtain the QCD sum rules,

$$\lambda_H^2 \exp\left(-\frac{M_H^2}{T^2}\right) = \frac{1}{\pi} \int_{\Delta^2}^{s_0} ds \text{Im}\Pi_{QCD}(s) \exp\left(-\frac{s}{T^2}\right). \quad (47)$$

Some typical and useful examples of the Borel transformation are:

$$\begin{aligned} \mathcal{B}[(P^2)^k] &= 0, \\ \mathcal{B}\left[\frac{\Gamma(k)}{(P^2)^k}\right] &= \frac{1}{(T^2)^{k-1}}, \\ \mathcal{B}\left[\frac{\Gamma(k)}{(s + P^2)^k}\right] &= \frac{1}{(T^2)^{k-1}} \exp\left(-\frac{s}{T^2}\right). \end{aligned} \quad (48)$$

It is evident that the Borel transformation kills any eventual subtraction terms in the correlation functions and suppresses exponentially the continuum contribution, therefore it improves the convergence of the dispersion integral. Furthermore, it suppresses factorially the higher-order operators in operator product expansion, which contain inverse powers of P^2 , thus justifies the truncation of the operator product expansion and favors a good convergent behavior.

Finally, we eliminate the pole residues λ_H to obtain the QCD sum rules for the ground state masses,

$$M_H^2 = \frac{-\frac{d}{d\tau} \int_{\Delta^2}^{s_0} ds \text{Im}\Pi_{QCD}(s) \exp(-\tau s)}{\int_{\Delta^2}^{s_0} ds \text{Im}\Pi_{QCD}(s) \exp(-\tau s)} \Big|_{\tau=\frac{1}{T^2}}. \quad (49)$$

In the QCDSR technique we make use of some phenomenological inputs, limiting the accuracy of the method to be around 10% – 20% [336]. The QCD sum rules have been extensively applied to study the X , Y , Z , T and P states [42, 43, 54, 56, 76].

3 Are QCD sum rules reliable to explore multiquark states

Any color-singlet four-quark and five-quark currents $J(x)$ can be written as $J(x) = J_A^i(x)J_B^i(x)$, where the $J_A^i(x)$ and $J_B^i(x)$ are color singlet clusters with $i = 1, 2, 3, \dots$, for example,

$$\begin{aligned} J_\mu(x) &= \frac{\varepsilon^{ijk}\varepsilon^{imn}}{\sqrt{2}} \left\{ u_j^T(x)C\gamma_5 c_k(x)\bar{d}_m(x)\gamma_\mu C\bar{c}_n^T(x) - u_j^T(x)C\gamma_\mu c_k(x)\bar{d}_m(x)\gamma_5 C\bar{c}_n^T(x) \right\}, \\ &= \frac{1}{2\sqrt{2}} \left\{ i\bar{c}i\gamma_5 c \bar{d}\gamma_\mu u - i\bar{c}\gamma_\mu c \bar{d}i\gamma_5 u + \bar{c}u \bar{d}\gamma_\mu \gamma_5 c - \bar{c}\gamma_\mu \gamma_5 u \bar{d}c \right. \\ &\quad \left. - i\bar{c}\gamma^\nu \gamma_5 c \bar{d}\sigma_{\mu\nu} u + i\bar{c}\sigma_{\mu\nu} c \bar{d}\gamma^\nu \gamma_5 u - i\bar{c}\sigma_{\mu\nu} \gamma_5 u \bar{d}\gamma^\nu c + i\bar{c}\gamma^\nu u \bar{d}\sigma_{\mu\nu} \gamma_5 c \right\}, \end{aligned} \quad (50)$$

for the four-quark current [56, 337], and

$$\begin{aligned} J(x) &= \varepsilon^{ila}\varepsilon^{ijk}\varepsilon^{lmn} u_j^T(x)C\gamma_5 d_k(x) u_m^T(x)C\gamma_5 c_n(x) C\bar{c}_a^T(x), \\ &= -\frac{1}{4}\mathcal{S}_{ud}\gamma_5 c \bar{c}u + \frac{1}{4}\mathcal{S}_{ud}\gamma^\lambda \gamma_5 c \bar{c}\gamma_\lambda u + \frac{1}{8}\mathcal{S}_{ud}\sigma^{\lambda\tau} \gamma_5 c \bar{c}\sigma_{\lambda\tau} u + \frac{1}{4}\mathcal{S}_{ud}\gamma^\lambda c \bar{c}\gamma_\lambda \gamma_5 u + \frac{i}{4}\mathcal{S}_{ud}c \bar{c}i\gamma_5 u \\ &\quad + \frac{1}{4}\mathcal{S}_{ud}\gamma_5 u \bar{c}c - \frac{1}{4}\mathcal{S}_{ud}\gamma^\lambda \gamma_5 u \bar{c}\gamma_\lambda c - \frac{1}{8}\mathcal{S}_{ud}\sigma^{\lambda\tau} \gamma_5 u \bar{c}\sigma_{\lambda\tau} c - \frac{1}{4}\mathcal{S}_{ud}\gamma^\lambda u \bar{c}\gamma_\lambda \gamma_5 c - \frac{i}{4}\mathcal{S}_{ud}u \bar{c}i\gamma_5 c, \end{aligned} \quad (51)$$

for the five-quark currents [338], where the components $\mathcal{S}_{ud}\Gamma c = \varepsilon^{ijk} u_i^T C\gamma_5 d_j \Gamma c_k$.

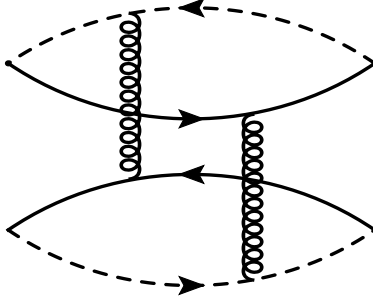


Figure 5: The nonfactorizable Feynman diagrams of the order $\mathcal{O}(\alpha_s^2)$ for the color singlet-singlet type currents, other diagrams obtained by interchanging of the heavy quark lines (dashed lines) and light quark lines (solid lines) are implied.

According to the pioneer works [339, 340, 341], in the coordinate space, we write the two-hadron-reducible contributions as

$$\Pi_{RE}(x) = \langle 0|T \{J_A^i(x)J_A^{j\dagger}(0)\} |0\rangle \langle 0|T \{J_B^i(x)J_B^{j\dagger}(0)\} |0\rangle, \quad (52)$$

and two-hadron-irreducible contributions as

$$\Pi_{IR}(x) = \langle 0|T \{J(x)J^\dagger(0)\} |0\rangle - \langle 0|T \{J_A^i(x)J_A^{j\dagger}(0)\} |0\rangle \langle 0|T \{J_B^i(x)J_B^{j\dagger}(0)\} |0\rangle. \quad (53)$$

At the phenomenological side of the correlation functions, we can write the two-hadron-reducible contributions as

$$\Pi_{RE}(p^2) = |\lambda_{AB}|^2 \frac{i}{(2\pi)^4} \int d^4q \frac{i}{q^2 - M_A^2} \frac{i}{(p-q)^2 - M_B^2}, \quad (54)$$

where the couplings

$$\langle 0|J_A^i(0)|A(q)\rangle \langle 0|J_B^i(0)|B(p-q)\rangle = \lambda_{AB}, \quad (55)$$

and the λ_{AB} could be estimated phenomenologically [339, 340, 341, 342].

In the correlation functions for the color singlet-singlet type currents [343, 344], Lucha, Melikhov and Sazdjian assert that the Feynman diagrams can be divided into or separated into factorizable diagrams and nonfactorizable diagrams in the color space in the operator product expansion, the contributions at the order $\mathcal{O}(\alpha_s^k)$ with $k \leq 1$, which are factorizable in the color space, are exactly canceled out by the meson-meson scattering states at the hadron side, the nonfactorizable diagrams, if have a Landau singularity, begin to make contributions to the tetraquark (molecular) states, the tetraquark (molecular) states begin to receive contributions at the order $\mathcal{O}(\alpha_s^2)$, see Fig.5.

In Ref.[345], we examine the assertion of Lucha, Melikhov and Sazdjian in details and use two examples for the currents $J_\mu(x)$ and $J_{\mu\nu}(x)$ to illustrate that the Landau equation is of no use in the QCD sum rule for the tetraquark molecular states, where

$$\begin{aligned} J_\mu(x) &= \frac{1}{\sqrt{2}} \left[\bar{u}(x) i \gamma_5 c(x) \bar{c}(x) \gamma_\mu d(x) + \bar{u}(x) \gamma_\mu c(x) \bar{c}(x) i \gamma_5 d(x) \right], \\ J_{\mu\nu}(x) &= \frac{1}{\sqrt{2}} \left[\bar{s}(x) \gamma_\mu c(x) \bar{c}(x) \gamma_\nu \gamma_5 s(x) - \bar{s}(x) \gamma_\nu \gamma_5 c(x) \bar{c}(x) \gamma_\mu s(x) \right]. \end{aligned} \quad (56)$$

Firstly, we cannot assert that the factorizable Feynman diagrams in color space are exactly canceled out by the meson-meson scattering states, because the meson-meson scattering state and tetraquark molecular state both have four valence quarks, which can be divided into or separated

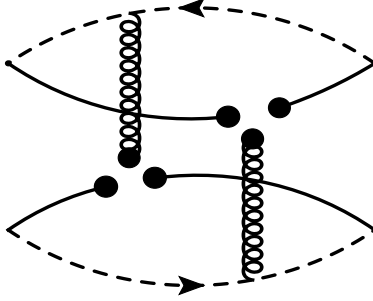


Figure 6: The nonfactorizable Feynman diagrams contribute to the vacuum condensates $\langle \bar{q}g_s\sigma Gq \rangle^2$ for the color singlet-singlet type currents, where the solid lines and dashed lines denote the light quarks and heavy quarks, respectively.

into two color-neutral clusters. We cannot distinguish which Feynman diagrams contribute to the meson-meson scattering state or tetraquark molecular state based on the two color-neutral clusters [345].

Secondly, the quarks and gluons are confined objects, they cannot be put on the mass-shell, it is questionable to assert that the Landau equation is applicable for the quark-gluon bound states [346].

If we insist on applying the Landau equation to study the Feynman diagrams, we should choose the pole masses rather than the \overline{MS} masses to warrant mass poles. As the tetraquark (molecular) states begin to receive contributions at the order $\mathcal{O}(\alpha_s^2)$ [343, 344], it is reasonable to take the pole masses \hat{m}_Q as,

$$\hat{m}_Q = m_Q(m_Q) \left[1 + \frac{4}{3} \frac{\alpha_s(m_Q)}{\pi} + f \left(\frac{\alpha_s(m_Q)}{\pi} \right)^2 + g \left(\frac{\alpha_s(m_Q)}{\pi} \right)^3 \right], \quad (57)$$

see Refs.[347, 348] for the explicit expressions of the f and g . If the Landau equation is applicable for the tetraquark (molecular) states, it is certainly applicable the traditional charmonium and bottomonium states. In the case of the c -quark (b -quark), the pole mass $\hat{m}_c = 1.67 \pm 0.07$ GeV ($\hat{m}_b = 4.78 \pm 0.06$ GeV) from the Particle Data Group [347], the Landau singularity appears at the s -channel $\sqrt{s} = \sqrt{p^2} = 2\hat{m}_c = 3.34 \pm 0.14$ GeV $> M_{\eta_c}/M_{J/\psi}$ ($2\hat{m}_b = 9.56 \pm 0.12$ GeV $> M_{\eta_b}/M_{\Upsilon}$). It is unreliable that the masses of the charmonium (bottomonium) states lie below the threshold $2\hat{m}_c$ ($2\hat{m}_b$) for the η_c and J/ψ (η_b and Υ) [345].

Thirdly, the nonfactorizable Feynman diagrams which have the Landau singularities begin to appear at the order $\mathcal{O}(\alpha_s^0/\alpha_s^1)$ rather than at the order $\mathcal{O}(\alpha_s^2)$, and make contributions to the tetraquark molecular states, if the assertion (the nonfactorizable Feynman diagrams which have Landau singularities make contributions to the tetraquark molecular states) of Lucha, Melikhov and Sazdjian is right.

The nonfactorizable contributions appear at the order $\mathcal{O}(\alpha_s)$ due to the operators $\bar{q}g_sGq\bar{q}g_sGq$, which come from the Feynman diagrams shown in Fig.6. If we insist on choosing the pole mass and applying the Landau equation to study the diagrams, we obtain a sub-leading Landau singularity at the s -channel $s = p^2 = 4\hat{m}_c^2$. From the operators $\bar{q}g_sGq\bar{q}g_sGq$, we obtain the vacuum condensate $\langle \bar{q}g_s\sigma Gq \rangle^2$, where the g_s^2 is absorbed into the vacuum condensate. The nonfactorizable Feynman diagrams appear at the order $\mathcal{O}(\alpha_s^0)$ or $\mathcal{O}(\alpha_s^1)$, not at the order $\mathcal{O}(\alpha_s^2)$ asserted in Refs.[343, 344].

Fourthly, the Landau equation serves as a kinematical equation in the momentum space, and does not depend on the factorizable and nonfactorizable properties of the Feynman diagrams in the color space.

In the leading order, the factorizable Feynman diagrams shown in Fig.7 can be divided into or separated into two color-neutral clusters, however, in the momentum space, they are nonfactoriz-

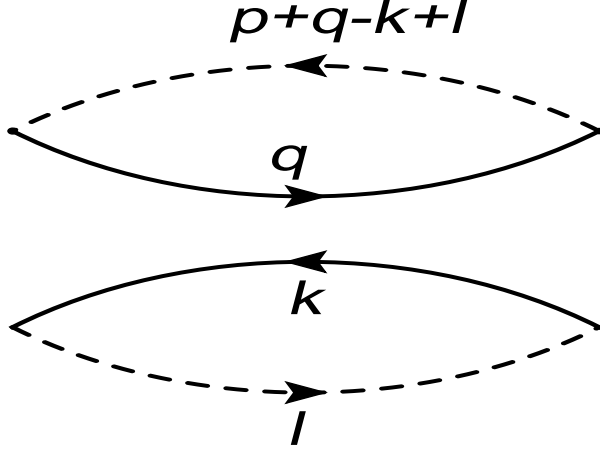


Figure 7: The Feynman diagrams for the lowest order contributions, where the solid lines and dashed lines represent the light quarks and heavy quarks, respectively.

able diagrams, the basic integrals are of the form,

$$\int d^4q d^4k d^4l \frac{1}{(p+q-k+l)^2 - m_c^2} \frac{1}{q^2 - m_q^2} \frac{1}{k^2 - m_q^2} \frac{1}{l^2 - m_c^2}. \quad (58)$$

If we choose the pole masses, there exists a Landau singularity at $s = p^2 = (\hat{m}_u + \hat{m}_d + \hat{m}_c + \hat{m}_c)^2$, which is just a signal of a four-quark intermediate state. We cannot assert that it is a signal of a two-meson scattering state or a tetraquark molecular state, because the meson-meson scattering state and tetraquark molecular state both have four valence quarks, q, \bar{q}, c and \bar{c} , which form two color-neutral clusters.

Fifthly, only formal QCD sum rules for the tetraquark (molecular) states are obtained based on the assertion of Lucha, Melikhov and Sazdjian in Refs.[343, 344], no feasible QCD sum rules are obtained up to now.

Sixthly, we carry out the operator product expansion in the deep Euclidean space, $-p^2 \rightarrow \infty$, then obtain the physical spectral densities at the quark-gluon level through dispersion relation [333, 334],

$$\rho_{QCD}(s) = \frac{1}{\pi} \text{Im} \Pi(s + i\epsilon) |_{\epsilon \rightarrow 0}, \quad (59)$$

where the $\Pi(s)$ denotes the correlation functions. The Landau singularities require that the squared momentum $p^2 = (\hat{m}_u + \hat{m}_d + \hat{m}_c + \hat{m}_c)^2$ in the Feynman diagrams, see Fig.7 and Eq.(58), it is questionable to perform the operator product expansion.

Seventhly, we choose the local four-quark or five-quark currents, while the traditional mesons and baryons are spatial extended objects and have mean spatial sizes $\sqrt{\langle r^2 \rangle} \neq 0$, for example, $\sqrt{\langle r^2 \rangle_{E, \Sigma_c^{++}}} = 0.48 \text{ fm}$, $\sqrt{\langle r^2 \rangle_{M, \Sigma_c^{++}}} = 0.83 \text{ fm}$, $\sqrt{\langle r^2 \rangle_{M, \Sigma_c^0}} = 0.81 \text{ fm}$ from the lattice QCD, where the subscripts E and M stand for the Electric and magnetic radii, respectively [349], $\sqrt{\langle r^2 \rangle_{M, \Sigma_c^{++}}} = 0.77 \text{ fm}$, $\sqrt{\langle r^2 \rangle_{M, \Sigma_c^0}} = 0.52 \text{ fm}$, $\sqrt{\langle r^2 \rangle_{M, \Sigma_c^+}} = 0.81 \text{ fm}$, $\sqrt{\langle r^2 \rangle_{M, \Xi_c^+}} = 0.55 \text{ fm}$, $\sqrt{\langle r^2 \rangle_{M, \Xi_c^0}} = 0.79 \text{ fm}$ from the self-consistent $SU(3)$ chiral quark-soliton model [350], $\sqrt{\langle r^2 \rangle_{D^+}} = 0.43 \text{ fm}$, $\sqrt{\langle r^2 \rangle_{D^0}} = 0.55 \text{ fm}$ from the light-front quark model [351], $\sqrt{\langle r^2 \rangle_{J/\psi}} = 0.41 \text{ fm}$, $\sqrt{\langle r^2 \rangle_{\chi_{c2}}} = 0.71 \text{ fm}$ from the screened potential model [82]. Local currents couple potentially to the compact objects having the average spatial sizes as that of the typical heavy mesons and baryons, not to two-particle scattering

states with average spatial size $\sqrt{\langle r^2 \rangle} \geq 1.0$ fm, which is too large to be interpolated by the local currents [352, 353].

Now we take a short digression to give a **short notice**. In the QCD sum rules, as we choose the local currents, the four-quark and five-quark states are all compact objects, they are $\bar{\mathbf{33}}$ -type, $\mathbf{11}$ -type or $\mathbf{88}$ -type tetraquark states, and $\bar{\mathbf{333}}$ -type or $\mathbf{11}$ -type pentaquark states, although we usually call the $\mathbf{11}$ -type states as the molecular states.

Now, let us write down the correlation functions $\Pi_{\mu\nu}(p)$ and $\Pi_{\mu\nu\alpha\beta}(p)$ for the two currents in Eq.(56),

$$\Pi_{\mu\nu}(p) = i \int d^4x e^{ip \cdot x} \langle 0 | T \{ J_\mu(x) J_\nu^\dagger(0) \} | 0 \rangle, \quad (60)$$

$$\Pi_{\mu\nu\alpha\beta}(p) = i \int d^4x e^{ip \cdot x} \langle 0 | T \{ J_{\mu\nu}(x) J_{\alpha\beta}^\dagger(0) \} | 0 \rangle. \quad (61)$$

If we assume the four-quark currents couple potentially both to the two-meson scattering states and molecular states, then we can express the $J_\mu(x)$ and $J_{\mu\nu}(x)$ in terms of the heavy meson fields,

$$\begin{aligned} J_\mu(x) &= \frac{1}{\sqrt{2}} \frac{f_D m_D^2}{m_c} f_{D^*} m_{D^*} [D^0(x) D_\mu^{*-}(x) + D_\mu^{*0}(x) D^-(x)] \\ &+ \frac{1}{\sqrt{2}} \frac{f_D m_D^2}{m_c} f_{D_0} [D^0(x) i \partial_\mu D_0^-(x) + i \partial_\mu D_0^0(x) D^-(x)] + \lambda_Z Z_{c,\mu}(x) + \dots, \end{aligned} \quad (62)$$

$$\begin{aligned} J_{\mu\nu}(x) &= \frac{1}{\sqrt{2}} f_{D_s^*} m_{D_s^*} f_{D_{s1}} m_{D_{s1}} [D_{s,\mu}^{*+}(x) D_{s1,\nu}^-(x) - D_{s1,\nu}^+(x) D_{s,\mu}^{*-}(x)] \\ &- \frac{1}{\sqrt{2}} f_{D_s^*} m_{D_s^*} f_{D_s} [D_{s,\mu}^{*+}(x) \partial_\nu D_s^-(x) - \partial_\nu D_s^+(x) D_{s,\mu}^{*-}(x)] \\ &+ \frac{1}{\sqrt{2}} f_{D_{s0}} f_{D_{s1}} m_{D_{s1}} [i \partial_\mu D_{s0}^+(x) D_{s1,\nu}^-(x) - D_{s1,\nu}^+(x) i \partial_\mu D_{s0}^-(x)] \\ &- \frac{1}{\sqrt{2}} f_{D_{s0}} f_{D_s} [i \partial_\mu D_{s0}^+(x) \partial_\nu D_s^-(x) - \partial_\nu D_s^+(x) i \partial_\mu D_{s0}^-(x)] \\ &- \frac{\lambda_{X^-}}{M_{X^-}} \varepsilon_{\mu\nu\alpha\beta} i \partial^\alpha X_c^{-\beta}(x) - \frac{\lambda_{X^+}}{M_{X^+}} [i \partial_\mu X_{c,\nu}^+(x) - i \partial_\nu X_{c,\mu}^+(x)] + \dots, \end{aligned} \quad (63)$$

where we have taken the standard definitions for the traditional mesons and pole residues of the tetraquark molecular states,

$$\langle 0 | J_\mu(0) | Z_c(p) \rangle = \lambda_Z \varepsilon_\mu(p), \quad (64)$$

$$\begin{aligned} \langle 0 | J_{\mu\nu}(0) | X_c^-(p) \rangle &= \frac{\lambda_{X^-}}{M_{X^-}} \varepsilon_{\mu\nu\alpha\beta} \varepsilon^\alpha(p) p^\beta, \\ \langle 0 | J_{\mu\nu}(0) | X_c^+(p) \rangle &= \frac{\lambda_{X^+}}{M_{X^+}} [\varepsilon_\mu(p) p_\nu - \varepsilon_\nu(p) p_\mu], \end{aligned} \quad (65)$$

where the Z_c , X^- and X^+ have the $J^{PC} = 1^{+-}$, 1^{-+} and 1^{++} , respectively, the ε_μ are the polarization vectors, we introduce the superscripts \mp to denote the parity.

It is straightforward to obtain the hadronic representation,

$$\Pi_{\mu\nu}(p) = \Pi(p^2) \left(-g_{\mu\nu} + \frac{p_\mu p_\nu}{p^2} \right) + \dots, \quad (66)$$

$$\begin{aligned} \Pi_{\mu\nu\alpha\beta}(p) &= \Pi_-(p^2) \left(g_{\mu\alpha} g_{\nu\beta} - g_{\mu\beta} g_{\nu\alpha} - g_{\mu\alpha} \frac{p_\nu p_\beta}{p^2} - g_{\nu\beta} \frac{p_\mu p_\alpha}{p^2} + g_{\mu\beta} \frac{p_\nu p_\alpha}{p^2} + g_{\nu\alpha} \frac{p_\mu p_\beta}{p^2} \right) \\ &+ \Pi_+(p^2) \left(-g_{\mu\alpha} \frac{p_\nu p_\beta}{p^2} - g_{\nu\beta} \frac{p_\mu p_\alpha}{p^2} + g_{\mu\beta} \frac{p_\nu p_\alpha}{p^2} + g_{\nu\alpha} \frac{p_\mu p_\beta}{p^2} \right), \end{aligned} \quad (67)$$

where

$$\begin{aligned}
\Pi(p^2) &= \frac{\lambda_Z^2}{M_Z^2 - p^2} + \Pi_{TW}(p^2) + \dots, \\
\Pi_-(p^2) &= P_-^{\mu\nu\alpha\beta} \Pi_{\mu\nu\alpha\beta}(p) = \frac{\lambda_{X^-}^2}{M_{X^-}^2 - p^2} + \Pi_{TW}^-(p^2) + \dots, \\
\Pi_+(p^2) &= P_+^{\mu\nu\alpha\beta} \Pi_{\mu\nu\alpha\beta}(p) = \frac{\lambda_{X^+}^2}{M_{X^+}^2 - p^2} + \dots,
\end{aligned} \tag{68}$$

we project out the components $\Pi_-(p^2)$ and $\Pi_+(p^2)$ by introducing the operators $P_-^{\mu\nu\alpha\beta}$ and $P_+^{\mu\nu\alpha\beta}$ respectively,

$$\begin{aligned}
P_-^{\mu\nu\alpha\beta} &= \frac{1}{6} \left(g^{\mu\alpha} - \frac{p^\mu p^\alpha}{p^2} \right) \left(g^{\nu\beta} - \frac{p^\nu p^\beta}{p^2} \right), \\
P_+^{\mu\nu\alpha\beta} &= \frac{1}{6} \left(g^{\mu\alpha} - \frac{p^\mu p^\alpha}{p^2} \right) \left(g^{\nu\beta} - \frac{p^\nu p^\beta}{p^2} \right) - \frac{1}{6} g^{\mu\alpha} g^{\nu\beta},
\end{aligned} \tag{69}$$

$$\begin{aligned}
\Pi_{TW}(p^2) &= \frac{\lambda_{DD^*}^2}{16\pi^2} \int_{\Delta_1^2}^{s_0} ds \frac{1}{s-p^2} \frac{\sqrt{\lambda(s, m_D^2, m_{D^*}^2)}}{s} \left[1 + \frac{\lambda(s, m_D^2, m_{D^*}^2)}{12sm_{D^*}^2} \right] \\
&+ \frac{\lambda_{DD_0}^2}{16\pi^2} \int_{\Delta_2^2}^{s_0} ds \frac{1}{s-p^2} \frac{\sqrt{\lambda(s, m_D^2, m_{D_0}^2)}}{s} \frac{\lambda(s, m_D^2, m_{D_0}^2)}{12s} + \dots,
\end{aligned} \tag{70}$$

$$\begin{aligned}
\Pi_{TW}^-(p^2) &= \frac{\lambda_{D_s^* D_{s1}}^2}{16\pi^2} \int_{\Delta_3^2}^{s_0} ds \frac{1}{s-p^2} \frac{\sqrt{\lambda(s, m_{D_s^*}^2, m_{D_{s1}}^2)}}{s} \left[1 + \frac{\lambda(s, m_{D_s^*}^2, m_{D_{s1}}^2)}{12sm_{D_s^*}^2} \frac{\lambda(s, m_{D_s^*}^2, m_{D_{s1}}^2)}{12sm_{D_{s1}}^2} \right] \\
&+ \frac{\lambda_{D_s^* D_s}^2}{16\pi^2} \int_{\Delta_4^2}^{s_0} ds \frac{1}{s-p^2} \frac{\sqrt{\lambda(s, m_{D_s^*}^2, m_{D_s}^2)}}{s} \frac{\lambda(s, m_{D_s^*}^2, m_{D_s}^2)}{12s} \\
&+ \frac{\lambda_{D_{s0} D_{s1}}^2}{16\pi^2} \int_{\Delta_5^2}^{s_0} ds \frac{1}{s-p^2} \frac{\sqrt{\lambda(s, m_{D_{s0}}^2, m_{D_{s1}}^2)}}{s} \frac{\lambda(s, m_{D_{s0}}^2, m_{D_{s1}}^2)}{12s} + \dots,
\end{aligned} \tag{71}$$

where $\lambda_{DD^*}^2 = \frac{f_D^2 m_D^4 f_{D^*}^2 m_{D^*}^2}{m_c^2}$, $\Delta_1^2 = (m_D + m_{D^*})^2$, $\lambda_{DD_0}^2 = \frac{f_D^2 m_D^4 f_{D_0}^2}{m_c^2}$, $\Delta_2^2 = (m_D + m_{D_0})^2$, $\lambda_{D_s^* D_{s1}}^2 = f_{D_s^*}^2 m_{D_s^*}^2 f_{D_{s1}}^2 m_{D_{s1}}^2$, $\Delta_3^2 = (m_{D_s^*} + m_{D_{s1}})^2$, $\lambda_{D_s^* D_s}^2 = f_{D_s^*}^2 m_{D_s^*}^2 f_{D_s}^2$, $\Delta_4^2 = (m_{D_s^*} + m_{D_s})^2$, $\lambda_{D_{s0} D_{s1}}^2 = f_{D_{s0}}^2 f_{D_{s1}}^2 m_{D_{s1}}^2$, $\Delta_5^2 = (m_{D_{s0}} + m_{D_{s1}})^2$ and $\lambda(a, b, c) = a^2 + b^2 + c^2 - 2ab - 2bc - 2ca$.

The traditional hidden-flavor mesons have the normal quantum numbers, $J^{PC} = 0^{-+}, 0^{++}, 1^{--}, 1^{+-}, 1^{++}, 2^{--}, 2^{-+}, 2^{++}, \dots$. The component $\Pi_-(p^2)$ receives contributions with the exotic quantum numbers $J^{PC} = 1^{-+}$, while the component $\Pi_+(p^2)$ receives contributions with the normal quantum numbers $J^{PC} = 1^{++}$. We choose the component $\Pi_-(p^2)$ with the exotic quantum numbers $J^{PC} = 1^{-+}$ and discard the component $\Pi_+(p^2)$ with the normal quantum numbers $J^{PC} = 1^{++}$. Thereafter, we will neglect the superscript $-$ in the X_c^- for simplicity.

According to the assertion of Lucha, Melikhov and Sazdjian [343, 344], all the contributions of the order $\mathcal{O}(\alpha_s^k)$ with $k \leq 1$ are exactly canceled out by the two-meson scattering states, we set

$$\begin{aligned}
\Pi(p^2) &= \Pi_{TW}(p^2) + \dots, \\
\Pi_-(p^2) &= \Pi_{TW}^-(p^2) + \dots,
\end{aligned} \tag{72}$$

at the hadron side [345]. Then let us take the quark-hadron duality below the continuum threshold s_0 and perform Borel transform with respect to the variable $P^2 = -p^2$ to obtain the QCD sum

rules:

$$\begin{aligned}
\Pi_{TW}(T^2) &= \frac{\lambda_{DD^*}^2}{16\pi^2} \int_{\Delta_1^2}^{s_0} ds \frac{\sqrt{\lambda(s, m_D^2, m_{D^*}^2)}}{s} \left[1 + \frac{\lambda(s, m_D^2, m_{D^*}^2)}{12sm_{D^*}^2} \right] \exp\left(-\frac{s}{T^2}\right) \\
&+ \frac{\lambda_{DD_0}^2}{16\pi^2} \int_{\Delta_2^2}^{s_0} ds \frac{\sqrt{\lambda(s, m_D^2, m_{D_0}^2)}}{s} \frac{\lambda(s, m_D^2, m_{D_0}^2)}{12s} \exp\left(-\frac{s}{T^2}\right) \\
&= \kappa \int_{4m_c^2}^{s_0} ds \rho_{Z, QCD}(s) \exp\left(-\frac{s}{T^2}\right), \tag{73}
\end{aligned}$$

$$\begin{aligned}
\Pi_{TW}^-(T^2) &= \frac{\lambda_{D_s^* D_{s1}}^2}{16\pi^2} \int_{\Delta_3^2}^{s_0} ds \frac{\sqrt{\lambda(s, m_{D_s^*}^2, m_{D_{s1}}^2)}}{s} \left[1 + \frac{\lambda(s, m_{D_s^*}^2, m_{D_{s1}}^2)}{12sm_{D_s^*}^2} \frac{\lambda(s, m_{D_s^*}^2, m_{D_{s1}}^2)}{12sm_{D_{s1}}^2} \right] \exp\left(-\frac{s}{T^2}\right) \\
&+ \frac{\lambda_{D_s^* D_s}^2}{16\pi^2} \int_{\Delta_4^2}^{s_0} ds \frac{\sqrt{\lambda(s, m_{D_s^*}^2, m_{D_s}^2)}}{s} \frac{\lambda(s, m_{D_s^*}^2, m_{D_s}^2)}{12s} \exp\left(-\frac{s}{T^2}\right) \\
&+ \frac{\lambda_{D_{s0} D_{s1}}^2}{16\pi^2} \int_{\Delta_5^2}^{s_0} ds \frac{\sqrt{\lambda(s, m_{D_{s0}}^2, m_{D_{s1}}^2)}}{s} \frac{\lambda(s, m_{D_{s0}}^2, m_{D_{s1}}^2)}{12s} \exp\left(-\frac{s}{T^2}\right) \\
&= \kappa \int_{4m_c^2}^{s_0} ds \rho_{X, QCD}(s) \exp\left(-\frac{s}{T^2}\right), \tag{74}
\end{aligned}$$

the explicit expressions of the QCD spectral densities $\rho_{Z, QCD}(s)$ and $\rho_{X, QCD}(s)$ are given in Ref.[345]. We introduce the parameter κ to measure the deviations from 1, if $\kappa \approx 1$, we can get the conclusion tentatively that the two-meson scattering states can saturate the QCD sum rules. Then we differentiate Eqs.(73)-(74) with respect to $\frac{1}{T^2}$, and obtain two additional QCD sum rules,

$$-\frac{d\Pi_{TW}(T^2)}{d(1/T^2)} = -\kappa \frac{d}{d(1/T^2)} \int_{4m_c^2}^{s_0} ds \rho_{Z, QCD}(s) \exp\left(-\frac{s}{T^2}\right), \tag{75}$$

$$-\frac{d\Pi_{TW}^-(T^2)}{d(1/T^2)} = -\kappa \frac{d}{d(1/T^2)} \int_{4m_c^2}^{s_0} ds \rho_{X, QCD}(s) \exp\left(-\frac{s}{T^2}\right). \tag{76}$$

Thereafter, we will denote the QCD sum rules in Eqs.(75)-(76) as the QCDSR I, and the QCD sum rules in Eqs.(73)-(74) as the QCDSR II.

On the other hand, if the two-meson scattering states cannot saturate the QCD sum rules, we have to introduce the tetraquark molecular states to saturate the QCD sum rules,

$$\lambda_{Z/X}^2 \exp\left(-\frac{M_{Z/X}^2}{T^2}\right) = \int_{4m_c^2}^{s_0} ds \rho_{Z/Z, QCD}(s) \exp\left(-\frac{s}{T^2}\right), \tag{77}$$

we differentiate Eq.(77) with respect to $\frac{1}{T^2}$, and obtain two QCD sum rules for the masses of the tetraquark molecular states,

$$M_{Z/X}^2 = \frac{-\frac{d}{d(1/T^2)} \int_{4m_c^2}^{s_0} ds \rho_{Z/X, QCD}(s) \exp\left(-\frac{s}{T^2}\right)}{\int_{4m_c^2}^{s_0} ds \rho_{Z/X, QCD}(s) \exp\left(-\frac{s}{T^2}\right)}. \tag{78}$$

In Fig.8, we plot the values of the κ with variations of the Borel parameters T^2 with the continuum threshold parameters $\sqrt{s_0} = 4.40$ GeV and 5.15 GeV for the $\bar{u}c\bar{c}d$ and $\bar{s}c\bar{c}s$ two-meson scattering states, respectively, where we normalize the values of the κ to be 1 at the points $T^2 =$

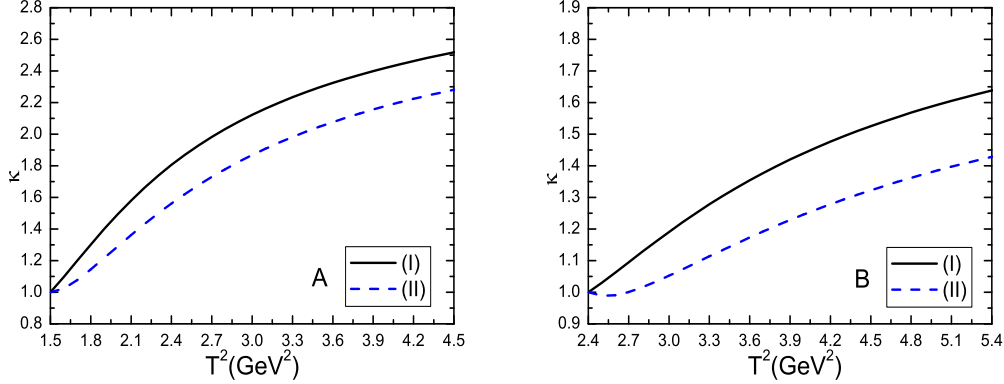


Figure 8: The κ with variations of the Borel parameters T^2 , where the A and B correspond to the $\bar{u}c\bar{c}d$ and $\bar{s}c\bar{c}s$ meson-meson scattering states, respectively, the (I) and (II) correspond to QCDSR I and II, respectively, the κ values are normalized to be 1 for the Borel parameters $T^2 = 1.5 \text{ GeV}^2$ and 2.4 GeV^2 , respectively.

1.5 GeV^2 and 2.4 GeV^2 for the $\bar{u}c\bar{c}d$ and $\bar{s}c\bar{c}s$ two-meson scattering states, respectively. From Fig.8, we can see that the values of the κ increase monotonically and quickly with the increase of the Borel parameters T^2 , no platform appears, which indicates that the QCD sum rules in Eqs.(73)-(74) obtained according to the assertion of Lucha, Melikhov and Sazdjian are unreasonable. Reasonable QCD sum rules lead to platforms flat enough or not flat enough, rather than no evidence of platforms, the two-meson scattering states cannot saturate the QCD sum rules.

We saturate the hadron side of the QCD sum rules with the tetraquark molecular states alone, and study the QCD sum rules shown in Eqs.(77)-(78). In Fig.9, we plot tetraquark molecule masses with variations of the Borel parameters T^2 . From the Fig.9, we observe that there appear Borel platforms in the Borel windows indeed, the relevant results are shown explicitly in Table 1, we adopt the energy scale formula $\mu = \sqrt{M_{X/Z}^2 - 4 \times (1.84 \text{ GeV})^2}$ to choose the best energy scales of the QCD spectral densities. The tetraquark molecular states alone can satisfy the QCD sum rules [345]. We obtain the prediction $M_Z = 3.89 \pm 0.09 \text{ GeV}$ and $M_X = 4.67 \pm 0.08 \text{ GeV}$, which are consistent with the $Z_c(3900)$ observed by the BESIII and Belle collaborations [154, 155] and the $X(4630)$ observed one-year latter by the LHCb collaboration [105]. If we have taken account of the light-flavor $SU(3)$ breaking effects of the energy scale formula, the fit between the theoretical calculation and experimental measurement would be better for the $X(4630)$.

The local currents do suppress but do not forbid the couplings between the four-quark currents and two-meson scattering states, as the overlaps of the wave-functions are very small [352], on the other hand, the quantum field theory does not forbid the couplings between the four-quark currents and two-meson scattering states if they have the same quantum numbers. We study the contributions of the intermediate meson-meson scattering states $D\bar{D}^*$, $J/\psi\pi$, $J/\psi\rho$, etc besides the tetraquark molecular state Z_c to the correlation function $\Pi_{\mu\nu}(p)$ as an example,

$$\Pi_{\mu\nu}(p) = -\frac{\hat{\lambda}_Z^2}{p^2 - \widehat{M}_Z^2 - \Sigma_{D\bar{D}^*}(p^2) - \Sigma_{J/\psi\pi}(p^2) - \Sigma_{J/\psi\rho}(p^2) + \dots} \tilde{g}_{\mu\nu}(p) + \dots, \quad (79)$$

where $\tilde{g}_{\mu\nu}(p) = -g_{\mu\nu} + \frac{p_\mu p_\nu}{p^2}$. We choose the bare quantities $\hat{\lambda}_Z$ and \widehat{M}_Z to absorb the divergences in the self-energies $\Sigma_{D\bar{D}^*}(p^2)$, $\Sigma_{J/\psi\pi}(p^2)$, $\Sigma_{J/\psi\rho}(p^2)$, etc. The renormalized energies satisfy the relation $p^2 - \widehat{M}_Z^2 - \overline{\Sigma}_{D\bar{D}^*}(p^2) - \overline{\Sigma}_{J/\psi\pi}(p^2) - \overline{\Sigma}_{J/\psi\rho}(p^2) + \dots = 0$, where the overlines above the self-energies denote that the divergent terms have been subtracted. As the tetraquark molecular

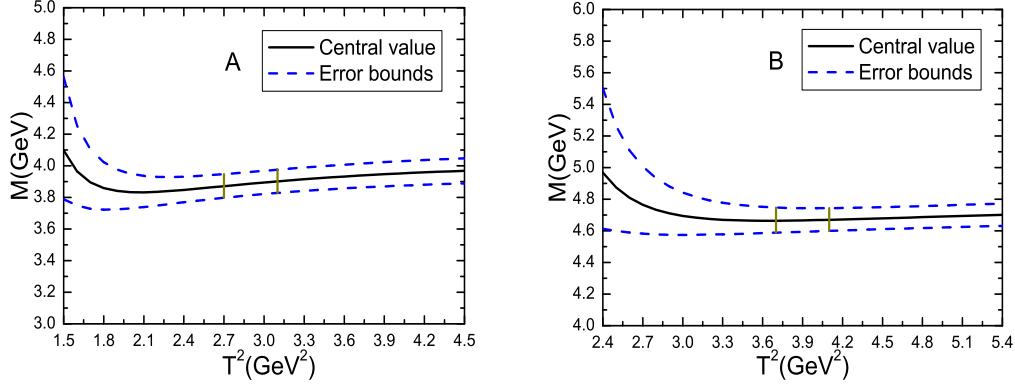


Figure 9: The masses with variations of the Borel parameters T^2 , where the A and B correspond to the $\bar{u}c\bar{c}d$ and $\bar{s}c\bar{c}s$ tetraquark molecular states, respectively, the regions between the two vertical lines are the Borel windows.

state Z_c is unstable, the relation should be modified, $p^2 - M_Z^2 - \text{Re}\bar{\Sigma}_{DD^*}(p^2) - \text{Re}\bar{\Sigma}_{J/\psi\pi}(p^2) - \text{Re}\bar{\Sigma}_{J/\psi\rho}(p^2) + \dots = 0$, and $-\text{Im}\bar{\Sigma}_{DD^*}(p^2) - \text{Im}\bar{\Sigma}_{J/\psi\pi}(p^2) - \text{Im}\bar{\Sigma}_{J/\psi\rho}(p^2) + \dots = \sqrt{p^2}\Gamma(p^2)$. The negative sign in front of the self-energies come from the special definitions in this article, if we redefine the self-energies, $\Sigma(p^2) \rightarrow -\Sigma(p^2)$ in Eq.(79), the negative sign can be removed. The renormalized self-energies contribute a finite imaginary part to modify the dispersion relation,

$$\Pi_{\mu\nu}(p) = -\frac{\lambda_Z^2}{p^2 - M_Z^2 + i\sqrt{p^2}\Gamma(p^2)}\tilde{g}_{\mu\nu}(p) + \dots \quad (80)$$

If we assign the $Z_c(3900)$ to be the $DD^* + D^*\bar{D}$ tetraquark molecular state with the $J^{PC} = 1^{+-}$ [76, 77, 78], the physical width $\Gamma_{Z_c(3900)}(M_Z^2) = (28.2 \pm 2.6)$ MeV from the Particle Data Group [347].

We can take into account the finite width effect by the following simple replacement of the hadronic spectral density,

$$\lambda_Z^2\delta(s - M_Z^2) \rightarrow \lambda_Z^2\frac{1}{\pi}\frac{M_Z\Gamma_Z(s)}{(s - M_Z^2)^2 + M_Z^2\Gamma_Z^2(s)}, \quad (81)$$

where

$$\Gamma_Z(s) = \Gamma_Z\frac{M_Z}{\sqrt{s}}\sqrt{\frac{s - (M_D + M_{D^*})^2}{M_Z^2 - (M_D + M_{D^*})^2}}. \quad (82)$$

Then the hadron sides of the QCD sum rules in Eq.(77) and Eq.(78) undergo the following changes,

$$\begin{aligned} \lambda_Z^2\exp\left(-\frac{M_Z^2}{T^2}\right) &\rightarrow \lambda_Z^2\int_{(m_D+m_{D^*})^2}^{s_0} ds\frac{1}{\pi}\frac{M_Z\Gamma_Z(s)}{(s - M_Z^2)^2 + M_Z^2\Gamma_Z^2(s)}\exp\left(-\frac{s}{T^2}\right), \\ &= (0.78 \sim 0.79)\lambda_Z^2\exp\left(-\frac{M_Z^2}{T^2}\right), \end{aligned} \quad (83)$$

$$\begin{aligned} \lambda_Z^2M_Z^2\exp\left(-\frac{M_Z^2}{T^2}\right) &\rightarrow \lambda_Z^2\int_{(m_D+m_{D^*})^2}^{s_0} ds s\frac{1}{\pi}\frac{M_Z\Gamma_Z(s)}{(s - M_Z^2)^2 + M_Z^2\Gamma_Z^2(s)}\exp\left(-\frac{s}{T^2}\right), \\ &= (0.80 \sim 0.81)\lambda_Z^2M_Z^2\exp\left(-\frac{M_Z^2}{T^2}\right), \end{aligned} \quad (84)$$

J^{PC}	$T^2(\text{GeV}^2)$	$\sqrt{s_0}(\text{GeV})$	$\mu(\text{GeV})$	pole	$M(\text{GeV})$	$\lambda(10^{-2}\text{GeV}^5)$
$1^{+-}(\bar{u}c\bar{c}d)$	2.7 – 3.1	4.40 ± 0.10	1.3	(40 – 63)%	3.89 ± 0.09	1.72 ± 0.30
$1^{-+}(\bar{s}c\bar{c}s)$	3.7 – 4.1	5.15 ± 0.10	2.9	(42 – 60)%	4.67 ± 0.08	6.87 ± 0.84

Table 1: The Borel windows, continuum threshold parameters, energy scales of the QCD spectral densities, pole contributions, masses and pole residues of the $\bar{u}c\bar{c}d$ and $\bar{s}c\bar{c}s$ tetraquark molecular states.

with the value $\sqrt{s_0} = 4.40 \text{ GeV}$. We can absorb the numerical factors $0.78 \sim 0.79$ and $0.80 \sim 0.81$ into the pole residue with the simple replacement $\lambda_Z \rightarrow 0.89\lambda_Z$ safely, the intermediate meson-loops cannot affect the mass M_Z significantly, but affect the pole residue remarkably, which are consistent with the fact that we obtain the masses of the tetraquark molecular states from a fraction, see Eq.(78).

We obtain the conclusion confidently that it is reliable to study the multi-quark states with the QCD sum rules, the contaminations from the two-particle scattering states play a tiny role. [345].

4 Energy scale dependence of the QCD sum rules

In calculating the Feynman diagrams, we usually adopt the dimensional regularization to regularize the divergences, and resort to wave-function, quark-mass and current renormalizations to absorb the ultraviolet divergences, and use the vacuum condensate redefinitions to absorb the infrared divergences. Thus, the correlation functions $\Pi(p^2)$ are free of divergences. And we expect to calculate the $\Pi(p^2)$ at any energy scale μ at which perturbative calculations are feasible, and the physical quantities are independent on the specified energy scale μ . Roughly speaking, the correlation functions $\Pi(p^2)$ are independent on the energy scale approximately,

$$\frac{d}{d\mu}\Pi(p^2) = 0, \quad (85)$$

at least the bare $\Pi(p^2)$ are independent on the energy scale.

We write the correlation functions $\Pi(p^2)$ for the hidden-charm (or hidden-bottom) four-quark currents, the most commonly chosen currents in studying the X , Y and Z states, in the Källén-Lehmann representation,

$$\Pi(p^2) = \int_{4m_Q^2(\mu)}^{s_0} ds \frac{\rho_{QCD}(s, \mu)}{s - p^2} + \int_{s_0}^{\infty} ds \frac{\rho_{QCD}(s, \mu)}{s - p^2}. \quad (86)$$

In fact, there are subtraction terms neglected at the right side of Eq.(86), which could be deleted after performing the Borel transformation. The $\Pi(p^2)$ should be independent on the energy scale we adopt to perform the operator product expansion, but which does not mean

$$\frac{d}{d\mu} \int_{4m_Q^2(\mu)}^{s_0} ds \frac{\rho_{QCD}(s, \mu)}{s - p^2} \rightarrow 0, \quad (87)$$

due to the two features inherited from the QCD sum rules:

- Perturbative corrections are neglected, even in the QCD sum rules for the traditional mesons, we cannot take into account the radiative corrections up to arbitrary orders, for example, we only have calculated the radiative corrections up to the order $\mathcal{O}(\alpha_s^2)$ for the pseudoscalar D/B mesons up to now [355, 356, 357]. The higher dimensional vacuum condensates are factorized into lower dimensional ones based on the vacuum saturation, for example,

$$\langle \bar{\psi}\Gamma\psi\bar{\psi}\Gamma\psi \rangle = \frac{1}{144} \langle \bar{\psi}\psi \rangle^2 [\text{Tr}(\Gamma)\text{Tr}(\Gamma) - \text{Tr}(\Gamma\Gamma)], \quad (88)$$

where $\psi = u, d$ or s , $\text{Tr} = \text{Tr}_D \text{Tr}_C$, the subscripts denote the Dirac spinor space and color space, respectively, therefore the energy scale dependence of the higher dimensional vacuum condensates is modified.

- Truncations s_0 which are physical quantities determined by the experimental data set in, the correlations between the thresholds $4m_Q^2(\mu)$ and continuum thresholds s_0 are unknown. Quark-hadron duality is just an assumption.

After performing the Borel transformation, we obtain the integrals

$$\int_{4m_Q^2(\mu)}^{s_0} ds \rho_{QCD}(s, \mu) \exp\left(-\frac{s}{T^2}\right), \quad (89)$$

which are sensitive to the Q -quark mass $m_Q(\mu)$, in other words, the energy scale μ . Variations of the energy scale μ can lead to changes of integral ranges $4m_Q^2(\mu) - s_0$ of the variable ds besides the QCD spectral densities $\rho_{QCD}(s, \mu)$, therefore changes of the Borel windows and predicted masses and pole residues. The strong fine-structure $\alpha_s = \frac{g_s^2}{4\pi}$ appear even in the tree-level,

$$\langle \bar{q} \gamma_\mu t^a q D_\eta g_s G_{\lambda\tau}^a \rangle = \frac{g_{\eta\lambda} g_{\mu\tau} - g_{\eta\tau} g_{\mu\lambda}}{27} \frac{\alpha_s}{4\pi} \langle \bar{q} q \rangle^2, \quad (90)$$

where $t^a = \frac{\lambda^a}{2}$. Thus we have to deal with the energy scale dependence of the QCD sum rules.

Let us take a short digression and perform some phenomenological analysis. We can describe the heavy four-quark systems $Q\bar{Q}q\bar{q}$ by a double-well potential with two light quarks $q\bar{q}$ lying in the two wells, respectively. In the heavy quark limit, the Q -quark serves as a static well potential and attracts with the light quark q to form a heavy diquark \mathcal{D}_{qQ}^i in color antitriplet,

$$q + Q \rightarrow \mathcal{D}_{qQ}^i, \quad (91)$$

or attracts with the light antiquark \bar{q} to form a meson-like color-singlet cluster (meson-like color-octet cluster),

$$\bar{q} + Q \rightarrow \bar{q}Q (\bar{q}\lambda^a Q), \quad (92)$$

the \bar{Q} -quark serves as another static well potential and attracts with the light antiquark \bar{q} to form a heavy antidiquark $\mathcal{D}_{\bar{q}\bar{Q}}^i$ in color triplet,

$$\bar{q} + \bar{Q} \rightarrow \mathcal{D}_{\bar{q}\bar{Q}}^i, \quad (93)$$

or attracts with the light quark q to form a heavy meson-like color-singlet cluster (meson-like color-octet-cluster),

$$q + \bar{Q} \rightarrow \bar{Q}q (\bar{Q}\lambda^a q). \quad (94)$$

Then

$$\begin{aligned} \mathcal{D}_{qQ}^i + \mathcal{D}_{\bar{q}\bar{Q}}^i &\rightarrow \mathbf{\bar{3}\bar{3}} - \text{type tetraquark states,} \\ \bar{q}Q + \bar{Q}q &\rightarrow \mathbf{11} - \text{type tetraquark states,} \\ \bar{q}\lambda^a Q + \bar{Q}\lambda^a q &\rightarrow \mathbf{88} - \text{type tetraquark states,} \end{aligned} \quad (95)$$

the two heavy quarks Q and \bar{Q} stabilize the four-quark systems $q\bar{q}Q\bar{Q}$, just as in the case of the $(\mu^- e^+)(\mu^+ e^-)$ molecule in QED [53].

We can also describe the hidden-charm (or hidden-bottom) five-quark systems $qq_1q_2Q\bar{Q}$ by a double-well potential. In the heavy quark limit, the Q -quark (\bar{Q} -quark) serves as a static well potential, the diquark $\mathcal{D}_{q_1q_2}^j$ and quark q lie in the two wells, respectively,

$$\begin{aligned} q_1 + q_2 + \bar{Q} &\rightarrow \mathcal{D}_{q_1q_2}^j + \bar{Q}^k \rightarrow \mathcal{T}_{q_1q_2\bar{Q}}^i, \\ q + Q &\rightarrow \mathcal{D}_{qQ}^i, \end{aligned} \quad (96)$$

or

$$\begin{aligned} q_1 + q_2 + Q &\rightarrow \mathcal{D}_{q_1 q_2}^j + Q^j \rightarrow q_1 q_2 Q, \\ q + \bar{Q} &\rightarrow q\bar{Q}, \end{aligned} \quad (97)$$

where the $\mathcal{T}_{q_1 q_2 \bar{Q}}^i$ denotes the heavy triquark in the color triplet. Then

$$\begin{aligned} \mathcal{D}_{qQ}^i + \mathcal{T}_{q_1 q_2 \bar{Q}}^i &\rightarrow \bar{\mathbf{3}}\bar{\mathbf{3}}\bar{\mathbf{3}} - \text{type pentaquark states}, \\ q_1 q_2 Q + \bar{Q}q &\rightarrow \mathbf{11} - \text{type pentaquark states}, \end{aligned} \quad (98)$$

Now we can see clearly that the heavy tetraquark states are characterized by the effective heavy quark masses \mathbb{M}_Q (or constituent quark masses) and the virtuality $V = \sqrt{M_{X/Y/Z}^2 - (2\mathbb{M}_Q)^2}$ (or bound energy not as robust) [76, 358, 359, 360].

In summary, the QCD sum rules have three typical energy scales μ^2 , T^2 , V^2 . It is natural to set the energy scale as,

$$\mu^2 = V^2 = \mathcal{O}(T^2), \quad (99)$$

and we obtain the energy scale formula [360],

$$\mu = \sqrt{M_{X/Y/Z/P}^2 - (2\mathbb{M}_Q)^2}, \quad (100)$$

which works very well for the tetraquark states and pentaquark states. It can improve the convergence of the operator product expansion remarkably and enhance the pole contributions remarkably.

We usually set the small u and d quark masses to be zero, and take account of the light-flavor $SU(3)$ breaking effects by introducing an effective s -quark mass \mathbb{M}_s , thus we reach the modified energy scale formula,

$$\mu = \sqrt{M_{X/Y/Z}^2 - (2\mathbb{M}_Q)^2 - \kappa \mathbb{M}_s}, \quad (101)$$

to choose the suitable energy scales of the QCD spectral densities [57, 77, 78, 164, 361], where the $\kappa = 0, 1$ and 2 denote the numbers of the s -quarks, the \mathbb{M}_Q and \mathbb{M}_s have universal values to be commonly used elsewhere.

We can rewrite the energy scale formula in Eq.(100) in the following form,

$$M_{X/Y/Z/P}^2 = \mu^2 + \text{Constants}, \quad (102)$$

where the Constants have the values $4\mathbb{M}_Q^2$ [362]. As we cannot obtain energy scale independent QCD sum rules, we conjecture that the predicted multi-quark masses and the pertinent energy scales of the QCD spectral densities have a Regge-trajectory-like relation, see Eq.(102), where the Constants are free parameters and fitted by the QCD sum rules. Direct calculations have proven that the Constants have universal values and work well. We take account of the light-flavor $SU(3)$ breaking effects, write down the modified energy scale formula [353],

$$M_{X/Y/Z/P}^2 = (\mu + \kappa \mathbb{M}_s)^2 + \text{Constants}. \quad (103)$$

In Ref.[56], we take the $X(3872)$ and $Z_c(3900)$ as the hidden-charm tetraquark with the $J^{PC} = 1^{++}$ and 1^{+-} , respectively, and explore the energy scale dependence of the QCD sum rules for the exotic states for the first time. In Fig.10, we plot the mass of the $Z_c(3900)$ with variations of the Borel parameter T^2 and energy scale μ for the threshold parameter $\sqrt{s_0} = 4.4 \text{ GeV}$. From the figure, we can see that the mass decreases monotonously with increase of the energy scale. The energy scale $\mu = 1.4 \text{ GeV}$ is the lowest energy scale to reproduce the experimental data [154, 155].

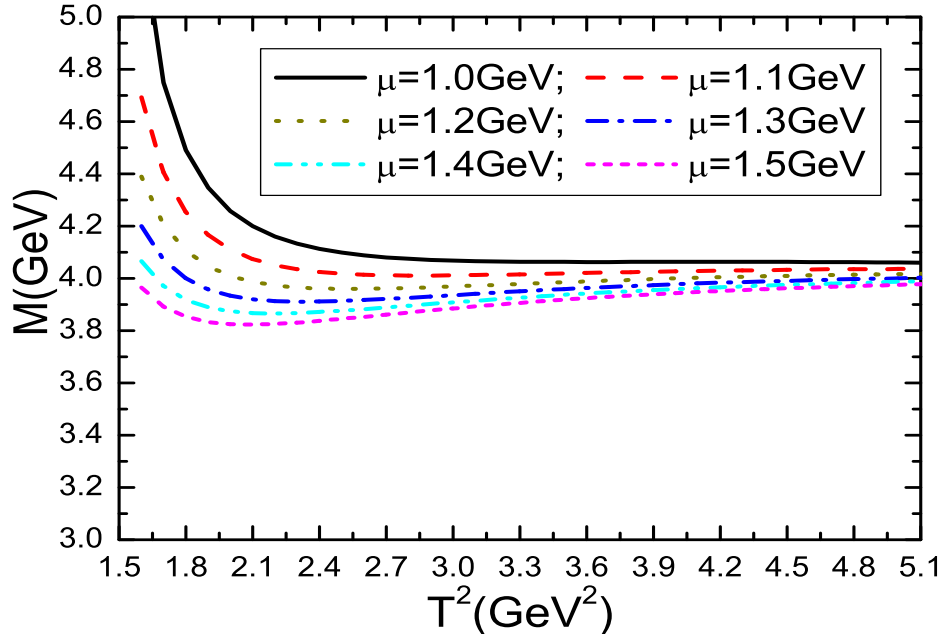


Figure 10: The mass with variation of the Borel parameter T^2 and energy scale μ for the $Z_c(3900)$.

There are three schemes to choose the input parameters at the QCD side of the QCD sum rules:

Scheme I. We take the energy scale formula and its modifications, see Eqs.(100)-(101), to choose the energy scales of the QCD spectral densities in a consistent way.

Scheme II. We take the \overline{MS} (modified-minimal-subtraction) masses for the heavy quarks $m_Q(m_Q)$, and take the light quark masses and vacuum condensates at the energy scale $\mu = 1$ GeV.

Scheme III. We take all the input parameters at the energy scale $\mu = 1$ GeV.

The **Scheme II** is taken in most QCD sum rules [42, 43, 54, 363, 364, 365, 366, 367, 368, 369, 370, 371, 372, 373, 374, 375, 376, 377, 378, 379, 380, 381, 382, 383, 384, 385, 386, 387, 388, 389, 390, 391, 392, 393, 394, 395, 396, 397, 398] ([399, 400, 401, 402, 403, 404, 405, 406, 407, 408, 409]), where the \overline{MS} masse $m_Q(m_Q)$ are smaller than (or equal to) the values from the Particle Data Group (with much smaller pole contributions) [91].

The **Scheme III** was taken in early works of Wang and his collaborators in 2009-2011 [410, 411, 412, 413, 414, 415, 416, 417, 418, 419, 420, 421], where many elegant four-quark currents were constructed originally.

In Ref.[422], we study the pentaquark molecular states in the three schemes in details and examine their advantages and shortcomings, in **Scheme I** and **III**, we truncate the operator product expansion up to the vacuum condensates of $D = 13$, while in **Scheme II**, we truncate the operator product expansion up to the vacuum condensates of $D = 10$, which is commonly adopted in this case.

We write down the correlation functions $\Pi(p)$, $\Pi_{\mu\nu}(p)$ and $\Pi_{\mu\nu\alpha\beta}(p)$ firstly,

$$\begin{aligned}\Pi(p) &= i \int d^4x e^{ip \cdot x} \langle 0 | T \{ J(x) \bar{J}(0) \} | 0 \rangle, \\ \Pi_{\mu\nu}(p) &= i \int d^4x e^{ip \cdot x} \langle 0 | T \{ J_\mu(x) \bar{J}_\nu(0) \} | 0 \rangle, \\ \Pi_{\mu\nu\alpha\beta}(p) &= i \int d^4x e^{ip \cdot x} \langle 0 | T \{ J_{\mu\nu}(x) \bar{J}_{\alpha\beta}(0) \} | 0 \rangle,\end{aligned}\quad (104)$$

where the currents $J(x) = J^{\bar{D}\Sigma_c}(x)$, $J_\mu(x) = J_\mu^{\bar{D}\Sigma_c^*}(x)$, $J_\mu^{\bar{D}^*\Sigma_c}(x)$, $J_{\mu\nu}(x) = J_{\mu\nu}^{\bar{D}^*\Sigma_c^*}(x)$,

$$\begin{aligned}J^{\bar{D}\Sigma_c}(x) &= \bar{c}(x) i \gamma_5 u(x) \varepsilon^{ijk} u_i^T(x) C \gamma_\alpha d_j(x) \gamma^\alpha \gamma_5 c_k(x), \\ J_\mu^{\bar{D}\Sigma_c^*}(x) &= \bar{c}(x) i \gamma_5 u(x) \varepsilon^{ijk} u_i^T(x) C \gamma_\mu d_j(x) c_k(x), \\ J_\mu^{\bar{D}^*\Sigma_c}(x) &= \bar{c}(x) \gamma_\mu u(x) \varepsilon^{ijk} u_i^T(x) C \gamma_\alpha d_j(x) \gamma^\alpha \gamma_5 c_k(x), \\ J_{\mu\nu}^{\bar{D}^*\Sigma_c^*}(x) &= \bar{c}(x) \gamma_\mu u(x) \varepsilon^{ijk} u_i^T(x) C \gamma_\nu d_j(x) c_k(x) + (\mu \leftrightarrow \nu).\end{aligned}\quad (105)$$

We separate the contributions for the molecular states with the $J^P = \frac{1}{2}^\pm, \frac{3}{2}^\pm$ and $\frac{5}{2}^\pm$ unambiguously, then we introduce the weight functions $\sqrt{s} \exp(-\frac{s}{T^2})$ and $\exp(-\frac{s}{T^2})$ to obtain the QCD sum rules at the hadron side,

$$\int_{4m_c^2}^{s_0} ds [\sqrt{s} \rho_{j,H}^1(s) + \rho_{j,H}^0(s)] \exp\left(-\frac{s}{T^2}\right) = 2M_- \lambda_j^-^2 \exp\left(-\frac{M_-^2}{T^2}\right), \quad (106)$$

$$\int_{4m_c^2}^{s_0} ds [\sqrt{s} \rho_{j,H}^1(s) - \rho_{j,H}^0(s)] \exp\left(-\frac{s}{T^2}\right) = 2M_+ \lambda_j^+^2 \exp\left(-\frac{M_+^2}{T^2}\right), \quad (107)$$

where the s_0 are the continuum threshold parameters and the T^2 are the Borel parameters, the $\rho_{j,H}^1(s)$ and $\rho_{j,H}^0(s)$ with the $j = \frac{1}{2}, \frac{3}{2}$ and $\frac{5}{2}$ are hadronic spectral densities, the λ_j^\pm are the pole residues.

We perform the operator product expansion to obtain the analytical QCD spectral densities $\rho_{j,QCD}^1(s)$ and $\rho_{j,QCD}^0(s)$ through dispersion relation, then we take the quark-hadron duality below the continuum thresholds s_0 and introduce the weight functions $\sqrt{s} \exp(-\frac{s}{T^2})$ and $\exp(-\frac{s}{T^2})$ to obtain the QCD sum rules:

$$2M_- \lambda_j^-^2 \exp\left(-\frac{M_-^2}{T^2}\right) = \int_{4m_c^2}^{s_0} ds [\sqrt{s} \rho_{j,QCD}^1(s) + \rho_{j,QCD}^0(s)] \exp\left(-\frac{s}{T^2}\right). \quad (108)$$

For the technical details, one can consult Ref.[422] or Sect.9.1.

We differentiate Eq.(108) with respect to $\tau = \frac{1}{T^2}$, then eliminate the pole residues to obtain the molecular masses,

$$M_-^2 = \frac{-\frac{d}{d\tau} \int_{4m_c^2}^{s_0} ds [\sqrt{s} \rho_{QCD}^1(s) + \rho_{QCD}^0(s)] \exp(-\tau s)}{\int_{4m_c^2}^{s_0} ds [\sqrt{s} \rho_{QCD}^1(s) + \rho_{QCD}^0(s)] \exp(-\tau s)}, \quad (109)$$

where $\rho_{QCD}^1(s) = \rho_{j,QCD}^1(s)$ and $\rho_{QCD}^0(s) = \rho_{j,QCD}^0(s)$.

We show the Borel windows T^2 , continuum threshold parameters s_0 , energy scales of the QCD spectral densities and pole contributions of the ground states explicitly in Table 2. In the **Scheme III**, the pole contributions are less than 25%, which are too small, and the **Scheme III** could be abandoned. On the other hand, the convergent behaviors of the operator product expansion have relation **Scheme I** > **Scheme II** > **Scheme III**.

	J^P	D	$\mu(\text{GeV})$	$T^2(\text{GeV}^2)$	$s_0(\text{GeV}^2)$	pole
$\bar{D}^0 \Sigma_c^+(2455)$	$\frac{1}{2}^-$	13	2.2	3.1 – 3.5	25.0 ± 1.0	(41 – 62)%
		10	1.0	2.7 – 3.1	24.5 ± 1.0	(38 – 63)%
		13	1.0	3.4 – 4.2	21.5 ± 1.0	(7 – 24)%
$\bar{D}^0 \Sigma_c^{*+}(2520)$	$\frac{3}{2}^-$	13	2.4	3.3 – 3.7	25.5 ± 1.0	(39 – 59)%
		10	1.0	2.8 – 3.2	25.5 ± 1.0	(40 – 64)%
		13	1.0	3.5 – 4.3	22.0 ± 1.0	(7 – 23)%
$\bar{D}^{*0} \Sigma_c^+(2455)$	$\frac{3}{2}^-$	13	2.5	3.3 – 3.7	26.5 ± 1.0	(40 – 60)%
		10	1.0	2.8 – 3.2	26.5 ± 1.0	(40 – 65)%
		13	1.0	3.7 – 4.6	23.0 ± 1.0	(5 – 19)%
$\bar{D}^{*0} \Sigma_c^{*+}(2520)$	$\frac{5}{2}^-$	13	2.6	3.4 – 3.8	27.0 ± 1.0	(39 – 59)%
		10	1.0	3.0 – 3.4	27.5 ± 1.0	(39 – 62)%
		13	1.0	3.5 – 4.4	23.5 ± 1.0	(7 – 25)%

Table 2: The truncations of the operator product expansion D , energy scales μ , Borel parameters T^2 , continuum threshold parameters s_0 and pole contributions for the hidden-charm pentaquark molecular states, where the $\mu = 1 \text{ GeV}$ denote the energy scale of the vacuum condensates, and the data are listed in **Scheme I**, **II**, **III** sequentially.

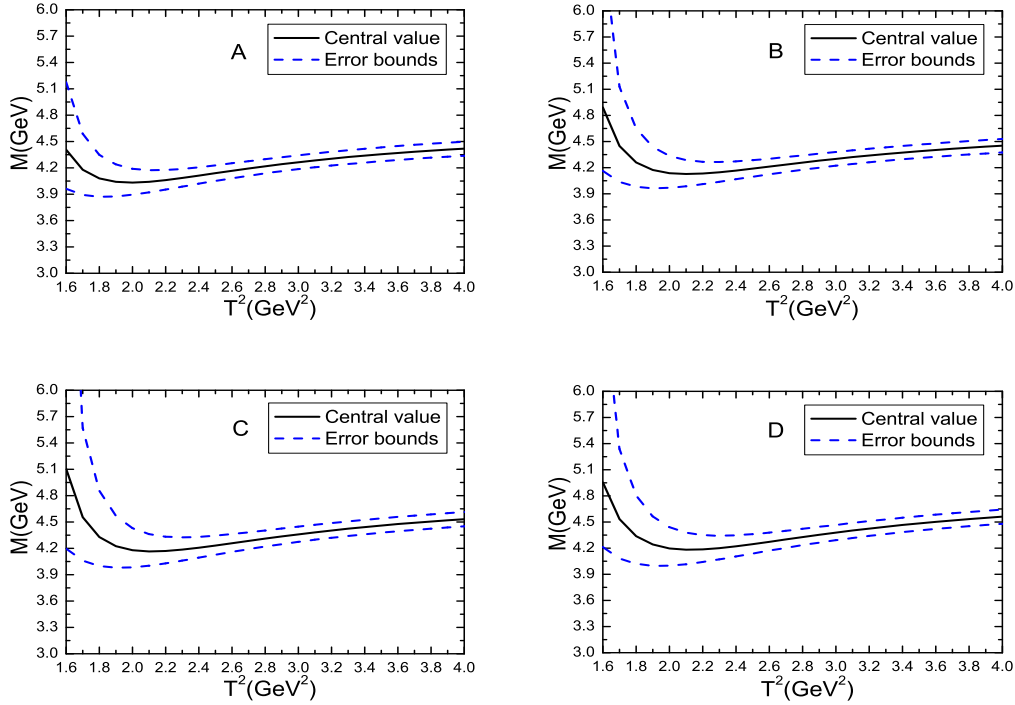


Figure 11: The masses of the molecular states with variations of the Borel parameter T^2 in the **Scheme I**, where the A , B , C and D denote the molecular states $\bar{D}\Sigma_c$, $\bar{D}\Sigma_c^*$, $\bar{D}^*\Sigma_c$ and $\bar{D}^*\Sigma_c^*$, respectively.

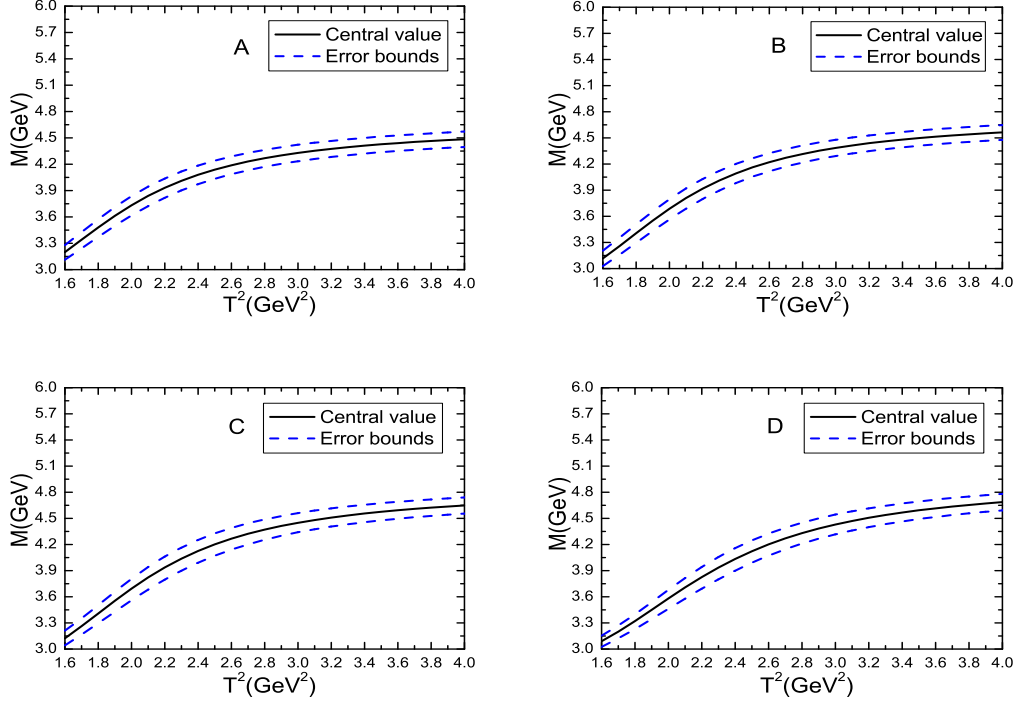


Figure 12: The masses of the molecular states with variations of the Borel parameter T^2 in the **Scheme II**, where the A , B , C and D denote the molecular states $\bar{D}\Sigma_c$, $\bar{D}\Sigma_c^*$, $\bar{D}^*\Sigma_c$ and $\bar{D}^*\Sigma_c^*$, respectively.

	J^P	D	$\mu(\text{GeV})$	$M(\text{GeV})$	$\lambda(10^{-3}\text{GeV}^6)$	Thresholds (MeV)
$\bar{D}^0 \Sigma_c^+(2455)$	$\frac{1}{2}^-$	13	2.2	$4.32^{+0.11}_{-0.11}$	$1.95^{+0.37}_{-0.33}$	4318
		10	1.0	$4.30^{+0.14}_{-0.17}$	$1.00^{+0.27}_{-0.24}$	
		13	1.0	$4.30^{+0.09}_{-0.10}$	$0.77^{+0.19}_{-0.15}$	
$\bar{D}^0 \Sigma_c^+(2520)$	$\frac{3}{2}^-$	13	2.4	$4.39^{+0.10}_{-0.11}$	$1.23^{+0.21}_{-0.20}$	4382
		10	1.0	$4.39^{+0.14}_{-0.17}$	$0.64^{+0.16}_{-0.15}$	
		13	1.0	$4.38^{+0.10}_{-0.09}$	$0.47^{+0.11}_{-0.09}$	
$\bar{D}^{*0} \Sigma_c^+(2455)$	$\frac{3}{2}^-$	13	2.5	$4.46^{+0.11}_{-0.12}$	$2.31^{+0.41}_{-0.38}$	4460
		10	1.0	$4.45^{+0.16}_{-0.20}$	$1.15^{+0.31}_{-0.29}$	
		13	1.0	$4.48^{+0.11}_{-0.10}$	$0.88^{+0.19}_{-0.18}$	
$\bar{D}^{*0} \Sigma_c^+(2520)$	$\frac{5}{2}^-$	13	2.6	$4.50^{+0.12}_{-0.12}$	$1.74^{+0.31}_{-0.28}$	4524
		10	1.0	$4.51^{+0.16}_{-0.19}$	$0.93^{+0.25}_{-0.22}$	
		13	1.0	$4.51^{+0.11}_{-0.10}$	$0.66^{+0.15}_{-0.12}$	

Table 3: The masses and pole residues of the hidden-charm pentaquark molecular states, where the data are listed in **Scheme I, II, III** sequentially.

At last, we take into account all uncertainties of the input parameters, and obtain the masses and pole residues of the molecular states, which are shown explicitly in Table 3 and Figs.11-12.

In Figs.11-12, we plot the masses at much larger ranges of the Borel parameters than the Borel windows. The predicted masses in the **Scheme I** decrease monotonously and quickly with increase of the Borel parameters at the region $T^2 \leq 2.0 \text{ GeV}^2$, then reach small platforms and increase slowly with increase of the Borel parameters. While the predicted masses in the **Scheme II** increase monotonously and quickly with increase of the Borel parameters at the region $T^2 < 2.6 \text{ GeV}^2$, then increase slowly with increase of the Borel parameters. It is obvious that the flatness of the platforms have relation **Scheme I** > **Scheme II**.

Both the predictions in the **Scheme I** and **II** support assigning the $P_c(4312)$ as the $\bar{D}\Sigma_c$ molecular state with the $J^P = \frac{1}{2}^-$, assigning the $P_c(4380)$ as the $\bar{D}\Sigma_c^*$ molecular state with the $J^P = \frac{3}{2}^-$, assigning the $P_c(4440/4457)$ as the $\bar{D}^*\Sigma_c$ molecular state with the $J^P = \frac{3}{2}^-$ or the $\bar{D}^*\Sigma_c^*$ molecular state with the $J^P = \frac{5}{2}^-$. However, if we take account of the vacuum condensates of the dimensions of $D = 11$ and 12 in the **Scheme II**, we would obtain a mass about 200 MeV larger than the corresponding one given in Table 3, so we prefer the **Scheme I** [422].

5 $\bar{\mathbf{3}}\mathbf{3}$ type hidden-heavy tetraquark states

The scattering amplitude for one-gluon exchange is proportional to,

$$\left(\frac{\lambda^a}{2}\right)_{ij} \left(\frac{\lambda^a}{2}\right)_{kl} = -\frac{1}{3}(\delta_{ij}\delta_{kl} - \delta_{il}\delta_{kj}) + \frac{1}{6}(\delta_{ij}\delta_{kl} + \delta_{il}\delta_{kj}), \quad (110)$$

the negative (positive) sign in front of the antisymmetric antitriplet $\bar{\mathbf{3}}$ (symmetric sextet $\mathbf{6}$) indicates the interaction is attractive (repulsive), which favors (disfavors) formation of the diquarks in color $\bar{\mathbf{3}}$ ($\mathbf{6}$). We usually construct the $\bar{\mathbf{3}}\mathbf{3}$ type color-singlet four-quark currents $J_{\bar{\mathbf{3}}\mathbf{3}}$ to interpolate the tetraquark states,

$$J_{\bar{\mathbf{3}}\mathbf{3}} = \varepsilon^{kij}\varepsilon^{kmn}q_i^T C\Gamma q'_j \bar{q}_m \Gamma' C\bar{q}_n'^T, \quad (111)$$

where the q and q' are the quarks, the Γ and Γ' are the Dirac γ -matrixes. The color factor has the relation,

$$\varepsilon^{kij}\varepsilon^{kmn} = \delta_{im}\delta_{jn} - \delta_{in}\delta_{jm}. \quad (112)$$

With the simple replacement,

$$\delta_{im}\delta_{jn} - \delta_{in}\delta_{jm} \rightarrow \delta_{im}\delta_{jn} + \delta_{in}\delta_{jm}, \quad (113)$$

we obtain the corresponding $\mathbf{6}\bar{\mathbf{6}}$ type currents $J_{\mathbf{6}\bar{\mathbf{6}}}$,

$$J_{\mathbf{6}\bar{\mathbf{6}}} = q_i^T C\Gamma q'_j \bar{q}_i \Gamma' C\bar{q}_j'^T + q_i^T C\Gamma q'_j \bar{q}_j \Gamma' C\bar{q}_i'^T. \quad (114)$$

If the $J_{\mathbf{6}\bar{\mathbf{6}}}$ type currents satisfy the Fermi-Dirac statistics, the quantum field theory does not forbid their existence. In fact, in the potential quark models, we usually take both the $\bar{\mathbf{3}}\mathbf{3}$ and $\mathbf{6}\bar{\mathbf{6}}$ diquark configurations, see Sect.2.5. The $\mathbf{6}\bar{\mathbf{6}}$ type currents are also widely used in literatures [30, 38, 111, 124, 177, 423, 424, 425, 426].

Or we construct the $\mathbf{8}\mathbf{8}$ type currents directly to interpolate the exotic states [392, 396, 427, 428, 429]. In Ref.[429], we assume the $Z_c(4200)$ as a color octet-octet type axial-vector molecule-like state, and construct the color octet-octet type axial-vector current to study its mass and width with the QCD sum rules, the numerical results support assigning the $Z_c(4200)$ to be the color octet-octet type molecule-like state with the $J^{PC} = 1^{+-}$. And we discuss the possible assignments of the $Z_c(3900)$, $Z_c(4200)$ and $Z(4430)$ as the $\bar{\mathbf{3}}\mathbf{3}$ type tetraquark states with $J^{PC} = 1^{+-}$.

5.1 Tetraquark states with positive parity

The attractive interactions favor formation of the diquarks in the color antitriplet, flavor antitriplet and spin singlet [269], while the most favored configurations are the scalar and axialvector diquark states [430, 431, 432, 433, 434, 435, 436]. The QCD sum rules indicate that the heavy-light scalar and axialvector diquark states have almost degenerate masses [430, 431, 432], while the masses of the light axialvector diquark states lie about (150–200) MeV above that of the light scalar diquark states [433, 434, 435, 436], if they have the same valence quarks.

The diquarks $\varepsilon^{ijk} q_j^T C \Gamma q'_k$ in the $\mathbf{\bar{3}}$ have five structures in the Dirac spinor space, where $C\Gamma = C\gamma_5, C, C\gamma_\mu\gamma_5, C\gamma_\mu$ and $C\sigma_{\mu\nu}$ for the scalar, pseudoscalar, vector, axialvector and tensor diquarks, respectively. In the non-relativistic quark model, a P-wave changes the parity by contributing a factor $(-)^L = -$ with the angular momentum $L = 1$. The $C\gamma_5$ and $C\gamma_\mu$ diquark states have the spin-parity $J^P = 0^+$ and 1^+ , respectively, the corresponding C and $C\gamma_\mu\gamma_5$ diquark states have the spin-parity $J^P = 0^-$ and 1^- , respectively, the effects of the P-waves are embodied in the underlined γ_5 in the $C\gamma_5\gamma_5$ and $C\gamma_\mu\gamma_5$. The tensor diquark states have both the $J^P = 1^+$ and 1^- components, we project out the 1^+ and 1^- components explicitly, and introduce the symbols \tilde{A} and \tilde{V} to represent them respectively. We would like to give an example on the heavy-light tensor diquarks to illustrate how to perform the projection.

Under parity transformation \hat{P} , the tensor diquarks have the properties,

$$\begin{aligned}\hat{P}\varepsilon^{ijk} q_j^T(x) C\sigma_{\mu\nu}\gamma_5 Q_k(x) \hat{P}^{-1} &= \varepsilon^{ijk} q_j^T(\tilde{x}) C\sigma^{\mu\nu}\gamma_5 Q_k(\tilde{x}), \\ \hat{P}\varepsilon^{ijk} q_j^T(x) C\sigma_{\mu\nu} Q_k(x) \hat{P}^{-1} &= -\varepsilon^{ijk} q_j^T(\tilde{x}) C\sigma^{\mu\nu} Q_k(\tilde{x}),\end{aligned}\quad (115)$$

where the four vectors $x^\mu = (t, \vec{x})$ and $\tilde{x}^\mu = (t, -\vec{x})$. We introduce the four vector $t^\mu = (1, \vec{0})$ and project out the 1^+ and 1^- components explicitly [437],

$$\begin{aligned}\hat{P}\varepsilon^{ijk} q_j^T(x) C\sigma_{\mu\nu}^t \gamma_5 Q_k(x) \hat{P}^{-1} &= +\varepsilon^{ijk} q_j^T(\tilde{x}) C\sigma_{\mu\nu}^t \gamma_5 Q_k(\tilde{x}), \\ \hat{P}\varepsilon^{ijk} q_j^T(x) C\sigma_{\mu\nu}^v \gamma_5 Q_k(x) \hat{P}^{-1} &= -\varepsilon^{ijk} q_j^T(\tilde{x}) C\sigma_{\mu\nu}^v \gamma_5 Q_k(\tilde{x}), \\ \hat{P}\varepsilon^{ijk} q_j^T(x) C\sigma_{\mu\nu}^v Q_k(x) \hat{P}^{-1} &= +\varepsilon^{ijk} q_j^T(\tilde{x}) C\sigma_{\mu\nu}^v Q_k(\tilde{x}), \\ \hat{P}\varepsilon^{ijk} q_j^T(x) C\sigma_{\mu\nu}^t Q_k(x) \hat{P}^{-1} &= -\varepsilon^{ijk} q_j^T(\tilde{x}) C\sigma_{\mu\nu}^t Q_k(\tilde{x}),\end{aligned}\quad (116)$$

where $\sigma_{\mu\nu}^t = \frac{i}{2}[\gamma_\mu^t, \gamma_\nu^t]$, $\sigma_{\mu\nu}^v = \frac{i}{2}[\gamma_\mu^v, \gamma_\nu^v]$, $\gamma_\mu^v = \gamma \cdot t t_\mu$, $\gamma_\mu^t = \gamma_\mu - \gamma \cdot t t_\mu$. We can also introduce the P-wave explicitly in the $C\gamma_5$ and $C\gamma_\mu$ diquarks and obtain the vector diquarks $\varepsilon^{ijk} q_j^T C\gamma_5 \overleftrightarrow{\partial}_\mu q'_k$ or tensor diquarks $\varepsilon^{ijk} q_j^T C\gamma_\mu \overleftrightarrow{\partial}_\nu q'_k$, where the derivative $\overleftrightarrow{\partial}_\mu = \overrightarrow{\partial}_\mu - \overleftarrow{\partial}_\mu$ embodies the P-wave effects.

We can also adopt the covariant derivative with the simple replacement $\partial_\mu \rightarrow D_\mu = \partial_\mu - ig_s G_\mu$, then the four-quark currents are gauge covariant, however, gluonic components are introduced, we have to deal with both valence quarks and gluons.

Now let us construct the $\mathbf{\bar{3}\bar{3}}$ -type four-quark currents to interpolate the hidden-charm tetraquark states with the $J^{PC} = 0^{++}, 1^{+-}, 1^{++}$ and 2^{++} ,

$$\begin{aligned}J_{SS}(x) &= \varepsilon^{ijk} \varepsilon^{imn} u_j^T(x) C\gamma_5 c_k(x) \bar{d}_m(x) \gamma_5 C\bar{c}_n^T(x), \\ J_{AA}(x) &= \varepsilon^{ijk} \varepsilon^{imn} u_j^T(x) C\gamma_\mu c_k(x) \bar{d}_m(x) \gamma^\mu C\bar{c}_n^T(x), \\ J_{\tilde{A}\tilde{A}}(x) &= \varepsilon^{ijk} \varepsilon^{imn} u_j^T(x) C\sigma_{\mu\nu}^v c_k(x) \bar{d}_m(x) \sigma_\nu^{\mu\nu} C\bar{c}_n^T(x), \\ J_{VV}(x) &= \varepsilon^{ijk} \varepsilon^{imn} u_j^T(x) C\gamma_\mu\gamma_5 c_k(x) \bar{d}_m(x) \gamma_5 \gamma^\mu C\bar{c}_n^T(x), \\ J_{\tilde{V}\tilde{V}}(x) &= \varepsilon^{ijk} \varepsilon^{imn} u_j^T(x) C\sigma_{\mu\nu}^t c_k(x) \bar{d}_m(x) \sigma_t^{\mu\nu} C\bar{c}_n^T(x), \\ J_{PP}(x) &= \varepsilon^{ijk} \varepsilon^{imn} u_j^T(x) C c_k(x) \bar{d}_m(x) C\bar{c}_n^T(x),\end{aligned}\quad (117)$$

$$\begin{aligned}
J_{-,\mu}^{SA}(x) &= \frac{\varepsilon^{ijk}\varepsilon^{imn}}{\sqrt{2}} \left[u_j^T(x) C \gamma_5 c_k(x) \bar{d}_m(x) \gamma_\mu C \bar{c}_n^T(x) - u_j^T(x) C \gamma_\mu c_k(x) \bar{d}_m(x) \gamma_5 C \bar{c}_n^T(x) \right], \\
J_{-,\mu\nu}^{AA}(x) &= \frac{\varepsilon^{ijk}\varepsilon^{imn}}{\sqrt{2}} \left[u_j^T(x) C \gamma_\mu c_k(x) \bar{d}_m(x) \gamma_\nu C \bar{c}_n^T(x) - u_j^T(x) C \gamma_\nu c_k(x) \bar{d}_m(x) \gamma_\mu C \bar{c}_n^T(x) \right], \\
J_{-,\mu\nu}^{S\tilde{A}}(x) &= \frac{\varepsilon^{ijk}\varepsilon^{imn}}{\sqrt{2}} \left[u_j^T(x) C \gamma_5 c_k(x) \bar{d}_m(x) \sigma_{\mu\nu} C \bar{c}_n^T(x) - u_j^T(x) C \sigma_{\mu\nu} c_k(x) \bar{d}_m(x) \gamma_5 C \bar{c}_n^T(x) \right], \\
J_{-,\mu}^{\tilde{A}A}(x) &= \frac{\varepsilon^{ijk}\varepsilon^{imn}}{\sqrt{2}} \left[u_j^T(x) C \sigma_{\mu\nu} \gamma_5 c_k(x) \bar{d}_m(x) \gamma^\nu C \bar{c}_n^T(x) - u_j^T(x) C \gamma^\nu c_k(x) \bar{d}_m(x) \gamma_5 \sigma_{\mu\nu} C \bar{c}_n^T(x) \right], \\
J_{-,\mu}^{\tilde{V}V}(x) &= \frac{\varepsilon^{ijk}\varepsilon^{imn}}{\sqrt{2}} \left[u_j^T(x) C \sigma_{\mu\nu} c^k(x) \bar{d}_m(x) \gamma_5 \gamma^\nu C \bar{c}_n^T(x) + u_j^T(x) C \gamma^\nu \gamma_5 c_k(x) \bar{d}_m(x) \sigma_{\mu\nu} C \bar{c}_n^T(x) \right], \\
J_{-,\mu\nu}^{VV}(x) &= \frac{\varepsilon^{ijk}\varepsilon^{imn}}{\sqrt{2}} \left[u_j^T(x) C \gamma_\mu \gamma_5 c_k(x) \bar{d}_m(x) \gamma_5 \gamma_\nu C \bar{c}_n^T(x) - u_j^T(x) C \gamma_\nu \gamma_5 c_k(x) \bar{d}_m(x) \gamma_5 \gamma_\mu C \bar{c}_n^T(x) \right], \\
J_{-,\mu}^{PV}(x) &= \frac{\varepsilon^{ijk}\varepsilon^{imn}}{\sqrt{2}} \left[u_j^T(x) C c_k(x) \bar{d}_m(x) \gamma_5 \gamma_\mu C \bar{c}_n^T(x) + u_j^T(x) C \gamma_\mu \gamma_5 c_k(x) \bar{d}_m(x) C \bar{c}_n^T(x) \right], \quad (118)
\end{aligned}$$

$$\begin{aligned}
J_{+,\mu}^{SA}(x) &= \frac{\varepsilon^{ijk}\varepsilon^{imn}}{\sqrt{2}} \left[u_j^T(x) C \gamma_5 c_k(x) \bar{d}_m(x) \gamma_\mu C \bar{c}_n^T(x) + u_j^T(x) C \gamma_\mu c_k(x) \bar{d}_m(x) \gamma_5 C \bar{c}_n^T(x) \right], \\
J_{+,\mu\nu}^{S\tilde{A}}(x) &= \frac{\varepsilon^{ijk}\varepsilon^{imn}}{\sqrt{2}} \left[u_j^T(x) C \gamma_5 c_k(x) \bar{d}_m(x) \sigma_{\mu\nu} C \bar{c}_n^T(x) + u_j^T(x) C \sigma_{\mu\nu} c_k(x) \bar{d}_m(x) \gamma_5 C \bar{c}_n^T(x) \right], \\
J_{+,\mu}^{\tilde{V}V}(x) &= \frac{\varepsilon^{ijk}\varepsilon^{imn}}{\sqrt{2}} \left[u_j^T(x) C \sigma_{\mu\nu} c_k(x) \bar{d}_m(x) \gamma_5 \gamma^\nu C \bar{c}_n^T(x) - u_j^T(x) C \gamma^\nu \gamma_5 c_k(x) \bar{d}_m(x) \sigma_{\mu\nu} C \bar{c}_n^T(x) \right], \\
J_{+,\mu}^{\tilde{A}A}(x) &= \frac{\varepsilon^{ijk}\varepsilon^{imn}}{\sqrt{2}} \left[u_j^T(x) C \sigma_{\mu\nu} \gamma_5 c_k(x) \bar{d}_m(x) \gamma^\nu C \bar{c}_n^T(x) + u_j^T(x) C \gamma^\nu c_k(x) \bar{d}_m(x) \gamma_5 \sigma_{\mu\nu} C \bar{c}_n^T(x) \right], \\
J_{+,\mu}^{PV}(x) &= \frac{\varepsilon^{ijk}\varepsilon^{imn}}{\sqrt{2}} \left[u_j^T(x) C c_k(x) \bar{d}_m(x) \gamma_5 \gamma_\mu C \bar{c}_n^T(x) - u_j^T(x) C \gamma_\mu \gamma_5 c_k(x) \bar{d}_m(x) C \bar{c}_n^T(x) \right], \\
J_{+,\mu\nu}^{AA}(x) &= \frac{\varepsilon^{ijk}\varepsilon^{imn}}{\sqrt{2}} \left[u_j^T(x) C \gamma_\mu c_k(x) \bar{d}_m(x) \gamma_\nu C \bar{c}_n^T(x) + u_j^T(x) C \gamma_\nu c_k(x) \bar{d}_m(x) \gamma_\mu C \bar{c}_n^T(x) \right], \\
J_{+,\mu\nu}^{VV}(x) &= \frac{\varepsilon^{ijk}\varepsilon^{imn}}{\sqrt{2}} \left[u_j^T(x) C \gamma_\mu \gamma_5 c_k(x) \bar{d}_m(x) \gamma_5 \gamma_\nu C \bar{c}_n^T(x) + u_j^T(x) C \gamma_\nu \gamma_5 c_k(x) \bar{d}_m(x) \gamma_5 \gamma_\mu C \bar{c}_n^T(x) \right], \quad (119)
\end{aligned}$$

where the subscripts \pm denote the positive and negative charge conjugation, respectively, the superscripts or subscripts P , S , $A(\tilde{A})$ and $V(\tilde{V})$ denote the pseudoscalar, scalar, axialvector and vector diquark and antidiquark operators, respectively [57]. With the simple replacements,

$$\begin{aligned}
u &\rightarrow q, \\
d &\rightarrow s, \quad (120)
\end{aligned}$$

where $q = u, d$, we obtain the corresponding currents for the $c\bar{c}q\bar{s}$ states [164]. Again, with the simple replacements,

$$\begin{aligned}
u &\rightarrow s, \\
d &\rightarrow s, \quad (121)
\end{aligned}$$

we obtain the corresponding currents for the $c\bar{c}s\bar{s}$ states [361].

We introduce the symbols,

$$\begin{aligned}
J(x) &= J_{SS}(x), J_{AA}(x), J_{\tilde{A}\tilde{A}}(x), J_{VV}(x), J_{\tilde{V}\tilde{V}}(x), J_{PP}(x), \\
J_\mu(x) &= J_{-, \mu}^{SA}(x), J_{-, \mu}^{\tilde{A}A}(x), J_{-, \mu}^{\tilde{V}V}(x), J_{-, \mu}^{PV}(x), J_{+, \mu}^{SA}(x), J_{+, \mu}^{\tilde{V}V}(x), J_{+, \mu}^{\tilde{A}A}(x), J_{+, \mu}^{PV}(x), \\
J_{\mu\nu}(x) &= J_{-, \mu\nu}^{AA}(x), J_{-, \mu\nu}^{S\tilde{A}}(x), J_{-, \mu\nu}^{VV}(x), J_{+, \mu\nu}^{S\tilde{A}}(x), J_{+, \mu\nu}^{AA}(x), J_{+, \mu\nu}^{VV}(x),
\end{aligned} \tag{122}$$

for simplicity.

Under parity transform \hat{P} , the currents have the properties,

$$\begin{aligned}
\hat{P}J(x)\hat{P}^{-1} &= +J(\tilde{x}), \\
\hat{P}J_\mu(x)\hat{P}^{-1} &= -J^\mu(\tilde{x}), \\
\hat{P}J_{\mu\nu}^{S\tilde{A}}(x)\hat{P}^{-1} &= -J_{S\tilde{A}}^{\mu\nu}(\tilde{x}), \\
\hat{P}J_{\mu\nu}^{AA/VV}(x)\hat{P}^{-1} &= +J_{AA/VV}^{\mu\nu}(\tilde{x}),
\end{aligned} \tag{123}$$

where $x^\mu = (t, \vec{x})$ and $\tilde{x}^\mu = (t, -\vec{x})$, and we have neglected other superscripts and subscripts of the currents.

The currents $J(x)$, $J_\mu(x)$ and $J_{\mu\nu}(x)$ have the symbolic quark constituent $\bar{c}\bar{c}\bar{d}u$ with the isospin $I = 1$ and $I_3 = 1$, other currents in the isospin multiplets can be constructed analogously, for example, we write down the isospin singlet current for the $J_{SS}(x)$ directly,

$$J_{SS}^{I=0}(x) = \frac{\varepsilon^{ijk}\varepsilon^{imn}}{\sqrt{2}} \left[u_j^T(x)C\gamma_5 c_k(x)\bar{u}_m(x)\gamma_5 C\bar{c}_n^T(x) + d_j^T(x)C\gamma_5 c_k(x)\bar{d}_m(x)\gamma_5 C\bar{c}_n^T(x) \right]. \tag{124}$$

In the isospin limit, the currents with the symbolic quark constituents $\bar{c}\bar{c}\bar{d}u$, $\bar{c}\bar{c}\bar{u}d$, $\bar{c}\bar{c}\frac{\bar{u}u-\bar{d}d}{\sqrt{2}}$, $\bar{c}\bar{c}\frac{\bar{u}u+\bar{d}d}{\sqrt{2}}$ couple potentially to the hidden-charm tetraquark states with degenerated masses, the currents with the isospins $I = 1$ and 0 lead to the same QCD sum rules. Thereafter, we will denote the Z_c states as the isospin triplet, and the X states as the isospin singlet,

$$\begin{aligned}
Z_c &: \bar{c}\bar{c}\bar{d}u, \bar{c}\bar{c}\bar{u}d, \bar{c}\bar{c}\frac{\bar{u}u-\bar{d}d}{\sqrt{2}}, \\
X &: \bar{c}\bar{c}\frac{\bar{u}u+\bar{d}d}{\sqrt{2}}.
\end{aligned} \tag{125}$$

Accordingly, the Z_{cs} states with the symbolic quark constituents $\bar{c}\bar{c}\bar{s}q$ and isospin $I = \frac{1}{2}$ have degenerated masses.

The currents with the symbolic quark constituents $\bar{c}\bar{c}\frac{\bar{u}u-\bar{d}d}{\sqrt{2}}$ and $\bar{c}\bar{c}\frac{\bar{u}u+\bar{d}d}{\sqrt{2}}$ have definite charge conjugation. We would like to assume that the $\bar{c}\bar{c}\bar{d}u$ type tetraquark states have the same charge conjugation as their charge-neutral cousins.

Under charge conjugation transform \hat{C} , the currents $J(x)$, $J_\mu(x)$ and $J_{\mu\nu}(x)$ have the properties,

$$\begin{aligned}
\hat{C}J(x)\hat{C}^{-1} &= +J(x) |_{u\leftrightarrow d}, \\
\hat{C}J_{\pm, \mu}(x)\hat{C}^{-1} &= \pm J_{\pm, \mu}(x) |_{u\leftrightarrow d}, \\
\hat{C}J_{\pm, \mu\nu}(x)\hat{C}^{-1} &= \pm J_{\pm, \mu\nu}(x) |_{u\leftrightarrow d},
\end{aligned} \tag{126}$$

where we have neglected other superscripts and subscripts.

Now we write down the correlation functions $\Pi(p)$, $\Pi_{\mu\nu}(p)$ and $\Pi_{\mu\nu\alpha\beta}(p)$,

$$\begin{aligned}
\Pi(p) &= i \int d^4x e^{ip \cdot x} \langle 0 | T \{ J(x) J^\dagger(0) \} | 0 \rangle, \\
\Pi_{\mu\nu}(p) &= i \int d^4x e^{ip \cdot x} \langle 0 | T \{ J_\mu(x) J_\nu^\dagger(0) \} | 0 \rangle, \\
\Pi_{\mu\nu\alpha\beta}(p) &= i \int d^4x e^{ip \cdot x} \langle 0 | T \{ J_{\mu\nu}(x) J_{\alpha\beta}^\dagger(0) \} | 0 \rangle.
\end{aligned} \tag{127}$$

At the hadron side, we insert a complete set of intermediate hadronic states with the same quantum numbers as the currents $J(x)$, $J_\mu(x)$ and $J_{\mu\nu}(x)$ into the correlation functions $\Pi(p)$, $\Pi_{\mu\nu}(p)$ and $\Pi_{\mu\nu\alpha\beta}(p)$ to obtain the hadronic representation [333, 334], and isolate the ground state hidden-charm tetraquark contributions,

$$\begin{aligned}
\Pi(p) &= \frac{\lambda_{Z^+}^2}{M_{Z^+}^2 - p^2} + \dots = \Pi_+(p^2), \\
\Pi_{\mu\nu}(p) &= \frac{\lambda_{Z^+}^2}{M_{Z^+}^2 - p^2} \left(-g_{\mu\nu} + \frac{p_\mu p_\nu}{p^2} \right) + \dots \\
&= \Pi_+(p^2) \left(-g_{\mu\nu} + \frac{p_\mu p_\nu}{p^2} \right) + \dots, \\
\Pi_{\mu\nu\alpha\beta}^{AA,-}(p) &= \frac{\lambda_{Z^+}^2}{M_{Z^+}^2 (M_{Z^+}^2 - p^2)} \left(p^2 g_{\mu\alpha} g_{\nu\beta} - p^2 g_{\mu\beta} g_{\nu\alpha} - g_{\mu\alpha} p_\nu p_\beta - g_{\nu\beta} p_\mu p_\alpha + g_{\mu\beta} p_\nu p_\alpha + g_{\nu\alpha} p_\mu p_\beta \right) \\
&\quad + \frac{\lambda_{Z^-}^2}{M_{Z^-}^2 (M_{Z^-}^2 - p^2)} \left(-g_{\mu\alpha} p_\nu p_\beta - g_{\nu\beta} p_\mu p_\alpha + g_{\mu\beta} p_\nu p_\alpha + g_{\nu\alpha} p_\mu p_\beta \right) + \dots \\
&= \tilde{\Pi}_+(p^2) \left(p^2 g_{\mu\alpha} g_{\nu\beta} - p^2 g_{\mu\beta} g_{\nu\alpha} - g_{\mu\alpha} p_\nu p_\beta - g_{\nu\beta} p_\mu p_\alpha + g_{\mu\beta} p_\nu p_\alpha + g_{\nu\alpha} p_\mu p_\beta \right) \\
&\quad + \tilde{\Pi}_-(p^2) \left(-g_{\mu\alpha} p_\nu p_\beta - g_{\nu\beta} p_\mu p_\alpha + g_{\mu\beta} p_\nu p_\alpha + g_{\nu\alpha} p_\mu p_\beta \right), \\
\Pi_{\mu\nu\alpha\beta}^{S\tilde{A},\pm}(p) &= \frac{\lambda_{Z^-}^2}{M_{Z^-}^2 (M_{Z^-}^2 - p^2)} \left(p^2 g_{\mu\alpha} g_{\nu\beta} - p^2 g_{\mu\beta} g_{\nu\alpha} - g_{\mu\alpha} p_\nu p_\beta - g_{\nu\beta} p_\mu p_\alpha + g_{\mu\beta} p_\nu p_\alpha + g_{\nu\alpha} p_\mu p_\beta \right) \\
&\quad + \frac{\lambda_{Z^+}^2}{M_{Z^+}^2 (M_{Z^+}^2 - p^2)} \left(-g_{\mu\alpha} p_\nu p_\beta - g_{\nu\beta} p_\mu p_\alpha + g_{\mu\beta} p_\nu p_\alpha + g_{\nu\alpha} p_\mu p_\beta \right) + \dots \\
&= \tilde{\Pi}_-(p^2) \left(p^2 g_{\mu\alpha} g_{\nu\beta} - p^2 g_{\mu\beta} g_{\nu\alpha} - g_{\mu\alpha} p_\nu p_\beta - g_{\nu\beta} p_\mu p_\alpha + g_{\mu\beta} p_\nu p_\alpha + g_{\nu\alpha} p_\mu p_\beta \right) \\
&\quad + \tilde{\Pi}_+(p^2) \left(-g_{\mu\alpha} p_\nu p_\beta - g_{\nu\beta} p_\mu p_\alpha + g_{\mu\beta} p_\nu p_\alpha + g_{\nu\alpha} p_\mu p_\beta \right), \\
\Pi_{\mu\nu\alpha\beta}^{AA,+}(p) &= \frac{\lambda_{Z^+}^2}{M_{Z^+}^2 - p^2} \left(\frac{\tilde{g}_{\mu\alpha} \tilde{g}_{\nu\beta} + \tilde{g}_{\mu\beta} \tilde{g}_{\nu\alpha}}{2} - \frac{\tilde{g}_{\mu\nu} \tilde{g}_{\alpha\beta}}{3} \right) + \dots, \\
&= \Pi_+(p^2) \left(\frac{\tilde{g}_{\mu\alpha} \tilde{g}_{\nu\beta} + \tilde{g}_{\mu\beta} \tilde{g}_{\nu\alpha}}{2} - \frac{\tilde{g}_{\mu\nu} \tilde{g}_{\alpha\beta}}{3} \right) + \dots,
\end{aligned} \tag{128}$$

where $\tilde{g}_{\mu\nu} = g_{\mu\nu} - \frac{p_\mu p_\nu}{p^2}$. We add the superscripts \pm in the $\Pi_{\mu\nu\alpha\beta}^{AA,-}(p)$, $\Pi_{\mu\nu\alpha\beta}^{S\tilde{A},\pm}(p)$ and $\Pi_{\mu\nu\alpha\beta}^{AA,+}(p)$ to denote the positive and negative charge conjugation, respectively, and add the superscripts (subscripts) \pm in the Z_c^\pm (the $\Pi_\pm(p^2)$ and $\tilde{\Pi}_\pm(p^2)$ components) to denote the positive and negative parity, respectively. And the $\Pi_{\mu\nu\alpha\beta}^{VV,\pm}(p)$ and $\Pi_{\mu\nu\alpha\beta}^{AA,\pm}(p)$ have the same tensor structures. The pole

Z_c	J^{PC}	Currents
$[uc]_S[\bar{d}\bar{c}]_S$	0^{++}	$J_{SS}(x)$
$[uc]_A[\bar{d}\bar{c}]_A$	0^{++}	$J_{AA}(x)$
$[uc]_{\bar{A}}[\bar{d}\bar{c}]_{\bar{A}}$	0^{++}	$J_{\bar{A}\bar{A}}(x)$
$[uc]_V[\bar{d}\bar{c}]_V$	0^{++}	$J_{VV}(x)$
$[uc]_{\bar{V}}[\bar{d}\bar{c}]_{\bar{V}}$	0^{++}	$J_{\bar{V}\bar{V}}(x)$
$[uc]_P[\bar{d}\bar{c}]_P$	0^{++}	$J_{PP}(x)$
$[uc]_S[\bar{d}\bar{c}]_A - [uc]_A[\bar{d}\bar{c}]_S$	1^{+-}	$J_{-}^{SA}(x)$
$[uc]_A[\bar{d}\bar{c}]_A$	1^{+-}	$J_{-,\mu\nu}^{AA}(x)$
$[uc]_S[\bar{d}\bar{c}]_{\bar{A}} - [uc]_{\bar{A}}[\bar{d}\bar{c}]_S$	1^{+-}	$J_{-}^{S\bar{A}}(x)$
$[uc]_{\bar{A}}[\bar{d}\bar{c}]_A - [uc]_A[\bar{d}\bar{c}]_{\bar{A}}$	1^{+-}	$J_{-,\mu\nu}^{\bar{A}A}(x)$
$[uc]_{\bar{V}}[\bar{d}\bar{c}]_V + [uc]_V[\bar{d}\bar{c}]_{\bar{V}}$	1^{+-}	$J_{-}^{\bar{V}V}(x)$
$[uc]_V[\bar{d}\bar{c}]_V$	1^{+-}	$J_{-,\mu\nu}^{\bar{V}V}(x)$
$[uc]_P[\bar{d}\bar{c}]_V + [uc]_V[\bar{d}\bar{c}]_P$	1^{+-}	$J_{-,\mu\nu}^{PV}(x)$
$[uc]_S[\bar{d}\bar{c}]_A + [uc]_A[\bar{d}\bar{c}]_S$	1^{++}	$J_{+}^{SA}(x)$
$[uc]_S[\bar{d}\bar{c}]_{\bar{A}} + [uc]_{\bar{A}}[\bar{d}\bar{c}]_S$	1^{++}	$J_{+,\mu\nu}^{S\bar{A}}(x)$
$[uc]_{\bar{V}}[\bar{d}\bar{c}]_V - [uc]_V[\bar{d}\bar{c}]_{\bar{V}}$	1^{++}	$J_{+,\mu\nu}^{\bar{V}V}(x)$
$[uc]_{\bar{A}}[\bar{d}\bar{c}]_A + [uc]_A[\bar{d}\bar{c}]_{\bar{A}}$	1^{++}	$J_{+,\mu\nu}^{\bar{A}A}(x)$
$[uc]_P[\bar{d}\bar{c}]_V - [uc]_V[\bar{d}\bar{c}]_P$	1^{++}	$J_{+,\mu\nu}^{PV}(x)$
$[uc]_A[\bar{d}\bar{c}]_A$	2^{++}	$J_{+,\mu\nu}^{AA}(x)$
$[uc]_V[\bar{d}\bar{c}]_V$	2^{++}	$J_{+,\mu\nu}^{\bar{V}V}(x)$

Table 4: The quark constituents and corresponding currents for the hidden-charm tetraquark states.

residues λ_{Z^\pm} are defined by

$$\begin{aligned}
\langle 0|J(0)|Z_c^+(p)\rangle &= \lambda_{Z^+}, \\
\langle 0|J_\mu(0)|Z_c^+(p)\rangle &= \lambda_{Z^+}\varepsilon_\mu, \\
\langle 0|J_{\pm,\mu\nu}^{S\bar{A}}(0)|Z_c^-(p)\rangle &= \tilde{\lambda}_{Z^-}\varepsilon_{\mu\nu\alpha\beta}\varepsilon^\alpha p^\beta, \\
\langle 0|J_{\pm,\mu\nu}^{S\bar{A}}(0)|Z_c^+(p)\rangle &= \tilde{\lambda}_{Z^+}(\varepsilon_\mu p_\nu - \varepsilon_\nu p_\mu), \\
\langle 0|J_{-,\mu\nu}^{AA/VV}(0)|Z_c^+(p)\rangle &= \tilde{\lambda}_{Z^+}\varepsilon_{\mu\nu\alpha\beta}\varepsilon^\alpha p^\beta, \\
\langle 0|J_{-,\mu\nu}^{AA/VV}(0)|Z_c^-(p)\rangle &= \tilde{\lambda}_{Z^-}(\varepsilon_\mu p_\nu - \varepsilon_\nu p_\mu), \\
\langle 0|J_{+,\mu\nu}^{AA/VV}(0)|Z_c^+(p)\rangle &= \lambda_{Z^+}\varepsilon_{\mu\nu},
\end{aligned} \tag{129}$$

where $\lambda_{Z^\pm} = \tilde{\lambda}_{Z^\pm}M_{Z^\pm}$, the $\varepsilon_{\mu/\alpha}$ and $\varepsilon_{\mu\nu}$ are the polarization vectors. We choose the components $\Pi_+(p^2)$ and $p^2\tilde{\Pi}_+(p^2)$ to study the hidden-charm tetraquark states.

In Table 4, we present the quark constituents and corresponding currents explicitly,

At the QCD side, we carry out the operator product expansion for the correlation functions $\Pi(p)$, $\Pi_{\mu\nu}(p)$ and $\Pi_{\mu\nu\alpha\beta}(p)$. For example, we contract the quark fields in the $\Pi_{\mu\nu}(p)$ with the

Wick's theorem, and obtain the results,

$$\begin{aligned}
\Pi_{\mu\nu}(p) &= -\frac{i\varepsilon^{ijk}\varepsilon^{imn}\varepsilon^{i'j'k'}\varepsilon^{i'm'n'}}{2} \int d^4x e^{ip\cdot x} \\
&\left\{ \text{Tr} \left[\gamma_5 S_Q^{kk'}(x) \gamma_5 C U_{jj'}^T(x) C \right] \text{Tr} \left[\gamma_\nu S_Q^{n' n}(-x) \gamma_\mu C D_{m'm}^T(-x) C \right] \right. \\
&+ \text{Tr} \left[\gamma_\mu S_Q^{kk'}(x) \gamma_\nu C U_{jj'}^T(x) C \right] \text{Tr} \left[\gamma_5 S_Q^{n' n}(-x) \gamma_5 C D_{m'm}^T(-x) C \right] \\
&\mp \text{Tr} \left[\gamma_\mu S_Q^{kk'}(x) \gamma_5 C U_{jj'}^T(x) C \right] \text{Tr} \left[\gamma_\nu S_Q^{n' n}(-x) \gamma_5 C D_{m'm}^T(-x) C \right] \\
&\left. \mp \text{Tr} \left[\gamma_5 S_Q^{kk'}(x) \gamma_\nu C U_{jj'}^T(x) C \right] \text{Tr} \left[\gamma_5 S_Q^{n' n}(-x) \gamma_\mu C D_{m'm}^T(-x) C \right] \right\}, \quad (130)
\end{aligned}$$

where the full quark propagators, $S^{ij}(x) = U^{ij}(x) = D^{ij}(x)$,

$$\begin{aligned}
S^{ij}(x) &= \frac{i\delta_{ij}\not{x}}{2\pi^2x^4} - \frac{\delta_{ij}m_s}{4\pi^2x^2} - \frac{\delta_{ij}\langle\bar{q}q\rangle}{12} + \frac{i\delta_{ij}\not{x}m_q\langle\bar{q}q\rangle}{48} - \frac{\delta_{ij}x^2\langle\bar{q}g_s\sigma Gq\rangle}{192} + \frac{i\delta_{ij}x^2\not{x}m_q\langle\bar{q}g_s\sigma Gq\rangle}{1152} \\
&- \frac{ig_s G_{\alpha\beta}^a t_{ij}^a (\not{x}\sigma^{\alpha\beta} + \sigma^{\alpha\beta}\not{x})}{32\pi^2x^2} - \frac{i\delta_{ij}x^2\not{x}g_s^2\langle\bar{q}q\rangle^2}{7776} - \frac{\delta_{ij}x^4\langle\bar{q}q\rangle\langle g_s^2GG\rangle}{27648} - \frac{1}{8}\langle\bar{q}_j\sigma^{\mu\nu}q_i\rangle\sigma_{\mu\nu} \\
&- \frac{1}{4}\langle\bar{q}_j\gamma^\mu q_i\rangle\gamma_\mu + \dots, \quad (131)
\end{aligned}$$

$$\begin{aligned}
S_Q^{ij}(x) &= \frac{i}{(2\pi)^4} \int d^4k e^{-ik\cdot x} \left\{ \frac{\delta_{ij}}{\not{k} - m_Q} - \frac{g_s G_{\alpha\beta}^n t_{ij}^n}{4} \frac{\sigma^{\alpha\beta}(\not{k} + m_Q) + (\not{k} + m_Q)\sigma^{\alpha\beta}}{(k^2 - m_Q^2)^2} \right. \\
&+ \left. \frac{g_s D_\alpha G_{\beta\lambda}^n t_{ij}^n (f^{\lambda\beta\alpha} + f^{\lambda\alpha\beta})}{3(k^2 - m_Q^2)^4} - \frac{g_s^2 (t^a t^b)_{ij} G_{\alpha\beta}^a G_{\mu\nu}^b (f^{\alpha\beta\mu\nu} + f^{\alpha\mu\beta\nu} + f^{\alpha\mu\nu\beta})}{4(k^2 - m_Q^2)^5} + \dots \right\}, \\
f^{\lambda\alpha\beta} &= (\not{k} + m_Q)\gamma^\lambda(\not{k} + m_Q)\gamma^\alpha(\not{k} + m_Q)\gamma^\beta(\not{k} + m_Q), \\
f^{\alpha\beta\mu\nu} &= (\not{k} + m_Q)\gamma^\alpha(\not{k} + m_Q)\gamma^\beta(\not{k} + m_Q)\gamma^\mu(\not{k} + m_Q)\gamma^\nu(\not{k} + m_Q), \quad (132)
\end{aligned}$$

$D_\alpha = \partial_\alpha - ig_s G_\alpha^n t^n$ [56, 438, 439], and the \mp correspond the currents $J_{+,\mu}^{SA}(x)$ and $J_{-,\mu}^{SA}(x)$, respectively. In Eq.(131), we retain the terms $\langle\bar{q}_j\sigma_{\mu\nu}q_i\rangle$ and $\langle\bar{q}_j\gamma_\mu q_i\rangle$ come from the Fierz transformation of the $\langle q_i\bar{q}_j\rangle$ to absorb the gluons emitted from the other quark lines to form $\langle\bar{q}_j g_s G_{\alpha\beta}^a t_{mn}^a \sigma_{\mu\nu} q_i\rangle$ and $\langle\bar{q}_j \gamma_\mu q_i D_\nu g_s G_{\alpha\beta}^a t_{mn}^a\rangle$ to extract the mixed condensate $\langle\bar{q}g_s\sigma Gq\rangle$ and four-quark condensate $g_s^2\langle\bar{q}q\rangle^2$, respectively [56], where $q = u, d$ or s . The condensate $g_s^2\langle\bar{q}q\rangle^2$ comes from the $\langle\bar{q}\gamma_\mu t^a q g_s D_\eta G_{\lambda\tau}^a\rangle$, $\langle\bar{q}_j D_\mu^\dagger D_\nu^\dagger D_\alpha^\dagger q_i\rangle$ and $\langle\bar{q}_j D_\mu D_\nu D_\alpha q_i\rangle$ rather than comes from the radiative $\mathcal{O}(\alpha_s)$ corrections to the $\langle\bar{q}q\rangle^2$.

In fact, the method of adopting the full propagators in Eq.(130) implies vacuum saturation implicitly, the factorization of the higher dimensional vacuum condensates, for example, see Eq.(88), is already performed. We calculate the higher dimensional vacuum condensates using the formula $t_{ij}^a t_{mn}^a = -\frac{1}{6}\delta_{ij}\delta_{mn} + \frac{1}{2}\delta_{jm}\delta_{in}$ rigorously.

Let us see Eq.(130) again, there are two Q -quark propagators and two q -quark propagators, if each Q -quark line emits a gluon and each q -quark line contributes a quark-antiquark pair, we obtain an operator $G_{\mu\nu} G_{\alpha\beta} \bar{u}u\bar{d}d$ (or $G_{\mu\nu} G_{\alpha\beta} \bar{q}q\bar{s}s$ or $G_{\mu\nu} G_{\alpha\beta} \bar{s}s\bar{s}s$), which is of dimension 10, see the Feynman diagram in Fig.6 for example. We should take account of the vacuum condensates at least up to dimension 10. The higher dimensional vacuum condensates are associated with the $\frac{1}{T^2}$, $\frac{1}{T^4}$ or $\frac{1}{T^6}$, which manifest themselves at small Borel parameter T^2 and play an important role in determining the Borel windows, where they play a minor important role. Therefore, we take account of the vacuum condensates $\langle\bar{q}q\rangle$, $\langle\frac{\alpha_s GG}{\pi}\rangle$, $\langle\bar{q}g_s\sigma Gq\rangle$, $\langle\bar{q}q\rangle^2$, $g_s^2\langle\bar{q}q\rangle^2$, $\langle\bar{q}q\rangle\langle\frac{\alpha_s GG}{\pi}\rangle$, $\langle\bar{q}q\rangle\langle\bar{q}g_s\sigma Gq\rangle$, $\langle\bar{q}g_s\sigma Gq\rangle^2$ and $\langle\bar{q}q\rangle^2\langle\frac{\alpha_s GG}{\pi}\rangle$, which are vacuum expectations of the quark-gluon operators of the order $\mathcal{O}(\alpha_s^k)$ with $k \leq 1$. We truncate the operator product expansion in such a way consistently and rigorously. The condensates $\langle g_s^3 GGG\rangle$, $\langle\frac{\alpha_s GG}{\pi}\rangle^2$, $\langle\frac{\alpha_s GG}{\pi}\rangle\langle\bar{q}g_s\sigma Gq\rangle$ have the

dimensions 6, 8, 9 respectively, but they are vacuum expectations of the quark-gluon operators of the order $\mathcal{O}(\alpha_s^{3/2})$, $\mathcal{O}(\alpha_s^2)$, $\mathcal{O}(\alpha_s^{3/2})$ respectively, and discarded. Furthermore, direct calculations indicate such contributions are tiny indeed [440].

We accomplish the integrals in Eqs.(130)-(132) sequentially by simply setting $d^4x d^4k d^4q \rightarrow d^Dx d^Dk d^Dq$ with $D = 4 - 2\epsilon$ to regularize the divergences, such a simple scheme misses many subtraction terms, which make no contribution in obtaining the imaginary parts through $p^2 \rightarrow p^2 + i\epsilon$. Finally, we obtain the QCD spectral densities $\rho_{QCD}(s)$ through dispersion relation.

Then we match the hadron side with the QCD side of the components $\Pi_+(p^2)$ and $p^2\tilde{\Pi}_+(p^2)$ of the correlation functions $\Pi(p)$, $\Pi_{\mu\nu}(p)$ and $\Pi_{\mu\nu\alpha\beta}(p)$ below the continuum thresholds s_0 and perform Borel transformation with respect to $P^2 = -p^2$ to obtain the QCD sum rules:

$$\lambda_{Z^+}^2 \exp\left(-\frac{M_{Z^+}^2}{T^2}\right) = \int_{4m_c^2}^{s_0} ds \rho_{QCD}(s) \exp\left(-\frac{s}{T^2}\right). \quad (133)$$

We derive Eq.(133) with respect to $\tau = \frac{1}{T^2}$, and obtain the QCD sum rules for the masses of the hidden-charm tetraquark states Z_c or X ,

$$M_{Z^+}^2 = -\frac{\int_{4m_c^2}^{s_0} ds \frac{d}{d\tau} \rho_{QCD}(s) \exp(-\tau s)}{\int_{4m_c^2}^{s_0} ds \rho_{QCD}(s) \exp(-\tau s)}. \quad (134)$$

Let us turn to the input parameters and write down the energy-scale dependence of the input parameters,

$$\begin{aligned} \langle \bar{q}q \rangle(\mu) &= \langle \bar{q}q \rangle(1\text{GeV}) \left[\frac{\alpha_s(1\text{GeV})}{\alpha_s(\mu)} \right]^{\frac{12}{33-2n_f}}, \\ \langle \bar{s}s \rangle(\mu) &= \langle \bar{s}s \rangle(1\text{GeV}) \left[\frac{\alpha_s(1\text{GeV})}{\alpha_s(\mu)} \right]^{\frac{12}{33-2n_f}}, \\ \langle \bar{q}g_s\sigma Gq \rangle(\mu) &= \langle \bar{q}g_s\sigma Gq \rangle(1\text{GeV}) \left[\frac{\alpha_s(1\text{GeV})}{\alpha_s(\mu)} \right]^{\frac{2}{33-2n_f}}, \\ \langle \bar{s}g_s\sigma Gs \rangle(\mu) &= \langle \bar{s}g_s\sigma Gs \rangle(1\text{GeV}) \left[\frac{\alpha_s(1\text{GeV})}{\alpha_s(\mu)} \right]^{\frac{2}{33-2n_f}}, \\ m_c(\mu) &= m_c(m_c) \left[\frac{\alpha_s(\mu)}{\alpha_s(m_c)} \right]^{\frac{12}{33-2n_f}}, \\ m_s(\mu) &= m_s(2\text{GeV}) \left[\frac{\alpha_s(\mu)}{\alpha_s(2\text{GeV})} \right]^{\frac{12}{33-2n_f}}, \\ \alpha_s(\mu) &= \frac{1}{b_0 t} \left[1 - \frac{b_1 \log t}{b_0^2 t} + \frac{b_1^2 (\log^2 t - \log t - 1) + b_0 b_2}{b_0^4 t^2} \right], \end{aligned} \quad (135)$$

where $t = \log \frac{\mu^2}{\Lambda_{QCD}^2}$, $b_0 = \frac{33-2n_f}{12\pi}$, $b_1 = \frac{153-19n_f}{24\pi^2}$, $b_2 = \frac{2857 - \frac{5033}{9}n_f + \frac{325}{27}n_f^2}{128\pi^3}$, $\Lambda_{QCD} = 210$ MeV, 292 MeV and 332 MeV for the flavors $n_f = 5, 4$ and 3, respectively [354, 441]. Because the c -quark is concerned, we choose the flavor number to be $n_f = 4$.

At the beginning points, we adopt the commonly-used values $\langle \bar{q}q \rangle = -(0.24 \pm 0.01 \text{ GeV})^3$, $\langle \bar{s}s \rangle = (0.8 \pm 0.1) \langle \bar{q}q \rangle$, $\langle \bar{q}g_s\sigma Gq \rangle = m_0^2 \langle \bar{q}q \rangle$, $\langle \bar{s}g_s\sigma Gs \rangle = m_0^2 \langle \bar{s}s \rangle$, $m_0^2 = (0.8 \pm 0.1) \text{ GeV}^2$, $\langle \frac{\alpha_s GG}{\pi} \rangle = (0.012 \pm 0.004) \text{ GeV}^4$ at the typical energy scale $\mu = 1 \text{ GeV}$ [333, 334, 438, 442], and adopt the \overline{MS} (modified-minimal-subtraction) masses $m_c(m_c) = (1.275 \pm 0.025) \text{ GeV}$ and $m_s(2\text{GeV}) = (0.095 \pm 0.005) \text{ GeV}$ from the Particle Data Group [354].

We apply the modified energy scale formula $\mu = \sqrt{M_{X/Y/Z}^2 - (2\mathbb{M}_c)^2 - \kappa \mathbb{M}_s}$ to choose the suitable energy scales of the QCD spectral densities [57, 164, 361], where the \mathbb{M}_c and \mathbb{M}_s are

the effective c and s -quark masses respectively, and have universal values to be commonly used elsewhere. We adopt the updated value $M_c = 1.82 \text{ GeV}$ [443], and take the collective light-flavor $SU(3)$ -breaking effects into account by introducing an effective s -quark mass $M_s = 0.20 \text{ GeV}$ (0.12 GeV) for the S-wave (P-wave) tetraquark states [77, 78, 163, 164, 361, 353, 444, 445, 446].

The continuum threshold parameters are not completely free parameters, and cannot be determined by the QCD sum rules themselves completely. We often consult the experimental data in choosing the continuum threshold parameters. The $Z_c(4430)$ can be assigned to be the first radial excitation of the $Z_c(3900)$ according to the analogous decays,

$$\begin{aligned} Z_c^\pm(3900) &\rightarrow J/\psi\pi^\pm, \\ Z_c^\pm(4430) &\rightarrow \psi'\pi^\pm, \end{aligned} \quad (136)$$

and the analogous mass gaps $M_{Z_c(4430)} - M_{Z_c(3900)} = 591 \text{ MeV}$ and $M_{\psi'} - M_{J/\psi} = 589 \text{ MeV}$ from the Particle Data Group [52, 173, 174, 347].

We tentatively choose the continuum threshold parameters as $\sqrt{s_0} = M_{X/Z} + 0.60 \text{ GeV}$ and vary the continuum threshold parameters s_0 and Borel parameters T^2 to satisfy the following four criteria:

- Pole dominance at the hadron side;
 - Convergence of the operator product expansion;
 - Appearance of the Borel platforms;
 - Satisfying the modified energy scale formula,
- via trial and error.

Thereafter, such criteria are taken for all the hidden-charm (hidden-bottom) tetraquark (molecular) states, hidden-charm (hidden-bottom) pentaquark (molecular) states, doubly-charm (doubly-bottom) tetraquark (molecular) states, doubly-charm (doubly-bottom) pentaquark (molecular) states, etc.

The pole dominance at the hadron side and convergence of the operator product expansion at the QCD side are two basic criteria, we should satisfy them to obtain reliable QCD sum rules. In the QCD sum rules for the hidden-charm tetraquark and pentaquark states, the largest power of the energy variable s in the QCD spectral densities $\rho_{QCD}(s) \sim s^4$ and s^5 , respectively, which make the integrals,

$$\int_{4m_c^2}^{s_0} ds s^4 \exp\left(-\frac{s}{T^2}\right), \quad \int_{4m_c^2}^{s_0} ds s^5 \exp\left(-\frac{s}{T^2}\right), \quad (137)$$

converge more slowly compared to the traditional hadrons, it is very difficult to satisfy the two basic criteria at the same time. We define the pole contributions (PC) by,

$$\text{PC} = \frac{\int_{4m_c^2}^{s_0} ds \rho_{QCD}(s) \exp\left(-\frac{s}{T^2}\right)}{\int_{4m_c^2}^{\infty} ds \rho_{QCD}(s) \exp\left(-\frac{s}{T^2}\right)}, \quad (138)$$

while we define the contributions of the vacuum condensates $D(n)$ of dimension n by,

$$D(n) = \frac{\int_{4m_c^2}^{s_0} ds \rho_{QCD,n}(s) \exp\left(-\frac{s}{T^2}\right)}{\int_{4m_c^2}^{s_0} ds \rho_{QCD}(s) \exp\left(-\frac{s}{T^2}\right)}, \quad (139)$$

or

$$D(n) = \frac{\int_{4m_c^2}^{\infty} ds \rho_{QCD,n}(s) \exp\left(-\frac{s}{T^2}\right)}{\int_{4m_c^2}^{\infty} ds \rho_{QCD}(s) \exp\left(-\frac{s}{T^2}\right)}. \quad (140)$$

Compared to the criterion in Eq.(140), the criterion in Eq.(139) is strong and leads to larger Borel parameter T^2 . If we only study the ground state contributions, the Eq.(139) is preferred.

$Z_c(X_c)$	J^{PC}	$T^2(\text{GeV}^2)$	$\sqrt{s_0}(\text{GeV})$	$\mu(\text{GeV})$	pole	$ D(10) $
$[uc]_S[\bar{d}\bar{c}]_S$	0^{++}	2.7 – 3.1	4.40 ± 0.10	1.3	(40 – 63)%	< 1%
$[uc]_A[\bar{d}\bar{c}]_A$	0^{++}	2.8 – 3.2	4.52 ± 0.10	1.5	(40 – 63)%	$\leq 1\%$
$[uc]_{\tilde{A}}[\bar{d}\bar{c}]_{\tilde{A}}$	0^{++}	3.1 – 3.5	4.55 ± 0.10	1.6	(42 – 62)%	< 1%
$[uc]_V[\bar{d}\bar{c}]_V$	0^{++}	3.7 – 4.1	5.22 ± 0.10	2.9	(41 – 60)%	$\ll 1\%$
$[uc]_{\tilde{V}}[\bar{d}\bar{c}]_{\tilde{V}}$	0^{++}	4.9 – 5.7	5.90 ± 0.10	3.9	(41 – 61)%	$\ll 1\%$
$[uc]_P[\bar{d}\bar{c}]_P$	0^{++}	5.2 – 6.0	6.03 ± 0.10	4.1	(40 – 60)%	$\ll 1\%$
$[uc]_S[\bar{d}\bar{c}]_A - [uc]_A[\bar{d}\bar{c}]_S$	1^{+-}	2.7 – 3.1	4.40 ± 0.10	1.4	(40 – 63)%	< 1%
$[uc]_A[\bar{d}\bar{c}]_A$	1^{+-}	3.3 – 3.7	4.60 ± 0.10	1.7	(40 – 59)%	$\ll 1\%$
$[uc]_S[\bar{d}\bar{c}]_{\tilde{A}} - [uc]_{\tilde{A}}[\bar{d}\bar{c}]_S$	1^{+-}	3.3 – 3.7	4.60 ± 0.10	1.7	(40 – 59)%	$\ll 1\%$
$[uc]_{\tilde{A}}[\bar{d}\bar{c}]_A - [uc]_A[\bar{d}\bar{c}]_{\tilde{A}}$	1^{+-}	3.2 – 3.6	4.60 ± 0.10	1.7	(41 – 61)%	$\ll 1\%$
$[uc]_{\tilde{V}}[\bar{d}\bar{c}]_V + [uc]_V[\bar{d}\bar{c}]_{\tilde{V}}$	1^{+-}	3.7 – 4.1	5.25 ± 0.10	2.9	(41 – 60)%	$\ll 1\%$
$[uc]_V[\bar{d}\bar{c}]_V$	1^{+-}	5.1 – 5.9	6.00 ± 0.10	4.1	(41 – 60)%	$\ll 1\%$
$[uc]_P[\bar{d}\bar{c}]_V + [uc]_V[\bar{d}\bar{c}]_P$	1^{+-}	5.1 – 5.9	6.00 ± 0.10	4.1	(41 – 60)%	$\ll 1\%$
$[uc]_S[\bar{d}\bar{c}]_A + [uc]_A[\bar{d}\bar{c}]_S$	1^{++}	2.7 – 3.1	4.40 ± 0.10	1.4	(40 – 62)%	$\ll 1\%$
$[uc]_S[\bar{d}\bar{c}]_{\tilde{A}} + [uc]_{\tilde{A}}[\bar{d}\bar{c}]_S$	1^{++}	3.3 – 3.7	4.60 ± 0.10	1.7	(40 – 59)%	$\ll 1\%$
$[uc]_{\tilde{V}}[\bar{d}\bar{c}]_V - [uc]_V[\bar{d}\bar{c}]_{\tilde{V}}$	1^{++}	2.8 – 3.2	4.62 ± 0.10	1.8	(40 – 63)%	< 2%
$[uc]_{\tilde{A}}[\bar{d}\bar{c}]_A + [uc]_A[\bar{d}\bar{c}]_{\tilde{A}}$	1^{++}	4.6 – 5.3	5.73 ± 0.10	3.7	(40 – 60)%	$\ll 1\%$
$[uc]_P[\bar{d}\bar{c}]_V - [uc]_V[\bar{d}\bar{c}]_P$	1^{++}	5.1 – 5.9	6.00 ± 0.10	4.1	(40 – 60)%	$\ll 1\%$
$[uc]_A[\bar{d}\bar{c}]_A$	2^{++}	3.3 – 3.7	4.65 ± 0.10	1.8	(40 – 60)%	< 1%
$[uc]_V[\bar{d}\bar{c}]_V$	2^{++}	5.0 – 5.8	5.95 ± 0.10	4.0	(40 – 60)%	$\ll 1\%$

Table 5: The Borel windows, continuum threshold parameters, energy scales of the QCD spectral densities, pole contributions, and the contributions of the vacuum condensates of dimension 10 for the ground state $c\bar{c}u\bar{d}$ tetraquark states [57].

X_c	J^{PC}	$T^2(\text{GeV}^2)$	$\sqrt{s_0}(\text{GeV})$	$\mu(\text{GeV})$	pole	$ D(10) $
$[sc]_S[\bar{s}\bar{c}]_S$	0^{++}	$3.1 - 3.5$	4.65 ± 0.10	1.4	(40 – 61)%	$\ll 1\%$
$[sc]_A[\bar{s}\bar{c}]_A$	0^{++}	$3.1 - 3.5$	4.70 ± 0.10	1.5	(39 – 60)%	$\ll 1\%$
$[sc]_{\tilde{A}}[\bar{s}\bar{c}]_{\tilde{A}}$	0^{++}	$3.4 - 3.9$	4.75 ± 0.10	1.6	(39 – 61)%	$\ll 1\%$
$[sc]_V[\bar{s}\bar{c}]_V$	0^{++}	$4.0 - 4.5$	5.40 ± 0.10	2.8	(41 – 60)%	$\ll 1\%$
$[sc]_{\tilde{V}}[\bar{s}\bar{c}]_{\tilde{V}}$	0^{++}	$5.2 - 6.1$	6.05 ± 0.10	3.7	(40 – 61)%	$\ll 1\%$
$[sc]_P[\bar{s}\bar{c}]_P$	0^{++}	$5.2 - 6.1$	6.10 ± 0.10	3.8	(40 – 61)%	$\ll 1\%$
$[sc]_S[\bar{s}\bar{c}]_S^*$	0^{++}	$2.8 - 3.2$	4.50 ± 0.10	1.3	(39 – 61)%	$\ll 1\%$
$[sc]_A[\bar{s}\bar{c}]_A^*$	0^{++}	$2.7 - 3.1$	4.55 ± 0.10	1.3	(39 – 62)%	$\leq 1\%$
$[sc]_{\tilde{A}}[\bar{s}\bar{c}]_{\tilde{A}}^*$	0^{++}	$3.0 - 3.5$	4.60 ± 0.10	1.4	(39 – 62)%	$\ll 1\%$
$[sc]_V[\bar{s}\bar{c}]_V^*$	0^{++}	$3.6 - 4.1$	5.25 ± 0.10	2.6	(40 – 62)%	$\ll 1\%$
$[sc]_{\tilde{V}}[\bar{s}\bar{c}]_{\tilde{V}}^*$	0^{++}	$4.7 - 5.4$	5.86 ± 0.10	3.5	(41 – 60)%	$\ll 1\%$
$[sc]_P[\bar{s}\bar{c}]_P^*$	0^{++}	$4.8 - 5.6$	5.95 ± 0.10	3.7	(40 – 61)%	$\ll 1\%$
$[sc]_S[\bar{s}\bar{c}]_A - [sc]_A[\bar{s}\bar{c}]_S$	1^{+-}	$3.2 - 3.7$	4.70 ± 0.10	1.5	(39 – 61)%	$\ll 1\%$
$[sc]_A[\bar{s}\bar{c}]_A$	1^{+-}	$3.4 - 3.8$	4.76 ± 0.10	1.6	(41 – 60)%	$\ll 1\%$
$[sc]_S[\bar{s}\bar{c}]_{\tilde{A}} - [sc]_{\tilde{A}}[\bar{s}\bar{c}]_S$	1^{+-}	$3.4 - 3.9$	4.76 ± 0.10	1.6	(39 – 61)%	$\ll 1\%$
$[sc]_{\tilde{A}}[\bar{s}\bar{c}]_A - [sc]_A[\bar{s}\bar{c}]_{\tilde{A}}$	1^{+-}	$3.4 - 3.8$	4.76 ± 0.10	1.6	(40 – 60)%	$\ll 1\%$
$[sc]_{\tilde{V}}[\bar{s}\bar{c}]_V + [sc]_V[\bar{s}\bar{c}]_{\tilde{V}}$	1^{+-}	$4.0 - 4.5$	5.40 ± 0.10	2.8	(40 – 60)%	$\ll 1\%$
$[sc]_V[\bar{s}\bar{c}]_V$	1^{+-}	$5.4 - 6.3$	6.16 ± 0.10	3.8	(41 – 61)%	$\ll 1\%$
$[sc]_P[\bar{s}\bar{c}]_V + [sc]_V[\bar{s}\bar{c}]_P$	1^{+-}	$4.6 - 5.3$	5.70 ± 0.10	3.2	(41 – 61)%	$\ll 1\%$
$[sc]_S[\bar{s}\bar{c}]_A + [sc]_A[\bar{s}\bar{c}]_S$	1^{++}	$3.2 - 3.6$	4.70 ± 0.10	1.5	(41 – 61)%	$\ll 1\%$
$[sc]_S[\bar{s}\bar{c}]_{\tilde{A}} + [sc]_{\tilde{A}}[\bar{s}\bar{c}]_S$	1^{++}	$3.4 - 3.9$	4.76 ± 0.10	1.6	(39 – 60)%	$\ll 1\%$
$[sc]_{\tilde{V}}[\bar{s}\bar{c}]_V - [sc]_V[\bar{s}\bar{c}]_{\tilde{V}}$	1^{++}	$3.2 - 3.6$	4.86 ± 0.10	1.9	(40 – 61)%	$\ll 1\%$
$[sc]_{\tilde{A}}[\bar{s}\bar{c}]_A + [sc]_A[\bar{s}\bar{c}]_{\tilde{A}}$	1^{++}	$4.9 - 5.8$	5.93 ± 0.10	3.5	(39 – 61)%	$\ll 1\%$
$[sc]_P[\bar{s}\bar{c}]_V - [sc]_V[\bar{s}\bar{c}]_P$	1^{++}	$4.6 - 5.4$	5.70 ± 0.10	3.2	(39 – 61)%	$\ll 1\%$
$[sc]_A[\bar{s}\bar{c}]_A$	2^{++}	$3.5 - 4.0$	4.82 ± 0.10	1.8	(40 – 60)%	$\ll 1\%$
$[sc]_V[\bar{s}\bar{c}]_V$	2^{++}	$5.1 - 6.0$	6.05 ± 0.10	3.7	(40 – 61)%	$\ll 1\%$

Table 6: The Borel windows, continuum threshold parameters, energy scales of the QCD spectral densities, pole contributions, and contributions of the vacuum condensates of dimension 10 for the ground state $cs\bar{c}\bar{s}$ tetraquark states [361].

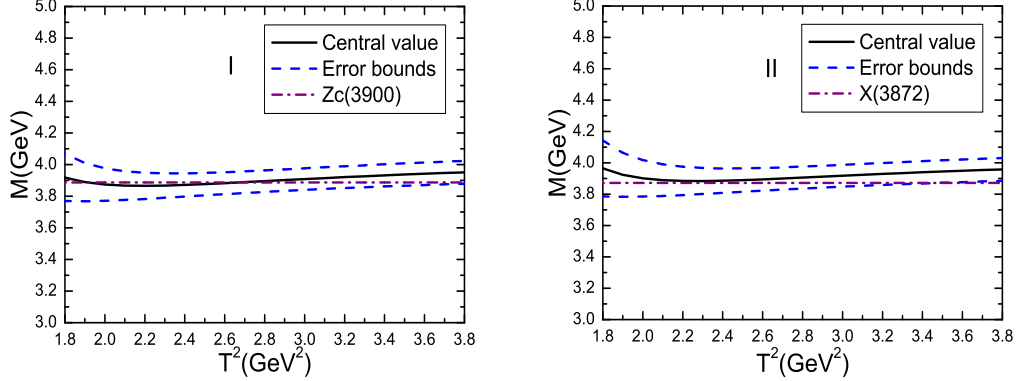


Figure 13: The masses of the $[uc]_S[\bar{d}\bar{c}]_A - [uc]_A[\bar{d}\bar{c}]_S$ (I) and $[uc]_S[\bar{d}\bar{c}]_A + [uc]_A[\bar{d}\bar{c}]_S$ (II) axialvector tetraquark states with variations of the Borel parameters T^2 .

After trial and error, we obtain the Borel windows, continuum threshold parameters, energy scales of the QCD spectral densities, pole contributions, and the contributions of the vacuum condensates of dimension 10, which are shown explicitly in Tables 5-6.

At the hadron side, the pole contributions are about (40 – 60)%, the pole dominance is well satisfied. It is more easy to obtain the pole contributions (40 – 60)% with the help of the modified energy scale formula. In Table 6, we provide two sets of data for the scalar tetraquark states, one set data is based on the continuum threshold parameters about $\sqrt{s_0} = M_X + 0.60 \pm 0.10$ GeV with the central values $\sqrt{s_0} < M_Y + 0.60$ GeV (the criterion is also adopted for the tetraquark states with the $J^{PC} = 1^{+-}, 1^{++}$ and 2^{++}), the other set data is based on the continuum threshold parameters about $\sqrt{s_0} = M_X + 0.55 \pm 0.10$ GeV with the central values $\sqrt{s_0} < M_Y + 0.55$ GeV, which will be characterized by the additional symbol * in Tables 6, 8 and 10.

At the QCD side, the contributions of the vacuum condensates of dimension 10 are $|D(10)| \leq 1\%$ or $\ll 1\%$ except for $|D(10)| < 2\%$ for the $[uc]_{\bar{V}}[\bar{d}\bar{c}]_V - [uc]_V[\bar{d}\bar{c}]_{\bar{V}}$ tetraquark state with the $J^{PC} = 1^{++}$, the convergent behavior of the operator product expansion is very good.

We take account of all the uncertainties of the input parameters and obtain the masses and pole residues of the scalar, axialvector and tensor hidden-charm tetraquark states, which are shown explicitly in Tables 7-8. From Tables 5-8, we could see clearly that the modified energy scale formula $\mu = \sqrt{M_{X/Y/Z}^2 - (2M_c)^2} - \kappa M_s$ is well satisfied. In Fig.13, we plot the masses of the $[uc]_S[\bar{d}\bar{c}]_A - [uc]_A[\bar{d}\bar{c}]_S$ and $[uc]_S[\bar{d}\bar{c}]_A + [uc]_A[\bar{d}\bar{c}]_S$ tetraquark states having the spin-parity $J^P = 1^+$ with variations of the Borel parameters at much larger ranges than the Borel widows as an example, there appear platforms in the Borel windows indeed.

In Tables 9-10, we present the possible assignments of the ground state hidden-charm tetraquark states, and revisit the assignments based on the tetraquark scenario. In Table 9, there are enough rooms to accommodate the $h_c(4000)$ and $\chi_{c1}(4010)$ in scenario of tetraquark states, as the central values of the predicted tetraquark masses happen to coincide with the experimental data from the LHCb collaboration [99]. We should bear in mind that the predictions were made **before** the experimental observation, therefore the calculations are robust [57]. While in the traditional charmonium scenario, the h'_c and χ'_{c1} have the masses 3956 MeV and 3953 MeV, respectively [98], there exist discrepancies about 50 – 60 MeV.

We suggest to study the two-body strong decays to diagnose those hidden-charm tetraquark

$Z_c(X_c)$	J^{PC}	$M_Z(\text{GeV})$	$\lambda_Z(\text{GeV}^5)$
$[uc]_S[\overline{dc}]_S$	0^{++}	3.88 ± 0.09	$(2.07 \pm 0.35) \times 10^{-2}$
$[uc]_A[\overline{dc}]_A$	0^{++}	3.95 ± 0.09	$(4.49 \pm 0.77) \times 10^{-2}$
$[uc]_{\tilde{A}}[\overline{dc}]_{\tilde{A}}$	0^{++}	3.98 ± 0.08	$(4.30 \pm 0.63) \times 10^{-2}$
$[uc]_V[\overline{dc}]_V$	0^{++}	4.65 ± 0.09	$(1.35 \pm 0.22) \times 10^{-1}$
$[uc]_{\tilde{V}}[\overline{dc}]_{\tilde{V}}$	0^{++}	5.35 ± 0.09	$(4.87 \pm 0.51) \times 10^{-1}$
$[uc]_P[\overline{dc}]_P$	0^{++}	5.49 ± 0.09	$(2.11 \pm 0.21) \times 10^{-1}$
$[uc]_S[\overline{dc}]_A - [uc]_A[\overline{dc}]_S$	1^{+-}	3.90 ± 0.08	$(2.09 \pm 0.33) \times 10^{-2}$
$[uc]_A[\overline{dc}]_A$	1^{+-}	4.02 ± 0.09	$(3.00 \pm 0.45) \times 10^{-2}$
$[uc]_S[\overline{dc}]_{\tilde{A}} - [uc]_{\tilde{A}}[\overline{dc}]_S$	1^{+-}	4.01 ± 0.09	$(3.02 \pm 0.45) \times 10^{-2}$
$[uc]_{\tilde{A}}[\overline{dc}]_A - [uc]_A[\overline{dc}]_{\tilde{A}}$	1^{+-}	4.02 ± 0.09	$(6.09 \pm 0.90) \times 10^{-2}$
$[uc]_{\tilde{V}}[\overline{dc}]_V + [uc]_V[\overline{dc}]_{\tilde{V}}$	1^{+-}	4.66 ± 0.10	$(1.18 \pm 0.21) \times 10^{-1}$
$[uc]_V[\overline{dc}]_V$	1^{+-}	5.46 ± 0.09	$(1.72 \pm 0.17) \times 10^{-1}$
$[uc]_P[\overline{dc}]_V + [uc]_V[\overline{dc}]_P$	1^{+-}	5.45 ± 0.09	$(1.87 \pm 0.19) \times 10^{-1}$
$[uc]_S[\overline{dc}]_A + [uc]_A[\overline{dc}]_S$	1^{++}	3.91 ± 0.08	$(2.10 \pm 0.34) \times 10^{-2}$
$[uc]_S[\overline{dc}]_{\tilde{A}} + [uc]_{\tilde{A}}[\overline{dc}]_S$	1^{++}	4.02 ± 0.09	$(3.01 \pm 0.45) \times 10^{-2}$
$[uc]_{\tilde{V}}[\overline{dc}]_V - [uc]_V[\overline{dc}]_{\tilde{V}}$	1^{++}	4.08 ± 0.09	$(3.67 \pm 0.67) \times 10^{-2}$
$[uc]_{\tilde{A}}[\overline{dc}]_A + [uc]_A[\overline{dc}]_{\tilde{A}}$	1^{++}	5.19 ± 0.09	$(2.12 \pm 0.24) \times 10^{-1}$
$[uc]_P[\overline{dc}]_V - [uc]_V[\overline{dc}]_P$	1^{++}	5.46 ± 0.09	$(1.89 \pm 0.19) \times 10^{-1}$
$[uc]_A[\overline{dc}]_A$	2^{++}	4.08 ± 0.09	$(4.67 \pm 0.68) \times 10^{-2}$
$[uc]_V[\overline{dc}]_V$	2^{++}	5.40 ± 0.09	$(2.32 \pm 0.25) \times 10^{-1}$

Table 7: The masses and pole residues of the ground state hidden-charm tetraquark states [57].

states [57, 361], for example,

$$\begin{aligned}
Z_c^\pm(1^{+-}) &\rightarrow \pi^\pm J/\psi, \pi^\pm \psi', \pi^\pm h_c, \rho^\pm \eta_c, (D\bar{D}^*)^\pm, (D^*\bar{D})^\pm, (D^*\bar{D}^*)^\pm, \\
Z_c^\pm(0^{++}) &\rightarrow \pi^\pm \eta_c, \pi^\pm \chi_{c1}, \rho^\pm J/\psi, \rho^\pm \psi', (D\bar{D})^\pm, (D^*\bar{D}^*)^\pm, \\
Z_c^\pm(1^{++}) &\rightarrow \pi^\pm \chi_{c1}, \rho^\pm J/\psi, \rho^\pm \psi', (D\bar{D}^*)^\pm, (D^*\bar{D})^\pm, (D^*\bar{D}^*)^\pm, \\
Z_c^\pm(2^{++}) &\rightarrow \pi^\pm \eta_c, \pi^\pm \chi_{c1}, \rho^\pm J/\psi, \rho^\pm \psi', (D\bar{D})^\pm, (D^*\bar{D}^*)^\pm, \tag{141}
\end{aligned}$$

$$\begin{aligned}
Z_c^0(1^{+-}) &\rightarrow \pi^0 J/\psi, \pi^0 \psi', \pi^0 h_c, \rho^0 \eta_c, (D\bar{D}^*)^0, (D^*\bar{D})^0, (D^*\bar{D}^*)^0, \\
Z_c^0(0^{++}) &\rightarrow \pi^0 \eta_c, \pi^0 \chi_{c1}, \rho^0 J/\psi, \rho^0 \psi', (D\bar{D})^0, (D^*\bar{D}^*)^0, \\
Z_c^0(1^{++}) &\rightarrow \pi^0 \chi_{c1}, \rho^0 J/\psi, \rho^0 \psi', (D\bar{D}^*)^0, (D^*\bar{D})^0, (D^*\bar{D}^*)^0, \\
Z_c^0(2^{++}) &\rightarrow \pi^0 \eta_c, \pi^0 \chi_{c1}, \rho^0 J/\psi, \rho^0 \psi', (D\bar{D})^0, (D^*\bar{D}^*)^0, \tag{142}
\end{aligned}$$

$$\begin{aligned}
X(1^{+-}) &\rightarrow \eta J/\psi, \eta \psi', \eta h_c, \omega \eta_c, (D\bar{D}^*)^0, (D^*\bar{D})^0, (D^*\bar{D}^*)^0, \\
X(0^{++}) &\rightarrow \eta \eta_c, \eta \chi_{c1}, \omega J/\psi, \omega \psi', (D\bar{D})^0, (D^*\bar{D}^*)^0, \\
X(1^{++}) &\rightarrow \eta \chi_{c1}, \omega J/\psi, \omega \psi', (D\bar{D}^*)^0, (D^*\bar{D})^0, (D^*\bar{D}^*)^0, \\
X(2^{++}) &\rightarrow \eta \eta_c, \eta \chi_{c1}, \omega J/\psi, \omega \psi', (D\bar{D})^0, (D^*\bar{D}^*)^0, \tag{143}
\end{aligned}$$

$$\begin{aligned}
X(1^{+-}) &\rightarrow \eta J/\psi, \eta \psi', \eta h_c, \phi \eta_c, D_s \bar{D}_s^*, D_s^* \bar{D}_s, D_s^* \bar{D}_s^*, \\
X(0^{++}) &\rightarrow \eta \eta_c, \eta \chi_{c1}, \phi J/\psi, \phi \psi', D_s \bar{D}_s, D_s^* \bar{D}_s^*, \\
X(1^{++}) &\rightarrow \eta \chi_{c1}, \phi J/\psi, \phi \psi', D_s \bar{D}_s^*, D_s^* \bar{D}_s, D_s^* \bar{D}_s^*, \\
X(2^{++}) &\rightarrow \eta \eta_c, \eta \chi_{c1}, \phi J/\psi, \phi \psi', D_s \bar{D}_s, D_s^* \bar{D}_s^*. \tag{144}
\end{aligned}$$

X_c	J^{PC}	$M_X(\text{GeV})$	$\lambda_X(\text{GeV}^5)$
$[sc]_S[\bar{s}\bar{c}]_S$	0^{++}	4.08 ± 0.09	$(3.18 \pm 0.52) \times 10^{-2}$
$[sc]_A[\bar{s}\bar{c}]_A$	0^{++}	4.13 ± 0.09	$(6.02 \pm 1.02) \times 10^{-2}$
$[sc]_{\bar{A}}[\bar{s}\bar{c}]_{\bar{A}}$	0^{++}	4.16 ± 0.09	$(5.83 \pm 0.87) \times 10^{-2}$
$[sc]_V[\bar{s}\bar{c}]_V$	0^{++}	4.82 ± 0.09	$(1.70 \pm 0.25) \times 10^{-1}$
$[sc]_{\bar{V}}[\bar{s}\bar{c}]_{\bar{V}}$	0^{++}	5.46 ± 0.10	$(5.37 \pm 0.58) \times 10^{-1}$
$[sc]_P[\bar{s}\bar{c}]_P$	0^{++}	5.54 ± 0.10	$(2.13 \pm 0.22) \times 10^{-1}$
$[sc]_S[\bar{s}\bar{c}]_{S^*}$	0^{++}	3.99 ± 0.09	$(2.41 \pm 0.42) \times 10^{-2}$
$[sc]_A[\bar{s}\bar{c}]_{A^*}$	0^{++}	4.04 ± 0.09	$(4.24 \pm 0.76) \times 10^{-2}$
$[sc]_{\bar{A}}[\bar{s}\bar{c}]_{\bar{A}^*}$	0^{++}	4.08 ± 0.08	$(4.39 \pm 0.69) \times 10^{-2}$
$[sc]_V[\bar{s}\bar{c}]_{V^*}$	0^{++}	4.70 ± 0.09	$(1.31 \pm 0.23) \times 10^{-1}$
$[sc]_{\bar{V}}[\bar{s}\bar{c}]_{\bar{V}^*}$	0^{++}	5.37 ± 0.11	$(4.41 \pm 0.47) \times 10^{-1}$
$[sc]_P[\bar{s}\bar{c}]_{P^*}$	0^{++}	5.47 ± 0.11	$(1.86 \pm 0.19) \times 10^{-1}$
$[sc]_S[\bar{s}\bar{c}]_A - [sc]_A[\bar{s}\bar{c}]_S$	1^{+-}	4.11 ± 0.10	$(2.91 \pm 0.48) \times 10^{-2}$
$[sc]_A[\bar{s}\bar{c}]_A$	1^{+-}	4.17 ± 0.08	$(3.65 \pm 0.55) \times 10^{-2}$
$[sc]_S[\bar{s}\bar{c}]_{\bar{A}} - [sc]_{\bar{A}}[\bar{s}\bar{c}]_S$	1^{+-}	4.17 ± 0.09	$(3.71 \pm 0.57) \times 10^{-2}$
$[sc]_{\bar{A}}[\bar{s}\bar{c}]_A - [sc]_A[\bar{s}\bar{c}]_{\bar{A}}$	1^{+-}	4.18 ± 0.09	$(7.50 \pm 1.12) \times 10^{-2}$
$[sc]_{\bar{V}}[\bar{s}\bar{c}]_V + [sc]_V[\bar{s}\bar{c}]_{\bar{V}}$	1^{+-}	4.82 ± 0.09	$(1.45 \pm 0.23) \times 10^{-1}$
$[sc]_V[\bar{s}\bar{c}]_V$	1^{+-}	5.57 ± 0.11	$(1.89 \pm 0.19) \times 10^{-1}$
$[sc]_P[\bar{s}\bar{c}]_V + [sc]_V[\bar{s}\bar{c}]_P$	1^{+-}	5.13 ± 0.10	$(1.33 \pm 0.16) \times 10^{-1}$
$[sc]_S[\bar{s}\bar{c}]_A + [sc]_A[\bar{s}\bar{c}]_S$	1^{++}	4.11 ± 0.09	$(2.88 \pm 0.46) \times 10^{-2}$
$[sc]_S[\bar{s}\bar{c}]_{\bar{A}} + [sc]_{\bar{A}}[\bar{s}\bar{c}]_S$	1^{++}	4.17 ± 0.09	$(3.67 \pm 0.57) \times 10^{-2}$
$[sc]_{\bar{V}}[\bar{s}\bar{c}]_V - [sc]_V[\bar{s}\bar{c}]_{\bar{V}}$	1^{++}	4.29 ± 0.09	$(5.49 \pm 0.92) \times 10^{-2}$
$[sc]_{\bar{A}}[\bar{s}\bar{c}]_A + [sc]_A[\bar{s}\bar{c}]_{\bar{A}}$	1^{++}	5.34 ± 0.10	$(2.52 \pm 0.30) \times 10^{-1}$
$[sc]_P[\bar{s}\bar{c}]_V - [sc]_V[\bar{s}\bar{c}]_P$	1^{++}	5.12 ± 0.10	$(1.33 \pm 0.17) \times 10^{-1}$
$[sc]_A[\bar{s}\bar{c}]_A$	2^{++}	4.24 ± 0.09	$(6.03 \pm 0.88) \times 10^{-2}$
$[sc]_V[\bar{s}\bar{c}]_V$	2^{++}	5.49 ± 0.11	$(2.43 \pm 0.26) \times 10^{-1}$

Table 8: The masses and pole residues of the ground state hidden-charm-hidden-strange tetraquark states [361].

$Z_c(X_c)$	J^{PC}	$M_{X/Z}(\text{GeV})$	Assignments	$Z'_c(X'_c)$
$[uc]_S[\overline{dc}]_S$	0^{++}	3.88 ± 0.09	? $X(3860)$	
$[uc]_A[\overline{dc}]_A$	0^{++}	3.95 ± 0.09	? $X(3915)$	
$[uc]_{\tilde{A}}[\overline{dc}]_{\tilde{A}}$	0^{++}	3.98 ± 0.08		
$[uc]_V[\overline{dc}]_V$	0^{++}	4.65 ± 0.09		
$[uc]_{\tilde{V}}[\overline{dc}]_{\tilde{V}}$	0^{++}	5.35 ± 0.09		
$[uc]_P[\overline{dc}]_P$	0^{++}	5.49 ± 0.09		
$[uc]_S[\overline{dc}]_A - [uc]_A[\overline{dc}]_S$	1^{+-}	3.90 ± 0.08	? $Z_c(3900)$? $Z_c(4430)$
$[uc]_A[\overline{dc}]_A$	1^{+-}	4.02 ± 0.09	? $Z_c(4020/4055)$? $Z_c(4600)$
$[uc]_S[\overline{dc}]_{\tilde{A}} - [uc]_{\tilde{A}}[\overline{dc}]_S$	1^{+-}	4.01 ± 0.09	? $Z_c(4020/4055)$? $Z_c(4600)$
$[uc]_{\tilde{A}}[\overline{dc}]_A - [uc]_A[\overline{dc}]_{\tilde{A}}$	1^{+-}	4.02 ± 0.09	? $Z_c(4020/4055)$? $Z_c(4600)$
$[uc]_{\tilde{V}}[\overline{dc}]_V + [uc]_V[\overline{dc}]_{\tilde{V}}$	1^{+-}	4.66 ± 0.10	? $Z_c(4600)$	
$[uc]_V[\overline{dc}]_V$	1^{+-}	5.46 ± 0.09		
$[uc]_P[\overline{dc}]_V + [uc]_V[\overline{dc}]_P$	1^{+-}	5.45 ± 0.09		
$[uc]_S[\overline{dc}]_A + [uc]_A[\overline{dc}]_S$	1^{++}	3.91 ± 0.08	? $X(3872)$	
$[uc]_S[\overline{dc}]_{\tilde{A}} + [uc]_{\tilde{A}}[\overline{dc}]_S$	1^{++}	4.02 ± 0.09	? $Z_c(4050)$	
$[uc]_{\tilde{V}}[\overline{dc}]_V - [uc]_V[\overline{dc}]_{\tilde{V}}$	1^{++}	4.08 ± 0.09	? $Z_c(4050)$	
$[uc]_{\tilde{A}}[\overline{dc}]_A + [uc]_A[\overline{dc}]_{\tilde{A}}$	1^{++}	5.19 ± 0.09		
$[uc]_P[\overline{dc}]_V - [uc]_V[\overline{dc}]_P$	1^{++}	5.46 ± 0.09		
$[uc]_A[\overline{dc}]_A$	2^{++}	4.08 ± 0.09	? $Z_c(4050)$	
$[uc]_V[\overline{dc}]_V$	2^{++}	5.40 ± 0.09		
$[uc]_A[\overline{dc}]_A$	1^{+-}	4.02 ± 0.09	? $h_c(4000)$	
$[uc]_S[\overline{dc}]_{\tilde{A}} - [uc]_{\tilde{A}}[\overline{dc}]_S$	1^{+-}	4.01 ± 0.09	? $h_c(4000)$	
$[uc]_{\tilde{A}}[\overline{dc}]_A - [uc]_A[\overline{dc}]_{\tilde{A}}$	1^{+-}	4.02 ± 0.09	? $h_c(4000)$	
$[uc]_S[\overline{dc}]_{\tilde{A}} + [uc]_{\tilde{A}}[\overline{dc}]_S$	1^{++}	4.02 ± 0.09	? $\chi_{c1}(4010)$	

Table 9: The possible assignments of the hidden-charm tetraquark states, the isospin limit is implied [57, 176, 361].

X_c	J^{PC}	$M_X(\text{GeV})$	Assignments	X'_c
$[sc]_S[\bar{s}\bar{c}]_S$	0^{++}	4.08 ± 0.09		
$[sc]_A[\bar{s}\bar{c}]_A$	0^{++}	4.13 ± 0.09		? $X(4700)$
$[sc]_{\tilde{A}}[\bar{s}\bar{c}]_{\tilde{A}}$	0^{++}	4.16 ± 0.09		? $X(4700)$
$[sc]_V[\bar{s}\bar{c}]_V$	0^{++}	4.82 ± 0.09		
$[sc]_{\tilde{V}}[\bar{s}\bar{c}]_{\tilde{V}}$	0^{++}	5.46 ± 0.10		
$[sc]_P[\bar{s}\bar{c}]_P$	0^{++}	5.54 ± 0.10		
$[sc]_S[\bar{s}\bar{c}]_S^*$	0^{++}	3.99 ± 0.09	? $X(3960)$? $X(4500)$
$[sc]_A[\bar{s}\bar{c}]_A^*$	0^{++}	4.04 ± 0.09		
$[sc]_{\tilde{A}}[\bar{s}\bar{c}]_{\tilde{A}}^*$	0^{++}	4.08 ± 0.08		
$[sc]_V[\bar{s}\bar{c}]_V^*$	0^{++}	4.70 ± 0.09	? $X(4700)$	
$[sc]_{\tilde{V}}[\bar{s}\bar{c}]_{\tilde{V}}^*$	0^{++}	5.37 ± 0.11		
$[sc]_P[\bar{s}\bar{c}]_P^*$	0^{++}	5.47 ± 0.11		
$[sc]_S[\bar{s}\bar{c}]_A - [sc]_A[\bar{s}\bar{c}]_S$	1^{+-}	4.11 ± 0.10		
$[sc]_A[\bar{s}\bar{c}]_A$	1^{+-}	4.17 ± 0.08		
$[sc]_S[\bar{s}\bar{c}]_{\tilde{A}} - [sc]_{\tilde{A}}[\bar{s}\bar{c}]_S$	1^{+-}	4.17 ± 0.09		
$[sc]_{\tilde{A}}[\bar{s}\bar{c}]_A - [sc]_A[\bar{s}\bar{c}]_{\tilde{A}}$	1^{+-}	4.18 ± 0.09		
$[sc]_{\tilde{V}}[\bar{s}\bar{c}]_V + [sc]_V[\bar{s}\bar{c}]_{\tilde{V}}$	1^{+-}	4.82 ± 0.09		
$[sc]_V[\bar{s}\bar{c}]_V$	1^{+-}	5.57 ± 0.11		
$[sc]_P[\bar{s}\bar{c}]_V + [sc]_V[\bar{s}\bar{c}]_P$	1^{+-}	5.13 ± 0.10		
$[sc]_S[\bar{s}\bar{c}]_A + [sc]_A[\bar{s}\bar{c}]_S$	1^{++}	4.11 ± 0.09	? $X(4140)$? $X(4685)$
$[sc]_S[\bar{s}\bar{c}]_{\tilde{A}} + [sc]_{\tilde{A}}[\bar{s}\bar{c}]_S$	1^{++}	4.17 ± 0.09	? $X(4140)$? $X(4685)$
$[sc]_{\tilde{V}}[\bar{s}\bar{c}]_V - [sc]_V[\bar{s}\bar{c}]_{\tilde{V}}$	1^{++}	4.29 ± 0.09	? $X(4274)$	
$[sc]_{\tilde{A}}[\bar{s}\bar{c}]_A + [sc]_A[\bar{s}\bar{c}]_{\tilde{A}}$	1^{++}	5.34 ± 0.10		
$[sc]_P[\bar{s}\bar{c}]_V - [sc]_V[\bar{s}\bar{c}]_P$	1^{++}	5.12 ± 0.10		
$[sc]_A[\bar{s}\bar{c}]_A$	2^{++}	4.24 ± 0.09		
$[sc]_V[\bar{s}\bar{c}]_V$	2^{++}	5.49 ± 0.11		

Table 10: The possible assignments of the hidden-charm-hidden-strange tetraquark states [361].

$Z_c(X_c)$	J^{PC}	$M_Z(\text{GeV})$	Assignments
$[uc]_S[\bar{s}\bar{c}]_S$	0^{++}	3.97 ± 0.09	
$[uc]_A[\bar{s}\bar{c}]_A$	0^{++}	4.04 ± 0.09	
$[uc]_{\bar{A}}[\bar{s}\bar{c}]_{\bar{A}}$	0^{++}	4.07 ± 0.08	
$[uc]_V[\bar{s}\bar{c}]_V$	0^{++}	4.74 ± 0.09	
$[uc]_{\bar{V}}[\bar{s}\bar{c}]_{\bar{V}}$	0^{++}	5.44 ± 0.09	
$[uc]_P[\bar{s}\bar{c}]_P$	0^{++}	5.58 ± 0.09	
$[uc]_S[\bar{s}\bar{c}]_{\bar{A}} - [uc]_A[\bar{s}\bar{c}]_S$	1^{+-}	3.99 ± 0.09	? $Z_{cs}(3985)$
$[uc]_A[\bar{s}\bar{c}]_A$	1^{+-}	4.11 ± 0.09	
$[uc]_S[\bar{s}\bar{c}]_{\bar{A}} - [uc]_{\bar{A}}[\bar{s}\bar{c}]_S$	1^{+-}	4.10 ± 0.09	? $Z_{cs}(4123)$
$[uc]_{\bar{A}}[\bar{s}\bar{c}]_A - [uc]_A[\bar{s}\bar{c}]_{\bar{A}}$	1^{+-}	4.11 ± 0.09	? $Z_{cs}(4123)$
$[uc]_{\bar{V}}[\bar{s}\bar{c}]_V + [uc]_V[\bar{s}\bar{c}]_{\bar{V}}$	1^{+-}	4.75 ± 0.10	
$[uc]_V[\bar{s}\bar{c}]_V$	1^{+-}	5.55 ± 0.09	
$[uc]_P[\bar{s}\bar{c}]_V + [uc]_V[\bar{s}\bar{c}]_P$	1^{+-}	5.54 ± 0.09	
$[uc]_S[\bar{s}\bar{c}]_A + [uc]_A[\bar{s}\bar{c}]_S$	1^{++}	3.99 ± 0.09	? $Z_{cs}(3985)$
$[uc]_S[\bar{s}\bar{c}]_{\bar{A}} + [uc]_{\bar{A}}[\bar{s}\bar{c}]_S$	1^{++}	4.11 ± 0.09	? $Z_{cs}(4123)$
$[uc]_{\bar{V}}[\bar{s}\bar{c}]_V - [uc]_V[\bar{s}\bar{c}]_{\bar{V}}$	1^{++}	4.17 ± 0.09	
$[uc]_{\bar{A}}[\bar{s}\bar{c}]_A + [uc]_A[\bar{s}\bar{c}]_{\bar{A}}$	1^{++}	5.28 ± 0.09	
$[uc]_P[\bar{s}\bar{c}]_V - [uc]_V[\bar{s}\bar{c}]_P$	1^{++}	5.55 ± 0.09	
$[uc]_A[\bar{s}\bar{c}]_A$	2^{++}	4.17 ± 0.09	
$[uc]_V[\bar{s}\bar{c}]_V$	2^{++}	5.49 ± 0.09	

Table 11: The possible assignments of the ground state hidden-charm tetraquark states with strangeness [163, 164].

The LHCb collaboration observed the $h_c(4000)$ and $\chi_{c1}(4010)$ in the $D^{*\pm}D^\mp$ mass spectrum [99], see the two-body strong decays of the Z_c^0 shown in Eq.(142).

As the $c\bar{c}q\bar{s}$ tetraquark states are concerned, we present the predictions based on the direct calculations plus light-flavor $SU(3)$ -breaking effects in Table 11 [163, 164]. In Ref.[163], we tentatively assign the $Z_c(4020/4025)$ as the $A\bar{A}$ -type hidden-charm tetraquark state with the $J^{PC} = 1^{+-}$ according to the analogous properties of the $Z_c(3900/3885)$ and $Z_{cs}(3985/4000)$, and study the $A\bar{A}$ -type tetraquark states without strange, with strange and with hidden-strange via the QCD sum rules in a consistent way. Then we study the hadronic coupling constants of the tetraquark states without strange and with strange via the QCD sum rules based on rigorous quark-hadron duality, and obtain the total decay widths,

$$\begin{aligned}
\Gamma_{Z_{cs}} &= 22.71 \pm 1.65 \text{ (or } \pm 6.60) \text{ MeV,} \\
\Gamma_{Z_c} &= 29.57 \pm 2.30 \text{ (or } \pm 9.20) \text{ MeV,}
\end{aligned}
\tag{145}$$

and suggest to search for the Z_{cs} state in the mass spectrum of the $h_c K$, $J/\psi K$, $\eta_c K^*$, $D^* \bar{D}_s^*$, $D_s^* \bar{D}^*$. Slightly later, the BESIII collaboration observed an evidence for the $Z_{cs}(4123)$ [162].

With the simple replacement,

$$c \rightarrow b, \tag{146}$$

we obtain the corresponding QCD sum rules for the hidden-bottom tetraquark states. And we would like to present the results from the QCD sum rules in Ref.[447].

In calculations, we use the energy scale formula $\mu = \sqrt{M_{X/Y/Z}^2 - (2M_b)^2}$ to determine the ideal energy scales of the QCD spectral densities and choose the continuum threshold parameters $\sqrt{s_0} = Z_b + 0.55 \pm 0.10 \text{ GeV}$ as a constraint to extract the masses and pole residues from the QCD sum rules. The predicted masses $10.61 \pm 0.09 \text{ GeV}$ and $10.62 \pm 0.09 \text{ GeV}$ for the 1^{+-} tetraquark states

Z_b	J^{PC}	$T^2(\text{GeV}^2)$	$\sqrt{s_0}(\text{GeV})$	$\mu(\text{GeV})$	pole	$ D(10) $
$[ub]_S[\overline{db}]_S$	0^{++}	7.0 – 8.0	11.16 ± 0.10	2.40	(44 – 66)%	$\leq 3\%$
$[ub]_A[\overline{db}]_A$	0^{++}	6.4 – 7.4	11.14 ± 0.10	2.30	(44 – 68)%	$\leq 11\%$
$[ub]_{\tilde{A}}[\overline{db}]_{\tilde{A}}$	0^{++}	7.2 – 8.2	11.17 ± 0.10	2.40	(45 – 66)%	$\leq 4\%$
$[ub]_{\tilde{V}}[\overline{db}]_{\tilde{V}}$	0^{++}	11.4 – 12.8	12.22 ± 0.10	5.40	(44 – 61)%	$\ll 1\%$
$[ub]_S[\overline{db}]_A - [ub]_A[\overline{db}]_S$	1^{+-}	7.0 – 8.0	11.16 ± 0.10	2.40	(44 – 66)%	$< 4\%$
$[ub]_A[\overline{db}]_A$	1^{+-}	7.1 – 8.1	11.17 ± 0.10	2.40	(44 – 65)%	$\leq 4\%$
$[ub]_{\tilde{A}}[\overline{db}]_A - [ub]_A[\overline{db}]_{\tilde{A}}$	1^{+-}	6.9 – 7.9	11.17 ± 0.10	2.40	(44 – 66)%	$\leq 7\%$
$[ub]_S[\overline{db}]_{\tilde{A}} - [ub]_{\tilde{A}}[\overline{db}]_S$	1^{+-}	7.1 – 8.1	11.17 ± 0.10	2.40	(44 – 66)%	$\leq 4\%$
$[ub]_S[\overline{db}]_A + [ub]_A[\overline{db}]_S$	1^{++}	7.1 – 8.1	11.18 ± 0.10	2.45	(44 – 65)%	$\leq 3\%$
$[ub]_{\tilde{V}}[\overline{db}]_V - [ub]_V[\overline{db}]_{\tilde{V}}$	1^{++}	6.8 – 7.8	11.19 ± 0.10	2.50	(44 – 66)%	$\leq 4\%$
$[ub]_{\tilde{A}}[\overline{db}]_A + [ub]_A[\overline{db}]_{\tilde{A}}$	1^{++}	9.7 – 11.1	11.99 ± 0.10	4.90	(44 – 63)%	$\ll 1\%$
$[ub]_A[\overline{db}]_A$	2^{++}	7.2 – 8.2	11.19 ± 0.10	2.50	(44 – 65)%	$< 4\%$

Table 12: The Borel parameters, continuum threshold parameters, energy scales of the QCD spectral densities, pole contributions, and the contributions of the vacuum condensates of dimension 10 for the ground state hidden-bottom tetraquark states.

Z_b	J^{PC}	$M_Z(\text{GeV})$	$\lambda_Z(\text{GeV}^5)$
$[ub]_S[\overline{db}]_S$	0^{++}	10.61 ± 0.09	$(1.10 \pm 0.17) \times 10^{-1}$
$[ub]_A[\overline{db}]_A$	0^{++}	10.60 ± 0.09	$(1.61 \pm 0.25) \times 10^{-1}$
$[ub]_{\tilde{A}}[\overline{db}]_{\tilde{A}}$	0^{++}	10.61 ± 0.09	$(1.81 \pm 0.27) \times 10^{-1}$
$[ub]_{\tilde{V}}[\overline{db}]_{\tilde{V}}$	0^{++}	11.66 ± 0.12	3.03 ± 0.31
$[ub]_S[\overline{db}]_A - [ub]_A[\overline{db}]_S$	1^{+-}	10.61 ± 0.09	$(1.08 \pm 0.16) \times 10^{-1}$
$[ub]_A[\overline{db}]_A$	1^{+-}	10.62 ± 0.09	$(1.07 \pm 0.16) \times 10^{-1}$
$[ub]_{\tilde{A}}[\overline{db}]_A - [ub]_A[\overline{db}]_{\tilde{A}}$	1^{+-}	10.62 ± 0.09	$(2.12 \pm 0.31) \times 10^{-1}$
$[ub]_S[\overline{db}]_{\tilde{A}} - [ub]_{\tilde{A}}[\overline{db}]_S$	1^{+-}	10.62 ± 0.09	$(1.08 \pm 0.16) \times 10^{-1}$
$[ub]_S[\overline{db}]_A + [ub]_A[\overline{db}]_S$	1^{++}	10.63 ± 0.09	$(1.17 \pm 0.17) \times 10^{-1}$
$[ub]_{\tilde{V}}[\overline{db}]_V - [ub]_V[\overline{db}]_{\tilde{V}}$	1^{++}	10.63 ± 0.09	$(1.22 \pm 0.20) \times 10^{-1}$
$[ub]_{\tilde{A}}[\overline{db}]_A + [ub]_A[\overline{db}]_{\tilde{A}}$	1^{++}	11.45 ± 0.14	$(8.52 \pm 1.02) \times 10^{-1}$
$[ub]_A[\overline{db}]_A$	2^{++}	10.65 ± 0.09	$(1.72 \pm 0.24) \times 10^{-1}$

Table 13: The masses and pole residues of the ground state hidden-bottom tetraquark states.

supports assigning the $Z_b(10610)$ and $Z_b(10650)$ to be the axialvector hidden-bottom tetraquark states with the $J^{PC} = 1^{+-}$, more theoretical and experimental works are still needed to assign the $Z_b(10610)$ and $Z_b(10650)$ unambiguously according to the partial decay widths.

5.2 Tetraquark states with the first radial excitation

In this sub-section, we would like to study the first radial excitations of the hidden-charm tetraquark states and make possible assignments of the exotic states. In Ref.[448], M. S. Maior de Sousa and R. Rodrigues da Silva suggest a theoretical scheme to study double pole QCD sum rules, and study the quarkonia $\rho(1S, 2S)$, $\psi(1S, 2S)$, $\Upsilon(1S, 2S)$ and $\psi_t(1S, 2S)$, the predicted hadron masses are not good enough, they adopt the experimental masses except for the $\psi_t(1S, 2S)$ to study the decay constants. In Ref.[174], we extend this scheme to study the $Z_c(3900)$ and $Z_c(4430)$ as the ground state and first radial excitation, respectively, and observed that it is impossible to reproduce the experimental masses at the same energy scale, just as in the case of the $\rho(1S, 2S)$, $\psi(1S, 2S)$ and $\Upsilon(1S, 2S)$ [448], we should resort to the energy scale formula, see Eq.(100), to choose the optimal energy scales independently.

In the following, we write down the correlation functions $\Pi_{\mu\nu}(p)$ and $\Pi_{\mu\nu\alpha\beta}(p)$ [176],

$$\begin{aligned}\Pi_{\mu\nu}(p) &= i \int d^4x e^{ip \cdot x} \langle 0 | T \{ J_\mu(x) J_\nu^\dagger(0) \} | 0 \rangle, \\ \Pi_{\mu\nu\alpha\beta}(p) &= i \int d^4x e^{ip \cdot x} \langle 0 | T \{ J_{\mu\nu}(x) J_{\alpha\beta}^\dagger(0) \} | 0 \rangle,\end{aligned}\quad (147)$$

where $J_\mu(x) = J_\mu^1(x)$, $J_\mu^2(x)$, $J_\mu^3(x)$, and $J_\mu^1(x) = J_{-\mu}^{SA}(x)$, $J_\mu^2(x) = J_{-\mu}^{\tilde{A}A}(x)$, $J_\mu^3(x) = J_{-\mu}^{\tilde{V}V}(x)$ and $J_{\mu\nu}(x) = J_{-\mu\nu}^{AA}(x)$, see Eq.(118).

At the hadron side, we insert a complete set of intermediate hadronic states with the same quantum numbers as the currents $J_\mu(x)$ and $J_{\mu\nu}(x)$ into the correlation functions $\Pi_{\mu\nu}(p)$ and $\Pi_{\mu\nu\alpha\beta}(p)$ to obtain the hadronic representation [333, 334], and isolate the ground state hidden-charm tetraquark contributions,

$$\begin{aligned}\Pi_{\mu\nu}(p) &= \frac{\lambda_Z^2}{m_Z^2 - p^2} \left(-g_{\mu\nu} + \frac{p_\mu p_\nu}{p^2} \right) + \dots \\ &= \Pi_Z(p^2) \left(-g_{\mu\nu} + \frac{p_\mu p_\nu}{p^2} \right) + \dots, \\ \Pi_{\mu\nu\alpha\beta}(p) &= \frac{\tilde{\lambda}_Z^2}{m_Z^2 - p^2} (p^2 g_{\mu\alpha} g_{\nu\beta} - p^2 g_{\mu\beta} g_{\nu\alpha} - g_{\mu\alpha} p_\nu p_\beta - g_{\nu\beta} p_\mu p_\alpha + g_{\mu\beta} p_\nu p_\alpha + g_{\nu\alpha} p_\mu p_\beta) \\ &\quad + \frac{\tilde{\lambda}_Y^2}{m_Y^2 - p^2} (-g_{\mu\alpha} p_\nu p_\beta - g_{\nu\beta} p_\mu p_\alpha + g_{\mu\beta} p_\nu p_\alpha + g_{\nu\alpha} p_\mu p_\beta) + \dots \\ &= \Pi_Z(p^2) (p^2 g_{\mu\alpha} g_{\nu\beta} - p^2 g_{\mu\beta} g_{\nu\alpha} - g_{\mu\alpha} p_\nu p_\beta - g_{\nu\beta} p_\mu p_\alpha + g_{\mu\beta} p_\nu p_\alpha + g_{\nu\alpha} p_\mu p_\beta) \\ &\quad + \Pi_Y(p^2) (-g_{\mu\alpha} p_\nu p_\beta - g_{\nu\beta} p_\mu p_\alpha + g_{\mu\beta} p_\nu p_\alpha + g_{\nu\alpha} p_\mu p_\beta),\end{aligned}\quad (149)$$

where the Z represents the axialvector tetraquark states, the Y represents the vector tetraquark states, the λ_Z , λ_Z and $\tilde{\lambda}_Y$ are the pole residues defined by,

$$\begin{aligned}\langle 0 | J_\mu(0) | Z_c(p) \rangle &= \lambda_Z \varepsilon_\mu, \\ \langle 0 | J_{\mu\nu}(0) | Z_c(p) \rangle &= \tilde{\lambda}_Z \varepsilon_{\mu\nu\alpha\beta} \varepsilon^\alpha p^\beta, \\ \langle 0 | J_{\mu\nu}(0) | Y(p) \rangle &= \tilde{\lambda}_Y (\varepsilon_\mu p_\nu - \varepsilon_\nu p_\mu),\end{aligned}\quad (150)$$

the antisymmetric tensor $\varepsilon_{0123} = -1$, the $\varepsilon_\mu(\lambda, p)$ are the polarization vectors.

Then we calculate all the Feynman diagrams in performing the operator product expansion to obtain the QCD spectral representations, and perform out the Borel transformation to get the QCD sum rules:

$$\lambda_Z^2 \exp\left(-\frac{M_Z^2}{T^2}\right) = \int_{4m_c^2}^{s_0} ds \rho_{QCD}(s) \exp\left(-\frac{s}{T^2}\right), \quad (151)$$

We derive Eq.(151) in regard to $\tau = \frac{1}{T^2}$, then obtain the tetraquark masses,

$$M_Z^2 = -\frac{\int_{4m_c^2}^{s_0} ds \frac{d}{d\tau} \rho(s) e^{-\tau s}}{\int_{4m_c^2}^{s_0} ds \rho_{QCD}(s) e^{-\tau s}}. \quad (152)$$

Thereafter, we will refer the QCD sum rules in Eq.(151) and Eq.(152) as QCDSR I.

If we take into account the contributions of the first radially excited tetraquark states Z'_c in the hadronic representation, we can obtain the QCD sum rules,

$$\lambda_Z^2 \exp\left(-\frac{M_Z^2}{T^2}\right) + \lambda_{Z'}^2 \exp\left(-\frac{M_{Z'}^2}{T^2}\right) = \int_{4m_c^2}^{s'_0} ds \rho_{QCD}(s) \exp\left(-\frac{s}{T^2}\right), \quad (153)$$

where the s'_0 is continuum threshold parameter, then we introduce the notations $\tau = \frac{1}{T^2}$, $D^n = \left(-\frac{d}{d\tau}\right)^n$, and resort to the subscripts 1 and 2 to represent the ground state tetraquark state Z_c and the first radially excited tetraquark state Z'_c respectively for simplicity. We rewrite the QCD sum rules as

$$\lambda_1^2 \exp(-\tau M_1^2) + \lambda_2^2 \exp(-\tau M_2^2) = \Pi_{QCD}(\tau), \quad (154)$$

here we introduce the subscript QCD to represent the QCD representation. We derive the QCD sum rules in Eq.(154) in regard to τ to obtain

$$\lambda_1^2 M_1^2 \exp(-\tau M_1^2) + \lambda_2^2 M_2^2 \exp(-\tau M_2^2) = D\Pi_{QCD}(\tau). \quad (155)$$

From Eqs.(154)-(155), we obtain the QCD sum rules,

$$\lambda_i^2 \exp(-\tau M_i^2) = \frac{(D - M_j^2) \Pi_{QCD}(\tau)}{M_i^2 - M_j^2}, \quad (156)$$

where the indexes $i \neq j$. Let us derive the QCD sum rules in Eq.(156) in regard to τ to obtain

$$\begin{aligned} M_i^2 &= \frac{(D^2 - M_j^2 D) \Pi_{QCD}(\tau)}{(D - M_j^2) \Pi_{QCD}(\tau)}, \\ M_i^4 &= \frac{(D^3 - M_j^2 D^2) \Pi_{QCD}(\tau)}{(D - M_j^2) \Pi_{QCD}(\tau)}. \end{aligned} \quad (157)$$

The squared masses M_i^2 satisfy the equation,

$$M_i^4 - bM_i^2 + c = 0, \quad (158)$$

where

$$\begin{aligned} b &= \frac{D^3 \otimes D^0 - D^2 \otimes D}{D^2 \otimes D^0 - D \otimes D}, \\ c &= \frac{D^3 \otimes D - D^2 \otimes D^2}{D^2 \otimes D^0 - D \otimes D}, \\ D^j \otimes D^k &= D^j \Pi_{QCD}(\tau) D^k \Pi_{QCD}(\tau), \end{aligned} \quad (159)$$

the indexes $i = 1, 2$ and $j, k = 0, 1, 2, 3$. Finally we solve above equation analytically to obtain two solutions [448, 174],

$$M_1^2 = \frac{b - \sqrt{b^2 - 4c}}{2}, \quad (160)$$

$$M_2^2 = \frac{b + \sqrt{b^2 - 4c}}{2}. \quad (161)$$

Thereafter, we will denote the QCD sum rules in Eq.(153) and Eqs.(160)-(161) as QCDSR II. In calculations, we observe that if we specify the energy scales of the spectral densities in the QCD representation, only one solution satisfies the energy scale formula $\mu = \sqrt{M_{X/Y/Z}^2 - (2\mathbb{M}_c)^2}$ in the QCDSR II, we have to abandon the other solution, i.e. the mass M_1 (M_Z). It is the unique feature of our works [174, 176], which is in contrast to Ref.[448].

The Okubo-Zweig-Iizuka supper-allowed decays

$$\begin{aligned} Z_c &\rightarrow J/\psi\pi, \\ Z'_c &\rightarrow \psi'\pi \\ Z''_c &\rightarrow \psi''\pi, \end{aligned} \quad (162)$$

are expected to take place easily. The energy gaps maybe have the relations $M_{Z'} - M_Z = m_{\psi'} - m_{J/\psi}$ and $M_{Z''} - M_{Z'} = m_{\psi''} - m_{\psi'}$. The charmonium masses are $m_{J/\psi} = 3.0969$ GeV, $m_{\psi'} = 3.686097$ GeV and $m_{\psi''} = 4.039$ GeV from the Particle Data Group [347], $m_{\psi'} - m_{J/\psi} = 0.59$ GeV, $m_{\psi''} - m_{J/\psi} = 0.94$ GeV, we can choose the continuum threshold parameters to be $\sqrt{s_0} = M_Z + 0.59$ GeV and $\sqrt{s'_0} = M_Z + 0.95$ GeV tentatively and vary the continuum threshold parameters and Borel parameters to satisfy the following four criteria in Sub-Sect 5.1.

After trial and error, we obtain the continuum threshold parameters, Borel windows, best energy scales, and the contributions of the ground states for the QCDSR I, see Table 14. In Table 14, we write the continuum threshold parameters as $s_0 = 21.0 \pm 1.0$ GeV² rather than as $s_0 = (4.58 \pm 0.11$ GeV)² for the $[uc]_{\bar{A}}[\bar{d}\bar{c}]_A - [uc]_A[\bar{d}\bar{c}]_{\bar{A}}$ and $[uc]_A[\bar{d}\bar{c}]_A$ tetraquark states to remain the same form as in Ref.[443]. Again we obtain the parameters for the QCDSR II using trial and error, see Table 15. We take the energy scale formula $\mu = \sqrt{M_{X/Y/Z}^2 - (2\mathbb{M}_c)^2}$ to obtain the ideal energy scales of the spectral densities [174, 176].

From Tables 14-15, we can see clearly that the contributions of the single-pole terms are about (40 – 60)% for the QCDSR I, the contributions of the two-pole terms are about (70 – 80)% for the QCDSR II, which satisfy the pole dominance very well. In the QCDSR II, the contributions of the ground states are about (30 – 45)%, which are much less than the ground state contributions in the QCDSR I, we prefer the QCDSR I for the ground states.

We take into account all the uncertainties, and obtain the masses and pole residues, which are shown in Tables 16-17. From those Tables, we can see that the ground state tetraquark masses from the QCDSR I and the radially excited tetraquark masses from the QCDSR II satisfy the energy scale formula $\mu = \sqrt{M_{X/Y/Z}^2 - (2\mathbb{M}_c)^2}$, where the updated value of the effective c -quark mass $\mathbb{M}_c = 1.82$ GeV is adopted [443]. In Table 17, we also present the central values of the ground state masses and pole residues extracted from the QCDSR II at the same energy scales. If we examine Table 17, we would observe the ground state masses cannot satisfy the energy scale formula, and should be discarded.

For example, in Fig.14, we plot the ground state masses from the QCDSR I and the first radially excited tetraquark masses from the QCDSR II with variations of the Borel parameters for the $[uc]_S[\bar{d}\bar{c}]_A - [uc]_A[\bar{d}\bar{c}]_S$ and $[uc]_{\bar{A}}[\bar{d}\bar{c}]_A - [uc]_A[\bar{d}\bar{c}]_{\bar{A}}$ states. From the figure, we observed that there indeed appear very flat platforms in the Borel windows.

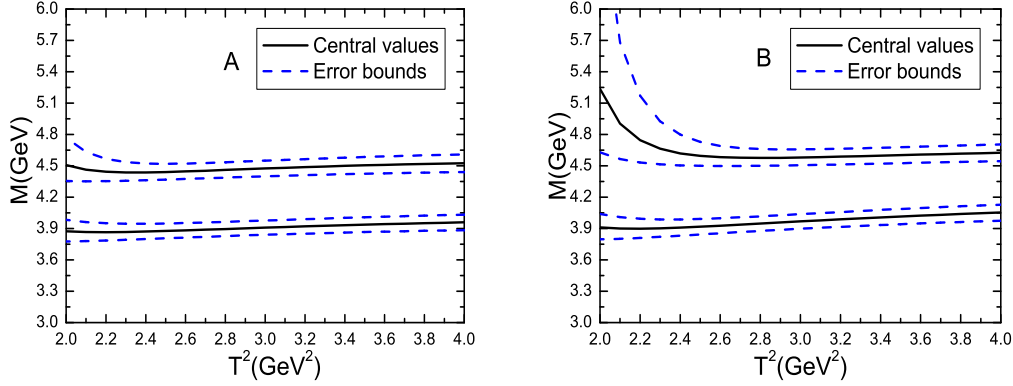


Figure 14: The masses with variations of the Borel parameters T^2 for the axialvector hidden-charm tetraquark states, the A and B represent the $[uc]_S[d\bar{c}]_A - [uc]_A[d\bar{c}]_S$, and $[uc]_{\bar{A}}[d\bar{c}]_A - [uc]_A[d\bar{c}]_{\bar{A}}$ tetraquark states, respectively.

Z_c	$T^2(\text{GeV}^2)$	s_0	$\mu(\text{GeV})$	pole
$[uc]_S[d\bar{c}]_A - [uc]_A[d\bar{c}]_S$	2.7 – 3.1	$(4.4 \pm 0.1 \text{ GeV})^2$	1.4	(40 – 63)%
$[uc]_{\bar{A}}[d\bar{c}]_A - [uc]_A[d\bar{c}]_{\bar{A}}$	3.2 – 3.6	$21.0 \pm 1.0 \text{ GeV}^2$	1.7	(40 – 60)%
$[uc]_{\bar{V}}[d\bar{c}]_V + [uc]_V[d\bar{c}]_{\bar{V}}$	3.7 – 4.1	$(5.25 \pm 0.10 \text{ GeV})^2$	2.9	(41 – 60)%
$[uc]_A[d\bar{c}]_A$	3.2 – 3.6	$21.0 \pm 1.0 \text{ GeV}^2$	1.7	(41 – 61)%

Table 14: The Borel parameters, continuum threshold parameters, energy scales of the QCD spectral densities and pole contributions for the QCDSR I.

We present the possible assignments explicitly in Table 9. The predicted mass $M_Z = 4.47 \pm 0.09 \text{ GeV}$ for the 2S tetraquark state $[uc]_S[d\bar{c}]_A - [uc]_A[d\bar{c}]_S$ exhibits very good agreement with the experimental data $(4475 \pm 7_{-25}^{+15}) \text{ MeV}$ from the LHCb collaboration [171], which is in favor of assigning the $Z_c(4430)$ as the first radial excitation of the $[uc]_S[d\bar{c}]_A - [uc]_A[d\bar{c}]_S$ with the $J^{PC} = 1^{+-}$ [174, 176].

The predicted mass $M_Z = 4.60 \pm 0.09 \text{ GeV}$ for the 2S tetraquark state $[uc]_{\bar{A}}[d\bar{c}]_A - [uc]_A[d\bar{c}]_{\bar{A}}$ and $M_Z = 4.58 \pm 0.09 \text{ GeV}$ for the 2S tetraquark state $[uc]_A[d\bar{c}]_A$ both exhibit very good agreement with the experimental data 4600 MeV from the LHCb collaboration [175], and the predicted mass $M_Z = 4.66 \pm 0.10 \text{ GeV}$ for the ground state $[uc]_{\bar{V}}[d\bar{c}]_V + [uc]_V[d\bar{c}]_{\bar{V}}$ is also compatible with the experimental data. In summary, there are three tetraquark state candidates with $J^{PC} = 1^{+-}$ for the $Z_c(4600)$.

The scheme of the QCDSR II and its modification have been applied extensively to study the

$Z_c + Z'_c$	$T^2(\text{GeV}^2)$	s_0	$\mu(\text{GeV})$	pole (Z_c)
$[uc]_S[d\bar{c}]_A - [uc]_A[d\bar{c}]_S$	2.7 – 3.1	$(4.85 \pm 0.10 \text{ GeV})^2$	2.6	(72 – 88)% ((35 – 52)%)
$[uc]_{\bar{A}}[d\bar{c}]_A - [uc]_A[d\bar{c}]_{\bar{A}}$	3.2 – 3.6	$(4.95 \pm 0.10 \text{ GeV})^2$	2.8	(64 – 80)% ((30 – 44)%)
$[uc]_A[d\bar{c}]_A$	3.2 – 3.6	$(4.95 \pm 0.10 \text{ GeV})^2$	2.8	(64 – 81)% ((29 – 43)%)

Table 15: The Borel parameters, continuum threshold parameters, energy scales of the QCD spectral densities and pole contributions for the QCDSR II.

Z_c	$ S_{uc}, S_{d\bar{c}}; S\rangle$	$M_Z(\text{GeV})$	$\lambda_Z(\text{GeV}^5)$
$[uc]_S[d\bar{c}]_A - [uc]_A[d\bar{c}]_S$	$ 0, 1; 1\rangle - 1, 0; 1\rangle$	3.90 ± 0.08	$(2.09 \pm 0.33) \times 10^{-2}$
$[uc]_{\bar{A}}[d\bar{c}]_A - [uc]_A[d\bar{c}]_{\bar{A}}$	$ 1^+, 1; 1\rangle - 1, 1^+; 1\rangle$	4.01 ± 0.09	$(5.96 \pm 0.94) \times 10^{-2}$
$[uc]_{\bar{V}}[d\bar{c}]_V + [uc]_V[d\bar{c}]_{\bar{V}}$	$ 1^-, 1; 1\rangle + 1, 1^-; 1\rangle$	4.66 ± 0.10	$(1.18 \pm 0.22) \times 10^{-1}$
$[uc]_A[d\bar{c}]_A$	$ 1, 1; 1\rangle$	4.00 ± 0.09	$(2.91 \pm 0.46) \times 10^{-2}$

Table 16: The masses and pole residues of the ground states Z_c from the QCDSR I, where the superscripts \pm represent the positive and negative parity components of the tensor diquarks, respectively.

$Z_c + Z'_c$	$M_Z(\text{GeV})$	$\lambda_Z(\text{GeV}^5)$	$M_{Z'}(\text{GeV})$	$\lambda_{Z'}(\text{GeV}^5)$
$[uc]_S[d\bar{c}]_A - [uc]_A[d\bar{c}]_S$	3.81	1.77×10^{-2}	4.47 ± 0.09	$(6.02 \pm 0.80) \times 10^{-2}$
$[uc]_{\bar{A}}[d\bar{c}]_A - [uc]_A[d\bar{c}]_{\bar{A}}$	3.78	3.94×10^{-2}	4.60 ± 0.09	$(1.35 \pm 0.18) \times 10^{-1}$
$[uc]_A[d\bar{c}]_A$	3.73	1.76×10^{-2}	4.58 ± 0.09	$(6.55 \pm 0.85) \times 10^{-2}$

Table 17: The masses and pole residues of the 1S states Z_c and 2S states Z'_c from the QCDSR II.

2S tetraquark states, such as the $Z_c(4430)$ [174, 176, 177, 449, 450], $Z_c(4600)$ [176, 177], $X(4500)$ (as the 2S state of the $X(3900)$) [451, 452], $X(4685)$ (as the 2S state of the $X(4140)$) [453], and $\Lambda_c(2S)$ and $\Xi_c(2S)$ [454], etc.

5.3 Tetraquark states with negative parity

In previous subsection, we study the hidden-heavy tetraquark states with the positive parity, in this subsection, we would like to study the hidden-heavy tetraquark states with the negative parity. Again we choose the diquarks without explicit P-waves as the elementary building blocks, for detailed discussions the diquark operators, see the beginning of the previous subsection. Compared to the vector tetraquark states, it is easy to analyze the pseudoscalar tetraquark states, and we would like present the results directly.

At first, let us write down the correlation functions $\Pi_{\mu\nu}(p)$ and $\Pi_{\mu\nu\alpha\beta}(p)$,

$$\begin{aligned}
\Pi_{\mu\nu}(p) &= i \int d^4x e^{ip \cdot x} \langle 0 | T \{ J_\mu(x) J_\nu^\dagger(0) \} | 0 \rangle, \\
\Pi_{\mu\nu\alpha\beta}(p) &= i \int d^4x e^{ip \cdot x} \langle 0 | T \{ J_{\mu\nu}(x) J_{\alpha\beta}^\dagger(0) \} | 0 \rangle,
\end{aligned} \tag{163}$$

where the currents

$$\begin{aligned}
J_\mu(x) &= J_{-, \mu}^{PA}(x), J_{+, \mu}^{PA}(x), J_{-, \mu}^{SV}(x), J_{+, \mu}^{SV}(x), J_{-, \mu}^{\tilde{V}A}(x), J_{+, \mu}^{\tilde{V}A}(x), J_{-, \mu}^{\tilde{A}V}(x), J_{+, \mu}^{\tilde{A}V}(x), \\
J_{\mu\nu}(x) &= J_{-, \mu\nu}^{S\tilde{V}}(x), J_{+, \mu\nu}^{S\tilde{V}}(x), J_{-, \mu\nu}^{P\tilde{A}}(x), J_{+, \mu\nu}^{P\tilde{A}}(x), J_{-, \mu\nu}^{AA}(x),
\end{aligned} \tag{164}$$

$$\begin{aligned}
J_{-,\mu}^{PA}(x) &= \frac{\varepsilon^{ijk}\varepsilon^{imn}}{\sqrt{2}} \left[u_j^T(x) C c_k(x) \bar{d}_m(x) \gamma_\mu C \bar{c}_n^T(x) - u_j^T(x) C \gamma_\mu c_k(x) \bar{d}_m(x) C \bar{c}_n^T(x) \right], \\
J_{+,\mu}^{PA}(x) &= \frac{\varepsilon^{ijk}\varepsilon^{imn}}{\sqrt{2}} \left[u_j^T(x) C c_k(x) \bar{d}_m(x) \gamma_\mu C \bar{c}_n^T(x) + u_j^T(x) C \gamma_\mu c_k(x) \bar{d}_m(x) C \bar{c}_n^T(x) \right], \\
J_{-,\mu}^{SV}(x) &= \frac{\varepsilon^{ijk}\varepsilon^{imn}}{\sqrt{2}} \left[u_j^T(x) C \gamma_5 c_k(x) \bar{d}_m(x) \gamma_5 \gamma_\mu C \bar{c}_n^T(x) + u_j^T(x) C \gamma_\mu \gamma_5 c_k(x) \bar{d}_m(x) \gamma_5 C \bar{c}_n^T(x) \right], \\
J_{+,\mu}^{SV}(x) &= \frac{\varepsilon^{ijk}\varepsilon^{imn}}{\sqrt{2}} \left[u_j^T(x) C \gamma_5 c_k(x) \bar{d}_m(x) \gamma_5 \gamma_\mu C \bar{c}_n^T(x) - u_j^T(x) C \gamma_\mu \gamma_5 c_k(x) \bar{d}_m(x) \gamma_5 C \bar{c}_n^T(x) \right],
\end{aligned} \tag{165}$$

$$\begin{aligned}
J_{-,\mu}^{\tilde{V}A}(x) &= \frac{\varepsilon^{ijk}\varepsilon^{imn}}{\sqrt{2}} \left[u_j^T(x) C \sigma_{\mu\nu} c_k(x) \bar{d}_m(x) \gamma^\nu C \bar{c}_n^T(x) - u_j^T(x) C \gamma^\nu c_k(x) \bar{d}_m(x) \sigma_{\mu\nu} C \bar{c}_n^T(x) \right], \\
J_{+,\mu}^{\tilde{V}A}(x) &= \frac{\varepsilon^{ijk}\varepsilon^{imn}}{\sqrt{2}} \left[u_j^T(x) C \sigma_{\mu\nu} c_k(x) \bar{d}_m(x) \gamma^\nu C \bar{c}_n^T(x) + u_j^T(x) C \gamma^\nu c_k(x) \bar{d}_m(x) \sigma_{\mu\nu} C \bar{c}_n^T(x) \right], \\
J_{-,\mu}^{\tilde{A}V}(x) &= \frac{\varepsilon^{ijk}\varepsilon^{imn}}{\sqrt{2}} \left[u_j^T(x) C \sigma_{\mu\nu} \gamma_5 c_k(x) \bar{d}_m(x) \gamma_5 \gamma^\nu C \bar{c}_n^T(x) + u_j^T(x) C \gamma^\nu \gamma_5 c_k(x) \bar{d}_m(x) \gamma_5 \sigma_{\mu\nu} C \bar{c}_n^T(x) \right], \\
J_{+,\mu}^{\tilde{A}V}(x) &= \frac{\varepsilon^{ijk}\varepsilon^{imn}}{\sqrt{2}} \left[u_j^T(x) C \sigma_{\mu\nu} \gamma_5 c_k(x) \bar{d}_m(x) \gamma_5 \gamma^\nu C \bar{c}_n^T(x) - u_j^T(x) C \gamma^\nu \gamma_5 c_k(x) \bar{d}_m(x) \gamma_5 \sigma_{\mu\nu} C \bar{c}_n^T(x) \right],
\end{aligned} \tag{166}$$

$$\begin{aligned}
J_{-,\mu\nu}^{S\tilde{V}}(x) &= \frac{\varepsilon^{ijk}\varepsilon^{imn}}{\sqrt{2}} \left[u_j^T(x) C \gamma_5 c_k(x) \bar{d}_m(x) \sigma_{\mu\nu} C \bar{c}_n^T(x) - u_j^T(x) C \sigma_{\mu\nu} c_k(x) \bar{d}_m(x) \gamma_5 C \bar{c}_n^T(x) \right], \\
J_{+,\mu\nu}^{S\tilde{V}}(x) &= \frac{\varepsilon^{ijk}\varepsilon^{imn}}{\sqrt{2}} \left[u_j^T(x) C \gamma_5 c_k(x) \bar{d}_m(x) \sigma_{\mu\nu} C \bar{c}_n^T(x) + u_j^T(x) C \sigma_{\mu\nu} c_k(x) \bar{d}_m(x) \gamma_5 C \bar{c}_n^T(x) \right], \\
J_{-,\mu\nu}^{P\tilde{A}}(x) &= \frac{\varepsilon^{ijk}\varepsilon^{imn}}{\sqrt{2}} \left[u_j^T(x) C c_k(x) \bar{d}_m(x) \gamma_5 \sigma_{\mu\nu} C \bar{c}_n^T(x) - u_j^T(x) C \sigma_{\mu\nu} \gamma_5 c_k(x) \bar{d}_m(x) C \bar{c}_n^T(x) \right], \\
J_{+,\mu\nu}^{P\tilde{A}}(x) &= \frac{\varepsilon^{ijk}\varepsilon^{imn}}{\sqrt{2}} \left[u_j^T(x) C c_k(x) \bar{d}_m(x) \gamma_5 \sigma_{\mu\nu} C \bar{c}_n^T(x) + u_j^T(x) C \sigma_{\mu\nu} \gamma_5 c_k(x) \bar{d}_m(x) C \bar{c}_n^T(x) \right],
\end{aligned} \tag{167}$$

$$J_{-,\mu\nu}^{AA}(x) = \frac{\varepsilon^{ijk}\varepsilon^{imn}}{\sqrt{2}} \left[u_j^T(x) C \gamma_\mu c_k(x) \bar{d}_m(x) \gamma_\nu C \bar{c}_n^T(x) - u_j^T(x) C \gamma_\nu c_k(x) \bar{d}_m(x) \gamma_\mu C \bar{c}_n^T(x) \right], \tag{168}$$

the subscripts \pm denote the positive and negative charge conjugation, respectively, the superscripts P , S , $A(\tilde{A})$ and $V(\tilde{V})$ denote the pseudoscalar, scalar, axialvector and vector diquark and antidiquark operators, respectively [360, 437, 443, 455, 456]. With the simple replacement,

$$\begin{aligned}
u &\rightarrow s, \\
d &\rightarrow s,
\end{aligned} \tag{169}$$

we reach the currents for the corresponding $c\bar{c}s\bar{s}$ currents [360, 456, 457].

Under parity transform \hat{P} , the current operators $J_\mu(x)$ and $J_{\mu\nu}(x)$ have the properties,

$$\begin{aligned}
\hat{P} J_\mu(x) \hat{P}^{-1} &= +J^\mu(\tilde{x}), \\
\hat{P} \tilde{J}_{\mu\nu}(x) \hat{P}^{-1} &= -\tilde{J}^{\mu\nu}(\tilde{x}), \\
\hat{P} J_{-,\mu\nu}^{AA}(x) \hat{P}^{-1} &= +J_{AA}^{,\mu\nu}(\tilde{x}),
\end{aligned} \tag{170}$$

according to the properties of the diquark operators,

$$\begin{aligned}\widehat{P}\varepsilon^{ijk}q_j^T(x)C\Gamma c_k(x)\widehat{P}^{-1} &= -\varepsilon^{ijk}q_j^T(\tilde{x})C\gamma^0\Gamma\gamma^0c_k(\tilde{x}), \\ \widehat{P}\varepsilon^{ijk}\bar{q}_j(x)\Gamma C\bar{c}_k^T(x)\widehat{P}^{-1} &= -\varepsilon^{ijk}\bar{q}_j(\tilde{x})\gamma^0\Gamma\gamma^0C\bar{c}_k^T(\tilde{x}),\end{aligned}\quad (171)$$

where $\tilde{J}_{\mu\nu}(x) = J_{-,\mu\nu}^{S\tilde{V}}(x)$, $J_{+,\mu\nu}^{S\tilde{V}}(x)$, $J_{-,\mu\nu}^{P\tilde{A}}(x)$, $J_{+,\mu\nu}^{P\tilde{A}}(x)$, $x^\mu = (t, \vec{x})$ and $\tilde{x}^\mu = (t, -\vec{x})$. For $\Gamma = 1, \gamma_5, \gamma_\mu, \gamma_\mu\gamma_5, \sigma_{\mu\nu}, \sigma_{\mu\nu}\gamma_5$, we obtain $\gamma^0\Gamma\gamma^0 = 1, -\gamma_5, \gamma^\mu, -\gamma^\mu\gamma_5, \sigma^{\mu\nu}, -\sigma^{\mu\nu}\gamma_5$. We rewrite Eq.(170) in more explicit form,

$$\begin{aligned}\widehat{P}J_i(x)\widehat{P}^{-1} &= -J_i(\tilde{x}), \\ \widehat{P}\tilde{J}_{ij}(x)\widehat{P}^{-1} &= -\tilde{J}_{ij}(\tilde{x}), \\ \widehat{P}J_{-,0i}^{AA}(x)\widehat{P}^{-1} &= -J_{AA,0i}^-(\tilde{x}),\end{aligned}\quad (172)$$

$$\begin{aligned}\widehat{P}J_0(x)\widehat{P}^{-1} &= +J_0(\tilde{x}), \\ \widehat{P}\tilde{J}_{0i}(x)\widehat{P}^{-1} &= +\tilde{J}_{0i}(\tilde{x}), \\ \widehat{P}J_{-,ij}^{AA}(x)\widehat{P}^{-1} &= +J_{AA,ij}^-(\tilde{x}),\end{aligned}\quad (173)$$

where $i, j = 1, 2, 3$.

Under charge conjugation transform \widehat{C} , the currents $J_\mu(x)$ and $J_{\mu\nu}(x)$ have the properties,

$$\begin{aligned}\widehat{C}J_{\pm,\mu}(x)\widehat{C}^{-1} &= \pm J_{\pm,\mu}(x) |_{u\leftrightarrow d}, \\ \widehat{C}J_{\pm,\mu\nu}(x)\widehat{C}^{-1} &= \pm J_{\pm,\mu\nu}(x) |_{u\leftrightarrow d}.\end{aligned}\quad (174)$$

The currents $J_\mu(x)$ and $J_{\mu\nu}(x)$ have the symbolic quark structure $\bar{c}c\bar{d}u$ with the isospin $I = 1$ and $I_3 = 1$. In the isospin limit, the currents with the symbolic quark structures

$$\bar{c}c\bar{d}u, \bar{c}c\bar{u}d, \bar{c}c\frac{\bar{u}u - \bar{d}d}{\sqrt{2}}, \bar{c}c\frac{\bar{u}u + \bar{d}d}{\sqrt{2}}\quad (175)$$

couple potentially to the hidden-charm tetraquark states with degenerated masses, the currents with the isospin $I = 1$ and 0 lead to the same QCD sum rules. Only the currents with the symbolic quark structures $\bar{c}c\frac{\bar{u}u - \bar{d}d}{\sqrt{2}}$ and $\bar{c}c\frac{\bar{u}u + \bar{d}d}{\sqrt{2}}$ have definite charge conjugation, and we assume that the tetraquark states $\bar{c}c\bar{d}u$ have the same charge conjugation as their neutral partners.

According to current-hadron duality, we obtain the hadronic representation,

$$\begin{aligned}
\Pi_{\mu\nu}(p) &= \frac{\lambda_{Y_-}^2}{M_{Y_-}^2 - p^2} \left(-g_{\mu\nu} + \frac{p_\mu p_\nu}{p^2} \right) + \dots \\
&= \Pi_-(p^2) \left(-g_{\mu\nu} + \frac{p_\mu p_\nu}{p^2} \right) + \dots, \\
\tilde{\Pi}_{\mu\nu\alpha\beta}(p) &= \frac{\lambda_{Y_-}^2}{M_{Y_-}^2 (M_{Y_-}^2 - p^2)} \left(p^2 g_{\mu\alpha} g_{\nu\beta} - p^2 g_{\mu\beta} g_{\nu\alpha} - g_{\mu\alpha} p_\nu p_\beta - g_{\nu\beta} p_\mu p_\alpha + g_{\mu\beta} p_\nu p_\alpha + g_{\nu\alpha} p_\mu p_\beta \right) \\
&\quad + \frac{\lambda_{Z_+}^2}{M_{Z_+}^2 (M_{Z_+}^2 - p^2)} \left(-g_{\mu\alpha} p_\nu p_\beta - g_{\nu\beta} p_\mu p_\alpha + g_{\mu\beta} p_\nu p_\alpha + g_{\nu\alpha} p_\mu p_\beta \right) + \dots \\
&= \tilde{\Pi}_-(p^2) \left(p^2 g_{\mu\alpha} g_{\nu\beta} - p^2 g_{\mu\beta} g_{\nu\alpha} - g_{\mu\alpha} p_\nu p_\beta - g_{\nu\beta} p_\mu p_\alpha + g_{\mu\beta} p_\nu p_\alpha + g_{\nu\alpha} p_\mu p_\beta \right) \\
&\quad + \tilde{\Pi}_+(p^2) \left(-g_{\mu\alpha} p_\nu p_\beta - g_{\nu\beta} p_\mu p_\alpha + g_{\mu\beta} p_\nu p_\alpha + g_{\nu\alpha} p_\mu p_\beta \right), \\
\Pi_{\mu\nu\alpha\beta}^{AA}(p) &= \frac{\lambda_{Z_+}^2}{M_{Z_+}^2 (M_{Z_+}^2 - p^2)} \left(p^2 g_{\mu\alpha} g_{\nu\beta} - p^2 g_{\mu\beta} g_{\nu\alpha} - g_{\mu\alpha} p_\nu p_\beta - g_{\nu\beta} p_\mu p_\alpha + g_{\mu\beta} p_\nu p_\alpha + g_{\nu\alpha} p_\mu p_\beta \right) \\
&\quad + \frac{\lambda_{Y_-}^2}{M_{Y_-}^2 (M_{Y_-}^2 - p^2)} \left(-g_{\mu\alpha} p_\nu p_\beta - g_{\nu\beta} p_\mu p_\alpha + g_{\mu\beta} p_\nu p_\alpha + g_{\nu\alpha} p_\mu p_\beta \right) + \dots \\
&= \tilde{\Pi}_+(p^2) \left(p^2 g_{\mu\alpha} g_{\nu\beta} - p^2 g_{\mu\beta} g_{\nu\alpha} - g_{\mu\alpha} p_\nu p_\beta - g_{\nu\beta} p_\mu p_\alpha + g_{\mu\beta} p_\nu p_\alpha + g_{\nu\alpha} p_\mu p_\beta \right) \\
&\quad + \tilde{\Pi}_-(p^2) \left(-g_{\mu\alpha} p_\nu p_\beta - g_{\nu\beta} p_\mu p_\alpha + g_{\mu\beta} p_\nu p_\alpha + g_{\nu\alpha} p_\mu p_\beta \right), \tag{176}
\end{aligned}$$

where the pole residues are defined by

$$\begin{aligned}
\langle 0 | J_\mu(0) | Y_c^-(p) \rangle &= \lambda_{Y_-} \varepsilon_\mu, \\
\langle 0 | \tilde{J}_{\mu\nu}(0) | Y_c^-(p) \rangle &= \frac{\lambda_{Y_-}}{M_{Y_-}} \varepsilon_{\mu\nu\alpha\beta} \varepsilon^\alpha p^\beta, \\
\langle 0 | \tilde{J}_{\mu\nu}(0) | Z_c^+(p) \rangle &= \frac{\lambda_{Z_+}}{M_{Z_+}} (\varepsilon_\mu p_\nu - \varepsilon_\nu p_\mu), \\
\langle 0 | J_{-, \mu\nu}^{AA}(0) | Z_c^+(p) \rangle &= \frac{\lambda_{Z_+}}{M_{Z_+}} \varepsilon_{\mu\nu\alpha\beta} \varepsilon^\alpha p^\beta, \\
\langle 0 | J_{-, \mu\nu}^{AA}(0) | Y_c^-(p) \rangle &= \frac{\lambda_{Y_-}}{M_{Y_-}} (\varepsilon_\mu p_\nu - \varepsilon_\nu p_\mu), \tag{177}
\end{aligned}$$

the $\varepsilon_{\mu/\alpha}$ and $\varepsilon_{\mu\nu}$ are the polarization vectors, we add the superscripts/subscripts \pm to denote the positive and negative parity, respectively. We choose the components $\Pi_-(p^2)$ and $p^2 \tilde{\Pi}_-(p^2)$ to explore the negative parity hidden-charm tetraquark states [455, 457].

At the QCD side, we calculate the vacuum condensates up to dimension 10 and take into account the vacuum condensates $\langle \bar{q}q \rangle$, $\langle \frac{\alpha_s GG}{\pi} \rangle$, $\langle \bar{q}g_s \sigma Gq \rangle$, $\langle \bar{q}q \rangle^2$, $g_s^2 \langle \bar{q}q \rangle^2$, $\langle \bar{q}q \rangle \langle \frac{\alpha_s GG}{\pi} \rangle$, $\langle \bar{q}q \rangle \langle \bar{q}g_s \sigma Gq \rangle$, $\langle \bar{q}g_s \sigma Gq \rangle^2$ and $\langle \bar{q}q \rangle^2 \langle \frac{\alpha_s GG}{\pi} \rangle$, which are vacuum expectations of the quark-gluon operators of the order $\mathcal{O}(\alpha_s^k)$ with $k \leq 1$ [455, 457].

We match the hadron side with the QCD side of the components $\Pi_-(p^2)$ and $p^2 \tilde{\Pi}_-(p^2)$ below the continuum thresholds s_0 with the help of spectral representation, and perform Borel transform with respect to $P^2 = -p^2$ to obtain the QCD sum rules:

$$\lambda_Y^2 \exp\left(-\frac{M_Y^2}{T^2}\right) = \int_{4m^2}^{s_0} ds \rho_{QCD}(s) \exp\left(-\frac{s}{T^2}\right), \tag{178}$$

Y_c	J^{PC}	$T^2(\text{GeV}^2)$	$\sqrt{s_0}(\text{GeV})$	$\mu(\text{GeV})$	pole
$[uc]_P[\overline{dc}]_A - [uc]_A[\overline{dc}]_P$	1^{--}	3.7 – 4.1	5.15 ± 0.10	2.9	(43 – 61)%
$[uc]_P[\overline{dc}]_A + [uc]_A[\overline{dc}]_P$	1^{++}	3.7 – 4.1	5.10 ± 0.10	2.8	(42 – 60)%
$[uc]_S[\overline{dc}]_V + [uc]_V[\overline{dc}]_S$	1^{--}	3.2 – 3.6	4.85 ± 0.10	2.4	(42 – 62)%
$[uc]_S[\overline{dc}]_V - [uc]_V[\overline{dc}]_S$	1^{++}	3.7 – 4.1	5.15 ± 0.10	2.9	(41 – 60)%
$[uc]_{\overline{V}}[\overline{dc}]_A - [uc]_A[\overline{dc}]_{\overline{V}}$	1^{--}	3.6 – 4.0	5.05 ± 0.10	2.7	(42 – 60)%
$[uc]_{\overline{V}}[\overline{dc}]_A + [uc]_A[\overline{dc}]_{\overline{V}}$	1^{++}	3.7 – 4.1	5.15 ± 0.10	2.9	(41 – 60)%
$[uc]_{\overline{A}}[\overline{dc}]_V + [uc]_V[\overline{dc}]_{\overline{A}}$	1^{--}	3.5 – 3.9	5.00 ± 0.10	2.6	(42 – 61)%
$[uc]_{\overline{A}}[\overline{dc}]_V - [uc]_V[\overline{dc}]_{\overline{A}}$	1^{++}	3.6 – 4.0	5.05 ± 0.10	2.7	(42 – 61)%
$[uc]_S[\overline{dc}]_{\overline{V}} - [uc]_{\overline{V}}[\overline{dc}]_S$	1^{--}	3.4 – 3.8	5.00 ± 0.10	2.6	(42 – 61)%
$[uc]_S[\overline{dc}]_{\overline{V}} + [uc]_{\overline{V}}[\overline{dc}]_S$	1^{++}	3.4 – 3.8	5.00 ± 0.10	2.6	(42 – 61)%
$[uc]_P[\overline{dc}]_{\overline{A}} - [uc]_{\overline{A}}[\overline{dc}]_P$	1^{--}	3.7 – 4.1	5.10 ± 0.10	2.8	(43 – 61)%
$[uc]_P[\overline{dc}]_{\overline{A}} + [uc]_{\overline{A}}[\overline{dc}]_P$	1^{++}	3.7 – 4.1	5.10 ± 0.10	2.8	(43 – 61)%
$[uc]_A[\overline{dc}]_A$	1^{--}	3.8 – 4.2	5.20 ± 0.10	3.0	(42 – 60)%

Table 18: The Borel parameters, continuum threshold parameters, energy scales of the QCD spectral densities and pole contributions for the ground state vector hidden-charm tetraquark states.

the explicit expressions of the QCD spectral densities $\rho(s)$ are neglected for simplicity.

We derive Eq.(178) with respect to $\tau = \frac{1}{T^2}$, and obtain the QCD sum rules for the masses of the vector hidden-charm tetraquark states Y_c ,

$$M_Y^2 = -\frac{\int_{4m_c^2}^{s_0} ds \frac{d}{d\tau} \rho(s) \exp(-\tau s)}{\int_{4m_c^2}^{s_0} ds \rho_{QCD}(s) \exp(-\tau s)}. \quad (179)$$

Perform the same procedure as in the previous subsection, we obtain the Borel windows, continuum threshold parameters, suitable energy scales of the QCD spectral densities and pole contributions, which are shown explicitly in Tables 18-19. From the Table, we can see clearly that the pole contributions are about (40 – 60)%, the central values are larger than 50%, the pole dominance is well satisfied. In calculations, we observe that the main contributions come from the perturbative terms, the higher dimensional condensates play a minor important role and the contributions $|D(10)| \ll 1\%$, the operator product expansion converges very good.

We take account of all the uncertainties of the relevant parameters and obtain the masses and pole residues of the hidden-charm-hidden-strange tetraquark states with the $J^{PC} = 1^{--}$ and 1^{++} , which are shown explicitly in Tables 20-21.

In Tables 22-23, we present the possible assignments of the hidden-charm tetraquark states with the $J^{PC} = 1^{--}$ and 1^{++} obtained in Refs.[455, 457]. Considering the large uncertainties, it is possible to assign the $X(4630)$ as the $[sc]_S[\overline{sc}]_{\overline{V}} + [sc]_{\overline{V}}[\overline{sc}]_S$ state with the $J^{PC} = 1^{++}$, which has a mass 4.68 ± 0.09 GeV, see Table 23. In Ref.[345], we prove that it is feasible and reliable to investigate the multiquark states in the framework of the QCD sum rules, and obtain the prediction for the mass of the $D_s^* \overline{D}_{s1} - D_{s1} \overline{D}_s^*$ molecular state with the exotic quantum numbers $J^{PC} = 1^{--}$, $M_X = 4.67 \pm 0.08$ GeV, which was obtained before the LHCb data and is compatible with the LHCb data. The $X(4630)$ maybe have two important Fock components.

After Ref.[455] has been published, the $Y(4500)$ was observed by the BESIII collaboration [147, 148, 151]. At the energy about 4.5 GeV, we obtain three hidden-charm tetraquark states with the $J^{PC} = 1^{--}$, the $[uc]_{\overline{V}}[\overline{uc}]_A + [dc]_{\overline{V}}[\overline{dc}]_A - [uc]_A[\overline{uc}]_{\overline{V}} - [dc]_A[\overline{dc}]_{\overline{V}}$, $[uc]_{\overline{A}}[\overline{uc}]_V + [dc]_{\overline{A}}[\overline{dc}]_V + [uc]_V[\overline{uc}]_{\overline{A}} + [dc]_V[\overline{dc}]_{\overline{A}}$ and $[uc]_S[\overline{uc}]_{\overline{V}} + [dc]_S[\overline{dc}]_{\overline{V}} - [uc]_{\overline{V}}[\overline{uc}]_S - [dc]_{\overline{V}}[\overline{dc}]_S$ tetraquark states have the masses 4.53 ± 0.07 GeV, 4.48 ± 0.08 GeV and 4.50 ± 0.09 GeV, respectively [455]. In Ref.[458], and investigate the two-body strong decays systematically. We obtain thirty QCD sum

Y_c	J^{PC}	$T^2(\text{GeV}^2)$	$\sqrt{s_0}(\text{GeV})$	$\mu(\text{GeV})$	pole
$[sc]_P[\overline{s\overline{c}}]_A - [sc]_A[\overline{s\overline{c}}]_P$	1^{--}	4.1 – 4.7	5.35 ± 0.10	2.9	(40 – 61)%
$[sc]_P[\overline{s\overline{c}}]_A + [sc]_A[\overline{s\overline{c}}]_P$	1^{++}	4.0 – 4.6	5.30 ± 0.10	2.8	(41 – 61)%
$[sc]_S[\overline{s\overline{c}}]_V + [sc]_V[\overline{s\overline{c}}]_S$	1^{--}	3.5 – 4.0	5.05 ± 0.10	2.5	(41 – 62)%
$[sc]_S[\overline{s\overline{c}}]_V - [sc]_V[\overline{s\overline{c}}]_S$	1^{++}	4.0 – 4.6	5.35 ± 0.10	2.9	(40 – 60)%
$[sc]_{\overline{V}}[\overline{s\overline{c}}]_A - [sc]_A[\overline{s\overline{c}}]_{\overline{V}}$	1^{--}	3.9 – 4.5	5.25 ± 0.10	2.7	(40 – 61)%
$[sc]_{\overline{V}}[\overline{s\overline{c}}]_A + [sc]_A[\overline{s\overline{c}}]_{\overline{V}}$	1^{++}	4.0 – 4.6	5.35 ± 0.10	2.9	(40 – 61)%
$[sc]_{\overline{A}}[\overline{s\overline{c}}]_V + [sc]_V[\overline{s\overline{c}}]_{\overline{A}}$	1^{--}	3.8 – 4.4	5.20 ± 0.10	2.7	(40 – 61)%
$[sc]_{\overline{A}}[\overline{s\overline{c}}]_V - [sc]_V[\overline{s\overline{c}}]_{\overline{A}}$	1^{++}	3.9 – 4.5	5.25 ± 0.10	2.7	(40 – 61)%
$[sc]_S[\overline{s\overline{c}}]_{\overline{V}} - [sc]_{\overline{V}}[\overline{s\overline{c}}]_S$	1^{--}	3.7 – 4.2	5.20 ± 0.10	2.7	(41 – 62)%
$[sc]_S[\overline{s\overline{c}}]_{\overline{V}} + [sc]_{\overline{V}}[\overline{s\overline{c}}]_S$	1^{++}	3.7 – 4.3	5.20 ± 0.10	2.7	(40 – 62)%
$[sc]_P[\overline{s\overline{c}}]_{\overline{A}} - [sc]_{\overline{A}}[\overline{s\overline{c}}]_P$	1^{--}	4.1 – 4.7	5.30 ± 0.10	2.8	(40 – 60)%
$[sc]_P[\overline{s\overline{c}}]_{\overline{A}} + [sc]_{\overline{A}}[\overline{s\overline{c}}]_P$	1^{++}	4.1 – 4.7	5.30 ± 0.10	2.8	(40 – 60)%
$[sc]_A[\overline{s\overline{c}}]_A$	1^{--}	4.2 – 4.9	5.40 ± 0.10	3.0	(40 – 60)%

Table 19: The Borel parameters, continuum threshold parameters, energy scales of the QCD spectral densities and pole contributions for the ground state hidden-charm-hidden-strange tetraquark states.

Y_c	J^{PC}	$M_Y(\text{GeV})$	$\lambda_Y(\text{GeV}^5)$
$[uc]_P[\overline{dc}]_A - [uc]_A[\overline{dc}]_P$	1^{--}	4.66 ± 0.07	$(7.19 \pm 0.84) \times 10^{-2}$
$[uc]_P[\overline{dc}]_A + [uc]_A[\overline{dc}]_P$	1^{++}	4.61 ± 0.07	$(6.69 \pm 0.80) \times 10^{-2}$
$[uc]_S[\overline{dc}]_V + [uc]_V[\overline{dc}]_S$	1^{--}	4.35 ± 0.08	$(4.32 \pm 0.61) \times 10^{-2}$
$[uc]_S[\overline{dc}]_V - [uc]_V[\overline{dc}]_S$	1^{++}	4.66 ± 0.09	$(6.67 \pm 0.82) \times 10^{-2}$
$[uc]_{\overline{V}}[\overline{dc}]_A - [uc]_A[\overline{dc}]_{\overline{V}}$	1^{--}	4.53 ± 0.07	$(1.03 \pm 0.14) \times 10^{-1}$
$[uc]_{\overline{V}}[\overline{dc}]_A + [uc]_A[\overline{dc}]_{\overline{V}}$	1^{++}	4.65 ± 0.08	$(1.13 \pm 0.15) \times 10^{-1}$
$[uc]_{\overline{A}}[\overline{dc}]_V + [uc]_V[\overline{dc}]_{\overline{A}}$	1^{--}	4.48 ± 0.08	$(9.47 \pm 1.27) \times 10^{-2}$
$[uc]_{\overline{A}}[\overline{dc}]_V - [uc]_V[\overline{dc}]_{\overline{A}}$	1^{++}	4.55 ± 0.07	$(1.06 \pm 0.14) \times 10^{-1}$
$[uc]_S[\overline{dc}]_{\overline{V}} - [uc]_{\overline{V}}[\overline{dc}]_S$	1^{--}	4.50 ± 0.09	$(4.78 \pm 0.66) \times 10^{-2}$
$[uc]_S[\overline{dc}]_{\overline{V}} + [uc]_{\overline{V}}[\overline{dc}]_S$	1^{++}	4.50 ± 0.09	$(4.79 \pm 0.66) \times 10^{-2}$
$[uc]_P[\overline{dc}]_{\overline{A}} - [uc]_{\overline{A}}[\overline{dc}]_P$	1^{--}	4.60 ± 0.07	$(6.32 \pm 0.74) \times 10^{-2}$
$[uc]_P[\overline{dc}]_{\overline{A}} + [uc]_{\overline{A}}[\overline{dc}]_P$	1^{++}	4.61 ± 0.08	$(6.36 \pm 0.74) \times 10^{-2}$
$[uc]_A[\overline{dc}]_A$	1^{--}	4.69 ± 0.08	$(6.65 \pm 0.81) \times 10^{-2}$

Table 20: The masses and pole residues of the ground state vector hidden-charm tetraquark states.

Y_c	J^{PC}	$M_Y(\text{GeV})$	$\lambda_Y(\text{GeV}^5)$
$[sc]_P[\overline{s\overline{c}}]_A - [sc]_A[\overline{s\overline{c}}]_P$	1^{--}	4.80 ± 0.08	$(8.97 \pm 1.09) \times 10^{-2}$
$[sc]_P[\overline{s\overline{c}}]_A + [sc]_A[\overline{s\overline{c}}]_P$	1^{-+}	4.75 ± 0.08	$(8.34 \pm 1.04) \times 10^{-2}$
$[sc]_S[\overline{s\overline{c}}]_V + [sc]_V[\overline{s\overline{c}}]_S$	1^{--}	4.53 ± 0.08	$(5.70 \pm 0.79) \times 10^{-2}$
$[sc]_S[\overline{s\overline{c}}]_V - [sc]_V[\overline{s\overline{c}}]_S$	1^{-+}	4.83 ± 0.09	$(8.39 \pm 1.05) \times 10^{-2}$
$[sc]_{\overline{V}}[\overline{s\overline{c}}]_A - [sc]_A[\overline{s\overline{c}}]_{\overline{V}}$	1^{--}	4.70 ± 0.08	$(1.32 \pm 0.18) \times 10^{-1}$
$[sc]_{\overline{V}}[\overline{s\overline{c}}]_A + [sc]_A[\overline{s\overline{c}}]_{\overline{V}}$	1^{-+}	4.81 ± 0.09	$(1.43 \pm 0.19) \times 10^{-1}$
$[sc]_{\overline{A}}[\overline{s\overline{c}}]_V + [sc]_V[\overline{s\overline{c}}]_{\overline{A}}$	1^{--}	4.65 ± 0.08	$(1.23 \pm 0.17) \times 10^{-1}$
$[sc]_{\overline{A}}[\overline{s\overline{c}}]_V - [sc]_V[\overline{s\overline{c}}]_{\overline{A}}$	1^{-+}	4.71 ± 0.08	$(1.34 \pm 0.17) \times 10^{-1}$
$[sc]_S[\overline{s\overline{c}}]_{\overline{V}} - [sc]_{\overline{V}}[\overline{s\overline{c}}]_S$	1^{--}	4.68 ± 0.09	$(6.22 \pm 0.82) \times 10^{-2}$
$[sc]_S[\overline{s\overline{c}}]_{\overline{V}} + [sc]_{\overline{V}}[\overline{s\overline{c}}]_S$	1^{-+}	4.68 ± 0.09	$(6.23 \pm 0.84) \times 10^{-2}$
$[sc]_P[\overline{s\overline{c}}]_{\overline{A}} - [sc]_{\overline{A}}[\overline{s\overline{c}}]_P$	1^{--}	4.75 ± 0.08	$(7.93 \pm 0.98) \times 10^{-2}$
$[sc]_P[\overline{s\overline{c}}]_{\overline{A}} + [sc]_{\overline{A}}[\overline{s\overline{c}}]_P$	1^{-+}	4.75 ± 0.08	$(7.94 \pm 0.97) \times 10^{-2}$
$[sc]_A[\overline{s\overline{c}}]_A$	1^{--}	4.85 ± 0.09	$(8.38 \pm 1.05) \times 10^{-2}$

Table 21: The masses and pole residues of the ground state hidden-charm-hidden-strange tetraquark states.

Y_c	J^{PC}	$M_Y(\text{GeV})$	Assignments
$[uc]_P[\overline{d\overline{c}}]_A - [uc]_A[\overline{d\overline{c}}]_P$	1^{--}	4.66 ± 0.07	? $Y(4660)$
$[uc]_P[\overline{d\overline{c}}]_A + [uc]_A[\overline{d\overline{c}}]_P$	1^{-+}	4.61 ± 0.07	
$[uc]_S[\overline{d\overline{c}}]_V + [uc]_V[\overline{d\overline{c}}]_S$	1^{--}	4.35 ± 0.08	? $Y(4360/4390)$
$[uc]_S[\overline{d\overline{c}}]_V - [uc]_V[\overline{d\overline{c}}]_S$	1^{-+}	4.66 ± 0.09	
$[uc]_{\overline{V}}[\overline{d\overline{c}}]_A - [uc]_A[\overline{d\overline{c}}]_{\overline{V}}$	1^{--}	4.53 ± 0.07	? $Y(4500)$
$[uc]_{\overline{V}}[\overline{d\overline{c}}]_A + [uc]_A[\overline{d\overline{c}}]_{\overline{V}}$	1^{-+}	4.65 ± 0.08	
$[uc]_{\overline{A}}[\overline{d\overline{c}}]_V + [uc]_V[\overline{d\overline{c}}]_{\overline{A}}$	1^{--}	4.48 ± 0.08	? $Y(4500)$
$[uc]_{\overline{A}}[\overline{d\overline{c}}]_V - [uc]_V[\overline{d\overline{c}}]_{\overline{A}}$	1^{-+}	4.55 ± 0.07	
$[uc]_S[\overline{d\overline{c}}]_{\overline{V}} - [uc]_{\overline{V}}[\overline{d\overline{c}}]_S$	1^{--}	4.50 ± 0.09	? $Y(4500)$
$[uc]_S[\overline{d\overline{c}}]_{\overline{V}} + [uc]_{\overline{V}}[\overline{d\overline{c}}]_S$	1^{-+}	4.50 ± 0.09	
$[uc]_P[\overline{d\overline{c}}]_{\overline{A}} - [uc]_{\overline{A}}[\overline{d\overline{c}}]_P$	1^{--}	4.60 ± 0.07	
$[uc]_P[\overline{d\overline{c}}]_{\overline{A}} + [uc]_{\overline{A}}[\overline{d\overline{c}}]_P$	1^{-+}	4.61 ± 0.08	
$[uc]_A[\overline{d\overline{c}}]_A$	1^{--}	4.69 ± 0.08	? $Y(4660)$

Table 22: The possible assignments of the hidden-charm tetraquark states, the isospin limit is implied.

Y_c	J^{PC}	M_Y (GeV)	Assignments
$[sc]_P[\overline{sc}]_A - [sc]_A[\overline{sc}]_P$	1^{--}	4.80 ± 0.08	? $Y(4790)$
$[sc]_P[\overline{sc}]_A + [sc]_A[\overline{sc}]_P$	1^{-+}	4.75 ± 0.08	
$[sc]_S[\overline{sc}]_V + [sc]_V[\overline{sc}]_S$	1^{--}	4.53 ± 0.08	
$[sc]_S[\overline{sc}]_V - [sc]_V[\overline{sc}]_S$	1^{-+}	4.83 ± 0.09	
$[sc]_{\tilde{V}}[\overline{sc}]_A - [sc]_A[\overline{sc}]_{\tilde{V}}$	1^{--}	4.70 ± 0.08	? $Y(4710)$
$[sc]_{\tilde{V}}[\overline{sc}]_A + [sc]_A[\overline{sc}]_{\tilde{V}}$	1^{-+}	4.81 ± 0.09	
$[sc]_{\tilde{A}}[\overline{sc}]_V + [sc]_V[\overline{sc}]_{\tilde{A}}$	1^{--}	4.65 ± 0.08	? $Y(4660)$
$[sc]_{\tilde{A}}[\overline{sc}]_V - [sc]_V[\overline{sc}]_{\tilde{A}}$	1^{-+}	4.71 ± 0.08	
$[sc]_S[\overline{sc}]_{\tilde{V}} - [sc]_{\tilde{V}}[\overline{sc}]_S$	1^{--}	4.68 ± 0.09	? $Y(4660)$
$[sc]_S[\overline{sc}]_{\tilde{V}} + [sc]_{\tilde{V}}[\overline{sc}]_S$	1^{-+}	4.68 ± 0.09	?? $X(4630)$
$[sc]_P[\overline{sc}]_{\tilde{A}} - [sc]_{\tilde{A}}[\overline{sc}]_P$	1^{--}	4.75 ± 0.08	
$[sc]_P[\overline{sc}]_{\tilde{A}} + [sc]_{\tilde{A}}[\overline{sc}]_P$	1^{-+}	4.75 ± 0.08	
$[sc]_A[\overline{sc}]_A$	1^{--}	4.85 ± 0.09	

Table 23: The possible assignments of the hidden-charm-hidden-strange tetraquark states.

rules for the hadronic coupling constants based on rigorous quark-hadron duality, then obtain the partial decay widths, therefore the total widths approximately, which are compatible with the experimental data of the $Y(4500)$ from the BESIII collaboration. In Ref.[?], we take the $Y(4500)$ as the $[uc]_{\tilde{A}}[\overline{uc}]_V + [dc]_{\tilde{A}}[\overline{dc}]_V + [uc]_V[\overline{uc}]_{\tilde{A}} + [dc]_V[\overline{dc}]_{\tilde{A}}$ tetraquark state, and study the three-body strong decay $Y(4500) \rightarrow D^{*-} D^{*0} \pi^+$ with the light-cone QCD sum rules.

If only the mass is concerned, the $Y(4660)$ can be assigned as the $[sc]_{\tilde{A}}[\overline{sc}]_V + [sc]_V[\overline{sc}]_{\tilde{A}}$, $[sc]_S[\overline{sc}]_{\tilde{V}} - [sc]_{\tilde{V}}[\overline{sc}]_S$, $[uc]_P[\overline{uc}]_A + [dc]_P[\overline{dc}]_A - [uc]_A[\overline{uc}]_P - [dc]_A[\overline{dc}]_P$ or $[uc]_A[\overline{uc}]_A + [dc]_A[\overline{dc}]_A$ tetraquark state, see Tables 22-23. In other words, the $Y(4660)$ maybe have several important Fock components, we have to study the strong decays in details to diagnose its nature. For example, if we assign $Y(4660) = [sc]_{\tilde{A}}[\overline{sc}]_V + [sc]_V[\overline{sc}]_{\tilde{A}}$ or $[sc]_S[\overline{sc}]_{\tilde{V}} - [sc]_{\tilde{V}}[\overline{sc}]_S$, then the strong decays $Y(4660) \rightarrow J/\psi f_0(980)$, $\eta_c \phi$, $\chi_{c0} \phi$, $D_s \overline{D}_s$, $D_s^* \overline{D}_s^*$, $D_s \overline{D}_s^*$, $D_s^* \overline{D}_s$, $J/\psi \pi^+ \pi^-$ and $\psi' \pi^+ \pi^-$ are Okubo-Zweig-Iizuka super-allowed, considering the intermediate process $f_0(980) \rightarrow \pi^+ \pi^-$. Up to now, only the decays $Y(4660) \rightarrow J/\psi \pi^+ \pi^-$, $\psi_2(3823) \pi^+ \pi^-$, $\Lambda_c^+ \Lambda_c^-$ and $D_s^+ D_{s1}^-$ have been observed [91], which cannot exclude the assignments $Y(4660) = [uc]_P[\overline{uc}]_A + [dc]_P[\overline{dc}]_A - [uc]_A[\overline{uc}]_P - [dc]_A[\overline{dc}]_P$ or $[uc]_A[\overline{uc}]_A + [dc]_A[\overline{dc}]_A$, as the decay $Y(4660) \rightarrow D_s^+ D_{s1}^-$ can take place through the re-scattering mechanism. We can investigate or search for the neutral Y_c tetraquark states with the $J^{PC} = 1^{--}$ and 1^{-+} through the two-body or three-body strong decays,

$$\begin{aligned}
Y_c(1^{--}) &\rightarrow \chi_{c0} \rho / \omega, J/\psi \pi^+ \pi^-, J/\psi K \overline{K}, \eta_c \rho / \omega, \chi_{c1} \rho / \omega, \\
Y_c(1^{-+}) &\rightarrow J/\psi \rho / \omega, h_c \rho / \omega.
\end{aligned} \tag{180}$$

Now let us turn to the pseudoscalar tetraquark states and write down the local currents,

$$J(x) = J_{AV}^+(x), J_{AV}^-(x), J_{PS}^+(x), J_{PS}^-(x), J_{TT}^+(x), J_{TT}^-(x), \tag{181}$$

$$\begin{aligned}
J_{AV}^+(x) &= \frac{\varepsilon^{ijk}\varepsilon^{imn}}{\sqrt{2}} \left[q_j^T(x) C \gamma_\mu c_k(x) \bar{q}'_m(x) \gamma_5 \gamma^\mu C \bar{c}_n^T(x) - q_j^T(x) C \gamma_\mu \gamma_5 c_k(x) \bar{q}'_m(x) \gamma^\mu C \bar{c}_n^T(x) \right], \\
J_{AV}^-(x) &= \frac{\varepsilon^{ijk}\varepsilon^{imn}}{\sqrt{2}} \left[q_j^T(x) C \gamma_\mu c_k(x) \bar{q}'_m(x) \gamma_5 \gamma^\mu C \bar{c}_n^T(x) + q_j^T(x) C \gamma_\mu \gamma_5 c_k(x) \bar{q}'_m(x) \gamma^\mu C \bar{c}_n^T(x) \right], \\
J_{PS}^+(x) &= \frac{\varepsilon^{ijk}\varepsilon^{imn}}{\sqrt{2}} \left[q_j^T(x) C c_k(x) \bar{q}'_m(x) \gamma_5 C \bar{c}_n^T(x) + q_j^T(x) C \gamma_5 c_k(x) \bar{q}'_m(x) C \bar{c}_n^T(x) \right], \\
J_{PS}^-(x) &= \frac{\varepsilon^{ijk}\varepsilon^{imn}}{\sqrt{2}} \left[q_j^T(x) C c_k(x) \bar{q}'_m(x) \gamma_5 C \bar{c}_n^T(x) - q_j^T(x) C \gamma_5 c_k(x) \bar{q}'_m(x) C \bar{c}_n^T(x) \right], \\
J_{TT}^+(x) &= \frac{\varepsilon^{ijk}\varepsilon^{imn}}{\sqrt{2}} \left[q_j^T(x) C \sigma_{\mu\nu} c_k(x) \bar{q}'_m(x) \gamma_5 \sigma^{\mu\nu} C \bar{c}_n^T(x) + q_j^T(x) C \sigma_{\mu\nu} \gamma_5 c_k(x) \bar{q}'_m(x) \sigma^{\mu\nu} C \bar{c}_n^T(x) \right], \\
J_{TT}^-(x) &= \frac{\varepsilon^{ijk}\varepsilon^{imn}}{\sqrt{2}} \left[q_j^T(x) C \sigma_{\mu\nu} c_k(x) \bar{q}'_m(x) \gamma_5 \sigma^{\mu\nu} C \bar{c}_n^T(x) - q_j^T(x) C \sigma_{\mu\nu} \gamma_5 c_k(x) \bar{q}'_m(x) \sigma^{\mu\nu} C \bar{c}_n^T(x) \right],
\end{aligned} \tag{182}$$

with $q, q' = u, d, s$, the superscripts \pm symbolize the positive and negative charge-conjugation, respectively, the subscripts P, S, V, A and T stand for the pseudoscalar, scalar, vector, axialvector and tensor diquarks, respectively [446].

Under parity transform \hat{P} , the $J(x)$ have the property,

$$\hat{P}J(x)\hat{P}^{-1} = -J(\tilde{x}). \tag{183}$$

Under charge-conjugation transform \hat{C} , the $J(x)$ have the property,

$$\hat{C}J^\pm(x)\hat{C}^{-1} = \pm J^\pm(x) |_{q \leftrightarrow q'}, \tag{184}$$

and we can prove that the current $J_{TT}^-(x) = 0$ through performing the Fierz-transformation. Again, we take the isospin limit $m_u = m_d$, the four-quark currents with the symbolic quark structures,

$$\bar{c}c\bar{d}u, \bar{c}c\bar{u}d, \bar{c}c\frac{\bar{u}u - \bar{d}d}{\sqrt{2}}, \bar{c}c\frac{\bar{u}u + \bar{d}d}{\sqrt{2}}, \tag{185}$$

couple potentially to the pseudoscalar tetraquark states with degenerated masses. And the four-quark currents with the symbolic quark structures,

$$\bar{c}c\bar{u}s, \bar{c}c\bar{s}d, \bar{c}c\bar{s}u, \bar{c}c\bar{s}d, \tag{186}$$

couple also potentially to the pseudoscalar tetraquark states with degenerated masses according to the isospin symmetry. And we obtain the QCD sum rules routinely.

In Table 24, we present the Borel windows, continuum threshold parameters, energy scales of the QCD spectral densities and pole contributions. From the Table, we can see distinctly that the pole contributions are about (40–60)% at the hadron side, while the central values are larger than 50%, the pole dominance criterion is satisfied very good. On the other hand, the higher vacuum condensates play a minor important role, the operator product expansion converge very well.

We take all the uncertainties of the input parameters into consideration and acquire the masses and pole residues, see Table 25. From Tables 24-25, we can see distinctly that the modified energy scale formula $\mu = \sqrt{M_{X/Y/Z}^2 - (2\mathbb{M}_c)^2} - k m_s(\mu)$ with $k = 0, 1$ or 2 is satisfied, where we subtract the small s -quark mass approximately to account for the small light flavor $SU(3)$ mass-breaking effects, which is slightly different from Eq.(101).

As can be seen distinctly from Table 25 that the lowest mass of the pseudoscalar hidden-charm tetraquark state with the symbolic quark constituents $c\bar{c}u\bar{d}$ is about 4.56 ± 0.08 GeV, which is much larger than the value $4239 \pm 18_{-10}^{+45}$ MeV from the LHCb collaboration [171]. In 2014, the

Z_c	J^{PC}	$T^2(\text{GeV}^2)$	$\sqrt{s_0}(\text{GeV})$	$\mu(\text{GeV})$	pole
$[uc]_A[d\bar{c}]_V - [uc]_V[d\bar{c}]_A$	0^{-+}	3.7 – 4.1	5.10 ± 0.10	2.7	(42 – 60)%
$[uc]_A[d\bar{c}]_V + [uc]_V[d\bar{c}]_A$	0^{--}	3.7 – 4.1	5.10 ± 0.10	2.8	(42 – 60)%
$[uc]_A[\bar{s}\bar{c}]_V - [uc]_V[\bar{s}\bar{c}]_A$	0^{-+}	3.7 – 4.1	5.15 ± 0.10	2.7	(43 – 61)%
$[uc]_A[\bar{s}\bar{c}]_V + [uc]_V[\bar{s}\bar{c}]_A$	0^{--}	3.7 – 4.1	5.15 ± 0.10	2.8	(43 – 61)%
$[sc]_A[\bar{s}\bar{c}]_V - [sc]_V[\bar{s}\bar{c}]_A$	0^{-+}	3.8 – 4.2	5.20 ± 0.10	2.7	(42 – 60)%
$[sc]_A[\bar{s}\bar{c}]_V + [sc]_V[\bar{s}\bar{c}]_A$	0^{--}	3.8 – 4.2	5.20 ± 0.10	2.8	(43 – 60)%
$[uc]_P[d\bar{c}]_S + [uc]_S[d\bar{c}]_P$	0^{-+}	3.7 – 4.1	5.10 ± 0.10	2.8	(42 – 60)%
$[uc]_P[d\bar{c}]_S - [uc]_S[d\bar{c}]_P$	0^{--}	3.7 – 4.1	5.10 ± 0.10	2.8	(42 – 60)%
$[uc]_P[\bar{s}\bar{c}]_S + [uc]_S[\bar{s}\bar{c}]_P$	0^{-+}	3.7 – 4.1	5.15 ± 0.10	2.8	(43 – 61)%
$[uc]_P[\bar{s}\bar{c}]_S - [uc]_S[\bar{s}\bar{c}]_P$	0^{--}	3.7 – 4.1	5.15 ± 0.10	2.8	(43 – 61)%
$[sc]_P[\bar{s}\bar{c}]_S + [sc]_S[\bar{s}\bar{c}]_P$	0^{-+}	3.8 – 4.2	5.20 ± 0.10	2.8	(43 – 61)%
$[sc]_P[\bar{s}\bar{c}]_S - [sc]_S[\bar{s}\bar{c}]_P$	0^{--}	3.8 – 4.2	5.20 ± 0.10	2.8	(43 – 61)%
$[uc]_T[d\bar{c}]_T + [uc]_T[d\bar{c}]_T$	0^{-+}	3.7 – 4.1	5.10 ± 0.10	2.7	(41 – 60)%
$[uc]_T[\bar{s}\bar{c}]_T + [uc]_T[\bar{s}\bar{c}]_T$	0^{-+}	3.7 – 4.1	5.15 ± 0.10	2.7	(43 – 61)%
$[sc]_T[\bar{s}\bar{c}]_T + [sc]_T[\bar{s}\bar{c}]_T$	0^{-+}	3.8 – 4.2	5.20 ± 0.10	2.7	(42 – 60)%

Table 24: The Borel parameters, continuum threshold parameters, energy scales of the QCD spectral densities and pole contributions for the pseudoscalar hidden-charm tetraquark states.

Z_c	J^{PC}	$M_Z(\text{GeV})$	$\lambda_Z(\text{GeV}^5)$
$[uc]_A[d\bar{c}]_V - [uc]_V[d\bar{c}]_A$	0^{-+}	4.56 ± 0.08	$(1.33 \pm 0.18) \times 10^{-1}$
$[uc]_A[d\bar{c}]_V + [uc]_V[d\bar{c}]_A$	0^{--}	4.58 ± 0.07	$(1.37 \pm 0.17) \times 10^{-1}$
$[uc]_A[\bar{s}\bar{c}]_V - [uc]_V[\bar{s}\bar{c}]_A$	0^{-+}	4.61 ± 0.08	$(1.41 \pm 0.19) \times 10^{-1}$
$[uc]_A[\bar{s}\bar{c}]_V + [uc]_V[\bar{s}\bar{c}]_A$	0^{--}	4.63 ± 0.08	$(1.45 \pm 0.19) \times 10^{-1}$
$[sc]_A[\bar{s}\bar{c}]_V - [sc]_V[\bar{s}\bar{c}]_A$	0^{-+}	4.66 ± 0.08	$(1.50 \pm 0.20) \times 10^{-1}$
$[sc]_A[\bar{s}\bar{c}]_V + [sc]_V[\bar{s}\bar{c}]_A$	0^{--}	4.67 ± 0.08	$(1.53 \pm 0.20) \times 10^{-1}$
$[uc]_P[d\bar{c}]_S + [uc]_S[d\bar{c}]_P$	0^{-+}	4.58 ± 0.07	$(6.92 \pm 0.86) \times 10^{-2}$
$[uc]_P[d\bar{c}]_S - [uc]_S[d\bar{c}]_P$	0^{--}	4.58 ± 0.07	$(6.91 \pm 0.86) \times 10^{-2}$
$[uc]_P[\bar{s}\bar{c}]_S + [uc]_S[\bar{s}\bar{c}]_P$	0^{-+}	4.63 ± 0.07	$(7.30 \pm 0.90) \times 10^{-2}$
$[uc]_P[\bar{s}\bar{c}]_S - [uc]_S[\bar{s}\bar{c}]_P$	0^{--}	4.63 ± 0.07	$(7.30 \pm 0.90) \times 10^{-2}$
$[sc]_P[\bar{s}\bar{c}]_S + [sc]_S[\bar{s}\bar{c}]_P$	0^{-+}	4.67 ± 0.08	$(7.73 \pm 0.97) \times 10^{-2}$
$[sc]_P[\bar{s}\bar{c}]_S - [sc]_S[\bar{s}\bar{c}]_P$	0^{--}	4.67 ± 0.08	$(7.73 \pm 0.96) \times 10^{-2}$
$[uc]_T[d\bar{c}]_T + [uc]_T[d\bar{c}]_T$	0^{-+}	4.57 ± 0.08	$(4.62 \pm 0.61) \times 10^{-1}$
$[uc]_T[\bar{s}\bar{c}]_T + [uc]_T[\bar{s}\bar{c}]_T$	0^{-+}	4.62 ± 0.08	$(4.89 \pm 0.63) \times 10^{-1}$
$[sc]_T[\bar{s}\bar{c}]_T + [sc]_T[\bar{s}\bar{c}]_T$	0^{-+}	4.67 ± 0.08	$(5.19 \pm 0.67) \times 10^{-1}$

Table 25: The masses and pole residues for the ground state pseudoscalar hidden-charm tetraquark states.

LHCb collaboration provided the first independent confirmation of the existence of the $Z_c(4430)$ in the $\psi'\pi^-$ mass spectrum and established its spin-parity to be $J^P = 1^+$ [?]. Furthermore, the LHCb collaboration observed a weak evidence for an additional resonance, the $Z_c(4240)$, in the $\psi'\pi^-$ mass spectrum with the preferred spin-parity $J^P = 0^-$, and the Breit-Wigner mass $M_Z = 4239 \pm 18_{-10}^{+45}$ MeV and width $\Gamma_Z = 220 \pm 47_{-74}^{+108}$ MeV, respectively with large uncertainties [172]. If the $Z_c(4240)$ is confirmed by further experimental research/detection in the future, it is an excellent candidate for the pseudoscalar hidden-charm tetraquark state with the spin-parity-charge-conjugation $J^{PC} = 0^{--}$.

In Ref.[425], Chen and Zhu study the hidden-charm tetraquark states with the symbolic quark constituents $c\bar{c}u\bar{d}$ in the framework of the QCD sum rules, and obtain the ground state masses 4.55 ± 0.11 GeV for the tetraquark states with the $J^{PC} = 0^{--}$, the masses 4.55 ± 0.11 GeV, 4.67 ± 0.10 GeV, 4.72 ± 0.10 GeV for the tetraquark states with the $J^{PC} = 0^{-+}$. The present predictions are consistent with their calculations, again, we should bear in mind that their interpolating currents and schemes in treating the operator product expansion and input parameters at the QCD side differ from the present work remarkably. Any current operator with the same quantum numbers and same quark structure as a Fock state in a hadron couples potentially to this hadron, so we can construct several current operators to interpolate a hadron, or construct a current operator to interpolate several hadrons.

From Table 25, we can see distinctly that the central values of the masses of the $J^{PC} = 0^{-+}$ tetraquark states with the symbolic quark constituents $uc\bar{d}\bar{c}$, $uc\bar{s}\bar{c}$, $sc\bar{s}\bar{c}$ are about $4.56 \sim 4.58$ GeV, $4.61 \sim 4.62$ GeV and $4.66 \sim 4.67$ GeV, respectively, the central values of the masses of the $J^{PC} = 0^{--}$ tetraquark states with the symbolic quark constituents $uc\bar{d}\bar{c}$, $uc\bar{s}\bar{c}$ and $sc\bar{s}\bar{c}$ are about 4.58 GeV, 4.63 GeV and 4.67 GeV, respectively. We can obtain the conclusion tentatively that the currents $J_{AV}^+(x)$, $J_{PS}^+(x)$ and $J_{TT}^+(x)$ couple potentially to three different pseudoscalar tetraquark states with almost degenerated masses, or to one pseudoscalar tetraquark state with three different Fock components; the currents $J_{AV}^-(x)$ and $J_{PS}^-(x)$ couple potentially to two different pseudoscalar tetraquark states with almost degenerated masses, or to one pseudoscalar tetraquark state with two different Fock components. As the currents with the same quantum numbers couple potentially to the pseudoscalar tetraquark states with almost degenerated masses, the mixing effects cannot improve the predictions remarkably if only the tetraquark masses are concerned. All in all, we obtain reasonable predictions for the masses of the pseudoscalar tetraquark states without strange, with strange and with hidden-strange, the central values are about $4.56 \sim 4.58$ GeV, $4.61 \sim 4.63$ GeV and $4.66 \sim 4.67$ GeV, respectively.

The following two-body strong decays of the pseudoscalar hidden-charm tetraquark states,

$$\begin{aligned}
Z_c(0^{--}) &\rightarrow \chi_{c1}\rho, \eta_c\rho, J/\psi a_1(1260), J/\psi\pi, D\bar{D}_0 + h.c., D^*\bar{D}_1 + h.c., D^*\bar{D} + h.c., \\
Z_c(0^{-+}) &\rightarrow \chi_{c0}\pi, \eta_c f_0(500), J/\psi\rho, D\bar{D}_0 + h.c., D^*\bar{D}_1 + h.c., D^*\bar{D} + h.c., \\
Z_{cs}(0^{--}) &\rightarrow \chi_{c1}K^*, \eta_c K^*, J/\psi K_1, J/\psi K, D_s\bar{D}_0 + h.c., D\bar{D}_{s0} + h.c., D_s^*\bar{D}_1 + h.c., \\
&\quad D^*\bar{D}_{s1} + h.c., D_s^*\bar{D} + h.c., D^*\bar{D}_s + h.c., \\
Z_{cs}(0^{-+}) &\rightarrow \chi_{c0}K, \eta_c K_0^*(700), J/\psi K^*, D_s\bar{D}_0 + h.c., D\bar{D}_{s0} + h.c., D_s^*\bar{D}_1 + h.c., \\
&\quad D^*\bar{D}_{s1} + h.c., D_s^*\bar{D} + h.c., D^*\bar{D}_s + h.c., \\
Z_{css}(0^{--}) &\rightarrow \chi_{c1}\phi, \eta_c\phi, J/\psi f_1, J/\psi\eta, D_s\bar{D}_{s0} + h.c., D_s^*\bar{D}_{s1} + h.c., D_s^*\bar{D}_s + h.c., \\
Z_{css}(0^{-+}) &\rightarrow \chi_{c0}\eta, \eta_c f_0(980), J/\psi\phi, D_s\bar{D}_{s0} + h.c., D_s^*\bar{D}_{s1} + h.c., D_s^*\bar{D}_s + h.c., \quad (187)
\end{aligned}$$

can take place through the Okubo-Zweig-Iizuka super-allowed fall-apart mechanism.

5.4 Tetraquark states with explicit P-wave

In the type-II diquark model [52], Maiani et al assign the $Y(4008)$, $Y(4260)$, $Y(4290/4220)$ and $Y(4630)$ as four tetraquark states with the $L = 1$ based on the effective spin-spin and spin-orbit interactions, see Eq.(31). In Ref.[276], A. Ali et al incorporate the dominant spin-spin, spin-orbit

$ S_{qc}, S_{\bar{q}\bar{c}}; S, L; J\rangle$	[52]	[276]	Currents
$ 0, 0; 0, 1; 1\rangle$	$Y(4008)$	$Y(4220)$	$J_\mu^1(x)$
$\frac{1}{\sqrt{2}}(1, 0; 1, 1; 1\rangle + 0, 1; 1, 1; 1\rangle)$	$Y(4260)$	$Y(4330)$	$J_{\mu\nu}(x)$
$ 1, 1; 0, 1; 1\rangle$	$Y(4290/4220)$	$Y(4390)$	$J_\mu^2(x)$
$ 1, 1; 2, 1; 1\rangle$	$Y(4630)$	$Y(4660)$	$J_\mu^3(x)$
$ 1, 1; 2, 3; 1\rangle$			

Table 26: The vector tetraquark states, possible assignments and the corresponding vector tetraquark currents, where the mixing effects are neglected.

and tensor interactions, see Eq.(32), and observe that the preferred assignments of the tetraquark states with $L = 1$ are the $Y(4220)$, $Y(4330)$, $Y(4390)$, $Y(4660)$. In the diquark model, the quantum numbers of the Y states are shown explicitly in Table 26, where the L is the angular momentum between the diquark and antidiquark, $\vec{S} = \vec{S}_{qc} + \vec{S}_{\bar{q}\bar{c}}$, $\vec{J} = \vec{S} + \vec{L}$.

We take the isospin limit, and construct the interpolating currents according the quantum numbers shown in Table 26,

$$\begin{aligned}
J_\mu^1(x) &= \frac{\varepsilon^{ijk}\varepsilon^{imn}}{\sqrt{2}} u^{Tj}(x) C \gamma_5 c^k(x) \overleftrightarrow{\partial}_\mu \bar{d}^m(x) \gamma_5 C \bar{c}^{Tn}(x), \\
J_\mu^2(x) &= \frac{\varepsilon^{ijk}\varepsilon^{imn}}{\sqrt{2}} u^{Tj}(x) C \gamma_\alpha c^k(x) \overleftrightarrow{\partial}_\mu \bar{d}^m(x) \gamma^\alpha C \bar{c}^{Tn}(x), \\
J_\mu^3(x) &= \frac{\varepsilon^{ijk}\varepsilon^{imn}}{2} \left[u^{Tj}(x) C \gamma_\mu c^k(x) \overleftrightarrow{\partial}_\alpha \bar{d}^m(x) \gamma^\alpha C \bar{c}^{Tn}(x) \right. \\
&\quad \left. + u^{Tj}(x) C \gamma^\alpha c^k(x) \overleftrightarrow{\partial}_\alpha \bar{d}^m(x) \gamma_\mu C \bar{c}^{Tn}(x) \right], \\
J_{\mu\nu}(x) &= \frac{\varepsilon^{ijk}\varepsilon^{imn}}{2\sqrt{2}} \left[u^{Tj}(x) C \gamma_5 c^k(x) \overleftrightarrow{\partial}_\mu \bar{d}^m(x) \gamma_\nu C \bar{c}^{Tn}(x) \right. \\
&\quad \left. + u^{Tj}(x) C \gamma_\nu c^k(x) \overleftrightarrow{\partial}_\mu \bar{d}^m(x) \gamma_5 C \bar{c}^{Tn}(x) \right. \\
&\quad \left. - u^{Tj}(x) C \gamma_5 c^k(x) \overleftrightarrow{\partial}_\nu \bar{d}^m(x) \gamma_\mu C \bar{c}^{Tn}(x) \right. \\
&\quad \left. - u^{Tj}(x) C \gamma_\mu c^k(x) \overleftrightarrow{\partial}_\nu \bar{d}^m(x) \gamma_5 C \bar{c}^{Tn}(x) \right]. \tag{188}
\end{aligned}$$

Under charge conjugation transform \hat{C} , the currents $J_\mu(x)$ and $J_{\mu\nu}(x)$ have the property,

$$\begin{aligned}
\hat{C} J_\mu(x) \hat{C}^{-1} &= -J_\mu(x), \\
\hat{C} J_{\mu\nu}(x) \hat{C}^{-1} &= -J_{\mu\nu}(x), \tag{189}
\end{aligned}$$

the currents have definite charge conjugation.

We choose the currents $J_\mu(x) = J_\mu^1(x)$, $J_\mu^2(x)$, $J_\mu^3(x)$ and $J_{\mu\nu}(x)$ and resort the correlation functions in Eqs.(163) to study the vector tetraquark states using the modified energy scale formula,

$$\begin{aligned}
\mu &= \sqrt{M_{X/Y/Z}^2 - (2M_c + 0.5 \text{ GeV})^2}, \\
&= \sqrt{M_{X/Y/Z}^2 - (4.1 \text{ GeV})^2}, \tag{190}
\end{aligned}$$

to determine the ideal energy scales of the QCD spectral densities, and reexamine the possible assignments of the Y states [459, 460]. The numerical results are shown explicitly in Tables 27-29.

The predicted mass $M_Y = 4.24 \pm 0.10 \text{ GeV}$ of the $|0, 0; 0, 1; 1\rangle$ tetraquark state is in excellent agreement with the experimental data $M_{Y(4220)} = 4222.0 \pm 3.1 \pm 1.4 \text{ MeV}$ from the BESIII collaboration [146], or $M_{Y(4260)} = 4230.0 \pm 8.0 \text{ MeV}$ from the Particle Data Group [347], which supports

$ S_{qc}, S_{\bar{q}\bar{c}}; S, L; J\rangle$	$\mu(\text{GeV})$	$T^2(\text{GeV}^2)$	$\sqrt{s_0}(\text{GeV})$	pole	$D(10)$
$ 0, 0; 0, 1; 1\rangle$	1.1	2.2 – 2.8	4.80 ± 0.10	(49 – 81)%	$\leq 1\%$
$ 1, 1; 0, 1; 1\rangle$	1.2	2.2 – 2.8	4.85 ± 0.10	(45 – 79)%	(1 – 5)%
$\frac{1}{\sqrt{2}}(1, 0; 1, 1; 1\rangle + 0, 1; 1, 1; 1\rangle)$	1.3	2.6 – 3.2	4.90 ± 0.10	(46 – 75)%	$\ll 1\%$
$ 1, 1; 2, 1; 1\rangle$	1.4	2.6 – 3.2	4.90 ± 0.10	(40 – 71)%	$\leq 1\%$

Table 27: The Borel windows T^2 , continuum threshold parameters s_0 , ideal energy scales, pole contributions of the ground states, and contributions of the vacuum condensates of dimension 10.

$ S_{qc}, S_{\bar{q}\bar{c}}; S, L; J\rangle$	$M_Y(\text{GeV})$	$\lambda_Y(10^{-2}\text{GeV}^6)$
$ 0, 0; 0, 1; 1\rangle$	4.24 ± 0.10	2.31 ± 0.45
$ 1, 1; 0, 1; 1\rangle$	4.28 ± 0.10	4.93 ± 1.00
$\frac{1}{\sqrt{2}}(1, 0; 1, 1; 1\rangle + 0, 1; 1, 1; 1\rangle)$	4.31 ± 0.10	2.99 ± 0.54
$ 1, 1; 2, 1; 1\rangle$	4.33 ± 0.10	7.35 ± 1.39

Table 28: The masses and pole residues of the vector tetraquark states.

assigning the $Y(4260/4220)$ as the $C\gamma_5 \otimes \overleftrightarrow{\partial}_\mu \otimes \gamma_5 C$ type vector tetraquark state. We obtain the **lowest vector hidden-charm tetraquark mass** up to now.

There have been other possible assignments for the $Y(4260)$ states, such as the hybrid states [261, 461, 462, 463, 464], molecular state [202, 204, 465, 466, 467], baryonium states [468, 469], hadro-charmonium state [470], interference effect [471, 472], etc.

From Tables 22 and 29, we can see explicitly that there are no rooms for the $Y(4008)$ and $Y(4750)$ in the vector hidden-charm tetraquark scenario. If we assign the $Y(4220/4230/4260)$ as the ground state, then we could assign the $Y(4750)$ as its first radial excitation according to the mass gap $M_{Y(4750)} - M_{Y(4260)} = 0.51 \text{ GeV}$.

We carry out the calculations routinely to obtain two QCD sum rules from the correlation functions, see Eq.(163), and currents, see Eq.(188),

$$\lambda_Y^2 \exp\left(-\frac{M_Y^2}{T^2}\right) = \int_{4m_c^2}^{s_0} ds \rho_{QCD}(s) \exp\left(-\frac{s}{T^2}\right), \quad (191)$$

$$\lambda_Y^2 \exp\left(-\frac{M_Y^2}{T^2}\right) + \lambda_{Y'}^2 \exp\left(-\frac{M_{Y'}^2}{T^2}\right) = \int_{4m_c^2}^{s'_0} ds \rho_{QCD}(s) \exp\left(-\frac{s}{T^2}\right), \quad (192)$$

where the s_0 and s'_0 correspond to the ground states Y and first radial excitations Y' , respectively.

We adopt the QCDSR II, see Eq.(153) and Eqs.(160)-(161), and obtain the Borel windows, continuum threshold parameters, suitable energy scales and pole contributions, which are shown

$ S_{qc}, S_{\bar{q}\bar{c}}; S, L; J\rangle$	$M_Y(\text{GeV})$	Assignments
$ 0, 0; 0, 1; 1\rangle$	4.24 ± 0.10	$Y(4220)$
$ 1, 1; 0, 1; 1\rangle$	4.28 ± 0.10	$Y(4220/4320)$
$\frac{1}{\sqrt{2}}(1, 0; 1, 1; 1\rangle + 0, 1; 1, 1; 1\rangle)$	4.31 ± 0.10	$Y(4320/4390)$
$ 1, 1; 2, 1; 1\rangle$	4.33 ± 0.10	$Y(4320/4390)$

Table 29: The possible assignments of the hidden-charm tetraquark states with explicit P-waves, the isospin limit is implied.

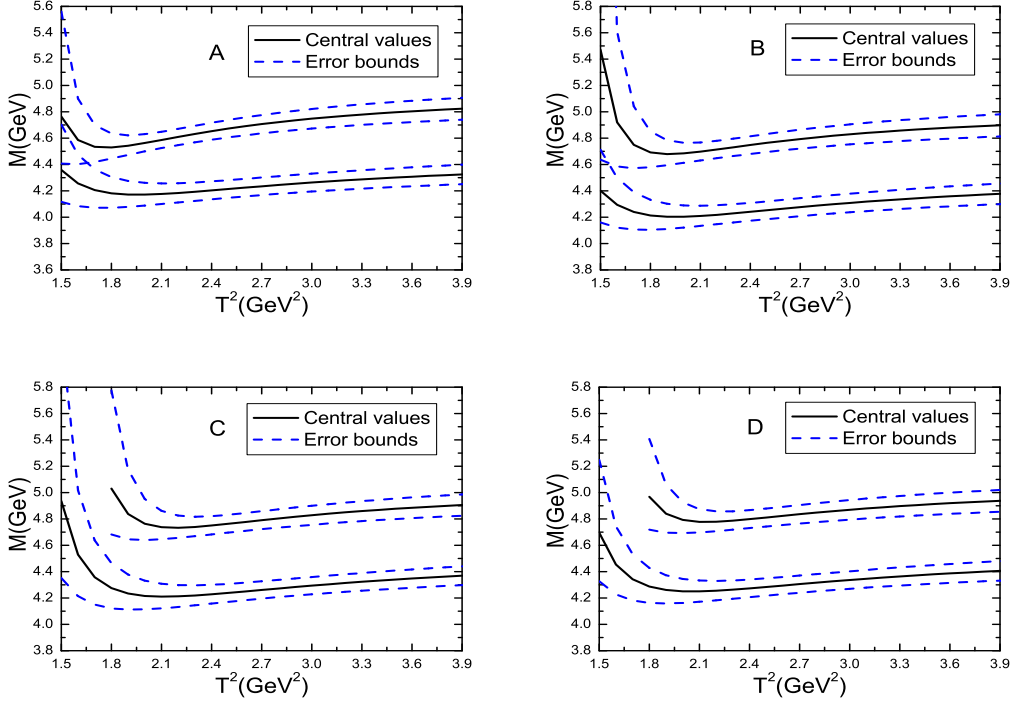


Figure 15: The masses of the vector tetraquark states with variations of the Borel parameters T^2 , where the A , B , C and D stand for the $|0, 0; 0, 1; 1\rangle$, $|1, 1; 0, 1; 1\rangle$, $\frac{1}{\sqrt{2}}(|1, 0; 1, 1; 1\rangle + |0, 1; 1, 1; 1\rangle)$ and $|1, 1; 2, 1; 1\rangle$ states, respectively; the lower lines and upper lines stand for the ground states and first radial excitations, respectively.

explicitly in Tables 30-31. From the tables, we can see explicitly that the pole contributions of the 1S states (the 1S plus 2S states) are about (40 – 60)% ((67 – 85)%), the pole dominance is satisfied very well. On the other hand, the contributions from the highest dimensional condensates play a minor important role, $|D(10)| < 3\%$ or $\ll 1\%$ ($< 1\%$ or $\ll 1\%$) for the 1S states (the 1S plus 2S states), the operator product expansion converges very good and better than that in our previous work [460], see Table 27.

From Tables 30-33, we can see explicitly that the modified energy scale formula, see Eq.(190), can be well satisfied, and the relations $\sqrt{s_0} = M_Y + 0.50 \sim 0.55 \pm 0.10 \text{ GeV}$ and $\sqrt{s'_0} = M_{Y'} + 0.40 \pm 0.10 \text{ GeV}$ are hold, see Eq.(162).

In Fig.15, we plot the masses of the 1P and 2P hidden-charm tetraquark states with the $J^{PC} = 1^{--}$. From the figure, we can see explicitly that there appear flat platforms in the Borel windows, the uncertainties come from the Borel parameters are rather small.

In Table 34, we present the possible assignments of the vector tetraquark states. From the table, we can see explicitly that there is a room to accommodate the $Y(4750)$, i.e. the $Y(4220/4260)$ and $Y(4750)$ can be assigned as the ground state and first radial excited state of the $C\gamma_5 \overset{\leftrightarrow}{\partial}_\mu \gamma_5 C$ type tetraquark states with the $J^{PC} = 1^{--}$, respectively [473].

We can study the corresponding hidden-bottom tetraquark states with the simple replacement $c \rightarrow b$ in Eq.(188). In Ref.[474], we observe that the $Y(10750)$ observed by the Belle collaboration [183] can be assigned as the $C\gamma_5 \otimes \overset{\leftrightarrow}{\partial}_\mu \otimes \gamma_5 C$ type hidden-bottom tetraquark state with the $J^{PC} = 1^{--}$.

$ S_{qc}, S_{\bar{q}\bar{c}}; S, L; J\rangle$	$\mu(\text{GeV})$	$T^2(\text{GeV}^2)$	$\sqrt{s_0}(\text{GeV})$	pole	$D(10)$
$ 0, 0; 0, 1; 1\rangle$	1.1	2.6 – 3.0	4.75 ± 0.10	(40 – 65)%	< 1%
$ 1, 1; 0, 1; 1\rangle$	1.2	2.5 – 2.9	4.80 ± 0.10	(39 – 64)%	< 3%
$\frac{1}{\sqrt{2}}(1, 0; 1, 1; 1\rangle + 0, 1; 1, 1; 1\rangle)$	1.3	3.0 – 3.4	4.85 ± 0.10	(38 – 60)%	$\ll 1\%$
$ 1, 1; 2, 1; 1\rangle$	1.3	2.7 – 3.1	4.85 ± 0.10	(39 – 63)%	< 1%

Table 30: The Borel windows T^2 , continuum threshold parameters s_0 , energy scales of the QCD spectral densities, contributions of the ground states, and values of the $D(10)$.

$ S_{qc}, S_{\bar{q}\bar{c}}; S, L; J\rangle$	$\mu(\text{GeV})$	$T^2(\text{GeV}^2)$	$\sqrt{s'_0}(\text{GeV})$	pole	$D(10)$
$ 0, 0; 0, 1; 1\rangle$	2.4	2.8 – 3.2	5.15 ± 0.10	(67 – 85)%	$\ll 1\%$
$ 1, 1; 0, 1; 1\rangle$	2.5	2.6 – 3.0	5.20 ± 0.10	(67 – 86)%	< 1%
$\frac{1}{\sqrt{2}}(1, 0; 1, 1; 1\rangle + 0, 1; 1, 1; 1\rangle)$	2.6	3.0 – 3.4	5.25 ± 0.10	(67 – 84)%	$\ll 1\%$
$ 1, 1; 2, 1; 1\rangle$	2.6	2.7 – 3.1	5.25 ± 0.10	(68 – 87)%	$\ll 1\%$

Table 31: The Borel windows T^2 , continuum threshold parameters s'_0 , energy scales of the QCD spectral densities, contributions of the ground states plus first radial excitations, and values of the $D(10)$.

$ S_{qc}, S_{\bar{q}\bar{c}}; S, L; J\rangle$	$M_Y(\text{GeV})$	$\lambda_Y(10^{-2}\text{GeV}^6)$
$ 0, 0; 0, 1; 1\rangle$	4.24 ± 0.09	2.28 ± 0.42
$ 1, 1; 0, 1; 1\rangle$	4.28 ± 0.09	4.80 ± 0.95
$\frac{1}{\sqrt{2}}(1, 0; 1, 1; 1\rangle + 0, 1; 1, 1; 1\rangle)$	4.31 ± 0.09	2.94 ± 0.50
$ 1, 1; 2, 1; 1\rangle$	4.33 ± 0.09	6.55 ± 1.19

Table 32: The masses and pole residues of the ground states.

$ S_{qc}, S_{\bar{q}\bar{c}}; S, L; J\rangle$	$M_Y(\text{GeV})$	$\lambda_Y(10^{-2}\text{GeV}^6)$
$ 0, 0; 0, 1; 1\rangle$	4.75 ± 0.10	8.19 ± 1.23
$ 1, 1; 0, 1; 1\rangle$	4.81 ± 0.10	18.3 ± 3.0
$\frac{1}{\sqrt{2}}(1, 0; 1, 1; 1\rangle + 0, 1; 1, 1; 1\rangle)$	4.85 ± 0.09	8.63 ± 1.22
$ 1, 1; 2, 1; 1\rangle$	4.86 ± 0.10	21.7 ± 3.4

Table 33: The masses and pole residues of the first radial excited states.

$ S_{qc}, S_{\bar{q}\bar{c}}; S, L; J\rangle$	$M_Y(\text{GeV})$	Assignments
$ 0, 0; 0, 1; 1\rangle$ (1P)	4.24 ± 0.09	$Y(4220/4260)$
$ 0, 0; 0, 1; 1\rangle$ (2P)	4.75 ± 0.10	$Y(4750)$
$ 1, 1; 0, 1; 1\rangle$ (1P)	4.28 ± 0.09	$Y(4220/4320)$
$ 1, 1; 0, 1; 1\rangle$ (2P)	4.81 ± 0.10	
$\frac{1}{\sqrt{2}}(1, 0; 1, 1; 1\rangle + 0, 1; 1, 1; 1\rangle)$ (1P)	4.31 ± 0.09	$Y(4320/4390)$
$\frac{1}{\sqrt{2}}(1, 0; 1, 1; 1\rangle + 0, 1; 1, 1; 1\rangle)$ (2P)	4.85 ± 0.09	
$ 1, 1; 2, 1; 1\rangle$ (1P)	4.33 ± 0.09	$Y(4320/4390)$
$ 1, 1; 2, 1; 1\rangle$ (2P)	4.86 ± 0.10	

Table 34: The masses of the vector tetraquark states and possible assignments, where the 1P and 2P denote the ground states and first radial excitations, respectively.

6 $\bar{3}3$ type doubly heavy tetraquark states

In 2016, the LHCb collaboration observed the doubly charmed baryon state Ξ_{cc}^{++} in the $\Lambda_c^+ K^- \pi^+ \pi^+$ mass spectrum and measured the mass, but did not determine the spin [475]. The Ξ_{cc}^{++} maybe have the spin $\frac{1}{2}$ or $\frac{3}{2}$, we can take the diquark $\varepsilon^{ijk} c_i^T C \gamma_\mu c_j$ as basic constituent to construct the current

$$J_{\Xi_{cc}}(x) = \varepsilon^{ijk} c_i^T(x) C \gamma_\mu c_j(x) \gamma_5 \gamma^\mu u_k(x), \quad (193)$$

or

$$J_{\Xi_{cc}}^\mu(x) = \varepsilon^{ijk} c_i^T(x) C \gamma^\mu c_j(x) u_k(x), \quad (194)$$

to study it with the QCD sum rules [476]. The observation of the doubly charmed baryon state Ξ_{cc}^{++} has led a renaissance in the doubly heavy tetraquark spectroscopy [477, 478]. For a $QQ\bar{q}\bar{q}'$ system, if the two Q -quarks are in long separation, the gluon exchange force between them would be screened by the two \bar{q} -quarks, then a loosely $Q\bar{q} - Q\bar{q}'$ type bound state is formed. If the two Q quarks are in short separation, the QQ pair forms a compact point-like color source in heavy quark limit, and attracts a $\bar{q}\bar{q}'$ pair, which serves as another compact point-like color source, then an exotic $QQ - \bar{q}\bar{q}'$ type tetraquark state is formed. The existence and stability of the $QQ\bar{q}\bar{q}'$ tetraquark states have been extensively discussed in early literatures based on the potential models [479, 480] and heavy quark symmetry [481],

In Ref.[482], we choose the currents $J_\mu(x)$ and $\eta_\mu(x)$ to study the doubly heavy tetraquark states with the $J^P = 1^+$, where

$$\begin{aligned} J_\mu(x) &= \varepsilon^{ijk} \varepsilon^{imn} Q_j^T(x) C \gamma_\mu Q_k(x) \bar{u}_m(x) \gamma_5 C \bar{s}_n^T(x), \\ \eta_\mu(x) &= \varepsilon^{ijk} \varepsilon^{imn} Q_j^T(x) C \gamma_\mu Q_k(x) \bar{u}_m(x) \gamma_5 C \bar{d}_n^T(x), \end{aligned} \quad (195)$$

$Q = c, b$, again, we choose the correlation functions $\Pi_{\mu\nu}$, see Eq.(127). The tetraquark states are spatial extended objects, not point-like objects, however, we choose the local currents to interpolate the tetraquark states and take all the quarks and antiquarks as the color sources, and neglect the finite size effects.

We rewrite the current $J_\mu(x)$ as

$$\begin{aligned} J_\mu(x) &= Q_j^T(x) C \gamma_\mu Q_k(x) [\bar{u}_j(x) \gamma_5 C \bar{s}_k^T(x) - \bar{u}_k(x) \gamma_5 C \bar{s}_j^T(x)] \\ &= \frac{1}{2} [Q_j^T(x) C \gamma_\mu Q_k(x) - Q_k^T(x) C \gamma_\mu Q_j(x)] [\bar{u}_j(x) \gamma_5 C \bar{s}_k^T(x) - \bar{u}_k(x) \gamma_5 C \bar{s}_j^T(x)] \quad (196) \end{aligned}$$

	$T^2(\text{GeV}^2)$	$\sqrt{s_0}(\text{GeV})$	$\mu(\text{GeV})$	pole	$M(\text{GeV})$	$\lambda(\text{GeV}^5)$
$cc\bar{u}\bar{d}$	2.6 – 3.0	4.45 ± 0.10	1.3	(39 – 63)%	3.90 ± 0.09	$(2.64 \pm 0.42) \times 10^{-2}$
$cc\bar{u}\bar{s}$	2.6 – 3.0	4.50 ± 0.10	1.3	(41 – 64)%	3.95 ± 0.08	$(2.88 \pm 0.46) \times 10^{-2}$
$bb\bar{u}\bar{d}$	6.9 – 7.7	11.14 ± 0.10	2.4	(41 – 60)%	10.52 ± 0.08	$(1.30 \pm 0.20) \times 10^{-1}$
$bb\bar{u}\bar{s}$	6.8 – 7.6	11.15 ± 0.10	2.4	(41 – 61)%	10.55 ± 0.08	$(1.33 \pm 0.20) \times 10^{-1}$
$cc\bar{u}\bar{d}$	2.6 – 3.0	4.40 ± 0.10	1.4	(39 – 62)%	3.85 ± 0.09	$(2.60 \pm 0.42) \times 10^{-2}$

Table 35: The Borel windows, continuum threshold parameters, ideal energy scales, pole contributions, masses and pole residues for the doubly heavy tetraquark states.

according to the identity $\varepsilon_{ijk} \varepsilon_{imn} = \delta_{jm} \delta_{kn} - \delta_{jn} \delta_{km}$ in the color space. The current $J_\mu(x)$ is of $\bar{\mathbf{3}} \otimes \mathbf{3}$ type in the color space, we can also construct the current $\tilde{J}_\mu(x)$ satisfying Fermi-Dirac statistics,

$$\tilde{J}_\mu(x) = \frac{1}{2} [Q_j^T(x) C \gamma_5 Q_k(x) + Q_k^T(x) C \gamma_5 Q_j(x)] [\bar{u}_j(x) \gamma_\mu C \bar{s}_k^T(x) + \bar{u}_k(x) \gamma_\mu C \bar{s}_j^T(x)] \quad (197)$$

which is of $\mathbf{6} \otimes \bar{\mathbf{6}}$ type in the color space, and differs from the corresponding current constructed in Ref.[483] slightly.

The color factor defined in Eq.(27) has the values, $\langle \hat{C}_i \cdot \hat{C}_j \rangle = -\frac{2}{3}$ and $\frac{1}{3}$ for the $\bar{\mathbf{3}}$ and $\mathbf{6}$ diquark $[qq]$, respectively. If we define $\hat{C}_{12} \cdot \hat{C}_{34} = (\hat{C}_1 + \hat{C}_2) \cdot (\hat{C}_3 + \hat{C}_4)$, then $\langle \hat{C}_{12} \cdot \hat{C}_{34} \rangle = -\frac{4}{3}$ and $-\frac{10}{3}$ for the $\bar{\mathbf{33}}$ and $\mathbf{6\bar{6}}$ type tetraquark states. The one-gluon exchange induced attractive (repulsive) interactions favors (disfavors) formation of the $\bar{\mathbf{3}}$ ($\mathbf{6}$) diquark state $Q_j^T C \gamma_\mu Q_k - Q_k^T C \gamma_\mu Q_j$ ($Q_j^T C \gamma_5 Q_k + Q_k^T C \gamma_5 Q_j$), while the $\mathbf{6\bar{6}}$ -type tetraquark states are expected to have much smaller masses than that of the $\bar{\mathbf{33}}$ -type tetraquark states according to the $\hat{C}_{12} \cdot \hat{C}_{34}$. Furthermore, the color magnetic interaction, see Eq.(28), leads to mixing between the $\mathbf{6\bar{6}}$ and $\bar{\mathbf{33}}$ tetraquark states. In Ref.[483], M. L. Du et al obtain degenerate masses for the $\mathbf{6\bar{6}}$ and $\bar{\mathbf{33}}$ based on the QCD sum rules. We should study this subject further.

After tedious but straightforward calculations, we obtain the QCD sum rules for the doubly-heavy tetraquark states [482], which are named as the T states in the *The Review of Particle Physics* [91]. According to the energy scale formula in Eq.(100), we suggest an energy scale formula,

$$\mu = \sqrt{M_T^2 - (2M_Q)^2} - \kappa m_s(\mu), \quad (198)$$

to determine the optimal energy scales.

There existed no experimental candidates for the doubly heavy tetraquark states when performing the calculations [482]. After careful examinations, we choose the effective heavy quark masses $M_c = 1.84 \text{ GeV}$ and $M_b = 5.12 \text{ GeV}$, and take into account the $SU(3)$ breaking effect by subtracting the $\kappa m_s(\mu)$. In Table 35, we present the Borel windows T^2 , continuum threshold parameters s_0 , optimal energy scales, pole contributions of the ground states, where the same parameters as the ones in the QCD sum rules for the $Z_c(3900)$ are chosen, see the last line.

We take into account all uncertainties of the input parameters, and obtain the values of the masses and pole residues of the Z_{QQ} , which are shown explicitly in Table 35 and Fig.16. From Fig.16, we can see that there appear platforms in the Borel windows shown in Table 35. And we suggested to search for the Z_{QQ} states in the Okubo-Zweig-Iizuka super-allowed two-body strong decays

$$Z_{cc\bar{u}\bar{d}} \rightarrow D^0 D^{*+}, D^+ D^{*0}, \quad (199)$$

$$Z_{cc\bar{u}\bar{s}} \rightarrow D^0 D_s^{*+}, D_s^+ D^{*0}, \quad (200)$$

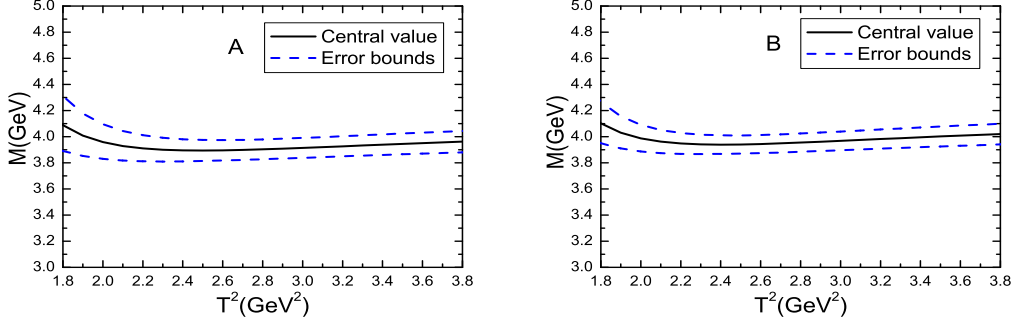


Figure 16: The masses with variations of the Borel parameter T^2 , where the A and B denote the tetraquark states $cc\bar{u}\bar{d}$ and $cc\bar{u}\bar{s}$, respectively.

and weak decays through $b \rightarrow c\bar{c}s$ at the quark level,

$$\begin{aligned} Z_{bb\bar{u}\bar{d}} &\rightarrow \bar{B}^0 B^{*-}, B^- \bar{B}^{*0} \rightarrow \gamma J/\psi K^- J/\psi \bar{K}^0, \\ Z_{bb\bar{u}\bar{s}} &\rightarrow \bar{B}_s^0 B^{*-}, B^- \bar{B}_s^{*0} \rightarrow \gamma J/\psi \phi J/\psi K^-. \end{aligned} \quad (201)$$

In 2021, the LHCb collaboration observed the exotic state $T_{cc}^+(3875)$ just below the $D^0 D^{*+}$ threshold [187, 188]. The Breit-Wigner mass and width are $\delta M_{BW} = -273 \pm 61 \pm 5_{-14}^{+11}$ KeV below the $D^0 D^{*+}$ threshold and $\Gamma_{BW} = 410 \pm 165 \pm 43_{-38}^{+18}$ KeV [187, 188]. While the Particle Data Group fit the Breit-Wigner mass and width to be 3874.83 ± 0.11 MeV and $0.410 \pm 0.165_{-0.057}^{+0.047}$ MeV, respectively [91]. The prediction $M_{Z_{cc\bar{u}\bar{d}}} = 3.90 \pm 0.09$ GeV is in excellent agreement with the LHCb data.

Before the LHCb data, several theoretical groups had made predictions for the T_{cc} masses [236, 245, 293, 299, 302, 308, 311, 317, 318, 477, 478, 482, 484, 485, 486, 487, 488, 489, 490, 491, 492, 493, 494, 495, 496, 497, 498, 499, 500, 501, 502], the predicted masses differ from each other in one way or the other.

In Ref.[484], we resort to the correlation functions $\Pi(p)$ and $\Pi_{\mu\nu\alpha\beta}(p)$ in Eq.(127) and currents

$$\begin{aligned} J(x) &= J_{\bar{u}\bar{d};0}(x), J_{\bar{u}\bar{s};0}(x), J_{\bar{s}\bar{s};0}(x), \\ J_{\mu\nu}(x) &= J_{\mu\nu;1}(x), J_{\mu\nu;2}(x), \\ J_{\mu\nu;1}(x) &= J_{\mu\nu;\bar{u}\bar{d};1}(x), J_{\mu\nu;\bar{u}\bar{s};1}(x), J_{\mu\nu;\bar{s}\bar{s};1}(x), \\ J_{\mu\nu;2}(x) &= J_{\mu\nu;\bar{u}\bar{d};2}(x), J_{\mu\nu;\bar{u}\bar{s};2}(x), J_{\mu\nu;\bar{s}\bar{s};2}(x), \end{aligned} \quad (202)$$

where

$$\begin{aligned} J_{\bar{u}\bar{d};0}(x) &= \varepsilon^{ijk} \varepsilon^{imn} c_j^T(x) C \gamma_\mu c_k(x) \bar{u}_m(x) \gamma^\mu C \bar{d}_n^T(x), \\ J_{\bar{u}\bar{s};0}(x) &= \varepsilon^{ijk} \varepsilon^{imn} c_j^T(x) C \gamma_\mu c_k(x) \bar{u}_m(x) \gamma^\mu C \bar{s}_n^T(x), \\ J_{\bar{s}\bar{s};0}(x) &= \varepsilon^{ijk} \varepsilon^{imn} c_j^T(x) C \gamma_\mu c_k(x) \bar{s}_m(x) \gamma^\mu C \bar{s}_n^T(x), \\ J_{\mu\nu;\bar{u}\bar{d};1}(x) &= \varepsilon^{ijk} \varepsilon^{imn} [c_j^T(x) C \gamma_\mu c_k(x) \bar{u}_m(x) \gamma_\nu C \bar{d}_n^T(x) - c_j^T(x) C \gamma_\nu c_k(x) \bar{u}_m(x) \gamma_\mu C \bar{d}_n^T(x)], \\ J_{\mu\nu;\bar{u}\bar{s};1}(x) &= \varepsilon^{ijk} \varepsilon^{imn} [c_j^T(x) C \gamma_\mu c_k(x) \bar{u}_m(x) \gamma_\nu C \bar{s}_n^T(x) - c_j^T(x) C \gamma_\nu c_k(x) \bar{u}_m(x) \gamma_\mu C \bar{s}_n^T(x)], \\ J_{\mu\nu;\bar{s}\bar{s};1}(x) &= \varepsilon^{ijk} \varepsilon^{imn} [c_j^T(x) C \gamma_\mu c_k(x) \bar{s}_m(x) \gamma_\nu C \bar{s}_n^T(x) - c_j^T(x) C \gamma_\nu c_k(x) \bar{s}_m(x) \gamma_\mu C \bar{s}_n^T(x)], \\ J_{\mu\nu;\bar{u}\bar{d};2}(x) &= \varepsilon^{ijk} \varepsilon^{imn} [c_j^T(x) C \gamma_\mu c_k(x) \bar{u}_m(x) \gamma_\nu C \bar{d}_n^T(x) + c_j^T(x) C \gamma_\nu c_k(x) \bar{u}_m(x) \gamma_\mu C \bar{d}_n^T(x)], \\ J_{\mu\nu;\bar{u}\bar{s};2}(x) &= \varepsilon^{ijk} \varepsilon^{imn} [c_j^T(x) C \gamma_\mu c_k(x) \bar{u}_m(x) \gamma_\nu C \bar{s}_n^T(x) + c_j^T(x) C \gamma_\nu c_k(x) \bar{u}_m(x) \gamma_\mu C \bar{s}_n^T(x)], \\ J_{\mu\nu;\bar{s}\bar{s};2}(x) &= \varepsilon^{ijk} \varepsilon^{imn} [c_j^T(x) C \gamma_\mu c_k(x) \bar{s}_m(x) \gamma_\nu C \bar{s}_n^T(x) + c_j^T(x) C \gamma_\nu c_k(x) \bar{s}_m(x) \gamma_\mu C \bar{s}_n^T(x)], \end{aligned} \quad (203)$$

to study the mass spectrum of the $J^P = 0^+, 1^\pm$ and 2^+ doubly charmed tetraquark states systematically, where the subscripts 0, 1 and 2 denote the spin $J = 0, 1$ and 2, respectively.

At the phenomenological side, we obtain the hadronic representation and isolate the ground state contributions,

$$\Pi(p) = \frac{\lambda_Z^2}{M_Z^2 - p^2} + \dots = \Pi_0(p^2), \quad (204)$$

$$\begin{aligned} \Pi_{\mu\nu\alpha\beta;1}(p) &= \frac{\lambda_Z^2}{M_Z^2 - p^2} (p^2 g_{\mu\alpha} g_{\nu\beta} - p^2 g_{\mu\beta} g_{\nu\alpha} - g_{\mu\alpha} p_\nu p_\beta - g_{\nu\beta} p_\mu p_\alpha + g_{\mu\beta} p_\nu p_\alpha + g_{\nu\alpha} p_\mu p_\beta) \\ &\quad + \frac{\lambda_Y^2}{M_Y^2 - p^2} (-g_{\mu\alpha} p_\nu p_\beta - g_{\nu\beta} p_\mu p_\alpha + g_{\mu\beta} p_\nu p_\alpha + g_{\nu\alpha} p_\mu p_\beta) + \dots, \\ &= \Pi_Z(p^2) (p^2 g_{\mu\alpha} g_{\nu\beta} - p^2 g_{\mu\beta} g_{\nu\alpha} - g_{\mu\alpha} p_\nu p_\beta - g_{\nu\beta} p_\mu p_\alpha + g_{\mu\beta} p_\nu p_\alpha + g_{\nu\alpha} p_\mu p_\beta) \\ &\quad + \Pi_Y(p^2) (-g_{\mu\alpha} p_\nu p_\beta - g_{\nu\beta} p_\mu p_\alpha + g_{\mu\beta} p_\nu p_\alpha + g_{\nu\alpha} p_\mu p_\beta), \end{aligned} \quad (205)$$

$$\begin{aligned} \Pi_{\mu\nu\alpha\beta;2}(p) &= \frac{\lambda_Z^2}{M_Z^2 - p^2} \left(\frac{\tilde{g}_{\mu\alpha} \tilde{g}_{\nu\beta} + \tilde{g}_{\mu\beta} \tilde{g}_{\nu\alpha}}{2} - \frac{\tilde{g}_{\mu\nu} \tilde{g}_{\alpha\beta}}{3} \right) + \dots, \\ &= \Pi_2(p^2) \left(\frac{\tilde{g}_{\mu\alpha} \tilde{g}_{\nu\beta} + \tilde{g}_{\mu\beta} \tilde{g}_{\nu\alpha}}{2} - \frac{\tilde{g}_{\mu\nu} \tilde{g}_{\alpha\beta}}{3} \right), \end{aligned} \quad (206)$$

where $\tilde{g}_{\mu\nu} = g_{\mu\nu} - \frac{p_\mu p_\nu}{p^2}$, the pole residues λ_Z and λ_Y are defined by

$$\begin{aligned} \langle 0|J(0)|Z_{0^+}(p) \rangle &= \lambda_Z, \\ \langle 0|J_{\mu\nu;1}(0)|Z_{1^+}(p) \rangle &= \tilde{\lambda}_Z \epsilon_{\mu\nu\alpha\beta} \varepsilon^\alpha p^\beta, \\ \langle 0|J_{\mu\nu;1}(0)|Y_{1^-}(p) \rangle &= \tilde{\lambda}_Y (\varepsilon_\mu p_\nu - \varepsilon_\nu p_\mu), \\ \langle 0|J_{\mu\nu;2}(0)|Z_{2^+}(p) \rangle &= \lambda_Z \varepsilon_{\mu\nu}, \end{aligned} \quad (207)$$

$\lambda_Y = \tilde{\lambda}_Y M_Y$, $\lambda_Z = \tilde{\lambda}_Z M_Z$, the ε_μ and $\varepsilon_{\mu\nu}$ are the polarization vectors.

We perform the calculations routinely, and obtain the QCD sum rules for the masses and pole residues from the components $\Pi_0(p^2)$, $\Pi_{1;A}(p^2)$, $\Pi_{1;V}(p^2)$ and $\Pi_2(p^2)$, respectively, where $\Pi_{1;A}(p^2) = p^2 \Pi_Z(p^2)$ and $\Pi_{1;V}(p^2) = p^2 \Pi_Y(p^2)$. Again, we take the modified energy scale formula in Eq.(198) to determine the best energy scale formula of the QCD spectral densities.

After trial and error, we obtain Borel windows T^2 , continuum threshold parameters s_0 , optimal energy scales, pole contributions, see Table 36. From the Table, we can see clearly that the pole dominance can be well satisfied. In calculations, we observe that for the 1^- tetraquark states, the operator product expansion is well convergent, while in the case of the 0^+ , 1^+ and 2^+ tetraquark states, the contributions of the vacuum condensates of dimensions 6, 8, 10 have the hierarchy $|D(6)| \gg |D(8)| \gg |D(10)|$, the operator product expansion is also convergent. At last, we take account of all uncertainties of the input parameters, and obtain the values of the masses and pole residues, which are shown explicitly in Table 36.

The centroids of the masses of the $C\gamma_\mu \otimes \gamma_\nu C$ type tetraquark states are

$$\begin{aligned} M_{C\gamma_\mu \otimes \gamma_\nu C}(cc\bar{u}\bar{d}) &= \frac{M_{cc\bar{u}\bar{d};0^+} + 3M_{cc\bar{u}\bar{d};1^+} + 5M_{cc\bar{u}\bar{d};2^+}}{9} = 3.92 \text{ GeV}, \\ M_{C\gamma_\mu \otimes \gamma_\nu C}(cc\bar{u}\bar{s}) &= \frac{M_{cc\bar{u}\bar{s};0^+} + 3M_{cc\bar{u}\bar{s};1^+} + 5M_{cc\bar{u}\bar{s};2^+}}{9} = 3.99 \text{ GeV}, \\ M_{C\gamma_\mu \otimes \gamma_\nu C}(cc\bar{s}\bar{s}) &= \frac{M_{cc\bar{s}\bar{s};0^+} + 3M_{cc\bar{s}\bar{s};1^+} + 5M_{cc\bar{s}\bar{s};2^+}}{9} = 4.04 \text{ GeV}, \end{aligned} \quad (208)$$

which are slightly larger than the centroids of the masses of the corresponding $C\gamma_\mu \otimes \gamma_5 C$ type tetraquark states,

$$\begin{aligned} M_{C\gamma_\mu \otimes \gamma_5 C}(cc\bar{u}\bar{d}) &= 3.90 \text{ GeV}, \\ M_{C\gamma_\mu \otimes \gamma_5 C}(cc\bar{u}\bar{s}) &= 3.95 \text{ GeV}, \end{aligned} \quad (209)$$

so the ground states are the $C\gamma_\mu \otimes \gamma_5 C$ type tetraquark states, which is consistent with our naive expectation that the axialvector (anti)diquarks have larger masses than the corresponding scalar (anti)diquarks. The lowest centroids $M_{cc\bar{u}\bar{d};0^+} = 3.87 \text{ GeV}$ and $M_{cc\bar{u}\bar{s};0^+} = 3.94 \text{ GeV}$ originate from the spin splitting, in other words, the spin-spin interaction between the doubly heavy diquark and the light antidiquark. In fact, the predicted masses have uncertainties, the centroids of the masses are not the super values, all values within uncertainties make sense.

The QCD sum rules indicate the masses of the light axialvector diquark states lie about (150 – 200) MeV above that of the light scalar diquark states [433, 434, 435, 436], if they have the same valence quarks. Therefore, the centroids of the masses of the $C\gamma_\mu \otimes \gamma_\nu C$ type tetraquark states should be larger than 4.0 GeV, the present calculations maybe under-estimate the doubly-heavy masses. If we make the simple replacement $m_s(\mu) \rightarrow \mathbb{M}_s$ in the modified energy scale formula in Eq.(198), the predictions should be improved.

The doubly charmed tetraquark states with the $J^P = 0^+, 1^+$ and 2^+ lie near the corresponding charmed meson pair thresholds, the decays to the charmed meson pairs are Okubo-Zweig-Iizuka super-allowed,

$$\begin{aligned} Z_{cc\bar{u}\bar{d};0^+} &\rightarrow D^0 D^+, \\ Z_{cc\bar{u}\bar{s};0^+} &\rightarrow D^0 D_s^+, \\ Z_{cc\bar{s}\bar{s};0^+} &\rightarrow D_s^+ D_s^+, \\ Z_{cc\bar{u}\bar{d};1^+} &\rightarrow D^0 D^{*+}, D^+ D^{*0}, \\ Z_{cc\bar{u}\bar{s};1^+} &\rightarrow D^0 D_s^{*+}, D_s^+ D^{*0}, \\ Z_{cc\bar{s}\bar{s};1^+} &\rightarrow D_s^+ D_s^{*+}, \\ Z_{cc\bar{u}\bar{d};2^+} &\rightarrow D^0 D^+, D^{*0} D^{*+}, \\ Z_{cc\bar{u}\bar{s};2^+} &\rightarrow D^0 D_s^+, \\ Z_{cc\bar{s}\bar{s};2^+} &\rightarrow D_s^+ D_s^+, \end{aligned} \quad (210)$$

but the available phase spaces are very small, the decays are kinematically depressed, the doubly charmed tetraquark states with the $J^P = 0^+, 1^+$ and 2^+ maybe have small widths. On the other hand, the doubly charmed tetraquark states with the $J^P = 1^-$ lie above the corresponding charmed meson pair thresholds, the decays to the charmed meson pairs are Okubo-Zweig-Iizuka super-allowed,

$$\begin{aligned} Y_{cc\bar{u}\bar{d};1^-} &\rightarrow D^0 D^+, D^0 D^{*+}, D^+ D^{*0}, \\ Y_{cc\bar{u}\bar{s};1^-} &\rightarrow D^0 D_s^+, D^0 D_s^{*+}, D_s^+ D^{*0}, \\ Y_{cc\bar{s}\bar{s};1^-} &\rightarrow D_s^+ D_s^+, D_s^+ D_s^{*+}, \end{aligned} \quad (211)$$

the available phase spaces are large, the decays are kinematically facilitated, the doubly charmed tetraquark states with the $J^P = 1^-$ should have large widths.

7 $\bar{3}3$ type fully heavy tetraquark states

The exotic states $Z_c(3900)$, $Z_c(4020)$, $Z_c(4430)$, $T(3885)$, $P_c(4380)$, $P_c(4450)$, $Z_b(10610)$, $Z_b(10650)$, \dots are excellent candidates for the multiquark states, which consist two heavy quarks and two or three light quarks, we have to deal with both the heavy and light degrees of freedom of the

	$T^2(\text{GeV}^2)$	$\sqrt{s_0}(\text{GeV})$	$\mu(\text{GeV})$	pole	$M(\text{GeV})$	$\lambda(\text{GeV}^5)$
$cc\bar{u}d(0^+)$	2.4 – 2.8	4.40 ± 0.10	1.2	(38 – 63)%	3.87 ± 0.09	$(3.90 \pm 0.63) \times 10^{-2}$
$cc\bar{u}\bar{s}(0^+)$	2.6 – 3.0	4.50 ± 0.10	1.3	(38 – 62)%	3.94 ± 0.10	$(4.92 \pm 0.89) \times 10^{-2}$
$cc\bar{s}\bar{s}(0^+)$	2.6 – 3.0	4.55 ± 0.10	1.3	(39 – 63)%	3.99 ± 0.10	$(5.31 \pm 0.99) \times 10^{-2}$
$cc\bar{u}d(1^+)$	2.6 – 3.0	4.45 ± 0.10	1.3	(39 – 62)%	3.90 ± 0.09	$(3.44 \pm 0.54) \times 10^{-2}$
$cc\bar{u}\bar{s}(1^+)$	2.6 – 3.0	4.50 ± 0.10	1.3	(40 – 64)%	3.96 ± 0.08	$(3.78 \pm 0.59) \times 10^{-2}$
$cc\bar{s}\bar{s}(1^+)$	2.7 – 3.1	4.55 ± 0.10	1.3	(39 – 62)%	4.02 ± 0.09	$(4.11 \pm 0.68) \times 10^{-2}$
$cc\bar{u}d(2^+)$	2.7 – 3.1	4.50 ± 0.10	1.4	(39 – 62)%	3.95 ± 0.09	$(5.67 \pm 0.90) \times 10^{-2}$
$cc\bar{u}\bar{s}(2^+)$	2.8 – 3.2	4.55 ± 0.10	1.4	(38 – 60)%	4.01 ± 0.09	$(6.27 \pm 1.02) \times 10^{-2}$
$cc\bar{s}\bar{s}(2^+)$	2.8 – 3.2	4.60 ± 0.10	1.4	(39 – 61)%	4.06 ± 0.09	$(6.78 \pm 1.12) \times 10^{-2}$
$cc\bar{u}d(1^-)$	3.3 – 3.9	5.20 ± 0.10	2.9	(50 – 73)%	4.66 ± 0.10	$(1.31 \pm 0.17) \times 10^{-1}$
$cc\bar{u}\bar{s}(1^-)$	3.4 – 4.0	5.25 ± 0.10	2.9	(49 – 71)%	4.73 ± 0.11	$(1.40 \pm 0.19) \times 10^{-1}$
$cc\bar{s}\bar{s}(1^-)$	3.7 – 4.3	5.30 ± 0.10	2.9	(49 – 72)%	4.78 ± 0.11	$(1.48 \pm 0.19) \times 10^{-1}$

Table 36: The Borel windows, continuum threshold parameters, optimal energy scales, pole contributions, masses and pole residues for the doubly charmed tetraquark states.

dynamics. If there exist multi-quark configurations consist of fully heavy quarks, the dynamics is much simple, and the $QQ\bar{Q}\bar{Q}$ tetraquark states have been studied extensively before the LHCb data [281, 290, 303, 306, 479, 504, 505, 506, 507, 508, 509, 510, 426, 511, 512, 513, 514].

The quarks have color $SU(3)$ symmetry, we can construct the tetraquark states according to the routine quark \rightarrow diquark \rightarrow tetraquark,

$$(\mathbf{3} \otimes \mathbf{3}) \otimes (\bar{\mathbf{3}} \otimes \bar{\mathbf{3}}) \rightarrow (\bar{\mathbf{3}} \oplus \mathbf{6}) \otimes (\mathbf{3} \oplus \bar{\mathbf{6}}) \rightarrow (\bar{\mathbf{3}} \otimes \mathbf{3}) \oplus (\mathbf{6} \otimes \bar{\mathbf{6}}) \rightarrow (\mathbf{1} \oplus \mathbf{8}) \oplus \dots \quad (212)$$

For the $\bar{\mathbf{3}}$ diquarks, only the operators $\varepsilon^{ijk}Q_j^T C\gamma_\mu Q_k$ and $\varepsilon^{ijk}Q_j^T C\sigma_{\mu\nu}Q_k$ could exist due to Fermi-Dirac statistics, and we usually take the $\varepsilon^{ijk}Q_j^T C\gamma_\mu Q_k$ operators to construct the four-quark currents $J(x)$ and $J_{\mu\nu}(x)$ [512, 513], where $J_{\mu\nu}(x) = J_{\mu\nu}^1(x), J_{\mu\nu}^2(x)$, and

$$\begin{aligned} J(x) &= \varepsilon^{ijk}\varepsilon^{imn}Q_j^T(x)C\gamma_\mu Q_k(x)\bar{Q}_m(x)\gamma^\mu C\bar{Q}_n^T(x), \\ J_{\mu\nu}^1(x) &= \varepsilon^{ijk}\varepsilon^{imn} \{Q_j^T(x)C\gamma_\mu Q_k(x)\bar{Q}_m(x)\gamma_\nu C\bar{Q}_n^T(x) - Q_j^T(x)C\gamma_\nu Q_k(x)\bar{Q}_m(x)\gamma_\mu C\bar{Q}_n^T(x)\}, \\ J_{\mu\nu}^2(x) &= \frac{\varepsilon^{ijk}\varepsilon^{imn}}{\sqrt{2}} \{Q_j^T(x)C\gamma_\mu Q_k(x)\bar{Q}_m(x)\gamma_\nu C\bar{Q}_n^T(x) + Q_j^T(x)C\gamma_\nu Q_k(x)\bar{Q}_m(x)\gamma_\mu C\bar{Q}_n^T(x)\}, \end{aligned} \quad (213)$$

then resort to the correlation functions $\Pi(p)$ and $\Pi_{\mu\nu\alpha\beta}(p)$ shown in Eq.(127) to obtain the QCD sum rules.

In Ref.[426], Chen et al choose the currents $\eta^i(x)$, $\eta_\mu^k(x)$ and $\eta_{\mu\nu}^j(x)$ with $i = 1, 2, 3, 4, 5$, $k = 1, 2$ and $j = 1, 2$, to interpolate the $QQ\bar{Q}\bar{Q}$ tetraquark states with the $J^{PC} = 0^{++}, 1^{+-}$ and 2^{++} , respectively,

$$\begin{aligned} \eta^i(x) &= Q_a^T(x)C\Gamma^i Q_b(x)\bar{Q}_a(x)\Gamma^i C\bar{Q}_b^T(x), \\ \eta_\mu^1(x) &= Q_a^T(x)C\gamma_\mu\gamma_5 Q_b(x)\bar{Q}_a(x)C\bar{Q}_b^T(x) - Q_a^T(x)CQ_b(x)\bar{Q}_a(x)\gamma_\mu\gamma_5 C\bar{Q}_b^T(x), \\ \eta_\mu^2(x) &= Q_a^T(x)C\sigma_{\mu\nu}\gamma_5 Q_b(x)\bar{Q}_a(x)\gamma^\nu C\bar{Q}_b^T(x) - Q_a^T(x)C\gamma^\nu Q_b(x)\bar{Q}_a(x)\sigma_{\mu\nu}\gamma_5 C\bar{Q}_b^T(x), \\ \eta_{\mu\nu}^j(x) &= Q_a^T(x)C\Gamma_\mu^j Q_b(x)\bar{Q}_a(x)\Gamma_\nu^j C\bar{Q}_b^T(x) + Q_a^T(x)C\Gamma_\nu^j Q_b(x)\bar{Q}_a(x)\Gamma_\mu^j C\bar{Q}_b^T(x), \end{aligned} \quad (214)$$

where $\Gamma^1 = \gamma_5$, $\Gamma^2 = \gamma_\mu\gamma_5$, $\Gamma^3 = \sigma_{\mu\nu}$, $\Gamma^4 = \gamma_\mu$, $\Gamma^5 = 1$, $\Gamma_\mu^1 = \gamma_\mu$, $\Gamma_\mu^2 = \gamma_\mu\gamma_5$, the a and b are color indexes. The $C\gamma_5$, C , $C\gamma_\mu\gamma_5$ are antisymmetric, while the $C\gamma_\mu$, $C\sigma_{\mu\nu}$, $C\sigma_{\mu\nu}\gamma_5$ are symmetric. The currents $\eta^{1/2/5}(x)$, $\eta_\mu^1(x)$ and $\eta_{\mu\nu}^2(x)$ are in the color $\mathbf{6\bar{6}}$ representation, while the currents $\eta^{3/4}(x)$,

$\eta_\mu^2(x)$ and $\eta_{\mu\nu}^1(x)$ are in the color $\bar{\mathbf{33}}$ representation. For more currents and predictions in Scheme II, one can consult Ref.[426].

At the hadron side, we isolating the ground state contributions and obtain the results [512, 513],

$$\Pi(p) = \frac{\lambda_X^2}{M_X^2 - p^2} + \dots = \Pi_S(p^2), \quad (215)$$

$$\begin{aligned} \Pi_{\mu\nu\alpha\beta}^1(p) &= \frac{\lambda_{Y^+}^2}{M_{Y^+}^2 (M_{Y^+}^2 - p^2)} (p^2 g_{\mu\alpha} g_{\nu\beta} - p^2 g_{\mu\beta} g_{\nu\alpha} - g_{\mu\alpha} p_\nu p_\beta - g_{\nu\beta} p_\mu p_\alpha + g_{\mu\beta} p_\nu p_\alpha + g_{\nu\alpha} p_\mu p_\beta) \\ &+ \frac{\lambda_{Y^-}^2}{M_{Y^-}^2 (M_{Y^-}^2 - p^2)} (-g_{\mu\alpha} p_\nu p_\beta - g_{\nu\beta} p_\mu p_\alpha + g_{\mu\beta} p_\nu p_\alpha + g_{\nu\alpha} p_\mu p_\beta) + \dots, \\ &= \Pi_A(p^2) (p^2 g_{\mu\alpha} g_{\nu\beta} - p^2 g_{\mu\beta} g_{\nu\alpha} - g_{\mu\alpha} p_\nu p_\beta - g_{\nu\beta} p_\mu p_\alpha + g_{\mu\beta} p_\nu p_\alpha + g_{\nu\alpha} p_\mu p_\beta) \\ &+ \Pi_V(p^2) (-g_{\mu\alpha} p_\nu p_\beta - g_{\nu\beta} p_\mu p_\alpha + g_{\mu\beta} p_\nu p_\alpha + g_{\nu\alpha} p_\mu p_\beta). \end{aligned} \quad (216)$$

$$\begin{aligned} \Pi_{\mu\nu\alpha\beta}^2(p) &= \frac{\lambda_X^2}{M_X^2 - p^2} \left(\frac{\tilde{g}_{\mu\alpha} \tilde{g}_{\nu\beta} + \tilde{g}_{\mu\beta} \tilde{g}_{\nu\alpha}}{2} - \frac{\tilde{g}_{\mu\nu} \tilde{g}_{\alpha\beta}}{3} \right) + \dots, \\ &= \Pi_T(p^2) \left(\frac{\tilde{g}_{\mu\alpha} \tilde{g}_{\nu\beta} + \tilde{g}_{\mu\beta} \tilde{g}_{\nu\alpha}}{2} - \frac{\tilde{g}_{\mu\nu} \tilde{g}_{\alpha\beta}}{3} \right) + \dots, \end{aligned} \quad (217)$$

where $\tilde{g}_{\mu\nu} = g_{\mu\nu} - \frac{p_\mu p_\nu}{p^2}$, we add the superscripts 1 and 2 to denote the spins, and define the pole residues λ_X and λ_Y with $\lambda_{Y^\pm} = \tilde{\lambda}_{Y^\pm} M_{Y^\pm}$,

$$\begin{aligned} \langle 0|J(0)|X(p) \rangle &= \lambda_X, \\ \langle 0|J_{\mu\nu}^1(0)|Y^+(p) \rangle &= \tilde{\lambda}_{Y^+} \varepsilon_{\mu\nu\alpha\beta} \varepsilon^\alpha p^\beta, \\ \langle 0|J_{\mu\nu}^1(0)|Y^-(p) \rangle &= \tilde{\lambda}_{Y^-} (\varepsilon_\mu p_\nu - \varepsilon_\nu p_\mu), \\ \langle 0|J_{\mu\nu}^2(0)|X(p) \rangle &= \lambda_X \varepsilon_{\mu\nu}, \end{aligned} \quad (218)$$

$\lambda_{Y^+} = \tilde{\lambda}_{Y^+} M_{Y^+}$ the ε_μ and $\varepsilon_{\mu\nu}$ are the polarization vectors, the superscripts \pm denote the positive and negative parity.

If we take into account the first radial excited states, we obtain

$$\begin{aligned} \Pi_{S/T}(p^2) &= \frac{\lambda_X^2}{M_X^2 - p^2} + \frac{\lambda_{X'}^2}{M_{X'}^2 - p^2} + \dots, \\ \Pi_{A/V}(p^2) &= \frac{\lambda_{Y^\pm}^2}{M_{Y^\pm}^2 (M_{Y^\pm}^2 - p^2)} + \frac{\lambda_{Y'^\pm}^2}{M_{Y'^\pm}^2 (M_{Y'^\pm}^2 - p^2)} + \dots. \end{aligned} \quad (219)$$

We project out the axialvector and vector components $\Pi_A(p^2)$ and $\Pi_V(p^2)$ by introducing the operators $P_A^{\mu\nu\alpha\beta}$ and $P_V^{\mu\nu\alpha\beta}$, respectively,

$$\begin{aligned} \tilde{\Pi}_A(p^2) &= p^2 \Pi_A(p^2) = P_A^{\mu\nu\alpha\beta} \Pi_{\mu\nu\alpha\beta}(p), \\ \tilde{\Pi}_V(p^2) &= p^2 \Pi_V(p^2) = P_V^{\mu\nu\alpha\beta} \Pi_{\mu\nu\alpha\beta}(p), \end{aligned} \quad (220)$$

where

$$\begin{aligned} P_A^{\mu\nu\alpha\beta} &= \frac{1}{6} \left(g^{\mu\alpha} - \frac{p^\mu p^\alpha}{p^2} \right) \left(g^{\nu\beta} - \frac{p^\nu p^\beta}{p^2} \right), \\ P_V^{\mu\nu\alpha\beta} &= \frac{1}{6} \left(g^{\mu\alpha} - \frac{p^\mu p^\alpha}{p^2} \right) \left(g^{\nu\beta} - \frac{p^\nu p^\beta}{p^2} \right) - \frac{1}{6} g^{\mu\alpha} g^{\nu\beta}. \end{aligned} \quad (221)$$

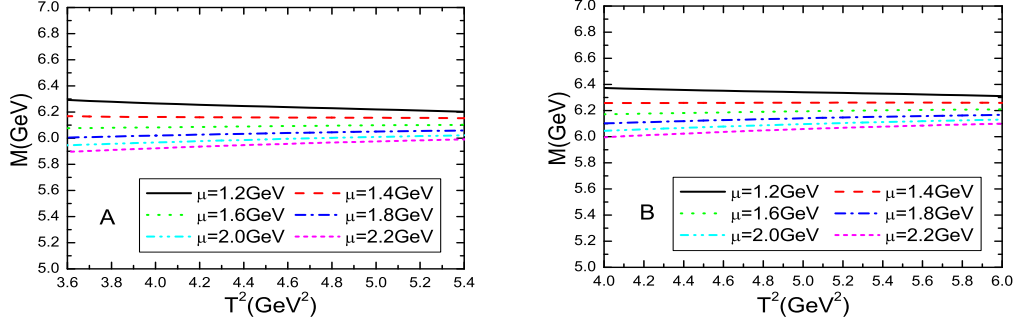


Figure 17: The masses of the $cc\bar{c}\bar{c}$ tetraquark states with variations of the energy scales and Borel parameters, where the A and B denote the $cc\bar{c}\bar{c}(0^{++})$ and $cc\bar{c}\bar{c}(2^{++})$, respectively.

	$T^2(\text{GeV}^2)$	$s_0(\text{GeV}^2)$	$\mu(\text{GeV})$	pole	$M_X(\text{GeV})$	$\lambda_X(\text{GeV}^5)$
$cc\bar{c}\bar{c}(0^{++})$	4.2 – 4.6	42 ± 1	2.0	(46 – 62)%	5.99 ± 0.08	$(3.72 \pm 0.54) \times 10^{-1}$
$cc\bar{c}\bar{c}(1^{+-})$	4.5 – 4.9	43 ± 1	2.0	(46 – 61)%	6.05 ± 0.08	$(2.97 \pm 0.44) \times 10^{-1}$
$cc\bar{c}\bar{c}(2^{++})$	4.6 – 5.2	44 ± 1	2.0	(46 – 63)%	6.09 ± 0.08	$(3.36 \pm 0.45) \times 10^{-1}$
$cc\bar{c}\bar{c}(1^{--})$	4.2 – 4.6	44 ± 1	2.0	(46 – 62)%	6.11 ± 0.08	$(1.82 \pm 0.33) \times 10^{-1}$
$bb\bar{b}\bar{b}(0^{++})$	13.0 – 13.6	374 ± 3	3.1	(49 – 61)%	18.84 ± 0.09	6.79 ± 1.27
$bb\bar{b}\bar{b}(1^{+-})$	13.3 – 13.9	374 ± 3	3.1	(48 – 60)%	18.84 ± 0.09	5.45 ± 1.01
$bb\bar{b}\bar{b}(2^{++})$	13.0 – 13.6	375 ± 3	3.1	(51 – 63)%	18.85 ± 0.09	5.55 ± 1.00
$bb\bar{b}\bar{b}(1^{--})$	11.7 – 12.3	376 ± 3	3.1	(47 – 60)%	18.89 ± 0.09	1.64 ± 0.36

Table 37: The Borel parameters, continuum threshold parameters, energy scales, pole contributions, masses and pole residues of the fully heavy tetraquark states.

Again we take the quark-hadron duality below the continuum thresholds s_0 and s'_0 , respectively, and perform Borel transform with respect to the variable $P^2 = -p^2$ to obtain the QCD sum rules:

$$\lambda_{X/Y}^2 \exp\left(-\frac{M_{X/Y}^2}{T^2}\right) = \int_{16m_c^2}^{s_0} ds \int_{z_i}^{z_f} dz \int_{t_i}^{t_f} dt \int_{r_i}^{r_f} dr \rho(s, z, t, r) \exp\left(-\frac{s}{T^2}\right), \quad (222)$$

$$\lambda_{X/Y}^2 \exp\left(-\frac{M_{X/Y}^2}{T^2}\right) + \lambda_{X'/Y'}^2 \exp\left(-\frac{M_{X'/Y'}^2}{T^2}\right) = \int_{16m_c^2}^{s'_0} ds \int_{z_i}^{z_f} dz \int_{t_i}^{t_f} dt \int_{r_i}^{r_f} dr \rho(s, z, t, r) \exp\left(-\frac{s}{T^2}\right), \quad (223)$$

where the QCD spectral densities $\rho(s, z, t, r) = \rho_S(s, z, t, r)$, $\rho_A(s, z, t, r)$, $\rho_V(s, z, t, r)$ and $\rho_T(s, z, t, r)$ [512, 513, 515].

In Fig.17, we plot the masses of the $cc\bar{c}\bar{c}$ tetraquark states with variations of the energy scales and Borel parameters for the threshold parameters $s_S^0 = 42 \text{ GeV}^2$ and $s_T^0 = 44 \text{ GeV}^2$. The predicted masses decrease monotonously and slowly with increase of the energy scales, the QCD sum rules are stable with variations of the Borel parameters at the energy scales $1.2 \text{ GeV} < \mu < 2.2 \text{ GeV}$. We choose the largest energy scale $\mu = 2.0 \text{ GeV}$ in Ref.[512]. In Refs.[512, 513], we obtain the predictions, see Table 37, where $M_{cc\bar{c}\bar{c}(0^{++})} < 2M_{J/\psi}$.

In 2020, the LHCb collaboration observed a broad structure above the $J/\psi J/\psi$ threshold ranging from 6.2 to 6.8 GeV and a narrow structure at about 6.9 GeV with the significance of

J^{PC}	$T^2(\text{GeV}^2)$	$\sqrt{s'_0}(\text{GeV})$	$\mu(\text{GeV})$	pole	$M_{X/Y}(\text{GeV})$	$\lambda_{X/Y}(10^{-1}\text{GeV}^5)$
$0^{++}(2S)$	4.4 – 4.8	6.80 ± 0.10	2.5	(65 – 79)%	6.48 ± 0.08	7.41 ± 1.12
$1^{+-}(2S)$	4.4 – 4.8	6.85 ± 0.10	2.5	(69 – 82)%	6.52 ± 0.08	5.56 ± 0.80
$2^{++}(2S)$	4.9 – 5.3	6.90 ± 0.10	2.5	(63 – 76)%	6.56 ± 0.08	5.92 ± 0.83
$1^{--}(2P)$	4.5 – 4.9	6.90 ± 0.10	2.2	(57 – 73)%	6.58 ± 0.09	3.46 ± 0.58

Table 38: The Borel parameters, continuum threshold parameters, energy scales, pole contributions, masses and pole residues of the 2S and 2P $cc\bar{c}\bar{c}$ tetraquark states.

J^{PC}	$M_1(\text{GeV})$	$M_2(\text{GeV})$	$M_3(\text{GeV})$	$M_4(\text{GeV})$
0^{++}	5.99 ± 0.08	6.48 ± 0.08	6.94 ± 0.08	7.36 ± 0.08
1^{+-}	6.05 ± 0.08	6.52 ± 0.08	6.96 ± 0.08	6.37 ± 0.08
2^{++}	6.09 ± 0.08	6.56 ± 0.08	7.00 ± 0.08	7.41 ± 0.08
1^{--}	6.11 ± 0.08	6.58 ± 0.09	7.02 ± 0.09	7.43 ± 0.09

Table 39: The masses of the $cc\bar{c}\bar{c}$ tetraquark states with the radial quantum numbers $n = 1, 2, 3$ and 4.

larger than 5σ in the $J/\psi J/\psi$ mass spectrum, and they also observed some vague structures around 7.2 GeV [132]. Accordingly, we obtain the masses of the 2S and 2P states from the QCDSR II from Eq.(223), and obtain the 3/4S and 3/4P masses by fitting the Regge trajectories,

$$M_n^2 = \alpha(n-1) + \alpha_0, \quad (224)$$

where the α and α_0 are constants, see Tables 38-39, which supports assigning the broad structure from 6.2 to 6.8 GeV in the di- J/ψ mass spectrum as the 2S or 2P tetraquark state, and assigning the narrow structure at about 6.9 GeV in the di- J/ψ mass spectrum as the 3S tetraquark state.

In 2023, the ATLAS collaboration observed a narrow resonance at about 6.9 GeV and a broader structure at much lower mass in the $J/\psi J/\psi$ channel, moreover, they observed a statistically significant excess at about 7.0 GeV in the $J/\psi\psi'$ channel [133]. In 2024, the CMS collaboration observed three resonant structures in the $J/\psi J/\psi$ mass spectrum, in the no-interference model, the measured Breit-Wigner masses and widths are [134],

$$\begin{aligned}
X(6600) : M &= 6552 \pm 10 \pm 12 \text{ MeV}, \Gamma = 124^{+32}_{-26} \pm 33 \text{ MeV}, \\
X(6900) : M &= 6927 \pm 9 \pm 4 \text{ MeV}, \Gamma = 122^{+24}_{-21} \pm 18 \text{ MeV}, \\
X(7300) : M &= 7287^{+20}_{-18} \pm 5 \text{ MeV}, \Gamma = 95^{+59}_{-40} \pm 19 \text{ MeV}.
\end{aligned} \quad (225)$$

In Ref.[135], we update the calculations by choosing the energy scale $\mu = 1.4 \text{ GeV}$, the lower bound in Fig.17 and choose the relation,

$$M_1 < \sqrt{s_0} < M_2 < \sqrt{s'_0} < M_3, \quad (226)$$

and obtain the predictions, see Tables 40-41, and make the possible assignments. see Table 42.

8 11 type hidden/doubly heavy tetraquark states

The $X(3872)$ and $Z_c(3900)$ lie at the $D\bar{D}^*$ threshold, the $T_{cc}(3875)$ lies at the DD^* threshold, the $X(3960)$ lies at the $D_s\bar{D}_s$ threshold, the $Z_c(4020)$ lies at the $D^*\bar{D}^*$ threshold, the $Z_{cs}(3985/4000)$ lies at $D\bar{D}_s^*$ or $D^*\bar{D}_s$ threshold, the $Z_{cs}(4123)$ lies at the $D^*\bar{D}_s^*$ threshold, the $Y(4260)$ lies at the

J^{PC}	$T^2(\text{GeV}^2)$	$\sqrt{s_0}(\text{GeV})$	$\mu(\text{GeV})$	pole	$M_{X/Y}(\text{GeV})$	$\lambda_{X/Y}(10^{-1}\text{GeV}^5)$
$0^{++}(1S)$	3.6 – 4.0	6.55 ± 0.10	1.4	(39 – 61)%	6.20 ± 0.10	2.68 ± 0.57
$1^{+-}(1S)$	3.8 – 4.2	6.60 ± 0.10	1.4	(40 – 61)%	6.24 ± 0.10	2.18 ± 0.44
$2^{++}(1S)$	4.0 – 4.4	6.65 ± 0.10	1.4	(39 – 60)%	6.27 ± 0.09	2.35 ± 0.46
$1^{--}(1P)$	3.2 – 3.6	6.70 ± 0.10	1.2	(39 – 63)%	6.33 ± 0.10	0.86 ± 0.24

Table 40: The Borel parameters, continuum threshold parameters, energy scales, pole contributions, masses and pole residues of the ground state tetraquark states.

J^{PC}	$T^2(\text{GeV}^2)$	$\sqrt{s_0'}(\text{GeV})$	$\mu(\text{GeV})$	pole	$M_{X/Y}(\text{GeV})$	$\lambda_{X/Y}(10^{-1}\text{GeV}^5)$
$0^{++}(2S)$	4.8 – 5.2	6.90 ± 0.10	2.4	(61 – 75)%	6.57 ± 0.09	8.12 ± 1.21
$1^{+-}(2S)$	5.2 – 5.6	7.00 ± 0.10	2.4	(61 – 75)%	6.64 ± 0.09	6.43 ± 0.88
$2^{++}(2S)$	5.3 – 5.7	7.05 ± 0.10	2.4	(62 – 75)%	6.69 ± 0.09	6.84 ± 0.92
$1^{--}(2P)$	5.0 – 5.4	7.10 ± 0.10	2.4	(60 – 74)%	6.74 ± 0.09	4.74 ± 0.71

Table 41: The Borel parameters, continuum threshold parameters, energy scales, pole contributions, masses and pole residues of the first radial excited tetraquark states.

J^{PC}	$M_1(\text{GeV})$	$M_2(\text{GeV})$	$M_3(\text{GeV})$	$M_4(\text{GeV})$
0^{++}	6.20 ± 0.10 ? $X(6220)$	6.57 ± 0.09 ? $X(6600/6620)$	6.92 ± 0.09 ? $X(6900)$	7.25 ± 0.09 ? $X(7220/7300)$
1^{+-}	6.24 ± 0.10 ? $X(6220)$	6.64 ± 0.09 ? $X(6600/6620)$	7.03 ± 0.09	7.40 ± 0.09
2^{++}	6.27 ± 0.09	6.69 ± 0.09	7.09 ± 0.09	7.46 ± 0.09
1^{--}	6.33 ± 0.10	6.74 ± 0.09	7.13 ± 0.09	7.50 ± 0.09

Table 42: The masses of the fully-charm tetraquark states with the radial quantum numbers $n = 1, 2, 3$ and 4. In the lower lines, we present the possible assignments.

$D\bar{D}_1$ threshold, naively, we expect that they consist of two color-neutral clusters, and they are molecular states, more precisely, they are the **11** type hidden-charm tetraquark states.

The **33** type four-quark currents could be reformed in a series of the **11** type four-quark currents through Fierz transformation [360, 516],

$$\begin{aligned}
2\sqrt{2}J_{1+}^\mu &= 2\varepsilon^{ijk}\varepsilon^{imn}\{u_j^T C\gamma_5 c_k \bar{d}_m \gamma^\mu C\bar{c}_n^T - u_j^T C\gamma^\mu c_k \bar{d}_m \gamma_5 C\bar{c}_n^T\}, \\
&= i\bar{c}i\gamma_5 c \bar{d}\gamma^\mu u - i\bar{c}\gamma^\mu c \bar{d}i\gamma_5 u + \bar{c}u \bar{d}\gamma^\mu \gamma_5 c - \bar{c}\gamma^\mu \gamma_5 u \bar{d}c - i\bar{c}\gamma_\nu \gamma_5 c \bar{d}\sigma^{\mu\nu} u \\
&\quad + i\bar{c}\sigma^{\mu\nu} c \bar{d}\gamma_\nu \gamma_5 u - i\bar{c}\sigma^{\mu\nu} \gamma_5 u \bar{d}\gamma_\nu c + i\bar{c}\gamma_\nu u \bar{d}\sigma^{\mu\nu} \gamma_5 c, \tag{227}
\end{aligned}$$

$$\begin{aligned}
2\sqrt{2}J_{1\pm}^{\mu\nu} &= 2\varepsilon^{ijk}\varepsilon^{imn}\{u_j^T C\gamma^\mu c_k \bar{d}_m \gamma^\nu C\bar{c}_n^T - u_j^T C\gamma^\nu c_k \bar{d}_m \gamma^\mu C\bar{c}_n^T\}, \\
&= i\bar{d}u \bar{c}\sigma^{\mu\nu} c + i\bar{d}\sigma^{\mu\nu} u \bar{c}c + i\bar{d}c \bar{c}\sigma^{\mu\nu} u + i\bar{d}\sigma^{\mu\nu} c \bar{c}u \\
&\quad - \bar{c}\sigma^{\mu\nu} \gamma_5 c \bar{d}i\gamma_5 u - \bar{c}i\gamma_5 c \bar{d}\sigma^{\mu\nu} \gamma_5 u - \bar{d}\sigma^{\mu\nu} \gamma_5 c \bar{c}i\gamma_5 u - \bar{d}i\gamma_5 c \bar{c}\sigma^{\mu\nu} \gamma_5 u \\
&\quad + i\varepsilon^{\mu\nu\alpha\beta} \bar{c}\gamma^\alpha \gamma_5 c \bar{d}\gamma^\beta u - i\varepsilon^{\mu\nu\alpha\beta} \bar{c}\gamma^\alpha c \bar{d}\gamma^\beta \gamma_5 u \\
&\quad + i\varepsilon^{\mu\nu\alpha\beta} \bar{c}\gamma^\alpha \gamma_5 u \bar{d}\gamma^\beta c - i\varepsilon^{\mu\nu\alpha\beta} \bar{c}\gamma^\alpha u \bar{d}\gamma^\beta \gamma_5 c, \tag{228}
\end{aligned}$$

$$\begin{aligned}
2\sqrt{2}J_{1-}^\mu &= 2\varepsilon^{ijk}\varepsilon^{imn}\{u_j^T Cc_k \bar{d}_m \gamma^\mu C\bar{c}_n^T - u_j^T C\gamma^\mu c_k \bar{d}_m C\bar{c}_n^T\}, \\
&= \bar{c}\gamma^\mu c \bar{d}u - \bar{c}c \bar{d}\gamma^\mu u + i\bar{c}\gamma^\mu \gamma_5 u \bar{d}i\gamma_5 c - i\bar{c}i\gamma_5 u \bar{d}\gamma^\mu \gamma_5 c \\
&\quad - i\bar{c}\gamma_\nu \gamma_5 c \bar{d}\sigma^{\mu\nu} \gamma_5 u + i\bar{c}\sigma^{\mu\nu} \gamma_5 c \bar{d}\gamma_\nu \gamma_5 u - i\bar{d}\gamma_\nu c \bar{c}\sigma^{\mu\nu} u + i\bar{d}\sigma^{\mu\nu} c \bar{c}\gamma_\nu u, \tag{229}
\end{aligned}$$

$$\begin{aligned}
2\sqrt{2}J_{1-+}^\mu &= 2\varepsilon^{ijk}\varepsilon^{imn}\{u_j^T Cc_k \bar{d}_m \gamma^\mu C\bar{c}_n^T + u_j^T C\gamma^\mu c_k \bar{d}_m C\bar{c}_n^T\}, \\
&= i\bar{c}i\gamma_5 c \bar{d}\gamma^\mu \gamma_5 u - i\bar{c}\gamma^\mu \gamma_5 c \bar{d}i\gamma_5 u - \bar{c}\gamma^\mu u \bar{d}c + \bar{c}u \bar{d}\gamma^\mu c \\
&\quad + i\bar{c}\sigma^{\mu\nu} c \bar{d}\gamma_\nu u - i\bar{c}\gamma_\nu c \bar{d}\sigma^{\mu\nu} u - i\bar{d}\gamma_\nu \gamma_5 c \bar{c}\sigma^{\mu\nu} \gamma_5 u + i\bar{d}\sigma^{\mu\nu} \gamma_5 c \bar{c}\gamma_\nu \gamma_5 u, \tag{230}
\end{aligned}$$

$$\begin{aligned}
2\sqrt{2}J_{1--}^\mu &= 2\varepsilon^{ijk}\varepsilon^{imn}\{s_j^T Cc_k \bar{s}_m \gamma^\mu C\bar{c}_n^T - s_j^T C\gamma^\mu c_k \bar{s}_m C\bar{c}_n^T\}, \\
&= \bar{c}\gamma^\mu c \bar{s}s - \bar{c}c \bar{s}\gamma^\mu s + i\bar{c}\gamma^\mu \gamma_5 s \bar{s}i\gamma_5 c - i\bar{c}i\gamma_5 s \bar{s}\gamma^\mu \gamma_5 c \\
&\quad - i\bar{c}\gamma_\nu \gamma_5 c \bar{s}\sigma^{\mu\nu} \gamma_5 s + i\bar{c}\sigma^{\mu\nu} \gamma_5 c \bar{s}\gamma_\nu \gamma_5 s - i\bar{s}\gamma_\nu c \bar{c}\sigma^{\mu\nu} s + i\bar{s}\sigma^{\mu\nu} c \bar{c}\gamma_\nu s, \tag{231}
\end{aligned}$$

$$\begin{aligned}
2\sqrt{2}J_{1-+}^\mu &= 2\varepsilon^{ijk}\varepsilon^{imn}\{s_j^T Cc_k \bar{s}_m \gamma^\mu C\bar{c}_n^T + s_j^T C\gamma^\mu c_k \bar{s}_m C\bar{c}_n^T\}, \\
&= i\bar{c}i\gamma_5 c \bar{s}\gamma^\mu \gamma_5 s - i\bar{c}\gamma^\mu \gamma_5 c \bar{s}i\gamma_5 s - \bar{c}\gamma^\mu s \bar{s}c + \bar{c}s \bar{s}\gamma^\mu c \\
&\quad + i\bar{c}\sigma^{\mu\nu} c \bar{s}\gamma_\nu s - i\bar{c}\gamma_\nu c \bar{s}\sigma^{\mu\nu} s - i\bar{s}\gamma_\nu \gamma_5 c \bar{c}\sigma^{\mu\nu} \gamma_5 s + i\bar{s}\sigma^{\mu\nu} \gamma_5 c \bar{c}\gamma_\nu \gamma_5 s, \tag{232}
\end{aligned}$$

$$\begin{aligned}
2\sqrt{2}J_{2+}^{\mu\nu} &= 2\varepsilon^{ijk}\varepsilon^{imn}\{u_j^T C\gamma^\mu c_k \bar{d}_m \gamma^\nu C\bar{c}_n^T + u_j^T C\gamma^\nu c_k \bar{d}_m \gamma^\mu C\bar{c}_n^T\}, \\
&= \bar{c}\gamma^\mu \gamma_5 c \bar{d}\gamma^\nu \gamma_5 u + \bar{c}\gamma^\nu \gamma_5 c \bar{d}\gamma^\mu \gamma_5 u - \bar{c}\gamma^\mu c \bar{d}\gamma^\nu u - \bar{c}\gamma^\nu c \bar{d}\gamma^\mu u + \bar{c}\gamma^\mu \gamma_5 u \bar{d}\gamma^\nu \gamma_5 c \\
&\quad + \bar{c}\gamma^\nu \gamma_5 u \bar{d}\gamma^\mu \gamma_5 c - \bar{c}\gamma^\mu u \bar{d}\gamma^\nu c - \bar{c}\gamma^\nu u \bar{d}\gamma^\mu c + g_{\alpha\beta} \bar{c}\sigma^{\mu\alpha} c \bar{d}\sigma^{\nu\beta} u + g_{\alpha\beta} \bar{c}\sigma^{\nu\alpha} c \bar{d}\sigma^{\mu\beta} u \\
&\quad + g_{\alpha\beta} \bar{c}\sigma^{\mu\alpha} u \bar{d}\sigma^{\nu\beta} c + g_{\alpha\beta} \bar{c}\sigma^{\nu\alpha} u \bar{d}\sigma^{\mu\beta} c + g^{\mu\nu} \bar{c}c \bar{d}u + g^{\mu\nu} \bar{c}i\gamma_5 c \bar{d}i\gamma_5 u + g^{\mu\nu} \bar{c}\gamma_\alpha c \bar{d}\gamma^\alpha u \\
&\quad - g^{\mu\nu} \bar{c}\gamma_\alpha \gamma_5 c \bar{d}\gamma^\alpha \gamma_5 u - \frac{1}{2}g^{\mu\nu} \bar{c}\sigma_{\alpha\beta} c \bar{d}\sigma^{\alpha\beta} u + g^{\mu\nu} \bar{c}u \bar{d}c + g^{\mu\nu} \bar{c}i\gamma_5 u \bar{d}i\gamma_5 c \\
&\quad + g^{\mu\nu} \bar{c}\gamma_\alpha u \bar{d}\gamma^\alpha c - g^{\mu\nu} \bar{c}\gamma_\alpha \gamma_5 u \bar{d}\gamma^\alpha \gamma_5 c - \frac{1}{2}g^{\mu\nu} \bar{c}\sigma_{\alpha\beta} u \bar{d}\sigma^{\alpha\beta} c, \tag{233}
\end{aligned}$$

$$\begin{aligned}
J_{0^{++}} &= \varepsilon^{ijk} \varepsilon^{imn} u_j^T C \gamma_\mu c_k \bar{d}_m \gamma^\mu C \bar{c}_n^T, \\
&= \bar{c} c \bar{d} u + \bar{c} i \gamma_5 c \bar{d} i \gamma_5 u + \frac{1}{2} \bar{c} \gamma_\alpha c \bar{d} \gamma^\alpha u - \frac{1}{2} \bar{c} \gamma_\alpha \gamma_5 c \bar{d} \gamma^\alpha \gamma_5 u \\
&\quad + \bar{c} u \bar{d} c + \bar{c} i \gamma_5 u \bar{d} i \gamma_5 c + \frac{1}{2} \bar{c} \gamma_\alpha u \bar{d} \gamma^\alpha c - \frac{1}{2} \bar{c} \gamma_\alpha \gamma_5 u \bar{d} \gamma^\alpha \gamma_5 c.
\end{aligned} \tag{234}$$

According to the quark-hadron duality, the $\bar{\mathbf{33}}$ and $\mathbf{11}$ type currents couple to the $\bar{\mathbf{33}}$ and $\mathbf{11}$ type tetraquark states, respectively. The $\bar{\mathbf{33}}$ type tetraquark states could be taken as a particular superposition of a series of the $\mathbf{11}$ type tetraquark states, while the $\mathbf{11}$ type tetraquark states could decay through the Okubo-Zweig-Iizuka super-allowed fall-apart mechanism. We usually use the identities in Eqs.(227)-(234) to analyze the strong decays [360, 516]. For example, the current in Eq.(227) couples potentially to the $Z_c(3900)$, in the nonrelativistic and heavy quark limit, the component $\bar{c} \sigma^{\mu\nu} \gamma_5 u \bar{d} \gamma_\nu c$ is reduced to the form,

$$\begin{aligned}
\bar{c} \sigma^{0j} \gamma_5 u \bar{d} \gamma_j c &\propto \xi_c^\dagger \sigma^j \zeta_u \chi_d^\dagger \vec{\sigma} \cdot \vec{k}_d \sigma^j \xi_c \propto \xi_c^\dagger \frac{\sigma^j}{2} \zeta_u \chi_d^\dagger \frac{\sigma^j}{2} \xi_c = \vec{S}_{D^*} \cdot \vec{S}_{D^*}, \\
\bar{c} \sigma^{ij} \gamma_5 u \bar{d} \gamma_j c &\propto \varepsilon^{ijk} \xi_c^\dagger \sigma^k \vec{\sigma} \cdot \vec{k}_u \zeta_u \chi_d^\dagger \vec{\sigma} \cdot \vec{k}_d \sigma^j \xi_c \propto \varepsilon^{ijk} \xi_c^\dagger \frac{\sigma^k}{2} \zeta_u \chi_d^\dagger \frac{\sigma^j}{2} \xi_c = \vec{S}_{D^*} \times \vec{S}_{D^*},
\end{aligned} \tag{235}$$

where the ξ, ζ, χ are the two-component spinors of the quark fields, the \vec{k} are the three-vectors of the quark fields, the σ^i are the pauli matrixes, and the \vec{S} are the spin operators. It is obvious that the currents $\bar{c} \sigma^{\mu\nu} \gamma_5 u \bar{d} \gamma_\nu c$ and $\bar{c} \gamma_\nu u \bar{d} \sigma^{\mu\nu} \gamma_5 c$ couple to the $J^P = 0^+$ and 1^+ ($D^* \bar{D}^*$) $^+$ states. However, the strong decays $Z_c^\pm(3900) \rightarrow (D^* \bar{D}^*)^\pm$ are kinematically forbidden.

8.1 11 type hidden heavy tetraquark states

Firstly, let us write down the correlation functions $\Pi(p)$, $\Pi_{\mu\nu}(p)$ and $\Pi_{\mu\nu\alpha\beta}(p)$,

$$\begin{aligned}
\Pi(p) &= i \int d^4 x e^{ip \cdot x} \langle 0 | T \{ J(x) J^\dagger(0) \} | 0 \rangle, \\
\Pi_{\mu\nu}(p) &= i \int d^4 x e^{ip \cdot x} \langle 0 | T \{ J_\mu(x) J_\nu^\dagger(0) \} | 0 \rangle, \\
\Pi_{\mu\nu\alpha\beta}(p) &= i \int d^4 x e^{ip \cdot x} \langle 0 | T \{ J_{\mu\nu}(x) J_{\alpha\beta}^\dagger(0) \} | 0 \rangle,
\end{aligned} \tag{236}$$

where the currents

$$\begin{aligned}
J(x) &= J_{D\bar{D}}(x), J_{D\bar{D}_s}(x), J_{D_s\bar{D}_s}(x), J_{D^*\bar{D}^*}(x), J_{D^*\bar{D}_s^*}(x), J_{D_s^*\bar{D}_s^*}(x), \\
J_\mu(x) &= J_{D\bar{D}^*,\pm,\mu}(x), J_{D\bar{D}_s^*,\pm,\mu}(x), J_{D_s\bar{D}_s^*,\pm,\mu}(x), \\
J_{\mu\nu}(x) &= J_{\pm,\mu\nu}(x), \\
J_{\pm,\mu\nu}(x) &= J_{D^*\bar{D}^*,\pm,\mu\nu}(x), J_{D^*\bar{D}_s^*,\pm,\mu\nu}(x), J_{D_s^*\bar{D}_s^*,\pm,\mu\nu}(x),
\end{aligned} \tag{237}$$

and

$$\begin{aligned}
J_{D\bar{D}}(x) &= \bar{q}(x) i \gamma_5 c(x) \bar{c}(x) i \gamma_5 q(x), \\
J_{D\bar{D}_s}(x) &= \bar{q}(x) i \gamma_5 c(x) \bar{c}(x) i \gamma_5 s(x), \\
J_{D_s\bar{D}_s}(x) &= \bar{s}(x) i \gamma_5 c(x) \bar{c}(x) i \gamma_5 s(x), \\
J_{D^*\bar{D}^*}(x) &= \bar{q}(x) \gamma_\mu c(x) \bar{c}(x) \gamma^\mu q(x), \\
J_{D^*\bar{D}_s^*}(x) &= \bar{q}(x) \gamma_\mu c(x) \bar{c}(x) \gamma^\mu s(x), \\
J_{D_s^*\bar{D}_s^*}(x) &= \bar{s}(x) \gamma_\mu c(x) \bar{c}(x) \gamma^\mu s(x),
\end{aligned} \tag{238}$$

$$\begin{aligned}
J_{D\bar{D}^*,+, \mu}(x) &= \frac{1}{\sqrt{2}} \left[\bar{u}(x) i\gamma_5 c(x) \bar{c}(x) \gamma_\mu d(x) - \bar{u}(x) \gamma_\mu c(x) \bar{c}(x) i\gamma_5 d(x) \right], \\
J_{D\bar{D}_s^*,+, \mu}(x) &= \frac{1}{\sqrt{2}} \left[\bar{q}(x) i\gamma_5 c(x) \bar{c}(x) \gamma_\mu s(x) - \bar{q}(x) \gamma_\mu c(x) \bar{c}(x) i\gamma_5 s(x) \right], \\
J_{D_s\bar{D}_s^*,+, \mu}(x) &= \frac{1}{\sqrt{2}} \left[\bar{s}(x) i\gamma_5 c(x) \bar{c}(x) \gamma_\mu s(x) - \bar{s}(x) \gamma_\mu c(x) \bar{c}(x) i\gamma_5 s(x) \right], \tag{239}
\end{aligned}$$

$$\begin{aligned}
J_{D\bar{D}^*,-, \mu}(x) &= \frac{1}{\sqrt{2}} \left[\bar{u}(x) i\gamma_5 c(x) \bar{c}(x) \gamma_\mu d(x) + \bar{u}(x) \gamma_\mu c(x) \bar{c}(x) i\gamma_5 d(x) \right], \\
J_{D\bar{D}_s^*,-, \mu}(x) &= \frac{1}{\sqrt{2}} \left[\bar{q}(x) i\gamma_5 c(x) \bar{c}(x) \gamma_\mu s(x) + \bar{q}(x) \gamma_\mu c(x) \bar{c}(x) i\gamma_5 s(x) \right], \\
J_{D_s\bar{D}_s^*,-, \mu}(x) &= \frac{1}{\sqrt{2}} \left[\bar{s}(x) i\gamma_5 c(x) \bar{c}(x) \gamma_\mu s(x) + \bar{s}(x) \gamma_\mu c(x) \bar{c}(x) i\gamma_5 s(x) \right], \tag{240}
\end{aligned}$$

$$\begin{aligned}
J_{D^*\bar{D}^*,-, \mu\nu}(x) &= \frac{1}{\sqrt{2}} \left[\bar{u}(x) \gamma_\mu c(x) \bar{c}(x) \gamma_\nu d(x) - \bar{u}(x) \gamma_\nu c(x) \bar{c}(x) \gamma_\mu d(x) \right], \\
J_{D^*\bar{D}_s^*,-, \mu\nu}(x) &= \frac{1}{\sqrt{2}} \left[\bar{q}(x) \gamma_\mu c(x) \bar{c}(x) \gamma_\nu s(x) - \bar{q}(x) \gamma_\nu c(x) \bar{c}(x) \gamma_\mu s(x) \right], \\
J_{D_s^*\bar{D}_s^*,-, \mu\nu}(x) &= \frac{1}{\sqrt{2}} \left[\bar{s}(x) \gamma_\mu c(x) \bar{c}(x) \gamma_\nu s(x) - \bar{s}(x) \gamma_\nu c(x) \bar{c}(x) \gamma_\mu s(x) \right], \tag{241}
\end{aligned}$$

$$\begin{aligned}
J_{D^*\bar{D}^*,+, \mu\nu}(x) &= \frac{1}{\sqrt{2}} \left[\bar{u}(x) \gamma_\mu c(x) \bar{c}(x) \gamma_\nu d(x) + \bar{u}(x) \gamma_\nu c(x) \bar{c}(x) \gamma_\mu d(x) \right], \\
J_{D^*\bar{D}_s^*,+, \mu\nu}(x) &= \frac{1}{\sqrt{2}} \left[\bar{q}(x) \gamma_\mu c(x) \bar{c}(x) \gamma_\nu s(x) + \bar{q}(x) \gamma_\nu c(x) \bar{c}(x) \gamma_\mu s(x) \right], \\
J_{D_s^*\bar{D}_s^*,+, \mu\nu}(x) &= \frac{1}{\sqrt{2}} \left[\bar{s}(x) \gamma_\mu c(x) \bar{c}(x) \gamma_\nu s(x) + \bar{s}(x) \gamma_\nu c(x) \bar{c}(x) \gamma_\mu s(x) \right], \tag{242}
\end{aligned}$$

and $q = u, d$. Again, we take the isospin limit, the currents with the symbolic quark structures $\bar{c}\bar{d}u$, $\bar{c}\bar{c}u\bar{d}$, $\bar{c}c\frac{\bar{u}u-\bar{d}d}{\sqrt{2}}$, $\bar{c}c\frac{\bar{u}u+\bar{d}d}{\sqrt{2}}$ couple potentially to the hidden-charm molecular states with degenerated masses, the currents with the isospin $I = 1$ and 0 lead to the same QCD sum rules [76, 77, 78, 358].

Under parity transform \hat{P} , the currents have the properties,

$$\begin{aligned}
\hat{P}J(x)\hat{P}^{-1} &= +J(\tilde{x}), \\
\hat{P}J_\mu(x)\hat{P}^{-1} &= -J^\mu(\tilde{x}), \\
\hat{P}J_{\pm, \mu\nu}(x)\hat{P}^{-1} &= +J_{\pm, \mu\nu}(\tilde{x}), \tag{243}
\end{aligned}$$

where $x^\mu = (t, \vec{x})$ and $\tilde{x}^\mu = (t, -\vec{x})$. Under charge conjugation transform \hat{C} , the currents $J(x)$, $J_\mu(x)$ and $J_{\mu\nu}(x)$ have the properties,

$$\begin{aligned}
\hat{C}J(x)\hat{C}^{-1} &= +J(x), \\
\hat{C}J_{\pm, \mu}(x)\hat{C}^{-1} &= \pm J_{\pm, \mu}(x), \\
\hat{C}J_{\pm, \mu\nu}(x)\hat{C}^{-1} &= \pm J_{\pm, \mu\nu}(x). \tag{244}
\end{aligned}$$

At the hadron side, we obtain the hadronic representation and isolate the ground state hidden-

charm molecule contributions [77, 78],

$$\begin{aligned}
\Pi(p) &= \frac{\lambda_{Z_+}^2}{M_{Z_+}^2 - p^2} + \dots = \Pi_+(p^2), \\
\Pi_{\mu\nu}(p) &= \frac{\lambda_{Z_+}^2}{M_{Z_+}^2 - p^2} \left(-g_{\mu\nu} + \frac{p_\mu p_\nu}{p^2} \right) + \dots \\
&= \Pi_+(p^2) \left(-g_{\mu\nu} + \frac{p_\mu p_\nu}{p^2} \right) + \dots, \\
\Pi_{-, \mu\nu\alpha\beta}(p) &= \frac{\lambda_{Z_+}^2}{M_{Z_+}^2 (M_{Z_+}^2 - p^2)} (p^2 g_{\mu\alpha} g_{\nu\beta} - p^2 g_{\mu\beta} g_{\nu\alpha} - g_{\mu\alpha} p_\nu p_\beta - g_{\nu\beta} p_\mu p_\alpha + g_{\mu\beta} p_\nu p_\alpha + g_{\nu\alpha} p_\mu p_\beta) \\
&\quad + \frac{\lambda_{Z_-}^2}{M_{Z_-}^2 (M_{Z_-}^2 - p^2)} (-g_{\mu\alpha} p_\nu p_\beta - g_{\nu\beta} p_\mu p_\alpha + g_{\mu\beta} p_\nu p_\alpha + g_{\nu\alpha} p_\mu p_\beta) + \dots \\
&= \tilde{\Pi}_+(p^2) (p^2 g_{\mu\alpha} g_{\nu\beta} - p^2 g_{\mu\beta} g_{\nu\alpha} - g_{\mu\alpha} p_\nu p_\beta - g_{\nu\beta} p_\mu p_\alpha + g_{\mu\beta} p_\nu p_\alpha + g_{\nu\alpha} p_\mu p_\beta) \\
&\quad + \tilde{\Pi}_-(p^2) (-g_{\mu\alpha} p_\nu p_\beta - g_{\nu\beta} p_\mu p_\alpha + g_{\mu\beta} p_\nu p_\alpha + g_{\nu\alpha} p_\mu p_\beta), \\
\Pi_{+, \mu\nu\alpha\beta}(p) &= \frac{\lambda_{Z_+}^2}{M_{Z_+}^2 - p^2} \left(\frac{\tilde{g}_{\mu\alpha} \tilde{g}_{\nu\beta} + \tilde{g}_{\mu\beta} \tilde{g}_{\nu\alpha}}{2} - \frac{\tilde{g}_{\mu\nu} \tilde{g}_{\alpha\beta}}{3} \right) + \dots, \\
&= \Pi_+(p^2) \left(\frac{\tilde{g}_{\mu\alpha} \tilde{g}_{\nu\beta} + \tilde{g}_{\mu\beta} \tilde{g}_{\nu\alpha}}{2} - \frac{\tilde{g}_{\mu\nu} \tilde{g}_{\alpha\beta}}{3} \right) + \dots, \tag{245}
\end{aligned}$$

where the Z represents the molecular states Z_c, X_c, Z_{cs} , etc. We add the subscripts \pm in the hidden-charm molecular states Z_\pm and the components $\Pi_\pm(p^2)$ and $\tilde{\Pi}_\pm(p^2)$ to represent the positive and negative parity contributions, respectively, and define the pole residues λ_{Z_\pm} ,

$$\begin{aligned}
\langle 0|J(0)|Z_+(p)\rangle &= \lambda_{Z_+}, \\
\langle 0|J_\mu(0)|Z_+(p)\rangle &= \lambda_{Z_+} \varepsilon_\mu, \\
\langle 0|J_{-, \mu\nu}(0)|Z_+(p)\rangle &= \tilde{\lambda}_{Z_+} \varepsilon_{\mu\nu\alpha\beta} \varepsilon^\alpha p^\beta, \\
\langle 0|J_{-, \mu\nu}(0)|Z_-(p)\rangle &= \tilde{\lambda}_{Z_-} (\varepsilon_\mu p_\nu - \varepsilon_\nu p_\mu), \\
\langle 0|J_{+, \mu\nu}(0)|Z_+(p)\rangle &= \lambda_{Z_+} \varepsilon_{\mu\nu}, \tag{246}
\end{aligned}$$

where $\lambda_{Z_\pm} = M_{Z_\pm} \tilde{\lambda}_{Z_\pm}$, the $\varepsilon_{\mu/\alpha}$ and $\varepsilon_{\mu\nu}$ are the polarization vectors of the molecular states. We choose the components $\Pi_+(p^2)$ and $p^2 \tilde{\Pi}_+(p^2)$ to study the scalar, axialvector and tensor hidden-charm molecular states. According to the discussions in Sect.3, we have no reason to worry about the contaminations from the two-meson scattering states.

At the QCD side, we carry out the operator product expansion up to the vacuum condensates of dimension 10, and take account of the vacuum condensates $\langle \bar{q}q \rangle$, $\langle \frac{\alpha_s GG}{\pi} \rangle$, $\langle \bar{q}g_s \sigma Gq \rangle$, $\langle \bar{q}q \rangle^2$, $g_s^2 \langle \bar{q}q \rangle^2$, $\langle \bar{q}q \rangle \langle \frac{\alpha_s GG}{\pi} \rangle$, $\langle \bar{q}q \rangle \langle \bar{q}g_s \sigma Gq \rangle$, $\langle \bar{q}g_s \sigma Gq \rangle^2$ and $\langle \bar{q}q \rangle^2 \langle \frac{\alpha_s GG}{\pi} \rangle$, where $q = u, d$ or s quark, just like in SubSect.5.1.

According to analogous routine of SubSect.5.1, we obtain the QCD sum rules:

$$\lambda_{Z_+}^2 \exp\left(-\frac{M_{Z_+}^2}{T^2}\right) = \int_{4m_c^2}^{s_0} ds \rho_{QCD}(s) \exp\left(-\frac{s}{T^2}\right), \tag{247}$$

and

$$M_{Z_+}^2 = -\frac{\int_{4m_c^2}^{s_0} ds \frac{d}{d\tau} \rho(s) \exp(-\tau s)}{\int_{4m_c^2}^{s_0} ds \rho(s) \exp(-\tau s)} \Big|_{\tau=\frac{1}{T^2}}. \tag{248}$$

$Z_c(X_c)$	J^{PC}	$T^2(\text{GeV}^2)$	$\sqrt{s_0}(\text{GeV})$	$\mu(\text{GeV})$	pole	$ D(10) $
DD	0^{++}	2.7 – 3.1	4.30 ± 0.10	1.3	(40 – 63)%	$\ll 1\%$
$D\bar{D}_s$	0^{++}	2.8 – 3.2	4.40 ± 0.10	1.3	(40 – 63)%	$\ll 1\%$
$D_s\bar{D}_s$	0^{++}	2.9 – 3.3	4.50 ± 0.10	1.3	(41 – 62)%	$\ll 1\%$
D^*D^*	0^{++}	2.8 – 3.2	4.55 ± 0.10	1.6	(40 – 62)%	$\leq 1\%$
$D^*\bar{D}_s^*$	0^{++}	2.9 – 3.3	4.65 ± 0.10	1.6	(41 – 63)%	$< 1\%$
$D_s^*\bar{D}_s^*$	0^{++}	3.1 – 3.5	4.75 ± 0.10	1.6	(40 – 61)%	$\ll 1\%$
$D\bar{D}^* - D^*\bar{D}$	1^{+-}	2.7 – 3.1	4.40 ± 0.10	1.3	(40 – 63)%	$\ll 1\%$
$D\bar{D}_s^* - D^*\bar{D}_s$	1^{+-}	2.9 – 3.3	4.55 ± 0.10	1.3	(41 – 63)%	$\ll 1\%$
$D_s\bar{D}_s^* - D_s^*\bar{D}_s$	1^{+-}	3.0 – 3.4	4.65 ± 0.10	1.3	(42 – 63)%	$\ll 1\%$
$D\bar{D}^* + D^*\bar{D}$	1^{+-}	2.7 – 3.1	4.40 ± 0.10	1.3	(40 – 63)%	$\ll 1\%$
$D\bar{D}_s^* + D^*\bar{D}_s$	1^{+-}	2.9 – 3.3	4.55 ± 0.10	1.3	(41 – 63)%	$\ll 1\%$
$D_s\bar{D}_s^* + D_s^*\bar{D}_s$	1^{+-}	3.0 – 3.4	4.65 ± 0.10	1.3	(42 – 63)%	$\ll 1\%$
D^*D^*	1^{+-}	3.0 – 3.4	4.55 ± 0.10	1.6	(42 – 63)%	$< 1\%$
$D^*\bar{D}_s^*$	1^{+-}	3.2 – 3.6	4.65 ± 0.10	1.6	(41 – 61)%	$\ll 1\%$
$D_s^*\bar{D}_s^*$	1^{+-}	3.3 – 3.7	4.75 ± 0.10	1.6	(42 – 61)%	$\ll 1\%$
D^*D^*	2^{++}	3.0 – 3.4	4.55 ± 0.10	1.6	(41 – 62)%	$< 1\%$
$D^*\bar{D}_s^*$	2^{++}	3.2 – 3.6	4.65 ± 0.10	1.6	(40 – 60)%	$\ll 1\%$
$D_s^*\bar{D}_s^*$	2^{++}	3.3 – 3.7	4.75 ± 0.10	1.6	(41 – 61)%	$\ll 1\%$

Table 43: The Borel parameters, continuum threshold parameters, energy scales of the QCD spectral densities, pole contributions, and the contributions of the vacuum condensates of dimension 10 for the ground states [77, 78].

In the heavy quark limit, we describe the $Q\bar{Q}q\bar{q}$ systems by a double-well potential model, the heavy quark Q (\bar{Q}) serves as a static well potential and attracts the light antiquark \bar{q} (q) to form a color-neutral cluster. We introduce the effective heavy quark mass \mathbb{M}_Q and divide the molecular states into both the heavy and light degrees of freedom, i.e. $2\mathbb{M}_Q$ and $\mu = \sqrt{M_{X/Y/Z}^2 - (2\mathbb{M}_Q)^2}$, respectively.

Analysis of the J/ψ and Υ mass spectrum with the famous Cornell potential or Coulomb-potential-plus-linear-potential leads to the constituent quark masses $m_c = 1.84 \text{ GeV}$ and $m_b = 5.17 \text{ GeV}$ [517], we can set the effective c -quark mass as the constituent quark mass $\mathbb{M}_c = m_c = 1.84 \text{ GeV}$. The old value $\mathbb{M}_c = 1.84 \text{ GeV}$ and updated value $\mathbb{M}_c = 1.85 \text{ GeV}$, which are fitted for the hidden-charm molecular states, are all consistent with the constituent quark mass $m_c = 1.84 \text{ GeV}$ [76, 358, 518]. We choose the value $\mathbb{M}_c = 1.84 \text{ GeV}$ to determine the ideal energy scales of the QCD spectral densities, and add an uncertainty $\delta\mu = \pm 0.1 \text{ GeV}$ to account for the difference between the values $\mathbb{M}_c = 1.84 \text{ GeV}$ and 1.85 GeV . Furthermore, we take the modified energy scale formula

$$\mu = \sqrt{M_{X/Y/Z}^2 - (2\mathbb{M}_c)^2 - k\mathbb{M}_s}, \quad (249)$$

with $k = 0, 1, 2$ and $\mathbb{M}_s = 0.2 \text{ GeV}$ to account for the light flavor $SU(3)$ breaking effects.

After trial and error, we obtain the Borel windows, continuum threshold parameters, energy scales of the QCD spectral densities, pole contributions, and the contributions of the vacuum condensates of dimension 10, which are shown explicitly in Table 43. At the hadron side, the pole contributions are about (40–60)%, while the central values are larger than 50%, the pole dominance condition is well satisfied. At the QCD side, the contributions of the vacuum condensates of dimension 10 are $|D(10)| \leq 1\%$ or $\ll 1\%$, the convergent behaviors of the operator product expansion are very good.

We take account of all the uncertainties of the input parameters, and obtain the masses and pole residues of the molecular states without strange, with strange and with hidden-strange, which

$Z_c(X_c)$	J^{PC}	$M_Z(\text{GeV})$	$\lambda_Z(\text{GeV}^5)$
DD	0^{++}	3.74 ± 0.09	$(1.61 \pm 0.23) \times 10^{-2}$
$D\bar{D}_s$	0^{++}	3.88 ± 0.10	$(1.98 \pm 0.30) \times 10^{-2}$
$D_s\bar{D}_s$	0^{++}	3.98 ± 0.10	$(2.36 \pm 0.45) \times 10^{-2}$
D^*D^*	0^{++}	4.02 ± 0.09	$(4.30 \pm 0.72) \times 10^{-2}$
$D^*\bar{D}_s^*$	0^{++}	4.10 ± 0.09	$(5.00 \pm 0.83) \times 10^{-2}$
$D_s^*\bar{D}_s^*$	0^{++}	4.20 ± 0.09	$(5.86 \pm 0.98) \times 10^{-2}$
$D\bar{D}^* - D^*\bar{D}$	1^{++}	3.89 ± 0.09	$(1.72 \pm 0.30) \times 10^{-2}$
$D\bar{D}_s^* - D^*\bar{D}_s$	1^{++}	3.99 ± 0.09	$(1.96 \pm 0.35) \times 10^{-2}$
$D_s\bar{D}_s^* - D_s^*\bar{D}_s$	1^{++}	4.07 ± 0.09	$(2.07 \pm 0.37) \times 10^{-2}$
$D\bar{D}^* + D^*\bar{D}$	1^{+-}	3.89 ± 0.09	$(1.72 \pm 0.30) \times 10^{-2}$
$D\bar{D}_s^* + D^*\bar{D}_s$	1^{+-}	3.99 ± 0.09	$(1.96 \pm 0.35) \times 10^{-2}$
$D_s\bar{D}_s^* + D_s^*\bar{D}_s$	1^{+-}	4.07 ± 0.09	$(2.07 \pm 0.37) \times 10^{-2}$
D^*D^*	1^{+-}	4.02 ± 0.09	$(2.33 \pm 0.35) \times 10^{-2}$
$D^*\bar{D}_s^*$	1^{+-}	4.11 ± 0.09	$(2.71 \pm 0.41) \times 10^{-2}$
$D_s^*\bar{D}_s^*$	1^{+-}	4.19 ± 0.09	$(3.12 \pm 0.47) \times 10^{-2}$
D^*D^*	2^{++}	4.02 ± 0.09	$(3.29 \pm 0.51) \times 10^{-2}$
$D^*\bar{D}_s^*$	2^{++}	4.11 ± 0.09	$(3.84 \pm 0.59) \times 10^{-2}$
$D_s^*\bar{D}_s^*$	2^{++}	4.19 ± 0.09	$(4.42 \pm 0.67) \times 10^{-2}$

Table 44: The masses and pole residues of the ground state hidden-charm molecular states [77, 78].

are shown explicitly in Table 44. From Tables 43–44, it is obvious that the modified energy scale formula in Eq.(249) is well satisfied [77, 78].

In Fig.18, we plot the masses of the axialvector molecular states $D\bar{D}^* + D^*\bar{D}$, $D\bar{D}^* - D^*\bar{D}$, $D\bar{D}_s^* + D^*\bar{D}_s$ and $D^*\bar{D}^*$ with variations of the Borel parameters at much larger ranges than the Borel widows as an example. From the figure, we can see plainly that there appear very flat platforms in the Borel windows indeed, where the regions between the two short vertical lines are the Borel windows.

In Fig.18, we also present the experimental values of the masses of the $Z_c(3900)$, $X_c(3872)$, $Z_{cs}(3985)$ and $Z_c(4020)$ [161, 520], the predicted masses are in excellent agreement with the experimental data. The calculations support assigning the $Z_c(3900)$, $X_c(3872)$, $Z_{cs}(3985)$ and $Z_c(4020)$ to be the $D\bar{D}^* + D^*\bar{D}$, $D\bar{D}^* - D^*\bar{D}$, $D\bar{D}_s^* + D^*\bar{D}_s$ and $D^*\bar{D}^*$ tetraquark molecular states with the quantum numbers $J^{PC} = 1^{+-}$, 1^{++} , 1^{+-} and 1^{+-} , respectively. In Table 45, we present the possible assignments of the ground state hidden-charm molecular states.

We could reproduce the experimental masses of the $X_c(3872)$, $Z_c(3900)$, $Z_{cs}(3985)$, $Z_{cs}(4123)$ and $Z_c(4020)$ both in the scenarios of tetraquark states and molecular states, see Tables 9-11 and 45, the tetraquark scenario can accommodate much more exotic X and Z states than the molecule scenario. Even in the tetraquark scenario, there are no rooms to accommodate the $X(3940)$, $X(4160)$, $Z_c(4100)$ and $Z_c(4200)$ without resorting to fine tuning. The $X(3940)$ and $X(4160)$ may be the conventional $\eta_c(3S)$ and $\eta_c(4S)$ states with the quantum numbers $J^{PC} = 0^{-+}$, respectively. The $Z_c(4100)$ may be a mixing scalar tetraquark state with the quantum numbers $J^{PC} = 0^{++}$, and the $Z_c(4200)$ may be an axialvector color-octet-color-octet type tetraquark state with the quantum numbers $J^{PC} = 1^{+-}$. For detailed discussions about this subject, one can consult Ref.[57].

The $Z_c(3900)$ and $Z_c(3885)$ have almost degenerated masses but quite different decay widths [154, 155, 157], they are taken as the same particle by the Particle Data Group [91], however, it is difficult to explain the large ratio,

$$R_{exp} = \frac{\Gamma(Z_c(3885) \rightarrow D\bar{D}^*)}{\Gamma(Z_c(3900) \rightarrow J/\psi\pi)} = 6.2 \pm 1.1 \pm 2.7, \quad (250)$$

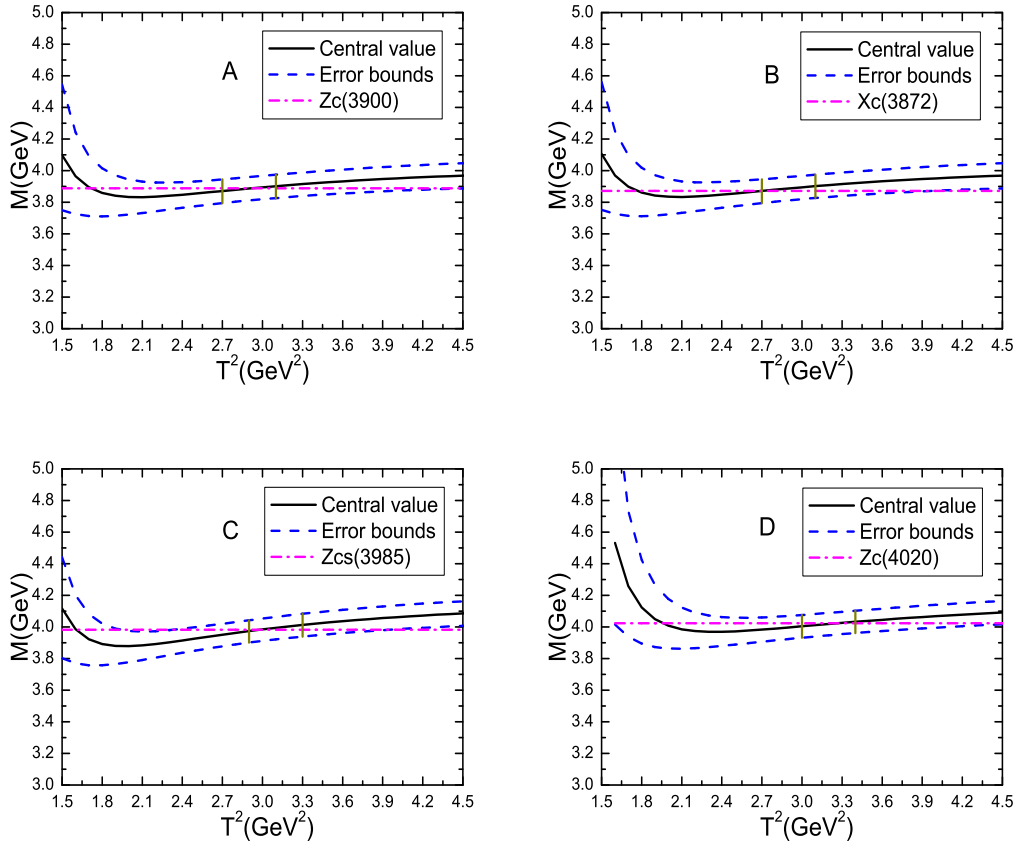


Figure 18: The masses of the molecular states with variations of the Borel parameters T^2 , where the A , B , C and D correspond to the axialvector molecular states $D\bar{D}^* + D^*\bar{D}$, $D\bar{D}^* - D^*\bar{D}$, $D\bar{D}_s^* + D^*\bar{D}_s$ and $D^*\bar{D}^*$, respectively.

$Z_c(X_c)$	J^{PC}	$M_Z(\text{GeV})$	Assignments
DD	0^{++}	3.74 ± 0.09	? $X(3960)$
$D\bar{D}_s$	0^{++}	3.88 ± 0.10	
$D_s\bar{D}_s$	0^{++}	3.98 ± 0.10	
$D^*\bar{D}^*$	0^{++}	4.02 ± 0.09	
$D^*\bar{D}_s^*$	0^{++}	4.10 ± 0.09	
$D_s^*\bar{D}_s^*$	0^{++}	4.20 ± 0.09	
$DD^* - \bar{D}^*D$	1^{++}	3.89 ± 0.09	? $X_c(3872)$
$D\bar{D}_s^* - D^*\bar{D}_s$	1^{++}	3.99 ± 0.09	
$D_s\bar{D}_s^* - D_s^*\bar{D}_s$	1^{++}	4.07 ± 0.09	
$DD^* + \bar{D}^*D$	1^{+-}	3.89 ± 0.09	? $Z_c(3900)$
$D\bar{D}_s^* + D^*\bar{D}_s$	1^{+-}	3.99 ± 0.09	? $Z_{cs}(3985/4000)$
$D_s\bar{D}_s^* + D_s^*\bar{D}_s$	1^{+-}	4.07 ± 0.09	
D^*D^*	1^{+-}	4.02 ± 0.09	? $Z_c(4020)$
$D^*\bar{D}_s^*$	1^{+-}	4.11 ± 0.09	? $Z_{cs}(4100/4123)$
$D_s^*\bar{D}_s^*$	1^{+-}	4.19 ± 0.09	
D^*D^*	2^{++}	4.02 ± 0.09	? $\mathbf{X}_2(4014)$
$D^*\bar{D}_s^*$	2^{++}	4.11 ± 0.09	
$D_s^*\bar{D}_s^*$	2^{++}	4.19 ± 0.09	

Table 45: The possible assignments of the ground state hidden-charm molecular states, the isospin limit is implied.

from the BESIII collaboration [157]. If we assign the $Z_c(3900)$ as the diquark-antidiquark type tetraquark state, and assign the $Z_c(3885)$ to be the $D\bar{D} + D^*\bar{D}$ molecular state, it is easy to explain the large ratio R_{exp} .

The $Z_{cs}(3985)$ observed by the BESIII collaboration near the $D_s^- D^{*0}$ and $D_s^{*-} D^0$ thresholds in the K^+ recoil-mass spectrum in the processes $e^+e^- \rightarrow K^+(D_s^- D^{*0} + D_s^{*-} D^0)$, its Breit-Wigner mass and width are $3985.2_{-2.0}^{+2.1} \pm 1.7$ MeV and $13.8_{-5.2}^{+8.1} \pm 4.9$ MeV respectively with an assignment of the spin-parity $J^P = 1^+$ [161]. The $Z_{cs}(4000)$ observed in the $J/\psi K^+$ mass spectrum by the LHCb collaboration has a mass of $4003 \pm 6_{-14}^{+4}$ MeV, a width of $131 \pm 15 \pm 26$ MeV, and the spin-parity $J^P = 1^+$ [105]. The $Z_{cs}(3885)$ and $Z_{cs}(4000)$ are two quite different particles, although they have almost degenerated masses.

In the $J/\psi K^+$ mass spectrum from the LHCb collaboration, there is a hint of a dip at the energy about 4.1 GeV [105], which maybe due to the $Z_{cs}^-(4123)$ observed by the BESIII collaboration with a mass about $(4123.5 \pm 0.7 \pm 4.7)$ MeV [162]. More experimental data are still needed to obtain a precise resolution.

After Ref.[77] was published, the Belle collaboration observed weak evidences for two structures in the $\gamma\psi(2S)$ invariant mass spectrum in the two-photon process $\gamma\gamma \rightarrow \gamma\psi(2S)$, one at $3922.4 \pm 6.5 \pm 2.0$ MeV with a width $22 \pm 17 \pm 4$ MeV, and another at $4014.3 \pm 4.0 \pm 1.5$ MeV with a width $4 \pm 11 \pm 6$ MeV [519]. The first structure is consistent with the $X(3915)$ or $\chi_{c2}(3930)$, the second one may be an exotic charmonium-like state. We present its possible assignment in Table 45.

In Table 44, the central values of the predicted molecule masses lie at the thresholds of the corresponding two-meson scattering states, where we have taken the currents having to color-neutral clusters, in each cluster, the constituents q and \bar{Q} (or Q and \bar{q}) are in relative S-wave, see Eq.(237).

Now let us see the possible outcome, if one of the color-neutral clusters has a relative P-wave between the constituents q and \bar{Q} (or Q and \bar{q}), as one of the possible assignments of the $Y(4260)$ is a $D\bar{D}_1$ molecular state with the $J^{PC} = 1^{--}$ [202, 204, 465, 466, 467].

For example, in the isospin limit, we write the valence quarks of the $D\bar{D}_1(2420)$ and $D^*\bar{D}_0^*(2400)$

molecular states symbolically as

$$\bar{u}d\bar{c}c, \frac{\bar{u}u - \bar{d}d}{\sqrt{2}}\bar{c}c, \bar{d}u\bar{c}c, \frac{\bar{u}u + \bar{d}d}{\sqrt{2}}\bar{c}c, \quad (251)$$

the isospin triplet and singlet have degenerate masses. We take the isospin limit to study those molecular states [518].

Again we resort to the correlation functions $\Pi_{\mu\nu}(p)$ in Eq.(236) with the currents $J_\mu(x) = J_\mu^1(x)$, $J_\mu^2(x)$, $J_\mu^3(x)$ and $J_\mu^4(x)$ to study the $D\bar{D}_1(2420)$ and $D^*\bar{D}_0^*(2400)$ molecular states, where

$$\begin{aligned} J_\mu^1(x) &= \frac{1}{\sqrt{2}} \{ \bar{u}(x)i\gamma_5 c(x)\bar{c}(x)\gamma_\mu\gamma_5 d(x) - \bar{u}(x)\gamma_\mu\gamma_5 c(x)\bar{c}(x)i\gamma_5 d(x) \}, \\ J_\mu^2(x) &= \frac{1}{\sqrt{2}} \{ \bar{u}(x)i\gamma_5 c(x)\bar{c}(x)\gamma_\mu\gamma_5 d(x) + \bar{u}(x)\gamma_\mu\gamma_5 c(x)\bar{c}(x)i\gamma_5 d(x) \}, \\ J_\mu^3(x) &= \frac{1}{\sqrt{2}} \{ \bar{u}(x)c(x)\bar{c}(x)\gamma_\mu d(x) + \bar{u}(x)\gamma_\mu c(x)\bar{c}(x)d(x) \}, \\ J_\mu^4(x) &= \frac{1}{\sqrt{2}} \{ \bar{u}(x)c(x)\bar{c}(x)\gamma_\mu d(x) - \bar{u}(x)\gamma_\mu c(x)\bar{c}(x)d(x) \}. \end{aligned} \quad (252)$$

Under charge conjugation transform \hat{C} , the currents $J_\mu(x)$ have the properties,

$$\begin{aligned} \hat{C}J_\mu^{1/3}(x)\hat{C}^{-1} &= -J_\mu^{1/3}(x)|_{u\leftrightarrow d}, \\ \hat{C}J_\mu^{2/4}(x)\hat{C}^{-1} &= +J_\mu^{2/4}(x)|_{u\leftrightarrow d}. \end{aligned} \quad (253)$$

According to the quark-hadron duality, we isolate the ground state contributions of the vector molecular states,

$$\Pi_{\mu\nu}(p) = \frac{\lambda_Y^2}{M_Y^2 - p^2} \left(-g_{\mu\nu} + \frac{p_\mu p_\nu}{p^2} \right) + \dots, \quad (254)$$

where the λ_Y are the pole residues.

We carry out the operator product expansion up to the vacuum condensates in a consistent way routinely [77, 78, 518], and obtain the QCD sum rules,

$$\lambda_Y^2 \exp\left(-\frac{M_Y^2}{T^2}\right) = \int_{4m_c^2}^{s_0} ds \rho_{QCD}(s) \exp\left(-\frac{s}{T^2}\right), \quad (255)$$

$$M_Y^2 = \frac{\int_{4m_c^2}^{s_0} ds \left(-\frac{d}{d\tau}\right) \rho_{QCD}(s) e^{-\tau s}}{\int_{4m_c^2}^{s_0} ds \rho_{QCD}(s) e^{-\tau s}}. \quad (256)$$

We adopt the energy scale formula in Eq.(249) to choose the best energy scales of the QCD spectral densities, and take the updated value $\mathbb{M}_c = 1.85$ GeV [518].

After trial and error, we obtain the Borel parameters, continuum threshold parameters, pole contributions and energy scales, see Table 46, where the central values of the pole contributions are larger than 50%, the pole dominance is well satisfied. In the Borel windows, the contributions $D_{10} \ll 1\%$, the operator product expansion is well convergent.

We take into account all uncertainties of the input parameters, and obtain the values of the masses and pole residues, which are also shown Table 46 [518].

The prediction $M_{D\bar{D}_1(1--)} = 4.36 \pm 0.08$ GeV is consistent with the experimental data $M_{Y(4390)} = 4391.6 \pm 6.3 \pm 1.0$ MeV from the BESIII collaboration within uncertainties [145], while the predictions $M_{D\bar{D}_1(1-+)} = 4.60 \pm 0.08$ GeV, $M_{D^*\bar{D}_0^*(1--)} = 4.78 \pm 0.07$ GeV and $M_{D^*\bar{D}_0^*(1-+)} = 4.73 \pm$

	$T^2(\text{GeV}^2)$	$\sqrt{s_0}(\text{GeV})$	pole	$\mu(\text{GeV})$	$M_Y(\text{GeV})$	$\lambda_Y(10^{-2}\text{GeV}^5)$
$DD_1(1^{--})$	3.2 – 3.6	4.9 ± 0.1	(45 – 65)%	2.3	4.36 ± 0.08	3.97 ± 0.54
$DD_1(1^{-+})$	3.5 – 3.9	5.1 ± 0.1	(44 – 63)%	2.7	4.60 ± 0.08	5.26 ± 0.65
$D^*D_0^*(1^{--})$	4.0 – 4.4	5.3 ± 0.1	(44 – 61)%	3.0	4.78 ± 0.07	7.56 ± 0.84
$D^*D_0^*(1^{-+})$	3.8 – 4.2	5.2 ± 0.1	(44 – 61)%	2.9	4.73 ± 0.07	6.83 ± 0.84

Table 46: The Borel parameters, continuum threshold parameters, pole contributions, energy scales, masses and pole residues of the vector molecular states.

0.07 GeV are much larger than upper bound of the experimental data $M_{Y(4390)} = 4218.4 \pm 4.0 \pm 0.9$ MeV and $M_{Y(4390)} = 4391.6 \pm 6.3 \pm 1.0$ MeV [145], moreover, they are much larger than the near thresholds $M_{D^+D_1(2420)^-} = 4293$ MeV, $M_{D^0D_1(2420)^0} = 4285$ MeV, $M_{D^{*+}D_0^*(2400)^-} = 4361$ MeV, $M_{D^{*0}D_0^*(2400)^0} = 4325$ MeV [521]. The present predictions only favor assigning the $Y(4390)$ to be the $DD_1(1^{--})$ molecular state.

In Ref.[371], Zhang and Huang study the $Q\bar{q}\bar{Q}'q$ type scalar, vector and axialvector molecular states with the QCD sum rules systematically by calculating the operator product expansion up to the vacuum condensates of dimension 6. The predicted molecule masses $M_{D^*D_0^*} = 4.26 \pm 0.07$ GeV and $M_{D\bar{D}_1} = 4.34 \pm 0.07$ GeV are consistent with the $Y(4220)$ and $Y(4390)$, respectively. However, they do not distinguish the charge conjugation of the molecular states and neglect the higher dimensional vacuum condensates.

In Ref.[367], Lee, Morita and Nielsen distinguish the charge conjugation, calculate the operator product expansion up to the vacuum condensates of dimension 6 including dimension 8 partly. They obtain the mass of the $D\bar{D}_1(2420)$ molecular state with the $J^{PC} = 1^{-+}$, $M_{D\bar{D}_1} = 4.19 \pm 0.22$ GeV, which differs from the prediction $M_{D\bar{D}_1} = 4.34 \pm 0.07$ GeV significantly [371].

In Refs.[367, 371], **Scheme II** is chosen, some higher dimensional vacuum condensates are neglected, which associate with $\frac{1}{T^2}$, $\frac{1}{T^4}$, $\frac{1}{T^6}$ in the QCD spectral densities and manifest themselves at small values of the T^2 , we have to choose large values of T^2 to warrant convergence of the operator product expansion. The higher dimensional vacuum condensates, see Fig.19, play an important role in determining the Borel windows therefore the ground state masses and pole residues, we should take them into account consistently. All in all, we expect that the QCD sum rules give much larger masses than the two-meson thresholds, and we should bear in mind that the continuum threshold parameters should not be large enough to include contaminations for the higher resonances [522].

In Ref.[468], Qiao assigns the $Y(4260)$ as the $\bar{\Lambda}_c\Lambda_c$ baryonium state with the $J^{PC} = 1^{--}$. In Ref.[469], Qiao includes the Σ_c^0 constituent, and suggests a triplet and a singlet baryonium states,

$$\begin{aligned}
& B_1^+ \equiv |\Lambda_c^+ \bar{\Sigma}_c^0 \rangle \\
\text{Triplet : } & B_1^0 \equiv \frac{1}{\sqrt{2}}(|\Lambda_c^+ \bar{\Lambda}_c^- \rangle - |\Sigma_c^0 \bar{\Sigma}_c^0 \rangle) \\
& B_1^- \equiv |\Lambda_c^- \Sigma_c^0 \rangle
\end{aligned} \tag{257}$$

and

$$\text{Singlet : } B_0^0 \equiv \frac{1}{\sqrt{2}}(|\Lambda_c^+ \bar{\Lambda}_c^- \rangle + |\Sigma_c^0 \bar{\Sigma}_c^0 \rangle), \tag{258}$$

then he assigns the $Z_c^\pm(4430)$ as the 2S B_1^\pm state with the $J^{PC} = 1^{+-}$, and the $Y(4360)$ ($Y(4660)$) as the 2S $\bar{\Lambda}_c\Lambda_c$ ($\bar{\Sigma}_c\Sigma_c$) baryonium state with the $J^{PC} = 1^{--}$.

We study the $\bar{\Lambda}_c\Lambda_c$ and $\bar{\Sigma}_c\Sigma_c$ type hidden-charm baryonium states via the QCD sum rules consistently by carrying out the operator product expansion up to the vacuum condensates of dimension 16 according to the counting roles in Sect.5.1, and observe that the $\bar{\Lambda}_c\Lambda_c$ state with

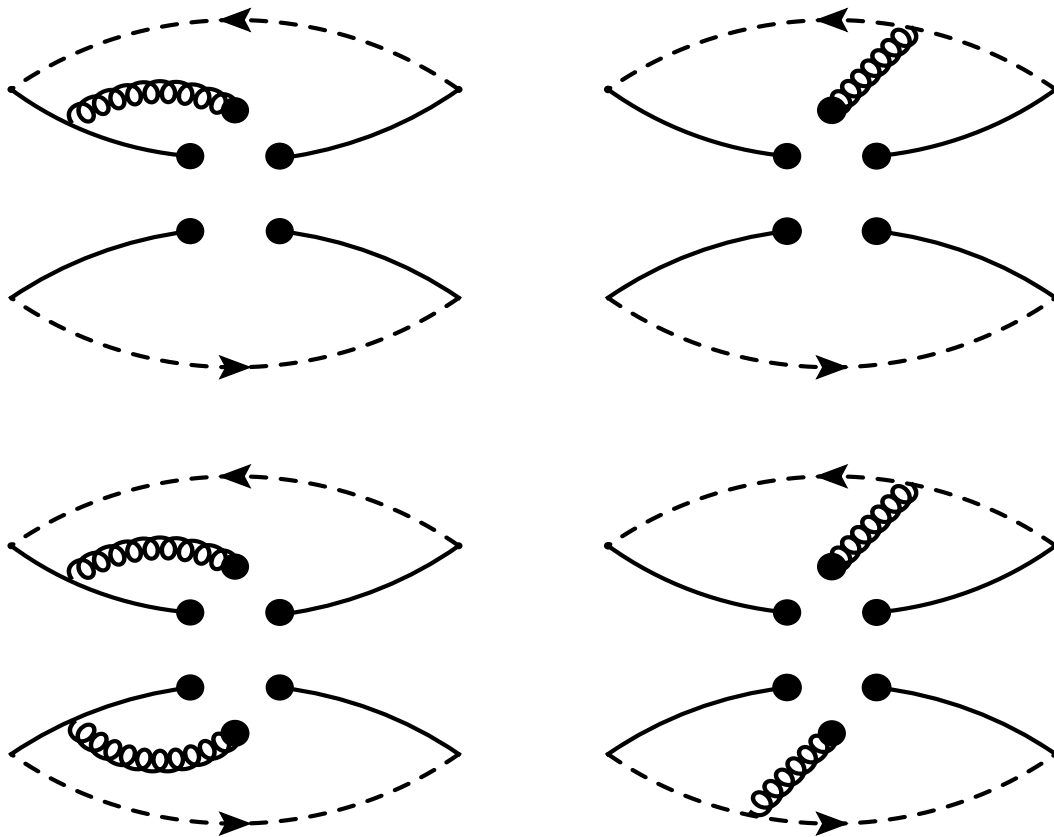


Figure 19: The Feynman diagrams contribute to the $\langle \bar{q}q \rangle \langle \bar{q}g_s \sigma Gq \rangle$ and $\langle \bar{q}g_s \sigma Gq \rangle^2$. Other diagrams obtained by interchanging of the light and heavy quark lines are implied.

the $J^P = 1^-$ and $\bar{\Sigma}_c \Sigma_c$ states with the $J^P = 0^-, 1^-$ lie at the corresponding baryon-antibaryon thresholds, respectively, while the $\bar{\Lambda}_c \Lambda_c$ states with the $J^P = 0^-, 1^+$ and $\bar{\Sigma}_c \Sigma_c$ states with the $J^P = 0^+, 1^+$ lie above the corresponding baryon-antibaryon thresholds, respectively, whose masses are all much larger than the $Y(4260)$ [523]. In Ref.[524], Wan, Tang and Qiao study the $\bar{\Lambda}_Q \Lambda_Q$ states with the $J^{PC} = 0^{++}, 0^{-+}, 1^{++}$ and 1^{--} via the QCD sum rules by taking account of the vacuum condensates up to dimension 12, and observe that only the baryonium states with the $J^{PC} = 0^{++}$ and 1^{--} could exist, they also obtain masses much larger than the corresponding $\bar{\Lambda}_Q \Lambda_Q$ thresholds, respectively. Such subjects need further studies to obtain definite conclusion.

8.2 11 type doubly heavy tetraquark states

Before and after the observation of the doubly-charmed tetraquark candidate $T_{cc}^+(3875)$, there have been several works on the doubly-charmed tetraquark (molecular) states.

If we perform Fierz rearrangements for the four-quark axialvector current $J_\mu(x)$ [482], see Eq.(195), we obtain a special superposition of the color singlet-singlet type currents,

$$\begin{aligned}
J_\mu(x) &= \varepsilon^{ijk} \varepsilon^{imn} Q_j^T(x) C \gamma_\mu Q_k(x) \bar{u}_m(x) \gamma_5 C \bar{d}_n^T(x), \\
&= \frac{i}{2} [\bar{u} i \gamma_5 Q \bar{d} \gamma_\mu Q - \bar{d} i \gamma_5 Q \bar{u} \gamma_\mu Q] + \frac{1}{2} [\bar{u} Q \bar{d} \gamma_\mu \gamma_5 Q - \bar{d} Q \bar{u} \gamma_\mu \gamma_5 Q] \\
&\quad - \frac{i}{2} [\bar{u} \sigma_{\mu\nu} \gamma_5 Q \bar{d} \gamma^\nu Q - \bar{d} \sigma_{\mu\nu} \gamma_5 Q \bar{u} \gamma^\nu Q] + \frac{i}{2} [\bar{u} \sigma_{\mu\nu} Q \bar{d} \gamma^\nu \gamma_5 Q - \bar{d} \sigma_{\mu\nu} Q \bar{u} \gamma^\nu \gamma_5 Q], \\
&= \frac{i}{2} J_\mu^1(x) + \frac{1}{2} J_\mu^2(x) - \frac{i}{2} J_\mu^3(x) + \frac{i}{2} J_\mu^4(x). \tag{259}
\end{aligned}$$

The currents $J_\mu^1(x)$, $J_\mu^2(x)$, $J_\mu^3(x)$ and $J_\mu^4(x)$ couple potentially to the color singlet-singlet type tetraquark states or two-meson scattering states. In fact, there exist spatial separations between the diquark and antidiquark pair, the currents $J_\mu(x)$ should be modified to $J_\mu(x, \epsilon)$,

$$J_\mu(x, \epsilon) = \varepsilon^{ijk} \varepsilon^{imn} Q_j^T(x) C \gamma_\mu Q_k(x) \bar{u}_m(x + \epsilon) \gamma_5 C \bar{d}_n^T(x + \epsilon), \tag{260}$$

where the four-vector $\epsilon^\alpha = (0, \vec{\epsilon})$. The spatial distance between the diquark and antidiquark pair maybe frustrate the Fierz rearrangements or recombination, although we usually take the local limit $\epsilon \rightarrow 0$, we should not take it for granted that the Fierz rearrangements are feasible [337], we cannot obtain the conclusion that the T_{cc}^+ has the $D^*D - DD^*$ Fock component according to the component $\bar{q} i \gamma_5 c \otimes \bar{q} \gamma_\mu c$ in Eq.(259). According to the predictions in Table 35, we can only obtain the conclusion tentatively that the T_{cc}^+ has a diquark-antidiquark type tetraquark Fock component with the spin-parity $J^P = 1^+$ and isospin $I = 0$ [482]. It is interesting to explore whether or not there exists a color singlet-singlet type Fock component.

Again, we resort to the correlation functions $\Pi(p)$, $\Pi_{\mu\nu}(p)$ and $\Pi_{\mu\nu\alpha\beta}(p)$ in Eq.(236), and construct the currents $J(x)$, $J_\mu(x)$ and $J_{\mu\nu}(x)$,

$$J(x) = J_{DD}(x), J_{DD_s}(x), J_{D_s D_s}(x), J_{D^* D^*}(x), J_{D^* D_s^*}(x), J_{D_s^* D_s^*}(x), \tag{261}$$

$$\begin{aligned}
J_\mu(x) &= J_{DD^*, L, \mu}(x), J_{DD^*, H, \mu}(x), J_{DD_s^*, L, \mu}(x), J_{DD_s^*, H, \mu}(x), J_{D_s D_s^*, \mu}(x), \\
&\quad J_{D_1 D_0^*, L, \mu}(x), J_{D_1 D_0^*, H, \mu}(x), J_{D_{s_1} D_0^*, L, \mu}(x), J_{D_{s_1} D_0^*, H, \mu}(x), J_{D_{s_1} D_{s_0}^*, \mu}(x), \tag{262}
\end{aligned}$$

$$\begin{aligned}
J_{\mu\nu}(x) &= J_{D^* D^*, L, \mu\nu}(x), J_{D^* D^*, H, \mu\nu}(x), J_{D^* D_s^*, L, \mu\nu}(x), J_{D^* D_s^*, H, \mu\nu}(x), J_{D_s^* D_s^*, L, \mu\nu}(x), \\
&\quad J_{D_s^* D_s^*, H, \mu\nu}(x), \tag{263}
\end{aligned}$$

$$\begin{aligned}
J_{DD}(x) &= \bar{u}(x)i\gamma_5c(x)\bar{d}(x)i\gamma_5c(x), \\
J_{DD_s}(x) &= \bar{q}(x)i\gamma_5c(x)\bar{s}(x)i\gamma_5c(x), \\
J_{D_sD_s}(x) &= \bar{s}(x)i\gamma_5c(x)\bar{s}(x)i\gamma_5c(x), \\
J_{D^*D^*}(x) &= \bar{u}(x)\gamma_\mu c(x)\bar{d}(x)\gamma^\mu c(x), \\
J_{D^*D_s^*}(x) &= \bar{q}(x)\gamma_\mu c(x)\bar{s}(x)\gamma^\mu c(x), \\
J_{D_s^*D_s^*}(x) &= \bar{s}(x)\gamma_\mu c(x)\bar{s}(x)\gamma^\mu c(x),
\end{aligned} \tag{264}$$

$$\begin{aligned}
J_{DD^*,L,\mu}(x) &= \frac{1}{\sqrt{2}}\left[\bar{u}(x)i\gamma_5c(x)\bar{d}(x)\gamma_\mu c(x) - \bar{u}(x)\gamma_\mu c(x)\bar{d}(x)i\gamma_5c(x)\right], \\
J_{DD^*,H,\mu}(x) &= \frac{1}{\sqrt{2}}\left[\bar{u}(x)i\gamma_5c(x)\bar{d}(x)\gamma_\mu c(x) + \bar{u}(x)\gamma_\mu c(x)\bar{d}(x)i\gamma_5c(x)\right], \\
J_{DD_s^*,L,\mu}(x) &= \frac{1}{\sqrt{2}}\left[\bar{q}(x)i\gamma_5c(x)\bar{s}(x)\gamma_\mu c(x) - \bar{q}(x)\gamma_\mu c(x)\bar{s}(x)i\gamma_5c(x)\right], \\
J_{DD_s^*,H,\mu}(x) &= \frac{1}{\sqrt{2}}\left[\bar{q}(x)i\gamma_5c(x)\bar{s}(x)\gamma_\mu c(x) + \bar{q}(x)\gamma_\mu c(x)\bar{s}(x)i\gamma_5c(x)\right], \\
J_{D_sD_s^*,\mu}(x) &= \bar{s}(x)i\gamma_5c(x)\bar{s}(x)\gamma_\mu c(x),
\end{aligned} \tag{265}$$

$$\begin{aligned}
J_{D_1D_0^*,L,\mu}(x) &= \frac{1}{\sqrt{2}}\left[\bar{u}(x)c(x)\bar{d}(x)\gamma_\mu\gamma_5c(x) + \bar{u}(x)\gamma_\mu\gamma_5c(x)\bar{d}(x)c(x)\right], \\
J_{D_1D_0^*,H,\mu}(x) &= \frac{1}{\sqrt{2}}\left[\bar{u}(x)c(x)\bar{d}(x)\gamma_\mu\gamma_5c(x) - \bar{u}(x)\gamma_\mu\gamma_5c(x)\bar{d}(x)c(x)\right], \\
J_{D_{s1}D_0^*,L,\mu}(x) &= \frac{1}{\sqrt{2}}\left[\bar{q}(x)c(x)\bar{s}(x)\gamma_\mu\gamma_5c(x) + \bar{q}(x)\gamma_\mu\gamma_5c(x)\bar{s}(x)c(x)\right], \\
J_{D_{s1}D_0^*,H,\mu}(x) &= \frac{1}{\sqrt{2}}\left[\bar{q}(x)c(x)\bar{s}(x)\gamma_\mu\gamma_5c(x) - \bar{q}(x)\gamma_\mu\gamma_5c(x)\bar{s}(x)c(x)\right], \\
J_{D_{s1}D_{s0}^*,\mu}(x) &= \bar{s}(x)c(x)\bar{s}(x)\gamma_\mu\gamma_5c(x),
\end{aligned} \tag{266}$$

$$\begin{aligned}
J_{D^*D^*,L,\mu\nu}(x) &= \frac{1}{\sqrt{2}}\left[\bar{u}(x)\gamma_\mu c(x)\bar{d}(x)\gamma_\nu c(x) - \bar{u}(x)\gamma_\nu c(x)\bar{d}(x)\gamma_\mu c(x)\right], \\
J_{D^*D^*,H,\mu\nu}(x) &= \frac{1}{\sqrt{2}}\left[\bar{u}(x)\gamma_\mu c(x)\bar{d}(x)\gamma_\nu c(x) + \bar{u}(x)\gamma_\nu c(x)\bar{d}(x)\gamma_\mu c(x)\right], \\
J_{D^*D_s^*,L,\mu\nu}(x) &= \frac{1}{\sqrt{2}}\left[\bar{q}(x)\gamma_\mu c(x)\bar{s}(x)\gamma_\nu c(x) - \bar{q}(x)\gamma_\nu c(x)\bar{s}(x)\gamma_\mu c(x)\right], \\
J_{D^*D_s^*,H,\mu\nu}(x) &= \frac{1}{\sqrt{2}}\left[\bar{q}(x)\gamma_\mu c(x)\bar{s}(x)\gamma_\nu c(x) + \bar{q}(x)\gamma_\nu c(x)\bar{s}(x)\gamma_\mu c(x)\right], \\
J_{D_s^*D_s^*,L,\mu\nu}(x) &= \frac{1}{\sqrt{2}}\left[\bar{s}(x)\gamma_\mu c(x)\bar{s}(x)\gamma_\nu c(x) - \bar{s}(x)\gamma_\nu c(x)\bar{s}(x)\gamma_\mu c(x)\right], \\
J_{D_s^*D_s^*,H,\mu\nu}(x) &= \frac{1}{\sqrt{2}}\left[\bar{s}(x)\gamma_\mu c(x)\bar{s}(x)\gamma_\nu c(x) + \bar{s}(x)\gamma_\nu c(x)\bar{s}(x)\gamma_\mu c(x)\right],
\end{aligned} \tag{267}$$

and $q = u, d$, we add the subscripts L and H to distinguish the lighter and heavier states in the same doublet due to the mixing effects, as direct calculations indicate that there exists such a tendency.

Under parity transform \hat{P} , the currents have the properties,

$$\begin{aligned}
\hat{P}J(x)\hat{P}^{-1} &= +J(\tilde{x}), \\
\hat{P}J_\mu(x)\hat{P}^{-1} &= -J^\mu(\tilde{x}), \\
\hat{P}J_{\mu\nu}(x)\hat{P}^{-1} &= +J^{\mu\nu}(\tilde{x}),
\end{aligned} \tag{268}$$

where $x^\mu = (t, \vec{x})$ and $\tilde{x}^\mu = (t, -\vec{x})$. We rewrite Eq.(268) in more explicit form,

$$\begin{aligned}\widehat{P}J_i(x)\widehat{P}^{-1} &= +J_i(\tilde{x}), \\ \widehat{P}J_{ij}(x)\widehat{P}^{-1} &= +J_{ij}(\tilde{x}),\end{aligned}\tag{269}$$

$$\begin{aligned}\widehat{P}J_0(x)\widehat{P}^{-1} &= -J_0(\tilde{x}), \\ \widehat{P}J_{0i}(x)\widehat{P}^{-1} &= -J_{0i}(\tilde{x}),\end{aligned}\tag{270}$$

where the space indexes $i, j = 1, 2, 3$. There are both positive and negative components, and they couple potentially to the axialvector/tensor and pseudoscalar/vector molecular states, respectively. We will introduce an superscript $-$ to denote the negative parity.

According to the quark-hadron duality, we obtain the hadronic representation and isolate the ground state contributions of the scalar, axialvector and tensor molecular states [78, 444],

$$\begin{aligned}\Pi(p) &= \frac{\lambda_T^2}{M_T^2 - p^2} + \dots = \Pi_T^0(p^2) + \dots, \\ \Pi_{\mu\nu}(p) &= \frac{\lambda_T^2}{M_T^2 - p^2} \left(-g_{\mu\nu} + \frac{p_\mu p_\nu}{p^2} \right) + \dots \\ &= \Pi_T^1(p^2) \left(-g_{\mu\nu} + \frac{p_\mu p_\nu}{p^2} \right) + \dots, \\ \Pi_{L,\mu\nu\alpha\beta}(p) &= \frac{\lambda_T^2}{M_T^2(M_T^2 - p^2)} (p^2 g_{\mu\alpha} g_{\nu\beta} - p^2 g_{\mu\beta} g_{\nu\alpha} - g_{\mu\alpha} p_\nu p_\beta - g_{\nu\beta} p_\mu p_\alpha + g_{\mu\beta} p_\nu p_\alpha + g_{\nu\alpha} p_\mu p_\beta) \\ &\quad + \frac{\lambda_{T-}^2}{M_{T-}^2(M_{T-}^2 - p^2)} (-g_{\mu\alpha} p_\nu p_\beta - g_{\nu\beta} p_\mu p_\alpha + g_{\mu\beta} p_\nu p_\alpha + g_{\nu\alpha} p_\mu p_\beta) + \dots \\ &= \widetilde{\Pi}_T^1(p^2) (p^2 g_{\mu\alpha} g_{\nu\beta} - p^2 g_{\mu\beta} g_{\nu\alpha} - g_{\mu\alpha} p_\nu p_\beta - g_{\nu\beta} p_\mu p_\alpha + g_{\mu\beta} p_\nu p_\alpha + g_{\nu\alpha} p_\mu p_\beta) \\ &\quad + \widetilde{\Pi}_T^{1,-}(p^2) (-g_{\mu\alpha} p_\nu p_\beta - g_{\nu\beta} p_\mu p_\alpha + g_{\mu\beta} p_\nu p_\alpha + g_{\nu\alpha} p_\mu p_\beta), \\ \Pi_{H,\mu\nu\alpha\beta}(p) &= \frac{\lambda_T^2}{M_T^2 - p^2} \left(\frac{\widetilde{g}_{\mu\alpha} \widetilde{g}_{\nu\beta} + \widetilde{g}_{\mu\beta} \widetilde{g}_{\nu\alpha}}{2} - \frac{\widetilde{g}_{\mu\nu} \widetilde{g}_{\alpha\beta}}{3} \right) + \dots, \\ &= \Pi_T^2(p^2) \left(\frac{\widetilde{g}_{\mu\alpha} \widetilde{g}_{\nu\beta} + \widetilde{g}_{\mu\beta} \widetilde{g}_{\nu\alpha}}{2} - \frac{\widetilde{g}_{\mu\nu} \widetilde{g}_{\alpha\beta}}{3} \right) + \dots,\end{aligned}\tag{271}$$

where the pole residues λ_T and λ_{T-} are defined by

$$\begin{aligned}\langle 0|J(0)|T_{cc}(p)\rangle &= \lambda_T, \\ \langle 0|J_\mu(0)|T_{cc}(p)\rangle &= \lambda_T \varepsilon_\mu, \\ \langle 0|J_{L,\mu\nu}(0)|T_{cc}(p)\rangle &= \tilde{\lambda}_T \varepsilon_{\mu\nu\alpha\beta} \varepsilon^\alpha p^\beta, \\ \langle 0|J_{L,\mu\nu}(0)|T_{cc}^-(p)\rangle &= \tilde{\lambda}_{T-} (\varepsilon_\mu p_\nu - \varepsilon_\nu p_\mu), \\ \langle 0|J_{H,\mu\nu}(0)|T_{cc}(p)\rangle &= \lambda_T \varepsilon_{\mu\nu},\end{aligned}\tag{272}$$

$\lambda_T = \tilde{\lambda}_T M_T$ and $\lambda_{T-} = \tilde{\lambda}_{T-} M_{T-}$, the $\varepsilon_\mu/\varepsilon_{\mu\nu}$ are the polarization vectors of the molecular states, we introduce the superscripts 0, 1 and 2 denote the spins of the molecular states. Thereafter, we choose the components $\Pi_T^{0/2}(p^2)$ and $p^2 \widetilde{\Pi}_T^1(p^2)$.

We accomplish the operator product expansion up to the vacuum condensates of dimension 10 and take account of the vacuum condensates $\langle \bar{q}q \rangle$, $\langle \frac{\alpha_s G G}{\pi} \rangle$, $\langle \bar{q}g_s \sigma G q \rangle$, $\langle \bar{q}q \rangle^2$, $\langle \bar{q}q \rangle \langle \frac{\alpha_s G G}{\pi} \rangle$,

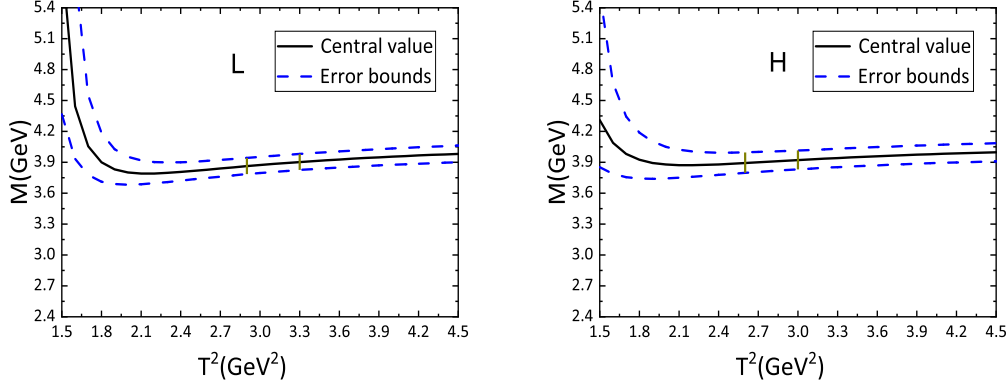


Figure 20: The masses with variations of the Borel parameters for the axialvector tetraquark molecular states, where the L and H denote the lighter and heavier DD^* states, respectively.

$\langle \bar{q}q \rangle \langle \bar{q}g_s \sigma Gq \rangle$, $\langle \bar{q}g_s \sigma Gq \rangle^2$ and $\langle \bar{q}q \rangle^2 \langle \frac{\alpha_s GG}{\pi} \rangle$ with the vacuum saturation in a consistent way [503], where $q = u, d$ or s [56, 57, 77, 78, 163, 164, 361, 361, 353, 444, 445, 446]. Again, we neglect the u and d quark masses, and take account of the terms $\propto m_s$ according to the light-flavor $SU(3)$ breaking effects.

Then we match the hadron side with the QCD side below the continuum thresholds s_0 , perform the Borel transform, and obtain two QCD sum rules,

$$\lambda_T^2 \exp\left(-\frac{M_T^2}{T^2}\right) = \int_{4m_c^2}^{s_0} ds \rho_{QCD}(s) \exp\left(-\frac{s}{T^2}\right), \quad (273)$$

$$M_T^2 = -\frac{\int_{4m_c^2}^{s_0} ds \frac{d}{d\tau} \rho_{QCD}(s) \exp(-\tau s)}{\int_{4m_c^2}^{s_0} ds \rho_{QCD}(s) \exp(-\tau s)} \Big|_{\tau=\frac{1}{T^2}}. \quad (274)$$

We take the modified energy scale formula shown in Eq.(249), and the effective c/s -quark masses $\mathbb{M}_c = 1.82 \text{ GeV}$ and $\mathbb{M}_s = 0.2 \text{ GeV}$ to determine the optimal energy scales of the QCD spectral densities. After trial and error, we obtain the Borel parameters, continuum threshold parameters, energy scales of the QCD spectral densities, pole contributions, and the contributions of the vacuum condensates of dimension 10, which are shown in Table 47. The pole contributions are about (40–60)% at the hadron side, the central values are larger than 50%, the pole dominance is satisfied very good. Moreover, the contributions of the vacuum condensates of dimension 10 are $|D(10)| < 1\%$ or $\ll 1\%$ at the QCD side, the operator product expansion converge very good.

We take account of all the uncertainties of the parameters, and obtain the masses and pole residues of the doubly-charmed molecular states without strange, with strange and with doubly-strange, which are presented explicitly in Table 48.

In Fig.20, as an example, we plot the masses of the axialvector doubly-charmed tetraquark molecular states $(D^*D - DD^*)_L$ and $(D^*D + DD^*)_H$ with variations of the Borel parameters at much larger ranges than the Borel widows. There appear very flat platforms in the Borel windows, the regions between the two short perpendicular lines.

There exist both a lighter state and a heavier state for the $cc\bar{u}\bar{d}$ and $cc\bar{q}\bar{s}$ tetraquark molecular states, the lighter state $(D^*D - DD^*)_L$ with the isospin $(I, I_3) = (0, 0)$ has a mass $3.88 \pm 0.11 \text{ GeV}$, which is in excellent agreement with the mass of the doubly-charmed tetraquark candidate T_{cc}^+ from the LHCb collaboration [187, 188], and supports assigning the T_{cc}^+ to be the $(D^*D - DD^*)_L$ molecular state, as the T_{cc}^+ has the isospin $I = 0$. In other words, the exotic state T_{cc}^+ maybe have a

T_{cc}	Isospin	$T^2(\text{GeV}^2)$	$\sqrt{s_0}(\text{GeV})$	$\mu(\text{GeV})$	pole	$ D(10) $
DD	1	2.6 – 3.0	4.30 ± 0.10	1.4	(40 – 64)%	$\ll 1\%$
DD_s	$\frac{1}{2}$	2.7 – 3.1	4.40 ± 0.10	1.4	(41 – 64)%	$\ll 1\%$
$D_s D_s$	0	2.8 – 3.2	4.50 ± 0.10	1.4	(41 – 63)%	$\ll 1\%$
$D^* D^*$	1	2.8 – 3.2	4.55 ± 0.10	1.7	(41 – 61)%	$< 1\%$
$D_s^* D^*$	$\frac{1}{2}$	2.9 – 3.3	4.65 ± 0.10	1.7	(42 – 62)%	$\ll 1\%$
$D_s^* D_s^*$	0	3.2 – 3.5	4.80 ± 0.10	1.8	(42 – 61)%	$\ll 1\%$
$D^* D - DD^*$	0	2.9 – 3.3	4.45 ± 0.10	1.4	(42 – 62)%	$\ll 1\%$
$D^* D + DD^*$	1	2.6 – 3.0	4.40 ± 0.10	1.4	(42 – 63)%	$\ll 1\%$
$D_s^* D - D_s D^*$	$\frac{1}{2}$	3.0 – 3.4	4.50 ± 0.10	1.5	(40 – 62)%	$< 1\%$
$D_s^* D + D_s D^*$	$\frac{1}{2}$	2.9 – 3.3	4.50 ± 0.10	1.5	(40 – 60)%	$\ll 1\%$
$D_s^* D_s$	0	3.0 – 3.4	4.60 ± 0.10	1.5	(41 – 63)%	$\ll 1\%$
$D_0^* D_1 - D_1 D_0^*$	0	5.6 – 7.0	6.35 ± 0.10	4.6	(41 – 60)%	$\ll 1\%$
$D_0^* D_1 + D_1 D_0^*$	1	4.7 – 6.1	5.90 ± 0.10	4.0	(42 – 61)%	$\ll 1\%$
$D_0^* D_{s1} - D_{s0}^* D_1$	$\frac{1}{2}$	5.8 – 7.2	6.50 ± 0.10	4.6	(43 – 60)%	$< 1\%$
$D_0^* D_{s1} + D_{s0}^* D_1$	$\frac{1}{2}$	4.7 – 6.1	6.05 ± 0.10	4.0	(42 – 62)%	$< 1\%$
$D_{s1} D_{s0}^*$	0	4.9 – 6.3	6.20 ± 0.10	4.0	(43 – 61)%	$< 1\%$
$D^* D^* - D^* D^*$	0	3.2 – 3.6	4.55 ± 0.10	1.7	(42 – 61)%	$< 1\%$
$D^* D^* + D^* D^*$	1	3.0 – 3.4	4.55 ± 0.10	1.7	(41 – 60)%	$< 1\%$
$D_s^* D^* - D_s^* D^*$	$\frac{1}{2}$	3.3 – 3.7	4.65 ± 0.10	1.7	(40 – 59)%	$\ll 1\%$
$D_s^* D^* + D_s^* D^*$	$\frac{1}{2}$	3.1 – 3.5	4.65 ± 0.10	1.7	(42 – 61)%	$< 1\%$
$D_s^* D_s^* - D_s^* D_s^*$	0	3.6 – 4.0	4.80 ± 0.10	1.8	(40 – 60)%	$\ll 1\%$
$D_s^* D_s^* + D_s^* D_s^*$	0	3.4 – 3.9	4.80 ± 0.10	1.8	(41 – 61)%	$< 1\%$

Table 47: The Borel parameters, continuum threshold parameters, energy scales of the QCD spectral densities, pole contributions, and the contributions of the vacuum condensates of dimension 10 for the doubly-charmed molecular states.

$(D^* D - DD^*)_L$ Fock component. The heavier state $(D^* D + DD^*)_H$ with the isospin $(I, I_3) = (1, 0)$ has a mass 3.90 ± 0.11 GeV, the central value lies slightly above the DD^* threshold, the strong decays to the final states $DD\pi$ are kinematically allowed but with small phase-space. If we choose the same input parameters, the DD^* molecular state with the isospin $I = 1$ has slightly larger mass than the corresponding molecule with the isospin $I = 0$, it is indeed that the isoscalar DD^* molecular state is lighter.

For the molecular states $(D_0^* D_1 + D_1 D_0^*)_L$, $(D_0^* D_1 - D_1 D_0^*)_H$, $(D_0^* D_{s1} + D_{s0}^* D_1)_L$ and $(D_0^* D_{s1} - D_{s0}^* D_1)_H$, there exists a P-wave in the color-singlet constituents, the P-wave is embodied implicitly in the underlined $\underline{\gamma}_5$ in the scalar currents $\bar{q}i\underline{\gamma}_5\underline{\gamma}_5 c$, $\bar{s}i\underline{\gamma}_5\underline{\gamma}_5 c$ and axialvector currents $\bar{q}\underline{\gamma}_\mu\underline{\gamma}_5 c$, $\bar{s}\underline{\gamma}_\mu\underline{\gamma}_5 c$, as multiplying $\underline{\gamma}_5$ to the pseudoscalar currents $\bar{q}i\underline{\gamma}_5 c$, $\bar{s}i\underline{\gamma}_5 c$ and vector currents $\bar{q}\underline{\gamma}_\mu c$, $\bar{s}\underline{\gamma}_\mu c$ changes their parity. We should introduce the spin-orbit interactions to account for the large mass gaps between the lighter and heavier states (L, H), i.e. $((D_0^* D_1 + D_1 D_0^*)_L, (D_0^* D_1 - D_1 D_0^*)_H), ((D_0^* D_{s1} + D_{s0}^* D_1)_L, (D_0^* D_{s1} - D_{s0}^* D_1)_H)$.

From Table 48, we can see explicitly that the $D_0^* D_1 - D_1 D_0^*$, $D_0^* D_1 + D_1 D_0^*$, $D_0^* D_{s1} - D_{s0}^* D_1$, $D_0^* D_{s1} + D_{s0}^* D_1$ and $D_{s1} D_{s0}^*$ doubly molecular states have much larger masses than the corresponding two-meson thresholds, just like in the case of the hidden-charm molecular states studied in previous sub-section, where there exist a relative P-wave in one of the color-neutral clusters.

T_{cc}	Isospin	$M_T(\text{GeV})$	$\lambda_T(\text{GeV}^5)$
DD	1	3.75 ± 0.09	$(1.48 \pm 0.23) \times 10^{-2}$
DD_s	$\frac{1}{2}$	3.85 ± 0.09	$(1.69 \pm 0.26) \times 10^{-2}$
$D_s D_s$	0	3.95 ± 0.09	$(2.00 \pm 0.32) \times 10^{-2}$
$D^* D^*$	1	4.04 ± 0.11	$(4.99 \pm 0.66) \times 10^{-2}$
$D_s^* D^*$	$\frac{1}{2}$	4.12 ± 0.10	$(5.74 \pm 0.78) \times 10^{-2}$
$D_s^* D_s^*$	0	4.22 ± 0.10	$(7.46 \pm 0.89) \times 10^{-2}$
$D^* D - \bar{D} D^*$	0	3.88 ± 0.11	$(1.92 \pm 0.29) \times 10^{-2}$
$D^* D + \bar{D} D^*$	1	3.90 ± 0.11	$(1.50 \pm 0.22) \times 10^{-2}$
$D_s^* D - D_s \bar{D}^*$	$\frac{1}{2}$	3.97 ± 0.10	$(2.40 \pm 0.41) \times 10^{-2}$
$D_s^* D + D_s \bar{D}^*$	$\frac{1}{2}$	3.98 ± 0.11	$(2.06 \pm 0.30) \times 10^{-2}$
$D_s^* D_s$	0	4.10 ± 0.12	$(2.31 \pm 0.45) \times 10^{-2}$
$D_0^* D_1 - D_1 D_0^*$	0	5.79 ± 0.15	$(2.13 \pm 0.19) \times 10^{-1}$
$D_0^* D_1 + D_1 D_0^*$	1	5.37 ± 0.13	$(1.30 \pm 0.11) \times 10^{-1}$
$D_0^* D_{s1} - D_{s0}^* D_1$	$\frac{1}{2}$	5.93 ± 0.27	$(2.80 \pm 0.33) \times 10^{-1}$
$D_0^* D_{s1} + D_{s0}^* D_1$	$\frac{1}{2}$	5.54 ± 0.20	$(1.51 \pm 0.16) \times 10^{-1}$
$D_{s1} D_{s0}^*$	0	5.67 ± 0.27	$(1.77 \pm 0.27) \times 10^{-1}$
$D^* D^* - \bar{D}^* D^*$	0	4.00 ± 0.11	$(2.47 \pm 0.32) \times 10^{-2}$
$D^* D^* + \bar{D}^* D^*$	1	4.02 ± 0.11	$(2.83 \pm 0.30) \times 10^{-2}$
$D_s^* D^* - D_s \bar{D}^*$	$\frac{1}{2}$	4.08 ± 0.10	$(2.81 \pm 0.40) \times 10^{-2}$
$D_s^* D^* + D_s \bar{D}^*$	$\frac{1}{2}$	4.10 ± 0.11	$(3.19 \pm 0.44) \times 10^{-2}$
$D_s^* D_s^* - D_s \bar{D}_s^*$	0	4.19 ± 0.09	$(3.49 \pm 0.49) \times 10^{-2}$
$D_s^* D_s^* + D_s \bar{D}_s^*$	0	4.20 ± 0.10	$(4.00 \pm 0.53) \times 10^{-2}$

Table 48: The masses and pole residues of the ground state doubly-charmed molecular states.

9 Hidden heavy pentaquark states

If a baryon current $J(x)$ has the spin-parity $J^P = \frac{1}{2}^+$, then the current $i\gamma_5 J(x)$ would have the spin-parity $J^P = \frac{1}{2}^-$, as multiplying $i\gamma_5$ changes the parity of the current $J(x)$ [525]. In 1993, Bagan et al took the infinite heavy quark limit to separate the contributions of the positive and negative parity heavy baryon states unambiguously [526]. In 1996, Jido et al introduced a novel approach to separate the contributions of the negative-parity light-flavor baryons from the positive-parity ones [527].

At first, we write down the correlation functions $\Pi_{\pm}(p)$,

$$\Pi_{\pm}(p) = i \int d^4x e^{ip \cdot x} \langle 0 | T \{ J_{\pm}(x) \bar{J}_{\pm}(0) \} | 0 \rangle, \quad (275)$$

where we add the subscripts \pm to denote the positive and negative parity, respectively, $J_- = i\gamma_5 J_+$. We decompose the correlation functions $\Pi_{\pm}(p)$,

$$\Pi_{\pm}(p) = \not{p} \Pi_1(p^2) \pm \Pi_0(p^2), \quad (276)$$

according to Lorentz covariance, because

$$\Pi_-(p) = -\gamma_5 \Pi_+(p) \gamma_5. \quad (277)$$

The currents J_+ couple to both the positive- and negative-parity baryons [525],

$$\langle 0 | J_+ | B^{\pm} \rangle \langle B^{\pm} | \bar{J}_+ | 0 \rangle = -\gamma_5 \langle 0 | J_- | B^{\pm} \rangle \langle B^{\pm} | \bar{J}_- | 0 \rangle \gamma_5, \quad (278)$$

where the B^{\pm} denote the positive and negative parity baryons, respectively.

According to the relation in Eq.(278), we obtain the hadronic representation [527],

$$\Pi_+(p) = \lambda_+^2 \frac{\not{p} + M_+}{M_+^2 - p^2} + \lambda_-^2 \frac{\not{p} - M_-}{M_-^2 - p^2} + \dots, \quad (279)$$

where the M_\pm are the baryon masses, the pole residues are defined by $\langle 0|J_\pm(0)|B^\pm(p)\rangle = \lambda_\pm U_\pm$, the U_\pm are the Dirac spinors.

If we take $\vec{p} = 0$, then

$$\begin{aligned} \lim_{\epsilon \rightarrow 0} \frac{\text{Im}\Pi_+(p_0 + i\epsilon)}{\pi} &= \lambda_+^2 \frac{\gamma_0 + 1}{2} \delta(p_0 - M_+) + \lambda_-^2 \frac{\gamma_0 - 1}{2} \delta(p_0 - M_-) + \dots \\ &= \gamma_0 A(p_0) + B(p_0) + \dots, \end{aligned} \quad (280)$$

where

$$\begin{aligned} A(p_0) &= \frac{1}{2} [\lambda_+^2 \delta(p_0 - M_+) + \lambda_-^2 \delta(p_0 - M_-)], \\ B(p_0) &= \frac{1}{2} [\lambda_+^2 \delta(p_0 - M_+) - \lambda_-^2 \delta(p_0 - M_-)], \end{aligned} \quad (281)$$

the contribution $A(p_0) + B(p_0)$ ($A(p_0) - B(p_0)$) contains contributions from the positive parity (negative parity) states only.

We carry out the operator product expansion at large $P^2 (= -p_0^2)$ region, then use the dispersion relation to obtain the spectral densities $\rho^A(p_0)$ and $\rho^B(p_0)$ at the quark-gluon level. At last, we introduce the weight functions $\exp\left[-\frac{p_0^2}{T^2}\right]$, $p_0^2 \exp\left[-\frac{p_0^2}{T^2}\right]$, and obtain the QCD sum rules,

$$\int_{\Delta}^{\sqrt{s_0}} dp_0 [A(p_0) + B(p_0)] \exp\left[-\frac{p_0^2}{T^2}\right] = \int_{\Delta}^{\sqrt{s_0}} dp_0 [\rho^A(p_0) + \rho^B(p_0)] \exp\left[-\frac{p_0^2}{T^2}\right], \quad (282)$$

$$\int_{\Delta}^{\sqrt{s_0}} dp_0 [A(p_0) + B(p_0)] p_0^2 \exp\left[-\frac{p_0^2}{T^2}\right] = \int_{\Delta}^{\sqrt{s_0}} dp_0 [\rho^A(p_0) + \rho^B(p_0)] p_0^2 \exp\left[-\frac{p_0^2}{T^2}\right], \quad (283)$$

where the Δ and $\sqrt{s_0}$ are the threshold and continuum threshold respectively [527]. Thereafter, such semi-analytical method was applied to study the heavy, doubly-heavy and triply-heavy baryons with the $J^P = \frac{1}{2}^\pm$ and $\frac{3}{2}^\pm$ [528, 529, 530, 531, 532, 533].

As the procedure introduced in Ref.[527] is semi-analytical, in 2016, we suggested an analytical procedure to study the pentaquark states [359]. For a correlation function $\Pi(p^2) = \Pi_-(p)$, at the hadron side, we obtain the spectral densities through the dispersion relation,

$$\begin{aligned} \frac{\text{Im}\Pi(s)}{\pi} &= \not{p} [\lambda_-^2 \delta(s - M_-^2) + \lambda_+^2 \delta(s - M_+^2)] + [M_- \lambda_-^2 \delta(s - M_-^2) - M_+ \lambda_+^2 \delta(s - M_+^2)], \\ &= \not{p} \rho_H^1(s) + \rho_H^0(s), \end{aligned} \quad (284)$$

where the subscript H denotes the hadron side, then we introduce the weight function $\exp\left(-\frac{s}{T^2}\right)$ to obtain the QCD sum rules at the hadron side,

$$\int_{\Delta^2}^{s_0} ds [\sqrt{s} \rho_H^1(s) + \rho_H^0(s)] \exp\left(-\frac{s}{T^2}\right) = 2M_- \lambda_-^2 \exp\left(-\frac{M_-^2}{T^2}\right), \quad (285)$$

$$\int_{\Delta^2}^{s_0} ds [\sqrt{s} \rho_H^1(s) - \rho_H^0(s)] \exp\left(-\frac{s}{T^2}\right) = 2M_+ \lambda_+^2 \exp\left(-\frac{M_+^2}{T^2}\right), \quad (286)$$

where the s_0 are the continuum threshold parameters and the T^2 are the Borel parameters. We separate the contributions of the negative parity pentaquark states from that of the positive parity pentaquark states unambiguously [359]. The calculations in the QCD side are analytical as we do not set $\vec{p} = 0$.

9.1 $\bar{3}\bar{3}\bar{3}$ type hidden heavy pentaquark states

Now, let us turn to the pentaquark states completely and write down the correlation functions $\Pi(p)$, $\Pi_{\mu\nu}(p)$ and $\Pi_{\mu\nu\alpha\beta}(p)$,

$$\begin{aligned}\Pi(p) &= i \int d^4x e^{ip \cdot x} \langle 0 | T \{ J(x) \bar{J}(0) \} | 0 \rangle, \\ \Pi_{\mu\nu}(p) &= i \int d^4x e^{ip \cdot x} \langle 0 | T \{ J_\mu(x) \bar{J}_\nu(0) \} | 0 \rangle, \\ \Pi_{\mu\nu\alpha\beta}(p) &= i \int d^4x e^{ip \cdot x} \langle 0 | T \{ J_{\mu\nu}(x) \bar{J}_{\alpha\beta}(0) \} | 0 \rangle,\end{aligned}\tag{287}$$

where

$$\begin{aligned}J(x) &= J^1(x), J^2(x), J^3(x), J^4(x), \\ J_\mu(x) &= J_\mu^1(x), J_\mu^2(x), J_\mu^3(x), J_\mu^4(x), \\ J_{\mu\nu}(x) &= J_{\mu\nu}^1(x), J_{\mu\nu}^2(x),\end{aligned}\tag{288}$$

$$\begin{aligned}J^1(x) &= \varepsilon^{ila} \varepsilon^{ijk} \varepsilon^{lmn} u_j^T(x) C \gamma_5 d_k(x) u_m^T(x) C \gamma_5 c_n(x) C \bar{c}_a^T(x), \\ J^2(x) &= \varepsilon^{ila} \varepsilon^{ijk} \varepsilon^{lmn} u_j^T(x) C \gamma_5 d_k(x) u_m^T(x) C \gamma_\mu c_n(x) \gamma_5 \gamma^\mu C \bar{c}_a^T(x), \\ J^3(x) &= \frac{\varepsilon^{ila} \varepsilon^{ijk} \varepsilon^{lmn}}{\sqrt{3}} [u_j^T(x) C \gamma_\mu u_k(x) d_m^T(x) C \gamma_5 c_n(x) + 2u_j^T(x) C \gamma_\mu d_k(x) u_m^T(x) C \gamma_5 c_n(x)] \gamma_5 \gamma^\mu C \bar{c}_a^T(x), \\ J^4(x) &= \frac{\varepsilon^{ila} \varepsilon^{ijk} \varepsilon^{lmn}}{\sqrt{3}} [u_j^T(x) C \gamma_\mu u_k(x) d_m^T(x) C \gamma^\mu c_n(x) + 2u_j^T(x) C \gamma_\mu d_k(x) u_m^T(x) C \gamma^\mu c_n(x)] C \bar{c}_a^T(x), \\ \\ J_\mu^1(x) &= \varepsilon^{ila} \varepsilon^{ijk} \varepsilon^{lmn} u_j^T(x) C \gamma_5 d_k(x) u_m^T(x) C \gamma_\mu c_n(x) C \bar{c}_a^T(x), \\ J_\mu^2(x) &= \frac{\varepsilon^{ila} \varepsilon^{ijk} \varepsilon^{lmn}}{\sqrt{3}} [u_j^T(x) C \gamma_\mu u_k(x) d_m^T(x) C \gamma_5 c_n(x) + 2u_j^T(x) C \gamma_\mu d_k(x) u_m^T(x) C \gamma_5 c_n(x)] C \bar{c}_a^T(x), \\ J_\mu^3(x) &= \frac{\varepsilon^{ila} \varepsilon^{ijk} \varepsilon^{lmn}}{\sqrt{3}} [u_j^T(x) C \gamma_\mu u_k(x) d_m^T(x) C \gamma_\alpha c_n(x) + 2u_j^T(x) C \gamma_\mu d_k(x) u_m^T(x) C \gamma_\alpha c_n(x)] \gamma_5 \gamma^\alpha C \bar{c}_a^T(x), \\ J_\mu^4(x) &= \frac{\varepsilon^{ila} \varepsilon^{ijk} \varepsilon^{lmn}}{\sqrt{3}} [u_j^T(x) C \gamma_\alpha u_k(x) d_m^T(x) C \gamma_\mu c_n(x) + 2u_j^T(x) C \gamma_\alpha d_k(x) u_m^T(x) C \gamma_\mu c_n(x)] \gamma_5 \gamma^\alpha C \bar{c}_a^T(x), \\ \\ J_{\mu\nu}^1(x) &= \frac{\varepsilon^{ila} \varepsilon^{ijk} \varepsilon^{lmn}}{\sqrt{6}} [u_j^T(x) C \gamma_\mu u_k(x) d_m^T(x) C \gamma_\nu c_n(x) + 2u_j^T(x) C \gamma_\mu d_k(x) u_m^T(x) C \gamma_\nu c_n(x)] \\ &\quad C \bar{c}_a^T(x) + (\mu \leftrightarrow \nu), \\ J_{\mu\nu}^2(x) &= \frac{1}{\sqrt{2}} \varepsilon^{ila} \varepsilon^{ijk} \varepsilon^{lmn} u_j^T(x) C \gamma_5 d_k(x) [u_m^T(x) C \gamma_\mu c_n(x) \gamma_5 \gamma_\nu C \bar{c}_a^T(x) \\ &\quad + u_m^T(x) C \gamma_\nu c_n(x) \gamma_5 \gamma_\mu C \bar{c}_a^T(x)],\end{aligned}\tag{289}$$

we choose the $C\gamma_5$ and $C\gamma_\mu$ diquarks in color $\bar{\mathbf{3}}$ as the basic constituents to construct the diquark-diquark-antiquark type currents $J(x)$, $J_\mu(x)$ and $J_{\mu\nu}(x)$ with the spin-parity $J^P = \frac{1}{2}^-, \frac{3}{2}^-$ and $\frac{5}{2}^-$, respectively, which are expected to couple potentially to the lowest pentaquark states [338, 359, 445].

In the currents $J(x)$, $J_\mu(x)$ and $J_{\mu\nu}(x)$, there are diquark constituents $\varepsilon^{ijk} u_j^T C \gamma_5 d_k$, $\varepsilon^{ijk} u_j^T C \gamma_\mu d_k$, $\varepsilon^{ijk} u_j^T C \gamma_\mu u_k$, $\varepsilon^{ijk} q_j^T C \gamma_5 c_k$, $\varepsilon^{ijk} q_j^T C \gamma_\mu c_k$ with $q = u, d$. If we use the S_L and S_H to represent the spins of the light and heavy diquarks respectively, the light diquarks $\varepsilon^{ijk} u_j^T C \gamma_5 d_k$, $\varepsilon^{ijk} u_j^T C \gamma_\mu d_k$

$[qq'][q''\bar{c}]\bar{c} (S_L, S_H, J_{LH}, J)$	J^P	Currents
$[ud][uc]\bar{c} (0, 0, 0, \frac{1}{2})$	$\frac{1}{2}^-$	$J^1(x)$
$[ud][uc]\bar{c} (0, 1, 1, \frac{1}{2})$	$\frac{1}{2}^-$	$J^2(x)$
$[uu][dc]\bar{c} + 2[ud][uc]\bar{c} (1, 0, 1, \frac{1}{2})$	$\frac{1}{2}^-$	$J^3(x)$
$[uu][dc]\bar{c} + 2[ud][uc]\bar{c} (1, 1, 0, \frac{1}{2})$	$\frac{1}{2}^-$	$J^4(x)$
$[ud][uc]\bar{c} (0, 1, 1, \frac{3}{2})$	$\frac{3}{2}^-$	$J_\mu^1(x)$
$[uu][dc]\bar{c} + 2[ud][uc]\bar{c} (1, 0, 1, \frac{3}{2})$	$\frac{3}{2}^-$	$J_\mu^2(x)$
$[uu][dc]\bar{c} + 2[ud][uc]\bar{c} (1, 1, 2, \frac{3}{2})$	$\frac{3}{2}^-$	$J_\mu^3(x)$
$[uu][dc]\bar{c} + 2[ud][uc]\bar{c} (1, 1, 2, \frac{3}{2})$	$\frac{3}{2}^-$	$J_\mu^4(x)$
$[uu][dc]\bar{c} + 2[ud][uc]\bar{c} (1, 1, 2, \frac{5}{2})$	$\frac{5}{2}^-$	$J_{\mu\nu}^1(x)$
$[ud][uc]\bar{c} (0, 1, 1, \frac{5}{2})$	$\frac{5}{2}^-$	$J_{\mu\nu}^2(x)$

Table 49: The quark structures of the currents, where the S_L and S_H denote the spins of the light and heavy diquarks respectively, $\vec{J}_{LH} = \vec{S}_L + \vec{S}_H$, $\vec{J} = \vec{J}_{LH} + \vec{J}_{\bar{c}}$, the $\vec{J}_{\bar{c}}$ is the angular momentum of the \bar{c} -quark.

and $\varepsilon^{ijk}u_j^T C\gamma_\mu u_k$ have the spins $S_L = 0, 1$ and 1 , respectively, the heavy diquarks $\varepsilon^{ijk}q_j^T C\gamma_5 c_k$ and $\varepsilon^{ijk}q_j^T C\gamma_\mu c_k$ have the spins $S_H = 0$ and 1 , respectively. A light diquark and a heavy diquark form a charmed tetraquark in color $\bar{\mathbf{3}}$ with the angular momentum $\vec{J}_{LH} = \vec{S}_L + \vec{S}_H$, which has the values $J_{LH} = 0, 1$ or 2 . The \bar{c} -quark operator $C\bar{c}_a^T$ has the spin-parity $J^P = \frac{1}{2}^-$, the \bar{c} -quark operator $\gamma_5\gamma_\mu C\bar{c}_a^T$ has the spin-parity $J^P = \frac{3}{2}^-$ due to the factor $\gamma_5\gamma_\mu$. The total angular momentums are $\vec{J} = \vec{J}_{LH} + \vec{J}_{\bar{c}}$ with the values $J = \frac{1}{2}, \frac{3}{2}$ or $\frac{5}{2}$, which are shown explicitly in Table 49. In Table 49, we present the quark structures of the currents explicitly. For example, in the current $J_{\mu\nu}^2(x)$, there are a scalar diquark $\varepsilon^{ijk}u_j^T(x)C\gamma_5 d_k(x)$ with the spin-parity $J^P = 0^+$, an axialvector diquark $\varepsilon^{lmn}u_m^T(x)C\gamma_\mu c_n(x)$ with the spin-parity $J^P = 1^+$, and an antiquark $\gamma_5\gamma_\nu C\bar{c}_a^T(x)$ with the spin-parity $J^P = \frac{3}{2}^-$, the total angular momentum is $J = \frac{5}{2}$.

Although the currents $J(x)$, $J_\mu(x)$ and $J_{\mu\nu}(x)$ have negative parity, but they couple potentially to the pentaquark states with positive parity, as multiplying $i\gamma_5$ to the currents $J(x)$, $J_\mu(x)$ and $J_{\mu\nu}(x)$ changes their parity [525, 526, 527, 528, 529, 530, 531, 532, 533].

Now we write down the current-pentaquark couplings explicitly,

$$\begin{aligned}
\langle 0|J(0)|P_{\frac{1}{2}}^-(p)\rangle &= \lambda_{\frac{1}{2}}^- U^-(p, s), \\
\langle 0|J(0)|P_{\frac{1}{2}}^+(p)\rangle &= \lambda_{\frac{1}{2}}^+ i\gamma_5 U^+(p, s),
\end{aligned} \tag{290}$$

$$\begin{aligned}
\langle 0|J_\mu(0)|P_{\frac{3}{2}}^-(p)\rangle &= \lambda_{\frac{3}{2}}^- U_\mu^-(p, s), \\
\langle 0|J_\mu(0)|P_{\frac{3}{2}}^+(p)\rangle &= \lambda_{\frac{3}{2}}^+ i\gamma_5 U_\mu^+(p, s), \\
\langle 0|J_\mu(0)|P_{\frac{1}{2}}^+(p)\rangle &= f_{\frac{1}{2}}^+ p_\mu U^+(p, s), \\
\langle 0|J_\mu(0)|P_{\frac{1}{2}}^-(p)\rangle &= f_{\frac{1}{2}}^- p_\mu i\gamma_5 U^-(p, s),
\end{aligned} \tag{291}$$

$$\begin{aligned}
\langle 0|J_{\mu\nu}(0)|P_{\frac{3}{2}}^-(p)\rangle &= \sqrt{2}\lambda_{\frac{3}{2}}^- U_{\mu\nu}^-(p, s), \\
\langle 0|J_{\mu\nu}(0)|P_{\frac{3}{2}}^+(p)\rangle &= \sqrt{2}\lambda_{\frac{3}{2}}^+ i\gamma_5 U_{\mu\nu}^+(p, s), \\
\langle 0|J_{\mu\nu}(0)|P_{\frac{3}{2}}^+(p)\rangle &= f_{\frac{3}{2}}^+ [p_\mu U_\nu^+(p, s) + p_\nu U_\mu^+(p, s)], \\
\langle 0|J_{\mu\nu}(0)|P_{\frac{3}{2}}^-(p)\rangle &= f_{\frac{3}{2}}^- i\gamma_5 [p_\mu U_\nu^-(p, s) + p_\nu U_\mu^-(p, s)], \\
\langle 0|J_{\mu\nu}(0)|P_{\frac{1}{2}}^-(p)\rangle &= g_{\frac{1}{2}}^- p_\mu p_\nu U^-(p, s), \\
\langle 0|J_{\mu\nu}(0)|P_{\frac{1}{2}}^+(p)\rangle &= g_{\frac{1}{2}}^+ p_\mu p_\nu i\gamma_5 U^+(p, s),
\end{aligned} \tag{292}$$

where the superscripts \pm denote the positive parity and negative parity, respectively, the subscripts $\frac{1}{2}$, $\frac{3}{2}$ and $\frac{5}{2}$ denote the spins of the pentaquark states, the λ , f and g are the pole residues.

The spinors $U^\pm(p, s)$ satisfy the Dirac equations $(\not{p} - M_\pm)U^\pm(p) = 0$, while the spinors $U_\mu^\pm(p, s)$ and $U_{\mu\nu}^\pm(p, s)$ satisfy the Rarita-Schwinger equations $(\not{p} - M_\pm)U_\mu^\pm(p) = 0$ and $(\not{p} - M_\pm)U_{\mu\nu}^\pm(p) = 0$, and relations $\gamma^\mu U_\mu^\pm(p, s) = 0$, $p^\mu U_\mu^\pm(p, s) = 0$, $\gamma^\mu U_{\mu\nu}^\pm(p, s) = 0$, $p^\mu U_{\mu\nu}^\pm(p, s) = 0$, $U_{\nu\mu}^\pm(p, s) = U_{\mu\nu}^\pm(p, s)$, respectively [359].

At the hadron side, we insert a complete set of intermediate pentaquark states with the same quantum numbers as the currents $J(x)$, $i\gamma_5 J(x)$, $J_\mu(x)$, $i\gamma_5 J_\mu(x)$, $J_{\mu\nu}(x)$ and $i\gamma_5 J_{\mu\nu}(x)$ into the correlation functions $\Pi(p)$, $\Pi_{\mu\nu}(p)$ and $\Pi_{\mu\nu\alpha\beta}(p)$ to obtain the hadronic representation, and isolate the lowest states of negative and positive parity hidden-charm pentaquark states [338, 359, 445]:

$$\begin{aligned}
\Pi(p) &= \lambda_{\frac{1}{2}}^{-2} \frac{\not{p} + M_-}{M_-^2 - p^2} + \lambda_{\frac{1}{2}}^{+2} \frac{\not{p} - M_+}{M_+^2 - p^2} + \dots, \\
&= \Pi_{\frac{1}{2}}^1(p^2) \not{p} + \Pi_{\frac{1}{2}}^0(p^2),
\end{aligned} \tag{293}$$

$$\begin{aligned}
\Pi_{\mu\nu}(p) &= \lambda_{\frac{3}{2}}^{-2} \frac{\not{p} + M_-}{M_-^2 - p^2} \left(-g_{\mu\nu} + \frac{\gamma_\mu \gamma_\nu}{3} + \frac{2p_\mu p_\nu}{3p^2} - \frac{p_\mu \gamma_\nu - p_\nu \gamma_\mu}{3\sqrt{p^2}} \right) \\
&\quad + \lambda_{\frac{3}{2}}^{+2} \frac{\not{p} - M_+}{M_+^2 - p^2} \left(-g_{\mu\nu} + \frac{\gamma_\mu \gamma_\nu}{3} + \frac{2p_\mu p_\nu}{3p^2} - \frac{p_\mu \gamma_\nu - p_\nu \gamma_\mu}{3\sqrt{p^2}} \right) \\
&\quad + f_{\frac{1}{2}}^{+2} \frac{\not{p} + M_+}{M_+^2 - p^2} p_\mu p_\nu + f_{\frac{1}{2}}^{-2} \frac{\not{p} - M_-}{M_-^2 - p^2} p_\mu p_\nu + \dots, \\
&= \left[\Pi_{\frac{3}{2}}^1(p^2) \not{p} + \Pi_{\frac{3}{2}}^0(p^2) \right] (-g_{\mu\nu}) + \dots,
\end{aligned} \tag{294}$$

$$\begin{aligned}
\Pi_{\mu\nu\alpha\beta}(p) &= 2\lambda_{\frac{5}{2}}^{-2} \frac{\not{p} + M_-}{M_-^2 - p^2} \left[\frac{\tilde{g}_{\mu\alpha}\tilde{g}_{\nu\beta} + \tilde{g}_{\mu\beta}\tilde{g}_{\nu\alpha}}{2} - \frac{\tilde{g}_{\mu\nu}\tilde{g}_{\alpha\beta}}{5} - \frac{1}{10} \left(\gamma_\mu\gamma_\alpha + \frac{\gamma_\mu p_\alpha - \gamma_\alpha p_\mu}{\sqrt{p^2}} - \frac{p_\mu p_\alpha}{p^2} \right) \tilde{g}_{\nu\beta} \right. \\
&\quad \left. - \frac{1}{10} \left(\gamma_\nu\gamma_\alpha + \frac{\gamma_\nu p_\alpha - \gamma_\alpha p_\nu}{\sqrt{p^2}} - \frac{p_\nu p_\alpha}{p^2} \right) \tilde{g}_{\mu\beta} + \dots \right] \\
&\quad + 2\lambda_{\frac{5}{2}}^{+2} \frac{\not{p} - M_+}{M_+^2 - p^2} \left[\frac{\tilde{g}_{\mu\alpha}\tilde{g}_{\nu\beta} + \tilde{g}_{\mu\beta}\tilde{g}_{\nu\alpha}}{2} - \frac{\tilde{g}_{\mu\nu}\tilde{g}_{\alpha\beta}}{5} - \frac{1}{10} \left(\gamma_\mu\gamma_\alpha + \frac{\gamma_\mu p_\alpha - \gamma_\alpha p_\mu}{\sqrt{p^2}} - \frac{p_\mu p_\alpha}{p^2} \right) \tilde{g}_{\nu\beta} \right. \\
&\quad \left. - \frac{1}{10} \left(\gamma_\nu\gamma_\alpha + \frac{\gamma_\nu p_\alpha - \gamma_\alpha p_\nu}{\sqrt{p^2}} - \frac{p_\nu p_\alpha}{p^2} \right) \tilde{g}_{\mu\beta} + \dots \right] \\
&\quad + f_{\frac{3}{2}}^{+2} \frac{\not{p} + M_+}{M_+^2 - p^2} \left[p_\mu p_\alpha \left(-g_{\nu\beta} + \frac{\gamma_\nu\gamma_\beta}{3} + \frac{2p_\nu p_\beta}{3p^2} - \frac{p_\nu\gamma_\beta - p_\beta\gamma_\nu}{3\sqrt{p^2}} \right) + \dots \right] \\
&\quad + f_{\frac{3}{2}}^{-2} \frac{\not{p} - M_-}{M_-^2 - p^2} \left[p_\mu p_\alpha \left(-g_{\nu\beta} + \frac{\gamma_\nu\gamma_\beta}{3} + \frac{2p_\nu p_\beta}{3p^2} - \frac{p_\nu\gamma_\beta - p_\beta\gamma_\nu}{3\sqrt{p^2}} \right) + \dots \right] \\
&\quad + g_{\frac{1}{2}}^{-2} \frac{\not{p} + M_-}{M_-^2 - p^2} p_\mu p_\nu p_\alpha p_\beta + g_{\frac{1}{2}}^{+2} \frac{\not{p} - M_+}{M_+^2 - p^2} p_\mu p_\nu p_\alpha p_\beta + \dots, \\
&= \left[\Pi_{\frac{5}{2}}^1(p^2) \not{p} + \Pi_{\frac{5}{2}}^0(p^2) \right] (g_{\mu\alpha}g_{\nu\beta} + g_{\mu\beta}g_{\nu\alpha}) + \dots, \tag{295}
\end{aligned}$$

where we have used the summations of the spinors [534],

$$\begin{aligned}
\sum_s U\bar{U} &= (\not{p} + M_\pm), \\
\sum_s U_\mu\bar{U}_\nu &= (\not{p} + M_\pm) \left(-g_{\mu\nu} + \frac{\gamma_\mu\gamma_\nu}{3} + \frac{2p_\mu p_\nu}{3p^2} - \frac{p_\mu\gamma_\nu - p_\nu\gamma_\mu}{3\sqrt{p^2}} \right), \\
\sum_s U_{\mu\nu}\bar{U}_{\alpha\beta} &= (\not{p} + M_\pm) \left\{ \frac{\tilde{g}_{\mu\alpha}\tilde{g}_{\nu\beta} + \tilde{g}_{\mu\beta}\tilde{g}_{\nu\alpha}}{2} - \frac{\tilde{g}_{\mu\nu}\tilde{g}_{\alpha\beta}}{5} - \frac{1}{10} \left(\gamma_\mu\gamma_\alpha + \frac{\gamma_\mu p_\alpha - \gamma_\alpha p_\mu}{\sqrt{p^2}} - \frac{p_\mu p_\alpha}{p^2} \right) \tilde{g}_{\nu\beta} \right. \\
&\quad - \frac{1}{10} \left(\gamma_\nu\gamma_\alpha + \frac{\gamma_\nu p_\alpha - \gamma_\alpha p_\nu}{\sqrt{p^2}} - \frac{p_\nu p_\alpha}{p^2} \right) \tilde{g}_{\mu\beta} - \frac{1}{10} \left(\gamma_\mu\gamma_\beta + \frac{\gamma_\mu p_\beta - \gamma_\beta p_\mu}{\sqrt{p^2}} - \frac{p_\mu p_\beta}{p^2} \right) \tilde{g}_{\nu\alpha} \\
&\quad \left. - \frac{1}{10} \left(\gamma_\nu\gamma_\beta + \frac{\gamma_\nu p_\beta - \gamma_\beta p_\nu}{\sqrt{p^2}} - \frac{p_\nu p_\beta}{p^2} \right) \tilde{g}_{\mu\alpha} \right\}, \tag{296}
\end{aligned}$$

and $p^2 = M_\pm^2$ on mass-shell. We study the components $\Pi_{\frac{1}{2}}^1(p^2)$, $\Pi_{\frac{1}{2}}^0(p^2)$, $\Pi_{\frac{3}{2}}^1(p^2)$, $\Pi_{\frac{3}{2}}^0(p^2)$, $\Pi_{\frac{5}{2}}^1(p^2)$, $\Pi_{\frac{5}{2}}^0(p^2)$ to avoid possible contaminations from other pentaquark states with different spins.

We obtain the spectral densities at the hadron side through dispersion relation,

$$\frac{\text{Im}\Pi_j^1(s)}{\pi} = \lambda_j^{-2} \delta(s - M_-^2) + \lambda_j^{+2} \delta(s - M_+^2) = \rho_{j,H}^1(s), \tag{297}$$

$$\frac{\text{Im}\Pi_j^0(s)}{\pi} = M_- \lambda_j^{-2} \delta(s - M_-^2) - M_+ \lambda_j^{+2} \delta(s - M_+^2) = \rho_{j,H}^0(s), \tag{298}$$

where $j = \frac{1}{2}, \frac{3}{2}, \frac{5}{2}$, the subscript H denotes the hadron side, then we introduce the weight functions $\sqrt{s} \exp(-\frac{s}{T^2})$ and $\exp(-\frac{s}{T^2})$ to obtain the QCD sum rules at the hadron side,

$$\int_{4m^2}^{s_0} ds [\sqrt{s} \rho_{j,H}^1(s) \pm \rho_{j,H}^0(s)] \exp\left(-\frac{s}{T^2}\right) = 2M_\mp \lambda_j^\mp \exp\left(-\frac{M_\mp^2}{T^2}\right), \tag{299}$$

where the s_0 are the continuum threshold parameters, the T^2 are the Borel parameters. We distinguish the contributions of the negative and positive parity pentaquark states unambiguously.

Now we briefly outline the operator product expansion. Firstly, we contract the u , d and c quark fields in the correlation functions $\Pi(p)$, $\Pi_{\mu\nu}(p)$ and $\Pi_{\mu\nu\alpha\beta}(p)$ with Wick theorem, for example,

$$\begin{aligned} \Pi(p) = & i \varepsilon^{ila} \varepsilon^{ijk} \varepsilon^{lmn} \varepsilon^{i'l'a'} \varepsilon^{i'j'k'} \varepsilon^{l'm'n'} \int d^4x e^{ip \cdot x} \\ & \left\{ -Tr \left[\gamma_5 D_{kk'}(x) \gamma_5 C U_{jj'}^T(x) C \right] Tr \left[\gamma_5 C_{nn'}(x) \gamma_5 C U_{mm'}^T(x) C \right] C C_{a'a}^T(-x) C \right. \\ & \left. + Tr \left[\gamma_5 D_{kk'}(x) \gamma_5 C U_{mj'}^T(x) C \gamma_5 C_{nn'}(x) \gamma_5 C U_{jm'}^T(x) C \right] C C_{a'a}^T(-x) C \right\}, \end{aligned} \quad (300)$$

for the current $J(x) = J^1(x)$, where the $U_{ij}(x)$, $D_{ij}(x)$ and $C_{ij}(x)$ are the full u , d and c quark propagators, respectively, see Eqs.(131)-(132). Then we compute all the integrals in the coordinate and momentum spaces sequentially to obtain the $\Pi(p)$, $\Pi_{\mu\nu}(p)$ and $\Pi_{\mu\nu\alpha\beta}(p)$ at the quark level, and finally we obtain the QCD spectral densities through dispersion relation,

$$\begin{aligned} \rho_{j,QCD}^1(s) &= \frac{\text{Im}\Pi_j^1(s)}{\pi}, \\ \rho_{j,QCD}^0(s) &= \frac{\text{Im}\Pi_j^0(s)}{\pi}, \end{aligned} \quad (301)$$

where $j = \frac{1}{2}, \frac{3}{2}, \frac{5}{2}$. In computing the integrals, we draw up all the Feynman diagrams from Eq.(300) and calculate them one by one. In Eq.(300), there are two c -quark propagators and three light quark propagators, if each c -quark line emits a gluon and each light quark line contributes a quark-antiquark pair, we obtain an operator $G_{\mu\nu} G_{\alpha\beta} \bar{u}u\bar{u}u\bar{d}d$, which is of dimension 13, see Fig.21. We should take account of the vacuum condensates at least up to dimension 13 in stead of dimension 10, which is adopted in most literatures. The vacuum condensates $\langle \bar{q}q \rangle^2 \langle \bar{q}g_s \sigma Gq \rangle$, $\langle \bar{q}q \rangle \langle \bar{q}g_s \sigma Gq \rangle^2$, $\langle \bar{q}q \rangle^3 \langle \frac{\alpha_s}{\pi} GG \rangle$ are of dimension 11 and 13 respectively, and come from the Feynman diagrams shown in Fig.21. Those vacuum condensates are associated with the $\frac{1}{T^2}$, $\frac{1}{T^4}$ and $\frac{1}{T^6}$, which manifest themselves at the small T^2 and play an important role in choosing the Borel windows. We take the truncations $n \leq 13$ and $k \leq 1$ in a consistent way, the quark-gluon operators of the orders $\mathcal{O}(\alpha_s^k)$ with $k > 1$ and dimension $n > 13$ are discarded.

In Refs.[359, 535, 536, 537, 538], we take the truncations $n \leq 10$ and $k \leq 1$ and discard the quark-gluon operators of the orders $\mathcal{O}(\alpha_s^k)$ with $k > 1$ and dimension $n > 10$. Sometimes we also neglected the vacuum condensates $\langle \frac{\alpha_s}{\pi} GG \rangle$, $\langle \bar{q}q \rangle \langle \frac{\alpha_s}{\pi} GG \rangle$, $\langle \bar{s}s \rangle \langle \frac{\alpha_s}{\pi} GG \rangle$, $\langle \bar{q}q \rangle^2 \langle \frac{\alpha_s}{\pi} GG \rangle$, $\langle \bar{q}q \rangle \langle \bar{s}s \rangle \langle \frac{\alpha_s}{\pi} GG \rangle$, $\langle \bar{s}s \rangle^2 \langle \frac{\alpha_s}{\pi} GG \rangle$, which are not associated with the $\frac{1}{T^2}$, $\frac{1}{T^4}$ and $\frac{1}{T^6}$ to manifest themselves at the small T^2 . Such an approximation would impair the predictive ability.

Then let us match the hadron side with the QCD side of the correlation functions, take the quark-hadron duality below the continuum thresholds s_0 , and obtain the QCD sum rules:

$$2M_{\mp} \lambda_{\mp}^{\mp 2} \exp\left(-\frac{M_{\mp}^2}{T^2}\right) = \int_{4m_c^2}^{s_0} ds \rho_{QCD,j}(s) \exp\left(-\frac{s}{T^2}\right), \quad (302)$$

where $\rho_{QCD,j}(s) = \sqrt{s} \rho_{QCD,j}^1(s) \pm \rho_{QCD,j}^0(s)$.

We derive Eq.(302) with respect to $\frac{1}{T^2}$, then eliminate the pole residues λ_{\mp}^{\mp} and obtain the QCD sum rules for the masses of the hidden-charm pentaquark states,

$$M_{\mp}^2 = \frac{-\int_{4m_c^2}^{s_0} ds \frac{d}{d(1/T^2)} \rho_{QCD,j}(s) \exp\left(-\frac{s}{T^2}\right)}{\int_{4m_c^2}^{s_0} ds \rho_{QCD,j}(s) \exp\left(-\frac{s}{T^2}\right)}. \quad (303)$$

With a simple replacement $c \rightarrow b$, we obtain the corresponding QCD sum rules for the hidden-bottom pentaquark states.

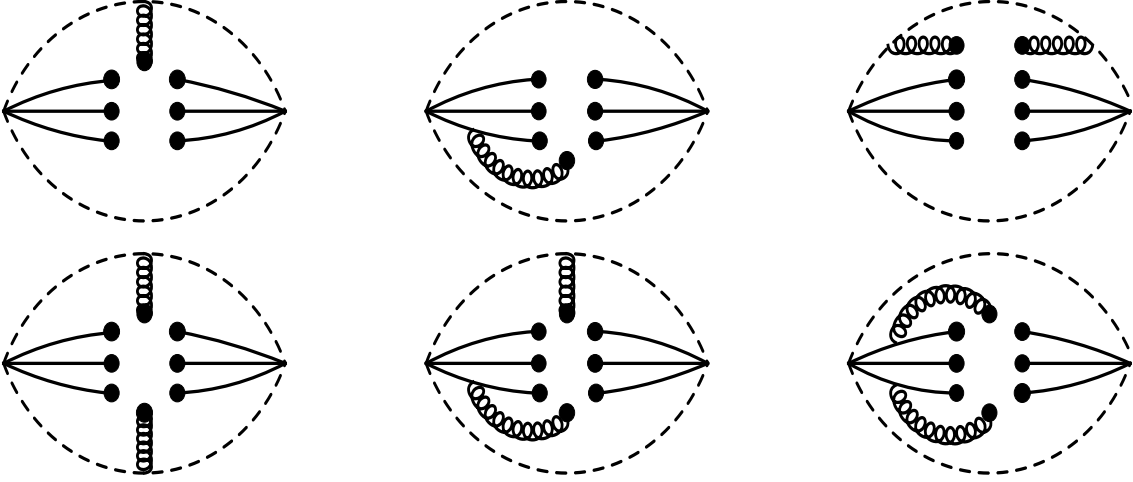


Figure 21: The diagrams contribute to the condensates $\langle \bar{q}q \rangle^2 \langle \bar{q}g_s \sigma Gq \rangle$, $\langle \bar{q}q \rangle \langle \bar{q}g_s \sigma Gq \rangle^2$, $\langle \bar{q}q \rangle^3 \langle \frac{\alpha_s}{\pi} GG \rangle$. Other diagrams obtained by interchanging of the c quark lines (dashed lines) or light quark lines (solid lines) are implied.

According to the discussions in Sect.4, we take the energy scale formula,

$$\mu = \sqrt{M_{X/Y/Z/P}^2 - (2M_Q)^2}, \quad (304)$$

to determine the best energy scales of the QCD spectral densities [338, 359, 535, 536, 537, 538], and choose the updated value of the effective c -quark mass $M_c = 1.82 \text{ GeV}$ [443].

After trial and error, we obtain the Borel windows T^2 , continuum threshold parameters s_0 , ideal energy scales of the QCD spectral densities, pole contributions of the ground states, and contributions of the vacuum condensates of dimension 13, which are shown explicitly in Table 50.

In Fig.22, we plot the contributions of the vacuum condensates of dimension 11 and 13 with variation of the Borel parameter T^2 for the hidden-charm pentaquark state $[ud][uc]\bar{c}$ $(0, 0, 0, \frac{1}{2})$ with the central values of the parameters shown in Table 50 as an example. The vacuum condensates of dimension 13 manifest themselves at the region $T^2 < 2 \text{ GeV}^2$, we should choose the value $T^2 > 2 \text{ GeV}^2$. While the vacuum condensates of dimension 11 manifest themselves at the region $T^2 < 2.6 \text{ GeV}^2$, which requires a larger Borel parameter $T^2 > 2.6 \text{ GeV}^2$ to warrant the convergence of the operator product expansion. The higher dimensional vacuum condensates play an important role in choosing the Borel windows, where they play an minor important role as the operator product expansion should be convergent, we should take them into account in a consistent way, for example, the $|D(13)|$ is less than 1%.

In Fig.23, we plot the mass of the hidden-charm pentaquark state $[ud][uc]\bar{c}$ $(0, 0, 0, \frac{1}{2})$ with variation of the Borel parameter T^2 for truncations of the operator product expansion up to the vacuum condensates of dimension 10 and 13, respectively. The vacuum condensates of dimension 11 and 13 play an important role to obtain stable QCD sum rules, we should take them into account.

In Table 50, the pole contributions are about (40 – 60)% and the contributions of the vacuum condensates of dimension 13 are $\leq 1\%$ or $\ll 1\%$, the pole dominance and convergence of the operator product expansion are all satisfied, **the two basic criteria of the QCD sum rules are satisfied for the first time in the case of the hidden-charm pentaquark states.**

We take into account all uncertainties of the input parameters, and obtain the masses and pole residues of the negative parity hidden-charm pentaquark states, which are shown explicitly in Table 51.

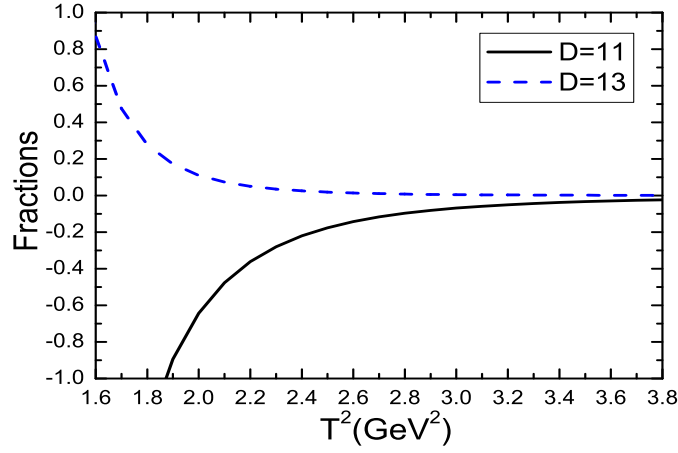


Figure 22: The contributions of the vacuum condensates of dimension 11 and 13 with variation of the Borel parameter T^2 for the hidden-charm pentaquark state $[ud][uc]\bar{c}$ $(0, 0, 0, \frac{1}{2})$.

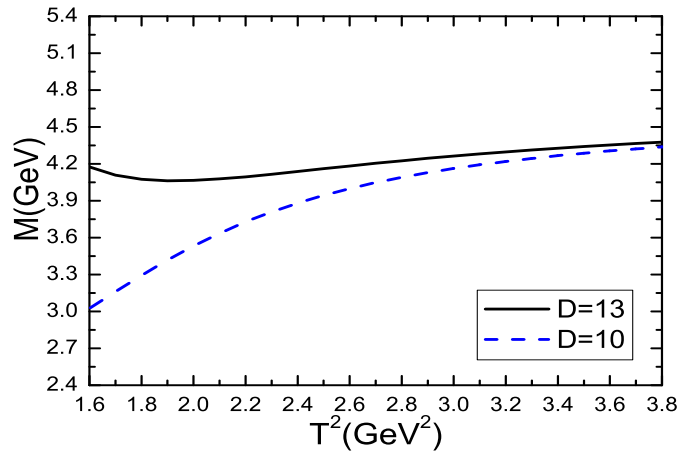


Figure 23: The mass with variation of the Borel parameter T^2 for the hidden-charm pentaquark state $[ud][uc]\bar{c}$ $(0, 0, 0, \frac{1}{2})$, the $D = 10, 13$ denote truncations of the operator product expansion.

	$T^2 \text{GeV}^2$	$\sqrt{s_0}(\text{GeV})$	$\mu(\text{GeV})$	pole	D_{13}
$J^1(x)$	3.1 – 3.5	4.96 ± 0.10	2.3	(41 – 62)%	$< 1\%$
$J^2(x)$	3.2 – 3.6	5.10 ± 0.10	2.6	(42 – 63)%	$< 1\%$
$J^3(x)$	3.2 – 3.6	5.11 ± 0.10	2.6	(42 – 63)%	$\ll 1\%$
$J^4(x)$	2.9 – 3.3	5.00 ± 0.10	2.4	(40 – 64)%	$\leq 1\%$
$J_\mu^1(x)$	3.1 – 3.5	5.03 ± 0.10	2.4	(42 – 63)%	$\leq 1\%$
$J_\mu^2(x)$	3.3 – 3.7	5.11 ± 0.10	2.6	(40 – 61)%	$\ll 1\%$
$J_\mu^3(x)$	3.4 – 3.8	5.26 ± 0.10	2.8	(42 – 62)%	$\ll 1\%$
$J_\mu^4(x)$	3.3 – 3.7	5.17 ± 0.10	2.7	(41 – 61)%	$< 1\%$
$J_{\mu\nu}^1(x)$	3.2 – 3.6	5.03 ± 0.10	2.4	(40 – 61)%	$\leq 1\%$
$J_{\mu\nu}^2(x)$	3.1 – 3.5	5.03 ± 0.10	2.4	(42 – 63)%	$\leq 1\%$

Table 50: The Borel windows, continuum threshold parameters, ideal energy scales, pole contributions, contributions of the vacuum condensates of dimension 13 for the hidden-charm pentaquark states.

The predicted masses $M_P = 4.31 \pm 0.11 \text{ GeV}$ for the ground state $[ud][uc]\bar{c}$ $(0, 0, 0, \frac{1}{2})$ pentaquark state and $M_P = 4.34 \pm 0.14 \text{ GeV}$ for the ground state $[uu][dc]\bar{c} + 2[ud][uc]\bar{c}$ $(1, 1, 0, \frac{1}{2})$ pentaquark state are both in excellent agreement with the experimental data $M_{P(4312)} = 4311.9 \pm 0.7_{-0.6}^{+6.8} \text{ MeV}$ from the LHCb collaboration [190], and support assigning the $P_c(4312)$ to be the hidden-charm pentaquark state with $J^P = \frac{1}{2}^-$.

After the work was published [338], the LHCb collaboration observed an evidence for a structure $P_c(4337)$ in the $J/\psi p$ and $J/\psi \bar{p}$ systems with a significance about $3.1 - 3.7\sigma$ depending on the J^P hypothesis [192], the Breit-Wigner mass and width are $4337_{-4-2}^{+7+2} \text{ MeV}$ and $29_{-12-14}^{+26+14} \text{ MeV}$ respectively. The $P_c(4337)$ can be assigned as the ground state $[uu][dc]\bar{c} + 2[ud][uc]\bar{c}$ $(1, 1, 0, \frac{1}{2})$ pentaquark state with the mass $4.34 \pm 0.14 \text{ GeV}$.

The predicted masses $M_P = 4.45 \pm 0.11 \text{ GeV}$ for the ground state $[ud][uc]\bar{c}$ $(0, 1, 1, \frac{1}{2})$ pentaquark state, $M_P = 4.46 \pm 0.11 \text{ GeV}$ for the ground state $[uu][dc]\bar{c} + 2[ud][uc]\bar{c}$ $(1, 0, 1, \frac{1}{2})$ pentaquark state and $M_P = 4.39 \pm 0.11$ for the ground state $[ud][uc]\bar{c}$ $(0, 1, 1, \frac{3}{2})$, $[uu][dc]\bar{c} + 2[ud][uc]\bar{c}$ $(1, 1, 2, \frac{5}{2})$, $[ud][uc]\bar{c}$ $(0, 1, 1, \frac{5}{2})$ pentaquark states are in excellent agreement (or compatible with) the experimental data $M_{P(4440)} = 4440.3 \pm 1.3_{-4.7}^{+4.1} \text{ MeV}$ from the LHCb collaboration [190], and support assigning the $P_c(4440)$ to be the hidden-charm pentaquark state with $J^P = \frac{1}{2}^-$, $\frac{3}{2}^-$ or $\frac{5}{2}^-$.

The predicted masses $M_P = 4.45 \pm 0.11 \text{ GeV}$ for the ground state $[ud][uc]\bar{c}$ $(0, 1, 1, \frac{1}{2})$ pentaquark state, $M_P = 4.46 \pm 0.11 \text{ GeV}$ for the ground state $[uu][dc]\bar{c} + 2[ud][uc]\bar{c}$ $(1, 0, 1, \frac{1}{2})$ pentaquark state and $M_P = 4.47 \pm 0.11 \text{ GeV}$ for the ground state $[uu][dc]\bar{c} + 2[ud][uc]\bar{c}$ $(1, 0, 1, \frac{3}{2})$ pentaquark states are in excellent agreement the experimental data $M_{P(4457)} = 4457.3 \pm 0.6_{-1.7}^{+4.1} \text{ MeV}$ from the LHCb collaboration [190], and support assigning the $P_c(4457)$ to be the hidden-charm pentaquark state with $J^P = \frac{1}{2}^-$ or $\frac{3}{2}^-$.

In Table 51, we present the possible assignments of the $P_c(4312)$, $P_c(4440)$ and $P_c(4457)$ explicitly as a summary. In Table 52, we compare the present predictions with our previous calculations [359, 535, 536, 537], where the vacuum condensates of dimension 11 and 13 were neglected, sometimes the vacuum condensates $\langle \frac{\alpha_s GG}{\pi} \rangle$, $\langle \bar{q}q \rangle \langle \frac{\alpha_s GG}{\pi} \rangle$ and $\langle \bar{q}q \rangle^2 \langle \frac{\alpha_s GG}{\pi} \rangle$ were also neglected. From the Table 52, we can see that in some cases the predicted masses change remarkably, while in other cases the predicted masses change slightly. In Ref.[359], we construct the current $\gamma_5 J_{\mu\nu}^2(x)$ to interpolate the hidden-charm tetraquark state with the $J^P = \frac{5}{2}^+$, which should be updated.

In Ref.[536], we construct the $J_{q_1 q_2 q_3}^{j_L j_H}(x)$ with the spin-parity $J^P = \frac{1}{2}^-$ to study the hidden-

$[qq'][q''c]\bar{c} (S_L, S_H, J_{LH}, J)$	$M(\text{GeV})$	$\lambda(10^{-3}\text{GeV}^6)$	Assignments	Currents
$[ud][uc]\bar{c} (0, 0, 0, \frac{1}{2})$	4.31 ± 0.11	1.40 ± 0.23	? $P_c(4312)$	$J^1(x)$
$[ud][uc]\bar{c} (0, 1, 1, \frac{1}{2})$	4.45 ± 0.11	3.02 ± 0.48	? $P_c(4440/4457)$	$J^2(x)$
$[uu][dc]\bar{c} + 2[ud][uc]\bar{c} (1, 0, 1, \frac{1}{2})$	4.46 ± 0.11	4.32 ± 0.71	? $P_c(4440/4457)$	$J^3(x)$
$[uu][dc]\bar{c} + 2[ud][uc]\bar{c} (1, 1, 0, \frac{1}{2})$	4.34 ± 0.14	3.23 ± 0.61	? $P_c(4312/\mathbf{4337})$	$J^4(x)$
$[ud][uc]\bar{c} (0, 1, 1, \frac{3}{2})$	4.39 ± 0.11	1.44 ± 0.23	? $P_c(4440)$	$J_\mu^1(x)$
$[uu][dc]\bar{c} + 2[ud][uc]\bar{c} (1, 0, 1, \frac{3}{2})$	4.47 ± 0.11	2.41 ± 0.38	? $P_c(4440/4457)$	$J_\mu^2(x)$
$[uu][dc]\bar{c} + 2[ud][uc]\bar{c} (1, 1, 2, \frac{3}{2})$	4.61 ± 0.11	5.13 ± 0.79		$J_\mu^3(x)$
$[uu][dc]\bar{c} + 2[ud][uc]\bar{c} (1, 1, 2, \frac{3}{2})$	4.52 ± 0.11	4.49 ± 0.72		$J_\mu^4(x)$
$[uu][dc]\bar{c} + 2[ud][uc]\bar{c} (1, 1, 2, \frac{5}{2})$	4.39 ± 0.11	1.94 ± 0.31	? $P_c(4440)$	$J_{\mu\nu}^1(x)$
$[ud][uc]\bar{c} (0, 1, 1, \frac{5}{2})$	4.39 ± 0.11	1.44 ± 0.23	? $P_c(4440)$	$J_{\mu\nu}^2(x)$

Table 51: The masses and pole residues of the hidden-charm pentaquark states.

$[qq'][q''c]\bar{c} (S_L, S_H, J_{LH}, J)$	Ref. [338]	Old calculations	Currents
$[ud][uc]\bar{c} (0, 0, 0, \frac{1}{2})$	4.31 ± 0.11	4.29 ± 0.13	$J^1(x)$
$[ud][uc]\bar{c} (0, 1, 1, \frac{1}{2})$	4.45 ± 0.11	4.30 ± 0.13	$J^2(x)$
$[uu][dc]\bar{c} + 2[ud][uc]\bar{c} (1, 0, 1, \frac{1}{2})$	4.46 ± 0.11	4.42 ± 0.12	$J^3(x)$
$[uu][dc]\bar{c} + 2[ud][uc]\bar{c} (1, 1, 0, \frac{1}{2})$	4.34 ± 0.14	4.35 ± 0.15	$J^4(x)$
$[ud][uc]\bar{c} (0, 1, 1, \frac{3}{2})$	4.39 ± 0.11	4.38 ± 0.13	$J_\mu^1(x)$
$[uu][dc]\bar{c} + 2[ud][uc]\bar{c} (1, 0, 1, \frac{3}{2})$	4.47 ± 0.11	4.39 ± 0.13	$J_\mu^2(x)$
$[uu][dc]\bar{c} + 2[ud][uc]\bar{c} (1, 1, 2, \frac{3}{2})$	4.61 ± 0.11	4.39 ± 0.14	$J_\mu^3(x)$
$[uu][dc]\bar{c} + 2[ud][uc]\bar{c} (1, 1, 2, \frac{3}{2})$	4.52 ± 0.11	4.39 ± 0.14	$J_\mu^4(x)$
$[uu][dc]\bar{c} + 2[ud][uc]\bar{c} (1, 1, 2, \frac{5}{2})$	4.39 ± 0.11		$J_{\mu\nu}^1(x)$
$[ud][uc]\bar{c} (0, 1, 1, \frac{5}{2})$	4.39 ± 0.11		$J_{\mu\nu}^2(x)$

Table 52: The masses (in unit of GeV) are compared with the old calculations [359, 535, 536, 537].

charm pentaquark states with the $J^P = \frac{1}{2}^\pm$ according to the rules,

$$\begin{aligned}
1_{q_1 q_2}^+ \otimes 0_{q_3 c}^+ \otimes \frac{1}{2_{\bar{c}}}^- &= \frac{1}{2_{q_1 q_2 q_3 c \bar{c}}}^- \oplus \frac{3}{2_{q_1 q_2 q_3 c \bar{c}}}^-, \\
1_{q_1 q_2}^+ \otimes 1_{q_3 c}^+ \otimes \frac{1}{2_{\bar{c}}}^- &= [0_{q_1 q_2 q_3 c}^+ \oplus 1_{q_1 q_2 q_3 c}^+ \oplus 2_{q_1 q_2 q_3 c}^+] \otimes \frac{1}{2_{\bar{c}}}^- \\
&= \frac{1}{2_{q_1 q_2 q_3 c \bar{c}}}^- \oplus \left[\frac{1}{2_{q_1 q_2 q_3 c \bar{c}}}^- \oplus \frac{3}{2_{q_1 q_2 q_3 c \bar{c}}}^- \right] \oplus \left[\frac{3}{2_{q_1 q_2 q_3 c \bar{c}}}^- \oplus \frac{5}{2_{q_1 q_2 q_3 c \bar{c}}}^- \right], \\
1_{q_1 q_2}^+ \otimes 0_{q_3 c}^+ \otimes \left[1^- \otimes \frac{1}{2_{\bar{c}}}^- \right] &= 1_{q_1 q_2}^+ \otimes 0_{q_3 c}^+ \otimes \left[\frac{1}{2_{\bar{c}}}^+ \oplus \frac{3}{2_{\bar{c}}}^+ \right] \\
&= \left[\frac{1}{2_{q_1 q_2 q_3 c \bar{c}}}^+ \oplus \frac{3}{2_{q_1 q_2 q_3 c \bar{c}}}^+ \right] \oplus \left[\frac{1}{2_{q_1 q_2 q_3 c \bar{c}}}^+ \oplus \frac{3}{2_{q_1 q_2 q_3 c \bar{c}}}^+ \oplus \frac{5}{2_{q_1 q_2 q_3 c \bar{c}}}^+ \right], \\
1_{q_1 q_2}^+ \otimes 1_{q_3 c}^+ \otimes \left[1^- \otimes \frac{1}{2_{\bar{c}}}^- \right] &= [0_{q_1 q_2 q_3 c}^+ \oplus 1_{q_1 q_2 q_3 c}^+ \oplus 2_{q_1 q_2 q_3 c}^+] \otimes \left[\frac{1}{2_{\bar{c}}}^+ \oplus \frac{3}{2_{\bar{c}}}^+ \right] \\
&= \frac{1}{2_{q_1 q_2 q_3 c \bar{c}}}^+ \oplus \left[\frac{1}{2_{q_1 q_2 q_3 c \bar{c}}}^+ \oplus \frac{3}{2_{q_1 q_2 q_3 c \bar{c}}}^+ \right] \oplus \left[\frac{3}{2_{q_1 q_2 q_3 c \bar{c}}}^+ \oplus \frac{5}{2_{q_1 q_2 q_3 c \bar{c}}}^+ \right] \\
&\quad \oplus \frac{3}{2_{q_1 q_2 q_3 c \bar{c}}}^+ \oplus \left[\frac{1}{2_{q_1 q_2 q_3 c \bar{c}}}^+ \oplus \frac{3}{2_{q_1 q_2 q_3 c \bar{c}}}^+ \oplus \frac{5}{2_{q_1 q_2 q_3 c \bar{c}}}^+ \right] \\
&\quad \oplus \left[\frac{1}{2_{q_1 q_2 q_3 c \bar{c}}}^+ \oplus \frac{3}{2_{q_1 q_2 q_3 c \bar{c}}}^+ \oplus \frac{5}{2_{q_1 q_2 q_3 c \bar{c}}}^+ \oplus \frac{7}{2_{q_1 q_2 q_3 c \bar{c}}}^+ \right], \tag{305}
\end{aligned}$$

where the 1^- denotes the additional P-wave and is embodied by a γ_5 in constructing the currents, the subscripts $q_1 q_2, q_3 c, \dots$ denote the quark constituents. The quark and antiquark have opposite parity, we usually take it for granted that the quarks (antiquarks) have positive (negative) parity, and the \bar{c} -quark has $J^P = \frac{1}{2}^-$.

We write down the currents $J_{q_1 q_2 q_3}^{jLjH}(x)$ explicitly,

$$\begin{aligned}
J_{uuu}^{11}(x) &= \varepsilon^{ila} \varepsilon^{ijk} \varepsilon^{lmn} u_j^T(x) C \gamma_\mu u_k(x) u_m^T(x) C \gamma^\mu c_n(x) C \bar{c}_a^T(x), \\
J_{uud}^{11}(x) &= \frac{\varepsilon^{ila} \varepsilon^{ijk} \varepsilon^{lmn}}{\sqrt{3}} [u_j^T(x) C \gamma_\mu u_k(x) d_m^T(x) C \gamma^\mu c_n(x) + 2u_j^T(x) C \gamma_\mu d_k(x) u_m^T(x) C \gamma^\mu c_n(x)] C \bar{c}_a^T(x), \\
J_{udd}^{11}(x) &= \frac{\varepsilon^{ila} \varepsilon^{ijk} \varepsilon^{lmn}}{\sqrt{3}} [d_j^T(x) C \gamma_\mu d_k(x) u_m^T(x) C \gamma^\mu c_n(x) + 2d_j^T(x) C \gamma_\mu u_k(x) d_m^T(x) C \gamma^\mu c_n(x)] C \bar{c}_a^T(x), \\
J_{ddd}^{11}(x) &= \varepsilon^{ila} \varepsilon^{ijk} \varepsilon^{lmn} d_j^T(x) C \gamma_\mu d_k(x) d_m^T(x) C \gamma^\mu c_n(x) C \bar{c}_a^T(x), \tag{306}
\end{aligned}$$

$$\begin{aligned}
J_{uus}^{11}(x) &= \frac{\varepsilon^{ila} \varepsilon^{ijk} \varepsilon^{lmn}}{\sqrt{3}} [u_j^T(x) C \gamma_\mu u_k(x) s_m^T(x) C \gamma^\mu c_n(x) + 2u_j^T(x) C \gamma_\mu s_k(x) u_m^T(x) C \gamma^\mu c_n(x)] C \bar{c}_a^T(x), \\
J_{uds}^{11}(x) &= \frac{\varepsilon^{ila} \varepsilon^{ijk} \varepsilon^{lmn}}{\sqrt{3}} [u_j^T(x) C \gamma_\mu d_k(x) s_m^T(x) C \gamma^\mu c_n(x) + u_j^T(x) C \gamma_\mu s_k(x) d_m^T(x) C \gamma^\mu c_n(x) \\
&\quad + d_j^T(x) C \gamma_\mu s_k(x) u_m^T(x) C \gamma^\mu c_n(x)] C \bar{c}_a^T(x), \\
J_{dds}^{11}(x) &= \frac{\varepsilon^{ila} \varepsilon^{ijk} \varepsilon^{lmn}}{\sqrt{3}} [d_j^T(x) C \gamma_\mu d_k(x) s_m^T(x) C \gamma^\mu c_n(x) + 2d_j^T(x) C \gamma_\mu s_k(x) d_m^T(x) C \gamma^\mu c_n(x)] C \bar{c}_a^T(x), \tag{307}
\end{aligned}$$

$$\begin{aligned}
J_{uss}^{11}(x) &= \frac{\varepsilon^{ila}\varepsilon^{ijk}\varepsilon^{lmn}}{\sqrt{3}} [s_j^T(x)C\gamma_\mu s_k(x)u_m^T(x)C\gamma^\mu c_n(x) + 2s_j^T(x)C\gamma_\mu u_k(x)s_m^T(x)C\gamma^\mu c_n(x)] C\bar{c}_a^T(x), \\
J_{dss}^{11}(x) &= \frac{\varepsilon^{ila}\varepsilon^{ijk}\varepsilon^{lmn}}{\sqrt{3}} [s_j^T(x)C\gamma_\mu s_k(x)d_m^T(x)C\gamma^\mu c_n(x) + 2s_j^T(x)C\gamma_\mu d_k(x)s_m^T(x)C\gamma^\mu c_n(x)] C\bar{c}_a^T(x),
\end{aligned} \tag{308}$$

$$J_{sss}^{11}(x) = \varepsilon^{ila}\varepsilon^{ijk}\varepsilon^{lmn}s_j^T(x)C\gamma_\mu s_k(x)s_m^T(x)C\gamma^\mu c_n(x)C\bar{c}_a^T(x), \tag{309}$$

$$\begin{aligned}
J_{uuu}^{10}(x) &= \frac{\varepsilon^{ila}\varepsilon^{ijk}\varepsilon^{lmn}}{\sqrt{3}} u_j^T(x)C\gamma_\mu u_k(x)u_m^T(x)C\gamma_5 c_n(x)\gamma_5\gamma^\mu C\bar{c}_a^T(x), \\
J_{uud}^{10}(x) &= \frac{\varepsilon^{ila}\varepsilon^{ijk}\varepsilon^{lmn}}{\sqrt{3}} [u_j^T(x)C\gamma_\mu u_k(x)d_m^T(x)C\gamma_5 c_n(x) + 2u_j^T(x)C\gamma_\mu d_k(x)u_m^T(x)C\gamma_5 c_n(x)] \gamma_5\gamma^\mu C\bar{c}_a^T(x), \\
J_{udd}^{10}(x) &= \frac{\varepsilon^{ila}\varepsilon^{ijk}\varepsilon^{lmn}}{\sqrt{3}} [d_j^T(x)C\gamma_\mu d_k(x)u_m^T(x)C\gamma_5 c_n(x) + 2d_j^T(x)C\gamma_\mu u_k(x)d_m^T(x)C\gamma_5 c_n(x)] \gamma_5\gamma^\mu C\bar{c}_a^T(x), \\
J_{ddd}^{10}(x) &= \frac{\varepsilon^{ila}\varepsilon^{ijk}\varepsilon^{lmn}}{\sqrt{3}} d_j^T(x)C\gamma_\mu d_k(x)d_m^T(x)C\gamma_5 c_n(x)\gamma_5\gamma^\mu C\bar{c}_a^T(x),
\end{aligned} \tag{310}$$

$$\begin{aligned}
J_{uus}^{10}(x) &= \frac{\varepsilon^{ila}\varepsilon^{ijk}\varepsilon^{lmn}}{\sqrt{3}} [u_j^T(x)C\gamma_\mu u_k(x)s_m^T(x)C\gamma_5 c_n(x) + 2u_j^T(x)C\gamma_\mu s_k(x)u_m^T(x)C\gamma_5 c_n(x)] \gamma_5\gamma^\mu C\bar{c}_a^T(x), \\
J_{uds}^{10}(x) &= \frac{\varepsilon^{ila}\varepsilon^{ijk}\varepsilon^{lmn}}{\sqrt{3}} [u_j^T(x)C\gamma_\mu d_k(x)s_m^T(x)C\gamma_5 c_n(x) + u_j^T(x)C\gamma_\mu s_k(x)d_m^T(x)C\gamma_5 c_n(x) \\
&\quad + d_j^T(x)C\gamma_\mu s_k(x)u_m^T(x)C\gamma_5 c_n(x)] \gamma_5\gamma^\mu C\bar{c}_a^T(x), \\
J_{dds}^{10}(x) &= \frac{\varepsilon^{ila}\varepsilon^{ijk}\varepsilon^{lmn}}{\sqrt{3}} [d_j^T(x)C\gamma_\mu d_k(x)s_m^T(x)C\gamma_5 c_n(x) + 2d_j^T(x)C\gamma_\mu s_k(x)d_m^T(x)C\gamma_5 c_n(x)] \gamma_5\gamma^\mu C\bar{c}_a^T(x),
\end{aligned} \tag{311}$$

$$\begin{aligned}
J_{uss}^{10}(x) &= \frac{\varepsilon^{ila}\varepsilon^{ijk}\varepsilon^{lmn}}{\sqrt{3}} [s_j^T(x)C\gamma_\mu s_k(x)u_m^T(x)C\gamma_5 c_n(x) + 2s_j^T(x)C\gamma_\mu u_k(x)s_m^T(x)C\gamma_5 c_n(x)] \gamma_5\gamma^\mu C\bar{c}_a^T(x), \\
J_{dss}^{10}(x) &= \frac{\varepsilon^{ila}\varepsilon^{ijk}\varepsilon^{lmn}}{\sqrt{3}} [s_j^T(x)C\gamma_\mu s_k(x)d_m^T(x)C\gamma_5 c_n(x) + 2s_j^T(x)C\gamma_\mu d_k(x)s_m^T(x)C\gamma_5 c_n(x)] \gamma_5\gamma^\mu C\bar{c}_a^T(x),
\end{aligned} \tag{312}$$

$$J_{sss}^{10}(x) = \frac{\varepsilon^{ila}\varepsilon^{ijk}\varepsilon^{lmn}}{\sqrt{3}} s_j^T(x)C\gamma_\mu s_k(x)s_m^T(x)C\gamma_5 c_n(x)\gamma_5\gamma^\mu C\bar{c}_a^T(x). \tag{313}$$

We take the isospin limit and classify the currents which couple to the pentaquark states with degenerate masses into the following 8 types,

$$\begin{aligned}
&J_{uuu,\mu}^{11}(x), J_{uud,\mu}^{11}(x), J_{udd,\mu}^{11}(x), J_{ddd,\mu}^{11}(x); \\
&J_{uus,\mu}^{11}(x), J_{uds,\mu}^{11}(x), J_{dds,\mu}^{11}(x); \\
&J_{uss,\mu}^{11}(x), J_{dss,\mu}^{11}(x); \\
&J_{sss,\mu}^{11}(x); \\
&J_{uuu,\mu}^{10}(x), J_{uud,\mu}^{10}(x), J_{udd,\mu}^{10}(x), J_{ddd,\mu}^{10}(x); \\
&J_{uus,\mu}^{10}(x), J_{uds,\mu}^{10}(x), J_{dds,\mu}^{10}(x); \\
&J_{uss,\mu}^{10}(x), J_{dss,\mu}^{10}(x); \\
&J_{sss,\mu}^{10}(x),
\end{aligned} \tag{314}$$

	$\mu(\text{GeV})$	$M_P(\text{GeV})$	$\lambda_P(\text{GeV}^6)$	$M_{B_{10}J/\psi(B_8J/\psi)}(\text{GeV})$
$P_{uuu}^{11\frac{1}{2}}\left(\frac{1}{2}^-\right)$	2.5	4.35 ± 0.15	$(3.72 \pm 0.76) \times 10^{-3}$	4.33 (4.04)
$P_{uus}^{11\frac{1}{2}}\left(\frac{1}{2}^-\right)$	2.6	4.47 ± 0.15	$(4.50 \pm 0.85) \times 10^{-3}$	4.48 (4.29)
$P_{uss}^{11\frac{1}{2}}\left(\frac{1}{2}^-\right)$	2.8	4.58 ± 0.14	$(5.43 \pm 0.96) \times 10^{-3}$	4.63 (4.41)
$P_{sss}^{11\frac{1}{2}}\left(\frac{1}{2}^-\right)$	3.0	4.68 ± 0.13	$(6.47 \pm 1.10) \times 10^{-3}$	4.77
$P_{uuu}^{10\frac{1}{2}}\left(\frac{1}{2}^-\right)$	2.5	4.42 ± 0.12	$(4.14 \pm 0.70) \times 10^{-3}$	4.33 (4.04)
$P_{uus}^{10\frac{1}{2}}\left(\frac{1}{2}^-\right)$	2.7	4.51 ± 0.11	$(4.97 \pm 0.79) \times 10^{-3}$	4.48 (4.29)
$P_{uss}^{10\frac{1}{2}}\left(\frac{1}{2}^-\right)$	2.9	4.60 ± 0.11	$(5.87 \pm 0.89) \times 10^{-3}$	4.63 (4.41)
$P_{sss}^{10\frac{1}{2}}\left(\frac{1}{2}^-\right)$	3.0	4.71 ± 0.11	$(6.84 \pm 1.00) \times 10^{-3}$	4.77
$P_{uu\bar{u}}^{11\frac{1}{2}}\left(\frac{1}{2}^+\right)$	2.8	4.56 ± 0.15	$(1.97 \pm 0.40) \times 10^{-3}$	4.33 (4.04)
$P_{uu\bar{s}}^{11\frac{1}{2}}\left(\frac{1}{2}^+\right)$	3.0	4.67 ± 0.14	$(2.42 \pm 0.47) \times 10^{-3}$	4.48 (4.29)
$P_{uss}^{11\frac{1}{2}}\left(\frac{1}{2}^+\right)$	3.1	4.78 ± 0.13	$(2.88 \pm 0.53) \times 10^{-3}$	4.63 (4.41)
$P_{sss}^{11\frac{1}{2}}\left(\frac{1}{2}^+\right)$	3.3	4.89 ± 0.13	$(3.44 \pm 0.61) \times 10^{-3}$	4.77
$P_{uu\bar{u}}^{10\frac{1}{2}}\left(\frac{1}{2}^+\right)$	3.6	5.12 ± 0.08	$(8.01 \pm 0.92) \times 10^{-3}$	4.33 (4.04)
$P_{uu\bar{s}}^{10\frac{1}{2}}\left(\frac{1}{2}^+\right)$	3.7	5.19 ± 0.08	$(8.92 \pm 1.05) \times 10^{-3}$	4.48 (4.29)
$P_{uss}^{10\frac{1}{2}}\left(\frac{1}{2}^+\right)$	3.8	5.26 ± 0.08	$(9.93 \pm 1.21) \times 10^{-3}$	4.63 (4.41)
$P_{sss}^{10\frac{1}{2}}\left(\frac{1}{2}^+\right)$	4.0	5.40 ± 0.08	$(12.17 \pm 1.28) \times 10^{-3}$	4.77

Table 53: The energy scales, masses and pole residues of the pentaquark states, where the B_{10} and B_8 denote the decuplet and octet baryons with the quark constituents $q_1 q_2 q_3$ respectively. We take the isospin limit, the pentaquark states $P_{uu\bar{u}}^{11\frac{1}{2}}\left(\frac{1}{2}^-\right)$, $P_{uud}^{11\frac{1}{2}}\left(\frac{1}{2}^-\right)$, $P_{udd}^{11\frac{1}{2}}\left(\frac{1}{2}^-\right)$ and $P_{ddd}^{11\frac{1}{2}}\left(\frac{1}{2}^-\right)$ have degenerate masses. Other states are implied.

and perform the operator product expansion up to the vacuum condensates of dimension 10 to obtain the QCD sum rules, the parameters and predictions are presented in Table 53.

In Ref.[537], we construct the currents $J_{q_1 q_2 q_3, \mu}^{j_L j_H j}(x)$ to interpolate the $J^P = \frac{3}{2}^\pm$ hidden-charm tetraquark states, where the superscripts j_L and j_H are the spins of the light diquark state and the charm (or heavy) diquark state, respectively, $\vec{j} = \vec{j}_H + \vec{j}_{\bar{c}}$, the $j_{\bar{c}}$ is the spin of the charm (or heavy) antiquark, the subscripts q_1, q_2, q_3 are the light quark constituents u, d or s . We write down the currents $J_{q_1 q_2 q_3, \mu}^{j_L j_H j}(x)$ explicitly,

$$\begin{aligned}
J_{uu\bar{u}, \mu}^{10\frac{1}{2}}(x) &= \frac{\varepsilon^{ila} \varepsilon^{ijk} \varepsilon^{lmn}}{\sqrt{3}} u_j^T(x) C \gamma_\mu u_k(x) u_m^T(x) C \gamma_5 c_n(x) C \bar{c}_a^T(x), \\
J_{uud, \mu}^{10\frac{1}{2}}(x) &= \frac{\varepsilon^{ila} \varepsilon^{ijk} \varepsilon^{lmn}}{\sqrt{3}} [u_j^T(x) C \gamma_\mu u_k(x) d_m^T(x) C \gamma_5 c_n(x) + 2u_j^T(x) C \gamma_\mu d_k(x) u_m^T(x) C \gamma_5 c_n(x)] C \bar{c}_a^T(x), \\
J_{udd, \mu}^{10\frac{1}{2}}(x) &= \frac{\varepsilon^{ila} \varepsilon^{ijk} \varepsilon^{lmn}}{\sqrt{3}} [d_j^T(x) C \gamma_\mu d_k(x) u_m^T(x) C \gamma_5 c_n(x) + 2d_j^T(x) C \gamma_\mu u_k(x) d_m^T(x) C \gamma_5 c_n(x)] C \bar{c}_a^T(x), \\
J_{ddd, \mu}^{10\frac{1}{2}}(x) &= \frac{\varepsilon^{ila} \varepsilon^{ijk} \varepsilon^{lmn}}{\sqrt{3}} d_j^T(x) C \gamma_\mu d_k(x) d_m^T(x) C \gamma_5 c_n(x) C \bar{c}_a^T(x), \tag{315}
\end{aligned}$$

$$\begin{aligned}
J_{uus,\mu}^{10\frac{1}{2}}(x) &= \frac{\varepsilon^{ila}\varepsilon^{ijk}\varepsilon^{lmn}}{\sqrt{3}} [u_j^T(x)C\gamma_\mu u_k(x)s_m^T(x)C\gamma_5 c_n(x) + 2u_j^T(x)C\gamma_\mu s_k(x)u_m^T(x)C\gamma_5 c_n(x)] C\bar{c}_a^T(x), \\
J_{uds,\mu}^{10\frac{1}{2}}(x) &= \frac{\varepsilon^{ila}\varepsilon^{ijk}\varepsilon^{lmn}}{\sqrt{3}} [u_j^T(x)C\gamma_\mu d_k(x)s_m^T(x)C\gamma_5 c_n(x) + u_j^T(x)C\gamma_\mu s_k(x)d_m^T(x)C\gamma_5 c_n(x) \\
&\quad + d_j^T(x)C\gamma_\mu s_k(x)u_m^T(x)C\gamma_5 c_n(x)] C\bar{c}_a^T(x), \\
J_{dds,\mu}^{10\frac{1}{2}}(x) &= \frac{\varepsilon^{ila}\varepsilon^{ijk}\varepsilon^{lmn}}{\sqrt{3}} [d_j^T(x)C\gamma_\mu d_k(x)s_m^T(x)C\gamma_5 c_n(x) + 2d_j^T(x)C\gamma_\mu s_k(x)d_m^T(x)C\gamma_5 c_n(x)] C\bar{c}_a^T(x),
\end{aligned} \tag{316}$$

$$\begin{aligned}
J_{uss,\mu}^{10\frac{1}{2}}(x) &= \frac{\varepsilon^{ila}\varepsilon^{ijk}\varepsilon^{lmn}}{\sqrt{3}} [s_j^T(x)C\gamma_\mu s_k(x)u_m^T(x)C\gamma_5 c_n(x) + 2s_j^T(x)C\gamma_\mu u_k(x)s_m^T(x)C\gamma_5 c_n(x)] C\bar{c}_a^T(x), \\
J_{dss,\mu}^{10\frac{1}{2}}(x) &= \frac{\varepsilon^{ila}\varepsilon^{ijk}\varepsilon^{lmn}}{\sqrt{3}} [s_j^T(x)C\gamma_\mu s_k(x)d_m^T(x)C\gamma_5 c_n(x) + 2s_j^T(x)C\gamma_\mu d_k(x)s_m^T(x)C\gamma_5 c_n(x)] C\bar{c}_a^T(x),
\end{aligned} \tag{317}$$

$$J_{sss,\mu}^{10\frac{1}{2}}(x) = \frac{\varepsilon^{ila}\varepsilon^{ijk}\varepsilon^{lmn}}{\sqrt{3}} s_j^T(x)C\gamma_\mu s_k(x)s_m^T(x)C\gamma_5 c_n(x)C\bar{c}_a^T(x), \tag{318}$$

$$\begin{aligned}
J_{u\bar{u}\bar{u},\mu}^{11\frac{1}{2}}(x) &= \varepsilon^{ila}\varepsilon^{ijk}\varepsilon^{lmn} u_j^T(x)C\gamma_\mu u_k(x)u_m^T(x)C\gamma_\alpha c_n(x)\gamma_5\gamma^\alpha C\bar{c}_a^T(x), \\
J_{u\bar{u}d,\mu}^{11\frac{1}{2}}(x) &= \frac{\varepsilon^{ila}\varepsilon^{ijk}\varepsilon^{lmn}}{\sqrt{3}} [u_j^T(x)C\gamma_\mu u_k(x)d_m^T(x)C\gamma_\alpha c_n(x) + 2u_j^T(x)C\gamma_\mu d_k(x)u_m^T(x)C\gamma_\alpha c_n(x)] \gamma_5\gamma^\alpha C\bar{c}_a^T(x), \\
J_{udd,\mu}^{11\frac{1}{2}}(x) &= \frac{\varepsilon^{ila}\varepsilon^{ijk}\varepsilon^{lmn}}{\sqrt{3}} [d_j^T(x)C\gamma_\mu d_k(x)u_m^T(x)C\gamma_\alpha c_n(x) + 2d_j^T(x)C\gamma_\mu u_k(x)d_m^T(x)C\gamma_\alpha c_n(x)] \gamma_5\gamma^\alpha C\bar{c}_a^T(x), \\
J_{ddd,\mu}^{11\frac{1}{2}}(x) &= \varepsilon^{ila}\varepsilon^{ijk}\varepsilon^{lmn} d_j^T(x)C\gamma_\mu d_k(x)d_m^T(x)C\gamma_\alpha c_n(x)\gamma_5\gamma^\alpha C\bar{c}_a^T(x),
\end{aligned} \tag{319}$$

$$\begin{aligned}
J_{u\bar{u}\bar{s},\mu}^{11\frac{1}{2}}(x) &= \frac{\varepsilon^{ila}\varepsilon^{ijk}\varepsilon^{lmn}}{\sqrt{3}} [u_j^T(x)C\gamma_\mu u_k(x)s_m^T(x)C\gamma_\alpha c_n(x) + 2u_j^T(x)C\gamma_\mu s_k(x)u_m^T(x)C\gamma_\alpha c_n(x)] \gamma_5\gamma^\alpha C\bar{c}_a^T(x), \\
J_{uds,\mu}^{11\frac{1}{2}}(x) &= \frac{\varepsilon^{ila}\varepsilon^{ijk}\varepsilon^{lmn}}{\sqrt{3}} [u_j^T(x)C\gamma_\mu d_k(x)s_m^T(x)C\gamma_\alpha c_n(x) + u_j^T(x)C\gamma_\mu s_k(x)d_m^T(x)C\gamma_\alpha c_n(x) \\
&\quad + d_j^T(x)C\gamma_\mu s_k(x)u_m^T(x)C\gamma_\alpha c_n(x)] \gamma_5\gamma^\alpha C\bar{c}_a^T(x), \\
J_{dds,\mu}^{11\frac{1}{2}}(x) &= \frac{\varepsilon^{ila}\varepsilon^{ijk}\varepsilon^{lmn}}{\sqrt{3}} [d_j^T(x)C\gamma_\mu d_k(x)s_m^T(x)C\gamma_\alpha c_n(x) + 2d_j^T(x)C\gamma_\mu s_k(x)d_m^T(x)C\gamma_\alpha c_n(x)] \gamma_5\gamma^\alpha C\bar{c}_a^T(x),
\end{aligned} \tag{320}$$

$$\begin{aligned}
J_{uss,\mu}^{11\frac{1}{2}}(x) &= \frac{\varepsilon^{ila}\varepsilon^{ijk}\varepsilon^{lmn}}{\sqrt{3}} [s_j^T(x)C\gamma_\mu s_k(x)u_m^T(x)C\gamma_\alpha c_n(x) + 2s_j^T(x)C\gamma_\mu u_k(x)s_m^T(x)C\gamma_\alpha c_n(x)] \gamma_5\gamma^\alpha C\bar{c}_a^T(x), \\
J_{dss,\mu}^{11\frac{1}{2}}(x) &= \frac{\varepsilon^{ila}\varepsilon^{ijk}\varepsilon^{lmn}}{\sqrt{3}} [s_j^T(x)C\gamma_\mu s_k(x)d_m^T(x)C\gamma_\alpha c_n(x) + 2s_j^T(x)C\gamma_\mu d_k(x)s_m^T(x)C\gamma_\alpha c_n(x)] \gamma_5\gamma^\alpha C\bar{c}_a^T(x),
\end{aligned} \tag{321}$$

$$J_{sss,\mu}^{11\frac{1}{2}}(x) = \varepsilon^{ila}\varepsilon^{ijk}\varepsilon^{lmn}s_j^T(x)C\gamma_\mu s_k(x)s_m^T(x)C\gamma_\alpha c_n(x)\gamma_5\gamma^\alpha C\bar{c}_a^T(x), \quad (322)$$

$$\begin{aligned} J_{uuu,\mu}^{11\frac{3}{2}}(x) &= \varepsilon^{ila}\varepsilon^{ijk}\varepsilon^{lmn}u_j^T(x)C\gamma_\alpha u_k(x)u_m^T(x)C\gamma_\mu c_n(x)\gamma_5\gamma^\alpha C\bar{c}_a^T(x), \\ J_{uud,\mu}^{11\frac{3}{2}}(x) &= \frac{\varepsilon^{ila}\varepsilon^{ijk}\varepsilon^{lmn}}{\sqrt{3}} [u_j^T(x)C\gamma_\alpha u_k(x)d_m^T(x)C\gamma_\mu c_n(x) + 2u_j^T(x)C\gamma_\alpha d_k(x)u_m^T(x)C\gamma_\mu c_n(x)] \gamma_5\gamma^\alpha C\bar{c}_a^T(x), \\ J_{udd,\mu}^{11\frac{3}{2}}(x) &= \frac{\varepsilon^{ila}\varepsilon^{ijk}\varepsilon^{lmn}}{\sqrt{3}} [d_j^T(x)C\gamma_\alpha d_k(x)u_m^T(x)C\gamma_\mu c_n(x) + 2d_j^T(x)C\gamma_\alpha u_k(x)d_m^T(x)C\gamma_\mu c_n(x)] \gamma_5\gamma^\alpha C\bar{c}_a^T(x), \\ J_{ddd,\mu}^{11\frac{3}{2}}(x) &= \varepsilon^{ila}\varepsilon^{ijk}\varepsilon^{lmn}d_j^T(x)C\gamma_\alpha d_k(x)d_m^T(x)C\gamma_\mu c_n(x)\gamma_5\gamma^\alpha C\bar{c}_a^T(x), \end{aligned} \quad (323)$$

$$\begin{aligned} J_{uus,\mu}^{11\frac{3}{2}}(x) &= \frac{\varepsilon^{ila}\varepsilon^{ijk}\varepsilon^{lmn}}{\sqrt{3}} [u_j^T(x)C\gamma_\alpha u_k(x)s_m^T(x)C\gamma_\mu c_n(x) + 2u_j^T(x)C\gamma_\alpha s_k(x)u_m^T(x)C\gamma_\mu c_n(x)] \gamma_5\gamma^\alpha C\bar{c}_a^T(x), \\ J_{uds,\mu}^{11\frac{3}{2}}(x) &= \frac{\varepsilon^{ila}\varepsilon^{ijk}\varepsilon^{lmn}}{\sqrt{3}} [u_j^T(x)C\gamma_\alpha d_k(x)s_m^T(x)C\gamma_\mu c_n(x) + u_j^T(x)C\gamma_\alpha s_k(x)d_m^T(x)C\gamma_\mu c_n(x) \\ &\quad + d_j^T(x)C\gamma_\alpha s_k(x)u_m^T(x)C\gamma_\mu c_n(x)] \gamma_5\gamma^\alpha C\bar{c}_a^T(x), \\ J_{dds,\mu}^{11\frac{3}{2}}(x) &= \frac{\varepsilon^{ila}\varepsilon^{ijk}\varepsilon^{lmn}}{\sqrt{3}} [d_j^T(x)C\gamma_\alpha d_k(x)s_m^T(x)C\gamma_\mu c_n(x) + 2d_j^T(x)C\gamma_\alpha s_k(x)d_m^T(x)C\gamma_\mu c_n(x)] \gamma_5\gamma^\alpha C\bar{c}_a^T(x), \end{aligned} \quad (324)$$

$$\begin{aligned} J_{uss,\mu}^{11\frac{3}{2}}(x) &= \frac{\varepsilon^{ila}\varepsilon^{ijk}\varepsilon^{lmn}}{\sqrt{3}} [s_j^T(x)C\gamma_\alpha s_k(x)u_m^T(x)C\gamma_\mu c_n(x) + 2s_j^T(x)C\gamma_\alpha u_k(x)s_m^T(x)C\gamma_\mu c_n(x)] \gamma_5\gamma^\alpha C\bar{c}_a^T(x), \\ J_{dss,\mu}^{11\frac{3}{2}}(x) &= \frac{\varepsilon^{ila}\varepsilon^{ijk}\varepsilon^{lmn}}{\sqrt{3}} [s_j^T(x)C\gamma_\alpha s_k(x)d_m^T(x)C\gamma_\mu c_n(x) + 2s_j^T(x)C\gamma_\alpha d_k(x)s_m^T(x)C\gamma_\mu c_n(x)] \gamma_5\gamma^\alpha C\bar{c}_a^T(x), \end{aligned} \quad (325)$$

$$J_{sss,\mu}^{11\frac{3}{2}}(x) = \varepsilon^{ila}\varepsilon^{ijk}\varepsilon^{lmn}s_j^T(x)C\gamma_\alpha s_k(x)s_m^T(x)C\gamma_\mu c_n(x)\gamma_5\gamma^\alpha C\bar{c}_a^T(x). \quad (326)$$

We take the isospin limit and classify the above thirty currents couple to the hidden-charm

pentaquark states with degenerate masses into the following twelve types,

$$\begin{aligned}
& J_{uu\bar{u},\mu}^{10\frac{1}{2}}(x), J_{uud,\mu}^{10\frac{1}{2}}(x), J_{udd,\mu}^{10\frac{1}{2}}(x), J_{ddd,\mu}^{10\frac{1}{2}}(x); \\
& J_{uus,\mu}^{10\frac{1}{2}}(x), J_{uds,\mu}^{10\frac{1}{2}}(x), J_{dds,\mu}^{10\frac{1}{2}}(x); \\
& J_{uss,\mu}^{10\frac{1}{2}}(x), J_{dss,\mu}^{10\frac{1}{2}}(x); \\
& J_{sss,\mu}^{10\frac{1}{2}}(x); \\
& J_{uu\bar{u},\mu}^{11\frac{1}{2}}(x), J_{uud,\mu}^{11\frac{1}{2}}(x), J_{udd,\mu}^{11\frac{1}{2}}(x), J_{ddd,\mu}^{11\frac{1}{2}}(x); \\
& J_{uus,\mu}^{11\frac{1}{2}}(x), J_{uds,\mu}^{11\frac{1}{2}}(x), J_{dds,\mu}^{11\frac{1}{2}}(x); \\
& J_{uss,\mu}^{11\frac{1}{2}}(x), J_{dss,\mu}^{11\frac{1}{2}}(x); \\
& J_{sss,\mu}^{11\frac{1}{2}}(x); \\
& J_{uu\bar{u},\mu}^{11\frac{3}{2}}(x), J_{uud,\mu}^{11\frac{3}{2}}(x), J_{udd,\mu}^{11\frac{3}{2}}(x), J_{ddd,\mu}^{11\frac{3}{2}}(x); \\
& J_{uus,\mu}^{11\frac{3}{2}}(x), J_{uds,\mu}^{11\frac{3}{2}}(x), J_{dds,\mu}^{11\frac{3}{2}}(x); \\
& J_{uss,\mu}^{11\frac{3}{2}}(x), J_{dss,\mu}^{11\frac{3}{2}}(x); \\
& J_{sss,\mu}^{11\frac{3}{2}}(x),
\end{aligned} \tag{327}$$

and perform the operator product expansion up to the vacuum condensates of dimension 10 to obtain the QCD sum rules, the parameters and predictions are presented in Table 54.

According to Figs.22-23, the vacuum condensates of the dimensions 11 and 13 play an important role, we should update the old calculations, just like in Ref.[338].

In Ref.[445], we extend our previous works [338, 535] to explore the possible assignment of the $P_{cs}(4459)$ as the $[ud][sc]\bar{c}$ $(0, 0, 0, \frac{1}{2})$ pentaquark state with the spin-parity $J^P = \frac{1}{2}^-$. We choose the current $J(x)$ and carry out the operator product expansion up to the vacuum condensates of dimension 13, where

$$J(x) = \varepsilon^{ila} \varepsilon^{ijk} \varepsilon^{lmn} u_j^T(x) C \gamma_5 d_k(x) s_m^T(x) C \gamma_5 c_n(x) C \bar{c}_a^T(x). \tag{328}$$

In calculations, we take the modified energy scale formula $\mu = \sqrt{M_P - (2M_c)^2} - m_s(\mu) = 2.4 \text{ GeV}$ to constraint the QCD spectral densities.

We obtain the Borel window $T^2 = 3.4 - 3.8 \text{ GeV}^2$ via trial and error, the pole contribution is about $(40 - 61)\%$, which is large enough to extract the pentaquark mass reliably. In Fig.24, we plot the contributions of the higher dimensional vacuum condensates with variation of the Borel parameter T^2 . The higher dimensional vacuum condensates manifest themselves at the region $T^2 < 2.5 \text{ GeV}^2$, we should choose the value $T^2 > 2.5 \text{ GeV}^2$. Their values decrease monotonously and quickly with the increase of the Borel parameter, in the Borel window $T^2 = 3.4 - 3.8 \text{ GeV}^2$, the contributions of the higher dimensional vacuum condensates are $D(8) = -(21 - 26)\%$, $D(9) = (6 - 8)\%$, $D(10) = (2 - 3)\%$, $D(11) = -(1 - 2)\%$, $D(13) \ll 1\%$, the convergent behavior is very good.

The higher dimensional vacuum condensates play an important role in obtaining the flat platform, especially those associated with the inverse Borel parameters $\frac{1}{T^2}$, $\frac{1}{T^4}$, $\frac{1}{T^6}$ and $\frac{1}{T^8}$. In Fig.25, we plot the predicted pentaquark mass with variation of the Borel parameter T^2 with the truncations of the operator product expansion up to the vacuum condensates of dimensions $n = 10$ and 13, respectively. From the figure, we can see that the vacuum condensates of dimensions 11 and 13 play an important role to obtain the flat platform, we should take them into account in a consistent way.

	$M_P(\text{GeV})$	$\lambda_P(10^{-3}\text{GeV}^6)$
$P_{uuu}^{10\frac{1}{2}}\left(\frac{3}{2}^{-}\right)$	4.39 ± 0.13	2.25 ± 0.40
$P_{uus}^{10\frac{1}{2}}\left(\frac{3}{2}^{-}\right)$	4.51 ± 0.12	2.75 ± 0.45
$P_{uss}^{10\frac{1}{2}}\left(\frac{3}{2}^{-}\right)$	4.60 ± 0.11	3.19 ± 0.50
$P_{sss}^{10\frac{1}{2}}\left(\frac{3}{2}^{-}\right)$	4.70 ± 0.11	3.78 ± 0.57
$P_{uu\bar{u}}^{11\frac{1}{2}}\left(\frac{3}{2}^{-}\right)$	4.39 ± 0.14	3.75 ± 0.68
$P_{uus}^{11\frac{1}{2}}\left(\frac{3}{2}^{-}\right)$	4.51 ± 0.12	4.64 ± 0.77
$P_{uss}^{11\frac{1}{2}}\left(\frac{3}{2}^{-}\right)$	4.62 ± 0.11	5.60 ± 0.88
$P_{sss}^{11\frac{1}{2}}\left(\frac{3}{2}^{-}\right)$	4.71 ± 0.11	6.47 ± 1.00
$P_{uuu}^{11\frac{3}{2}}\left(\frac{3}{2}^{-}\right)$	4.39 ± 0.14	3.74 ± 0.70
$P_{uus}^{11\frac{3}{2}}\left(\frac{3}{2}^{-}\right)$	4.52 ± 0.12	4.64 ± 0.79
$P_{uss}^{11\frac{3}{2}}\left(\frac{3}{2}^{-}\right)$	4.61 ± 0.12	5.52 ± 0.90
$P_{sss}^{11\frac{3}{2}}\left(\frac{3}{2}^{-}\right)$	4.72 ± 0.11	6.52 ± 1.02
$P_{uuu}^{10\frac{1}{2}}\left(\frac{3}{2}^{+}\right)$	4.51 ± 0.13	0.99 ± 0.19
$P_{uus}^{10\frac{1}{2}}\left(\frac{3}{2}^{+}\right)$	4.60 ± 0.12	1.21 ± 0.22
$P_{uss}^{10\frac{1}{2}}\left(\frac{3}{2}^{+}\right)$	4.72 ± 0.11	1.45 ± 0.25
$P_{sss}^{10\frac{1}{2}}\left(\frac{3}{2}^{+}\right)$	4.81 ± 0.12	1.71 ± 0.29
$P_{uu\bar{u}}^{11\frac{1}{2}}\left(\frac{3}{2}^{+}\right)$	4.91 ± 0.09	5.04 ± 0.68
$P_{uus}^{11\frac{1}{2}}\left(\frac{3}{2}^{+}\right)$	4.99 ± 0.09	5.83 ± 0.82
$P_{uss}^{11\frac{1}{2}}\left(\frac{3}{2}^{+}\right)$	5.08 ± 0.09	6.72 ± 0.98
$P_{sss}^{11\frac{1}{2}}\left(\frac{3}{2}^{+}\right)$	5.18 ± 0.09	7.73 ± 1.10
$P_{uuu}^{11\frac{3}{2}}\left(\frac{3}{2}^{+}\right)$	5.14 ± 0.08	7.86 ± 0.91
$P_{uus}^{11\frac{3}{2}}\left(\frac{3}{2}^{+}\right)$	5.21 ± 0.08	8.79 ± 1.07
$P_{uss}^{11\frac{3}{2}}\left(\frac{3}{2}^{+}\right)$	5.28 ± 0.08	9.91 ± 1.25
$P_{sss}^{11\frac{3}{2}}\left(\frac{3}{2}^{+}\right)$	5.36 ± 0.08	11.20 ± 1.42

Table 54: The masses and pole residues of the hidden-charm pentaquark states with the $J^P = \frac{3}{2}^{\pm}$.

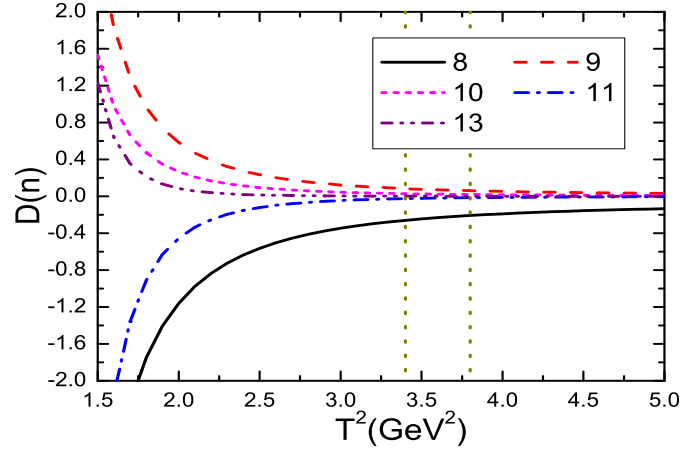


Figure 24: The contributions of the higher dimensional vacuum condensates $D(n)$ with variation of the Borel parameter T^2 , where the $n = 8, 9, 10, 11$ and 13 , the region between the two vertical lines is the Borel window.

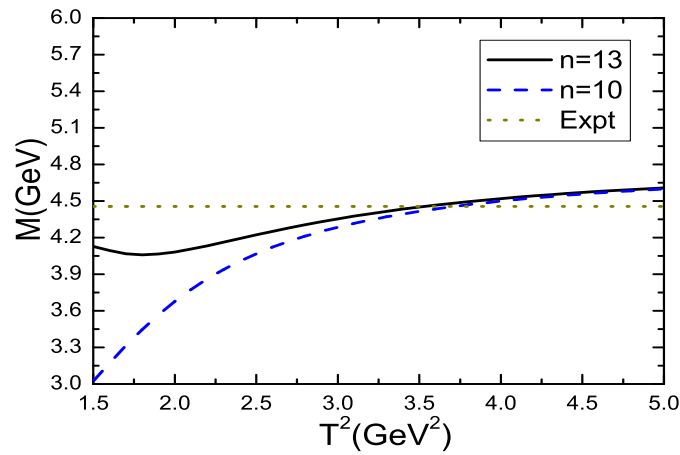


Figure 25: The predicted mass with variation of the Borel parameter T^2 , where the $n = 10$ and 13 denote truncations of the operator product expansion, the expt denotes the experimental value.

$[qq'][q''\bar{c}](S_L, S_H, J_{LH}, J)$	New analysis [338]	u or $d \rightarrow s$	Assignments
$[ud][uc]\bar{c} (0, 0, 0, \frac{1}{2})$	4.31 ± 0.11	4.46 ± 0.11	? $P_{cs}(4459)$
$[ud][uc]\bar{c} (0, 1, 1, \frac{1}{2})$	4.45 ± 0.11	4.60 ± 0.11	
$[uu][dc]\bar{c} + 2[ud][uc]\bar{c} (1, 0, 1, \frac{1}{2})$	4.46 ± 0.11	4.61 ± 0.11	
$[uu][dc]\bar{c} + 2[ud][uc]\bar{c} (1, 1, 0, \frac{1}{2})$	4.34 ± 0.14	4.49 ± 0.14	
$[ud][uc]\bar{c} (0, 1, 1, \frac{3}{2})$	4.39 ± 0.11	4.54 ± 0.11	
$[uu][dc]\bar{c} + 2[ud][uc]\bar{c} (1, 0, 1, \frac{3}{2})$	4.47 ± 0.11	4.62 ± 0.11	
$[uu][dc]\bar{c} + 2[ud][uc]\bar{c} (1, 1, 2, \frac{3}{2})$	4.61 ± 0.11	4.76 ± 0.11	
$[uu][dc]\bar{c} + 2[ud][uc]\bar{c} (1, 1, 2, \frac{5}{2})$	4.52 ± 0.11	4.67 ± 0.11	
$[uu][dc]\bar{c} + 2[ud][uc]\bar{c} (1, 1, 2, \frac{7}{2})$	4.39 ± 0.11	4.54 ± 0.11	
$[ud][uc]\bar{c} (0, 1, 1, \frac{5}{2})$	4.39 ± 0.11	4.54 ± 0.11	

Table 55: The masses (in unit of GeV) of the pentaquark states with the strangeness $S = -1$, where the S_L and S_H denote the spins of the light diquarks and heavy diquarks respectively, $\vec{J}_{LH} = \vec{S}_L + \vec{S}_H$, $\vec{J} = \vec{J}_{LH} + \vec{J}_{\bar{c}}$, the $\vec{J}_{\bar{c}}$ is the angular momentum of the \bar{c} -quark.

At last, we obtain the mass and pole residue,

$$\begin{aligned}
M_P &= 4.47 \pm 0.11 \text{ GeV}, \\
\lambda_P &= (1.86 \pm 0.31) \times 10^{-3} \text{ GeV}^6.
\end{aligned} \tag{329}$$

The predicted mass $M_P = 4.47 \pm 0.11$ GeV is in excellent agreement with the experimental data $4458.8 \pm 2.9_{-1.1}^{+4.7}$ MeV from the LHCb collaboration [191], and supports assigning the $P_{cs}(4459)$ as the $[ud][sc]\bar{c} (0, 0, 0, \frac{1}{2})$ pentaquark state with the spin-parity $J^P = \frac{1}{2}^-$. In Ref.[338], we observe that the $P_c(4312)$ can be assigned to be the $[ud][uc]\bar{c} (0, 0, 0, \frac{1}{2})$ pentaquark state with the spin-parity $J^P = \frac{1}{2}^-$. The flavor $SU(3)$ mass-breaking effect is about $\Delta = m_s = 147$ MeV, the estimations presented in Table 55 are reasonable and reliable. In Refs.[536, 537], we study the $J^P = \frac{1}{2}^\pm$ and $\frac{3}{2}^\pm$ hidden-charm pentaquark states with the strangeness $S = 0, -1, -2$ and -3 in a systematic way by carrying out the operator product expansion up to the vacuum condensates of dimension 10 and choosing the old value $M_c = 1.80$ GeV, and observe that the flavor $SU(3)$ mass-breaking effects are $\Delta = (90 - 130)$ MeV for the negative-parity pentaquark states. The new analysis supports a larger flavor $SU(3)$ mass-breaking effect.

9.2 11 type hidden heavy pentaquark states

In Ref.[539], Chen et al construct the color singlet-singlet type currents,

$$\begin{aligned}
J_\mu^{\bar{D}^* \Sigma_c}(x) &= \bar{c}(x) \gamma_\mu d(x) \varepsilon^{ijk} u_i^T(x) C \gamma_\nu u_j(x) \gamma^\nu \gamma_5 c_k(x), \\
J_\mu^{\bar{D} \Sigma_c^*}(x) &= \bar{c}(x) \gamma_5 d(x) \varepsilon^{ijk} u_i^T(x) C \gamma_\mu u_j(x) c_k(x),
\end{aligned} \tag{330}$$

$$\begin{aligned}
J_{\mu\nu}^{\bar{D}^* \Sigma_c^*}(x) &= \bar{c}(x) \gamma_\mu d(x) \varepsilon^{ijk} u_i^T(x) C \gamma_\nu u_j(x) \gamma_5 c_k(x) + (\mu \leftrightarrow \nu), \\
J_{\mu\nu}^{\bar{D} \Sigma_c^*}(x) &= \bar{c}(x) \gamma_\mu \gamma_5 d(x) \varepsilon^{ijk} u_i^T(x) C \gamma_\nu u_j(x) c_k(x) + (\mu \leftrightarrow \nu), \\
J_{\mu\nu}^{\bar{D}^* \Lambda_c}(x) &= \bar{c}(x) \gamma_\mu u(x) \varepsilon^{ijk} u_i^T(x) C \gamma_\nu \gamma_5 d_j(x) c(x) + (\mu \leftrightarrow \nu),
\end{aligned} \tag{331}$$

for the first time, and take the currents $J_\mu^{\bar{D}^* \Sigma_c}(x)$ and $J_{\mu\nu}^{\bar{D} \Sigma_c^*}(x)$ to study the $P_c(4380)$ and $P_c(4450)$ by carrying out the operator product expansion up to the vacuum condensates of dimension 8. Thereafter, the color singlet-singlet type currents were used to interpolate the pentaquark molecular states [353, 422, 540, 541, 542, 543, 544, 545, 546]. However, in those works, the isospins of the

currents are not specified and should be improved, as the two-body strong decays to the final states $J/\psi p$ and $J/\psi \Lambda$ conserve Isospins.

The u and d quarks have the isospin $I = \frac{1}{2}$, i.e. $\widehat{I}u = \frac{1}{2}u$ and $\widehat{I}d = -\frac{1}{2}d$, where the \widehat{I} is the isospin operator. Then the $\bar{D}^0, \bar{D}^{*0}, \bar{D}^-, \bar{D}^{*-}, \bar{D}_s^-, \bar{D}_s^{*-}, \Sigma_c^+, \Sigma_c^{*+}, \Sigma_c^{++}, \Sigma_c^{*++}, \Xi_c^{\prime 0}, \Xi_c^{\prime *0}, \Xi_c^{\prime +}, \Xi_c^{\prime *+}, \Xi_c^0, \Xi_c^+$ and Λ_c^+ correspond to the eigenstates $|\frac{1}{2}, \frac{1}{2}\rangle, |\frac{1}{2}, \frac{1}{2}\rangle, |\frac{1}{2}, -\frac{1}{2}\rangle, |\frac{1}{2}, -\frac{1}{2}\rangle, |0, 0\rangle, |0, 0\rangle, |1, 0\rangle, |1, 0\rangle, |1, 1\rangle, |1, 1\rangle, |\frac{1}{2}, -\frac{1}{2}\rangle, |\frac{1}{2}, -\frac{1}{2}\rangle, |\frac{1}{2}, \frac{1}{2}\rangle, |\frac{1}{2}, \frac{1}{2}\rangle, |\frac{1}{2}, -\frac{1}{2}\rangle, |\frac{1}{2}, \frac{1}{2}\rangle$ and $|0, 0\rangle$ in the isospin space $|I, I_3\rangle$, respectively. We construct the color-singlet currents to interpolate them,

$$\begin{aligned}
J^{\bar{D}^0}(x) &= \bar{c}(x)i\gamma_5 u(x), \\
J^{\bar{D}^-}(x) &= \bar{c}(x)i\gamma_5 d(x), \\
J_{\bar{D}_s^-}(x) &= \bar{c}(x)i\gamma_5 s(x), \\
J_\mu^{\bar{D}^{*0}}(x) &= \bar{c}(x)\gamma_\mu u(x), \\
J_\mu^{\bar{D}^{*-}}(x) &= \bar{c}(x)\gamma_\mu d(x), \\
J_{\bar{D}_s^{*-}}(x) &= \bar{c}(x)\gamma_\mu s(x),
\end{aligned} \tag{332}$$

$$\begin{aligned}
J^{\Sigma_c^+}(x) &= \varepsilon^{ijk} u_i^T(x) C \gamma_\mu d_j(x) \gamma^\mu \gamma_5 c_k(x), \\
J^{\Sigma_c^{*+}}(x) &= \varepsilon^{ijk} u_i^T(x) C \gamma_\mu u_j(x) \gamma^\mu \gamma_5 c_k(x), \\
J_\mu^{\Sigma_c^{*+}}(x) &= \varepsilon^{ijk} u_i^T(x) C \gamma_\mu d_j(x) c_k(x), \\
J_\mu^{\Sigma_c^{*++}}(x) &= \varepsilon^{ijk} u_i^T(x) C \gamma_\mu u_j(x) c_k(x),
\end{aligned} \tag{333}$$

$$\begin{aligned}
J^{\Xi_c^{\prime 0}}(x) &= \varepsilon^{ijk} d_i^T(x) C \gamma_\mu s_j(x) \gamma^\mu \gamma_5 c_k(x), \\
J_\mu^{\Xi_c^{\prime *0}}(x) &= \varepsilon^{ijk} d_i^T(x) C \gamma_\mu s_j(x) c_k(x), \\
J^{\Xi_c^{\prime +}}(x) &= \varepsilon^{ijk} u_i^T(x) C \gamma_\mu s_j(x) \gamma^\mu \gamma_5 c_k(x), \\
J_\mu^{\Xi_c^{\prime *+}}(x) &= \varepsilon^{ijk} u_i^T(x) C \gamma_\mu s_j(x) c_k(x),
\end{aligned} \tag{334}$$

$$\begin{aligned}
J_{\Xi_c^0}(x) &= \varepsilon^{ijk} d_i^T(x) C \gamma_5 s_j(x) c_k(x), \\
J_{\Xi_c^+}(x) &= \varepsilon^{ijk} u_i^T(x) C \gamma_5 s_j(x) c_k(x), \\
J_{\Lambda_c^+}(x) &= \varepsilon^{ijk} u_i^T(x) C \gamma_5 d_j(x) c_k(x).
\end{aligned} \tag{335}$$

Accordingly, we construct the color singlet-singlet type five-quark currents to interpolate the $\bar{D}^{(*)}\Sigma_c^{(*)}, \bar{D}^{(*)}\Xi_c^{(*)}, \bar{D}^{(*)}\Xi_c^{\prime}$ and $\bar{D}^{(*)}\Lambda_c$ type pentaquark states, where the $\bar{D}^{(*)}, \Sigma_c^{(*)}, \Xi_c^{(*)}, \Xi_c^{\prime}$ and Λ_c represent the color-singlet clusters having the same quantum numbers as the physical states $\bar{D}^{(*)}, \Sigma_c^{(*)}, \Xi_c^{(*)}, \Xi_c^{\prime}$ and Λ_c respectively except for the masses,

$$\begin{aligned}
J(x) &= J_{\frac{1}{2}}^{\bar{D}^{\Sigma_c}}(x), J_{\frac{3}{2}}^{\bar{D}^{\Sigma_c}}(x), J_0^{\bar{D}^{\Xi_c^{\prime}}}(x), J_1^{\bar{D}^{\Xi_c^{\prime}}}(x), \\
&J_0^{\bar{D}^{\Xi_c^{\prime}}}(x), J_1^{\bar{D}^{\Xi_c^{\prime}}}(x), J_{\frac{1}{2}}^{\bar{D}^{\Lambda_c}}(x), J_{\frac{3}{2}}^{\bar{D}^{\Xi_c^{\prime}}}(x), J_0^{\bar{D}^{\Lambda_c}}(x), \\
J_\mu(x) &= J_{\frac{1}{2};\mu}^{\bar{D}^{\Sigma_c^*}}(x), J_{\frac{3}{2};\mu}^{\bar{D}^{\Sigma_c^*}}(x), J_{\frac{1}{2};\mu}^{\bar{D}^{\Sigma_c}}(x), J_{\frac{3}{2};\mu}^{\bar{D}^{\Sigma_c}}(x), \\
&J_{0;\mu}^{\bar{D}^{\Xi_c^{\prime *}}}(x), J_{1;\mu}^{\bar{D}^{\Xi_c^{\prime *}}}(x), J_{0;\mu}^{\bar{D}^{\Xi_c^{\prime}}}(x), J_{1;\mu}^{\bar{D}^{\Xi_c^{\prime}}}(x), \\
&J_{0;\mu}^{\bar{D}^{\Xi_c^{\prime}}}(x), J_{1;\mu}^{\bar{D}^{\Xi_c^{\prime}}}(x), J_{\frac{1}{2};\mu}^{\bar{D}^{\Lambda_c}}(x), J_{\frac{3}{2};\mu}^{\bar{D}^{\Xi_c^{\prime}}}(x), J_{0;\mu}^{\bar{D}^{\Lambda_c}}(x), \\
J_{\mu\nu}(x) &= J_{\frac{1}{2};\mu\nu}^{\bar{D}^{\Sigma_c^*}}(x), J_{\frac{3}{2};\mu\nu}^{\bar{D}^{\Sigma_c^*}}(x), J_{0;\mu\nu}^{\bar{D}^{\Xi_c^{\prime *}}}(x), J_{1;\mu\nu}^{\bar{D}^{\Xi_c^{\prime *}}}(x),
\end{aligned} \tag{336}$$

$$\begin{aligned}
J_{\frac{1}{2}}^{\bar{D}\Sigma_c}(x) &= \frac{1}{\sqrt{3}}J^{\bar{D}^0}(x)J^{\Sigma_c^+}(x) - \sqrt{\frac{2}{3}}J^{\bar{D}^-}(x)J^{\Sigma_c^{++}}(x), \\
J_{\frac{3}{2}}^{\bar{D}\Sigma_c}(x) &= \sqrt{\frac{2}{3}}J^{\bar{D}^0}(x)J^{\Sigma_c^+}(x) + \frac{1}{\sqrt{3}}J^{\bar{D}^-}(x)J^{\Sigma_c^{++}}(x), \\
J_{\frac{1}{2};\mu}^{\bar{D}\Sigma_c^*}(x) &= \frac{1}{\sqrt{3}}J^{\bar{D}^0}(x)J_{\mu}^{\Sigma_c^{*+}}(x) - \sqrt{\frac{2}{3}}J^{\bar{D}^-}(x)J_{\mu}^{\Sigma_c^{*++}}(x), \\
J_{\frac{3}{2};\mu}^{\bar{D}\Sigma_c^*}(x) &= \sqrt{\frac{2}{3}}J^{\bar{D}^0}(x)J_{\mu}^{\Sigma_c^{*+}}(x) + \frac{1}{\sqrt{3}}J^{\bar{D}^-}(x)J_{\mu}^{\Sigma_c^{*++}}(x), \tag{337}
\end{aligned}$$

$$\begin{aligned}
J_{\frac{1}{2};\mu}^{\bar{D}^*\Sigma_c}(x) &= \frac{1}{\sqrt{3}}J_{\mu}^{\bar{D}^{*0}}(x)J^{\Sigma_c^+}(x) - \sqrt{\frac{2}{3}}J_{\mu}^{\bar{D}^{*-}}(x)J^{\Sigma_c^{++}}(x), \\
J_{\frac{3}{2};\mu}^{\bar{D}^*\Sigma_c}(x) &= \sqrt{\frac{2}{3}}J_{\mu}^{\bar{D}^{*0}}(x)J^{\Sigma_c^+}(x) + \frac{1}{\sqrt{3}}J_{\mu}^{\bar{D}^{*-}}(x)J^{\Sigma_c^{++}}(x), \\
J_{\frac{1}{2};\mu\nu}^{\bar{D}^*\Sigma_c^*}(x) &= \frac{1}{\sqrt{3}}J_{\mu}^{\bar{D}^{*0}}(x)J_{\nu}^{\Sigma_c^{*+}}(x) - \sqrt{\frac{2}{3}}J_{\mu}^{\bar{D}^{*-}}(x)J_{\nu}^{\Sigma_c^{*++}}(x) + (\mu \leftrightarrow \nu), \\
J_{\frac{3}{2};\mu\nu}^{\bar{D}^*\Sigma_c^*}(x) &= \sqrt{\frac{2}{3}}J_{\mu}^{\bar{D}^{*0}}(x)J_{\nu}^{\Sigma_c^{*+}}(x) + \frac{1}{\sqrt{3}}J_{\mu}^{\bar{D}^{*-}}(x)J_{\nu}^{\Sigma_c^{*++}}(x) + (\mu \leftrightarrow \nu), \tag{338}
\end{aligned}$$

$$\begin{aligned}
J_0^{\bar{D}\Xi'_c}(x) &= \frac{1}{\sqrt{2}}J^{\bar{D}^0}(x)J^{\Xi'_c{}^0}(x) - \frac{1}{\sqrt{2}}J^{\bar{D}^-}(x)J^{\Xi'_c{}^+}(x), \\
J_1^{\bar{D}\Xi'_c}(x) &= \frac{1}{\sqrt{2}}J^{\bar{D}^0}(x)J^{\Xi'_c{}^0}(x) + \frac{1}{\sqrt{2}}J^{\bar{D}^-}(x)J^{\Xi'_c{}^+}(x), \\
J_{0;\mu}^{\bar{D}\Xi'_c}(x) &= \frac{1}{\sqrt{2}}J^{\bar{D}^0}(x)J_{\mu}^{\Xi'_c{}^0}(x) - \frac{1}{\sqrt{2}}J^{\bar{D}^-}(x)J_{\mu}^{\Xi'_c{}^+}(x), \\
J_{1;\mu}^{\bar{D}\Xi'_c}(x) &= \frac{1}{\sqrt{2}}J^{\bar{D}^0}(x)J_{\mu}^{\Xi'_c{}^0}(x) + \frac{1}{\sqrt{2}}J^{\bar{D}^-}(x)J_{\mu}^{\Xi'_c{}^+}(x), \tag{339}
\end{aligned}$$

$$\begin{aligned}
J_{0;\mu}^{\bar{D}^*\Xi'_c}(x) &= \frac{1}{\sqrt{2}}J_{\mu}^{\bar{D}^{*0}}(x)J^{\Xi'_c{}^0}(x) - \frac{1}{\sqrt{2}}J_{\mu}^{\bar{D}^{*-}}(x)J^{\Xi'_c{}^+}(x), \\
J_{1;\mu}^{\bar{D}^*\Xi'_c}(x) &= \frac{1}{\sqrt{2}}J_{\mu}^{\bar{D}^{*0}}(x)J^{\Xi'_c{}^0}(x) + \frac{1}{\sqrt{2}}J_{\mu}^{\bar{D}^{*-}}(x)J^{\Xi'_c{}^+}(x), \\
J_{0;\mu\nu}^{\bar{D}^*\Xi'_c}(x) &= \frac{1}{\sqrt{2}}J_{\mu}^{\bar{D}^{*0}}(x)J_{\nu}^{\Xi'_c{}^0}(x) - \frac{1}{\sqrt{2}}J_{\mu}^{\bar{D}^{*-}}(x)J_{\nu}^{\Xi'_c{}^+}(x) + (\mu \leftrightarrow \nu), \\
J_{1;\mu\nu}^{\bar{D}^*\Xi'_c}(x) &= \frac{1}{\sqrt{2}}J_{\mu}^{\bar{D}^{*0}}(x)J_{\nu}^{\Xi'_c{}^0}(x) + \frac{1}{\sqrt{2}}J_{\mu}^{\bar{D}^{*-}}(x)J_{\nu}^{\Xi'_c{}^+}(x) + (\mu \leftrightarrow \nu), \tag{340}
\end{aligned}$$

$$\begin{aligned}
J_0^{\bar{D}\Xi_c}(x) &= \frac{1}{\sqrt{2}}J^{\bar{D}^0}(x)J^{\Xi_c{}^0}(x) - \frac{1}{\sqrt{2}}J^{\bar{D}^-}(x)J^{\Xi_c{}^+}(x), \\
J_1^{\bar{D}\Xi_c}(x) &= \frac{1}{\sqrt{2}}J^{\bar{D}^0}(x)J^{\Xi_c{}^0}(x) + \frac{1}{\sqrt{2}}J^{\bar{D}^-}(x)J^{\Xi_c{}^+}(x), \\
J_{\frac{1}{2}}^{\bar{D}\Lambda_c}(x) &= J^{\bar{D}^0}(x)J^{\Lambda_c^+}(x), \\
J_{\frac{1}{2}}^{\bar{D}_s\Xi_c}(x) &= J^{\bar{D}_s^-}(x)J^{\Xi_c^+}(x), \\
J_0^{\bar{D}_s\Lambda_c}(x) &= J^{\bar{D}_s^-}(x)J^{\Lambda_c^+}(x), \tag{341}
\end{aligned}$$

$$\begin{aligned}
J_{0;\mu}^{\bar{D}^* \Xi_c}(x) &= \frac{1}{\sqrt{2}} J_{\mu}^{\bar{D}^{*0}}(x) J^{\Xi_c^0}(x) - \frac{1}{\sqrt{2}} J_{\mu}^{\bar{D}^{*-}}(x) J^{\Xi_c^+}(x), \\
J_{1;\mu}^{\bar{D}^* \Xi_c}(x) &= \frac{1}{\sqrt{2}} J_{\mu}^{\bar{D}^{*0}}(x) J^{\Xi_c^0}(x) + \frac{1}{\sqrt{2}} J_{\mu}^{\bar{D}^{*-}}(x) J^{\Xi_c^+}(x), \\
J_{\frac{1}{2};\mu}^{\bar{D}^* \Lambda_c}(x) &= J_{\mu}^{\bar{D}^{*0}}(x) J^{\Lambda_c^+}(x), \\
J_{\frac{1}{2};\mu}^{\bar{D}_s^* \Xi_c}(x) &= J_{\mu}^{\bar{D}_s^{*-}}(x) J^{\Xi_c^+}(x), \\
J_{0;\mu}^{\bar{D}_s^* \Lambda_c}(x) &= J_{\mu}^{\bar{D}_s^{*-}}(x) J^{\Lambda_c^+}(x),
\end{aligned} \tag{342}$$

the subscripts $\frac{1}{2}$, $\frac{3}{2}$, 0 and 1 represent the isospins I [353, 547, 548, 549]. They are the isospin eigenstates $|I, I_3\rangle = |\frac{1}{2}, \frac{1}{2}\rangle, |\frac{3}{2}, \frac{1}{2}\rangle, |1, 0\rangle$ or $|0, 0\rangle$.

For example, from Eq.(337), we obtain the relations,

$$\begin{aligned}
J^{\bar{D}^0}(x) J^{\Sigma_c^+}(x) &= \frac{1}{\sqrt{3}} J_{\frac{1}{2}}^{\bar{D}^{\Sigma_c}}(x) + \sqrt{\frac{2}{3}} J_{\frac{3}{2}}^{\bar{D}^{\Sigma_c}}(x), \\
J^{\bar{D}^-}(x) J^{\Sigma_c^{++}}(x) &= \frac{1}{\sqrt{3}} J_{\frac{3}{2}}^{\bar{D}^{\Sigma_c}}(x) - \sqrt{\frac{2}{3}} J_{\frac{1}{2}}^{\bar{D}^{\Sigma_c}}(x),
\end{aligned} \tag{343}$$

the currents $J^{\bar{D}^0}(x) J^{\Sigma_c^+}(x)$ and $J^{\bar{D}^-}(x) J^{\Sigma_c^{++}}(x)$ have both the isospin $(I, I_3) = (\frac{1}{2}, \frac{1}{2})$ and $(\frac{3}{2}, \frac{1}{2})$ components, and couple potentially to the pentaquark molecular states with the isospins $(\frac{1}{2}, \frac{1}{2})$ and $(\frac{3}{2}, \frac{1}{2})$, which decay to the final states $J/\psi p$ and $J/\psi \Delta^+$, respectively. As the $P_c(4312)$, $P_c(4380)$, $P_c(4440)$, $P_c(4457)$ and $P_c(4337)$ are observed in the $J/\psi p$ mass spectrum, it is better to choose the current $J_{\frac{1}{2}}^{\bar{D}^{\Sigma_c}}(x)$ with the definite Isospin, we prefer the color singlet-singlet type currents with the definite isospins [353, 547, 548, 549]. Although the mass splitting between the isospin cousins is of several 10-MeV in most cases, in some cases, the mass splitting can be as large as 150 MeV, see Table 57.

We resort to the correlation functions $\Pi(p)$, $\Pi_{\mu\nu}(p)$ and $\Pi_{\mu\alpha\beta}(p)$ in Eq.(287), and perform analogous analysis to obtain the QCD sum rules for the masses and pole residues like Eqs.(302)-(303),

$$2M_- \lambda_j^- \exp\left(-\frac{M_-^2}{T^2}\right) = \int_{4m_c^2}^{s_0} ds \rho_{QCD,j}(s) \exp\left(-\frac{s}{T^2}\right), \tag{344}$$

$$M_-^2 = \frac{-\int_{4m_c^2}^{s_0} ds \frac{d}{d(1/T^2)} \rho_{QCD,j}(s) \exp\left(-\frac{s}{T^2}\right)}{\int_{4m_c^2}^{s_0} ds \rho_{QCD,j}(s) \exp\left(-\frac{s}{T^2}\right)}, \tag{345}$$

where $j = \frac{1}{2}$, $\frac{3}{2}$ and $\frac{5}{2}$, the pole residues are defined by,

$$\begin{aligned}
\langle 0 | J(0) | P_{\frac{1}{2}}^-(p) \rangle &= \lambda_{\frac{1}{2}}^- U^-(p, s), \\
\langle 0 | J(0) | P_{\frac{1}{2}}^+(p) \rangle &= \lambda_{\frac{1}{2}}^+ i\gamma_5 U^+(p, s),
\end{aligned} \tag{346}$$

$$\begin{aligned}
\langle 0 | J_{\mu}(0) | P_{\frac{3}{2}}^-(p) \rangle &= \lambda_{\frac{3}{2}}^- U_{\mu}^-(p, s), \\
\langle 0 | J_{\mu}(0) | P_{\frac{3}{2}}^+(p) \rangle &= \lambda_{\frac{3}{2}}^+ i\gamma_5 U_{\mu}^+(p, s),
\end{aligned} \tag{347}$$

$$\begin{aligned}
\langle 0 | J_{\mu\nu}(0) | P_{\frac{5}{2}}^-(p) \rangle &= \sqrt{2} \lambda_{\frac{5}{2}}^- U_{\mu\nu}^-(p, s), \\
\langle 0 | J_{\mu\nu}(0) | P_{\frac{5}{2}}^+(p) \rangle &= \sqrt{2} \lambda_{\frac{5}{2}}^+ i\gamma_5 U_{\mu\nu}^+(p, s),
\end{aligned} \tag{348}$$

the $U^\pm(p, s)$, $U_\mu^\pm(p, s)$ and $U_{\mu\nu}^\pm(p, s)$ are the Dirac and Rarita-Schwinger spinors, satisfy the relations in Eq.(296).

As we study the color singlet-singlet type pentaquark states, it is better to choose the updated values $\mathbb{M}_c = 1.85 \pm 0.01 \text{ GeV}$ and $\mathbb{M}_s = 0.2 \text{ GeV}$ to determine the optimal energy scales of the QCD spectral densities with the formula [518],

$$\mu = \sqrt{M_{X/Y/Z/P}^2 - (2\mathbb{M}_c)^2 - k\mathbb{M}_s}. \quad (349)$$

After trial and error, we obtain the Borel windows, continuum threshold parameters, energy scales and pole contributions, see Table 56, the pole contributions are about or slightly larger than (40 – 60)%, we obtain the **largest pole contributions** up to now. In the Borel windows, the highest dimensional condensate contributions $|D(12)|$ and $|D(13)|$ are approximately zero, the most important contributions are mainly from the lowest order contributions $\langle \bar{q}q \rangle$, $\langle \bar{q}q \rangle^2$ and $\langle \bar{q}g_s\sigma Gq \rangle \langle \bar{q}q \rangle$. The operator product expansion converges very well.

Then we calculate the uncertainties of the masses and pole residues, which are shown in Table 57. The central value of the mass of the $\bar{D}\Sigma_c$ molecular state with the $IJ^P = \frac{1}{2}\frac{1}{2}^-$ is 4.31 GeV, it is only about 10 MeV below the $\bar{D}^0\Sigma_c^+$ threshold, we assign it as the $P_c(4312)$ tentatively. For the $\bar{D}\Sigma_c$ molecular state with the $IJ^P = \frac{3}{2}\frac{1}{2}^-$, the central value of the mass is 4.33 GeV, which is about 10 MeV above the $\bar{D}^-\Sigma_c^{++}$ threshold, we tentatively assign it as the $\bar{D}\Sigma_c$ resonance, the isospin cousin of the $P_c(4312)$.

In a similar way, we assign the $P_c(4380)$, $P_c(4440)$ and $P_c(4457)$ as the $\bar{D}\Sigma_c^*$, $\bar{D}^*\Sigma_c$ and $\bar{D}^*\Sigma_c^*$ molecular states with the $IJ^P = \frac{1}{2}\frac{3}{2}^-$, $\frac{1}{2}\frac{3}{2}^-$ and $\frac{1}{2}\frac{5}{2}^-$, respectively. For the molecular states (resonances) $\bar{D}\Sigma_c^*$ with the $IJ^P = \frac{3}{2}\frac{3}{2}^-$, $\bar{D}^*\Sigma_c$ with the $IJ^P = \frac{3}{2}\frac{3}{2}^-$ and $\bar{D}^*\Sigma_c^*$ with the $IJ^P = \frac{3}{2}\frac{5}{2}^-$, the central values of the masses are about 20 MeV, 10 MeV and 90 MeV above the corresponding meson-baryon thresholds, respectively.

If we choose the same input parameters, the color singlet-singlet type pentaquark states with the isospin $I = \frac{3}{2}$ (1) have slightly larger masses than the corresponding ones with the isospin $I = \frac{1}{2}$ (0).

The $P_c(4312)$, $P_c(4380)$, $P_c(4440)$ and $P_c(4457)$ can be assigned as the $\bar{D}\Sigma_c$, $\bar{D}\Sigma_c^*$, $\bar{D}^*\Sigma_c$ and $\bar{D}^*\Sigma_c^*$ molecular states with the isospin $I = \frac{1}{2}$ respectively, since the two-body strong decays $P_c \rightarrow J/\psi p$ conserve isospin. If the assignments are robust, there exist four slightly higher molecular states $\bar{D}\Sigma_c$, $\bar{D}\Sigma_c^*$, $\bar{D}^*\Sigma_c$ and $\bar{D}^*\Sigma_c^*$ with the isospin $I = \frac{3}{2}$, we can search for the four resonances in the $J/\psi\Delta^+$ mass spectrum, as the two-body strong decays $P_c \rightarrow J/\psi\Delta^+$ also conserve isospin, the J/ψ , p and Δ have the isospins $I = 0$, $\frac{1}{2}$ and $\frac{3}{2}$, respectively.

The $\bar{D}^*\Xi_c'$ and $\bar{D}^*\Xi_c^*$ molecular states lie about 0.1 GeV and 0.2 GeV above the $P_{cs}(4459)$ respectively, the $P_{cs}(4459)$ is unlikely to be the $\bar{D}^*\Xi_c'$ or $\bar{D}^*\Xi_c^*$ molecular state. The mass of the $\bar{D}\Xi_c'$ molecular state with the isospin $I = 1$ is $4.45_{-0.08}^{+0.07}$ GeV, which is near the value 4459 MeV, but lies slightly above the corresponding meson-baryon threshold, it is as a resonance, from the decay channel $P_{cs}(4459) \rightarrow J/\psi\Lambda$ [191], the isospin of the $P_{cs}(4459)$ is zero, which excludes assigning the $P_{cs}(4459)$ as the $\bar{D}\Xi_c^*$ molecular state with the isospin $I = 1$. The mass of the $\bar{D}\Xi_c^*$ molecular state with the isospin $I = 0$ is $4.46_{-0.07}^{+0.07}$ GeV, which is in very good agreement with the $P_{cs}(4459)$, it is very good to assign the $P_{cs}(4459)$ as the $\bar{D}\Xi_c^*$ molecular state with the isospin $I = 0$ and the spin-parity $J^P = \frac{3}{2}^-$. The predications also favor assigning the $P_{cs}(4459)$ as the $\bar{D}^*\Xi_c$ molecular state with the spin-parity $J^P = \frac{3}{2}^-$ and isospin $I = 0$.

The predictions support assigning the $P_{cs}(4338)$ as the $\bar{D}\Xi_c$ molecular state with the spin-parity $J^P = \frac{1}{2}^-$ and isospin $I = 0$, the observation of its cousin with the isospin $I = 1$ in the $J/\psi\Sigma^0/\eta_c\Sigma^0$ mass spectrum would decipher the inner structure of the $P_{cs}(4338)$. However, there exists no candidate for the $P_c(4337)$ [192].

	IJ^P	$T^2(\text{GeV}^2)$	$\sqrt{s_0}(\text{GeV})$	$\mu(\text{GeV})$	PC
$\bar{D}\Sigma_c$	$\frac{1}{2}\frac{1}{2}^-$	3.2 – 3.8	5.00 ± 0.10	2.2	(42 – 60)%
$\bar{D}\Sigma_c$	$\frac{3}{2}\frac{1}{2}^-$	2.8 – 3.4	4.98 ± 0.10	2.2	(44 – 65)%
$\bar{D}\Sigma_c^*$	$\frac{1}{2}\frac{3}{2}^-$	3.3 – 3.9	5.06 ± 0.10	2.3	(42 – 60)%
$\bar{D}\Sigma_c^*$	$\frac{3}{2}\frac{3}{2}^-$	2.9 – 3.5	5.03 ± 0.10	2.4	(44 – 64)%
$\bar{D}^*\Sigma_c$	$\frac{1}{2}\frac{3}{2}^-$	3.3 – 3.9	5.12 ± 0.10	2.5	(42 – 60)%
$\bar{D}^*\Sigma_c$	$\frac{3}{2}\frac{3}{2}^-$	3.0 – 3.6	5.10 ± 0.10	2.5	(41 – 61)%
$\bar{D}^*\Sigma_c^*$	$\frac{1}{2}\frac{5}{2}^-$	3.2 – 3.8	5.08 ± 0.10	2.5	(43 – 60)%
$\bar{D}^*\Sigma_c^*$	$\frac{3}{2}\frac{5}{2}^-$	3.0 – 3.6	5.24 ± 0.10	2.8	(42 – 61)%
$\bar{D}\Xi'_c$	$0\frac{1}{2}^-$	3.4 – 4.0	5.12 ± 0.10	2.2	(41 – 58)%
$\bar{D}\Xi'_c$	$1\frac{1}{2}^-$	3.2 – 3.8	5.14 ± 0.10	2.3	(43 – 61)%
$\bar{D}\Xi_c^*$	$0\frac{3}{2}^-$	3.4 – 4.0	5.15 ± 0.10	2.3	(43 – 60)%
$\bar{D}\Xi_c^*$	$1\frac{3}{2}^-$	3.3 – 3.9	5.22 ± 0.10	2.4	(44 – 62)%
$\bar{D}^*\Xi'_c$	$0\frac{3}{2}^-$	3.5 – 4.1	5.26 ± 0.10	2.5	(42 – 59)%
$\bar{D}^*\Xi'_c$	$1\frac{3}{2}^-$	3.4 – 4.0	5.31 ± 0.10	2.6	(43 – 60)%
$\bar{D}^*\Xi_c^*$	$0\frac{5}{2}^-$	3.6 – 4.2	5.31 ± 0.10	2.6	(42 – 58)%
$\bar{D}^*\Xi_c^*$	$1\frac{5}{2}^-$	3.4 – 4.0	5.35 ± 0.10	2.6	(44 – 61)%
$\bar{D}\Xi_c$	$0\frac{1}{2}^-$	3.2 – 3.8	5.00 ± 0.10	2.1	(41 – 60)%
$\bar{D}\Xi_c$	$1\frac{1}{2}^-$	3.1 – 3.7	5.09 ± 0.10	2.3	(42 – 61)%
$\bar{D}\Lambda_c$	$\frac{1}{2}\frac{1}{2}^-$	3.2 – 3.8	5.11 ± 0.10	2.5	(42 – 60)%
$\bar{D}_s\Xi_c$	$\frac{1}{2}\frac{1}{2}^-$	3.2 – 3.8	5.15 ± 0.10	2.2	(41 – 59)%
$\bar{D}_s\Lambda_c$	$0\frac{1}{2}^-$	3.2 – 3.8	5.13 ± 0.10	2.3	(43 – 61)%
$\bar{D}^*\Xi_c$	$0\frac{3}{2}^-$	3.2 – 3.8	5.10 ± 0.10	2.3	(43 – 61)%
$\bar{D}^*\Xi_c$	$1\frac{3}{2}^-$	3.3 – 3.9	5.27 ± 0.10	2.6	(43 – 61)%
$\bar{D}^*\Lambda_c$	$\frac{1}{2}\frac{3}{2}^-$	3.3 – 3.9	5.23 ± 0.10	2.7	(41 – 61)%
$\bar{D}_s^*\Xi_c$	$\frac{1}{2}\frac{3}{2}^-$	3.3 – 3.9	5.28 ± 0.10	2.4	(42 – 59)%
$\bar{D}_s^*\Lambda_c$	$0\frac{3}{2}^-$	3.2 – 3.8	5.14 ± 0.10	2.4	(42 – 60)%

Table 56: The Borel parameters, continuum threshold parameters, energy scales and pole contributions for the color singlet-singlet type pentaquark states.

	IJP	$M(\text{GeV})$	$\lambda(10^{-3}\text{GeV}^6)$	Assignments	Thresholds (MeV)
$\bar{D}\Sigma_c$	$\frac{1}{2}\frac{1}{2}^-$	$4.31^{+0.07}_{-0.07}$	$3.25^{+0.43}_{-0.41}$	$P_c(4312)$	4321
$\bar{D}\Sigma_c$	$\frac{3}{2}\frac{1}{2}^-$	$4.33^{+0.09}_{-0.08}$	$1.97^{+0.28}_{-0.26}$		4321
$\bar{D}\Sigma_c^*$	$\frac{1}{2}\frac{3}{2}^-$	$4.38^{+0.07}_{-0.07}$	$1.97^{+0.26}_{-0.24}$	$P_c(4380)$	4385
$\bar{D}\Sigma_c^*$	$\frac{3}{2}\frac{3}{2}^-$	$4.41^{+0.08}_{-0.08}$	$1.24^{+0.17}_{-0.16}$		4385
$\bar{D}^*\Sigma_c$	$\frac{1}{2}\frac{3}{2}^-$	$4.44^{+0.07}_{-0.08}$	$3.60^{+0.47}_{-0.44}$	$P_c(4440)$	4462
$\bar{D}^*\Sigma_c$	$\frac{3}{2}\frac{3}{2}^-$	$4.47^{+0.09}_{-0.09}$	$2.31^{+0.33}_{-0.31}$		4462
$\bar{D}^*\Sigma_c^*$	$\frac{1}{2}\frac{5}{2}^-$	$4.46^{+0.08}_{-0.08}$	$4.05^{+0.54}_{-0.50}$	$P_c(4457)$	4527
$\bar{D}^*\Sigma_c^*$	$\frac{3}{2}\frac{5}{2}^-$	$4.62^{+0.09}_{-0.09}$	$2.40^{+0.37}_{-0.35}$		4527
$\bar{D}\Xi'_c$	$0\frac{1}{2}^-$	$4.43^{+0.07}_{-0.07}$	$3.02^{+0.39}_{-0.37}$		4446
$\bar{D}\Xi'_c$	$1\frac{1}{2}^-$	$4.45^{+0.07}_{-0.08}$	$2.50^{+0.33}_{-0.31}$		4446
$\bar{D}\Xi_c^*$	$0\frac{3}{2}^-$	$4.46^{+0.07}_{-0.07}$	$1.71^{+0.22}_{-0.21}$	$P_{cs}(4459)$	4513
$\bar{D}\Xi_c^*$	$1\frac{3}{2}^-$	$4.53^{+0.07}_{-0.07}$	$1.56^{+0.20}_{-0.19}$		4513
$\bar{D}^*\Xi'_c$	$0\frac{3}{2}^-$	$4.57^{+0.07}_{-0.07}$	$3.41^{+0.43}_{-0.41}$		4588
$\bar{D}^*\Xi'_c$	$1\frac{3}{2}^-$	$4.62^{+0.08}_{-0.08}$	$3.05^{+0.39}_{-0.37}$		4588
$\bar{D}^*\Xi_c^*$	$0\frac{5}{2}^-$	$4.64^{+0.07}_{-0.07}$	$4.36^{+0.54}_{-0.51}$		4655
$\bar{D}^*\Xi_c^*$	$1\frac{5}{2}^-$	$4.67^{+0.08}_{-0.08}$	$3.25^{+0.41}_{-0.39}$		4655
$\bar{D}\Xi_c$	$0\frac{1}{2}^-$	$4.34^{+0.07}_{-0.07}$	$1.43^{+0.19}_{-0.18}$? $P_{cs}(4338)$	4337
$\bar{D}\Xi_c$	$1\frac{1}{2}^-$	$4.46^{+0.07}_{-0.07}$	$1.37^{+0.19}_{-0.18}$		4337
$\bar{D}\Lambda_c$	$\frac{1}{2}\frac{1}{2}^-$	$4.46^{+0.07}_{-0.08}$	$1.47^{+0.20}_{-0.18}$		4151
$\bar{D}_s\Xi_c$	$\frac{1}{2}\frac{1}{2}^-$	$4.54^{+0.07}_{-0.07}$	$1.58^{+0.21}_{-0.20}$		4437
$\bar{D}_s\Lambda_c$	$0\frac{1}{2}^-$	$4.48^{+0.07}_{-0.07}$	$1.57^{+0.21}_{-0.20}$		4255
$\bar{D}^*\Xi_c$	$0\frac{3}{2}^-$	$4.46^{+0.07}_{-0.07}$	$1.55^{+0.20}_{-0.19}$? $P_{cs}(4459)$	4479
$\bar{D}^*\Xi_c$	$1\frac{3}{2}^-$	$4.63^{+0.08}_{-0.08}$	$1.69^{+0.22}_{-0.21}$		4479
$\bar{D}^*\Lambda_c$	$\frac{1}{2}\frac{3}{2}^-$	$4.59^{+0.08}_{-0.08}$	$1.67^{+0.22}_{-0.21}$		4293
$\bar{D}_s^*\Xi_c$	$\frac{1}{2}\frac{3}{2}^-$	$4.65^{+0.08}_{-0.08}$	$1.66^{+0.22}_{-0.21}$		4580
$\bar{D}_s^*\Lambda_c$	$0\frac{3}{2}^-$	$4.50^{+0.07}_{-0.07}$	$1.52^{+0.21}_{-0.19}$		4398

Table 57: The masses, pole residues and assignments for the color singlet-singlet type pentaquark states, where the thresholds denote the corresponding thresholds of the meson-baryon scattering states.

10 Singly-heavy tetraquark and pentaquark states

10.1 Singly-heavy tetraquark states

The $X_0(2900)$ and $X_1(2900)$ observed in the D^-K^+ mass spectrum are the first exotic structures with fully open flavor [95, 96], they have the valence quarks $ud\bar{c}\bar{s}$. The $T_{c\bar{s}}^0(2900)$ and $T_{c\bar{s}}^{++}(2900)$ are observed in the $D_s^+\pi^-$ and $D_s^+\pi^+$ mass spectra, respectively [120, 121], they have the valence quarks $c\bar{s}u\bar{d}$ and $c\bar{s}u\bar{d}$, respectively.

Based on the predicted masses of the AA -type scalar tetraquark states from the QCD sum rules [57, 550],

$$\begin{aligned} M_{qq\bar{q}\bar{q}} &= 1.86 \pm 0.11 \text{ GeV}, \\ M_{ss\bar{s}\bar{s}} &= 2.08 \pm 0.13 \text{ GeV}, \\ M_{cq\bar{c}\bar{q}} &= 3.95 \pm 0.09 \text{ GeV}, \end{aligned} \quad (350)$$

we estimate the mass of the AA -type $cs\bar{u}\bar{d}$ tetraquark state crudely,

$$M_{cs\bar{u}\bar{d}} = \frac{M_{qq\bar{q}\bar{q}} + M_{ss\bar{s}\bar{s}} + 2M_{cq\bar{c}\bar{q}}}{4} = 2.96 \pm 0.11 \text{ GeV}, \quad (351)$$

which is consistent with the mass of the $X_0(2900)$ within uncertainties [109].

In Ref.[109], we construct the AA and SS -type scalar currents,

$$\begin{aligned} J_{AA}(x) &= \varepsilon^{ijk} \varepsilon^{imn} s_j^T(x) C \gamma_\alpha c_k(x) \bar{u}_m(x) \gamma^\alpha C \bar{d}_n^T(x), \\ J_{SS}(x) &= \varepsilon^{ijk} \varepsilon^{imn} s_j^T(x) C \gamma_5 c_k(x) \bar{u}_m(x) \gamma_5 C \bar{d}_n^T(x), \end{aligned} \quad (352)$$

to study the $cs\bar{u}\bar{d}$ tetraquark states with the correlation function $\Pi(p)$, see Eq.(127). We carry out the operator product expansion up to the vacuum condensates of dimension-11 and assume vacuum saturation for the higher dimensional vacuum condensates according to the routine in Sect.5.1. As there are three q -quark lines and one Q -quark line, if each Q -quark line emits a gluon and each q -quark line contributes a quark-antiquark pair, we obtain a quark-gluon operator $g_s G_{\mu\nu} \bar{q}q\bar{q}q\bar{s}s$, which is of dimension 11, and leads to the vacuum condensates $\langle \bar{q}q \rangle^2 \langle \bar{s}g_s \sigma G s \rangle$ and $\langle \bar{q}q \rangle \langle \bar{s}s \rangle \langle \bar{q}g_s \sigma G q \rangle$.

We obtain the QCD sum rules routinely, at the QCD side, we choose the flavor numbers $n_f = 4$ and the typical energy scale $\mu = 1 \text{ GeV}$. After trial and error, we obtain the Borel windows and continuum threshold parameters, therefore the pole contributions of the ground states and the convergent behaviors of the operator product expansion, see Table 58. In the Borel windows, the pole contributions are about (38 – 67)%, the central values exceed 52%. The contributions of the vacuum condensates $|D(11)|$ are about (2 – 4)% and (0 – 1)% for the AA and SS -type tetraquark states, respectively.

At last, we obtain the values of the masses and pole residues, which are also shown in Table 58. In Fig.26, we plot the masses of the AA and SS -type scalar $cs\bar{u}\bar{d}$ tetraquark states with variations of the Borel parameters T^2 in much larger ranges than the Borel windows, there appear platforms in the Borel windows indeed.

The predicted mass $M_{AA} = 2.91 \pm 0.12 \text{ GeV}$ is consistent with the experimental value $2866 \pm 7 \text{ MeV}$ from the LHCb collaboration [95, 96], and supports assigning the $X_0(2900)$ to be the AA -type $cs\bar{u}\bar{d}$ tetraquark state with the spin-parity $J^P = 0^+$. While the predicted mass $M_{SS} = 3.05 \pm 0.10 \text{ GeV}$ lies above the experimental value $2866 \pm 7 \text{ MeV}$ [95, 96].

In Ref.[551], we construct the $A\bar{A}$ -type currents to study the ground state mass spectrum of the tetraquark states with strange and doubly-strange via the QCD sum rules to verify the inner structures of the $T_{c\bar{s}}(2900)$, where

$$\begin{aligned} J(x) &= J_s^0(x), J_{ss}^0(x), \\ J_{\mu\nu}(x) &= J_{s,\mu\nu}^1(x), J_{ss,\mu\nu}^1(x), J_{s,\mu\nu}^2(x), J_{ss,\mu\nu}^2(x), \end{aligned} \quad (353)$$

	$T^2(\text{GeV}^2)$	$\sqrt{s_0}(\text{GeV})$	pole	$ D(11) $	$M(\text{GeV})$	$\lambda(\text{GeV}^5)$
$[cs]_A[\bar{u}\bar{d}]_A$	1.9 – 2.3	3.5 ± 0.1	(38 – 67)%	(2 – 4)%	2.91 ± 0.12	$(1.60 \pm 0.33) \times 10^{-2}$
$[cs]_S[\bar{u}\bar{d}]_S$	2.1 – 2.5	3.6 ± 0.1	(39 – 66)%	(0 – 1)%	3.05 ± 0.10	$(1.20 \pm 0.21) \times 10^{-2}$

Table 58: The Borel windows, continuum threshold parameters, pole contributions, contributions of the vacuum condensates of dimension 11, masses and pole residues for the scalar tetraquark states.

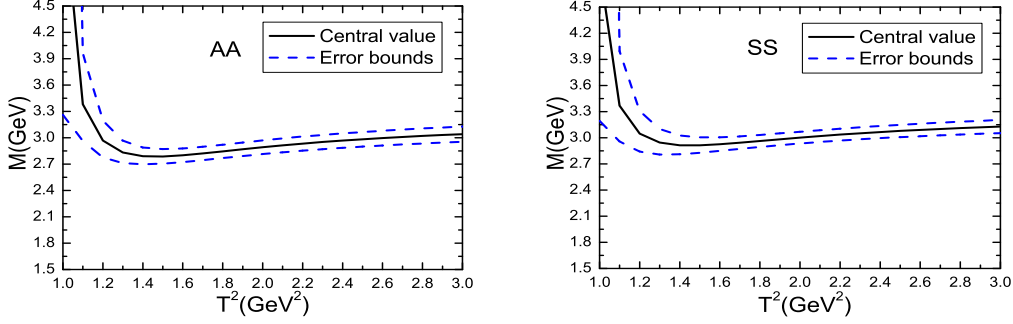


Figure 26: The masses of the AA and SS -type tetraquark states with variations of the Borel parameters T^2 .

$$\begin{aligned}
J_s^0(x) &= \varepsilon^{ijk} \varepsilon^{imn} u_j^T(x) C \gamma_\mu c_k(x) \bar{d}_m(x) \gamma^\mu C \bar{s}_n^T(x), \\
J_{ss}^0(x) &= \varepsilon^{ijk} \varepsilon^{imn} u_j^T(x) C \gamma_\mu c_k(x) \bar{s}_m(x) \gamma^\mu C \bar{s}_n^T(x), \\
J_{s,\mu\nu}^1(x) &= \varepsilon^{ijk} \varepsilon^{imn} [u_j^T(x) C \gamma_\mu c_k(x) \bar{d}_m(x) \gamma_\nu C \bar{s}_n^T(x) - u_j^T(x) C \gamma_\nu c_k(x) \bar{d}_m(x) \gamma_\mu C \bar{s}_n^T(x)], \\
J_{ss,\mu\nu}^1(x) &= \varepsilon^{ijk} \varepsilon^{imn} [u_j^T(x) C \gamma_\mu c_k(x) \bar{s}_m(x) \gamma_\nu C \bar{s}_n^T(x) - u_j^T(x) C \gamma_\nu c_k(x) \bar{s}_m(x) \gamma_\mu C \bar{s}_n^T(x)], \\
J_{s,\mu\nu}^2(x) &= \varepsilon^{ijk} \varepsilon^{imn} [u_j^T(x) C \gamma_\mu c_k(x) \bar{d}_m(x) \gamma_\nu C \bar{s}_n^T(x) + u_j^T(x) C \gamma_\nu c_k(x) \bar{d}_m(x) \gamma_\mu C \bar{s}_n^T(x)], \\
J_{ss,\mu\nu}^2(x) &= \varepsilon^{ijk} \varepsilon^{imn} [u_j^T(x) C \gamma_\mu c_k(x) \bar{s}_m(x) \gamma_\nu C \bar{s}_n^T(x) + u_j^T(x) C \gamma_\nu c_k(x) \bar{s}_m(x) \gamma_\mu C \bar{s}_n^T(x)],
\end{aligned} \tag{354}$$

the superscripts 0, 1 and 2 denote the spins. With a simple replacement $u \leftrightarrow d$, we obtain the corresponding currents in the same isospin multiplets. In the isospin limit, the tetraquark states in the same multiplets have the same masses.

Again, we resort to the correlation functions $\Pi(p)$ and $\Pi_{\mu\nu\alpha\beta}(p)$, see Eq.(127), and obtain the ground state contributions according to hadron representations in Eqs.(204)-(206), and obtain the QCD sum rules routinely, again we take the flavor numbers $n_f = 4$ and the typical energy scale $\mu = 1.0 \text{ GeV}$.

After trial and error, we obtain the Borel windows, continuum threshold parameters and pole contributions, see Table 59, where the pole contributions are 38% – 66% and the central values for the six states are larger than 50%, furthermore, the vacuum condensate show a descending trend $|D(6)| > |D(8)| > |D(9)| > |D(10)| \sim |D(11)| \sim 0$. At last, we obtain the masses and pole residues, which are also shown in Table 59.

In Table 59, the predicted mass of the $J^P = 0^+$ state $cu\bar{d}\bar{s}$, $M = 2.92 \pm 0.12 \text{ GeV}$, is in very good agreement with the experimental values $M = 2.892 \pm 0.014 \pm 0.015 \text{ GeV}$ and $2.921 \pm 0.017 \pm 0.020 \text{ GeV}$ from the LHCb collaboration [120, 121], and supports assigning the $T_{c\bar{s}}(2900)$ to be the

	J^P	$T^2(\text{GeV}^2)$	$\sqrt{s_0}(\text{GeV})$	pole	$M_T(\text{GeV})$	$\lambda_T(10^{-2}\text{GeV}^5)$
$cu\bar{d}\bar{s}$	0^+	1.9 – 2.3	3.50 ± 0.10	(40 – 65)%	2.92 ± 0.12	1.62 ± 0.33
$cu\bar{d}\bar{s}$	1^+	2.2 – 2.6	3.65 ± 0.10	(40 – 62)%	3.10 ± 0.10	1.59 ± 0.27
$cu\bar{d}\bar{s}$	2^+	2.5 – 2.9	3.95 ± 0.10	(42 – 61)%	3.40 ± 0.10	3.51 ± 0.55
$cu\bar{s}\bar{s}$	0^+	2.0 – 2.4	3.60 ± 0.10	(38 – 66)%	3.02 ± 0.12	2.72 ± 0.43
$cu\bar{s}\bar{s}$	1^+	2.3 – 2.7	3.75 ± 0.10	(40 – 65)%	3.20 ± 0.10	2.64 ± 0.33
$cu\bar{s}\bar{s}$	2^+	2.6 – 3.0	4.05 ± 0.10	(41 – 64)%	3.49 ± 0.10	5.70 ± 0.65

Table 59: The spin-parity, Borel parameters, continuum threshold parameters, pole contributions, masses and pole residues of the tetraquark states.

$A\bar{A}$ -type $c\bar{s}q\bar{q}$ tetraquark states with the spin-parity $J^P = 0^+$.

10.2 Single-heavy pentaquark states

In 2017, the LHCb collaboration observed five narrow structures $\Omega_c(3000)$, $\Omega_c(3050)$, $\Omega_c(3066)$, $\Omega_c(3090)$ and $\Omega_c(3119)$ [552]. Also in 2017, the Belle collaboration confirmed the $\Omega_c(3000)$, $\Omega_c(3050)$, $\Omega_c(3066)$ and $\Omega_c(3090)$ in the $\Xi_c^+ K^-$ decay mode [553]. In 2023, the LHCb collaboration observed the $\Omega_c(3185)$ and $\Omega_c(3327)$ in the $\Xi_c^+ K^-$ mass spectrum [554], which lie near the $D\Xi$ and $D^*\Xi$ thresholds, respectively, the measured Breit-Wigner masses and decay widths are

$$\begin{aligned} \Omega_c(3185) : M &= 3185.1 \pm 1.7_{-0.9}^{+7.4} \pm 0.2 \text{ MeV}, \Gamma = 50 \pm 7_{-20}^{+10} \text{ MeV}, \\ \Omega_c(3327) : M &= 3327.1 \pm 1.2_{-1.3}^{+0.1} \pm 0.2 \text{ MeV}, \Gamma = 20 \pm 5_{-1}^{+13} \text{ MeV}. \end{aligned} \quad (355)$$

As early as 2005, the Belle collaboration tentatively assigned the $\Sigma_c^0(2800)$, $\Sigma_c^+(2800)$ and $\Sigma_c^{++}(2800)$ in the $\Lambda_c^+ \pi^{-/0/+}$ mass spectra as the isospin triplet states with the spin-parity $J^P = \frac{3}{2}^-$ [555], the measured masses and decay widths are

$$\begin{aligned} \Sigma_c^0(2800) : M &= M_{\Lambda^+} + 515.4_{-3.1-6.0}^{+3.2+2.1} \text{ MeV}, \Gamma = 61_{-13-13}^{+18+22} \text{ MeV}, \\ \Sigma_c^+(2800) : M &= M_{\Lambda^+} + 505.4_{-4.6-2.0}^{+5.8+12.4} \text{ MeV}, \Gamma = 62_{-23-38}^{+37+52} \text{ MeV}, \\ \Sigma_c^{++}(2800) : M &= M_{\Lambda^+} + 514.5_{-3.1-4.9}^{+3.4+2.8} \text{ MeV}, \Gamma = 75_{-13-11}^{+18+12} \text{ MeV}. \end{aligned} \quad (356)$$

In 2008, the BaBar collaboration observed the $\Sigma_c^0(2800)$ in the $\Lambda_c^+ \pi^-$ mass spectrum with the possible spin-parity $J^P = \frac{1}{2}^-$ [556], the mass and decay width are,

$$\Sigma_c^0(2800) : M = 2846 \pm 8 \pm 10 \text{ MeV}, \Gamma = 86_{-22}^{+33} \pm 7 \text{ MeV}. \quad (357)$$

In 2007, the BaBar collaboration observed the $\Lambda_c(2940)$ in the $D^0 p$ invariant mass spectrum [557]. Subsequently, the Belle collaboration verified the $\Lambda_c(2940)$ in the decay mode $\Lambda_c(2940) \rightarrow \Sigma_c(2455)\pi$ [558]. In 2017, the LHCb collaboration determined the spin-parity of the $\Lambda(2940)^+$ to be $J^P = \frac{3}{2}^-$ in analyzing the process $\Lambda_b^0 \rightarrow D^0 p \pi^-$ [559]. The measured masses and decay widths are,

$$\begin{aligned} \Lambda_c(2940) : M &= 2939.8 \pm 1.3 \pm 1.0 \text{ MeV}, \Gamma = 17.5 \pm 5.0 \pm 5.9 \text{ MeV} \quad (\text{BaBar}), \\ \Lambda_c(2940) : M &= 2938.0 \pm 1.3_{-4.0}^{+2.0} \text{ MeV}, \Gamma = 13_{-5-7}^{+8+27} \text{ MeV} \quad (\text{Belle}), \\ \Lambda_c(2940) : M &= 2944.8_{-2.5}^{+3.5} \pm 0.4_{-4.6}^{+0.1} \text{ MeV}, \Gamma = 27.7_{-6.0}^{+8.2} \pm 0.9_{-10.4}^{+5.2} \text{ MeV} \quad (\text{LHCb}). \end{aligned} \quad (358)$$

In 2023, the Belle collaboration investigated the decays $\bar{B}^0 \rightarrow \Sigma_c(2455)^{0,++}\pi^\pm \bar{p}$ and found a new structure $\Lambda_c^+(2910)$ in the $\Sigma_c(2455)^{0,++}\pi^\pm$ mass spectrum [560], the mass and decay width are,

$$\Lambda_c(2910) : M = 2913.8 \pm 5.6 \pm 3.8 \text{ MeV}, \Gamma = 51.8 \pm 20.0 \pm 18.8 \text{ MeV}. \quad (359)$$

The $\Sigma_c(2800)$, $\Lambda_c(2940)$ and $\Lambda_c(2910)$ lie near the $D^{(*)}N$ thresholds, and they might be the $D^{(*)}N$ molecular states. For example, we can assign the $\Sigma_c(2800)$ as the DN molecular (bound) state [561, 562, 563, 564], and assign the $\Lambda_c(2940)$ as the D^*N molecular state [562, 564, 565, 566, 567, 568, 569]. We would like to study the color singlet-singlet type charmed pentaquark states and explore the possible assignments in the scenario of molecular states.

Again, we write down the correlation functions $\Pi(p)$, $\Pi_{\mu\nu}(p)$ and $\Pi_{\mu\nu\alpha\beta}(p)$ explicitly for convenience,

$$\begin{aligned}\Pi(p) &= i \int d^4x e^{ip \cdot x} \langle 0 | T \{ J(x) \bar{J}(0) \} | 0 \rangle, \\ \Pi_{\mu\nu}(p) &= i \int d^4x e^{ip \cdot x} \langle 0 | T \{ J_\mu(x) \bar{J}_\nu(0) \} | 0 \rangle, \\ \Pi_{\mu\nu\alpha\beta}(p) &= i \int d^4x e^{ip \cdot x} \langle 0 | T \{ J_{\mu\nu}(x) \bar{J}_{\alpha\beta}(0) \} | 0 \rangle,\end{aligned}\quad (360)$$

where

$$\begin{aligned}J(x) &= J_{[1,0]}^{DN}(x), J_{[0,0]}^{DN}(x), J_{[1,0]}^{D\Xi}(x), J_{[0,0]}^{D\Xi}(x), J_{|\frac{1}{2}, \pm\frac{1}{2}}^{D_s\Xi}(x), \\ J_\mu(x) &= J_{[1,0]}^{D^*N}(x), J_{[0,0]}^{D^*N}(x), J_{[1,0]}^{D^*\Xi}(x), J_{[0,0]}^{D^*\Xi}(x), J_{|\frac{1}{2}, \pm\frac{1}{2}}^{D_s^*\Xi}(x), J_{[1,0]}^{D\Xi^*}(x), J_{[0,0]}^{D\Xi^*}(x), J_{|\frac{1}{2}, \pm\frac{1}{2}}^{D_s\Xi^*}(x), \\ J_{\mu\nu}(x) &= J_{[1,0]}^{D^*\Xi^*}(x), J_{[0,0]}^{D^*\Xi^*}(x), J_{|\frac{1}{2}, \pm\frac{1}{2}}^{D_s^*\Xi^*}(x),\end{aligned}\quad (361)$$

$$\begin{aligned}J_{[1,0]}^{DN}(x) &= \frac{1}{\sqrt{2}} J_{|\frac{1}{2}, -\frac{1}{2}}^{D^0}(x) J_{|\frac{1}{2}, \frac{1}{2}}^{N^+}(x) + \frac{1}{\sqrt{2}} J_{|\frac{1}{2}, \frac{1}{2}}^{D^+}(x) J_{|\frac{1}{2}, -\frac{1}{2}}^{N^0}(x), \\ J_{[0,0]}^{DN}(x) &= \frac{1}{\sqrt{2}} J_{|\frac{1}{2}, -\frac{1}{2}}^{D^0}(x) J_{|\frac{1}{2}, \frac{1}{2}}^{N^+}(x) - \frac{1}{\sqrt{2}} J_{|\frac{1}{2}, \frac{1}{2}}^{D^+}(x) J_{|\frac{1}{2}, -\frac{1}{2}}^{N^0}(x), \\ J_{[1,0]}^{D\Xi}(x) &= \frac{1}{\sqrt{2}} J_{|\frac{1}{2}, -\frac{1}{2}}^{D^0}(x) J_{|\frac{1}{2}, \frac{1}{2}}^{\Xi^0}(x) + \frac{1}{\sqrt{2}} J_{|\frac{1}{2}, \frac{1}{2}}^{D^+}(x) J_{|\frac{1}{2}, -\frac{1}{2}}^{\Xi^-}(x), \\ J_{[0,0]}^{D\Xi}(x) &= \frac{1}{\sqrt{2}} J_{|\frac{1}{2}, -\frac{1}{2}}^{D^0}(x) J_{|\frac{1}{2}, \frac{1}{2}}^{\Xi^0}(x) - \frac{1}{\sqrt{2}} J_{|\frac{1}{2}, \frac{1}{2}}^{D^+}(x) J_{|\frac{1}{2}, -\frac{1}{2}}^{\Xi^-}(x), \\ J_{|\frac{1}{2}, \pm\frac{1}{2}}^{D_s\Xi}(x) &= J_{[0,0]}^{D_s^+}(x) J_{|\frac{1}{2}, \pm\frac{1}{2}}^{\Xi^{0/-}}(x),\end{aligned}\quad (362)$$

$$\begin{aligned}J_{[1,0]}^{D^*N}(x) &= \frac{1}{\sqrt{2}} J_{|\frac{1}{2}, -\frac{1}{2}}^{D^{*0}}(x) J_{|\frac{1}{2}, \frac{1}{2}}^{N^+}(x) + \frac{1}{\sqrt{2}} J_{|\frac{1}{2}, \frac{1}{2}}^{D^{*+}}(x) J_{|\frac{1}{2}, -\frac{1}{2}}^{N^0}(x), \\ J_{[0,0]}^{D^*N}(x) &= \frac{1}{\sqrt{2}} J_{|\frac{1}{2}, -\frac{1}{2}}^{D^{*0}}(x) J_{|\frac{1}{2}, \frac{1}{2}}^{N^+}(x) - \frac{1}{\sqrt{2}} J_{|\frac{1}{2}, \frac{1}{2}}^{D^{*+}}(x) J_{|\frac{1}{2}, -\frac{1}{2}}^{N^0}(x), \\ J_{[1,0]}^{D^*\Xi}(x) &= \frac{1}{\sqrt{2}} J_{|\frac{1}{2}, -\frac{1}{2}}^{D^{*0}}(x) J_{|\frac{1}{2}, \frac{1}{2}}^{\Xi^0}(x) + \frac{1}{\sqrt{2}} J_{|\frac{1}{2}, \frac{1}{2}}^{D^{*+}}(x) J_{|\frac{1}{2}, -\frac{1}{2}}^{\Xi^-}(x), \\ J_{[0,0]}^{D^*\Xi}(x) &= \frac{1}{\sqrt{2}} J_{|\frac{1}{2}, -\frac{1}{2}}^{D^{*0}}(x) J_{|\frac{1}{2}, \frac{1}{2}}^{\Xi^0}(x) - \frac{1}{\sqrt{2}} J_{|\frac{1}{2}, \frac{1}{2}}^{D^{*+}}(x) J_{|\frac{1}{2}, -\frac{1}{2}}^{\Xi^-}(x), \\ J_{|\frac{1}{2}, \pm\frac{1}{2}}^{D_s^*\Xi}(x) &= J_{[0,0]}^{D_s^{*+}}(x) J_{|\frac{1}{2}, \pm\frac{1}{2}}^{\Xi^{0/-}}(x), \\ J_{[1,0]}^{D\Xi^*}(x) &= \frac{1}{\sqrt{2}} J_{|\frac{1}{2}, -\frac{1}{2}}^{D^0}(x) J_{|\frac{1}{2}, \frac{1}{2}}^{\Xi^{*0}}(x) + \frac{1}{\sqrt{2}} J_{|\frac{1}{2}, \frac{1}{2}}^{D^+}(x) J_{|\frac{1}{2}, -\frac{1}{2}}^{\Xi^{*-}}(x), \\ J_{[0,0]}^{D\Xi^*}(x) &= \frac{1}{\sqrt{2}} J_{|\frac{1}{2}, -\frac{1}{2}}^{D^0}(x) J_{|\frac{1}{2}, \frac{1}{2}}^{\Xi^{*0}}(x) - \frac{1}{\sqrt{2}} J_{|\frac{1}{2}, \frac{1}{2}}^{D^+}(x) J_{|\frac{1}{2}, -\frac{1}{2}}^{\Xi^{*-}}(x), \\ J_{|\frac{1}{2}, \pm\frac{1}{2}}^{D_s\Xi^*}(x) &= J_{[0,0]}^{D_s^+}(x) J_{|\frac{1}{2}, \pm\frac{1}{2}}^{\Xi^{*0/-}}(x),\end{aligned}\quad (363)$$

$$\begin{aligned}
J_{|1,0\rangle}^{D^*\Xi^*}(x) &= \frac{1}{\sqrt{2}}J_{|\frac{1}{2},-\frac{1}{2}\rangle}^{D^{*0}}(x)J_{|\frac{1}{2},\frac{1}{2}\rangle}^{\Xi^{*0}}(x) + \frac{1}{\sqrt{2}}J_{|\frac{1}{2},\frac{1}{2}\rangle}^{D^{*+}}(x)J_{|\frac{1}{2},-\frac{1}{2}\rangle}^{\Xi^{*-}}(x), \\
J_{|0,0\rangle}^{D^*\Xi^*}(x) &= \frac{1}{\sqrt{2}}J_{|\frac{1}{2},-\frac{1}{2}\rangle}^{D^{*0}}(x)J_{|\frac{1}{2},\frac{1}{2}\rangle}^{\Xi^{*0}}(x) - \frac{1}{\sqrt{2}}J_{|\frac{1}{2},\frac{1}{2}\rangle}^{D^{*+}}(x)J_{|\frac{1}{2},-\frac{1}{2}\rangle}^{\Xi^{*-}}(x), \\
J_{|\frac{1}{2},\pm\frac{1}{2}\rangle}^{D_s^*\Xi^*}(x) &= J_{|0,0\rangle}^{D_s^{*+}}(x)J_{|\frac{1}{2},\pm\frac{1}{2}\rangle}^{\Xi^{*0/-}}(x),
\end{aligned} \tag{364}$$

and

$$\begin{aligned}
J_{|\frac{1}{2},-\frac{1}{2}\rangle}^{D^0}(x) &= \bar{u}(x)i\gamma_5c(x), \\
J_{|\frac{1}{2},\frac{1}{2}\rangle}^{D^+}(x) &= -\bar{d}(x)i\gamma_5c(x), \\
J_{|0,0\rangle}^{D_s^+}(x) &= \bar{s}(x)i\gamma_5c(x), \\
J_{|\frac{1}{2},-\frac{1}{2}\rangle}^{D^{*0}}(x) &= \bar{u}(x)\gamma_\mu c(x), \\
J_{|\frac{1}{2},\frac{1}{2}\rangle}^{D^{*+}}(x) &= -\bar{d}(x)\gamma_\mu c(x), \\
J_{|0,0\rangle}^{D_s^{*+}}(x) &= \bar{s}(x)\gamma_\mu c(x),
\end{aligned} \tag{365}$$

$$\begin{aligned}
J_{|\frac{1}{2},\frac{1}{2}\rangle}^{N^+}(x) &= \varepsilon^{ijk}u_i^T(x)C\gamma_\mu u_j(x)\gamma^\mu\gamma_5d_k(x), \\
J_{|\frac{1}{2},-\frac{1}{2}\rangle}^{N^0}(x) &= \varepsilon^{ijk}d_i^T(x)C\gamma_\mu d_j(x)\gamma^\mu\gamma_5u_k(x), \\
J_{|\frac{1}{2},\frac{1}{2}\rangle}^{\Xi^0}(x) &= \varepsilon^{ijk}s_i^T(x)C\gamma_\mu s_j(x)\gamma^\mu\gamma_5u_k(x), \\
J_{|\frac{1}{2},-\frac{1}{2}\rangle}^{\Xi^-}(x) &= \varepsilon^{ijk}s_i^T(x)C\gamma_\mu s_j(x)\gamma^\mu\gamma_5d_k(x), \\
J_{|\frac{1}{2},\frac{1}{2}\rangle}^{\Xi^{*0}}(x) &= \varepsilon^{ijk}s_i^T(x)C\gamma_\mu s_j(x)u_k(x), \\
J_{|\frac{1}{2},-\frac{1}{2}\rangle}^{\Xi^{*-}}(x) &= \varepsilon^{ijk}s_i^T(x)C\gamma_\mu s_j(x)d_k(x),
\end{aligned} \tag{366}$$

the subscripts $|1,0\rangle$, $|0,0\rangle$, $|\frac{1}{2},\frac{1}{2}\rangle$ and $|\frac{1}{2},-\frac{1}{2}\rangle$ are isospin indexes $|I,I_3\rangle$, we choose the convention $|\frac{1}{2},\frac{1}{2}\rangle = -\bar{d}$ [570].

The currents $J(0)$, $J_\mu(0)$ and $J_{\mu\nu}(0)$ couple potentially to the $J^P = \frac{1}{2}^\mp, \frac{3}{2}^\mp$ and $\frac{5}{2}^\mp$ singly-charmed molecular states $P_{\frac{1}{2}}^\mp$, $P_{\frac{3}{2}}^\mp$, and $P_{\frac{5}{2}}^\mp$, respectively,

$$\begin{aligned}
\langle 0|J(0)|P_{\frac{1}{2}}^-(p)\rangle &= \lambda_{\frac{1}{2}}^-U^-(p,s), \\
\langle 0|J(0)|P_{\frac{1}{2}}^+(p)\rangle &= \lambda_{\frac{1}{2}}^+i\gamma_5U^+(p,s), \\
\langle 0|J_\mu(0)|P_{\frac{3}{2}}^-(p)\rangle &= \lambda_{\frac{3}{2}}^-U_\mu^-(p,s), \\
\langle 0|J_\mu(0)|P_{\frac{3}{2}}^+(p)\rangle &= \lambda_{\frac{3}{2}}^+i\gamma_5U_\mu^+(p,s), \\
\langle 0|J_{\mu\nu}(0)|P_{\frac{5}{2}}^-(p)\rangle &= \lambda_{\frac{5}{2}}^-U_{\mu\nu}^-(p,s), \\
\langle 0|J_{\mu\nu}(0)|P_{\frac{5}{2}}^+(p)\rangle &= \lambda_{\frac{5}{2}}^+i\gamma_5U_{\mu\nu}^+(p,s),
\end{aligned} \tag{367}$$

for more details, see Sect.9.1.

At the hadron side, we isolate the ground state hadronic representation,

$$\begin{aligned}
\Pi(p) &= \lambda_{\frac{1}{2}}^{-2} \frac{\not{p} + M_-}{M_-^2 - p^2} + \lambda_{\frac{1}{2}}^{+2} \frac{\not{p} - M_+}{M_+^2 - p^2} + \dots, \\
&= \Pi_{\frac{1}{2}}^1(p^2)\not{p} + \Pi_{\frac{1}{2}}^0(p^2),
\end{aligned} \tag{368}$$

$$\begin{aligned}
\Pi_{\mu\nu}(p) &= \lambda_{\frac{3}{2}}^{-2} \frac{\not{p} + M_-}{M_-^2 - p^2} \left(-g_{\mu\nu} + \frac{\gamma_\mu \gamma_\nu}{3} + \frac{2p_\mu p_\nu}{3p^2} - \frac{p_\mu \gamma_\nu - p_\nu \gamma_\mu}{3\sqrt{p^2}} \right) \\
&\quad + \lambda_{\frac{3}{2}}^{+2} \frac{\not{p} - M_+}{M_+^2 - p^2} \left(-g_{\mu\nu} + \frac{\gamma_\mu \gamma_\nu}{3} + \frac{2p_\mu p_\nu}{3p^2} - \frac{p_\mu \gamma_\nu - p_\nu \gamma_\mu}{3\sqrt{p^2}} \right) + \dots, \\
&= -\Pi_{\frac{3}{2}}^1(p^2) \not{p} g_{\mu\nu} - \Pi_{\frac{3}{2}}^0(p^2) g_{\mu\nu} + \dots, \tag{369}
\end{aligned}$$

$$\begin{aligned}
\Pi_{\mu\nu\alpha\beta}(p) &= \lambda_{\frac{5}{2}}^{+2} \frac{\not{p} + M_+}{M_+^2 - p^2} \left[\frac{\tilde{g}_{\mu\alpha} \tilde{g}_{\nu\beta} + \tilde{g}_{\mu\beta} \tilde{g}_{\nu\alpha}}{2} - \frac{\tilde{g}_{\mu\nu} \tilde{g}_{\alpha\beta}}{5} - \frac{1}{10} (\gamma_\alpha \gamma_\mu + \dots) \tilde{g}_{\nu\beta} + \dots \right] \\
&\quad + \lambda_{\frac{5}{2}}^{-2} \frac{\not{p} - M_-}{M_-^2 - p^2} \left[\frac{\tilde{g}_{\mu\alpha} \tilde{g}_{\nu\beta} + \tilde{g}_{\mu\beta} \tilde{g}_{\nu\alpha}}{2} - \frac{\tilde{g}_{\mu\nu} \tilde{g}_{\alpha\beta}}{5} + \dots \right] + \dots, \\
&= \Pi_{\frac{5}{2}}^1(p^2) \not{p} \frac{g_{\mu\alpha} g_{\nu\beta} + g_{\mu\beta} g_{\nu\alpha}}{2} + \Pi_{\frac{5}{2}}^0(p^2) \frac{g_{\mu\alpha} g_{\nu\beta} + g_{\mu\beta} g_{\nu\alpha}}{2} + \dots. \tag{370}
\end{aligned}$$

We choose the components $\Pi_{\frac{1}{2}}^1(p^2)$, $\Pi_{\frac{1}{2}}^0(p^2)$, $\Pi_{\frac{3}{2}}^1(p^2)$, $\Pi_{\frac{3}{2}}^0(p^2)$, $\Pi_{\frac{5}{2}}^1(p^2)$ and $\Pi_{\frac{5}{2}}^0(p^2)$ to explore the spin-parity $J^P = \frac{1}{2}^-$, $\frac{3}{2}^-$ and $\frac{5}{2}^-$ states, respectively. Again see Sect.9.1 for technical details in tensor analysis.

Again we obtain the spectral densities through dispersion relation,

$$\begin{aligned}
\frac{\text{Im}\Pi_j^1(s)}{\pi} &= \lambda_j^{-2} \delta(s - M_-^2) + \lambda_j^{+2} \delta(s - M_+^2) = \rho_{j,H}^1(s), \\
\frac{\text{Im}\Pi_j^0(s)}{\pi} &= M_- \lambda_j^{-2} \delta(s - M_-^2) - M_+ \lambda_j^{+2} \delta(s - M_+^2) = \rho_{j,H}^0(s), \tag{371}
\end{aligned}$$

where $j = \frac{1}{2}, \frac{3}{2}, \frac{5}{2}$, the subscript H denotes the hadron side, then we introduce the weight functions $\sqrt{s} \exp(-\frac{s}{T^2})$ and $\exp(-\frac{s}{T^2})$ to obtain the QCD sum rules at the hadron side,

$$\int_{m_c^2}^{s_0} ds [\sqrt{s} \rho_{j,H}^1(s) + \rho_{j,H}^0(s)] \exp\left(-\frac{s}{T^2}\right) = 2M_- \lambda_j^{-2} \exp\left(-\frac{M_-^2}{T^2}\right), \tag{372}$$

which are free from contaminations of the positive-parity molecular states.

At the QCD side, we accomplish the operator product expansion with the full light-quark propagators and full heavy-quark propagator up to the vacuum condensates of dimension 13 in a consistent way, and obtain the QCD spectral densities through dispersion relation,

$$\frac{\text{Im}\Pi_j(s)}{\pi} = \not{p} \rho_{j,QCD}^1(s) + \rho_{j,QCD}^0(s), \tag{373}$$

where $j = \frac{1}{2}, \frac{3}{2}, \frac{5}{2}$. See Sect.5.1 for technical details.

At last, we obtain the QCD sum rules,

$$2M_- \lambda_j^{-2} \exp\left(-\frac{M_-^2}{T^2}\right) = \int_{m_c^2}^{s_0} ds [\sqrt{s} \rho_{j,QCD}^1(s) + \rho_{j,QCD}^0(s)] \exp\left(-\frac{s}{T^2}\right). \tag{374}$$

We differentiate Eq.(374) with respect to $\tau = \frac{1}{T^2}$, then eliminate the pole residues to obtain the QCD sum rules for the masses,

$$M_-^2 = \frac{-\frac{d}{d\tau} \int_{m_c^2}^{s_0} ds [\sqrt{s} \rho_{QCD}^1(s) + \rho_{QCD}^0(s)] \exp(-\tau s)}{\int_{m_c^2}^{s_0} ds [\sqrt{s} \rho_{QCD}^1(s) + \rho_{QCD}^0(s)] \exp(-\tau s)}, \tag{375}$$

	J^P	Isospin	μ	$T^2(\text{GeV}^2)$	$\sqrt{s_0}(\text{GeV})$	pole	$ D(13) $
DN	$\frac{1}{2}^-$	0	2.1	1.9 – 2.3	3.45 ± 0.10	(41 – 70)%	4.9%
DN	$\frac{1}{2}^-$	1	2.1	1.9 – 2.3	3.45 ± 0.10	(41 – 70)%	4.9%
$D\Xi$	$\frac{1}{2}^-$	0	2.2	2.3 – 2.7	3.85 ± 0.10	(41 – 67)%	1.2%
$D\Xi$	$\frac{1}{2}^-$	1	2.2	2.3 – 2.7	3.85 ± 0.10	(41 – 67)%	1.2%
$D_s\Xi$	$\frac{1}{2}^-$	$\frac{1}{2}$	2.2	2.4 – 2.8	3.95 ± 0.10	(41 – 65)%	0.9%
D^*N	$\frac{3}{2}^-$	0	2.3	2.1 – 2.5	3.60 ± 0.10	(37 – 64)%	1.2%
D^*N	$\frac{3}{2}^-$	1	2.3	2.1 – 2.5	3.60 ± 0.10	(37 – 64)%	1.2%
$D^*\Xi$	$\frac{3}{2}^-$	0	2.4	2.5 – 2.9	4.00 ± 0.10	(38 – 62)%	0.3%
$D^*\Xi$	$\frac{3}{2}^-$	1	2.4	2.5 – 2.9	4.00 ± 0.10	(38 – 62)%	0.3%
$D_s^*\Xi$	$\frac{3}{2}^-$	$\frac{1}{2}$	2.4	2.5 – 2.9	4.05 ± 0.10	(38 – 62)%	0.3%
$D\Xi^*$	$\frac{3}{2}^-$	0	2.5	2.5 – 2.9	4.10 ± 0.10	(41 – 66)%	0.5%
$D\Xi^*$	$\frac{3}{2}^-$	1	2.5	2.5 – 2.9	4.10 ± 0.10	(41 – 66)%	0.5%
$D_s\Xi^*$	$\frac{3}{2}^-$	$\frac{1}{2}$	2.5	2.6 – 3.0	4.20 ± 0.10	(40 – 64)%	0.5%
$D^*\Xi^*$	$\frac{5}{2}^-$	0	2.6	2.6 – 3.0	4.20 ± 0.10	(41 – 64)%	0.4%
$D^*\Xi^*$	$\frac{5}{2}^-$	1	2.6	2.6 – 3.0	4.20 ± 0.10	(41 – 64)%	0.4%
$D_s^*\Xi^*$	$\frac{5}{2}^-$	$\frac{1}{2}$	2.6	2.8 – 3.2	4.30 ± 0.10	(40 – 63)%	0.2%

Table 60: The spin-parity, isospin, energy scales μ , Borel parameters T^2 , continuum threshold parameters s_0 , pole contributions and vacuum condensates $|D(13)|$ for the charmed pentaquark molecular states.

where the spectral densities $\rho_{QCD}^1(s) = \rho_{j,QCD}^1(s)$ and $\rho_{QCD}^0(s) = \rho_{j,QCD}^0(s)$.

We take the quark flavor number $n_f = 4$ and resort to the modified energy scale formula

$$\mu = \sqrt{M_P^2 - M_c^2 - k M_s}, \quad (376)$$

to choose the ideal energy scales of the QCD spectral densities, where $M_P = M_-$, the effective c -quark mass $M_c = 1.82 \text{ GeV}$ and effective s -quark mass $M_s = 0.2 \text{ GeV}$, the k is the number of the s -quark in the currents/states, see Sect.8.1 for details.

Routinely, we obtain the Borel windows, continuum threshold parameters, energy scales of the QCD spectral densities, and the contributions of the $D(13)$, see Table 60, where the pole dominance is well satisfied. On the other hand, the highest dimensional vacuum condensate contributions have the relation $|D(11)| \gg |D(12)| > |D(13)|$, the operator product expansion is convergent very well.

At last, we obtain the masses and pole residues of the pentaquark molecular states, see Table 61. From Tables 60-61, it is obvious that the modified energy scale formula $\mu = \sqrt{M_P^2 - M_c^2 - k M_s}$ is satisfied in most cases. The energy scales $\sqrt{M_P^2 - M_c^2 - 3M_s}$ for the $D_s\Xi$, $D_s^*\Xi$ and $D_s\Xi^*$ states are smaller than the energy scales $\sqrt{M_P^2 - M_c^2 - 2M_s}$ for the corresponding $D\Xi$, $D^*\Xi$ and $D\Xi^*$ states, respectively, we choose the same energy scales $\sqrt{M_P^2 - M_c^2 - 2M_s}$ for those cousins, as larger masses correspond to larger energy scales naively.

The predicted masses $2.81_{-0.16}^{+0.13} \text{ GeV}$ and $3.19_{-0.13}^{+0.11} \text{ GeV}$ for the DN and $D\Xi$ molecular states with the $J^P = \frac{1}{2}^-$ support assigning the $\Sigma_c(2800)$ and $\Omega_c(3185)$ as the DN and $D\Xi$ molecule states, respectively. The predicted mass $3.35_{-0.13}^{+0.11} \text{ GeV}$ of the $D^*\Xi$ molecular state with the $J^P = \frac{3}{2}^-$ supports assigning the $\Omega_c(3327)$ as the $D^*\Xi$ molecular state. The predicted mass $2.96_{-0.13}^{+0.14} \text{ GeV}$ for the D^*N molecular state is consistent with the $\Lambda_c(2940)/\Lambda_c(2910)$ within uncertainties, which does not exclude the possibility that they are molecular states.

	J^P	Isospin	$M(\text{GeV})$	$\lambda(10^{-4}\text{GeV}^6)$	Thresholds (MeV)	Assignments
DN	$\frac{1}{2}^-$	0	$2.81^{+0.13}_{-0.16}$	$7.98^{+1.98}_{-1.56}$	2806	
DN	$\frac{1}{2}^-$	1	$2.81^{+0.13}_{-0.16}$	$7.98^{+1.98}_{-1.56}$	2806	? $\Sigma_c(2800)$
$D\Xi$	$\frac{1}{2}^-$	0	$3.19^{+0.11}_{-0.13}$	$14.22^{+2.74}_{-2.40}$	3186	? $\Omega_c(3185)$
$D\Xi$	$\frac{1}{2}^-$	1	$3.19^{+0.11}_{-0.13}$	$14.22^{+2.74}_{-2.40}$	3186	
$D_s\Xi$	$\frac{1}{2}^-$	$\frac{1}{2}$	$3.28^{+0.12}_{-0.12}$	$16.04^{+3.04}_{-2.66}$	3287	
D^*N	$\frac{3}{2}^-$	0	$2.96^{+0.13}_{-0.14}$	$8.87^{+1.84}_{-1.59}$	2947	?? $\Lambda_c(2940)/\Lambda_c(2910)$
D^*N	$\frac{3}{2}^-$	1	$2.96^{+0.13}_{-0.14}$	$8.87^{+1.84}_{-1.59}$	2947	
$D^*\Xi$	$\frac{3}{2}^-$	0	$3.35^{+0.11}_{-0.13}$	$15.89^{+2.93}_{-2.56}$	3327	? $\Omega_c(3327)$
$D^*\Xi$	$\frac{3}{2}^-$	1	$3.35^{+0.11}_{-0.13}$	$15.89^{+2.93}_{-2.56}$	3327	
$D_s^*\Xi$	$\frac{3}{2}^-$	$\frac{1}{2}$	$3.44^{+0.11}_{-0.11}$	$17.24^{+3.06}_{-2.66}$	3430	
$D\Xi^*$	$\frac{3}{2}^-$	0	$3.41^{+0.11}_{-0.12}$	$10.67^{+1.92}_{-1.68}$	3399	
$D\Xi^*$	$\frac{3}{2}^-$	1	$3.41^{+0.11}_{-0.12}$	$10.67^{+1.92}_{-1.68}$	3399	
$D_s\Xi^*$	$\frac{3}{2}^-$	$\frac{1}{2}$	$3.51^{+0.11}_{-0.13}$	$11.93^{+2.11}_{-1.85}$	3500	
$D^*\Xi^*$	$\frac{5}{2}^-$	0	$3.54^{+0.11}_{-0.12}$	$10.93^{+1.94}_{-1.71}$	3540	
$D^*\Xi^*$	$\frac{5}{2}^-$	1	$3.54^{+0.11}_{-0.12}$	$10.93^{+1.94}_{-1.71}$	3540	
$D_s^*\Xi^*$	$\frac{5}{2}^-$	$\frac{1}{2}$	$3.65^{+0.11}_{-0.11}$	$12.91^{+2.19}_{-1.93}$	3644	

Table 61: The masses, pole residues, (corresponding meson-baryon) thresholds and possible assignments for the charmed pentaquark molecular states.

In Ref.[566], J. R. Zhang studies the $\Sigma_c(2800)$ and $\Lambda_c(2940)$ as the S -wave DN and D^*N molecule candidates respectively with the QCD sum rules, obtains the masses 3.64 ± 0.33 GeV and 3.73 ± 0.35 GeV for the S -wave DN state with the $J^P = \frac{1}{2}^-$ and S -wave D^*N state with the $J^P = \frac{3}{2}^-$, respectively, which are somewhat bigger than the experimental data for the $\Sigma_c(2800)$ and $\Lambda_c(2940)$, respectively, and differ from the present calculations significantly. J. R. Zhang chooses **Scheme II**, while we choose **Scheme I**.

Taking the $D\Xi$ ($D^*\Xi$) pentaquark molecular states with the $J^P = \frac{1}{2}^-$ ($\frac{3}{2}^-$) as an example, we obtain a symmetric isotriplet $|1, 1\rangle$, $|1, 0\rangle$, $|1, -1\rangle$ and an antisymmetric isosinglet $|0, 0\rangle$. The $\Omega_c(3185)$ ($\Omega_c(3327)$) is a good candidate for the $D\Xi$ ($D^*\Xi$) molecular state with the isospin $|0, 0\rangle$. We expect to search for the molecular states with the isospin $|1, 1\rangle$ and $|1, -1\rangle$ in the $\Xi_c^+ \bar{K}^0$ and $\Xi_c^0 \bar{K}^-$ mass spectra respectively to shed light on the nature of the $\Omega_c(3185)$ ($\Omega_c(3327)$).

Other interpretations also exist, the $\Sigma_c(2800)$ could be assigned as overlap of the $\Sigma_c(2813)$ and $\Sigma_c(2840)$ [571] or P-wave charmed baryon state with the $J^P = \frac{1}{2}^- / \frac{3}{2}^- / \frac{5}{2}^-$ [572, 573, 574]. Cheng et al suggest that the $\Sigma_c(2800)$ is not possible to be $J^P = \frac{1}{2}^-$ charmed baryon state [575]. The $\Lambda_c(2940)^+$ is most likely to be the $J^P = \frac{1}{2}^-$ or $\frac{3}{2}^-$ (2P) state [575, 576, 577]. And the $\Lambda_c(2910)^+$ is probably the $J^P = \frac{1}{2}^-$ (2P) [578] or $\frac{5}{2}^-$ (1P) state [579]. The $\Omega_c(3185)$ lies in the region of the 2S state [580, 581], while the $\Omega_c(3327)$ is a good candidate for the 2S Ω_c state [581] or D-wave Ω_c baryon state with the $J^P = \frac{1}{2}^+ / \frac{3}{2}^+ / \frac{5}{2}^+$ [580, 582, 583].

In Ref.[?], we study the axialvector-diquark-scalar-diquark-antiquark type charmed pentaquark states with $J^P = \frac{3}{2}^\pm$ with the QCD sum rules by carrying out the operator product expansion up to the vacuum condensates of dimension 13 in a consistent way. In calculations, we separate the contributions of the negative parity and positive parity pentaquark states unambiguously, and choose three sets input parameters to study the masses and pole residues of the charmed pentaquark states $uuuc\bar{u}$ and $sssc\bar{s}$ in details. Then we estimate the masses of the charmed pentaquark states

$ssuc\bar{u}$, $susc\bar{u}$, $ssdc\bar{d}$ and $sdsd\bar{c}$ with $J^P = \frac{3}{2}^-$ to be 3.15 ± 0.13 GeV according to the $SU(3)$ breaking effects, which is compatible with the $\Omega_c(3050)$, $\Omega_c(3066)$, $\Omega_c(3090)$, $\Omega_c(3119)$.

With a simple replacement $c \rightarrow b$, we obtain the corresponding QCD sum rules for the single-bottom pentaquark molecular states, see Eqs.(374)-(375). In Ref.[584], we choose the current

$$J(x) = \bar{u}(x)i\gamma_5 s(x)\varepsilon^{ijk}u_i^T(x)C\gamma_\alpha d_j(x)\gamma^\alpha\gamma_5 b_k(x), \quad (377)$$

to interpolate the molecular states with the $J^P = \frac{1}{2}^\pm$, the prediction supports assigning the $\Xi_b(6227)$ as the pentaquark molecular state with the $J^P = \frac{1}{2}^-$.

In Ref.[585], we construct the $\mathbf{\bar{3}\bar{3}\bar{3}}$ type currents,

$$\begin{aligned} J_{SS}(x) &= \varepsilon^{ila}\varepsilon^{ijk}\varepsilon^{lmn}s_j^T(x)C\gamma_5 u_k(x)s_m^T(x)C\gamma_5 c_n(x)C\bar{u}_a^T(x), \\ J_{AA}(x) &= \varepsilon^{ila}\varepsilon^{ijk}\varepsilon^{lmn}s_j^T(x)C\gamma_\mu u_k(x)s_m^T(x)C\gamma^\mu c_n(x)C\bar{u}_a^T(x), \end{aligned} \quad (378)$$

to interpolate the charmed pentaquark states $susc\bar{u}$ with the $J^P = \frac{1}{2}^\pm$. The predicted support assigning the excited Ω_c states from the LHCb collaboration as the $\bar{S}\bar{S}$ or $\bar{A}\bar{A}$ -type pentaquark states with the $J^P = \frac{1}{2}^-$ and the mass about 3.08 GeV. We group the quark flavors as $[su][sc]\bar{u}$ to construct the currents, if we group the quark flavors as $[ss][cu]\bar{u}$, the $\bar{S}\bar{S}$ -type current will vanish due to Fermi-Dirac statistics, but the $\bar{A}\bar{A}$ -type current survives and leads to almost degenerated mass according to the $SU(3)$ symmetry.

In Ref.[586], we study the $\mathbf{\bar{3}\bar{3}\bar{3}}$ type charmed pentaquark states with the $J^P = \frac{3}{2}^\pm$ via the QCD sum rules. We distinguish the isospins in constructing the interpolating currents via two clusters, a diquark $q_j^T C\gamma_\mu q_k'' (D_i)$ plus a triquark $q_m''' C\gamma_5 c_n C\bar{q}_a^T (T_{mna})$, which have the properties,

$$\begin{aligned} \hat{I}^2 \varepsilon_{ijk}q_j^T C\gamma_\mu q_k' &= 1(1+1)\varepsilon_{ijk}q_j^T C\gamma_\mu q_k', \\ \hat{I}^2 \varepsilon_{ijk}q_j^T C\gamma_\mu s_j &= \frac{1}{2}\left(\frac{1}{2}+1\right)\varepsilon_{ijk}q_j^T C\gamma_\mu s_j, \\ \hat{I}^2 \varepsilon_{ijk}s_j^T C\gamma_\mu s_j' &= 0(0+1)\varepsilon_{ijk}s_j^T C\gamma_\mu s_j', \\ \hat{I}^2 u_m^T C\gamma_5 c_n C\bar{d}_a^T &= 1(1+1)u_m^T C\gamma_5 c_n C\bar{d}_a^T, \\ \hat{I}^2 d_m^T C\gamma_5 c_n C\bar{u}_a^T &= 1(1+1)d_m^T C\gamma_5 c_n C\bar{u}_a^T, \\ \hat{I}^2 [u_m^T C\gamma_5 c_n C\bar{u}_a^T - d_m^T C\gamma_5 c_n C\bar{d}_a^T] &= 1(1+1)[u_m^T C\gamma_5 c_n C\bar{u}_a^T - d_m^T C\gamma_5 c_n C\bar{d}_a^T], \\ \hat{I}^2 [u_m^T C\gamma_5 c_n C\bar{u}_a^T + d_m^T C\gamma_5 c_n C\bar{d}_a^T] &= 0(0+1)[u_m^T C\gamma_5 c_n C\bar{u}_a^T + d_m^T C\gamma_5 c_n C\bar{d}_a^T], \\ \hat{I}^2 q_m^T C\gamma_5 c_n C\bar{s}_a^T &= \frac{1}{2}\left(\frac{1}{2}+1\right)q_m^T C\gamma_5 c_n C\bar{s}_a^T, \\ \hat{I}^2 s_m^T C\gamma_5 c_n C\bar{q}_a^T &= \frac{1}{2}\left(\frac{1}{2}+1\right)s_m^T C\gamma_5 c_n C\bar{q}_a^T, \\ \hat{I}^2 s_m^T C\gamma_5 c_n C\bar{s}_a^T &= 0(0+1)s_m^T C\gamma_5 c_n C\bar{s}_a^T, \end{aligned} \quad (379)$$

with $q, q' = u, d$, the \hat{I}^2 is the isospin operator. The diquark clusters D_i and triquark clusters T_{mna} have the isospins $I = 1, \frac{1}{2}$ or 0. We could obtain some mass relations based on the $SU(3)$ breaking effects of the u, d, s quarks, the mass relation among the diquark clusters D_i is $m_{I=0} - m_{I=\frac{1}{2}} = m_{I=\frac{1}{2}} - m_{I=1}$, while the mass relation among the triquark clusters T_{mna} is $m_{I=0} - m_{I=\frac{1}{2}} = m_{I=\frac{1}{2}} - m_{I=1}$, if the hidden-flavor (for u and d) isospin singlet $u_m^T C\gamma_5 c_n C\bar{u}_a^T + d_m^T C\gamma_5 c_n C\bar{d}_a^T$ is excluded. Moreover, the isospin triplet $u_m^T C\gamma_5 c_n C\bar{u}_a^T - d_m^T C\gamma_5 c_n C\bar{d}_a^T$ and isospin singlet $u_m^T C\gamma_5 c_n C\bar{u}_a^T + d_m^T C\gamma_5 c_n C\bar{d}_a^T$ are expected to have degenerate masses, which can be inferred from the tiny mass difference between the vector mesons $\rho^0(770)$ and $\omega(780)$. In fact, if we choose the currents $J_\mu(x) = \bar{u}(x)\gamma_\mu u(x) - \bar{d}(x)\gamma_\mu d(x)$ and $\bar{u}(x)\gamma_\mu u(x) + \bar{d}(x)\gamma_\mu d(x)$ to interpolate the $\rho^0(770)$ and $\omega(780)$, respectively, we obtain the same QCD sum rules.

We write down the currents explicitly,

$$J_{q'q''q'''_{\bar{q},\mu}(x)} = \varepsilon^{ila}\varepsilon^{ijk}\varepsilon^{lmn}q_j'^T(x)C\gamma_\mu q_k''(x)q_m'''T(x)C\gamma_5 c_n(x)C\bar{q}_a^T(x), \quad (381)$$

and study the charmed pentaquark states $uuuc\bar{u}$ and $sssc\bar{s}$ with the QCD sum rules in details. Then we estimate the masses of the charmed pentaquark states $ssuc\bar{u}$, $susc\bar{u}$, $ssdc\bar{d}$ and $sdsc\bar{d}$ with $J^P = \frac{3}{2}^-$ to be 3.15 ± 0.13 GeV according to the $SU(3)$ breaking effects, which is compatible with the experimental values of the masses of the $\Omega_c(3050)$, $\Omega_c(3066)$, $\Omega_c(3090)$, $\Omega_c(3119)$.

11 Strong decays of exotic states

In Refs.[587, 588], we suggest rigorous quark-hadron duality to calculate the hadronic coupling constants in the two-body strong decays of the tetraquark states with the QCD sum rules. At first, we write down the three-point correlation functions $\Pi(p, q)$ firstly,

$$\Pi(p, q) = i^2 \int d^4x d^4y e^{ipx} e^{iqy} \langle 0 | T \left\{ J_B(x) J_C(y) J_A^\dagger(0) \right\} | 0 \rangle, \quad (382)$$

where the currents $J_A(0)$ interpolate the tetraquark states A , the $J_B(x)$ and $J_C(y)$ interpolate the conventional mesons B and C , respectively,

$$\begin{aligned} \langle 0 | J_A(0) | A(p') \rangle &= \lambda_A, \\ \langle 0 | J_B(0) | B(p) \rangle &= \lambda_B, \\ \langle 0 | J_C(0) | C(q) \rangle &= \lambda_C, \end{aligned} \quad (383)$$

the λ_A , λ_B and λ_C are the pole residues or decay constants.

At the hadron side, we insert a complete set of intermediate hadronic states with the same quantum numbers as the current operators $J_A(0)$, $J_B(x)$, $J_C(y)$ into the three-point correlation functions $\Pi(p, q)$ and isolate the ground state contributions to obtain the result [588],

$$\begin{aligned} \Pi(p, q) &= \frac{\lambda_A \lambda_B \lambda_C G_{ABC}}{(m_A^2 - p'^2)(m_B^2 - p^2)(m_C^2 - q^2)} + \frac{1}{(m_A^2 - p'^2)(m_B^2 - p^2)} \int_{s_C^0}^{\infty} dt \frac{\rho_{AC'}(p'^2, p^2, t)}{t - q^2} \\ &+ \frac{1}{(m_A^2 - p'^2)(m_C^2 - q^2)} \int_{s_B^0}^{\infty} dt \frac{\rho_{AB'}(p'^2, t, q^2)}{t - p^2} \\ &+ \frac{1}{(m_B^2 - p^2)(m_C^2 - q^2)} \int_{s_A^0}^{\infty} dt \frac{\rho_{A'B}(t, p^2, q^2) + \rho_{A'C}(t, p^2, q^2)}{t - p'^2} + \dots \\ &= \Pi(p'^2, p^2, q^2), \end{aligned} \quad (384)$$

where $p' = p + q$, the G_{ABC} are the hadronic coupling constants defined by

$$\langle B(p)C(q) | A(p') \rangle = iG_{ABC}, \quad (385)$$

the four functions $\rho_{AC'}(p'^2, p^2, t)$, $\rho_{AB'}(p'^2, t, q^2)$, $\rho_{A'B}(t', p^2, q^2)$ and $\rho_{A'C}(t', p^2, q^2)$ have complex dependence on the transitions between the ground states and the higher resonances or the continuum states.

We rewrite the correlation functions $\Pi_H(p'^2, p^2, q^2)$ at the hadron side as

$$\begin{aligned} \Pi_H(p'^2, p^2, q^2) &= \int_{\Delta^2}^{s_A^0} ds' \int_{\Delta_s^2}^{s_B^0} ds \int_{\Delta_u^2}^{u_C^0} du \frac{\rho_H(s', s, u)}{(s' - p'^2)(s - p^2)(u - q^2)} \\ &+ \int_{s_A^0}^{\infty} ds' \int_{\Delta_s^2}^{s_B^0} ds \int_{\Delta_u^2}^{u_C^0} du \frac{\rho_H(s', s, u)}{(s' - p'^2)(s - p^2)(u - q^2)} + \dots, \end{aligned} \quad (386)$$

through dispersion relation, where the $\rho_H(s', s, u)$ are the hadronic spectral densities,

$$\rho_H(s', s, u) = \lim_{\epsilon_3 \rightarrow 0} \lim_{\epsilon_2 \rightarrow 0} \lim_{\epsilon_1 \rightarrow 0} \frac{\text{Im}_{s'} \text{Im}_s \text{Im}_u \Pi_H(s' + i\epsilon_3, s + i\epsilon_2, u + i\epsilon_1)}{\pi^3}, \quad (387)$$

where the Δ_s^2 and Δ_u^2 are the thresholds, the s_A^0, s_B^0, u_C^0 are the continuum thresholds.

Now we carry out the operator product expansion at the QCD side, and write the correlation functions $\Pi_{QCD}(p'^2, p^2, q^2)$ as

$$\Pi_{QCD}(p'^2, p^2, q^2) = \int_{\Delta_s^2}^{s_B^0} ds \int_{\Delta_u^2}^{u_C^0} du \frac{\rho_{QCD}(p'^2, s, u)}{(s-p^2)(u-q^2)} + \dots, \quad (388)$$

through dispersion relation, where the $\rho_{QCD}(p'^2, s, u)$ are the QCD spectral densities,

$$\rho_{QCD}(p'^2, s, u) = \lim_{\epsilon_2 \rightarrow 0} \lim_{\epsilon_1 \rightarrow 0} \frac{\text{Im}_s \text{Im}_u \Pi_{QCD}(p'^2, s + i\epsilon_2, u + i\epsilon_1)}{\pi^2}. \quad (389)$$

However, the QCD spectral densities $\rho_{QCD}(s', s, u)$ do not exist,

$$\begin{aligned} \rho_{QCD}(s', s, u) &= \lim_{\epsilon_3 \rightarrow 0} \lim_{\epsilon_2 \rightarrow 0} \lim_{\epsilon_1 \rightarrow 0} \frac{\text{Im}_{s'} \text{Im}_s \text{Im}_u \Pi_{QCD}(s' + i\epsilon_3, s + i\epsilon_2, u + i\epsilon_1)}{\pi^3} \\ &= 0, \end{aligned} \quad (390)$$

because

$$\lim_{\epsilon_3 \rightarrow 0} \frac{\text{Im}_{s'} \Pi_{QCD}(s' + i\epsilon_3, p^2, q^2)}{\pi} = 0. \quad (391)$$

Thereafter we will write the QCD spectral densities $\rho_{QCD}(p'^2, s, u)$ as $\rho_{QCD}(s, u)$ for simplicity.

We match the hadron side of the correlation functions with the QCD side of the correlation functions, and carry out the integral over ds' firstly to obtain the solid duality [587],

$$\int_{\Delta_s^2}^{s_B^0} ds \int_{\Delta_u^2}^{u_C^0} du \frac{\rho_{QCD}(s, u)}{(s-p^2)(u-q^2)} = \int_{\Delta_s^2}^{s_B^0} ds \int_{\Delta_u^2}^{u_C^0} du \frac{1}{(s-p^2)(u-q^2)} \left[\int_{\Delta^2}^{\infty} ds' \frac{\rho_H(s', s, u)}{s' - p'^2} \right], \quad (392)$$

the Δ^2 denotes the thresholds $(\Delta_s + \Delta_u)^2$. Now we write down the quark-hadron duality explicitly,

$$\begin{aligned} \int_{\Delta_s^2}^{s_B^0} ds \int_{\Delta_u^2}^{u_C^0} du \frac{\rho_{QCD}(s, u)}{(s-p^2)(u-q^2)} &= \int_{\Delta_s^2}^{s_B^0} ds \int_{\Delta_u^2}^{u_C^0} du \int_{\Delta^2}^{\infty} ds' \frac{\rho_H(s', s, u)}{(s' - p'^2)(s - p^2)(u - q^2)} \\ &= \frac{\lambda_A \lambda_B \lambda_C G_{ABC}}{(m_A^2 - p'^2)(m_B^2 - p^2)(m_C^2 - q^2)} + \frac{C_{A'B} + C_{A'C}}{(m_B^2 - p^2)(m_C^2 - q^2)}. \end{aligned} \quad (393)$$

No approximation is needed, we do not need the continuum threshold parameter s_A^0 in the s' channel, as we match the hadron side with the QCD side below the continuum thresholds s_0 and u_0 to obtain rigorous quark-hadron duality, and we take account of the continuum contributions in the s' channel.

In Ref.[383, 589], Nielsen et al approximate the hadron side of the correlation functions as

$$\Pi_H(p'^2, p^2, q^2) = \frac{\lambda_A \lambda_B \lambda_C G_{ABC}}{(m_A^2 - p'^2)(m_B^2 - p^2)(m_C^2 - q^2)} + \frac{B_H}{(s'_0 - p'^2)(m_C^2 - q^2)}, \quad (394)$$

then match them with the QCD side below the continuum threshold s_0 by taking the chiral limit $m_C^2 \rightarrow 0$ and $q^2 \rightarrow 0$ sequentially, where the B_H stand for the pole-continuum transitions, and

we have changed their notations into the present form for convenience. Although Nielsen et al take account of the continuum contributions by introducing a parameter s'_0 in the s' channel phenomenologically, they neglect the continuum contributions in the u channel at the hadron side by hand. Such an approximation is also adopted in Refs.[43, 590, 591, 592].

There is another scheme to study the strong hadronic coupling constants with the correlation functions $\Pi(p, p')$,

$$\Pi(p, p') = i^2 \int d^4x d^4y e^{-ipx} e^{ip'y} \langle 0 | T \left\{ J_B(y) J_C(0) J_A^\dagger(x) \right\} | 0 \rangle. \quad (395)$$

At the QCD side, a double dispersion relation,

$$\Pi(p^2, p'^2, q^2) = \int_{\Delta_s^2}^{s_0} ds \int_{\Delta_{s'}^2}^{s'_0} ds' \frac{\rho(s, s', q^2)}{(s - p^2)(s' - p'^2)} + \dots, \quad (396)$$

with $q = p' - p$ is adopted [402, 409]. However, we cannot obtain the QCD spectral densities $\rho(s, s', q^2)$. Such a scheme is also adopted in the case of pentaquark states [593, 594].

We can introduce the parameters $C_{AC'}$, $C_{AB'}$, $C_{A'B}$ and $C_{A'C}$ to parameterize the net effects,

$$\begin{aligned} C_{AC'} &= \int_{s_C^0}^{\infty} dt \frac{\rho_{AC'}(p'^2, p^2, t)}{t - q^2}, \\ C_{AB'} &= \int_{s_B^0}^{\infty} dt \frac{\rho_{AB'}(p'^2, t, q^2)}{t - p^2}, \\ C_{A'B} &= \int_{s_A^0}^{\infty} dt \frac{\rho_{A'B}(t, p^2, q^2)}{t - p'^2}, \\ C_{A'C} &= \int_{s_A^0}^{\infty} dt \frac{\rho_{A'C}(t, p^2, q^2)}{t - p'^2}. \end{aligned} \quad (397)$$

In numerical calculations, we take the relevant functions $C_{A'B}$ and $C_{A'C}$ as free parameters, and choose suitable values to eliminate the contaminations from the higher resonances and continuum states to obtain the stable QCD sum rules with the variations of the Borel parameters.

If the B are charmonium or bottomonium states, we set $p'^2 = p^2$ and perform the double Borel transform with respect to the variables $P^2 = -p^2$ and $Q^2 = -q^2$, respectively to obtain the QCD sum rules,

$$\begin{aligned} &\frac{\lambda_A \lambda_B \lambda_C G_{ABC}}{m_A^2 - m_B^2} \left[\exp\left(-\frac{m_B^2}{T_1^2}\right) - \exp\left(-\frac{m_A^2}{T_1^2}\right) \right] \exp\left(-\frac{m_C^2}{T_2^2}\right) + \\ &(C_{A'B} + C_{A'C}) \exp\left(-\frac{m_B^2}{T_1^2} - \frac{m_C^2}{T_2^2}\right) = \int_{\Delta_s^2}^{s_B^0} ds \int_{\Delta_u^2}^{u_C^0} du \rho_{QCD}(s, u) \exp\left(-\frac{s}{T_1^2} - \frac{u}{T_2^2}\right) \end{aligned} \quad (398)$$

where the T_1^2 and T_2^2 are the Borel parameters. If the B are open-charm or open-bottom mesons, we set $p'^2 = 4p^2$ and perform the double Borel transform with respect to the variables $P^2 = -p^2$ and $Q^2 = -q^2$, respectively to obtain the QCD sum rules,

$$\begin{aligned} &\frac{\lambda_A \lambda_B \lambda_C G_{ABC}}{4(\tilde{m}_A^2 - m_B^2)} \left[\exp\left(-\frac{m_B^2}{T_1^2}\right) - \exp\left(-\frac{\tilde{m}_A^2}{T_1^2}\right) \right] \exp\left(-\frac{m_C^2}{T_2^2}\right) + \\ &(C_{A'B} + C_{A'C}) \exp\left(-\frac{m_B^2}{T_1^2} - \frac{m_C^2}{T_2^2}\right) = \int_{\Delta_s^2}^{s_B^0} ds \int_{\Delta_u^2}^{u_C^0} du \rho_{QCD}(s, u) \exp\left(-\frac{s}{T_1^2} - \frac{u}{T_2^2}\right) \end{aligned} \quad (399)$$

where $\tilde{m}_A^2 = \frac{m_A^2}{4}$. Or set $p'^2 = p^2$, just like in the first case. The scheme based on the rigorous quark-hadron duality is adopted in Refs.[58, 163, 595, 596, 597, 598, 599, 600, 601, 602, 603, 604].

11.1 Strong decays of the $Y(4500)$ as an example

In this sub-section, we would like use a typical example to illustrate the procedure in details.

After Ref.[455] was published, the $Y(4500)$ was observed by the BESIII collaboration [147, 148, 151]. At the energy about 4.5 GeV, we obtain three hidden-charm tetraquark states with the $J^{PC} = 1^{--}$, the $[uc]_{\bar{V}}[\bar{u}\bar{c}]_A + [dc]_{\bar{V}}[\bar{d}\bar{c}]_A - [uc]_A[\bar{u}\bar{c}]_{\bar{V}} - [dc]_A[\bar{d}\bar{c}]_{\bar{V}}$, $[uc]_{\bar{A}}[\bar{u}\bar{c}]_V + [dc]_{\bar{A}}[\bar{d}\bar{c}]_V + [uc]_V[\bar{u}\bar{c}]_{\bar{A}} + [dc]_V[\bar{d}\bar{c}]_{\bar{A}}$ and $[uc]_S[\bar{u}\bar{c}]_{\bar{V}} + [dc]_S[\bar{d}\bar{c}]_{\bar{V}} - [uc]_{\bar{V}}[\bar{u}\bar{c}]_S - [dc]_{\bar{V}}[\bar{d}\bar{c}]_S$ tetraquark states have the masses 4.53 ± 0.07 GeV, 4.48 ± 0.08 GeV and 4.50 ± 0.09 GeV, respectively [455], see Table 22. In Ref.[458], we study their two-body strong decays systematically,

$$\Pi_{\mu}^{\bar{D}D\bar{A}V}(p, q) = i^2 \int d^4x d^4y e^{ip \cdot x} e^{iq \cdot y} \langle 0 | T \left\{ J^{\bar{D}}(x) J^D(y) J_{-, \mu}^{\bar{A}V \dagger}(0) \right\} | 0 \rangle, \quad (400)$$

$$\Pi_{\alpha\mu}^{\bar{D}^*D\bar{A}V}(p, q) = i^2 \int d^4x d^4y e^{ip \cdot x} e^{iq \cdot y} \langle 0 | T \left\{ J_{\alpha}^{\bar{D}^*}(x) J^D(y) J_{-, \mu}^{\bar{A}V \dagger}(0) \right\} | 0 \rangle, \quad (401)$$

$$\Pi_{\alpha\beta\mu}^{\bar{D}^*D^*\bar{A}V}(p, q) = i^2 \int d^4x d^4y e^{ip \cdot x} e^{iq \cdot y} \langle 0 | T \left\{ J_{\alpha}^{\bar{D}^*}(x) J_{\beta}^{D^*}(y) J_{-, \mu}^{\bar{A}V \dagger}(0) \right\} | 0 \rangle, \quad (402)$$

$$\Pi_{\alpha\mu}^{\bar{D}_0D^*\bar{A}V}(p, q) = i^2 \int d^4x d^4y e^{ip \cdot x} e^{iq \cdot y} \langle 0 | T \left\{ J^{\bar{D}_0}(x) J_{\alpha}^{D^*}(y) J_{-, \mu}^{\bar{A}V \dagger}(0) \right\} | 0 \rangle, \quad (403)$$

$$\Pi_{\alpha\mu}^{\bar{D}_1D\bar{A}V}(p, q) = i^2 \int d^4x d^4y e^{ip \cdot x} e^{iq \cdot y} \langle 0 | T \left\{ J_{\alpha}^{\bar{D}_1}(x) J^D(y) J_{-, \mu}^{\bar{A}V \dagger}(0) \right\} | 0 \rangle, \quad (404)$$

$$\Pi_{\alpha\mu}^{\eta_c\omega\bar{A}V}(p, q) = i^2 \int d^4x d^4y e^{ip \cdot x} e^{iq \cdot y} \langle 0 | T \left\{ J^{\eta_c}(x) J_{\alpha}^{\omega}(y) J_{-, \mu}^{\bar{A}V \dagger}(0) \right\} | 0 \rangle, \quad (405)$$

$$\Pi_{\alpha\beta\mu}^{J/\psi\omega\bar{A}V}(p, q) = i^2 \int d^4x d^4y e^{ip \cdot x} e^{iq \cdot y} \langle 0 | T \left\{ J_{\alpha}^{J/\psi}(x) J_{\beta}^{\omega}(y) J_{-, \mu}^{\bar{A}V \dagger}(0) \right\} | 0 \rangle, \quad (406)$$

$$\Pi_{\alpha\mu}^{\chi_{c0}\omega\bar{A}V}(p, q) = i^2 \int d^4x d^4y e^{ip \cdot x} e^{iq \cdot y} \langle 0 | T \left\{ J^{\chi_{c0}}(x) J_{\alpha}^{\omega}(y) J_{-, \mu}^{\bar{A}V \dagger}(0) \right\} | 0 \rangle, \quad (407)$$

$$\Pi_{\alpha\beta\mu}^{\chi_{c1}\omega\bar{A}V}(p, q) = i^2 \int d^4x d^4y e^{ip \cdot x} e^{iq \cdot y} \langle 0 | T \left\{ J_{\alpha}^{\chi_{c1}}(x) J_{\beta}^{\omega}(y) J_{-, \mu}^{\bar{A}V \dagger}(0) \right\} | 0 \rangle, \quad (408)$$

$$\Pi_{\alpha\mu}^{J/\psi f_0\bar{A}V}(p, q) = i^2 \int d^4x d^4y e^{ip \cdot x} e^{iq \cdot y} \langle 0 | T \left\{ J_{\alpha}^{J/\psi}(x) J^{f_0}(y) J_{-, \mu}^{\bar{A}V \dagger}(0) \right\} | 0 \rangle. \quad (409)$$

With the simple replacement $\bar{A}V \rightarrow \tilde{V}A$, we obtain the corresponding correlation functions for the current $J_{-, \mu}^{\tilde{V}A}$.

$$\Pi_{\mu\nu}^{\bar{D}D\tilde{S}\tilde{V}}(p, q) = i^2 \int d^4x d^4y e^{ip \cdot x} e^{iq \cdot y} \langle 0 | T \left\{ J^{\bar{D}}(x) J^D(y) J_{-, \mu\nu}^{\tilde{S}\tilde{V} \dagger}(0) \right\} | 0 \rangle, \quad (410)$$

$$\Pi_{\alpha\mu\nu}^{\bar{D}^*DS\tilde{V}}(p, q) = i^2 \int d^4x d^4y e^{ip \cdot x} e^{iq \cdot y} \langle 0|T \left\{ J_{\alpha}^{\bar{D}^*}(x) J^D(y) J_{-\mu\nu}^{S\tilde{V}\dagger}(0) \right\} |0\rangle, \quad (411)$$

$$\Pi_{\alpha\beta\mu\nu}^{\bar{D}^*D^*S\tilde{V}}(p, q) = i^2 \int d^4x d^4y e^{ip \cdot x} e^{iq \cdot y} \langle 0|T \left\{ J_{\alpha}^{\bar{D}^*}(x) J_{\beta}^{D^*}(y) J_{-\mu\nu}^{S\tilde{V}\dagger}(0) \right\} |0\rangle, \quad (412)$$

$$\Pi_{\alpha\mu\nu}^{\bar{D}_0D^*S\tilde{V}}(p, q) = i^2 \int d^4x d^4y e^{ip \cdot x} e^{iq \cdot y} \langle 0|T \left\{ J^{\bar{D}_0}(x) J_{\alpha}^{D^*}(y) J_{-\mu\nu}^{S\tilde{V}\dagger}(0) \right\} |0\rangle, \quad (413)$$

$$\Pi_{\alpha\mu\nu}^{\bar{D}_1DS\tilde{V}}(p, q) = i^2 \int d^4x d^4y e^{ip \cdot x} e^{iq \cdot y} \langle 0|T \left\{ J_{\alpha}^{\bar{D}_1}(x) J^D(y) J_{-\mu\nu}^{S\tilde{V}\dagger}(0) \right\} |0\rangle, \quad (414)$$

$$\Pi_{\alpha\mu\nu}^{\eta_c\omega S\tilde{V}}(p, q) = i^2 \int d^4x d^4y e^{ip \cdot x} e^{iq \cdot y} \langle 0|T \left\{ J^{\eta_c}(x) J_{\alpha}^{\omega}(y) J_{-\mu\nu}^{S\tilde{V}\dagger}(0) \right\} |0\rangle, \quad (415)$$

$$\Pi_{\alpha\beta\mu\nu}^{J/\psi\omega S\tilde{V}}(p, q) = i^2 \int d^4x d^4y e^{ip \cdot x} e^{iq \cdot y} \langle 0|T \left\{ J_{\alpha}^{J/\psi}(x) J_{\beta}^{\omega}(y) J_{-\mu\nu}^{S\tilde{V}\dagger}(0) \right\} |0\rangle, \quad (416)$$

$$\Pi_{\alpha\mu\nu}^{\chi_{c0}\omega S\tilde{V}}(p, q) = i^2 \int d^4x d^4y e^{ip \cdot x} e^{iq \cdot y} \langle 0|T \left\{ J^{\chi_{c0}}(x) J_{\alpha}^{\omega}(y) J_{-\mu\nu}^{S\tilde{V}\dagger}(0) \right\} |0\rangle, \quad (417)$$

$$\Pi_{\alpha\beta\mu\nu}^{\chi_{c1}\omega S\tilde{V}}(p, q) = i^2 \int d^4x d^4y e^{ip \cdot x} e^{iq \cdot y} \langle 0|T \left\{ J_{\alpha}^{\chi_{c1}}(x) J_{\beta}^{\omega}(y) J_{-\mu\nu}^{S\tilde{V}\dagger}(0) \right\} |0\rangle, \quad (418)$$

$$\Pi_{\alpha\mu\nu}^{J/\psi f_0 S\tilde{V}}(p, q) = i^2 \int d^4x d^4y e^{ip \cdot x} e^{iq \cdot y} \langle 0|T \left\{ J_{\alpha}^{J/\psi}(x) J^{f_0}(y) J_{-\mu\nu}^{S\tilde{V}\dagger}(0) \right\} |0\rangle, \quad (419)$$

where the currents

$$\begin{aligned} J^{\bar{D}}(x) &= \bar{c}(x) i\gamma_5 u(x), \\ J^D(y) &= \bar{u}(y) i\gamma_5 c(y), \\ J_{\alpha}^{\bar{D}^*}(x) &= \bar{c}(x) \gamma_{\alpha} u(x), \\ J_{\beta}^{D^*}(y) &= \bar{u}(y) \gamma_{\beta} c(y), \\ J^{\bar{D}_0}(x) &= \bar{c}(x) u(x), \\ J_{\alpha}^{\bar{D}_1}(x) &= \bar{c}(x) \gamma_{\alpha} \gamma_5 u(x), \end{aligned} \quad (420)$$

$$\begin{aligned} J^{\eta_c}(x) &= \bar{c}(x) i\gamma_5 c(x), \\ J_{\alpha}^{J/\psi}(x) &= \bar{c}(x) \gamma_{\alpha} c(x), \\ J^{\chi_{c0}}(x) &= \bar{c}(x) c(x), \\ J_{\alpha}^{\chi_{c1}}(x) &= \bar{c}(x) \gamma_{\alpha} \gamma_5 c(x), \end{aligned} \quad (421)$$

$$\begin{aligned}
J_\alpha^\omega(y) &= \frac{\bar{u}(y)\gamma_\alpha u(y) + \bar{d}(y)\gamma_\alpha d(y)}{\sqrt{2}}, \\
J^{f_0}(y) &= \frac{\bar{u}(y)u(y) + \bar{d}(y)d(y)}{\sqrt{2}}, \tag{422}
\end{aligned}$$

$$\begin{aligned}
J_{-,\mu}^{\tilde{A}V}(x) &= \frac{\varepsilon^{ijk}\varepsilon^{imn}}{2} \left[u_j^T(x)C\sigma_{\mu\nu}\gamma_5 c_k(x)\bar{u}_m(x)\gamma_5\gamma^\nu C\bar{c}_n^T(x) + d_j^T(x)C\sigma_{\mu\nu}\gamma_5 c_k(x)\bar{d}_m(x)\gamma_5\gamma^\nu C\bar{c}_n^T(x) \right. \\
&\quad \left. + u_j^T(x)C\gamma^\nu\gamma_5 c_k(x)\bar{u}_m(x)\gamma_5\sigma_{\mu\nu}C\bar{c}_n^T(x) + d_j^T(x)C\gamma^\nu\gamma_5 c_k(x)\bar{d}_m(x)\gamma_5\sigma_{\mu\nu}C\bar{c}_n^T(x) \right], \tag{423}
\end{aligned}$$

$$\begin{aligned}
J_{-,\mu}^{\tilde{V}A}(x) &= \frac{\varepsilon^{ijk}\varepsilon^{imn}}{2} \left[u_j^T(x)C\sigma_{\mu\nu}c_k(x)\bar{u}_m(x)\gamma^\nu C\bar{c}_n^T(x) + d_j^T(x)C\sigma_{\mu\nu}c_k(x)\bar{d}_m(x)\gamma^\nu C\bar{c}_n^T(x) \right. \\
&\quad \left. - u_j^T(x)C\gamma^\nu c_k(x)\bar{u}_m(x)\sigma_{\mu\nu}C\bar{c}_n^T(x) - d_j^T(x)C\gamma^\nu c_k(x)\bar{d}_m(x)\sigma_{\mu\nu}C\bar{c}_n^T(x) \right], \tag{424}
\end{aligned}$$

$$\begin{aligned}
J_{-,\mu\nu}^{S\tilde{V}}(x) &= \frac{\varepsilon^{ijk}\varepsilon^{imn}}{2} \left[u_j^T(x)C\gamma_5 c_k(x)\bar{u}_m(x)\sigma_{\mu\nu}C\bar{c}_n^T(x) + d_j^T(x)C\gamma_5 c_k(x)\bar{d}_m(x)\sigma_{\mu\nu}C\bar{c}_n^T(x) \right. \\
&\quad \left. - u_j^T(x)C\sigma_{\mu\nu}c_k(x)\bar{u}_m(x)\gamma_5 C\bar{c}_n^T(x) - d_j^T(x)C\sigma_{\mu\nu}c_k(x)\bar{d}_m(x)\gamma_5 C\bar{c}_n^T(x) \right]. \tag{425}
\end{aligned}$$

According to quark-hadron duality, we obtain the hadron representation and isolate the ground state contributions explicitly,

$$\Pi_\mu^{\bar{D}D\tilde{A}V}(p, q) = \Pi_{\bar{D}D\tilde{A}V}(p'^2, p^2, q^2) i(p - q)_\mu + \dots, \tag{426}$$

$$\Pi_{\alpha\mu}^{\bar{D}^*D\tilde{A}V}(p, q) = \Pi_{\bar{D}^*D\tilde{A}V}(p'^2, p^2, q^2) (-i\varepsilon_{\alpha\mu\lambda\tau}p^\lambda q^\tau) + \dots, \tag{427}$$

$$\Pi_{\alpha\beta\mu}^{\bar{D}^*D^*\tilde{A}V}(p, q) = \Pi_{\bar{D}^*D^*\tilde{A}V}(p'^2, p^2, q^2) (-ig_{\alpha\beta}p_\mu) + \dots, \tag{428}$$

$$\Pi_{\alpha\mu}^{\bar{D}_0D^*\tilde{A}V}(p, q) = \Pi_{\bar{D}_0D^*\tilde{A}V}(p'^2, p^2, q^2) (-ig_{\alpha\mu}p \cdot q) + \dots, \tag{429}$$

$$\Pi_{\alpha\mu}^{\bar{D}_1D\tilde{A}V}(p, q) = \Pi_{\bar{D}_1D\tilde{A}V}(p'^2, p^2, q^2) g_{\alpha\mu} + \dots, \tag{430}$$

$$\Pi_{\alpha\mu}^{\eta_c\omega\tilde{A}V}(p, q) = \Pi_{\eta_c\omega\tilde{A}V}(p'^2, p^2, q^2) (i\varepsilon_{\alpha\mu\lambda\tau}p^\lambda q^\tau) + \dots, \tag{431}$$

$$\Pi_{\alpha\beta\mu}^{J/\psi\omega\tilde{A}V}(p, q) = \Pi_{J/\psi\omega\tilde{A}V}(p'^2, p^2, q^2) (ig_{\alpha\beta}p_\mu) + \dots, \tag{432}$$

$$\Pi_{\alpha\mu}^{\chi_{c0}\omega\tilde{A}V}(p, q) = \Pi_{\chi_{c0}\omega\tilde{A}V}(p'^2, p^2, q^2) ig_{\alpha\mu} + \dots, \tag{433}$$

$$\Pi_{\alpha\beta\mu}^{\chi_{c1}\omega\tilde{A}V}(p, q) = \Pi_{\chi_{c1}\omega\tilde{A}V}(p'^2, p^2, q^2) (\varepsilon_{\alpha\beta\mu\lambda}p^\lambda p \cdot q) + \dots, \tag{434}$$

$$\Pi_{\alpha\mu}^{J/\psi f_0 \tilde{A}V}(p, q) = \Pi_{J/\psi f_0 \tilde{A}V}(p'^2, p^2, q^2) (-ig_{\alpha\mu}) + \dots, \quad (435)$$

other ground state contributions are given in Ref.[458], where

$$\Pi_{\bar{D}D\tilde{A}V}(p'^2, p^2, q^2) = \frac{\lambda_{\bar{D}D\tilde{A}V}}{(m_Y^2 - p'^2)(m_D^2 - p^2)(m_D^2 - q^2)} + \frac{C_{\bar{D}D\tilde{A}V}}{(m_D^2 - p^2)(m_D^2 - q^2)} + \dots, \quad (436)$$

$$\Pi_{\bar{D}^*D\tilde{A}V}(p'^2, p^2, q^2) = \frac{\lambda_{\bar{D}^*D\tilde{A}V}}{(m_Y^2 - p'^2)(m_{D^*}^2 - p^2)(m_D^2 - q^2)} + \frac{C_{\bar{D}^*D\tilde{A}V}}{(m_{D^*}^2 - p^2)(m_D^2 - q^2)} + \dots, \quad (437)$$

$$\Pi_{\bar{D}^*D^*\tilde{A}V}(p'^2, p^2, q^2) = \frac{\lambda_{\bar{D}^*D^*\tilde{A}V}}{(m_Y^2 - p'^2)(m_{D^*}^2 - p^2)(m_{D^*}^2 - q^2)} + \frac{C_{\bar{D}^*D^*\tilde{A}V}}{(m_{D^*}^2 - p^2)(m_{D^*}^2 - q^2)} + \dots, \quad (438)$$

$$\Pi_{\bar{D}_0D^*\tilde{A}V}(p'^2, p^2, q^2) = \frac{\lambda_{\bar{D}_0D^*\tilde{A}V}}{(m_Y^2 - p'^2)(m_{D_0}^2 - p^2)(m_{D^*}^2 - q^2)} + \frac{C_{\bar{D}_0D^*\tilde{A}V}}{(m_{D_0}^2 - p^2)(m_{D^*}^2 - q^2)} + \dots, \quad (439)$$

$$\Pi_{\bar{D}_1D\tilde{A}V}(p'^2, p^2, q^2) = \frac{\lambda_{\bar{D}_1D\tilde{A}V}}{(m_Y^2 - p'^2)(m_{D_1}^2 - p^2)(m_D^2 - q^2)} + \frac{C_{\bar{D}_1D\tilde{A}V}}{(m_{D_1}^2 - p^2)(m_D^2 - q^2)} + \dots, \quad (440)$$

$$\Pi_{\eta_c\omega\tilde{A}V}(p'^2, p^2, q^2) = \frac{\lambda_{\eta_c\omega\tilde{A}V}}{(m_Y^2 - p'^2)(m_{\eta_c}^2 - p^2)(m_\omega^2 - q^2)} + \frac{C_{\eta_c\omega\tilde{A}V}}{(m_{\eta_c}^2 - p^2)(m_\omega^2 - q^2)} + \dots, \quad (441)$$

$$\Pi_{J/\psi\omega\tilde{A}V}(p'^2, p^2, q^2) = \frac{\lambda_{J/\psi\omega\tilde{A}V}}{(m_Y^2 - p'^2)(m_{J/\psi}^2 - p^2)(m_\omega^2 - q^2)} + \frac{C_{J/\psi\omega\tilde{A}V}}{(m_{J/\psi}^2 - p^2)(m_\omega^2 - q^2)} + \dots, \quad (442)$$

$$\Pi_{\chi_{c0}\omega\tilde{A}V}(p'^2, p^2, q^2) = \frac{\lambda_{\chi_{c0}\omega\tilde{A}V}}{(m_Y^2 - p'^2)(m_{\chi_{c0}}^2 - p^2)(m_\omega^2 - q^2)} + \frac{C_{\chi_{c0}\omega\tilde{A}V}}{(m_{\chi_{c0}}^2 - p^2)(m_\omega^2 - q^2)} + \dots, \quad (443)$$

$$\Pi_{\chi_{c1}\omega\tilde{A}V}(p'^2, p^2, q^2) = \frac{\lambda_{\chi_{c1}\omega\tilde{A}V}}{(m_Y^2 - p'^2)(m_{\chi_{c1}}^2 - p^2)(m_\omega^2 - q^2)} + \frac{C_{\chi_{c1}\omega\tilde{A}V}}{(m_{\chi_{c1}}^2 - p^2)(m_\omega^2 - q^2)} + \dots, \quad (444)$$

$$\begin{aligned} \Pi_{J/\psi f_0 \tilde{A}V}(p'^2, p^2, q^2) &= \frac{\lambda_{J/\psi f_0 \tilde{A}V}}{(m_Y^2 - p'^2)(m_{J/\psi}^2 - p^2)(m_{f_0}^2 - q^2)} + \frac{C_{J/\psi f_0 \tilde{A}V}}{(m_{J/\psi}^2 - p^2)(m_{f_0}^2 - q^2)} \\ &+ \dots \end{aligned} \quad (445)$$

With the simple replacements $\tilde{A}V \rightarrow \tilde{V}A$ and $S\tilde{V}$, we obtain the corresponding components $\Pi(p'^2, p^2, q^2)$ for the currents $J_{-, \mu}^{\tilde{V}A}(0)$ and $J_{-, \mu\nu}^{S\tilde{V}}(0)$, except for the component $\Pi_{\eta_c \omega S\tilde{V}}(p'^2, p^2, q^2)$,

$$\begin{aligned} \Pi_{\eta_c \omega S\tilde{V}}(p'^2, p^2, q^2) &= \frac{\lambda_{\eta_c \omega S\tilde{V}}}{(m_Y^2 - p'^2)(m_{\eta_c}^2 - p^2)(m_\omega^2 - q^2)} + \frac{C_{\eta_c \omega S\tilde{V}}}{(m_{\eta_c}^2 - p^2)(m_\omega^2 - q^2)} \\ &+ \frac{\bar{\lambda}_{\eta_c \omega S\tilde{A}}}{(m_X^2 - p'^2)(m_{\eta_c}^2 - p^2)(m_\omega^2 - q^2)} + \dots \end{aligned} \quad (446)$$

Where we introduce the collective notations to simplify the expressions,

$$\begin{aligned} \lambda_{\tilde{D}D\tilde{A}V} &= \frac{f_{\tilde{D}}^2 m_{\tilde{D}}^4}{m_c^2} \lambda_{\tilde{A}V} G_{\tilde{D}D\tilde{A}V}, \\ \lambda_{\tilde{D}^*D\tilde{A}V} &= \frac{f_{\tilde{D}^*} m_{\tilde{D}^*} f_{\tilde{D}} m_{\tilde{D}}^2}{m_c} \lambda_{\tilde{A}V} G_{\tilde{D}^*D\tilde{A}V}, \\ \lambda_{\tilde{D}^*D^*\tilde{A}V} &= f_{\tilde{D}^*}^2 m_{\tilde{D}^*}^2 \lambda_{\tilde{A}V} G_{\tilde{D}^*D^*\tilde{A}V}, \\ \lambda_{\tilde{D}_0D^*\tilde{A}V} &= f_{\tilde{D}_0} m_{\tilde{D}_0} f_{\tilde{D}^*} m_{\tilde{D}^*} \lambda_{\tilde{A}V} G_{\tilde{D}_0D^*\tilde{A}V}, \\ \lambda_{\tilde{D}_1D\tilde{A}V} &= \frac{f_{\tilde{D}_1} m_{\tilde{D}_1} f_{\tilde{D}} m_{\tilde{D}}^2}{m_c} \lambda_{\tilde{A}V} G_{\tilde{D}_1D\tilde{A}V}, \end{aligned} \quad (447)$$

$$\begin{aligned} \lambda_{\eta_c \omega \tilde{A}V} &= \frac{f_{\eta_c} m_{\eta_c}^2 f_\omega m_\omega}{2m_c} \lambda_{\tilde{A}V} G_{\eta_c \omega \tilde{A}V}, \\ \lambda_{J/\psi \omega \tilde{A}V} &= f_{J/\psi} m_{J/\psi} f_\omega m_\omega \lambda_{\tilde{A}V} G_{J/\psi \omega \tilde{A}V} \left(1 + \frac{m_\omega^2}{m_Y^2} - \frac{m_{J/\psi}^2}{m_Y^2} \right), \\ \lambda_{\chi_{c0} \omega \tilde{A}V} &= f_{\chi_{c0}} m_{\chi_{c0}} f_\omega m_\omega \lambda_{\tilde{A}V} G_{\chi_{c0} \omega \tilde{A}V}, \\ \lambda_{\chi_{c1} \omega \tilde{A}V} &= f_{\chi_{c1}} m_{\chi_{c1}} f_\omega m_\omega \lambda_{\tilde{A}V} G_{\chi_{c1} \omega \tilde{A}V}, \\ \lambda_{J/\psi f_0 \tilde{A}V} &= f_{J/\psi} m_{J/\psi} f_{f_0} m_{f_0} \lambda_{\tilde{A}V} G_{J/\psi f_0 \tilde{A}V}. \end{aligned} \quad (448)$$

With the simple replacements $\tilde{A}V \rightarrow \tilde{V}A$ and $S\tilde{V}$, we obtain the collective notations λ for the currents $J_{-, \mu}^{\tilde{V}A}(0)$ and $J_{-, \mu\nu}^{S\tilde{V}}(0)$, except for the $\lambda_{\eta_c \omega S\tilde{V}}$, $\lambda_{J/\psi \omega S\tilde{V}}$, $\lambda_{\chi_{c1} \omega S\tilde{V}}$, where

$$\begin{aligned} \lambda_{\eta_c \omega S\tilde{V}} &= \frac{f_{\eta_c} m_{\eta_c}^2 f_\omega m_\omega^3}{2m_c} \lambda_{S\tilde{V}} G_{\eta_c \omega S\tilde{V}}, \\ \lambda_{J/\psi \omega S\tilde{V}} &= f_{J/\psi} m_{J/\psi} f_\omega m_\omega \lambda_{S\tilde{V}} G_{J/\psi \omega S\tilde{V}}, \\ \lambda_{\chi_{c1} \omega S\tilde{V}} &= f_{\chi_{c1}} m_{\chi_{c1}}^3 f_\omega m_\omega \lambda_{S\tilde{V}} G_{\chi_{c1} \omega S\tilde{V}}, \end{aligned} \quad (449)$$

and

$$\bar{\lambda}_{\eta_c \omega S\tilde{A}} = \frac{f_{\eta_c} m_{\eta_c}^2 f_\omega m_\omega}{2m_c} \bar{\lambda}_{S\tilde{A}} \bar{G}_{\eta_c \omega S\tilde{A}}. \quad (450)$$

And we define the decay constants and pole residues,

$$\begin{aligned} \langle 0 | J^D(0) | D(p) \rangle &= \frac{f_D m_D^2}{m_c}, \\ \langle 0 | J_\alpha^{D^*}(0) | D^*(p) \rangle &= f_{D^*} m_{D^*} \xi_\alpha, \\ \langle 0 | J^{D_0}(0) | D_0(p) \rangle &= f_{D_0} m_{D_0}, \\ \langle 0 | J_\alpha^{D_1}(0) | D_1(p) \rangle &= f_{D_1} m_{D_1} \xi_\alpha, \end{aligned} \quad (451)$$

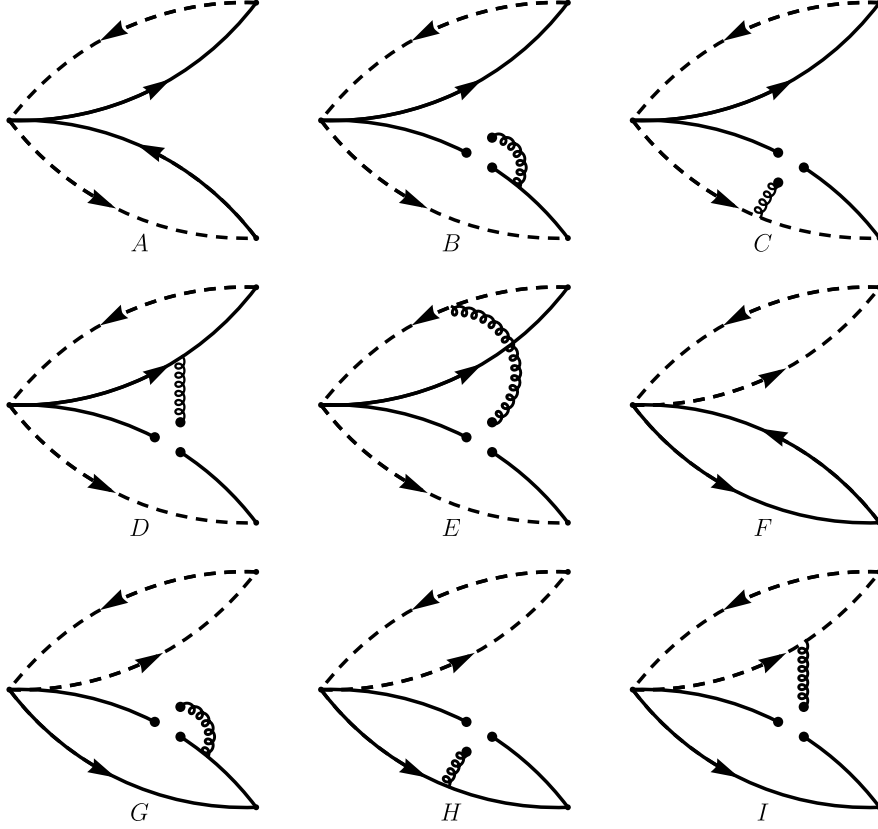


Figure 27: The connected and disconnected Feynman diagrams, where the dashed (solid) lines denote the heavy (light) quark lines, the interchanges of the heavy (light) quark lines are implied.

etc [458]. And we define the hadronic coupling constants,

$$\begin{aligned}
\langle \bar{D}(p)D(q)|Y_{\tilde{A}V}(p')\rangle &= (p-q) \cdot \varepsilon G_{\bar{D}D\tilde{A}V}, \\
\langle \bar{D}(p)D(q)|Y_{\tilde{V}A}(p')\rangle &= (p-q) \cdot \varepsilon G_{\bar{D}D\tilde{V}A}, \\
\langle \bar{D}(p)D(q)|Y_{S\tilde{V}}(p')\rangle &= -i(p-q) \cdot \varepsilon G_{\bar{D}DS\tilde{V}},
\end{aligned} \tag{452}$$

$$\begin{aligned}
\langle \bar{D}^*(p)D(q)|Y_{\tilde{A}V}(p')\rangle &= -\varepsilon^{\lambda\tau\rho\sigma} p_\lambda \xi_\tau^* p'_\rho \varepsilon_\sigma G_{\bar{D}^*D\tilde{A}V}, \\
\langle \bar{D}^*(p)D(q)|Y_{\tilde{V}A}(p')\rangle &= \varepsilon^{\lambda\tau\rho\sigma} p_\lambda \xi_\tau^* p'_\rho \varepsilon_\sigma G_{\bar{D}^*D\tilde{V}A}, \\
\langle \bar{D}^*(p)D(q)|Y_{S\tilde{V}}(p')\rangle &= -i\varepsilon^{\lambda\tau\rho\sigma} p_\lambda \xi_\tau^* p'_\rho \varepsilon_\sigma G_{\bar{D}^*DS\tilde{V}},
\end{aligned} \tag{453}$$

etc [458].

In Eq.(446), there are contributions come from both the $J^{PC} = 1^{+-}$ and 1^{--} tetraquark states, and we cannot choose the pertinent structures to exclude the contaminations from the $J^{PC} = 1^{+-}$ tetraquark state X , so we include it at the hadron side. The unknown parameters $C_{\bar{D}D\tilde{A}V}$, $C_{\bar{D}^*D\tilde{A}V}$, $C_{\bar{D}^*D^*\tilde{A}V}$, etc, parameterize the complex interactions among the excitations in the p'^2 channels and the ground state charmed meson pairs or charmonium plus ω . It is difficult to choose the pertinent tensor structures in Eqs.(426)-(446) to obtain good QCD sum rules without contamination, we have to reach the satisfactory results via trial and error.

At the QCD side, we accomplish the operator product expansion up to the vacuum condensates of dimension 5 and take account of both the connected and disconnected Feynman diagrams in the

color space, see Fig.27 (in Refs.[43, 383, 589, 590, 591], only the connected Feynman diagrams are taken into account, i.e. the D , E and I in Fig.27), and choose the components $\Pi_H(p^2, p^2, q^2)$ to study the hadronic coupling constants G_H based on the rigorous quark-hadron duality [587, 588].

Then we set $p^2 = p^2$ in the components $\Pi(p^2, p^2, q^2)$, and carry out the double Borel transform with respect to the variables $P^2 = -p^2$ and $Q^2 = -q^2$ respectively, and set $T_1^2 = T_2^2 = T^2$ to obtain thirty QCD sum rules,

$$\begin{aligned} & \frac{\lambda_{\bar{D}D\tilde{A}V}}{m_Y^2 - m_D^2} \left[\exp\left(-\frac{m_D^2}{T^2}\right) - \exp\left(-\frac{m_Y^2}{T^2}\right) \right] \exp\left(-\frac{m_D^2}{T^2}\right) + C_{\bar{D}D\tilde{A}V} \exp\left(-\frac{m_D^2}{T^2} - \frac{m_D^2}{T^2}\right) \\ & = \Pi_{\bar{D}D\tilde{A}V}^{QCD}(T^2), \end{aligned} \quad (454)$$

$$\begin{aligned} & \frac{\lambda_{\bar{D}^*D\tilde{A}V}}{m_Y^2 - m_{D^*}^2} \left[\exp\left(-\frac{m_{D^*}^2}{T^2}\right) - \exp\left(-\frac{m_Y^2}{T^2}\right) \right] \exp\left(-\frac{m_{D^*}^2}{T^2}\right) + C_{\bar{D}^*D\tilde{A}V} \exp\left(-\frac{m_{D^*}^2}{T^2} - \frac{m_{D^*}^2}{T^2}\right) \\ & = \Pi_{\bar{D}^*D\tilde{A}V}^{QCD}(T^2), \end{aligned} \quad (455)$$

$$\begin{aligned} & \frac{\lambda_{\bar{D}^*D^*\tilde{A}V}}{m_Y^2 - m_{D^*}^2} \left[\exp\left(-\frac{m_{D^*}^2}{T^2}\right) - \exp\left(-\frac{m_Y^2}{T^2}\right) \right] \exp\left(-\frac{m_{D^*}^2}{T^2}\right) + C_{\bar{D}^*D^*\tilde{A}V} \exp\left(-\frac{m_{D^*}^2}{T^2} - \frac{m_{D^*}^2}{T^2}\right) \\ & = \Pi_{\bar{D}^*D^*\tilde{A}V}^{QCD}(T^2), \end{aligned} \quad (456)$$

$$\begin{aligned} & \frac{\lambda_{\bar{D}_0D^*\tilde{A}V}}{m_Y^2 - m_{D_0}^2} \left[\exp\left(-\frac{m_{D_0}^2}{T^2}\right) - \exp\left(-\frac{m_Y^2}{T^2}\right) \right] \exp\left(-\frac{m_{D_0}^2}{T^2}\right) + C_{\bar{D}_0D^*\tilde{A}V} \exp\left(-\frac{m_{D_0}^2}{T^2} - \frac{m_{D_0}^2}{T^2}\right) \\ & = \Pi_{\bar{D}_0D^*\tilde{A}V}^{QCD}(T^2), \end{aligned} \quad (457)$$

$$\begin{aligned} & \frac{\lambda_{\bar{D}_1D\tilde{A}V}}{m_Y^2 - m_{D_1}^2} \left[\exp\left(-\frac{m_{D_1}^2}{T^2}\right) - \exp\left(-\frac{m_Y^2}{T^2}\right) \right] \exp\left(-\frac{m_{D_1}^2}{T^2}\right) + C_{\bar{D}_1D\tilde{A}V} \exp\left(-\frac{m_{D_1}^2}{T^2} - \frac{m_{D_1}^2}{T^2}\right) \\ & = \Pi_{\bar{D}_1D\tilde{A}V}^{QCD}(T^2), \end{aligned} \quad (458)$$

$$\begin{aligned} & \frac{\lambda_{\eta_c\omega\tilde{A}V}}{m_Y^2 - m_{\eta_c}^2} \left[\exp\left(-\frac{m_{\eta_c}^2}{T^2}\right) - \exp\left(-\frac{m_Y^2}{T^2}\right) \right] \exp\left(-\frac{m_\omega^2}{T^2}\right) + C_{\eta_c\omega\tilde{A}V} \exp\left(-\frac{m_{\eta_c}^2}{T^2} - \frac{m_\omega^2}{T^2}\right) \\ & = \Pi_{\eta_c\omega\tilde{A}V}^{QCD}(T^2), \end{aligned} \quad (459)$$

$$\begin{aligned} & \frac{\lambda_{J/\psi\omega\tilde{A}V}}{m_Y^2 - m_{J/\psi}^2} \left[\exp\left(-\frac{m_{J/\psi}^2}{T^2}\right) - \exp\left(-\frac{m_Y^2}{T^2}\right) \right] \exp\left(-\frac{m_\omega^2}{T^2}\right) + C_{J/\psi\omega\tilde{A}V} \exp\left(-\frac{m_{J/\psi}^2}{T^2} - \frac{m_\omega^2}{T^2}\right) \\ & = \Pi_{J/\psi\omega\tilde{A}V}^{QCD}(T^2), \end{aligned} \quad (460)$$

$$\begin{aligned} & \frac{\lambda_{\chi_{c0}\omega\tilde{A}V}}{m_Y^2 - m_{\chi_{c0}}^2} \left[\exp\left(-\frac{m_{\chi_{c0}}^2}{T^2}\right) - \exp\left(-\frac{m_Y^2}{T^2}\right) \right] \exp\left(-\frac{m_\omega^2}{T^2}\right) + C_{\chi_{c0}\omega\tilde{A}V} \exp\left(-\frac{m_{\chi_{c0}}^2}{T^2} - \frac{m_\omega^2}{T^2}\right) \\ & = \Pi_{\chi_{c0}\omega\tilde{A}V}^{QCD}(T^2), \end{aligned} \quad (461)$$

$$\begin{aligned} & \frac{\lambda_{\chi_{c1}\omega\tilde{A}V}}{m_Y^2 - m_{\chi_{c1}}^2} \left[\exp\left(-\frac{m_{\chi_{c1}}^2}{T^2}\right) - \exp\left(-\frac{m_Y^2}{T^2}\right) \right] \exp\left(-\frac{m_\omega^2}{T^2}\right) + C_{\chi_{c1}\omega\tilde{A}V} \exp\left(-\frac{m_{\chi_{c1}}^2}{T^2} - \frac{m_\omega^2}{T^2}\right) \\ &= \Pi_{\chi_{c1}\omega\tilde{A}V}^{QCD}(T^2), \end{aligned} \quad (462)$$

$$\begin{aligned} & \frac{\lambda_{J/\psi f_0\tilde{A}V}}{m_Y^2 - m_{J/\psi}^2} \left[\exp\left(-\frac{m_{J/\psi}^2}{T^2}\right) - \exp\left(-\frac{m_Y^2}{T^2}\right) \right] \exp\left(-\frac{m_{f_0}^2}{T^2}\right) + C_{J/\psi f_0\tilde{A}V} \exp\left(-\frac{m_{J/\psi}^2}{T^2} - \frac{m_{f_0}^2}{T^2}\right) \\ &= \Pi_{J/\psi f_0\tilde{A}V}^{QCD}(T^2). \end{aligned} \quad (463)$$

With the simple replacements $\tilde{A}V \rightarrow \tilde{V}A$ and $S\tilde{V}$, we obtain the QCD sum rules for the $J_{-\mu}^{\tilde{V}A}(0)$ and $J_{-\mu\nu}^{S\tilde{V}}(0)$, except for the $\eta_c\omega$ channel,

$$\begin{aligned} & \frac{\lambda_{\eta_c\omega S\tilde{V}}}{m_Y^2 - m_{\eta_c}^2} \left[\exp\left(-\frac{m_{\eta_c}^2}{T^2}\right) - \exp\left(-\frac{m_Y^2}{T^2}\right) \right] \exp\left(-\frac{m_\omega^2}{T^2}\right) + C_{\eta_c\omega S\tilde{V}} \exp\left(-\frac{m_{\eta_c}^2}{T^2} - \frac{m_\omega^2}{T^2}\right) \\ &+ \frac{\bar{\lambda}_{\eta_c\omega S\tilde{A}}}{m_X^2 - m_{\eta_c}^2} \left[\exp\left(-\frac{m_{\eta_c}^2}{T^2}\right) - \exp\left(-\frac{m_X^2}{T^2}\right) \right] \exp\left(-\frac{m_\omega^2}{T^2}\right) = \Pi_{\eta_c\omega S\tilde{V}}^{QCD}(T^2), \end{aligned} \quad (464)$$

the explicit expressions of the QCD side are given in Ref.[458].

We take the unknown parameters $C_{\bar{D}D\tilde{A}V}$, $C_{\bar{D}^*D\tilde{A}V}$, $C_{\bar{D}^*D^*\tilde{A}V}$, \dots as free parameters, and adjust the suitable values to obtain flat Borel platforms for the hadronic coupling constants [458],

$$\begin{aligned} C_{\bar{D}D\tilde{A}V} &= 0.00045 \text{ GeV}^5 \times T^2, \\ C_{\bar{D}^*D\tilde{A}V} &= -0.000003 \text{ GeV}^4 \times T^2, \\ C_{\bar{D}^*D^*\tilde{A}V} &= 0.0001 \text{ GeV}^5 \times T^2, \\ C_{\bar{D}_0D^*\tilde{A}V} &= 0.000055 \text{ GeV}^4 \times T^2, \\ C_{\bar{D}_1D\tilde{A}V} &= 0.0031 \text{ GeV}^6 \times T^2, \\ C_{\eta_c\omega\tilde{A}V} &= -0.000082 \text{ GeV}^4 \times T^2, \\ C_{J/\psi\omega\tilde{A}V} &= 0.0, \\ C_{\chi_{c0}\omega\tilde{A}V} &= 0.00085 \text{ GeV}^6 \times T^2, \\ C_{\chi_{c1}\omega\tilde{A}V} &= -0.000019 \text{ GeV}^3 \times T^2, \\ C_{J/\psi f_0\tilde{A}V} &= 0.00085 \text{ GeV}^6 \times T^2, \end{aligned} \quad (465)$$

$$\begin{aligned} C_{\bar{D}D\tilde{V}A} &= 0.0000015 \text{ GeV}^5 \times T^2, \\ C_{\bar{D}^*D\tilde{V}A} &= 0.000038 \text{ GeV}^4 \times T^2, \\ C_{\bar{D}^*D^*\tilde{V}A} &= 0.0000054 \text{ GeV}^5 \times T^2, \\ C_{\bar{D}_0D^*\tilde{V}A} &= 0.00264 \text{ GeV}^6 \times T^2, \\ C_{\bar{D}_1D\tilde{V}A} &= 0.000055 \text{ GeV}^4 \times T^2, \\ C_{\eta_c\omega\tilde{V}A} &= -0.00006 \text{ GeV}^4 \times T^2, \\ C_{J/\psi\omega\tilde{V}A} &= 0.0, \\ C_{\chi_{c0}\omega\tilde{V}A} &= 0.00087 \text{ GeV}^6 \times T^2, \\ C_{\chi_{c1}\omega\tilde{V}A} &= -0.000018 \text{ GeV}^3 \times T^2, \\ C_{J/\psi f_0\tilde{V}A} &= 0.00075 \text{ GeV}^6 \times T^2, \end{aligned} \quad (466)$$

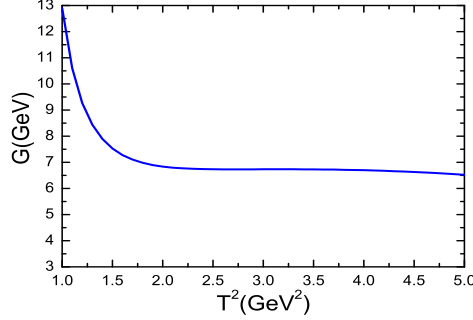


Figure 28: The hadron-coupling constant $G_{\bar{D}_1 D \bar{A} V}$ via the Borel parameter.

$$\begin{aligned}
C_{\bar{D} D S \tilde{V}} &= 0.00014 \text{ GeV}^6 + 0.00002 \text{ GeV}^4 \times T^2, \\
C_{\bar{D}^* D S \tilde{V}} &= 0.0000006 \text{ GeV}^3 \times T^2, \\
C_{\bar{D}^* D^* S \tilde{V}} &= -0.000002 \text{ GeV}^4 \times T^2, \\
C_{\bar{D}_0 D^* S \tilde{V}} &= 0.0012 \text{ GeV}^7 + 0.000164 \text{ GeV}^5 \times T^2, \\
C_{\bar{D}_1 D S \tilde{V}} &= 0.0017 \text{ GeV}^7 + 0.000205 \text{ GeV}^5 \times T^2, \\
C_{\eta_c \omega S \tilde{V}} &= 0.00014 \text{ GeV}^7, \\
\bar{\lambda}_{\eta_c \omega S \tilde{A}} &= 0.0012 \text{ GeV}^7 \times T^2, \\
C_{J/\psi \omega S \tilde{V}} &= -0.0005 \text{ GeV}^6 - 0.0000216 \text{ GeV}^4 \times T^2, \\
C_{\chi_{c0} \omega S \tilde{V}} &= -0.0018 \text{ GeV}^7 - 0.000156 \text{ GeV}^5 \times T^2, \\
C_{\chi_{c1} \omega S \tilde{V}} &= 0.0012 \text{ GeV}^8 + 0.00015 \text{ GeV}^6 \times T^2, \\
C_{J/\psi f_0 S \tilde{V}} &= 0.0005 \text{ GeV}^7 + 0.00006 \text{ GeV}^5 \times T^2,
\end{aligned} \tag{467}$$

the Borel windows are shown explicitly in Table 62. We obtain uniform flat platforms $T_{max}^2 - T_{min}^2 = 1 \text{ GeV}^2$, where the max and min denote the maximum and minimum, respectively. In calculations, we choose quark flavor numbers $n_f = 4$, and evolve all the input parameters to the energy scale $\mu = 1 \text{ GeV}$. For detailed information about the parameters, one can consult Ref.[458].

In Fig.28, we plot the $G_{\bar{D}_1 D \bar{A} V}$ with variation of the Borel parameter at a large interval as an example, in the Borel window, there appears very flat platform indeed.

We estimate the uncertainties of the hadronic coupling constants routinely. For an input parameter ξ , $\xi = \bar{\xi} + \delta\xi$, the left side can be written as $\lambda_{\bar{A} V} f_{\bar{D}} f_D G_{\bar{D} D \bar{A} V} = \bar{\lambda}_{\bar{A} V} \bar{f}_{\bar{D}} \bar{f}_D \bar{G}_{\bar{D} D \bar{A} V} + \delta \lambda_{\bar{A} V} f_{\bar{D}} f_D G_{\bar{D} D \bar{A} V}$, $C_{\bar{D} D \bar{A} V} = \bar{C}_{\bar{D} D \bar{A} V} + \delta C_{\bar{D} D \bar{A} V}$, \dots , where

$$\delta \lambda_{\bar{A} V} f_{\bar{D}} f_D G_{\bar{D} D \bar{A} V} = \bar{\lambda}_{\bar{A} V} \bar{f}_{\bar{D}} \bar{f}_D \bar{G}_{\bar{D} D \bar{A} V} \left(\frac{\delta f_{\bar{D}}}{\bar{f}_{\bar{D}}} + \frac{\delta f_D}{\bar{f}_D} + \frac{\delta \lambda_{\bar{A} V}}{\bar{\lambda}_{\bar{A} V}} + \frac{\delta G_{\bar{D} D \bar{A} V}}{\bar{G}_{\bar{D} D \bar{A} V}} \right), \tag{468}$$

\dots . We set $\delta C_{\bar{D} D \bar{A} V} = 0$, $\frac{\delta f_{\bar{D}}}{\bar{f}_{\bar{D}}} = \frac{\delta f_D}{\bar{f}_D} = \frac{\delta \lambda_{\bar{A} V}}{\bar{\lambda}_{\bar{A} V}} = \frac{\delta G_{\bar{D} D \bar{A} V}}{\bar{G}_{\bar{D} D \bar{A} V}}$, \dots approximately.

After taking into account the uncertainties, we obtain the values of the hadronic coupling constants, which are shown explicitly in Table 62, then we obtain the partial decay widths directly, and show them explicitly in Table 63.

Channels	$T^2(\text{GeV}^2)$	G
$\bar{D}D\tilde{A}V$	3.8 – 4.8	2.11 ± 0.10
$\bar{D}^*D\tilde{A}V$	4.7 – 5.7	$(4.49 \pm 0.15) \times 10^{-2} \text{ GeV}^{-1}$
$\bar{D}^*D^*\tilde{A}V$	4.1 – 5.1	0.95 ± 0.04
$\bar{D}_0D^*\tilde{A}V$	4.4 – 5.4	$0.30 \pm 0.01 \text{ GeV}^{-1}$
$\bar{D}_1D\tilde{A}V$	2.5 – 3.5	$6.73 \pm 0.31 \text{ GeV}$
$\eta_c\omega\tilde{A}V$	3.7 – 4.7	$-(0.35 \pm 0.03) \text{ GeV}^{-1}$
$J/\psi\omega\tilde{A}V$	— — —	0.0
$\chi_{c0}\omega\tilde{A}V$	3.8 – 4.8	$2.72 \pm 0.20 \text{ GeV}$
$\chi_{c1}\omega\tilde{A}V$	5.2 – 6.2	$-(0.25 \pm 0.01) \text{ GeV}^{-2}$
$J/\psi f_0\tilde{A}V$	3.8 – 4.8	$2.51 \pm 0.15 \text{ GeV}$
$\bar{D}D\tilde{V}A$	4.4 – 5.4	$-(4.02 \pm 0.16) \times 10^{-2}$
$\bar{D}^*D\tilde{V}A$	4.0 – 5.0	$0.30 \pm 0.01 \text{ GeV}^{-1}$
$\bar{D}^*D^*\tilde{V}A$	4.6 – 5.6	$-(6.00 \pm 0.20) \times 10^{-2}$
$\bar{D}_0D^*\tilde{V}A$	2.6 – 3.6	$8.00 \pm 0.37 \text{ GeV}$
$\bar{D}_1D\tilde{V}A$	2.8 – 3.8	$0.30 \pm 0.01 \text{ GeV}^{-1}$
$\eta_c\omega\tilde{V}A$	5.3 – 6.3	$-(0.40 \pm 0.03) \text{ GeV}^{-1}$
$J/\psi\omega\tilde{V}A$	— — —	0.0
$\chi_{c0}\omega\tilde{V}A$	3.0 – 4.0	$2.56 \pm 0.19 \text{ GeV}$
$\chi_{c1}\omega\tilde{V}A$	5.4 – 6.4	$-(0.24 \pm 0.01) \text{ GeV}^{-2}$
$J/\psi f_0\tilde{V}A$	4.6 – 5.6	$2.60 \pm 0.15 \text{ GeV}$
$\bar{D}DS\tilde{V}$	2.5 – 3.5	0.60 ± 0.06
$\bar{D}^*DS\tilde{V}$	4.7 – 5.7	$-(7.00 \pm 0.24) \times 10^{-2} \text{ GeV}^{-1}$
$\bar{D}^*D^*S\tilde{V}$	4.0 – 5.0	0.18 ± 0.01
$\bar{D}_0D^*S\tilde{V}$	3.3 – 4.3	$2.23 \pm 0.24 \text{ GeV}$
$\bar{D}_1DS\tilde{V}$	3.5 – 4.5	$4.21 \pm 0.37 \text{ GeV}$
$\eta_c\omega S\tilde{V}$	2.8 – 3.8	$1.71 \pm 0.31 \text{ GeV}^{-1}$
$J/\psi\omega S\tilde{V}$	3.7 – 4.7	$-(1.08 \pm 0.19)$
$\chi_{c0}\omega S\tilde{V}$	4.4 – 5.4	$-(5.56 \pm 0.97) \text{ GeV}$
$\chi_{c1}\omega S\tilde{V}$	3.1 – 4.1	0.29 ± 0.04
$J/\psi f_0S\tilde{V}$	3.5 – 4.5	$0.47 \pm 0.14 \text{ GeV}$

Table 62: The Borel parameters and hadronic coupling constants.

Channels	$\Gamma(\text{MeV})$
$Y_{\tilde{A}V} \rightarrow \bar{D}^0 D^0, D^- D^+$	22.5 ± 2.1
$Y_{\tilde{A}V} \rightarrow \frac{\bar{D}^{0*} D^0 - \bar{D}^0 D^{*0}}{\sqrt{2}}, \frac{\bar{D}^- D^+ - \bar{D}^- D^{*+}}{\sqrt{2}}$	0.08 ± 0.01
$Y_{\tilde{A}V} \rightarrow \bar{D}^{*0} D^{*0}, \bar{D}^{*-} D^{*+}$	9.93 ± 0.84
$Y_{\tilde{A}V} \rightarrow \frac{\bar{D}_0^0 D^{*0} - \bar{D}^{*0} D_0^0}{\sqrt{2}}, \frac{\bar{D}_0^- D^{*+} - \bar{D}^{*-} D_0^+}{\sqrt{2}}$	1.92 ± 0.13
$Y_{\tilde{A}V} \rightarrow \frac{\bar{D}_1^0 D^0 - \bar{D}^0 D_1^0}{\sqrt{2}}, \frac{\bar{D}_1^- D^+ - \bar{D}^- D_1^+}{\sqrt{2}}$	59.7 ± 5.5
$Y_{\tilde{A}V} \rightarrow \eta_c \omega$	3.83 ± 0.66
$Y_{\tilde{A}V} \rightarrow J/\psi \omega$	0.0
$Y_{\tilde{A}V} \rightarrow \chi_{c0} \omega$	11.3 ± 1.7
$Y_{\tilde{A}V} \rightarrow \chi_{c1} \omega$	24.4 ± 1.9
$Y_{\tilde{A}V} \rightarrow J/\psi f_0(500)$	13.9 ± 1.7
$Y_{\tilde{V}A} \rightarrow \bar{D}^0 D^0, D^- D^+$	0.009 ± 0.001
$Y_{\tilde{V}A} \rightarrow \frac{\bar{D}^{0*} D^0 - \bar{D}^0 D^{*0}}{\sqrt{2}}, \frac{\bar{D}^- D^+ - \bar{D}^- D^{*+}}{\sqrt{2}}$	3.88 ± 0.26
$Y_{\tilde{V}A} \rightarrow \bar{D}^{*0} D^{*0}, \bar{D}^{*-} D^{*+}$	0.047 ± 0.003
$Y_{\tilde{V}A} \rightarrow \frac{\bar{D}_0^0 D^{*0} - \bar{D}^{*0} D_0^0}{\sqrt{2}}, \frac{\bar{D}_0^- D^{*+} - \bar{D}^{*-} D_0^+}{\sqrt{2}}$	66.3 ± 6.1
$Y_{\tilde{V}A} \rightarrow \frac{\bar{D}_1^0 D^0 - \bar{D}^0 D_1^0}{\sqrt{2}}, \frac{\bar{D}_1^- D^+ - \bar{D}^- D_1^+}{\sqrt{2}}$	4.10 ± 0.27
$Y_{\tilde{V}A} \rightarrow \eta_c \omega$	5.65 ± 0.85
$Y_{\tilde{V}A} \rightarrow J/\psi \omega$	0.0
$Y_{\tilde{V}A} \rightarrow \chi_{c0} \omega$	11.1 ± 1.6
$Y_{\tilde{V}A} \rightarrow \chi_{c1} \omega$	29.9 ± 2.5
$Y_{\tilde{V}A} \rightarrow J/\psi f_0(500)$	15.2 ± 1.8
$Y_{S\tilde{V}} \rightarrow \bar{D}^0 D^0, D^- D^+$	1.88 ± 0.38
$Y_{S\tilde{V}} \rightarrow \frac{\bar{D}^{0*} D^0 - \bar{D}^0 D^{*0}}{\sqrt{2}}, \frac{\bar{D}^- D^+ - \bar{D}^- D^{*+}}{\sqrt{2}}$	0.20 ± 0.01
$Y_{S\tilde{V}} \rightarrow \frac{\bar{D}^{0*} D^0 - \bar{D}^0 D^{*0}}{\sqrt{2}}, \frac{\bar{D}^- D^+ - \bar{D}^- D^{*+}}{\sqrt{2}}$	0.38 ± 0.04
$Y_{S\tilde{V}} \rightarrow \frac{\bar{D}_0^0 D^{*0} - \bar{D}^{*0} D_0^0}{\sqrt{2}}, \frac{\bar{D}_0^- D^{*+} - \bar{D}^{*-} D_0^+}{\sqrt{2}}$	4.51 ± 0.97
$Y_{S\tilde{V}} \rightarrow \frac{\bar{D}_1^0 D^0 - \bar{D}^0 D_1^0}{\sqrt{2}}, \frac{\bar{D}_1^- D^+ - \bar{D}^- D_1^+}{\sqrt{2}}$	24.4 ± 4.3
$Y_{S\tilde{V}} \rightarrow \eta_c \omega$	96.0 ± 34.8
$Y_{S\tilde{V}} \rightarrow J/\psi \omega$	18.0 ± 6.3
$Y_{S\tilde{V}} \rightarrow \chi_{c0} \omega$	49.4 ± 17.2
$Y_{S\tilde{V}} \rightarrow \chi_{c1} \omega$	2.76 ± 0.76
$Y_{S\tilde{V}} \rightarrow J/\psi f_0(500)$	0.49 ± 0.29

Table 63: The partial decay widths.

At last, we saturate the total widths with the summary of partial decay widths,

$$\begin{aligned}\Gamma(Y_{\tilde{A}V}) &= 241.6 \pm 9.0 \text{ MeV}, \\ \Gamma(Y_{\tilde{V}A}) &= 210.6 \pm 9.4 \text{ MeV}, \\ \Gamma(Y_{S\tilde{V}}) &= 229.4 \pm 39.9 \text{ MeV}.\end{aligned}\tag{469}$$

The widths of the $Y(4484)$, $Y(4469)$ and $Y(4544)$ are $111.1 \pm 30.1 \pm 15.2 \text{ MeV}$, $246.3 \pm 36.7 \pm 9.4 \text{ MeV}$ and $116.1 \pm 33.5 \pm 1.7 \text{ MeV}$, respectively, from the BESIII collaboration [147, 148, 151], which are compatible with the theoretical predictions in magnitude.

From Table 63, we obtain the typical decay modes. For the $Y_{\tilde{A}V}$ state, the decays,

$$Y_{\tilde{A}V} \rightarrow \frac{\bar{D}_1^0 D^0 - \bar{D}^0 D_1^0}{\sqrt{2}}, \frac{\bar{D}_1^- D^+ - \bar{D}^- D_1^+}{\sqrt{2}},\tag{470}$$

have the largest partial decay width $59.7 \pm 5.5 \text{ MeV}$; while the decay,

$$Y_{\tilde{A}V} \rightarrow J/\psi\omega,\tag{471}$$

has zero partial decay width. For the $Y_{\tilde{V}A}$ state, the decays,

$$Y_{\tilde{V}A} \rightarrow \frac{\bar{D}_0^0 D^{*0} - \bar{D}^{*0} D_0^0}{\sqrt{2}}, \frac{\bar{D}_0^- D^{*+} - \bar{D}^{*-} D_0^+}{\sqrt{2}},\tag{472}$$

have the largest partial decay width $66.3 \pm 6.1 \text{ MeV}$; while the decay,

$$Y_{\tilde{V}A} \rightarrow J/\psi\omega,\tag{473}$$

has zero partial decay width. For the $Y_{S\tilde{V}}$ state, the decay,

$$Y_{S\tilde{V}} \rightarrow \eta_c\omega,\tag{474}$$

has the largest partial decay width $96.0 \pm 34.8 \text{ MeV}$; while the decay,

$$Y_{S\tilde{V}} \rightarrow J/\psi\omega,\tag{475}$$

has the partial decay width $18.0 \pm 6.3 \text{ MeV}$. We can search for the $Y(4500)$ in those typical decays to diagnose its nature.

11.2 Light-cone QCD sum rules for the $Y(4500)$ as an example

The light-cone QCD sum rules have been applied extensively to study the two-body strong decays of the tetraquark (molecular) states [117, 399, 404, 605, 606, 607, 608], where only the ground state contributions are isolated, and an unknown parameter is introduced by hand to parameterize the higher resonance contributions, then the Ioffe-Smilga-type trick,

$$1 - T^2 \frac{d}{dT^2},\tag{476}$$

is adopted to subtract this parameter [609, 610]. The Ioffe-Smilga-type trick was suggested to deal with the traditional hadrons, where there exists a triangle Feynman diagram. In the case of tetraquark (molecular) states, we deal with two disconnected loop diagrams approximately, see Fig.27, we would like not to resort to the Ioffe-Smilga trick, and write down the higher resonance contributions explicitly.

We would like to use an example to illustrate how to study the strong decays of the tetraquark states via the light-cone QCD sum rules. In the following, we write down the three-point correlation function $\Pi_{\mu\alpha\beta}(p)$,

$$\Pi_{\mu\alpha\beta}(p, q) = i^2 \int d^4x d^4y e^{-ip \cdot x} e^{-iq \cdot y} \langle 0 | T \left\{ J_\mu^Y(0) J_\alpha^{D^{*+}}(x) J_\beta^{\bar{D}^{*0}}(y) \right\} | \pi(r) \rangle, \quad (477)$$

where

$$\begin{aligned} J_\mu^Y(0) &= \frac{\varepsilon^{ijk} \varepsilon^{imn}}{2} \left[u_j^T(0) C \sigma_{\mu\nu} \gamma_5 c_k(0) \bar{u}_m(0) \gamma_5 \gamma^\nu C \bar{c}_n^T(0) + u_j^T(0) C \gamma^\nu \gamma_5 c_k(0) \bar{u}_m(0) \gamma_5 \sigma_{\mu\nu} C \bar{c}_n^T(0) \right. \\ &\quad \left. + d_j^T(x) C \sigma_{\mu\nu} \gamma_5 c_k(0) \bar{d}_m(0) \gamma_5 \gamma^\nu C \bar{c}_n^T(0) + d_j^T(0) C \gamma^\nu \gamma_5 c_k(0) \bar{d}_m(0) \gamma_5 \sigma_{\mu\nu} C \bar{c}_n^T(0) \right], \\ J_\alpha^{D^{*+}}(y) &= \bar{d}(x) \gamma_\alpha c(x), \\ J_\beta^{\bar{D}^{*0}}(x) &= \bar{c}(y) \gamma_\beta u(y), \end{aligned} \quad (478)$$

interpolate the $Y(4500)$, \bar{D}^* and D^* , respectively [611], the $|\pi(r)\rangle$ is the external π state.

At the hadron side, we insert a complete set of intermediate hadronic states with the same quantum numbers as the interpolating currents into the three-point correlation function, and isolate the ground state contributions,

$$\begin{aligned} \Pi_{\mu\alpha\beta}(p, q) &= \lambda_Y f_{D^*}^2 M_{D^*}^2 \frac{-iG_\pi r_\tau + iG_Y p'_\tau}{(M_Y^2 - p^2)(M_{D^*}^2 - p^2)(M_{D^*}^2 - q^2)} \varepsilon^{\rho\sigma\lambda\tau} \left(-g_{\mu\rho} + \frac{p'_\mu p'_\rho}{p'^2} \right) \\ &\quad \left(-g_{\alpha\sigma} + \frac{p_\alpha p_\sigma}{p^2} \right) \left(-g_{\lambda\beta} + \frac{q_\lambda q_\beta}{q^2} \right) + \dots, \end{aligned} \quad (479)$$

where $p' = p + q + r$, the decay constants λ_Y , f_{D^*} , $f_{\bar{D}^*}$ and hadronic coupling constants G_π , G_Y are defined by,

$$\begin{aligned} \langle 0 | J_\mu^Y(0) | Y_c(p') \rangle &= \lambda_Y \varepsilon_\mu, \\ \langle 0 | J_\alpha^{D^{*+}\dagger}(0) | \bar{D}^*(p) \rangle &= f_{\bar{D}^*} M_{\bar{D}^*} \xi_\alpha, \\ \langle 0 | J_\beta^{\bar{D}^{*0}\dagger}(0) | D^*(q) \rangle &= f_{D^*} M_{D^*} \zeta_\beta, \end{aligned} \quad (480)$$

$$\langle Y_c(p') | \bar{D}^*(p) D^*(q) \pi(r) \rangle = G_\pi \varepsilon^{\rho\sigma\lambda\tau} \varepsilon_\rho^* \xi_\sigma \zeta_\lambda r_\tau - G_Y \varepsilon^{\rho\sigma\lambda\tau} \varepsilon_\rho^* \xi_\sigma \zeta_\lambda p'_\tau, \quad (481)$$

the ε_μ , ξ_α and ζ_β are polarization vectors of the $Y(4500)$, \bar{D}^* and D^* , respectively. In the isospin limit, $m_u = m_d$, $f_{D^*} = f_{\bar{D}^*}$ and $M_{D^*} = M_{\bar{D}^*}$.

We multiply Eq.(479) with the tensor $\varepsilon_{\theta\omega}^{\alpha\beta}$ and obtain

$$\begin{aligned} \tilde{\Pi}_{\mu\theta\omega}(p, q) &= \varepsilon_{\theta\omega}^{\alpha\beta} \Pi_{\mu\alpha\beta}(p, q) \\ &= \lambda_Y f_{D^*}^2 M_{D^*}^2 \frac{iG_\pi (g_{\mu\omega} r_\theta - g_{\mu\theta} r_\omega) - iG_Y (g_{\mu\omega} p'_\theta - g_{\mu\theta} p'_\omega)}{(M_Y^2 - p'^2)(M_{D^*}^2 - p^2)(M_{D^*}^2 - q^2)} + \dots. \end{aligned} \quad (482)$$

Again, we take the isospin limit, then $\tilde{\Pi}_{\mu\theta\omega}(p, q) = \tilde{\Pi}_{\mu\theta\omega}(q, p)$, and we write down the relevant components explicitly,

$$\begin{aligned} \tilde{\Pi}_{\mu\theta\omega}(p, q) &= [i\Pi_\pi(p'^2, p^2, q^2) - i\Pi_Y(p'^2, p^2, q^2)] (g_{\mu\omega} r_\theta - g_{\mu\theta} r_\omega) \\ &\quad + i\Pi_Y(p'^2, p^2, q^2) (g_{\mu\omega} q_\theta - g_{\mu\theta} q_\omega) + \dots, \end{aligned} \quad (483)$$

where

$$\begin{aligned} \Pi_\pi(p'^2, p^2, q^2) &= \frac{\lambda_Y f_{D^*}^2 M_{D^*}^2 G_\pi}{(M_Y^2 - p'^2)(M_{D^*}^2 - p^2)(M_{D^*}^2 - q^2)} + \dots, \\ \Pi_Y(p'^2, p^2, q^2) &= \frac{\lambda_Y f_{D^*}^2 M_{D^*}^2 G_Y}{(M_Y^2 - p'^2)(M_{D^*}^2 - p^2)(M_{D^*}^2 - q^2)} + \dots. \end{aligned} \quad (484)$$

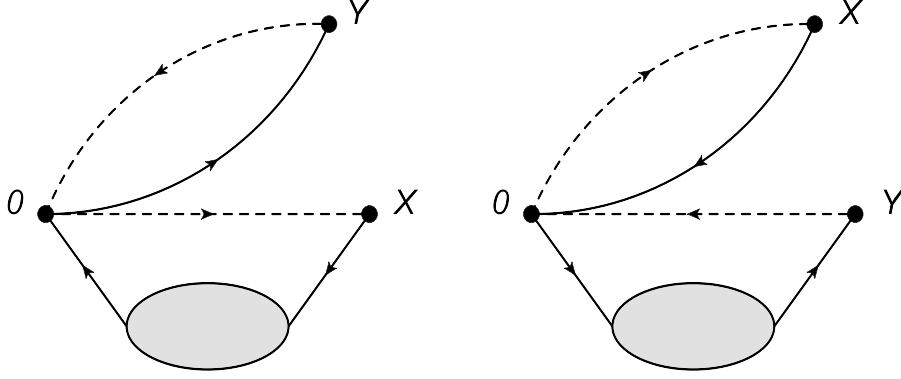


Figure 29: The lowest order Feynman diagrams, where the dashed (solid) lines denote the heavy (light) quark lines, the ovals denote the external π^+ meson.

Then we choose the tensor structures $g_{\mu\omega}r_\theta - g_{\mu\theta}r_\omega$ and $g_{\mu\omega}q_\theta - g_{\mu\theta}q_\omega$ to study the hadronic coupling constants G_π and G_Y , respectively. We obtain the hadronic spectral densities $\rho_H(s', s, u)$ through triple dispersion relation,

$$\Pi_H(p'^2, p^2, q^2) = \int_{\Delta_s'^2}^{\infty} ds' \int_{\Delta_s^2}^{\infty} ds \int_{\Delta_u^2}^{\infty} du \frac{\rho_H(s', s, u)}{(s' - p'^2)(s - p^2)(u - q^2)}, \quad (485)$$

where the $\Delta_s'^2$, Δ_s^2 and Δ_u^2 are the thresholds, and we add the subscript H to represent the hadron side.

We carry out the operator product expansion up to the vacuum condensates of dimension 5 and neglect the tiny gluon condensate contributions [587, 588],

$$\begin{aligned} \Pi_\pi(p^2, q'^2, q^2) &= f_\pi m_c \int_0^1 du \varphi_\pi(u) \left[\int_0^1 dx x \bar{x} \frac{\Gamma(\epsilon - 1)}{2\pi^2 (p^2 - \tilde{m}_c^2)^{\epsilon-1}} - \frac{2m_c \langle \bar{q}q \rangle}{3(p^2 - m_c^2)} \right. \\ &\quad \left. + \frac{m_c^3 \langle \bar{q}g_s \sigma Gq \rangle}{3(p^2 - m_c^2)^3} \right] \frac{1}{(q + ur)^2 - m_c^2} \\ &\quad + \frac{f_\pi m_\pi^2}{m_u + m_d} \int_0^1 du \varphi_5(u) \bar{u} \left[\int_0^1 dx x \bar{x} \frac{\Gamma(\epsilon - 1)}{2\pi^2 (p^2 - \tilde{m}_c^2)^{\epsilon-1}} - \frac{2m_c \langle \bar{q}q \rangle}{3(p^2 - m_c^2)} \right. \\ &\quad \left. + \frac{m_c^3 \langle \bar{q}g_s \sigma Gq \rangle}{3(p^2 - m_c^2)^3} \right] \frac{1}{(q + ur)^2 - m_c^2} \\ &\quad - \frac{f_\pi m_c^2 \langle \bar{q}g_s \sigma Gq \rangle}{36} \int_0^1 du \varphi_\pi(u) \frac{1}{(p^2 - m_c^2)((q + ur)^2 - m_c^2)^2} \\ &\quad + \frac{f_\pi m_\pi^2 m_c \langle \bar{q}g_s \sigma Gq \rangle}{36(m_u + m_d)} \int_0^1 du \varphi_5(u) \bar{u} \frac{1}{(p^2 - m_c^2)((q + ur)^2 - m_c^2)^2}, \quad (486) \end{aligned}$$

$$\begin{aligned}
\Pi_Y(p^2, q'^2, q^2) &= \frac{f_\pi m_\pi^2}{m_u + m_d} \int_0^1 du \varphi_5(u) \left[\int_0^1 dx x \bar{x} \frac{\Gamma(\epsilon - 1)}{2\pi^2 (p^2 - \tilde{m}_c^2)^{\epsilon-1}} - \frac{2m_c \langle \bar{q}q \rangle}{3(p^2 - m_c^2)} \right. \\
&\quad \left. + \frac{m_c^3 \langle \bar{q}g_s \sigma Gq \rangle}{3(p^2 - m_c^2)^3} \right] \frac{1}{(q + ur)^2 - m_c^2} \\
&\quad + \frac{f_\pi m_\pi^2 m_c \langle \bar{q}g_s \sigma Gq \rangle}{36(m_u + m_d)} \int_0^1 du \varphi_5(u) \frac{1}{(p^2 - m_c^2)((q + ur)^2 - m_c^2)^2} \\
&\quad + f_{3\pi} m_\pi^2 \int_0^1 dx \bar{x} \left[\frac{3\Gamma(\epsilon)}{8\pi^2 (p^2 - \tilde{m}_c^2)^\epsilon} - \frac{p^2}{2\pi^2 (p^2 - \tilde{m}_c^2)} \right] \frac{1}{q^2 - m_c^2} \\
&\quad - f_{3\pi} m_\pi^2 \int_0^1 dx x \bar{x} \left[\frac{\Gamma(\epsilon - 1)}{2\pi^2 (p^2 - \tilde{m}_c^2)^{\epsilon-1}} + \frac{p^2 \Gamma(\epsilon)}{2\pi^2 (p^2 - \tilde{m}_c^2)^\epsilon} \right] \frac{1}{(q^2 - m_c^2)^2} \\
&\quad - f_{3\pi} m_\pi^2 \int_0^1 dx x \left[\frac{3\Gamma(\epsilon)}{8\pi^2 (p^2 - \tilde{m}_c^2)^\epsilon} + \frac{p^2}{4\pi^2 (p^2 - \tilde{m}_c^2)} \right] \frac{1}{q^2 - m_c^2}, \tag{487}
\end{aligned}$$

where $q' = q + r$, $\bar{u} = 1 - u$, $\bar{x} = 1 - x$, $\tilde{m}_c^2 = \frac{m_c^2}{x}$, $(q - ur)^2 - m_c^2 = (1 - u)q^2 + u(q + r)^2 - u\bar{u}m_\pi^2 - m_c^2$. And we have used the π light-cone distribution functions [612],

$$\begin{aligned}
\langle 0 | \bar{d}(0) \gamma_\mu \gamma_5 u(x) | \pi(r) \rangle &= i f_\pi r_\mu \int_0^1 du e^{-iur \cdot x} \varphi_\pi(u) + \dots, \\
\langle 0 | \bar{d}(0) \sigma_{\mu\nu} \gamma_5 u(x) | \pi(r) \rangle &= \frac{i}{6} \frac{f_\pi m_\pi^2}{m_u + m_d} (r_\mu x_\nu - r_\nu x_\mu) \int_0^1 du e^{-iur \cdot x} \varphi_\sigma(u), \\
\langle 0 | \bar{d}(0) i \gamma_5 u(x) | \pi(r) \rangle &= \frac{f_\pi m_\pi^2}{m_u + m_d} \int_0^1 du e^{-iur \cdot x} \varphi_5(u), \tag{488}
\end{aligned}$$

and the approximation,

$$\langle 0 | \bar{d}(x_1) \sigma_{\mu\nu} \gamma_5 g_s G_{\alpha\beta}(x_2) u(x_3) | \pi(r) \rangle = i f_{3\pi} (r_\mu r_\alpha g_{\nu\beta} + r_\nu r_\beta g_{\mu\alpha} - r_\nu r_\alpha g_{\mu\beta} - r_\mu r_\beta g_{\nu\alpha}), \tag{489}$$

for the twist-3 quark-gluon light-cone distribution functions with the value $f_{3\pi} = 0.0035 \text{ GeV}^2$ at the energy scale $\mu = 1 \text{ GeV}$ [612, 613]. Such terms proportional to m_π^2 and their contributions are greatly suppressed, and we also neglect the twist-4 light-cone distribution functions due to their small contributions. According to the Gell-Mann-Oakes-Renner relation $\frac{f_\pi m_\pi^2}{m_u + m_d} = -\frac{2\langle \bar{q}q \rangle}{f_\pi}$, we take account of the Chiral enhanced contributions fully in Eqs.(486)-(487).

In Fig.29, we draw the lowest order Feynman diagrams as example to illustrate the operator product expansion.

In the soft limit $r_\mu \rightarrow 0$, $(q + r)^2 = q^2$, we can set $\Pi_{\pi/Y}(p^2, q'^2, q^2) = \Pi_{\pi/Y}(p^2, q^2)$, then we obtain the QCD spectral densities $\rho_{QCD}(s, u)$ through double dispersion relation,

$$\Pi_{\pi/Y}^{QCD}(p^2, q^2) = \int_{\Delta_s^2}^\infty ds \int_{\Delta_u^2}^\infty du \frac{\rho_{QCD}(s, u)}{(s - p^2)(u - q^2)}, \tag{490}$$

we add the superscript (subscript) QCD to stand for the QCD side.

We match the hadron side with the QCD side below the continuum thresholds s_0 and u_0 to acquire rigorous quark-hadron duality [587, 588],

$$\int_{\Delta_s^2}^{s_0} ds \int_{\Delta_u^2}^{u_0} du \frac{\rho_{QCD}(s, u)}{(s - p^2)(u - q^2)} = \int_{\Delta_s^2}^{s_0} ds \int_{\Delta_u^2}^{u_0} du \left[\int_{\Delta_s'^2}^\infty ds' \frac{\rho_H(s', s, u)}{(s' - p'^2)(s - p^2)(u - q^2)} \right], \tag{491}$$

and we carry out the integral over ds' firstly, then

$$\begin{aligned}
\Pi_H(p'^2, p^2, q^2) &= \frac{\lambda_Y f_{D^*}^2 M_{D^*}^2 G_{\pi/Y}}{(M_Y^2 - p'^2)(M_{D^*}^2 - p^2)(M_{D^*}^2 - q^2)} + \int_{s'_0}^{\infty} ds' \frac{\tilde{\rho}_H(s', M_{D^*}^2, M_{D^*}^2)}{(s' - p'^2)(M_{D^*}^2 - p^2)(M_{D^*}^2 - q^2)} \\
&\quad + \dots, \\
&= \frac{\lambda_Y f_{D^*}^2 M_{D^*}^2 G_{\pi/Y}}{(M_Y^2 - p'^2)(M_{D^*}^2 - p^2)(M_{D^*}^2 - q^2)} + \frac{C_{\pi/Y}}{(M_{D^*}^2 - p^2)(M_{D^*}^2 - q^2)} + \dots, \quad (492)
\end{aligned}$$

where $\rho_H(s', s, u) = \tilde{\rho}_H(s', s, u)\delta(s - M_{D^*}^2)\delta(u - M_{D^*}^2)$, and we introduce the parameters $C_{\pi/Y}$ to parameterize the contributions concerning the higher resonances and continuum states in the s' channel,

$$C_{\pi/Y} = \int_{s'_0}^{\infty} ds' \frac{\tilde{\rho}_H(s', M_{D^*}^2, M_{D^*}^2)}{s' - p'^2}. \quad (493)$$

As the strong interactions among the ground states π , D^* , \bar{D}^* and excited Y' states are complex, and we have no knowledge about the corresponding four-hadron contact vertex. In practical calculations, we can take the unknown functions $C_{\pi/Y}$ as free parameters and adjust the values to acquire flat platforms for the hadronic coupling constants $G_{\pi/Y}$ with variations of the Borel parameters. Such a method works well in the case of three-hadron contact vertexes [587, 588], and we expect it also works in the present work.

In Eq.(479) and Eq.(482), there exist three poles in the limit $p'^2 \rightarrow M_Y^2$, $p^2 \rightarrow M_{D^*}^2$ and $q^2 \rightarrow M_{D^*}^2$. According to the relation $M_Y \approx M_{\bar{D}^*} + M_{D^*}$, we set $p'^2 = 4q^2$ and perform double Borel transform with respect to the variables $P^2 = -p^2$ and $Q^2 = -q^2$ respectively, then we set $T_1^2 = T_2^2 = T^2$ to obtain two QCD sum rules,

$$\begin{aligned}
&\frac{\lambda_{Y D^* D^*} G_{\pi}}{4(\widetilde{M}_Y^2 - M_{D^*}^2)} \left[\exp\left(-\frac{M_{D^*}^2}{T^2}\right) - \exp\left(-\frac{\widetilde{M}_Y^2}{T^2}\right) \right] \exp\left(-\frac{M_{D^*}^2}{T^2}\right) + C_{\pi} \exp\left(-\frac{M_{D^*}^2 + M_{D^*}^2}{T^2}\right) \\
&= f_{\pi} m_c \int_{m_c^2}^{s_0} ds \int_0^1 du \varphi_{\pi}(u) \left[\frac{1}{2\pi^2} \int_{x_i}^1 dx x \bar{x} (s - \tilde{m}_c^2) - \left(\frac{2m_c \langle \bar{q}q \rangle}{3} - \frac{m_c^3 \langle \bar{q}g_s \sigma Gq \rangle}{6T^4} \right) \delta(s - m_c^2) \right] \\
&\exp\left(-\frac{s + m_c^2 + u\bar{u}m_{\pi}^2}{T^2}\right) \\
&+ \frac{f_{\pi} m_{\pi}^2}{m_u + m_d} \int_{m_c^2}^{s_0} ds \int_0^1 du \varphi_5(u) \bar{u} \left[\frac{1}{2\pi^2} \int_{x_i}^1 dx x \bar{x} (s - \tilde{m}_c^2) - \left(\frac{2m_c \langle \bar{q}q \rangle}{3} - \frac{m_c^3 \langle \bar{q}g_s \sigma Gq \rangle}{6T^4} \right) \delta(s - m_c^2) \right] \\
&\exp\left(-\frac{s + m_c^2 + u\bar{u}m_{\pi}^2}{T^2}\right) + \frac{f_{\pi} m_c^2 \langle \bar{q}g_s \sigma Gq \rangle}{36T^2} \int_0^1 du \varphi_{\pi}(u) \exp\left(-\frac{2m_c^2 + u\bar{u}m_{\pi}^2}{T^2}\right) \\
&- \frac{f_{\pi} m_{\pi}^2 m_c \langle \bar{q}g_s \sigma Gq \rangle}{36(m_u + m_d)T^2} \int_0^1 du \varphi_5(u) \bar{u} \exp\left(-\frac{2m_c^2 + u\bar{u}m_{\pi}^2}{T^2}\right), \quad (494)
\end{aligned}$$

$$\begin{aligned}
& \frac{\lambda_{YD^*D^*}G_Y}{4(\widetilde{M}_Y^2 - M_{D^*}^2)} \left[\exp\left(-\frac{M_{D^*}^2}{T^2}\right) - \exp\left(-\frac{\widetilde{M}_Y^2}{T^2}\right) \right] \exp\left(-\frac{M_{D^*}^2}{T^2}\right) + C_Y \exp\left(-\frac{M_{D^*}^2 + M_{\bar{D}^*}^2}{T^2}\right) \\
&= \frac{f_\pi m_\pi^2}{m_u + m_d} \int_{m_c^2}^{s_0} ds \int_0^1 du \varphi_5(u) \left[\frac{1}{2\pi^2} \int_{x_i}^1 dx x \bar{x} (s - \tilde{m}_c^2) - \left(\frac{2m_c \langle \bar{q}q \rangle}{3} - \frac{m_c^3 \langle \bar{q}g_s \sigma Gq \rangle}{6T^4} \right) \delta(s - m_c^2) \right] \\
&\exp\left(-\frac{s + m_c^2 + u\bar{u}m_\pi^2}{T^2}\right) - \frac{f_\pi m_\pi^2 m_c \langle \bar{q}g_s \sigma Gq \rangle}{36(m_u + m_d)T^2} \int_0^1 du \varphi_5(u) \exp\left(-\frac{2m_c^2 + u\bar{u}m_\pi^2}{T^2}\right) \\
&- \frac{f_{3\pi} m_\pi^2}{2\pi^2} \int_{m_c^2}^{s_0} ds \int_{x_i}^1 dx \bar{x} \left[\frac{3}{4} + s \delta(s - \tilde{m}_c^2) \right] \exp\left(-\frac{s + m_c^2}{T^2}\right) \\
&- \frac{f_{3\pi} m_\pi^2}{2\pi^2 T^2} \int_{m_c^2}^{s_0} ds \int_{x_i}^1 dx x \bar{x} \tilde{m}_c^2 \exp\left(-\frac{s + m_c^2}{T^2}\right) \\
&+ \frac{f_{3\pi} m_\pi^2}{4\pi^2} \int_{m_c^2}^{s_0} ds \int_{x_i}^1 dx x \left[\frac{3}{2} - s \delta(s - \tilde{m}_c^2) \right] \exp\left(-\frac{s + m_c^2}{T^2}\right), \tag{495}
\end{aligned}$$

where $\lambda_{YD^*D^*} = \lambda_Y f_{D^*}^2 M_{D^*}^2$, $\widetilde{M}_Y^2 = \frac{M_Y^2}{4}$ and $x_i = \frac{m_c^2}{s}$.

In calculations, we fit the free parameters as $C_\pi = 0.00101(T^2 - 3.6 \text{ GeV}^2) \text{ GeV}^4$ and $C_Y = 0.00089(T^2 - 3.2 \text{ GeV}^2) \text{ GeV}^4$ to acquire uniform flat Borel platforms $T_{max}^2 - T_{min}^2 = 1 \text{ GeV}^2$. The Borel windows are $T_\pi^2 = (4.6 - 5.6) \text{ GeV}^2$ and $T_Y^2 = (4.4 - 5.4) \text{ GeV}^2$, where the subscripts π and Y represent the corresponding channels. In Fig.30, we plot the hadronic coupling constants G_π and G_Y with variations of the Borel parameters. In the Borel windows, there appear very flat platforms indeed.

We obtain the hadronic coupling constants routinely,

$$\begin{aligned}
G_\pi &= 15.9 \pm 0.5 \text{ GeV}^{-1}, \\
G_Y &= 10.4 \pm 0.6 \text{ GeV}^{-1}, \tag{496}
\end{aligned}$$

by setting

$$\delta \bar{\lambda}_Y \bar{f}_{D^*} \bar{f}_{\bar{D}^*} \bar{G}_{\pi/Y} = \bar{\lambda}_Y \bar{f}_{D^*} \bar{f}_{\bar{D}^*} \bar{G}_{\pi/Y} \frac{4\delta G_{\pi/Y}}{\bar{G}_{\pi/Y}}. \tag{497}$$

It is direct to obtain the partial decay width,

$$\begin{aligned}
\Gamma(Y(4500) \rightarrow D^* \bar{D}^* \pi^+) &= \frac{1}{24\pi M_Y} \int dk^2 (2\pi)^4 \delta^4(p' - k - p) \frac{d^3 \vec{k}}{(2\pi)^3 2k_0} \frac{d^3 \vec{p}}{(2\pi)^3 2p_0} \\
&(2\pi)^4 \delta^4(k - q - r) \frac{d^3 \vec{q}}{(2\pi)^3 2q_0} \frac{d^3 \vec{r}}{(2\pi)^3 2r_0} \Sigma |T|^2 \\
&= 6.43_{-0.76}^{+0.80} \text{ MeV}, \tag{498}
\end{aligned}$$

where $T = \langle Y_c(p') | \bar{D}^*(p) D^*(q) \pi(r) \rangle$.

The partial decay width $\Gamma(Y(4500) \rightarrow D^* \bar{D}^* \pi^+) = 6.43_{-0.76}^{+0.80} \text{ MeV}$ is much smaller than the total width $\Gamma = 246.3 \pm 36.7 \pm 9.4 \text{ MeV}$ from the BESIII collaboration [148].

The three-body strong decays of the $Y(4230)$ are also studied in this scheme [614], this scheme could be applied to the two-body strong decays of the tetraquark (molecular) states straightforwardly.

Acknowledgements

This work is supported by National Natural Science Foundation, Grant Number 11775079.

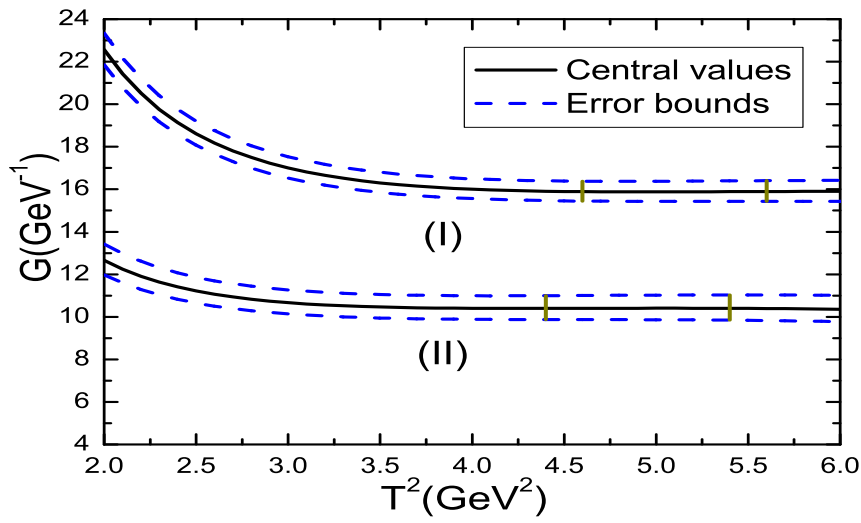


Figure 30: The hadronic coupling constants with variations of the Borel parameters T^2 , where the (I) and (II) denote the G_π and G_Y , respectively, the regions between the two vertical lines are the Borel windows.

References

- [1] M. Gell-Mann, *A Schematic Model of Baryons and Mesons*, Phys. Lett. **8** (1964) 214.
- [2] R. L. Jaffe, *Multi-Quark Hadrons. 1. The Phenomenology of $Q^2\bar{Q}^2$ Mesons*, Phys. Rev. **D15** (1977) 267.
- [3] R. L. Jaffe, *Multi-Quark Hadrons. 2. Methods*, Phys. Rev. **D15** (1977) 281.
- [4] D. Strottman, *Multi-Quark Baryons and the MIT Bag Model*, Phys. Rev. **D20** (1979) 748.
- [5] H. J. Lipkin, *New Possibilities for Exotic Hadrons: Anticharmed Strange Baryons*, Phys. Lett. **B195** (1987) 484.
- [6] R. L. Jaffe and K. Johnson, *Unconventional States of Confined Quarks and Gluons*, Phys. Lett. **B60** (1976) 201.
- [7] K. L. Au, D. Morgan and M. R. Pennington, *Meson Dynamics Beyond the Quark Model: A Study of Final State Interactions*, Phys. Rev. **D35** (1987) 1633.
- [8] T. Barnes, F. E. Close and F. de Viron, *$Q\bar{Q}G$ Hermaphrodite Mesons in the MIT Bag Model*, Nucl. Phys. **B224** (1983) 241.
- [9] S. K. Choi et al, *Observation of a narrow charmonium-like state in exclusive $B^+ \rightarrow K^+\pi^+\pi^- J/\psi$ decays*, Phys. Rev. Lett. **91** (2003) 262001.
- [10] J. D. Weinstein and N. Isgur, *Do Multi-Quark Hadrons Exist?*, Phys. Rev. Lett. **48** (1982) 659.
- [11] J. D. Weinstein and N. Isgur, *$K\bar{K}$ Molecules*, Phys. Rev. **D41** (1990) 2236.
- [12] N. N. Achasov, V. V. Gubin and V. I. Shevchenko, *Production of scalar $K\bar{K}$ molecules in ϕ radiative decays*, Phys. Rev. **D56** (1997) 203.
- [13] M. Boglione and M. R. Pennington, *Dynamical generation of scalar mesons*, Phys. Rev. **D65** (2002) 114010.
- [14] L. Maiani, F. Piccinini, A. D. Polosa and V. Riquer, *A New look at scalar mesons*, Phys. Rev. Lett. **93** (2004) 212002.
- [15] R. L. Jaffe and F. Wilczek, *Diquarks and exotic spectroscopy*, Phys. Rev. Lett. **91** (2003) 232003.
- [16] T. V. Brito, F. S. Navarra, M. Nielsen and M. E. Bracco, *QCD sum rule approach for the light scalar mesons as four-quark states*, Phys. Lett. **B608** (2005) 69.
- [17] Z. G. Wang and W. M. Yang, *Analysis the $f_0(980)$ and $a_0(980)$ mesons as four-quark states with the QCD sum rules*, Eur. Phys. J. **C42** (2005) 89.
- [18] Z. G. Wang, W. M. Yang and S. L. Wan, *Analysis the 0^{++} nonet mesons as four-quark states with the QCD sum rules*, J. Phys. **G31** (2005) 971.
- [19] H. J. Lee, *A QCD sum rule study of the light scalar meson*, Eur. Phys. J. **A30** (2006) 423.
- [20] H. J. Lee and N. I. Kochelev, *Instanton interpolating current for sigma-tetraquark*, Phys. Lett. **B642** (2006) 358.
- [21] S. Groote, J. G. Korner and D. Niinepuu, *Perturbative $\mathcal{O}(\alpha_s)$ corrections to the correlation functions of light tetraquark currents*, Phys. Rev. **D90** (2014) 054028.

- [22] Z. G. Wang, *Analysis of the scalar nonet mesons with QCD sum rules*, Eur. Phys. J. **C76** (2016) 427.
- [23] S. S. Agaev, K. Azizi and H. Sundu, *The strong decays of the light scalar mesons $f_0(500)$ and $f_0(980)$* , Phys. Lett. **B784** (2018) 266.
- [24] S. S. Agaev, K. Azizi and H. Sundu, *The nonet of the light scalar tetraquarks: The mesons $a_0(980)$ and $K_0^*(800)$* , Phys. Lett. **B789** (2019) 405.
- [25] S. Weinberg, *Tetraquark Mesons in Large- N Quantum Chromodynamics*, Phys. Rev. Lett. **110** (2013) 261601.
- [26] C. Amsler and N. A. Tornqvist, *Mesons beyond the naive quark model*, Phys. Rept. **389** (2004) 61.
- [27] F. E. Close and N. A. Tornqvist, *Scalar mesons above and below 1-GeV*, J. Phys. **G28** (2002) R249.
- [28] E. Klempt and A. Zaitsev, *Glueballs, Hybrids, Multiquarks. Experimental facts versus QCD inspired concepts*, Phys. Rept. **454** (2007) 1.
- [29] A. Hosaka, T. Iijima, K. Miyabayashi, Y. Sakai and S. Yasui, *Exotic hadrons with heavy flavors: X , Y , Z , and related states*, Prog. Theor. Exp. Phys. **2016** (2016) 062C01.
- [30] H. X. Chen, W. Chen, X. Liu and S. L. Zhu, *The hidden-charm pentaquark and tetraquark states*, Phys. Rept. **639** (2016) 1.
- [31] R. F. Lebed, R. E. Mitchell and E. S. Swanson, *Heavy-Quark QCD Exotica*, Prog. Part. Nucl. Phys. **93** (2017) 143.
- [32] A. Ali, J. S. Lange and S. Stone, *Exotics: Heavy Pentaquarks and Tetraquarks*, Prog. Part. Nucl. Phys. **97** (2017) 123.
- [33] A. Esposito, A. Pilloni and A. D. Polosa, *Multiquark Resonances*, Phys. Rept. **668** (2017) 1.
- [34] F. K. Guo, C. Hanhart, U. G. Meissner, Q. Wang, Q. Zhao and B. S. Zou, *Hadronic molecules*, Rev. Mod. Phys. **90** (2018) 015004.
- [35] S. L. Olsen and T. Skwarnicki, *Nonstandard heavy mesons and baryons: Experimental evidence*, Rev. Mod. Phys. **90** (2018) 015003.
- [36] M. Karliner, J. L. Rosner and T. Skwarnicki, *Multiquark States*, Ann. Rev. Nucl. Part. Sci. **68** (2018) 17.
- [37] N. Brambilla, S. Eidelman, C. Hanhart, A. Nefediev, C. P. Shen, C. E. Thomas, A. Vairo and C. Z. Yuan, *The XYZ states: experimental and theoretical status and perspectives*, Phys. Rept. **873** (2020) 1.
- [38] Y. R. Liu, H. X. Chen, W. Chen, X. Liu and S. L. Zhu, *Pentaquark and Tetraquark states*, Prog. Part. Nucl. Phys. **107** (2019) 237.
- [39] H. X. Chen, W. Chen, X. Liu, Y. R. Liu and S. L. Zhu, *An updated review of the new hadron states*, Rept. Prog. Phys. **86** (2023) 026201.
- [40] L. Meng, B. Wang, G. J. Wang and S. L. Zhu, *Chiral perturbation theory for heavy hadrons and chiral effective field theory for heavy hadronic molecules*, Phys. Rept. **1019** (2023) 1.

- [41] M. Z. Liu, Y. W. Pan, Z. W. Liu, T. W. Wu, J. X. Lu and L. S. Geng, *Three ways to decipher the nature of exotic hadrons: Multiplets, three-body hadronic molecules, and correlation functions*, Phys. Rept. **1108** (2025) 1.
- [42] M. Nielsen, F. S. Navarra and S. H. Lee, *New Charmonium States in QCD Sum Rules: A Concise Review*, Phys. Rept. **497** (2010) 41.
- [43] R. M. Albuquerque, J. M. Dias, K. P. Khemchandani, A. M. Torres, F. S. Navarra, M. Nielsen and C. M. Zanetti, *QCD sum rules approach to the X, Y and Z states*, J. Phys. **G46** (2019) 093002.
- [44] K. Abe et al, *Evidence for $X(3872) \rightarrow \gamma J/\psi$ and the sub-threshold decay $X(3872) \rightarrow \omega J/\psi$* , hep-ex/0505037.
- [45] B. Aubert et al, *Search for $B^+ \rightarrow X(3872)K^+$, $X(3872) \rightarrow J/\psi\gamma$* , Phys. Rev. **D74** (2006) 071101.
- [46] B. Aubert et al, *Evidence for $X(3872) \rightarrow \psi(2S)\gamma$ in $B^\pm \rightarrow X(3872)K^\pm$ decays, and a study of $B \rightarrow c\bar{c}\gamma K$* , Phys. Rev. Lett. **102** (2009) 132001.
- [47] A. Abulencia et al, *Analysis of the Quantum Numbers J^{PC} of the $X(3872)$ Particle*, Phys. Rev. Lett. **98** (2007) 132002.
- [48] S. K. Choi et al, *Bounds on the width, mass difference and other properties of $X(3872) \rightarrow \pi^+\pi^-J/\psi$ decays*, Phys. Rev. **D84** (2011) 052004.
- [49] R Aaij et al, *Determination of the $X(3872)$ meson quantum numbers*, Phys. Rev. Lett. **110** (2013) 222001.
- [50] R Aaij et al, *Quantum numbers of the $X(3872)$ state and orbital angular momentum in its $\rho^0 J/\psi$ decay*, Phys. Rev. **D92** (2015) 011102.
- [51] L. Maiani, F. Piccinini, A. D. Polosa and V. Riquer, *Diquark-antidiquarks with hidden or open charm and the nature of $X(3872)$* , Phys. Rev. **D71** (2005) 014028.
- [52] L. Maiani, F. Piccinini, *The $Z(4430)$ and a New Paradigm for Spin Interactions in Tetraquarks*, A. D. Polosa and V. Riquer, Phys. Rev. **D89** (2014) 114010.
- [53] S. J. Brodsky, D. S. Hwang and R. F. Lebed, *Dynamical Picture for the Formation and Decay of the Exotic XYZ Mesons*, Phys. Rev. Lett. **113** (2014) 112001.
- [54] R. D. Matheus, S. Narison, M. Nielsen and J. M. Richard, *Can the $X(3872)$ be a 1^{++} four-quark state?*, Phys. Rev. **D75** (2007) 014005.
- [55] D. Ebert, R. N. Faustov and V. O. Galkin, *Masses of heavy tetraquarks in the relativistic quark model*, Phys. Lett. **B634** (2006) 214.
- [56] Z. G. Wang and T. Huang, *Analysis of the $X(3872)$, $Z_c(3900)$ and $Z_c(3885)$ as axial-vector tetraquark states with QCD sum rules*, Phys. Rev. **D89** (2014) 054019.
- [57] Z. G. Wang, *Analysis of the hidden-charm tetraquark mass spectrum with the QCD sum rules*, Phys. Rev. **D102** (2020) 014018.
- [58] Z. G. Wang, *Decipher the width of the $X(3872)$ via the QCD sum rules*, Phys. Rev. **D109** (2024) 014017.
- [59] Y. R. Liu, X. Liu, W. Z. Deng and S. L. Zhu, *Is $X(3872)$ Really a Molecular State?*, Eur. Phys. J. **C56** (2008) 63.

- [60] N. A. Tornqvist, *Isospin breaking of the narrow charmonium state of Belle at 3872 MeV as a deuson*, Phys. Lett. **B590** (2004) 209.
- [61] E. S. Swanson, *Short range structure in the X(3872)*, Phys. Lett. **B588** (2004) 189.
- [62] S. Swanson, *Diagnostic decays of the X(3872)*, Phys. Lett. **B598** (2004) 197.
- [63] S. Fleming, M. Kusunoki, T. Mehen and U. v. Kolck, *Pion interactions in the X(3872)*, Phys. Rev. **D76** (2007) 034006.
- [64] C. Bignamini, B. Grinstein, F. Piccinini, A. D. Polosa and C. Sabelli, *Is the X(3872) Production Cross Section at Tevatron Compatible with a Hadron Molecule Interpretation?*, Phys. Rev. Lett. **103** (2009) 162001.
- [65] F. E. Close and P. R. Page, *The $D^{*0}\bar{D}^0$ threshold resonance*, Phys. Lett. **B578** (2004) 119.
- [66] D. Gamermann, J. Nieves, E. Oset and E. R. Arriola, *Couplings in coupled channels versus wave functions: application to the X(3872) resonance*, Phys. Rev. **D81** (2010) 014029.
- [67] M. B. Voloshin, *Interference and binding effects in decays of possible molecular component of X(3872)*, Phys. Lett. **B579** (2004) 316.
- [68] F. K. Guo, C. Hidalgo-Duque, J. Nieves and M. P. Valderrama, *Consequences of Heavy Quark Symmetries for Hadronic Molecules*, Phys. Rev. **D88** (2013) 054007.
- [69] C. Y. Wong, *Molecular states of heavy quark mesons*, Phys. Rev. **C69** (2004) 055202.
- [70] M. T. AlFiky, F. Gabbiani and A. A. Petrov, *X(3872): Hadronic molecules in effective field theory*, Phys. Lett. **B640** (2006) 238.
- [71] J. Nieves and M. P. Valderrama, *The Heavy Quark Spin Symmetry Partners of the X(3872)*, Phys. Rev. **D86** (2012) 056004.
- [72] C. Hanhart, Y. S. Kalashnikova, A. E. Kudryavtsev and A. V. Nefediev, *Reconciling the X(3872) with the near-threshold enhancement in the $D^0\bar{D}^{*0}$ final state*, Phys. Rev. **D76** (2007) 034007.
- [73] Y. S. Kalashnikova, *Coupled-channel model for charmonium levels and an option for X(3872)*, Phys. Rev. **D72** (2005) 034010.
- [74] P. Artoisenet and E. Braaten, *Production of the X(3872) at the Tevatron and the LHC*, Phys. Rev. **D81** (2010) 114018.
- [75] Y. B. Dong, A. Faessler, T. Gutsche and V. E. Lyubovitskij, *Estimate for the $X(3872) \rightarrow \gamma J/\psi$ decay width*, Phys. Rev. **D77** (2008) 094013.
- [76] Z. G. Wang and T. Huang, *Possible assignments of the X(3872), $Z_c(3900)$ and $Z_b(10610)$ as axial-vector molecular states*, Eur. Phys. J. **C74** (2014) 2891.
- [77] Z. G. Wang, *Analysis of the Hidden-charm Tetraquark molecule mass spectrum with the QCD sum rules*, Int. J. Mod. Phys. **A36** (2021) 2150107.
- [78] Q. Xin and Z. G. Wang, *Analysis of the X(3960) and related tetraquark molecular states via the QCD sum rules*, AAPPS Bull. **32** (2022) 37.
- [79] E. J. Eichten, K. Lane and C. Quigg, *New states above charm threshold*, Phys. Rev. **D73** (2006) 014014.

- [80] T. Barnes and S. Godfrey, *Charmonium options for the X(3872)*, Phys. Rev. **D69** (2004) 054008.
- [81] M. Suzuki, *The X(3872) boson: Molecule or charmonium*, Phys. Rev. **D72** (2005) 114013.
- [82] B. Q. Li and K. T. Chao, *Higher Charmonia and X, Y, Z states with Screened Potential*, Phys. Rev. **D79** (2009) 094004.
- [83] D. V. Bugg, *Reinterpreting several narrow resonances as threshold cusps*, Phys. Lett. **B598** (2004) 8.
- [84] S. K. Choi et al, *Observation of a near-threshold $\omega J/\psi$ mass enhancement in exclusive $B \rightarrow K\omega J/\psi$ decays*, Phys. Rev. Lett. **94** (2005) 182002.
- [85] B. Aubert et al, *Observation of $Y(3940) \rightarrow J/\psi\omega$ in $B \rightarrow J/\psi\omega K$ at BABAR*, Phys. Rev. Lett. **101** (2008) 082001.
- [86] P. del Amo Sanchez et al, *Evidence for the decay $X(3872) \rightarrow J/\psi\omega$* , Phys. Rev. **D82** (2010) 011101.
- [87] K. Abe et al, *Observation of a new charmonium state in double charmonium production in e^+e^- annihilation at $\sqrt{s} \approx 10.6$ GeV*, Phys. Rev. Lett. **98** (2007) 082001.
- [88] K. Abe et al, *Search for new charmonium states in the processes $e^+e^- \rightarrow J/\psi D^{(*)}\bar{D}^{(*)}$ at $\sqrt{s} \approx 10.6$ GeV*, Phys. Rev. Lett. **100** (2008) 202001.
- [89] S. Uehara et al, *Observation of a charmonium-like enhancement in the $\gamma\gamma \rightarrow \omega J/\psi$ process*, Phys. Rev. Lett. **104** (2010) 092001.
- [90] J. P. Lees et al, *Study of $X(3915) \rightarrow J/\psi\omega$ in two-photon collisions*, Phys. Rev. **D86** (2012) 072002.
- [91] S. Navas et al, *The Review of Particle Physics (2024)*, Phys. Rev. **D110** (2024) 030001.
- [92] S. Uehara et al, *Observation of a χ'_{c2} candidate in $\gamma\gamma \rightarrow D\bar{D}$ production at Belle*, Phys. Rev. Lett. **96** (2006) 082003.
- [93] B. Aubert et al, *Observation of the $\chi_{c2}(2P)$ meson in the reaction $\gamma\gamma \rightarrow D\bar{D}$ at BABAR*, Phys. Rev. **D81** (2010) 092003.
- [94] K. Chilikin et al, *Observation of an alternative $\chi_{c0}(2P)$ candidate in $e^+e^- \rightarrow J/\psi D\bar{D}$* , Phys. Rev. **D95** (2017) 112003.
- [95] R. Aaij et al, *Model-independent study of structure in $B^+ \rightarrow D^+D^-K^+$ decays*, Phys. Rev. Lett. **125** (2020) 242001.
- [96] R. Aaij et al, *Amplitude analysis of the $B^+ \rightarrow D^+D^-K^+$ decay*, Phys. Rev. **D102** (2020) 112003.
- [97] R. Aaij et al, *Observation of a resonant structure near the $D_s^+D_s^-$ threshold in the $B^+ \rightarrow D_s^+D_s^-K^+$ decay*, Phys. Rev. Lett. **131** (2023) 071901.
- [98] T. Barnes, S. Godfrey and E. S. Swanson, *Higher charmonia*, Phys. Rev. **D72** (2005) 054026.
- [99] R. Aaij et al, *Observation of new charmonium(-like) states in $B^+ \rightarrow D^{*\pm}D^\mp K^+$* , Phys. Rev. Lett. **133** (2024) 131902.
- [100] T. Aaltonen et al, *Evidence for a Narrow Near-Threshold Structure in the $J/\psi\phi$ Mass Spectrum in $B^+ \rightarrow J/\psi\phi K^+$ Decays*, Phys. Rev. Lett. **102** (2009) 242002.

- [101] T. Aaltonen et al, *Observation of the $Y(4140)$ structure in the $J/\psi\phi$ Mass Spectrum in $B^\pm \rightarrow J/\psi\phi K^\pm$ Decays*, Mod. Phys. Lett. **A32** (2017) 1750139.
- [102] S. Chatrchyan et al, *Observation of a peaking structure in the $J/\psi\phi$ mass spectrum from $B^\pm \rightarrow J/\psi\phi K^\pm$ decays*, Phys. Lett. **B734** (2014) 261.
- [103] R. Aaij et al, *Observation of $J/\psi\phi$ structures consistent with exotic states from amplitude analysis of $B^+ \rightarrow J/\psi\phi K^+$ decays*, Phys. Rev. Lett. **118** (2017) 022003.
- [104] R. Aaij et al, *Amplitude analysis of $B^+ \rightarrow J/\psi\phi K^+$ decays*, Phys. Rev. **D95** (2017) 012002.
- [105] R. Aaij et al, *Observation of new resonances decaying to $J/\psi K^+$ and $J/\psi\phi$* , Phys. Rev. Lett. **127** (2021) 082001.
- [106] R. Aaij et al, *Amplitude analysis of $B^+ \rightarrow \psi(2S)K^+\pi^+\pi^-$ decays*, arXiv: 2407.12475 [hep-ex].
- [107] C. P. Shen et al, *Evidence for a new resonance and search for the $Y(4140)$ in $\gamma\gamma \rightarrow \phi J/\psi$* , Phys. Rev. Lett. **104** (2010) 112004.
- [108] M. Karliner and J. L. Rosner, *First exotic hadron with open heavy flavor: $c\bar{s}\bar{u}\bar{d}$ tetraquark*, Phys. Rev. **D102** (2020) 094016.
- [109] Z. G. Wang, *Analysis of the $X_0(2900)$ as the scalar tetraquark state via the QCD sum rules*, Int. J. Mod. Phys. **A35** (2020) 2050187.
- [110] J. R. Zhang, *Open-charm tetraquark candidate: Note on $X_0(2900)$* , Phys. Rev. **D103** (2021) 054019.
- [111] H. X. Chen, W. Chen, R. R. Dong and N. Su, *$X_0(2900)$ and $X_1(2900)$: Hadronic Molecules or Compact Tetraquarks*, Chin. Phys. Lett. **37** (2020) 101201.
- [112] X. G. He, W. Wang and R. L. Zhu, *Open-charm tetraquark X_c and open-bottom tetraquark X_b* , Eur. Phys. J. **C80** (2020) 1026.
- [113] Q. F. Lu, D. Y. Chen and Y. B. Dong, *Open charm and bottom tetraquarks in an extended relativized quark model*, Phys. Rev. **D102** (2020) 074021.
- [114] M. Z. Liu, J. J. Xie and L. S. Geng, *$X_0(2866)$ as a $D^*\bar{K}^*$ molecular state*, Phys. Rev. **D102** (2020) 091502.
- [115] M. W. Hu, X. Y. Lao, P. Ling and Q. Wang, *$X_0(2900)$ and its heavy quark spin partners in molecular picture*, Chin. Phys. **C45** (2021) 021003.
- [116] R. Molina and E. Oset, *Molecular picture for the $X_0(2866)$ as a $D^*\bar{K}^*$ $J^P = 0^+$ state and related $1^+, 2^+$ states*, Phys. Lett. **B811** (2020) 135870.
- [117] S. S. Agaev, K. Azizi and H. Sundu, *New scalar resonance $X_0(2900)$ as a molecule: mass and width*, J. Phys. **G48** (2021) 085012.
- [118] R. M. Albuquerque, S. Narison, D. Rabetiariivony and G. Randriamanatrika, *$X_{0,1}(2900)$ and (D^-K^+) invariant mass from QCD Laplace sum rules at NLO*, Nucl. Phys. **A1007** (2021) 122113.
- [119] X. H. Liu, M. J. Yan, H. W. Ke, G. Li and J. J. Xie, *Triangle singularity as the origin of $X_0(2900)$ and $X_1(2900)$ observed in $B^+ \rightarrow D^+D^-K^+$* , Eur. Phys. J. **C80** (2020) 1178.
- [120] R. Aaij et al, *First Observation of a Doubly Charged Tetraquark and Its Neutral Partner*, Phys. Rev. Lett. **131** (2023) 041902.

- [121] R. Aaij et al, *Amplitude analysis of $B^0 \rightarrow \bar{D}^0 D_s^+ \pi^-$ and $B^+ \rightarrow D^- D_s^+ \pi^+$ decays*, Phys. Rev. **D108** (2023) 012017.
- [122] V. M. Abazov et al, *Evidence for a $B_s^0 \pi^\pm$ State*, Phys. Rev. Lett. **117** (2016) 022003.
- [123] Z. G. Wang, *Analysis of the $X(5568)$ as scalar tetraquark state in the diquark-antidiquark model with QCD sum rules*, Commun. Theor. Phys. **66** (2016) 335.
- [124] W. Chen, H. X. Chen, X. Liu, T. G. Steele and S. L. Zhu, *Decoding the $X(5568)$ as a fully open-flavor $\text{sub}\bar{d}$ tetraquark state*, Phys. Rev. Lett. **117** (2016) 022002.
- [125] S. S. Agaev, K. Azizi and H. Sundu, *Mass and decay constant of the newly observed exotic $X(5568)$ state*, Phys. Rev. **D93** (2016) 074024.
- [126] W. Wang and R. L. Zhu, *Can $X(5568)$ be a tetraquark state?*, Chin. Phys. **C40** (2016) 093101.
- [127] C. M. Zanetti, M. Nielsen and K. P. Khemchandani, *QCD sum rule study of a charged bottom-strange scalar meson*, Phys. Rev. **D93** (2016) 096011.
- [128] R. Aaij et al, *Search for structure in the $B_s^0 \pi^\pm$ invariant mass spectrum*, Phys. Rev. Lett. **117** (2016) 152003.
- [129] A. M. Sirunyan et al, *Search for the $X(5568)$ state decaying into $B_s^0 \pi^\pm$ in proton-proton collisions at $\sqrt{s} = 8$ TeV*, Phys. Rev. Lett. **120** (2018) 202005.
- [130] M. Aaboud et al, *Search for a Structure in the $B_s^0 \pi^\pm$ Invariant Mass Spectrum with the ATLAS Experiment*, Phys. Rev. Lett. **120** (2018) 202007.
- [131] T. Aaltonen et al, *A search for the exotic meson $X(5568)$ with the Collider Detector at Fermilab*, Phys. Rev. Lett. **120** (2018) 202006.
- [132] R. Aaij et al, *Observation of structure in the J/ψ -pair mass spectrum*, Sci. Bull. **65** (2020) 1983.
- [133] G. Aad et al, *Observation of an Excess of Dicharmonium Events in the Four-Muon Final State with the ATLAS Detector* Phys. Rev. Lett. **131** (2023) 151902.
- [134] A. Hayrapetyan et al, *New Structures in the $J/\psi J/\psi$ Mass Spectrum in Proton-Proton Collisions at $\sqrt{s} = 13$ TeV*, Phys. Rev. Lett. **132** (2024) 111901.
- [135] Z. G. Wang, *Analysis of the $X(6600)$, $X(6900)$, $X(7300)$ and related tetraquark states with the QCD sum rules*, Nucl. Phys. **B985** (2022) 115983.
- [136] Z. G. Wang, *Analysis of the mass and width of the $X^*(3860)$ with QCD sum rules*, Eur. Phys. J. **A53** (2017) 192.
- [137] B. Aubert et al, *Observation of a Broad Structure in the $\pi^+ \pi^- J/\psi$ Mass Spectrum around 4.26 GeV/c²*, Phys. Rev. Lett. **95** (2005) 142001.
- [138] C. Z. Yuan et al, *Measurement of $e^+ e^- \rightarrow \pi^+ \pi^- J/\psi$ Cross Section via Initial State Radiation at Belle*, Phys. Rev. Lett. **99** (2007) 182004.
- [139] Q. He et al, *Confirmation of the $Y(4260)$ Resonance Production in ISR*, Phys. Rev. **D74** (2006) 091104.
- [140] X. L. Wang et al, *Observation of Two Resonant Structures in $e^+ e^- \rightarrow \pi^+ \pi^- \psi(2S)$ via Initial State Radiation at Belle*, Phys. Rev. Lett. **99** (2007) 142002.

- [141] X. L. Wang et al, *Measurement of $e^+e^- \rightarrow \pi^+\pi^-\psi(2S)$ via Initial State Radiation at Belle*, Phys. Rev. **D91** (2015) 112007.
- [142] J. P. Lees et al, *Study of the reaction $e^+e^- \rightarrow \psi(2S)\pi^-\pi^-$ via initial state radiation at BaBar*, Phys. Rev. **D89** (2014) 111103.
- [143] G. Pakhlova et al, *Observation of a near-threshold enhancement in the $e^+e^- \rightarrow \Lambda_c^+\Lambda_c^-$ cross section using initial-state radiation*, Phys. Rev. Lett. **101** (2008) 172001.
- [144] M. Ablikim et al, *Study of $e^+e^- \rightarrow \omega\chi_{cJ}$ at center-of-mass energies from 4.21 to 4.42 GeV*, Phys. Rev. Lett. **114** (2015) 092003.
- [145] M. Ablikim et al, *Evidence of Two Resonant Structures in $e^+e^- \rightarrow \pi^+\pi^-h_c$* , Phys. Rev. Lett. **118** (2017) 092002.
- [146] M. Ablikim et al, *Precise measurement of the $e^+e^- \rightarrow \pi^+\pi^-J/\psi$ cross section at center-of-mass energies from 3.77 to 4.60 GeV*, Phys. Rev. Lett. **118** (2017) 092001.
- [147] M. Ablikim et al, *Observation of the $Y(4230)$ and a new structure in $e^+e^- \rightarrow K^+K^-J/\psi$* , Chin. Phys. **C46** (2022) 111002.
- [148] M. Ablikim et al, *Observation of Three Charmoniumlike States with $J^{PC} = 1^{--}$ in $e^+e^- \rightarrow D^{*0}D^{*-}\pi^+$* Phys. Rev. Lett. **130** (2023) 121901.
- [149] M. Ablikim et al, *Precise measurement of the $e^+e^- \rightarrow D_s^{*+}D_s^{*-}$ cross sections at center-of-mass energies from threshold to 4.95 GeV*, Phys. Rev. Lett. **131** (2023) 151903.
- [150] M. Ablikim et al, *Observation of a vector charmoniumlike state at 4.7 GeV/ c^2 and search for Z_{cs} in $e^+e^- \rightarrow K^+K^-J/\psi$* , Phys. Rev. Lett. **131** (2023) 211902.
- [151] M. Ablikim et al, *Observation of structures in the processes $e^+e^- \rightarrow \omega\chi_{c1}$ and $\omega\chi_{c2}$* , Phys. Rev. Lett. **132** (2024) 161901.
- [152] M. Ablikim et al, *Study of $e^+e^- \rightarrow \omega X(3872)$ and $\gamma X(3872)$ from 4.66 to 4.95 GeV*, Phys. Rev. **D110** (2024) 012006.
- [153] M. Ablikim et al, *Measurement of Energy-Dependent Pair-Production Cross Section and Electromagnetic Form Factors of a Charmed Baryon*, Phys. Rev. Lett. **131** (2023) 191901.
- [154] M. Ablikim et al, *Observation of a charged charmoniumlike structure in $e^+e^- \rightarrow \pi^+\pi^-J/\psi$ at $\sqrt{s} = 4.26$ GeV*, Phys. Rev. Lett. **110** (2013) 252001.
- [155] Z. Q. Liu et al, *Study of $e^+e^- \rightarrow \pi^+\pi^-J/\psi$ and Observation of a Charged Charmonium-like State at Belle*, Phys. Rev. Lett. **110** (2013) 252002.
- [156] T. Xiao, S. Dobbs, A. Tomaradze and K. K. Seth, *Observation of the Charged Hadron $Z_c^\pm(3900)$ and Evidence for the Neutral $Z_c^0(3900)$ in $e^+e^- \rightarrow \pi^+\pi^-J/\psi$ at $\sqrt{s} = 4170$ MeV*, Phys. Lett. **B727** (2013) 366.
- [157] M. Ablikim et al, *Observation of a charged $(D\bar{D}^*)^\pm$ mass peak in $e^+e^- \rightarrow \pi D\bar{D}^*$ at $\sqrt{s} = 4.26$ GeV*, Phys. Rev. Lett. **112** (2014) 022001.
- [158] M. Ablikim et al, *Determination of spin and parity of the $Z_c(3900)$* , Phys. Rev. Lett. **119** (2017) 072001.
- [159] M. Ablikim et al, *Observation of a charged charmoniumlike structure in $e^+e^- \rightarrow (D^*\bar{D}^*)^\pm\pi^\mp$ at $\sqrt{s} = 4.26$ GeV*, Phys. Rev. Lett. **112** (2014) 132001.

- [160] M. Ablikim et al, *Observation of a charged charmoniumlike structure $Z_c(4020)$ and search for the $Z_c(3900)$ in $e^+e^- \rightarrow \pi^+\pi^-h_c$* , Phys. Rev. Lett. **111** (2013) 242001.
- [161] M. Ablikim et al, *Observation of a near-threshold structure in the K^+ recoil-mass spectra in $e^+e^- \rightarrow K^+(D_s^-D^{*0} + D_s^{*-}D^0)$* , Phys. Rev. Lett. **126** (2021) 102001.
- [162] M. Ablikim et al, *Search for hidden-charm tetraquark with strangeness in $e^+e^- \rightarrow K^+D_s^{*-}D^{*0} + c.c.$* , Chin. Phys. **C47** (2023) 033001.
- [163] Z. G. Wang, *Strange cousin of $Z_c(4020/4025)$ as a tetraquark state*, Chin. Phys. **C46** (2022) 123106.
- [164] Z. G. Wang, *Analysis of $Z_{cs}(3985)$ as the axialvector tetraquark state*, Chin. Phys. **C45** (2021) 073107.
- [165] R. Mizuk et al, *Observation of two resonance-like structures in the $\pi^+\chi_{c1}$ mass distribution in exclusive $\bar{B}^0 \rightarrow K^-\pi^+\chi_{c1}$ decays*, Phys. Rev. **D78** (2008) 072004.
- [166] J. P. Lees et al, *Search for the $Z_1(4050)^+$ and $Z_2(4250)^+$ states in $\bar{B}^0 \rightarrow \chi_{c1}K^-\pi^+$ and $B^+ \rightarrow \chi_{c1}K_S^0\pi^+$* , Phys. Rev. **D85** (2012) 052003.
- [167] R. Aaij et al, *Evidence for an $\eta_c(1S)\pi^-$ resonance in $B^0 \rightarrow \eta_c(1S)K^+\pi^-$ decays*, Eur. Phys. J. **C78** (2018) 1019.
- [168] S. K. Choi et al, *Observation of a resonance-like structure in the $\pi^\pm\psi'$ mass distribution in exclusive $B \rightarrow K\pi^\pm\psi'$ decays*, Phys. Rev. Lett. **100** (2008) 142001.
- [169] R. Mizuk et al, *Dalitz analysis of $B \rightarrow K\pi^+\psi'$ decays and the $Z(4430)^+$* , Phys. Rev. **D80** (2009) 031104.
- [170] K. Chilikin et al, *Experimental constraints on the spin and parity of the $Z(4430)^+$* , Phys. Rev. **D88** (2013) 074026.
- [171] R. Aaij et al, *Observation of the resonant character of the $Z(4430)^-$ state*, Phys. Rev. Lett. **112** (2014) 222002.
- [172] S. H. Lee, A. Mihara, F. S. Navarra and M. Nielsen, *QCD sum rules study of the meson $Z^+(4430)$* , Phys. Lett. **B661** (2008) 28.
- [173] M. Nielsen and F. S. Navarra, *Charged Exotic Charmonium States*, Mod. Phys. Lett. **A29** (2014) 1430005.
- [174] Z. G. Wang, *Analysis of the $Z(4430)$ as the first radial excitation of the $Z_c(3900)$* , Commun. Theor. Phys. **63** (2015) 325.
- [175] R. Aaij et al, *Model-independent observation of exotic contributions to $B^0 \rightarrow J/\psi K^+\pi^-$ decays*, Phys. Rev. Lett. **122** (2019) 152002.
- [176] Z. G. Wang, *Axialvector tetraquark candidates for the $Z_c(3900)$, $Z_c(4020)$, $Z_c(4430)$, $Z_c(4600)$* , Chin. Phys. **C44** (2020) 063105.
- [177] H. X. Chen and W. Chen, *Settling the $Z_c(4600)$ in the charged charmonium-like family*, Phys. Rev. **D99** (2019) 074022.
- [178] K. Chilikin et al, *Observation of a new charged charmoniumlike state in $\bar{B}^0 \rightarrow J/\psi K^-\pi^+$ decays*, Phys. Rev. **D90** (2014) 112009.
- [179] R. Aaij et al, *Model-independent observation of exotic contributions to $B^0 \rightarrow J/\psi K^+\pi^-$ decays*, Phys. Rev. Lett. **122** (2019) 152002.

- [180] I. Adachi et al, *Observation of two charged bottomonium-like resonances*, arXiv:1105.4583 [hep-ex].
- [181] A. Bondar et al, *Observation of two charged bottomonium-like resonances in $\Upsilon(5S)$ decays*, Phys. Rev. Lett. **108** (2012) 122001.
- [182] P. Krokovny et al, *First Observation of the $Z_b^0(10610)$ in a Dalitz Analysis of $\Upsilon(5S) \rightarrow \Upsilon(nS)\pi^0\pi^0$* , Phys. Rev. **D88** (2013) 052016.
- [183] A. Abdesselam et al, *Observation of a new structure near 10.75 GeV in the energy dependence of the $e^+e^- \rightarrow \Upsilon(nS)\pi^+\pi^-$ ($n = 1, 2, 3$) cross sections*, JHEP **10** (2019) 220.
- [184] I. Adachi et al, *Observation of $e^+e^- \rightarrow \omega\chi_{bJ}(1P)$ and search for $X_b \rightarrow \omega\Upsilon(1S)$ at \sqrt{s} near 10.75 GeV*, Phys. Rev. Lett. **130** (2023) 091902
- [185] I. Adachi et al, *Study of $Y(10753)$ decays to $\pi^+\pi^-\Upsilon(nS)$ final states at Belle II*, JHEP **07** (2024) 116.
- [186] I. Adachi et al, *Search for the $e^+e^- \rightarrow \eta_b(1S)\omega$ and $e^+e^- \rightarrow \chi_{b0}(1P)\omega$ processes at $\sqrt{s} = 10.745$ GeV*, Phys. Rev. **D109** (2024) 072013.
- [187] R. Aaij et al, *Observation of an exotic narrow doubly charmed tetraquark*, Nature Phys. **18** (2022) 751.
- [188] R. Aaij et al, *Study of the doubly charmed tetraquark T_{cc}^+* , Nature Commun. **13** (2022) 3351.
- [189] R. Aaij et al, *Observation of J/ψ Resonances Consistent with Pentaquark States in $\Lambda_b^0 \rightarrow J/\psi K^- p$ Decays*, Phys. Rev. Lett. **115** (2015) 072001.
- [190] R. Aaij et al, *Observation of a narrow pentaquark state, $P_c(4312)^+$, and of two-peak structure of the $P_c(4450)^+$* , Phys. Rev. Lett. **122** (2019) 222001.
- [191] R. Aaij et al, *Evidence of a $J/\psi\Lambda$ structure and observation of excited Ξ^- states in the $\Xi_b^- \rightarrow J/\psi\Lambda K^-$ decay*, Sci. Bull. **66** (2021) 1278.
- [192] R. Aaij et al, *Evidence for a new structure in the $J/\psi p$ and $J/\psi\bar{p}$ systems in $\bar{B}_s^0 \rightarrow J/\psi p\bar{p}$ decays*, Phys. Rev. Lett. **128** (2022) 062001.
- [193] R. Aaij et al, *Observation of a $J/\psi\Lambda$ resonance consistent with a strange pentaquark candidate in $B^- \rightarrow J/\psi\Lambda\bar{p}$ decays* Phys. Rev. Lett. **131** (2023) 031901.
- [194] F. K. Guo, X. H. Liu and S. Sakai, *Threshold cusps and triangle singularities in hadronic reactions*, Prog. Part. Nucl. Phys. **112** (2020) 103757.
- [195] D. V. Bugg, *How Resonances can synchronise with Thresholds*, J. Phys. **G35** (2008) 075005.
- [196] E. S. Swanson, *Z_b and Z_c Exotic States as Coupled Channel Cusps*, Phys. Rev. **D91** (2015) 034009.
- [197] E. S. Swanson, *Cusps and Exotic Charmonia*, Int. J. Mod. Phys. **E25** (2016) 1642010.
- [198] D. Y. Chen and X. Liu, *$Z_b(10610)$ and $Z_b(10650)$ structures produced by the initial single pion emission in the $\Upsilon(5S)$ decays*, Phys. Rev. **D84** (2011) 094003.
- [199] D. Y. Chen, X. Liu and T. Matsuki, *Reproducing the $Z_c(3900)$ structure through the initial-single-pion-emission mechanism*, Phys. Rev. **D88** (2013) 036008.
- [200] X. K. Dong, F. K. Guo and B. S. Zou, *Explaining the Many Threshold Structures in the Heavy-Quark Hadron Spectrum*, Phys. Rev. Lett. **126** (2021) 152001.

- [201] X. H. Liu and G. Li, *Exploring the threshold behavior and implications on the nature of $Y(4260)$ and $Z_c(3900)$* , Phys. Rev. **D88** (2013) 014013.
- [202] Q. Wang, C. Hanhart and Q. Zhao, *Decoding the riddle of $Y(4260)$ and $Z_c(3900)$* , Phys. Rev. Lett. **111** (2013) 132003.
- [203] Q. Wang, C. Hanhart and Q. Zhao, *Systematic study of the singularity mechanism in heavy quarkonium decays*, Phys. Lett. **B725** (2013) 106.
- [204] M. Cleven, Q. Wang, F. K. Guo, C. Hanhart, U. G. Meissner and Q. Zhao, *$Y(4260)$ as the first S -wave open charm vector molecular state?*, Phys. Rev. **D90** (2014) 074039.
- [205] M. Albaladejo, F. K. Guo, C. Hidalgo-Duque and J. Nieves, *$Z_c(3900)$: What has been really seen?*, Phys. Lett. **B755** (2016) 337.
- [206] F. K. Guo, C. Hanhart, Q. Wang and Q. Zhao, *Could the near-threshold XYZ states be simply kinematic effects?*, Phys. Rev. **D91** (2015) 051504.
- [207] A. P. Szczepaniak, *Triangle Singularities and XYZ Quarkonium Peaks*, Phys. Lett. **B747** (2015) 410.
- [208] Y. H. Chen, M. L. Du and F. K. Guo, *Precise determination of the pole position of the exotic $Z_c(3900)$* , Sci. China Phys. Mech. Astron. **67** (2024) 291011.
- [209] B. A. Li, *Is $X(3872)$ a possible candidate of hybrid meson?*, Phys. Lett. **B605** (2005) 306.
- [210] X. H. Liu, Q. Zhao and F. E. Close, *Search for tetraquark candidate $Z(4430)$ in meson photoproduction*, Phys. Rev. **D77** (2008) 094005.
- [211] X. Y. Wang, J. He, X. R. Chen, Q. J. Wang and X. M. Zhu, *Pion-induced production of hidden-charm pentaquarks $P_c(4312)$, $P_c(4440)$ and $P_c(4457)$* , Phys. Lett. **B797** (2019) 134862.
- [212] J. A. Oller, E. Oset and A. Ramos, *Chiral unitary approach to meson-meson and meson-baryon interactions and nuclear applications*, Prog. Part. Nucl. Phys. **45** (2000) 157.
- [213] T. Hyodo, D. Jido and A. Hosaka, *Compositeness of dynamically generated states in a chiral unitary approach*, Phys. Rev. **C85** (2012) 015201.
- [214] D. Gamermann and E. Oset, *Axial resonances in the open and hidden charm sectors*, Eur. Phys. J. **A33** (2007) 119.
- [215] R. Molina and E. Oset, *The $Y(3940)$, $Z(3930)$ and the $X(4160)$ as dynamically generated resonances from the vector-vector interaction*, Phys. Rev. **D80** (2009) 114013.
- [216] F. Aceti, M. Bayar, E. Oset, A. Martinez Torres, K. P. Khemchandani, J. M. Dias, F. S. Navarra and M. Nielsen, *Prediction of an $I = 1$ DD^* state and relationship to the claimed $Z_c(3900)$, $Z_c(3885)$* , Phys. Rev. **D90** (2014) 016003.
- [217] J. M. Dias, F. Aceti and E. Oset, *Study of $B\bar{B}^*$ and $B^*\bar{B}^*$ interactions in $I = 1$ and relationship to the $Z_b(10610)$, $Z_b(10650)$ states*, Phys. Rev. **D91** (2015) 076001.
- [218] J. J. Wu, R. Molina, E. Oset and B. S. Zou, *Dynamically generated N^* and Λ^* resonances in the hidden charm sector around 4.3 GeV*, Phys. Rev. **C84** (2011) 015202.
- [219] C. W. Xiao, J. Nieves and E. Oset, *Combining heavy quark spin and local hidden gauge symmetries in the dynamical generation of hidden charm baryons*, Phys. Rev. **D88** (2013) 056012.

- [220] L. Roca, J. Nieves and E. Oset, *The LHCb pentaquark as a $\bar{D}^*\Sigma_c - \bar{D}^*\Sigma_c^*$ molecular state*, Phys. Rev. **D92** (2015) 094003.
- [221] T. Uchino, W. H. Liang and E. Oset, *Baryon states with hidden charm in the extended local hidden gauge approach*, Eur. Phys. J. **A52** (2016) 43.
- [222] C. W. Xiao, J. Nieves and E. Oset, *Heavy quark spin symmetric molecular states from $\bar{D}^{(*)}\Sigma_c^{(*)}$ and other coupled channels in the light of the recent LHCb pentaquarks*, Phys. Rev. **D100** (2019) 014021.
- [223] T. Hyodo, *Structure of Near-Threshold s -Wave Resonances*, T. Hyodo, Phys. Rev. Lett. **111** (2013) 132002.
- [224] Z. H. Guo and J. A. Oller, *Probabilistic interpretation of compositeness relation for resonances*, Phys. Rev. **D93** (2016) 096001.
- [225] Y. Kamiya and T. Hyodo, *Structure of near-threshold quasibound states*, Phys. Rev. **C93** (2016) 035203.
- [226] X. W. Kang, Z. H. Guo and J. A. Oller, *General considerations on the nature of $Z_b(10610)$ and $Z_b(10650)$ from their pole positions*, Phys. Rev. **D94** (2016) 014012.
- [227] Y. Li, F. K. Guo, J. Y. Pang and J. J. Wu, *Generalization of Weinberg's compositeness relations*, Phys. Rev. **D105** (2022) L071502.
- [228] J. He, *The $Z_c(3900)$ as a resonance from the $D\bar{D}^*$ interaction*, Phys. Rev. **D92** (2015) 034004.
- [229] J. He, *$\bar{D}\Sigma_c^*$ and $\bar{D}^*\Sigma_c$ interactions and the LHCb hidden-charmed pentaquarks*, Phys. Lett. **B753** (2016) 547.
- [230] P. G. Ortega, J. Segovia, D. R. Entem and F. Fernandez, *The Z_c structures in a coupled-channels model*, Eur. Phys. J. **C79** (2019) 78.
- [231] H. W. Ke, X. Q. Li, Y. L. Shi, G. L. Wang and X. H. Yuan, *Is $Z_b(10610)$ a Molecular State?*, JHEP **04** (2012) 056.
- [232] H. W. Ke, M. Li, X. H. Liu and X. Q. Li, *Study on possible molecular states composed of $\Lambda_c\bar{D}(\Lambda_b B)$ and $\Sigma_c\bar{D}(\Sigma_b B)$ within the Bethe-Salpeter framework*, Phys. Rev. **D101** (2020) 014024.
- [233] M. J. Zhao, Z. Y. Wang, C. Wang and X. H. Guo, *Investigation of the possible $D\bar{D}^*/B\bar{B}^*$ and $DD^*/\bar{B}\bar{B}^*$ molecule states*, Phys. Rev. **D105** (2022) 096016.
- [234] J. Nieves and M. P. Valderrama, *Deriving the existence of $B\bar{B}^*$ bound states from the $X(3872)$ and Heavy Quark Symmetry*, Phys. Rev. **D84** (2011) 056015.
- [235] M. Z. Liu, T. W. Wu, J. J. Xie, M. P. Valderrama and L. S. Geng, *$D\Xi$ and $D^*\Xi$ molecular states from one boson exchange*, Phys. Rev. **D98** (2018) 014014.
- [236] M. Z. Liu, T. W. Wu, M. P. Valderrama, J. J. Xie and L. S. Geng, *Heavy-quark spin and flavor symmetry partners of the $X(3872)$* , Phys. Rev. **D99** (2019) 094018.
- [237] M. Z. Liu, Y. W. Pan, F. Z. Peng, M. S. Sanchez, L. S. Geng, A. Hosaka and M. P. Valderrama, *Emergence of a complete heavy-quark spin symmetry multiplet: seven molecular pentaquarks in light of the latest LHCb analysis*, Phys. Rev. Lett. **122** (2019) 242001.
- [238] M. Z. Liu, Y. W. Pan and L. S. Geng, *Can discovery of hidden charm strange pentaquark states help determine the spins of $P_c(4440)$ and $P_c(4457)$?*, Phys. Rev. **D103** (2021) 034003.

- [239] X. Liu, Z. G. Luo, Y. R. Liu and S. L. Zhu, *X(3872) and Other Possible Heavy Molecular States*, Eur. Phys. J. **C61** (2009) 411.
- [240] G. J. Ding, *Are $Y(4260)$ and $Z_2^+(4250)$ D_1D or D^0D Hadronic Molecules?*, Phys. Rev. **D79** (2009) 014001.
- [241] I. W. Lee, A. Faessler, T. Gutsche and V. E. Lyubovitskij, *X(3872) as a molecular DD^* state in a potential model*, Phys. Rev. **D80** (2009) 094005.
- [242] Z. F. Sun, J. He, X. Liu, Z. G. Luo and S. L. Zhu, *$Z_b(10610)^\pm$ and $Z_b(10650)^\pm$ as the $B^*\bar{B}$ and $B^*\bar{B}^*$ molecular states*, Phys. Rev. **D84** (2011) 054002.
- [243] Z. C. Yang, Z. F. Sun, J. He, X. Liu and S. L. Zhu, *The possible hidden-charm molecular baryons composed of anti-charmed meson and charmed baryon*, Chin. Phys. **C36** (2012) 6.
- [244] S. Ohkoda, Y. Yamaguchi, S. Yasui, K. Sudoh and A. Hosaka, *Exotic mesons with double charm and bottom flavor*, Phys. Rev. **D86** (2012) 034019.
- [245] N. Li, Z. F. Sun, X. Liu and S. L. Zhu, *Coupled-channel analysis of the possible $D^{(*)}D^{(*)}$, $\bar{B}^{(*)}\bar{B}^{(*)}$ and $D^{(*)}\bar{B}^{(*)}$ molecular states*, Phys. Rev. **D88** (2013) 114008.
- [246] H. Xu, B. Wang, Z. W. Liu and X. Liu, *DD^* potentials in chiral perturbation theory and possible molecular states*, Phys. Rev. **D99** (2019) 014027.
- [247] L. Meng, B. Wang, G. J. Wang and S. L. Zhu, *The hidden charm pentaquark states and $\Sigma_c\bar{D}^{(*)}$ interaction in chiral perturbation theory*, Phys. Rev. **D100** (2019) 014031.
- [248] B. Wang, L. Meng and S. L. Zhu, *Hidden-charm and hidden-bottom molecular pentaquarks in chiral effective field theory*, JHEP **11** (2019) 108.
- [249] M. Z. Liu, T. W. Wu, M. S. Sanchez, M. P. Valderrama, L. S. Geng and J. J. Xie, *Spin-parities of the $P_c(4440)$ and $P_c(4457)$ in the one-boson-exchange model*, Phys. Rev. **D103** (2021) 054004.
- [250] S. Y. Yu and X. W. Kang, *Nature of X(3872) from its radiative decay*, Phys. Lett. **B848** (2024) 138404.
- [251] E. Braaten and M. Kusunoki, *Low-energy universality and the new charmonium resonance at 3870-MeV*, Phys. Rev. **D69** (2004) 074005.
- [252] P. G. Ortega, J. Segovia, D. R. Entem and F. Fernandez, *Coupled channel approach to the structure of the X(3872)*, Phys. Rev. **D81** (2010) 054023.
- [253] S. Coito, G. Rupp and E. van Beveren, *X(3872) is not a true molecule*, Eur. Phys. J. **C73** (2013) 2351.
- [254] P. G. Ortega, J. Segovia, D. R. Entem and F. Fernandez, *Charmonium resonances in the 3.9 GeV/c² energy region and the X(3915)/X(3930) puzzle*, Phys. Lett. **B778** (2018) 5.
- [255] J. Ferretti and E. Santopinto, *Threshold corrections of $\chi_c(2P)$ and $\chi_b(3P)$ states and $J/\psi\rho$ and $J/\psi\omega$ transitions of the X(3872) in a coupled-channel model*, Phys. Lett. **B789** (2019) 550.
- [256] Y. S. Kalashnikova and A. V. Nefediev, *X(3872) in the molecular model*, Phys. Usp. **62** (2019) 568.
- [257] Y. Yamaguchi, A. Hosaka, S. Takeuchi and M. Takizawa, *Heavy hadronic molecules with pion exchange and quark core couplings: a guide for practitioners*, J. Phys. **G47** (2020) 053001.

- [258] Q. Deng, R. H. Ni, Q. Li and X. H. Zhong, *Charmonia in an unquenched quark model*, Phys. Rev. **D110** (2024) 056034.
- [259] E. Braaten, *How the $Z_c(3900)$ Reveals the Spectra of Quarkonium Hybrid and Tetraquark Mesons*, Phys. Rev. Lett. **111** (2013) 162003.
- [260] E. Braaten, C. Langmack, D. H. Smith, *Selection Rules for Hadronic Transitions of XYZ Mesons*, Phys. Rev. Lett. **112** (2014) 222001.
- [261] E. Braaten, C. Langmack and D. H. Smith, *Born-Oppenheimer Approximation for the XYZ Mesons*, Phys. Rev. **D90** (2014) 014044.
- [262] M. Berwein, N. Brambilla, J. T. Castella and A. Vairo, *Quarkonium Hybrids with Nonrelativistic Effective Field Theories*, Phys. Rev. **D92** (2015) 114019.
- [263] R. Oncala and J. Soto, *Heavy Quarkonium Hybrids: Spectrum, Decay and Mixing*, Phys. Rev. **D96** (2017) 014004.
- [264] N. Brambilla, W. K. Lai, J. Segovia, J. T. Castella and A. Vairo, *Spin structure of heavy-quark hybrids*, Phys. Rev. **D99** (2019) 014017.
- [265] K. J. Juge, J. Kuti and C. J. Morningstar, *Ab initio study of hybrid $\bar{b}gb$ mesons*, Phys. Rev. Lett. **82** (1999) 4400.
- [266] G. S. Bali, B. Bolder, N. Eicker, T. Lippert, B. Orth, P. Ueberholz, K. Schilling and T. Struckmann, *Static potentials and glueball masses from QCD simulations with Wilson sea quarks*, Phys. Rev. **D62** (2000) 054503.
- [267] G. S. Bali, H. Neff, T. Duessel, T. Lippert and K. Schilling, *Observation of String Breaking in QCD*, Phys. Rev. **D71** (2005) 114513.
- [268] M. Foster and C. Michael, *Hadrons with a heavy colour-adjoint particle*, Phys. Rev. **D59** (2009) 094509.
- [269] R. L. Jaffe, *Exotica*, Phys. Rept. **409** (2005) 1.
- [270] R. Faccini, L. Maiani, F. Piccinini, A. Pilloni, A. D. Polosa and V. Riquer, *A $J^{PG} = 1^{++}$ Charged Resonance in the $Y(4260)$ to $\pi^+\pi^-J/\psi$ Decay?*, Phys. Rev. **D87** (2013) 111102.
- [271] L. Maiani, V. Riquer, F. Piccinini and A. D. Polosa, *Four Quark Interpretation of $Y(4260)$* , Phys. Rev. **D72** (2005) 031502.
- [272] N. V. Drenska, R. Faccini and A. D. Polosa, *Exotic Hadrons with Hidden Charm and Strangeness*, Phys. Rev. **D79** (2009) 077502.
- [273] R. F. Lebed and A. D. Polosa, *$\chi_{c0}(3915)$ As the Lightest $c\bar{c}s\bar{s}$ State*, Phys. Rev. **D93** (2016) 094024.
- [274] L. Maiani, A. D. Polosa and V. Riquer, *Interpretation of Axial Resonances in $J/\psi\phi$ at LHCb*, Phys. Rev. **D94** (2016) 054026.
- [275] L. Maiani, A. D. Polosa and V. Riquer, *A Theory of X and Z Multiquark Resonances*, Phys. Lett. **B778** (2018) 247.
- [276] A. Ali, L. Maiani, A. V. Borisov, I. Ahmed, M. Jamil Aslam, A. Y. Parkhomenko, A. D. Polosa and A. Rehman, *A New Look at the Y Tetraquarks and Ω_c Baryons in the Diquark Model* Eur. Phys. J. **C78** (2018) 29.

- [277] L. Maiani, A. D. Polosa and V. Riquer, *The new resonances $Z_{cs}(3985)$ and $Z_{cs}(4003)$ (almost) fill two tetraquark nonets of broken $SU(3)_f$* , Sci. Bull. **66** (2021) 1616.
- [278] H. Hogaasen, J. M. Richard and P. Sorba, *A Chromomagnetic mechanism for the $X(3872)$ resonance*, Phys. Rev. **D73** (2006) 054013.
- [279] F. Buccella, H. Hogaasen, J. M. Richard and P. Sorba, *Chromomagnetism, flavour symmetry breaking and S -wave tetraquarks*, Eur. Phys. J. **C49** (2007) 743.
- [280] L. Zhao, W. Z. Deng and S. L. Zhu, *Hidden-Charm Tetraquarks and Charged Z_c States*, Phys. Rev. **D90** (2014) 094031.
- [281] J. Wu, Y. R. Liu, K. Chen, X. Liu and S. L. Zhu, *Heavy-flavored tetraquark states with the $QQ\bar{Q}\bar{Q}$ configuration*, Phys. Rev. **D97** (2018) 094015.
- [282] T. Guo, J. Li, J. Zhao and L. He, *Mass spectra of doubly heavy tetraquarks in an improved chromomagnetic interaction model*, Phys. Rev. **D105** (2022) 014021.
- [283] R. F. Lebed, *Spectroscopy of Exotic Hadrons Formed from Dynamical Diquarks*, Phys. Rev. **D96** (2017) 116003.
- [284] J. F. Giron and R. F. Lebed, *The Dynamical Diquark Model: First Numerical Results*, JHEP **05** (2019) 061.
- [285] J. F. Giron, R. F. Lebed and C. T. Peterson, *The Dynamical Diquark Model: Fine Structure and Isospin*, JHEP **01** (2020) 124.
- [286] J. F. Giron and R. F. Lebed, *Spectrum of p -wave hidden-charm exotic mesons in the diquark model*, Phys. Rev. **D101** (2020) 074032.
- [287] J. F. Giron and R. F. Lebed, *Spectrum of the hidden-bottom and the hidden-charm-strange exotics in the dynamical diquark model*, Phys. Rev. **D102** (2020) 014036.
- [288] R. F. Lebed and S. R. Martinez, *T_{cc} in the diabatic diquark model: Effects of D^*D isospin*, Phys. Rev. **D110** (2024) 034033.
- [289] Q. F. Lu and Y. B. Dong, *$X(4140)$, $X(4274)$, $X(4500)$, and $X(4700)$ in the relativized quark model*, Phys. Rev. **D94** (2016) 074007.
- [290] M. N. Anwar, J. Ferretti and E. Santopinto, *Spectroscopy of the hidden-charm $[qc][\bar{q}\bar{c}]$ and $[sc][\bar{s}\bar{c}]$ tetraquarks*, Phys. Rev. **D98** (2018) 094015.
- [291] M. A. Bedolla, J. Ferretti, C. D. Roberts and E. Santopinto, *Spectrum of fully-heavy tetraquarks from a diquark+antidiquark perspective*, Eur. Phys. J. **C80** (2020) 1004.
- [292] J. Ferretti and E. Santopinto, *Hidden-charm and bottom tetra- and pentaquarks with strangeness in the hadro-quarkonium and compact tetraquark models*, JHEP **04** (2020) 119.
- [293] Q. F. Lu, D. Y. Chen and Y. B. Dong, *Masses of doubly heavy tetraquarks $T_{QQ'}$ in a relativized quark model*, Phys. Rev. **D102** (2020) 034012.
- [294] G. L. Yu, Z. Y. Li, Z. G. Wang, J. Lu and M. Yan, *The S - and P -wave fully charmed tetraquark states and their radial excitations*, Eur. Phys. J. **C83** (2023) 416.
- [295] W. C. Dong and Z. G. Wang, *Going in quest of potential tetraquark interpretations for the newly observed states in light of the diquark-antidiquark scenarios*, Phys. Rev. **D107** (2023) 074010.

- [296] G. L. Yu, Z. Y. Li, Z. G. Wang, B. Wu and Z. Zhou, *The ground states of hidden-charm tetraquarks and their radial excitations*, Eur. Phys. J. **C84** (2024) 1130.
- [297] W. C. Dong and Z. G. Wang, *Hunting for the prospective T_{cc} family based on the diquark-antidiquark configuration*, arXiv: 2407.19383 [hep-ph].
- [298] D. Ebert, R. N. Faustov and V. O. Galkin, *Masses of heavy tetraquarks in the relativistic quark model*, Phys. Lett. **B634** (2006) 214.
- [299] D. Ebert, R. N. Faustov, V. O. Galkin and W. Lucha, *Masses of tetraquarks with two heavy quarks in the relativistic quark model*, Phys. Rev. **D76** (2007) 114015.
- [300] D. Ebert, R. N. Faustov and V. O. Galkin, *Excited heavy tetraquarks with hidden charm*, Eur. Phys. J. **C58** (2008) 399.
- [301] R. N. Faustov, V. O. Galkin, E. M. Savchenko, *Masses of the $QQ\bar{Q}\bar{Q}$ tetraquarks in the relativistic diquark-antidiquark picture*, Phys. Rev. **D102** (2020) 114030.
- [302] J. Vijande, F. Fernandez, A. Valcarce and B. Silvestre-Brac, *Tetraquarks in a chiral constituent quark model*, Eur. Phys. J. **A19** (2004) 383.
- [303] N. Barnea, J. Vijande and A. Valcarce, *Four-quark spectroscopy within the hyperspherical formalism*, Phys. Rev. **D73** (2006) 054004.
- [304] J. Vijande, E. Weissma, N. Barnea and A. Valcarce, *Do $c\bar{c}n\bar{n}$ bound states exist?*, Phys. Rev. **D76** (2007) 094022.
- [305] Y. R. Liu and Z. Y. Zhang, *$X(3872)$ and the bound state problem of $D^0\bar{D}^{*0}$ (\bar{D}^0D^{*0}) in a chiral quark model*, Phys. Rev. **C79** (2009) 035206.
- [306] G. J. Wang, L. Meng and S. L. Zhu, *Spectrum of the fully-heavy tetraquark state $QQ\bar{Q}'\bar{Q}'$* , Phys. Rev. **D100** (2019) 096013.
- [307] G. Yang, J. L. Ping and J. Segovia, *Tetra- and penta-quark structures in the constituent quark model*, Symmetry **12** (2020) 1869.
- [308] S. Noh, W. Park and S. H. Lee, *The Doubly-heavy Tetraquarks ($qq'\bar{Q}\bar{Q}'$) in a Constituent Quark Model with a Complete Set of Harmonic Oscillator Bases*, Phys. Rev. **D103** (2021) 114009.
- [309] Z. Zhao, K. Xu, A. Kaewsnod, X. Liu, A. Limphirat and Y. Yan, *Study of charmoniumlike and fully-charm tetraquark spectroscopy*, Phys. Rev. **D103** (2021) 116027.
- [310] C. R. Deng, J. L. Ping, H. X. Huang and F. Wang, *Hidden charmed states and multibody color flux-tube dynamics*, Phys. Rev. **D98** (2018) 014026.
- [311] C. R. Deng, H. Chen and J. L. Ping, *Systematical investigation on the stability of doubly heavy tetraquark states*, Eur. Phys. J. **A56** (2020) 9.
- [312] C. Michael, *Adjoint Sources in Lattice Gauge Theory*, Nucl. Phys. **B259** (1985) 58.
- [313] B. Blossier, M. D. Morte, G. v. Hippel, T. Mendes and R. Sommer, *On the generalized eigenvalue method for energies and matrix elements in lattice field theory*, JHEP **04** (2009) 094.
- [314] S. Prelovsek, C. B. Lang, L. Leskovec and D. Mohler, *Study of the Z_c^+ channel using lattice QCD*, Phys. Rev. **D91** (2015) 014504.

- [315] M. Padmanath, C. B. Lang and S. Prelovsek, *X(3872) and Y(4140) using diquark-antidiquark operators with lattice QCD*, Phys. Rev. **D92** (2015) 034501.
- [316] A. Francis, R. J. Hudspith, R. Lewis and K. Maltman, *Lattice Prediction for Deeply Bound Doubly Heavy Tetraquarks*, Phys. Rev. Lett. **118** (2017) 142001.
- [317] G. K. C. Cheung, C. E. Thomas, J. J. Dudek and R. G. Edwards, *Tetraquark operators in lattice QCD and exotic flavour states in the charm sector*, JHEP **11** (2017) 033.
- [318] P. Junnarkar, N. Mathur and M. Padmanath, *Study of doubly heavy tetraquarks in Lattice QCD*, Phys. Rev. **D99** (2019) 034507.
- [319] L. Leskovec, S. Meinel, M. Pflaumer and M. Wagner, *Lattice QCD investigation of a doubly-bottom $\bar{b}bud$ tetraquark with quantum numbers $I(J^P) = 0(1^+)$* , Phys. Rev. **D100** (2019) 014503.
- [320] A. Francis, R. J. Hudspith, R. Lewis and K. Maltman, *Evidence for charm-bottom tetraquarks and the mass dependence of heavy-light tetraquark states from lattice QCD*, Phys. Rev. **D99** (2019) 054505.
- [321] A. Francis, *Lattice perspectives on doubly heavy tetraquarks*, Prog. Part. Nucl. Phys. **140** (2025) 104143.
- [322] P. Bicudo, *Tetraquarks and pentaquarks in lattice QCD with light and heavy quarks*, Phys. Rept. **1039** (2023) 1.
- [323] M. Luscher, *Two particle states on a torus and their relation to the scattering matrix*, Nucl. Phys. **B354** (1991) 531.
- [324] M. Luscher, *Signatures of unstable particles in finite volume*, Nucl. Phys. **B364** (1991) 237.
- [325] R. A. Briceno, J. J. Dudek and R. D. Young, *Scattering processes and resonances from lattice QCD*, Rev. Mod. Phys. **90** (2018) 025001.
- [326] S. Prelovsek and L. Leskovec, *Evidence for X(3872) from DD^* scattering on the lattice*, Phys. Rev. Lett. **111** (2013) 192001.
- [327] Y. Chen et al, *Low-energy Scattering of $(D\bar{D}^*)^\pm$ System And the Resonance-like Structure $Z_c(3900)$* , Phys. Rev. **D89** (2014) 094506.
- [328] M. Padmanath and S. Prelovsek, *Signature of a Doubly Charm Tetraquark Pole in DD^* Scattering on the Lattice*, Phys. Rev. Lett. **129** (2022) 032002.
- [329] S. Chen, C. Shi, Y. Chen, M. Gong, Z. Liu, W. Sun and R. Zhang, *$T_{cc}^+(3875)$ relevant DD^* scattering from $N_f = 2$ lattice QCD*, Phys. Lett. **B833** (2022) 137391.
- [330] M. L. Du, A. Filin, V. Baru, X. K. Dong, E. Epelbaum, F. K. Guo, C. Hanhart, A. Nefediev, J. Nieves and Q. Wang, *Role of left-hand cut contributions on pole extractions from lattice data: Case study for $T_{cc}(3875)^+$* , Phys. Rev. Lett. **131** (2023) 131903.
- [331] S. Aoki, T. Doi, T. Hatsuda, Y. Ikeda, T. Inoue, N. Ishii, K. Murano, H. Nemura and K. Sasaki, *Lattice QCD approach to Nuclear Physics*, PTEP *2012* (2012) 01A105.
- [332] Y. Lyu, S. Aoki, T. Doi, T. Hatsuda, Y. Ikeda and J. Meng, *Doubly Charmed Tetraquark T^{+cc} from Lattice QCD near Physical Point* Phys. Rev. Lett. **131** (2023) 161901.
- [333] M. A. Shifman, A. I. Vainshtein and V. I. Zakharov, *QCD and Resonance Physics. Theoretical Foundations*, Nucl. Phys. **B147** (1979) 385.

- [334] M. A. Shifman, A. I. Vainshtein and V. I. Zakharov, *QCD and Resonance Physics: Applications*, Nucl. Phys. **B147** (1979) 448.
- [335] B.L. Ioffe, *Calculation of Baryon Masses in Quantum Chromodynamics*, Nucl. Phys. **B188** (1981) 317.
- [336] D. B. Leinweber, *QCD sum rules for skeptics* Annals Phys. **254** (1997) 328.
- [337] Z. G. Wang, *Two-particle contributions and nonlocal effects in the QCD sum rules for the axial vector tetraquark candidate $Z_c(3900)$* , Int. J. Mod. Phys. **A35** (2020) 2050138.
- [338] Z. G. Wang, *Analysis of the $P_c(4312)$, $P_c(4440)$, $P_c(4457)$ and related hidden-charm pentaquark states with QCD sum rules*, Int. J. Mod. Phys. **A35** (2020) 2050003.
- [339] Y. Kondo, O. Morimatsu and T. Nishikawa, *Two-hadron-irreducible QCD sum rule for pentaquark baryon*, Phys. Lett. **B611** (2005) 93.
- [340] S. H. Lee, H. Kim and Y. Kwon, *Parity of $\Theta^+(1540)$ from QCD sum rules*, Phys. Lett. **B609** (2005) 252.
- [341] H. J. Lee and N. I. Kochelev, *On the $\pi\pi$ contribution to the QCD sum rules for the light tetraquark*, Phys. Rev. **D78** (2008) 076005.
- [342] H. X. Chen, A. Hosaka, H. Toki and S. L. Zhu, *Light Scalar Meson $\sigma(600)$ in QCD Sum Rule with Continuum*, Phys. Rev. **D81** (2010) 114034.
- [343] W. Lucha, D. Melikhov and H. Sazdjian, *Tetraquark-adequate formulation of QCD sum rules*, Phys. Rev. **D100** (2019) 014010.
- [344] W. Lucha, D. Melikhov and H. Sazdjian, *Tetraquark-adequate QCD sum rules for quark-exchange processes*, Phys. Rev. **D100** (2019) 074029.
- [345] Z. G. Wang, *Landau equation and QCD sum rules for the tetraquark molecular states*, Phys. Rev. **D101** (2020) 074011.
- [346] L. D. Landau, *On analytic properties of vertex parts in quantum field theory*, Nucl. Phys. **13** (1959) 181.
- [347] M. Tanabashi et al, *The Review of Particle Physics*, Phys. Rev. **D98** (2018) 030001.
- [348] N. Gray, D. J. Broadhurst, W. Grafe and K. Schilcher, *Three Loop Relation of Quark (Modified) \overline{MS} and Pole Masses*, Z. Phys. **C48** (1990) 673.
- [349] K. U. Can, G. Erkol, B. Isildak, M. Oka and T. Takahashi, *Electromagnetic structure of charmed baryons in Lattice QCD*, PoS LATTICE2014 (2015) 157.
- [350] J. Y. Kim and H. C. Kim, *Electromagnetic form factors of singly heavy baryons in the self-consistent $SU(3)$ chiral quark-soliton model*, Phys. Rev. **D97** (2018) 114009.
- [351] C. W. Hwang, *Charge radii of light and heavy mesons*, Eur. Phys. J. **C23** (2002) 585.
- [352] Z. G. Wang, *Comment on "OPE and quark-hadron duality for two-point functions of tetraquark currents in $1/N_c$ expansion"*, arXiv:2102.07520 [hep-ph].
- [353] Z. G. Wang and Q. Xin, *Analysis of the hidden-charm pentaquark molecular states with and without strangeness via the QCD sum rules*, Chin. Phys. **C45** (2021) 123105.
- [354] J. Beringer et al, *Review of Particle Physics*, Phys. Rev. **D86** (2012) 010001.

- [355] Z. G. Wang, *Analysis of the masses and decay constants of the heavy-light mesons with QCD sum rules*, Eur. Phys. J. **C75** (2015) 427.
- [356] K. G. Chetyrkin and M. Steinhauser, *Three loop nondiagonal current correlators in QCD and NLO corrections to single top quark production*, Phys. Lett. **B502** (2001) 104.
- [357] K. G. Chetyrkin and M. Steinhauser, *Heavy-light current correlators at order α_s^2 in QCD and HQET*, Eur. Phys. J. **C21** (2001) 319.
- [358] Z. G. Wang, *Reanalysis of the $Y(3940)$, $Y(4140)$, $Z_c(4020)$, $Z_c(4025)$ and $Z_b(10650)$ as molecular states with QCD sum rules*, Eur. Phys. J. **C74** (2014) 2963.
- [359] Z. G. Wang, *Analysis of $P_c(4380)$ and $P_c(4450)$ as pentaquark states in the diquark model with QCD sum rules*, Eur. Phys. J. **C76** (2016) 70.
- [360] Z. G. Wang, *Analysis of the $Z_c(4020)$, $Z_c(4025)$, $Y(4360)$ and $Y(4660)$ as vector tetraquark states with QCD sum rules*, Eur. Phys. J. **C74** (2014) 2874.
- [361] Z. G. Wang, *Analysis of the hidden-charm-hidden-strange tetraquark mass spectrum via the QCD sum rules*, Nucl. Phys. **1007** (2024) 116661.
- [362] Z. G. Wang, *Analysis of the tetraquark and hexaquark molecular states with the QCD sum rules*, Commun. Theor. Phys. **73** (2021) 065201.
- [363] S. H. Lee, A. Mihara, F. S. Navarra and M. Nielsen, *QCD sum rules study of the meson $Z^+(4430)$* , Phys. Lett. **B661** (2008) 28.
- [364] S. H. Lee, K. Morita and M. Nielsen, *Width of exotics from QCD sum rules: Tetraquarks or molecules?*, Phys. Rev. **D78** (2008) 076001.
- [365] S. H. Lee, M. Nielsen and U. Wiedner, *$D_s D^*$ molecule as an axial meson*, J. Korean Phys. Soc. **55** (2009) 424.
- [366] M. E. Bracco, S. H. Lee, M. Nielsen, R. Rodrigues da Silva, *The Meson $Z^+(4430)$ as a tetraquark state*, Phys. Lett. **B671** (2009) 240.
- [367] S. H. Lee, K. Morita and M. Nielsen, *Can the $\pi^+ \chi_{c1}$ resonance structures be $D^* \bar{D}^*$ and $D_1 \bar{D}$ molecules?*, Nucl. Phys. **A815** (2009) 29.
- [368] R. M. Albuquerque and M. Nielsen, *QCD sum rules study of the $J^{PC} = 1^{--}$ charmonium Y mesons*, Nucl. Phys. **A815** (2009) 53; Nucl. Phys. **A857** (2011) 48.
- [369] R. M. Albuquerque, M. E. Bracco and M. Nielsen, *A QCD sum rule calculation for the $Y(4140)$ narrow structure*, Phys. Lett. **B678** (2009) 186.
- [370] R. D. Matheus, F. S. Navarra, M. Nielsen and C. M. Zanetti, *QCD Sum Rules for the $X(3872)$ as a mixed molecule-charmonium state*, Phys. Rev. **D80** (2009) 056002.
- [371] J. R. Zhang and M. Q. Huang, *$\{Q\bar{q}\}\{\bar{Q}^{(\prime)}q\}$ molecular states*, Phys. Rev. **D80** (2009) 056004.
- [372] J. R. Zhang and M. Q. Huang, *$(Q\bar{s})^{(*)}(\bar{Q}s)^{(*)}$ molecular states from QCD sum rules: a view on $Y(4140)$* , J. Phys. **G37** (2010) 025005.
- [373] J. R. Zhang and M. Q. Huang, *$\{Q\bar{s}\}\{\bar{Q}^{(\prime)}s\}$ molecular states in QCD sum rules*, Commun. Theor. Phys. **54** (2010) 1075.
- [374] W. Chen and S. L. Zhu, *Possible $J^{PC} = 0^{--}$ Charmonium-like State*, Phys. Rev. **D81** (2010) 105018.

- [375] M. Nielsen and C. M. Zanetti, *Radiative decay of the $X(3872)$ as a mixed molecule-charmonium state in QCD Sum Rules*, Phys. Rev. **D82** (2010) 116002.
- [376] S. Narison, F. S. Navarra and M. Nielsen, *On the nature of the $X(3872)$ from QCD*, Phys. Rev. **D83** (2011) 016004.
- [377] R. M. Albuquerque, M. Nielsen, R. Rodrigues da Silva, *Exotic 1^{--} States in QCD Sum Rules*, Phys. Rev. **D84** (2011) 116004.
- [378] J. M. Dias, S. Narison, F. S. Navarra, M. Nielsen and J. M. Richard, *Relation between $T_{cc,bb}$ and $X_{c,b}$ from QCD*, Phys. Lett. **B703** (2011) 274.
- [379] S. I. Finazzo, X. Liu and M. Nielsen, *QCD sum rule calculation for the charmonium-like structures in the $J/\psi\phi$ and $J/\psi\omega$ invariant mass spectra*, Phys. Lett. **B701** (2011) 101.
- [380] J. R. Zhang, M. Zhong and M. Q. Huang, *Could $Z_b(10610)$ be a $B^*\bar{B}$ molecular state?*, Phys. Lett. **B704** (2011) 312.
- [381] W. Chen and S. L. Zhu, *The Vector and Axial-Vector Charmonium-like States*, Phys. Rev. **D83** (2011) 034010.
- [382] C. Y. Cui, Y. L. Liu and M. Q. Huang, *Investigating different structures of the $Z_b(10610)$ and $Z_b(10650)$* , Phys. Rev. **D85** (2012) 074014.
- [383] J. M. Dias, F. S. Navarra, M. Nielsen and C. M. Zanetti, *$Z_c^+(3900)$ decay width in QCD sum rules*, Phys. Rev. **D88** (2013) 016004.
- [384] W. Chen, H. Y. Jin, R. T. Kleiv, T. G. Steele, M. Wang and Q. Xu, *QCD Sum-Rule Interpretation of $X(3872)$ with $J^{PC} = 1^{++}$ Mixtures of Hybrid Charmonium and $\bar{D}D^*$ Molecular Currents*, Phys. Rev. **D88** (2013) 045027.
- [385] J. R. Zhang, *Improved QCD sum rule study of $Z_c(3900)$ as a $\bar{D}D^*$ molecular state*, Phys. Rev. **D87** (2013) 116004.
- [386] C. F. Qiao and L. Tang, *Estimating the mass of the hidden charm $1^+(1^+)$ tetraquark state via QCD sum rules* Eur. Phys. J. **C74** (2014) 3122.
- [387] C. F. Qiao and L. Tang, *Interpretation of $Z_c(4025)$ as the hidden charm tetraquark states via QCD Sum Rules*, Eur. Phys. J. **C74** (2014) 2810.
- [388] W. Chen, T. G. Steele, H. X. Chen and S. L. Zhu, *Mass spectra of Z_c and Z_b exotic states as hadron molecules*, Phys. Rev. **D92** (2015) 054002.
- [389] R. Albuquerque, S. Narison, F. Fanomezana, A. Rabemananjara, D. Rabetiarivony and G. Randriamanatrika, *XYZ-like Spectra from Laplace Sum Rule at N^2LO in the Chiral Limit*, Int. J. Mod. Phys. **A31** (2016) 1650196.
- [390] L. Tang and C. F. Qiao, *Tetraquark States with Open Flavors*, Eur. Phys. J. **C76** (2016) 558.
- [391] R. Albuquerque, S. Narison, D. Rabetiarivony and G. Randriamanatrika, *XYZ- SU_3 Breakings from Laplace Sum Rules at Higher Orders*, Int. J. Mod. Phys. **A33** (2018) 1850082.
- [392] L. Tang, B. D. Wan, K. Maltman and C. F. Qiao, *Doubly Heavy Tetraquarks in QCD Sum Rules*, Phys. Rev. **D101** (2020) 094032.
- [393] R. M. Albuquerque, S. Narison, A. Rabemananjara, D. Rabetiarivony and G. Randriamanatrika, *Doubly-hidden scalar heavy molecules and tetraquarks states from QCD at NLO*, Phys. Rev. **D102** (2020) 094001.

- [394] B. D. Wan and C. F. Qiao, *About the exotic structure of Z_{cs}* , Nucl. Phys. **B968** (2021) 115450.
- [395] W. Chen, T. G. Steele and S. L. Zhu, *Exotic open-flavor $bc\bar{q}\bar{q}$, $bc\bar{s}\bar{s}$ and $qc\bar{q}\bar{b}$, $sc\bar{s}\bar{b}$ tetraquark states*, Phys. Rev. **D89** (2014) 054037.
- [396] B. C. Yang, L. Tang and C. F. Qiao, *Scalar Fully-heavy Tetraquark States $QQ'\bar{Q}\bar{Q}'$ in QCD Sum Rules*, Eur. Phys. J. **C81** (2021) 324.
- [397] J. R. Zhang, 0^+ *fully-charmed tetraquark states*, Phys. Rev. **D103** (2021) 014018.
- [398] R. M. Albuquerque, S. Narison and D. Rabetiarivony, *Z_c -like spectra from QCD Laplace sum rules at NLO*, Phys. Rev. **D103** (2021) 074015.
- [399] S. S. Agaev, K. Azizi and H. Sundu, *Strong $Z_c^+(3900) \rightarrow J/\psi\pi^+$; $\eta_c\rho^+$ decays in QCD*, Phys. Rev. **D93** (2016) 074002.
- [400] U. Ozdem and K. Azizi, *Magnetic and quadrupole moments of the $Z_c(3900)$* , Phys. Rev. **D96** (2017) 074030.
- [401] S. S. Agaev, K. Azizi and H. Sundu, *Treating $Z_c(3900)$ and $Z(4430)$ as the ground-state and first radially excited tetraquarks*, Phys. Rev. **D96** (2017) 034026.
- [402] H. Sundu, S. S. Agaev and K. Azizi, *New charged resonance $Z_c(4100)$: the spectroscopic parameters and width*, Eur. Phys. J. **C79** (2019) 215.
- [403] S. S. Agaev, K. Azizi, B. Barsbay and H. Sundu, *The doubly charmed pseudoscalar tetraquarks $T_{cc;\bar{s}\bar{s}}^{++}$ and $T_{cc;\bar{d}\bar{s}}^{++}$* , Nucl. Phys. **B939** (2019) 130.
- [404] S. Agaev, K. Azizi and H. Sundu, *Four-quark exotic mesons*, Turk. J. Phys. **44** (2020) 95.
- [405] U. Ozdem and K. Azizi, *Magnetic dipole moment of the $Z_{cs}(3985)$ state: diquark-antidiquark and molecular pictures*, Eur. Phys. J. Plus **136** (2021) 968.
- [406] U. Ozdem and A. K. Yildirim, *Magnetic dipole moments of the $Z_c(4020)^+$, $Z_c(4200)^+$, $Z_{cs}(4000)^+$ and $Z_{cs}(4220)^+$ states in light-cone QCD*, Phys. Rev. **D104** (2021) 054017.
- [407] K. Azizi and N. Er, *The newly observed $Z_{cs}(3985)^-$ state: in vacuum and a dense medium*, Eur. Phys. J. **C81** (2021) 61.
- [408] S. S. Agaev, K. Azizi and H. Sundu, *Hadronic molecule model for the doubly charmed state T_{cc}^+* , JHEP **06** (2022) 057.
- [409] S. S. Agaev, K. Azizi and H. Sundu, *Newly observed exotic doubly charmed meson T_{cc}^+* , Nucl. Phys. **B975** (2022) 115650.
- [410] Z. G. Wang, *Mass spectrum of the vector hidden charmed and bottomed tetraquark states*, J. Phys. **G36** (2009) 085002.
- [411] Z. G. Wang, *Mass spectrum of the scalar hidden charmed and bottomed tetraquark states*, Phys. Rev. **D79** (2009) 094027.
- [412] Z. G. Wang, *Analysis of the $Y(4140)$ with QCD sum rules*, Eur. Phys. J. **C63** (2009) 115.
- [413] Z. G. Wang, Z. C. Liu and X. H. Zhang, *Analysis of the $Y(4140)$ and related molecular states with QCD sum rules*, Eur. Phys. J. **C64** (2009) 373.
- [414] Z. G. Wang, *Possible tetraquark state in the $\pi^+\chi_{c1}$ invariant mass distribution*, Eur. Phys. J. **C59** (2009) 675.

- [415] Z. G. Wang, *Another tetraquark structure in the $\pi^+\chi_{c1}$ invariant mass distribution*, Eur. Phys. J. **C62** (2009) 375.
- [416] Z. G. Wang, *Reanalysis of the mass spectrum of the scalar hidden charm and hidden bottom tetraquark states*, Eur. Phys. J. **C67** (2010) 411.
- [417] Z. G. Wang and X. H. Zhang, *Analysis of the pseudoscalar partner of the $Y(4660)$ and related bound states*, Eur. Phys. J. **C66** (2010) 419.
- [418] Z. G. Wang, *Mass spectrum of the axial-vector hidden charmed and hidden bottom tetraquark states*, Eur. Phys. J. **C70** (2010) 139.
- [419] Z. G. Wang, *Analysis of the $X(4350)$ as a scalar $\bar{c}c$ and $D_s^*\bar{D}_s^*$ mixing state with QCD sum rules*, Phys. Lett. **B690** (2010) 403.
- [420] Z. G. Wang and X. H. Zhang, *Analysis of $Y(4660)$ and related bound states with QCD sum rules*, Commun. Theor. Phys. **54** (2010) 323.
- [421] Z. G. Wang, *Analysis of the $Y(4274)$ with QCD sum rules*, Int. J. Mod. Phys. **A26** (2011) 4929.
- [422] Z. G. Wang, *Analysis of the $\bar{D}\Sigma_c$, $\bar{D}^*\Sigma_c^*$, $\bar{D}^*\Sigma_c$ and $\bar{D}^*\Sigma_c^*$ pentaquark molecular states with QCD sum rules*, Int. J. Mod. Phys. **A34** (2019) 1950097.
- [423] H. X. Chen, A. Hosaka and S. L. Zhu, *Light Scalar Tetraquark Mesons in the QCD Sum Rule*, Phys. Rev. **D76** (2007) 094025.
- [424] W. Chen, H. X. Chen, X. Liu, T. G. Steele and S. L. Zhu, *Mass spectra for $qc\bar{q}\bar{c}$, $sc\bar{s}\bar{c}$, $qb\bar{q}\bar{b}$, $sb\bar{s}\bar{b}$ tetraquark states with $J^{PC} = 0^{++}$ and 2^{++}* , Phys. Rev. **D96** (2017) 114017.
- [425] W. Chen and S. L. Zhu, *The Possible $J^{PC} = 0^{--}$ Charmonium-like State*, Phys. Rev. **D81** (2010) 105018.
- [426] W. Chen, H. X. Chen, X. Liu, T. G. Steele and S. L. Zhu, *Hunting for exotic doubly hidden-charm/bottom tetraquark states*, Phys. Lett. **B773** (2017) 247.
- [427] Z. G. Wang, *Analysis of the $Y(2175)$ as a tetraquark state with QCD sum rules*, Nucl. Phys. **A791** (2007) 106.
- [428] Z. G. Wang, *Analysis of the mass and width of the $Y(4274)$ as axialvector molecule-like state*, Eur. Phys. J. **C77** (2017) 174.
- [429] Z. G. Wang, *Analysis of the $Z_c(4200)$ as axial-vector molecule-like state*, Int. J. Mod. Phys. **A30** (2015) 1550168.
- [430] Z. G. Wang, *Analysis of the scalar and axial-vector heavy diquark states with QCD sum rules*, Eur. Phys. J. **C71** (2011) 1524.
- [431] L. Tang and X. Q. Li, *Discussions on Stability of Diquarks*, Chin. Phys. **C36** (2012) 578.
- [432] R. T. Kleiv, T. G. Steele, A. L. Zhang and I. Blokland, *Heavy-light diquark masses from QCD sum rules and constituent diquark models of tetraquarks*, Phys. Rev. **D87** (2013) 125018.
- [433] Z. G. Wang, *Analysis of the light-flavor scalar and axial-vector diquark states with QCD sum rules*, Commun. Theor. Phys. **59** (2013) 451.
- [434] H. G. Dosch, M. Jamin and B. Stech, *Diquarks, QCD Sum Rules and Weak Decays*, Z. Phys. **C42** (1989) 167.

- [435] M. Jamin and M. Neubert, *Diquark Decay Constants From QCD Sum Rules*, Phys. Lett. **B238** (1990) 387.
- [436] A. L. Zhang, T. Huang and T. G. Steele, *Diquark and light four-quark states*, Phys. Rev. **D76** (2007) 036004.
- [437] Z. G. Wang, *Scalar or vector tetraquark state candidate: $Z_c(4100)$* , Commun. Theor. Phys. **71** (2019) 1319.
- [438] L. J. Reinders, H. Rubinstein and S. Yazaki, *Hadron Properties from QCD Sum Rules*, Phys. Rept. **127** (1985) 1.
- [439] P. Pascual and R. Tarrach, *QCD : renormalization for the practitioner* Lect. Notes Phys. **194** (1984) 1.
- [440] X. W. Wang, Z. G. Wang and G. L. Yu, *Study of $\Lambda_c\Lambda_c$ dibaryon and $\Lambda_c\bar{\Lambda}_c$ baryonium states via QCD sum rules*, Eur. Phys. J. **A57** (2021) 275.
- [441] S. Narison and R. Tarrach, *Higher Dimensional Renormalization Group Invariant Vacuum Condensates in Quantum Chromodynamics*, Phys. Lett. **B125** (1983) 217.
- [442] P. Colangelo and A. Khodjamirian, *QCD sum rules, a modern perspective*, arXiv: hep-ph/0010175.
- [443] Z. G. Wang, *Tetraquark state candidates: $Y(4260)$, $Y(4360)$, $Y(4660)$ and $Z_c(4020/4025)$* , Eur. Phys. J. **C76** (2016) 387.
- [444] Q. Xin and Z. G. Wang, *Analysis of the doubly-charmed tetraquark molecular states with the QCD sum rules*, Eur. Phys. J. **A58** (2022) 110.
- [445] Z. G. Wang, *Analysis of the $P_{cs}(4459)$ as the hidden-charm pentaquark state with QCD sum rules*, Int. J. Mod. Phys. **A36** (2021) 2150071.
- [446] Z. G. Wang and Q. Xin, *Analysis of the pseudoscalar hidden-charm tetraquark states with the QCD sum rules*, Nucl. Phys. **B978** (2022) 115761.
- [447] Z. G. Wang, *Analysis of the hidden-bottom tetraquark mass spectrum with the QCD sum rules*, Eur. Phys. J. **C79** (2019) 489.
- [448] M. S. Maior de Sousa and R. Rodrigues da Silva, *The $\rho(1S, 2S)$, $\psi(1S, 2S)$, $\Upsilon(1S, 2S)$ and $\psi_t(1S, 2S)$ mesons in a double pole QCD Sum Rule*, Braz. J. Phys. **46** (2016) 730.
- [449] S. S. Agaev, K. Azizi and H. Sundu, *Treating $Z_c(3900)$ and $Z(4430)$ as the ground-state and first radially excited tetraquarks*, Phys. Rev. **D96** (2017) 034026.
- [450] K. Azizi and N. Er, *Modifications on parameters of $Z(4430)$ in a dense medium*, Phys. Lett. **B811** (2020) 135979.
- [451] Z. G. Wang, *Scalar tetraquark state candidates: $X(3915)$, $X(4500)$ and $X(4700)$* , Eur. Phys. J. **C77** (2017) 78.
- [452] Z. G. Wang, *Reanalysis of the $X(3915)$, $X(4500)$ and $X(4700)$ with QCD sum rules*, Eur. Phys. J. **A53** (2017) 19.
- [453] Z. G. Wang, *Assignments of the $X(4140)$, $X(4500)$, $X(4630)$ and $X(4685)$ Based on the QCD Sum Rules*, Adv. High Energy Phys. **2021** (2021) 4426163.
- [454] Z. G. Wang and H. J. Wang, *Analysis of the $1S$ and $2S$ states of Λ_Q and Ξ_Q with QCD sum rules*, Chin. Phys. **C45** (2021) 013109.

- [455] Z. G. Wang, *Analysis of the vector hidden-charm tetraquark states without explicit P-waves via the QCD sum rules*, Nucl. Phys. **B973** (2021) 115592.
- [456] Z. G. Wang, *Vector tetraquark state candidates: $Y(4260/4220)$, $Y(4360/4320)$, $Y(4390)$ and $Y(4660/4630)$* , Eur. Phys. J. **C78** (2018) 518.
- [457] Z. G. Wang, *Analysis of the vector hidden-charm-hidden-strange tetraquark states with implicit P-waves via the QCD sum rules*, Nucl. Phys. **1007** (2024) 116661.
- [458] Z. G. Wang, *Strong decays of the vector tetraquark states with the masses about 4.5 GeV via the QCD sum rules*, Nucl. Phys. **B1005** (2024) 116580.
- [459] Z. G. Wang, *Lowest vector tetraquark states: $Y(4260/4220)$ or $Z_c(4100)$* , Eur. Phys. J. **C78** (2018) 933.
- [460] Z. G. Wang, *Analysis of the vector tetraquark states with P-waves between the diquarks and antidiquarks via the QCD sum rules*, Eur. Phys. J. **C79** (2019) 29.
- [461] S. L. Zhu, *The Possible interpretations of $Y(4260)$* , Phys. Lett. **B625** (2005) 212.
- [462] F. E. Close and P. R. Page, *Gluonic charmonium resonances at BaBar and BELLE?*, Phys. Lett. **B628** (2005) 215.
- [463] E. Kou and O. Pene, *Suppressed decay into open charm for the $Y(4260)$ being an hybrid*, Phys. Lett. **B631** (2005) 164.
- [464] L. Liu et al, *Excited and exotic charmonium spectroscopy from lattice QCD*, JHEP **07** (2012) 126.
- [465] G. J. Ding, *Are $Y(4260)$ and $Z_2^+(4250)$ D_1D or D_0D^* Hadronic Molecules?*, Phys. Rev. **D79** (2009) 014001.
- [466] X. K. Dong, F. K. Guo and B. S. Zou, *A survey of heavy-antiheavy hadronic molecules*, Progr. Phys. **41** (2021) 65.
- [467] T. W. Chiu and T. H. Hsieh, *$Y(4260)$ on the lattice*, Phys. Rev. **D73** (2006) 094510.
- [468] C. F. Qiao, *One explanation for the exotic state $Y(4260)$* , Phys. Lett. **B639** (2006) 263.
- [469] C. F. Qiao, *A Uniform description of the states recently observed at B-factories*, J. Phys. **G35** (2008) 075008.
- [470] X. Li and M. B. Voloshin, *$Y(4260)$ and $Y(4360)$ as mixed hadrocharmonium*, Mod. Phys. Lett. **A29** (2014) 1450060.
- [471] D. Y. Chen, J. He and X. Liu, *Nonresonant explanation for the $Y(4260)$ structure observed in the $e^+e^- \rightarrow J/\psi\pi^+\pi^-$ process*, Phys. Rev. **D83** (2011) 054021.
- [472] D. Y. Chen, X. Liu, X. Q. Li and H. W. Ke, *Unified Fano-like interference picture for charmoniumlike states $Y(4008)$, $Y(4260)$ and $Y(4360)$* , Phys. Rev. **D93** (2016) 014011.
- [473] Z. G. Wang, *Ground states and first radial excitations of vector tetraquark states with explicit P-waves via QCD sum rules*, Chin. Phys. **C48** (2024) 103103.
- [474] Z. G. Wang, *Vector hidden-bottom tetraquark candidate: $Y(10750)$* , Chin. Phys. **C43** (2019) 123102.
- [475] R. Aaij et al, *Observation of the doubly charmed baryon Ξ_{cc}^{++}* , Phys. Rev. Lett. **119** (2017) 112001.

- [476] Z. G. Wang, *Analysis of the doubly heavy baryon states and pentaquark states with QCD sum rules*, Eur. Phys. J. **C78** (2018) 826.
- [477] M. Karliner and J. L. Rosner, *Discovery of doubly-charmed Ξ_{cc} baryon implies a stable $bb\bar{u}\bar{d}$ tetraquark*, Phys. Rev. Lett. **119** (2017) 202001.
- [478] E. J. Eichten and C. Quigg, *Heavy-quark symmetry implies stable heavy tetraquark mesons $Q_i Q_j \bar{q}_k \bar{q}_l$* , Phys. Rev. Lett. **119** (2017) 202002.
- [479] J. P. Ader, J. M. Richard and P. Taxil, *Do narrow heavy multiquark states exist?*, Phys. Rev. **D25** (1982) 2370.
- [480] S. Zouzou, B. Silvestre-Brac, C. Gignoux and J. M. Richard, *Four-quark bound states*, Z. Phys. **C30** (1986) 457.
- [481] A. V. Manohar and M. B. Wise, *Exotic $QQ\bar{q}\bar{q}$ states in QCD*, Nucl. Phys. **B399** (1993) 17.
- [482] Z. G. Wang, *Analysis of the axialvector doubly heavy tetraquark states with QCD sum rules*, Acta Phys. Polon. **B49** (2018) 1781.
- [483] M. L. Du, W. Chen, X. L. Chen and S. L. Zhu, *Exotic $QQ\bar{q}\bar{q}$, $QQ\bar{q}\bar{s}$ and $QQ\bar{s}\bar{s}$ states*, Phys. Rev. **D87** (2013) 014003.
- [484] Z. G. Wang and Z. H. Yan, *Analysis of the scalar, axialvector, vector, tensor doubly charmed tetraquark states with QCD sum rules*, Eur. Phys. J. **C78** (2018) 19.
- [485] M. A. Moinester, *How to search for doubly charmed baryons and tetraquarks*, Z. Phys. **A355** (1996) 349.
- [486] S. Pepin, F. Stancu, M. Genovese and J. M. Richard, *Tetraquarks with color blind forces in chiral quark models*, Phys. Lett. **B393** (1997) 119.
- [487] B. A. Gelman and S. Nussinov, *Does a narrow tetraquark $cc\bar{u}\bar{d}$ state exist?*, Phys. Lett. **B551** (2003) 296.
- [488] D. Janc and M. Rosina, *The $T_{cc} = DD^*$ molecular state*, Few Body Syst. **35** (2004) 175.
- [489] F. S. Navarra, M. Nielsen and S. H. Lee, *QCD sum rules study of $QQ\bar{u}\bar{d}$ mesons*, Phys. Lett. **B649** (2007) 166.
- [490] Z. G. Wang, Y. M. Xu and H. J. Wang, *Analysis of the scalar doubly heavy tetraquark states with QCD sum rules*, Commun. Theor. Phys. **55** (2011) 1049.
- [491] J. Vijande, E. Weissman, A. Valcarce and N. Barnea, *Are there compact heavy four-quark bound states?*, Phys. Rev. **D76** (2007) 094027.
- [492] S. H. Lee and S. Yasui, *Stable multiquark states with heavy quarks in a diquark model*, Eur. Phys. J. **C64** (2009) 283.
- [493] Y. Yang, C. Deng, J. Ping and T. Goldman, *S-wave $QQ\bar{q}\bar{q}$ state in the constituent quark model*, Phys. Rev. **D80** (2009) 114023.
- [494] S. Q. Luo, K. Chen, X. Liu, Y. R. Liu and S. L. Zhu, *Exotic tetraquark states with the $qq\bar{Q}\bar{Q}$ configuration*, Eur. Phys. J. **C77** (2017) 709.
- [495] W. Park, S. Noh and S. H. Lee, *Masses of the doubly heavy tetraquarks in a constituent quark model*, Nucl. Phys. **A 983** (2019) 1.

- [496] L. Maiani, A. D. Polosa and V. Riquer, *Hydrogen bond of QCD in doubly heavy baryons and tetraquarks*, Phys. Rev. **D100** (2019) 074002.
- [497] G. Yang, J. Ping and J. Segovia, *Doubly-heavy tetraquarks*, Phys. Rev. **D101** (2020) 014001.
- [498] E. Braaten, L. P. He and A. Mohapatra, *Masses of doubly heavy tetraquarks with error bars*, Phys. Rev. **D103** (2021) 016001.
- [499] D. Gao, D. Jia and Y. J. Sun, *Masses of doubly heavy tetraquarks $QQ\bar{n}\bar{q}$ with $J^P = 1^+$* , Mod. Phys. Lett. **A37** (2022) 2250223.
- [500] J. B. Cheng, S. Y. Li, Y. R. Liu, Z. G. Si and T. Yao, *Double-heavy tetraquark states with heavy diquark-antiquark symmetry*, Chin. Phys. **C45** (2021) 043102.
- [501] R. N. Faustov, V. O. Galkin and E. M. Savchenko, *Heavy tetraquarks in the relativistic quark model*, Universe **7** (2021) 94.
- [502] Y. Ikeda et al, *Charmed Tetraquarks T_{cc} and T_{cs} from Dynamical Lattice QCD Simulations*, Phys. Lett. **B729** (2014) 85.
- [503] Z. G. Wang, *Does vacuum saturation work for the higher-dimensional vacuum condensates in the QCD sum rules?*, Int. J. Mod. Phys. **A36** (2021) 2150246.
- [504] Y. Iwasaki, *Is a State $c\bar{c}c\bar{c}$ Found at 6.0 GeV?*, Phys. Rev. Lett. **36** (1976) 1266.
- [505] K. T. Chao, *The $cc\bar{c}\bar{c}$ (Diquark-Anti-Diquark) States in e^+e^- Annihilation*, Z. Phys. **C7** (1981) 317.
- [506] A. M. Badalyan, B. L. Ioffe and A. V. Smilga, *Four-quark states in heavy quark systems*, Nucl. Phys. **B281** (1987) 85.
- [507] A. V. Berezhnoy, A. V. Luchinsky and A. A. Novoselov, *Tetraquarks Composed of 4 Heavy Quarks*, Phys. Rev. **D86** (2012) 034004.
- [508] M. Karliner, J. L. Rosner and S. Nussinov, *$QQ\bar{Q}\bar{Q}$ states: masses, production, and decays*, Phys. Rev. **D95** (2017) 034011.
- [509] V. R. Debastiani and F. S. Navarra, *A non-relativistic model for the $cc\bar{c}\bar{c}$ tetraquark*, Chin. Phys. **C43** (2019) 013105.
- [510] M. S. Liu, Q. F. Lu, X. H. Zhong and Q. Zhao, *All-heavy tetraquarks*, Phys. Rev. **D100** (2019) 016006.
- [511] R. J. Lloyd and J. P. Vary, *All charm tetraquarks*, Phys. Rev. **D70** (2004) 014009.
- [512] Z. G. Wang, *Analysis of the $QQ\bar{Q}\bar{Q}$ tetraquark states with QCD sum rules*, Eur. Phys. J. **C77** (2017) 432.
- [513] Z. G. Wang and Z. Y. Di, *Analysis of the vector and axialvector $QQ\bar{Q}\bar{Q}$ tetraquark states with QCD sum rules*, Acta Phys. Polon. **B50** (2019) 1335.
- [514] M. N. Anwar, J. Ferretti, F. K. Guo, E. Santopinto and B. S. Zou, *Spectroscopy and decays of the fully-heavy tetraquarks*, Eur. Phys. J. **C78** (2018) 647.
- [515] Z. G. Wang, *Tetraquark candidates in the LHCb's $di\text{-}J/\psi$ mass spectrum*, Chin. Phys. **C44** (2020) 113106.
- [516] Z. G. Wang, *Reanalysis of the $Z_c(4020)$, $Z_c(4025)$, $Z(4050)$ and $Z(4250)$ as tetraquark states with QCD sum rules*, Commun. Theor. Phys. **63** (2015) 466.

- [517] E. J. Eichten and C. Quigg, *Mesons with Beauty and Charm: New Horizons in Spectroscopy*, Phys. Rev. **D99** (2019) 054025.
- [518] Z. G. Wang, *Analysis of the $Y(4220)$ and $Y(4390)$ as molecular states with QCD sum rules*, Chin. Phys. **C41** (2017) 083103.
- [519] X. L. Wang et al, *The study of $\gamma\gamma \rightarrow \gamma\psi(2S)$ at Belle*, Phys. Rev. **D105** (2022) 112011.
- [520] P. A. Zyla et al, *Review of Particle Physics*, PTEP **2020** (2020) 083C01.
- [521] C. Patrignani et al, *Review of Particle Physics*, Chin. Phys. **C40** (2016) 100001.
- [522] Z. G. Wang, *Comment on "Zc-like spectra from QCD Laplace sum rules at NLO"*, arXiv:2202.06058 [hep-ph].
- [523] X. W. Wang and Z. G. Wang, *Search for the Charmed Baryonium and Dibaryon Structures via the QCD Sum Rules*, Adv. High Energy Phys. **2022** (2022) 6224597.
- [524] B. D. Wan, L. Tang and C. F. Qiao, *Hidden-bottom and -charm hexaquark states in QCD sum rules*, Eur. Phys. J. **C80** (2020) 121.
- [525] Y. Chung, H. G. Dosch, M. Kremer and D. Schall, *Baryon Sum Rules and Chiral Symmetry Breaking*, Nucl. Phys. **B197** (1982) 55.
- [526] E. Bagan, M. Chabab, H. G. Dosch and S. Narison, *Baryon sum rules in the heavy quark effective theory*, Phys. Lett. **B301**, 243 (1993).
- [527] D. Jido, N. Kodama and M. Oka, *Negative parity nucleon resonance in the QCD sum rule*, Phys. Rev. **D54** (1996) 4532.
- [528] Z. G. Wang, *Reanalysis of the heavy baryon states Ω_b , Ω_c , Ξ'_b , Ξ'_c , Σ_b and Σ_c with QCD sum rules*, Phys. Lett. **B685** (2010) 59.
- [529] Z. G. Wang, *Analysis of the $\frac{1}{2}^+$ doubly heavy baryon states with QCD sum rules*, Eur. Phys. J. **A45** (2010) 267.
- [530] Z. G. Wang, *Analysis of the $\frac{3}{2}^+$ heavy and doubly heavy baryon states with QCD sum rules*, Eur. Phys. J. **C68** (2010) 459.
- [531] Z. G. Wang, *Analysis of the $\frac{1}{2}^\pm$ antitriplet heavy baryon states with QCD sum rules*, Eur. Phys. J. **C68** (2010) 479.
- [532] Z. G. Wang, *Analysis of the $\frac{1}{2}^-$ and $\frac{3}{2}^-$ heavy and doubly heavy baryon states with QCD sum rules*, Eur. Phys. J. **A47** (2011) 81.
- [533] Z. G. Wang, *Analysis of the Triply Heavy Baryon States with QCD Sum Rules*, Commun. Theor. Phys. **58** (2012) 723.
- [534] Shi-Zhong Huang, *Free particles and fields of high spins (in chinese)*, Anhui peoples Publishing House, 2006.
- [535] Z. G. Wang and T. Huang *Analysis of the $\frac{1}{2}^\pm$ pentaquark states in the diquark model with QCD sum rules*, Eur. Phys. J. **C76** (2016) 43.
- [536] Z. G. Wang, *Analysis of the $\frac{1}{2}^\pm$ pentaquark states in the diquark-diquark-antiquark model with QCD sum rules*, Eur. Phys. J. **C76** (2016) 142.

- [537] Z. G. Wang, *Analysis of the $\frac{3}{2}^{\pm}$ pentaquark states in the diquark-diquark-antiquark model with QCD sum rules*, Nucl. Phys. **B913** (2016) 163.
- [538] J. X. Zhang, Z. G. Wang and Z. Y. Di, *Analysis of the $\frac{3}{2}^{\pm}$ pentaquark states in the diquark model with QCD sum rules*, Acta Phys. Polon. **B48** (2017) 2013.
- [539] H. X. Chen, W. Chen, X. Liu, T. G. Steele and S. L. Zhu, *Towards exotic hidden-charm pentaquarks in QCD*, Phys. Rev. Lett. **115** (2015) 172001.
- [540] H. X. Chen, E. L. Cui, W. Chen, T. G. Steele, X. Liu and S. L. Zhu, *QCD sum rule study of hidden-charm pentaquarks*, Eur. Phys. J. **C76** (2016) 572.
- [541] K. Azizi, Y. Sarac and H. Sundu, *Analysis of $P_c^+(4380)$ and $P_c^+(4450)$ as pentaquark states in the molecular picture with QCD sum rules*, Phys. Rev. **D95** (2017) 094016.
- [542] K. Azizi, Y. Sarac and H. Sundu, *Strong Decay of $P_c(4380)$ Pentaquark in a Molecular Picture*, Phys. Lett. **B782** (2018) 694.
- [543] H. X. Chen, W. Chen and S. L. Zhu, *Possible interpretations of the $P_c(4312)$, $P_c(4440)$, and $P_c(4457)$* , Phys. Rev. **D100** (2019) 051501.
- [544] J. R. Zhang, *Exploring a $\Sigma_c\bar{D}$ state: with focus on $P_c(4312)^+$* , Eur. Phys. J. **C79** (2019) 1001.
- [545] H. X. Chen, W. Chen, X. Liu and X. H. Liu, *Establishing the first hidden-charm pentaquark with strangeness*, Eur. Phys. J. **C81** (2021) 409.
- [546] K. Azizi, Y. Sarac and H. Sundu, *Properties of the $P_c(4312)$ pentaquark and its bottom partner*, Chin. Phys. **C45** (2021) 053103.
- [547] X. W. Wang, Z. G. Wang, G. L. Yu and Q. Xin, *Isospin eigenstates of the color singlet-singlet-type pentaquark states*, Sci. China Phys. Mech. Astron. **65** (2022) 291011.
- [548] X. W. Wang and Z. G. Wang, *Study of isospin eigenstates of the pentaquark molecular states with strangeness*, Int. J. Mod. Phys. **A37** (2022) 2250189.
- [549] X. W. Wang and Z. G. Wang, *Analysis of $P_{cs}(4338)$ and related pentaquark molecular states via QCD sum rules*, Chin. Phys. **C47** (2023) 013109.
- [550] Z. G. Wang, *Light tetraquark state candidates*, Adv. High Energy Phys. **2020** (2020) 6438730.
- [551] X. S. Yang, Q. Xin and Z. G. Wang, *Analysis of the $T_{c\bar{s}}(2900)$ and related tetraquark states with the QCD sum rules*, Int. J. Mod. Phys. **A38** (2023) 2350056.
- [552] R. Aaij et al, *Observation of five new narrow Ω_c^0 states decaying to $\Xi_c^+ K^-$* , Phys. Rev. Lett. **118** (2017) 182001.
- [553] J. Yelton et al, *Observation of Excited Ω_c Charmed Baryons in e^+e^- Collisions*, Phys. Rev. **D97** (2018) 051102.
- [554] R. Aaij et al, *Observation of new Ω_c^0 states decaying to the $\Xi_c^+ K^-$ final state*, Phys. Rev. Lett. **131** (2023) 131902.
- [555] R. Mizuk et al, *Observation of an Isotriplet of Excited Charmed Baryons Decaying to $\Lambda_c^+ \pi$* , Phys. Rev. Lett. **94** (2005) 122002.
- [556] B. Aubert et al, *Measurements of $\mathcal{B}(\bar{B}^0 \rightarrow \Lambda_c^+ \bar{p})$ and $\mathcal{B}(B^- \rightarrow \Lambda_c^+ \bar{p} \pi^-)$ and Studies of $\Lambda_c^+ \pi^-$ Resonances*, Phys. Rev. **D78** (2008) 112003.

- [557] B. Aubert et al, *Observation of a Charmed Baryon Decaying to $D^0 p$ at a Mass Near $2.94 \text{ GeV}/c^2$* , Phys. Rev. Lett. **98** (2007) 012001.
- [558] K. Abe et al, *Experimental Constraints on the Spin and Parity of the $\Lambda_c(2880)$* , Phys. Rev. Lett. **98** (2007) 262001.
- [559] R. Aaij et al, *Study of the $D^0 p$ amplitude in $\Lambda_b^0 \rightarrow D^0 p \pi^-$ decays*, JHEP **05** (2017) 030.
- [560] Y. B. Li et al, *Evidence of a new excited charmed baryon decaying to $\Sigma_c(2455)^{0,++} \pi^\pm$* , Phys. Rev. Lett. **130** (2023) 031901.
- [561] S. Sakai, F. K. Guo and B. Kubis, *Extraction of ND scattering lengths from the $\Lambda_b \rightarrow \pi^- p D^0$ decay and properties of the $\Sigma_c(2800)^+$* , Phys. Lett. **B808** (2020) 135623.
- [562] L. F. Zhao, H. X. Huang and J. L. Ping, *ND and NB systems in quark delocalization color screening model*, Eur. Phys. J. **A53** (2017) 28.
- [563] Z. Y. Wang, J. J. Qi, X. H. Guo and K. W. Wei, *Study of molecular ND bound states in the Bethe-Salpeter equation approach*, Phys. Rev. **D97** (2018) 094025.
- [564] M. J. Yan, F. Z. Peng and M. P. Valderrama, *Molecular charmed baryons and pentaquarks from light-meson exchange saturation*, Phys. Rev. **D109** (2024) 014023.
- [565] Y. Yan, X. H. Hu, Y. H. Wu, H. X. Huang and J. L. Ping, *Molecular state interpretation of charmed baryons in the quark model*, Eur. Phys. J. **C83** (2023) 524.
- [566] J. R. Zhang, *S -wave $D^{(*)}N$ molecular states: $\Sigma_c(2800)$ and $\Lambda_c(2940)^+?$* , Phys. Rev. **D89** (2014) 096006.
- [567] Z. L. Zhang, Z. W. Liu, S. Q. Luo, F. L. Wang, B. Wang and H. Xu, *$\Lambda_c(2910)$ and $\Lambda_c(2940)$ as the conventional baryons dressed with the D^*N channel*, Phys. Rev. **D107** (2023) 034036.
- [568] B. Wang, L. Meng and S. L. Zhu, *$D^{(*)}N$ interaction and the structure of $\Sigma_c(2800)$ and $\Lambda_c(2940)$ in chiral effective field theory*, Phys. Rev. **D101** (2020) 094035.
- [569] Y. Huang, J. He, J. J. Xie and L. S. Geng, *Production of the $\Lambda_c(2940)$ by kaon-induced reactions on a proton target*, Phys. Rev. **D99** (2019) 014045.
- [570] Q. Xin, X. S. Yang and Z. G. Wang, *The singly charmed pentaquark molecular states via the QCD sum rules*, Int. J. Mod. Phys. **A38** (2023) 2350123.
- [571] K. L. Wang and X. H. Zhong, *Toward establishing the low-lying P -wave excited Σ_c baryon states*, Chin. Phys. **C46** (2022) 023103.
- [572] K. L. Wang, Y. X. Yao, X. H. Zhong and Q. Zhao, *Strong and radiative decays of the low-lying S - and P -wave singly heavy baryons*, Phys. Rev. **D96** (2017) 116016.
- [573] H. M. Yang and H. X. Chen, *P -wave charmed baryons of the $SU(3)$ flavor 6_F* , Phys. Rev. **D104** (2021) 034037.
- [574] D. J. Jia, W. N. Liu and A. Hosaka, *Regge behaviors in orbitally excited spectroscopy of charmed and bottom baryons*, Phys. Rev. **D101** (2020) 034016.
- [575] H. Y. Cheng and C. W. Chiang, *Quantum numbers of Ω_c states and other charmed baryons*, Phys. Rev. **D95** (2017) 094018.
- [576] S. Q. Luo, B. Chen, Z. W. Liu and X. Liu, *Resolving the low mass puzzle of $\Lambda_c(2940)^+$* , Eur. Phys. J. **C80** (2020) 301.

- [577] Q. F. Lu, Z. Y. Wang and X. H. Zhong, *Strong decay of $\Lambda_c(2940)$ as a $2P$ state in the Λ_c family*, Eur. Phys. J. **C78** (2018) 599.
- [578] K. Azizi, Y. Sarac and H. Sundu, *Interpretation of the $\Lambda_c(2910)^+$ baryon newly seen by Belle Collaboration and its possible bottom partner*, Eur. Phys. J. **C82** (2022) 920.
- [579] W. J. Wang, L. Y. Xiao and X. H. Zhong, *The strong decays of the low-lying ρ -mode $1P$ -wave singly heavy baryons*, Phys. Rev. **D106** (2022) 074020.
- [580] G. L. Yu, M. Yan, Z. Y. Li, Z. G. Wang and J. Lu, *Strong decay properties of single heavy baryons Λ_Q , Σ_Q and Ω_Q* , Int. J. Mod. Phys. **A38** (2023) 2350082.
- [581] M. Karliner and J. L. Rosner, *Excited Ω_c baryons as $2S$ states*, Phys. Rev. **D108** (2023) 014006.
- [582] S. Q. Luo and X. Liu, *The newly observed $\Omega_c(3327)$: A good candidate for a D -wave charmed baryon*, Phys. Rev. **D107** (2023) 074041.
- [583] Z. G. Wang, F. Lu and Y. Liu, *Analysis of the D -wave Σ -type charmed baryon states with the QCD sum rules*, Eur. Phys. J. **C83** (2023) 689.
- [584] H. J. Wang, Z. Y. Di and Z. G. Wang, *Analysis of the $\Xi_b(6227)$ as the $\frac{1}{2}^\pm$ Pentaquark Molecular States with QCD Sum Rules*, Int. J. Theor. Phys. **59** (2020) 3124.
- [585] H. J. Wang, Z. Y. Di and Z. G. Wang, *Analysis of the excited Ω_c states as the $\frac{1}{2}^\pm$ pentaquark states with QCD sum rules*, Commun. Theor. Phys. **73** (2021) 035201.
- [586] Z. G. Wang and J. X. Zhang, *Possible pentaquark candidates: new excited Ω_c states*, Eur. Phys. J. **C78** (2018) 503.
- [587] Z. G. Wang and J. X. Zhang, *The decay width of the $Z_c(3900)$ as an axialvector tetraquark state in solid quark-hadron duality*, Eur. Phys. J. **C78** (2018) 14.
- [588] Z. G. Wang, *Strong decays of the $Y(4660)$ as a vector tetraquark state in solid quark-hadron duality*, Eur. Phys. J. **C79** (2019) 184.
- [589] F. S. Navarra and M. Nielsen, *$X(3872) \rightarrow J/\psi\pi^+\pi^-$ and $X(3872) \rightarrow J/\psi\pi^+\pi^-\pi^0$ decay widths from QCD sum rules*, Phys. Lett. **B639** (2006) 272.
- [590] Z. G. Wang and T. Huang, *The $Z_b(10610)$ and $Z_b(10650)$ as axial-vector tetraquark states in the QCD sum rules*, Nucl. Phys. **A930** (2014) 63.
- [591] J. M. Dias, K. P. Khemchandani, A. M. Torres, M. Nielsen and C. M. Zanetti, *A QCD sum rule calculation of the $X^\pm(5568) \rightarrow B_s^0\pi^\pm$ decay width*, Phys. Lett. **B758** (2016) 235.
- [592] W. Chen, T. G. Steele, H. X. Chen and S. L. Zhu, *$Z_c(4200)^+$ decay width as a charmonium-like tetraquark state*, Eur. Phys. J. **C75** (2015) 358.
- [593] K. Azizi, Y. Sarac and H. Sundu, *Investigation of $P_{cs}(4459)^0$ pentaquark via its strong decay to $\Lambda J/\psi$* Phys. Rev. **D103** (2021) 094033.
- [594] K. Azizi, Y. Sarac and H. Sundu, *Investigation of a candidate spin- $\frac{1}{2}$ hidden-charm triple strange pentaquark state P_{csss}* , Phys. Rev. **D107** (2023) 014023.
- [595] Z. G. Wang, *Analysis of strong decays of the $Z_c(4600)$ with the QCD sum rules*, Int. J. Mod. Phys. **A34** (2019) 1950110.
- [596] Z. G. Wang and Z. Y. Di, *Analysis of the mass and width of the $X(4140)$ as axialvector tetraquark state*, Eur. Phys. J. **C79** (2019) 72.

- [597] Z. G. Wang, *Revisit the $X(4274)$ as the Axialvector Tetraquark State*, Acta Phys. Polon. **B51** (2020) 435.
- [598] Z. G. Wang and X. Wang, *Analysis of the strong decays of the $P_c(4312)$ as a pentaquark molecular state with QCD sum rules*, Chin. Phys. **C44** (2020) 103102.
- [599] Z. G. Wang, H. J. Wang and Q. Xin, *The hadronic coupling constants of the lowest hidden-charm pentaquark state with the QCD sum rules in rigorous quark-hadron duality*, Chin. Phys. **C45** (2021) 063104.
- [600] Y. J. Xu, Y. L. Liu and M. Q. Huang, *The magnetic moment of $P_c(4312)$ as a $\bar{D}\Sigma_c$ molecular state*, Eur. Phys. J. **C81** (2021) 421.
- [601] Z. G. Wang, *Decay widths of $Z_{cs}(3985/4000)$ based on rigorous quark-hadron duality*, Chin. Phys. **C46** (2022) 103106.
- [602] Z. G. Wang and X. S. Yang, *The two-body strong decays of the fully-charm tetraquark states*, AAPPs Bull. **34** (2024) 5.
- [603] X. W. Wang and Z. G. Wang, *Strong decays of the $P_c(4312)$ and its isospin cousin via the QCD sum rules*, Chin. Phys. **C48** (2024) 053102.
- [604] X. W. Wang and Z. G. Wang, *Strong decays of $P_{cs}(4338)$ and its high isospin cousin via QCD sum rules*, Phys. Rev. **D110** (2024) 014008.
- [605] S. S. Agaev, K. Azizi and H. Sundu, *Exploring the resonances $X(4140)$ and $X(4274)$ through their decay channels*, Phys. Rev. **D95** (2017) 114003.
- [606] S. S. Agaev, K. Azizi and H. Sundu, *Spectroscopic parameters and decays of the resonance $Z_b(10610)$* , Eur. Phys. J. **C77** (2017) 836.
- [607] H. Sundu, S. S. Agaev and K. Azizi, *Resonance $Y(4660)$ as a vector tetraquark and its strong decay channels*, Phys. Rev. **D98** (2018) 054021.
- [608] Y. Xie and H. Sun, *Investigate the strong coupling of $g_{XJ/\psi\phi}$ in $X(4500) \rightarrow J/\psi\phi$ by using the three-point sum rules and the light-cone sum rules*, Nucl. Phys. **B1000** (2024) 116471.
- [609] B. L. Ioffe and A. V. Smilga, *Nucleon Magnetic Moments and Magnetic Properties of Vacuum in QCD*, Nucl. Phys. **B232** (1984) 109.
- [610] V. M. Belyaev, V. M. Braun, A. Khodjamirian and R. Ruckl, *$D^*D\pi$ and $B^*B\pi$ couplings in QCD*, Phys. Rev. **D51** (1995) 6177.
- [611] Z. G. Wang, *Analysis of the decay $Y(4500) \rightarrow D^*\bar{D}^*\pi$ with the light-cone QCD sum rules*, Nucl. Phys. **B993** (2023) 116265.
- [612] P. Ball, *Theoretical update of pseudoscalar meson distribution amplitudes of higher twist: The Nonsinglet case*, JHEP **01** (1999) 010.
- [613] V. M. Braun and I. E. Filyanov, *Conformal Invariance and Pion Wave Functions of Non-leading Twist*, Z. Phys. **C48** (1990) 239.
- [614] Z. G. Wang, *Three-body strong decays of the $Y(4230)$ via the light-cone QCD sum rules*, Int. J. Mod. Phys. **A38** (2023) 2350175.